

**VOLUME 9, NUMBER 1      JANUARY 2011**

**ISSN:1548-5390 PRINT,1559-176X ONLINE**



**JOURNAL  
OF CONCRETE  
AND APPLICABLE  
MATHEMATICS  
EUDOXUS PRESS,LLC**

**GUEST EDITORS: HIKMET CAGLAR, LEVENT CUHACI,  
GURSEL HACIBEKIROGLU and MEHMET OZER  
SPECIAL ISSUE IV: “CHAOS and COMPLEX SYSTEMS 2010”**

**SCOPE AND PRICES OF THE JOURNAL**  
**Journal of Concrete and Applicable Mathematics**

A quartely international publication of **Eudoxus Press,LLC**

**Editor in Chief: George Anastassiou**  
Department of Mathematical Sciences,  
University of Memphis  
Memphis, TN 38152, U.S.A.  
ganastss@memphis.edu

The main purpose of the "Journal of Concrete and Applicable Mathematics" is to publish high quality original research articles from all subareas of Non-Pure and/or Applicable Mathematics and its many real life applications, as well connections to other areas of Mathematical Sciences, as long as they are presented in a Concrete way. It welcomes also related research survey articles and book reviews. A sample list of connected mathematical areas with this publication includes and is not restricted to: Applied Analysis, Applied Functional Analysis, Probability theory, Stochastic Processes, Approximation Theory, O.D.E, P.D.E, Wavelet, Neural Networks, Difference Equations, Summability, Fractals, Special Functions, Splines, Asymptotic Analysis, Fractional Analysis, Inequalities, Moment Theory, Numerical Functional Analysis, Tomography, Asymptotic Expansions, Fourier Analysis, Applied Harmonic Analysis, Integral Equations, Signal Analysis, Numerical Analysis, Optimization, Operations Research, Linear Programming, Fuzzyness, Mathematical Finance, Stochastic Analysis, Game Theory, Math. Physics aspects, Applied Real and Complex Analysis, Computational Number Theory, Graph Theory, Combinatorics, Computer Science Math. related topics, combinations of the above, etc. In general any kind of Concretely presented Mathematics which is Applicable fits to the scope of this journal. Working Concretely and in Applicable Mathematics has become a main trend in many recent years, so we can understand better and deeper and solve the important problems of our real and scientific world. "Journal of Concrete and Applicable Mathematics" is a peer-reviewed International Quarterly Journal. We are calling for papers for possible publication. The contributor should send three copies of the contribution to the editor in-Chief typed in TEX, LATEX double spaced. [ See: Instructions to Contributors]

**Journal of Concrete and Applicable Mathematics(JCAAM)**  
**ISSN:1548-5390 PRINT, 1559-176X ONLINE.**

is published in January, April, July and October of each year by

**EUDOXUS PRESS,LLC,**  
1424 Beaver Trail Drive, Cordova, TN38016, USA,  
Tel.001-901-751-3553  
anastassioug@yahoo.com  
<http://www.EudoxusPress.com>.

**Visit also [www.msci.memphis.edu/~ganastss/jcaam](http://www.msci.memphis.edu/~ganastss/jcaam).**  
**Webmaster: Ray Clapsadle**

**Annual Subscription Current Prices:** For USA and Canada, Institutional: Print \$400, Electronic \$250, Print and Electronic \$450. Individual: Print \$150, Electronic

\$80,Print &Electronic \$200.For any other part of the world add \$50 more to the above prices for Print.

Single article PDF file for individual \$15.Single issue in PDF form for individual \$60.

No credit card payments.Only certified check,money order or international check in US dollars are acceptable.

Combination orders of any two from JoCAAA,JCAAM,JAFA receive 25% discount,all three receive 30% discount.

**Copyright**©2011 by Eudoxus Press,LLC all rights reserved.JCAAM is printed in USA.

**JCAAM is reviewed and abstracted by AMS Mathematical Reviews,MATHSCI,and Zentralblatt MATH.**

It is strictly prohibited the reproduction and transmission of any part of JCAAM and in any form and by any means without the written permission of the publisher.It is only allowed to educators to Xerox articles for educational purposes.The publisher assumes no responsibility for the content of published papers.

***JCAAM IS A JOURNAL OF RAPID PUBLICATION***

---

## Editorial Board

### Associate Editors

---

#### Editor in -Chief:

George Anastassiou  
Department of Mathematical Sciences  
The University Of Memphis  
Memphis, TN 38152, USA  
tel. 901-678-3144, fax 901-678-2480  
e-mail ganastss@memphis.edu  
www.msci.memphis.edu/~anastasg/anlyjour.htm  
Areas: Approximation Theory,  
Probability, Moments, Wavelet,  
Neural Networks, Inequalities, Fuzzyness.

#### Associate Editors:

1) Ravi Agarwal  
Florida Institute of Technology  
Applied Mathematics Program  
150 W. University Blvd.  
Melbourne, FL 32901, USA  
agarwal@fit.edu  
Differential Equations, Difference  
Equations,  
Inequalities

2) Drumi D. Bainov  
Medical University of Sofia  
P.O. Box 45, 1504 Sofia, Bulgaria  
drumibainov@yahoo.com  
Differential Equations, Optimal Control,  
Numerical Analysis, Approximation Theory

3) Carlo Bardaro  
Dipartimento di Matematica & Informatica  
Universita' di Perugia  
Via Vanvitelli 1  
06123 Perugia, ITALY  
tel. +390755855034, +390755853822,  
fax +390755855024  
bardaro@unipg.it ,  
bardaro@dipmat.unipg.it  
Functional Analysis and Approximation Th.,  
Summability, Signal Analysis, Integral  
Equations,  
Measure Th., Real Analysis

4) Francoise Bastin  
Institute of Mathematics  
University of Liege  
4000 Liege

21) Gustavo Alberto Perla Menzala  
National Laboratory of Scientific Computation  
LNCC/MCT  
Av. Getulio Vargas 333  
25651-075 Petropolis, RJ  
Caixa Postal 95113, Brasil  
and

Federal University of Rio de Janeiro  
Institute of Mathematics  
RJ, P.O. Box 68530 Rio de Janeiro, Brasil  
perla@lncc.br and perla@im.ufrj.br  
Phone 55-24-22336068, 55-21-25627513 Ext 224  
FAX 55-24-22315595  
Hyperbolic and Parabolic Partial Differential  
Equations,  
Exact controllability, Nonlinear Lattices and  
Global  
Attractors, Smart Materials

22) Ram N. Mohapatra  
Department of Mathematics  
University of Central Florida  
Orlando, FL 32816-1364  
tel. 407-823-5080  
ramm@pegasus.cc.ucf.edu  
Real and Complex analysis, Approximation Th.,  
Fourier Analysis, Fuzzy Sets and Systems

23) Rainer Nagel  
Arbeitsbereich Funktionalanalysis  
Mathematisches Institut  
Auf der Morgenstelle 10  
D-72076 Tuebingen  
Germany  
tel. 49-7071-2973242  
fax 49-7071-294322  
rana@fa.uni-tuebingen.de  
evolution equations, semigroups, spectral th.,  
positivity

24) Panos M. Pardalos  
Center for Appl. Optimization  
University of Florida  
303 Weil Hall  
P.O. Box 116595  
Gainesville, FL 32611-6595  
tel. 352-392-9011  
pardalos@ufl.edu  
Optimization, Operations Research



BELGIUM

f.bastin@ulg.ac.be  
Functional Analysis,Wavelets

5) Yeol Je Cho  
Department of Mathematics Education  
College of Education  
Gyeongsang National University  
Chinju 660-701

KOREA

tel.055-751-5673 Office,  
055-755-3644 home,  
fax 055-751-6117  
yjcho@nongae.gsnu.ac.kr  
Nonlinear operator Th.,Inequalities,  
Geometry of Banach Spaces

6) Sever S.Dragomir  
School of Communications and Informatics  
Victoria University of Technology  
PO Box 14428  
Melbourne City M.C  
Victoria 8001,Australia  
tel 61 3 9688 4437,fax 61 3 9688 4050  
sever.dragomir@vu.edu.au,  
sever@sci.vu.edu.au  
Math.Analysis,Inequalities,Approximation  
Th.,  
Numerical Analysis, Geometry of Banach  
Spaces,  
Information Th. and Coding

7) Angelo Favini  
Università di Bologna  
Dipartimento di Matematica  
Piazza di Porta San Donato 5  
40126 Bologna, ITALY  
tel.++39 051 2094451  
fax.++39 051 2094490  
favini@dm.unibo.it  
Partial Differential Equations, Control  
Theory,  
Differential Equations in Banach Spaces

8) Claudio A. Fernandez  
Facultad de Matematicas  
Pontificia Universidad Católica de Chile  
Vicuna Mackenna 4860  
Santiago, Chile  
tel.++56 2 354 5922  
fax.++56 2 552 5916  
cfernand@mat.puc.cl  
Partial Differential Equations,  
Mathematical Physics,  
Scattering and Spectral Theory

25) Svetlozar T.Rachev  
Dept.of Statistics and Applied Probability  
Program

University of California,Santa Barbara  
CA 93106-3110,USA  
tel.805-893-4869  
rachev@pstat.ucsb.edu

AND

Chair of Econometrics and Statistics  
School of Economics and Business Engineering  
University of Karlsruhe  
Kollegium am Schloss,Bau II,20.12,R210  
Postfach 6980,D-76128,Karlsruhe,Germany  
tel.011-49-721-608-7535  
rachev@lsoe.uni-karlsruhe.de  
Mathematical and Empirical Finance,  
Applied Probability, Statistics and Econometrics

26) John Michael Rassias  
University of Athens  
Pedagogical Department  
Section of Mathematics and Infomatics  
20, Hippocratous Str., Athens, 106 80, Greece

Address for Correspondence

4, Agamemnonos Str.  
Aghia Paraskevi, Athens, Attikis 15342 Greece  
jrassias@primedu.uoa.gr  
jrassias@tellas.gr  
Approximation Theory,Functional Equations,  
Inequalities, PDE

27) Paolo Emilio Ricci  
Universita' degli Studi di Roma "La Sapienza"  
Dipartimento di Matematica-Istituto  
"G.Castelnuovo"  
P.le A.Moro,2-00185 Roma,ITALY  
tel.++39 0649913201,fax ++39 0644701007  
riccip@uniroma1.it,Paoloemilio.Ricci@uniroma1.it  
Orthogonal Polynomials and Special functions,  
Numerical Analysis, Transforms,Operational  
Calculus,  
Differential and Difference equations

28) Cecil C.Rousseau  
Department of Mathematical Sciences  
The University of Memphis  
Memphis,TN 38152,USA  
tel.901-678-2490,fax 901-678-2480  
ccrousse@memphis.edu  
Combinatorics,Graph Th.,  
Asymptotic Approximations,  
Applications to Physics

29) Tomasz Rychlik

- 9) A.M.Fink  
Department of Mathematics  
Iowa State University  
Ames, IA 50011-0001, USA  
tel.515-294-8150  
fink@math.iastate.edu  
Inequalities, Ordinary Differential Equations
- 10) Sorin Gal  
Department of Mathematics  
University of Oradea  
Str.Armatei Romane 5  
3700 Oradea, Romania  
galso@uoradea.ro  
Approximation Th., Fuzzyness, Complex Analysis
- 11) Jerome A. Goldstein  
Department of Mathematical Sciences  
The University of Memphis,  
Memphis, TN 38152, USA  
tel.901-678-2484  
jgoldste@memphis.edu  
Partial Differential Equations, Semigroups of Operators
- 12) Heiner H. Gonska  
Department of Mathematics  
University of Duisburg  
Duisburg, D-47048  
Germany  
tel.0049-203-379-3542 office  
gonska@informatik.uni-duisburg.de  
Approximation Th., Computer Aided Geometric Design
- 13) Dmitry Khavinson  
Department of Mathematical Sciences  
University of Arkansas  
Fayetteville, AR 72701, USA  
tel.(479)575-6331, fax(479)575-8630  
dmitry@uark.edu  
Potential Th., Complex Analysis, Holomorphic PDE,  
Approximation Th., Function Th.
- 14) Virginia S. Kiryakova  
Institute of Mathematics and Informatics  
Bulgarian Academy of Sciences  
Sofia 1090, Bulgaria  
virginia@diogenes.bg  
Special Functions, Integral Transforms, Fractional Calculus
- 15) Hans-Bernd Knoop  
Institute of Mathematics  
Polish Academy of Sciences  
Chopina 12, 87100 Torun, Poland  
T.Rychlik@impan.gov.pl  
Mathematical Statistics, Probabilistic Inequalities
- 30) Bl. Sendov  
Institute of Mathematics and Informatics  
Bulgarian Academy of Sciences  
Sofia 1090, Bulgaria  
bsendov@bas.bg  
Approximation Th., Geometry of Polynomials, Image Compression
- 31) Igor Shevchuk  
Faculty of Mathematics and Mechanics  
National Taras Shevchenko  
University of Kyiv  
252017 Kyiv  
UKRAINE  
shevchuk@univ.kiev.ua  
Approximation Theory
- 32) H.M. Srivastava  
Department of Mathematics and Statistics  
University of Victoria  
Victoria, British Columbia V8W 3P4  
Canada  
tel.250-721-7455 office, 250-477-6960 home,  
fax 250-721-8962  
harimsri@math.uvic.ca  
Real and Complex Analysis, Fractional Calculus and Appl.,  
Integral Equations and Transforms, Higher Transcendental Functions and Appl., q-Series and q-Polynomials, Analytic Number Th.
- 33) Stevo Stevic  
Mathematical Institute of the Serbian Acad. of Science  
Knez Mihailova 35/I  
11000 Beograd, Serbia  
sstevic@ptt.yu; sstevo@matf.bg.ac.yu  
Complex Variables, Difference Equations, Approximation Th., Inequalities
- 34) Ferenc Szidarovszky  
Dept. Systems and Industrial Engineering  
The University of Arizona  
Engineering Building, 111  
PO.Box 210020  
Tucson, AZ 85721-0020, USA  
szidar@sie.arizona.edu  
Numerical Methods, Game Th., Dynamic Systems,

Institute of Mathematics  
Gerhard Mercator University  
D-47048 Duisburg  
Germany  
tel.0049-203-379-2676  
knoop@math.uni-duisburg.de  
Approximation Theory, Interpolation

16) Jerry Koliha  
Dept. of Mathematics & Statistics  
University of Melbourne  
VIC 3010, Melbourne  
Australia  
koliha@unimelb.edu.au  
Inequalities, Operator Theory,  
Matrix Analysis, Generalized Inverses

17) Mustafa Kulenovic  
Department of Mathematics  
University of Rhode Island  
Kingston, RI 02881, USA  
kulenm@math.uri.edu  
Differential and Difference Equations

18) Gerassimos Ladas  
Department of Mathematics  
University of Rhode Island  
Kingston, RI 02881, USA  
gladas@math.uri.edu  
Differential and Difference Equations

19) V. Lakshmikantham  
Department of Mathematical Sciences  
Florida Institute of Technology  
Melbourne, FL 32901  
e-mail: lakshmik@fit.edu  
Ordinary and Partial Differential  
Equations,  
Hybrid Systems, Nonlinear Analysis

20) Rupert Lasser  
Institut für Biomathematik & Biomertie, GSF  
-National Research Center for environment  
and health  
Ingolstaedter Landstr.1  
D-85764 Neuherberg, Germany  
lasser@gsf.de  
Orthogonal Polynomials, Fourier Analysis,  
Mathematical Biology

Multicriteria Decision making,  
Conflict Resolution, Applications  
in Economics and Natural Resources  
Management

35) Gancho Tachev  
Dept. of Mathematics  
Univ. of Architecture, Civil Eng. and Geodesy  
1 Hr. Smirnenski Blvd  
BG-1421 Sofia, Bulgaria  
gtt\_fte@uacg.bg  
Approximation Theory

36) Manfred Tasche  
Department of Mathematics  
University of Rostock  
D-18051 Rostock  
Germany  
manfred.tasche@mathematik.uni-rostock.de  
Approximation Th., Wavelet, Fourier Analysis,  
Numerical Methods, Signal Processing,  
Image Processing, Harmonic Analysis

37) Chris P. Tsokos  
Department of Mathematics  
University of South Florida  
4202 E. Fowler Ave., PHY 114  
Tampa, FL 33620-5700, USA  
profcp@math.usf.edu, profcp@chumal.cas.usf.edu  
Stochastic Systems, Biomathematics,  
Environmental Systems, Reliability Th.

38) Lutz Volkmann  
Lehrstuhl II für Mathematik  
RWTH-Aachen  
Templergraben 55  
D-52062 Aachen  
Germany  
volkm@math2.rwth-aachen.de  
Complex Analysis, Combinatorics, Graph Theory

## Preface

These **six** special issues, which constitute the proceedings of the symposium 3rd International Interdisciplinary Chaos Symposium on CHAOS and COMPLEX SYSTEMS - CCS2010 (21-24 May 2010), have tried to create a forum for the exchange of information and experience in the exciting interdisciplinary field of chaos. However the conference was more in the Applied Mathematics, Social Sciences and Physics direction centered.

The view of the organizers concerning international resonance of the conference has been fulfilled: approximately 200 scientists from 21 different countries (Algeria, Bulgaria, Croatia, Denmark, France, Germany, Greece, Iran, Italy, Jordan, Lebanon, Malaysia, Pakistan, Republic of Serbia, Russia, Sultanate of Oman, Tunisia, Turkey, Ukraine, United Kingdom and United States of America) have participated. Good relations to research institutes of these countries might be of great importance for science and applications in different fields of Chaos.

On behalf of the Organizing Committee we would like to express our thanks to the Scientific Committee, the Program Committee and to all who have contributed to this conference for their support and advice. We are also grateful to the invited lecturers Prof. Henry D.I. Abarbanel, Prof. David S. Byrne, Prof. George Anastassiou, Prof. Zidong Wang, Prof. Turgut Ozis and Prof. Markus J. Aschwanden.

Special thanks are due to Rector Prof. Dursun Kocer and Vice Rector Prof. Cetin Bolcal for their close support, advice and incentive encouraging.

Our thanks are also due to the Istanbul Kultur University, which was hosting this symposium and provided all of its facilities.

Finally, we are grateful to the Editor-in-Chief, Prof. George Anastassiou for accepting this volume for publication.

Hikmet Caglar, PhD in Mathematics, [s.caglar@iku.edu.tr](mailto:s.caglar@iku.edu.tr)  
Levent Cuhaci, PhD in Computer Science, [l.cuhaci@iku.edu.tr](mailto:l.cuhaci@iku.edu.tr)  
Gursel Hacibekiroglu, PhD in Physics, [g.hacibekiroglu@iku.edu.tr](mailto:g.hacibekiroglu@iku.edu.tr)  
Mehmet Ozer, PhD in Physics, [m.ozar@iku.edu.tr](mailto:m.ozar@iku.edu.tr)

Istanbul Kultur University, Faculty of Science and Letters, Istanbul, Turkey

# TEMPORAL AND THREE DIMENSIONAL SPATIAL ANALYSIS OF EARTHQUAKE ACTIVITY BETWEEN 1970 AND 2010 ALONG THE NORTH ANATOLIAN FAULT ZONE, TURKEY

**Serkan ÖZTÜRK**

Gümüşhane University, Department of Geophysics, TR-29100, Gümüşhane, Turkey

Tel: +90 456 233 74 25 - 26

e-mail: seko6134@hotmail.com

## ABSTRACT

Characteristics of seismic activity from 1970 to 2010 along the North Anatolian Fault Zone (NAFZ) are analyzed to make a statistical assessment by using the Gutenberg-Richter  $b$ -value, seismic quiescence  $Z$ -value, fractal dimension  $D_c$ -value, and spatial, temporal and magnitude distributions. Magnitude completeness,  $M_c$ , changes between 2.7 and 2.9 in all parts of the NAFZ. Frequency-magnitude distribution of the earthquakes is well represented by the Gutenberg-Richter law with a  $b$ -value typically close to 1. A strong decrease in temporal distribution of  $b$ -value is observed before the great main shocks.  $D_c$ -values are relatively large and the seismic activity is more clustered at larger scales for all parts of the NAFZ. From the standard normal deviate  $Z$ -value test, eight significant anomalous zones are centered at 41.08°N-28.58°E (around Silivri), 41.47°N-29.51°E (in the Black Sea), 40.69°N-29.78°E (including Izmit), 40.26°N-26.46°E (around Gelibolu, Canakkale), 40.59°N-31.03°E (including Duzce fault), 40.86°N-35.30°E (around Amasya), 39.48°N-39.74°E (around Erzincan), and 39.06°N-40.50°E (around Bingöl).

**Keywords:** *Seismicity, North Anatolian Fault Zone,  $b$ -value,  $D_c$ -value,  $Z$ -value.*

## 1. INTRODUCTION

The variation of the seismic patterns in space and time in the North Anatolian Fault Zone (NAFZ), Turkey, is analyzed statistically and physically by many authors and some significant results are obtained [e.g., 1,2,3,4,5]. The NAFZ is one of the most seismically active regions of Turkey. The NAFZ is a major tectonic feature with a well-defined fault trace and an established history of seismicity. Because of topography and water resources, the fault zone is a relatively densely populated, agricultural area dotted by many villages and small towns. Most intermediate and large magnitude earthquakes occurring along the North Anatolian Fault (NAF) have produced surface breaks. Activity of the NAF during the 20<sup>th</sup> century began with the destructive Erzincan earthquake in 1939 in northeast Turkey and it migrated westwards by a series of earthquakes in 1942, 1943, 1944, 1951, 1957 and 1967 [6,7].

At the turn of the previous century, two destructive earthquakes occurred on the western continuation of the NAFZ in northwestern Turkey. The 17 August 1999,  $M_w$  7.4, Izmit earthquake ruptured the NAFZ along a 125-km segment, which extended from Golyaka, Duzce, in the east through the Izmit Bay into the Sea of Marmara in the west. The 12 November 1999,  $M_w$  7.2, Duzce earthquake ruptured a segment about 50 km long, further to the east [8]. These two earthquakes are the latest in a sequence of large events that have ruptured an approximately 1000-km-long section of the NAFZ. This sequence began with the 1939 Erzincan earthquake in the northeastern part of Turkey, followed by a generally westward migration of earthquakes [6,7].

This work aims to identify the seismicity behaviors in the North Anatolian Fault Zone in order to better understand the earthquake properties in this significant area. For this purpose, this study is addressed the mapping of size-scaling distributions such as spatial, temporal and magnitude distribution of seismic activity, completeness magnitude  $M_c$  and  $b$ -values with time, seismic quiescence  $Z$ -value, fractal dimension  $D_c$  and the correlation of results with the structural elements which carry high risk for the region.

## 2. DATA AND ACTIVE TECTONICS OF THE NORTH ANATOLIAN FAULT ZONE

A part of the database used in this study is taken from Öztürk [9]. Öztürk [9] developed some relationships between different magnitude scales ( $m_b$ -body wave magnitude,  $M_S$ -surface wave magnitude,  $M_L$ -local magnitude,  $M_D$ -duration magnitude) in order to prepare a homogenous earthquake catalogue from different data sets. For this purpose, he used the catalogue data from the website of the International Seismological Centre (ISC) for the time period from 1970 to 1973 and Bogazici University, Kandilli Observatory and Research Institute (KOERI) for the time interval 1974 and 2005. He prepared a homogenous instrumental data catalogue for  $M_D$  magnitude using these relationships. This homogeneous catalogue for duration magnitude includes 73530 earthquakes whose magnitudes are equal to or larger than 1.4, which occurred in Turkey between 1970 and 2006. Öztürk [9] used the empirical relations in order to get a homogenous catalogue from 1970 to 2006 and so this relatively smaller magnitude level  $M_D > 1.4$  is obtained. For the time period between 2006 and 2010, KOERI catalogue is also used. The bounds of the region analyzed in this study are provided from Öztürk [9]. Since Öztürk [9] made a detailed zonation, a part of these seismic source zones is considered in this study. The North Anatolian Fault Zone is selected as an area of investigation in this study. According to Öztürk [9], region 20 (region 1 in this study) covers the Marmara part of the North Anatolian Fault Zone (MNAFZ), region 21 (region 2 in this study) is the Anatolian part of the North Anatolian Fault Zone (ANAFZ) and region 24 (region 3 in this study) is the Eastern part of the North Anatolian Fault Zone (ENAFZ). The major tectonic structures of the region adopted from Şaroğlu et al. [10] and the zones from Öztürk [9] are shown in Figure 1.

There are total 2804 events in these three regions between 2006 and 2010. The time interval considered for the present work is 1970 to 2010. The magnitudes in the used catalogue are  $M_D$ -duration magnitude. Thus, the final data catalogue for region 1 (9884 events), region 2 (4669 events) and region 3 (2645 events) consists of 17198 earthquakes in total (depth < 70 km) with magnitudes greater than or equal to 1.4. Epicenter distributions of whole earthquakes ( $M_D \geq 1.4$ ) and the principal main shocks ( $M_D \geq 5.5$ ) in the study region are shown in Figure 2.

The North Anatolian Fault Zone is one of the best-known strike-slip faults in the world because of its remarkable seismic activity, extremely well developed surface expression and importance for the tectonics of eastern Mediterranean region [11]. The NAFZ is a very active structure, and according to geodesy it accommodates 24-30 mm/yr of dextral motion [12]. The NAFZ is an approximately 1500 km-long, broadly arc-shaped, dextral strike-slip fault system that extends from eastern Turkey in the east to the north Aegean in the west. It is predominantly a single zone of a few hundred meters to 40 km wide. Along much of its length, this fault zone consists of a few shorter sub-parallel fault strands that sometimes display an anatomizing pattern [11]. To the east, the NAFZ forms a typical triple-junction and joins with the sinistral East Anatolian Fault Zone at Karlıova. The NAFZ does not terminate at the Karlıova triple junction but, continues towards south east. During the past 60 years, NAFZ has produced earthquakes along different sections in a system manner that is atypical of long faults. Beginning with 1939 Erzincan earthquake ( $M=7.9$  to  $8.0$ ), which produced about 350 km of ground rupture, the NAFZ ruptured by nine moderate to large earthquakes ( $M > 6.7$ ), and formed more than 1000 km surface rupture along the fault. Most of the earthquakes occurred sequentially in a westward progression. These include 26 December 1939 Erzincan ( $M=7.9$  to  $8.0$ ), 20 December 1942 Erbaa-Niksar ( $M=7.1$ ), 26 November 1943 Tosya ( $M=7.6$ ), 1 February 1944 Bolu-Gerede ( $M=7.3$ ), 13 August 1951 Çankırı ( $M=6.9$ ), 26 May 1957 Abant ( $M=7.0$ ), 22 July 1967 Mudurnu valley ( $M=7.1$ ), 13 March 1992 Erzincan ( $M=6.8$ ), 17 August 1999 Izmit ( $M=7.4$ ), and 12 November 1999 Düzce ( $M=7.2$ ) earthquakes [11].

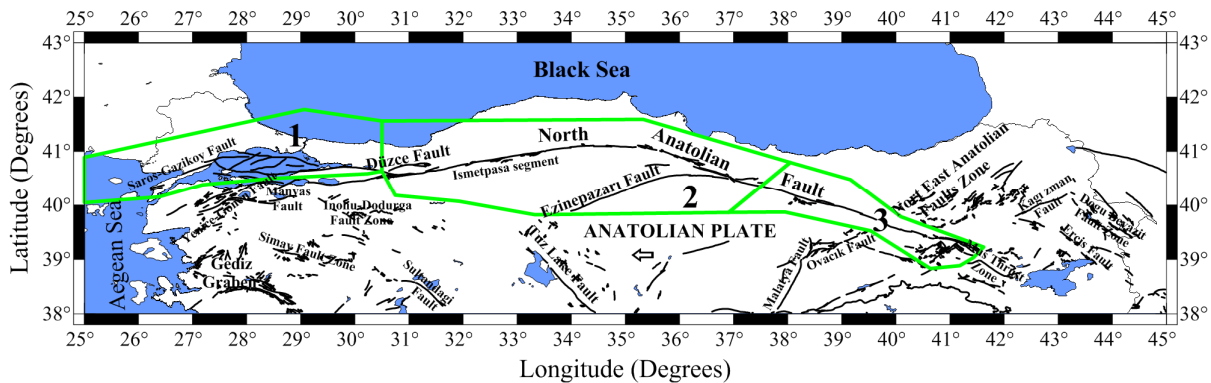


Figure 1. Tectonic structures and seismic source zones in the North Anatolian Fault Zone. Faults were modified from Şaroğlu et al. [10] and the seismic regions from Öztürk [9]. (1: Marmara part of the North Anatolian Fault Zone, 2: Anatolian part of the North Anatolian Fault Zone, 3: Eastern part of the North Anatolian Fault Zone).

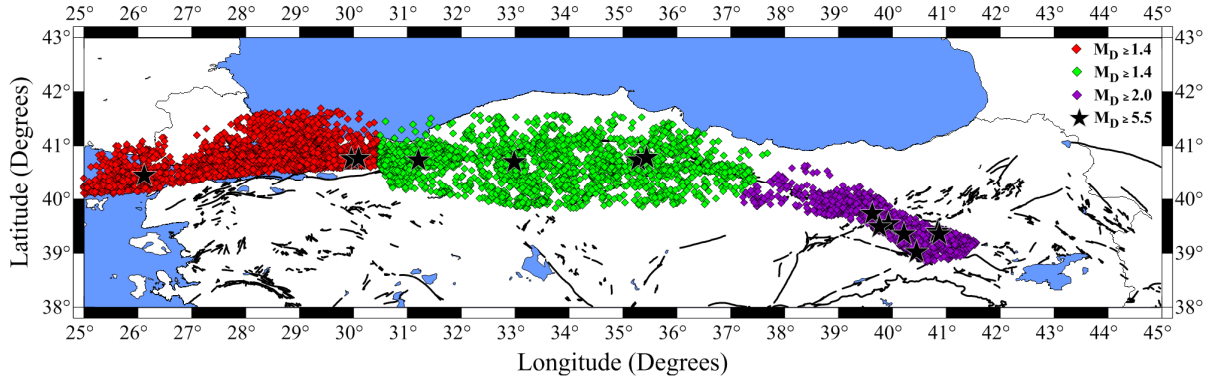


Figure 2. Seismicity in the North Anatolian Fault Zone including all earthquakes with  $M_D \geq 1.4$  and depth  $< 70$  km between February 1970 and December 2009. Stars represent the principal main shocks with  $M_D \geq 5.5$ .

### 3. DEFINITION OF THE THEORETICAL BACKGROUND

A number of seismicity parameters are used in order to characterize the seismic behavior along the North Anatolian Fault Zone. These parameters are size-scaling parameters (such as slope of recurrence curve  $b$ -value), temporal and spatial distribution of earthquakes with characteristic of fractal correlation dimension,  $D_c$ , and seismic quiescence  $Z$ -value as well as the histograms of temporal, spatial and magnitude distribution.

#### 3.1. Magnitude-frequency relation ( $b$ -value) and completeness magnitude ( $M_c$ value)

Size distribution of earthquakes in most cases is well described by the Gutenberg and Richter [13] relationship:

$$\log_{10} N(M) = a - bM \quad (1)$$

where  $N(M)$  is the cumulative number of earthquakes with magnitudes equal to or larger than  $M$ ,  $b$  describes the slope of the size distribution of events, and  $a$  is proportional to the seismicity rate.  $b$ -value is one of the most widely used statistical parameters to describe the size scaling properties of seismicity. Utsu [14] summarized that  $b$ -values change roughly in the range 0.5 to 1.5, depending on the different region. However, on average, the regional scale estimates of  $b$ -value are approximately equal to 1 [15]. The maximum likelihood method provides the least biased estimate of  $b$ -value [16]:

$$b = 2.303 / (M_{mean} - M_{min} + 0.05) \quad (2)$$

where  $M_{mean}$  is the mean magnitude of events and  $M_{min}$  is the minimum magnitude of completeness in the earthquake catalogue. Accurate estimates of local changes of  $M_{min}$  can be made if relatively large numbers (100 or so) of local observations are available for analysis [17]. The value 0.05 in Eq. (2) is a correction constant that compensates for round off errors. The 95% confidence limits on the estimates of  $b$ -value are  $\pm 1.96b / \sqrt{n}$ , where  $n$  is the number of earthquakes used to make the estimate. This yields confidence limits on  $b$ -value of  $\pm 0.1$ -0.2 for a typical sample consisting of  $n=100$  earthquakes.

The magnitude above which all events have been recorded is important for all seismicity-based studies because it is frequently necessary to use the maximum number of events available for high-quality results. The estimate of the magnitude of completeness ( $M_c$ ) is based on the assumption of Gutenberg Richter's power-law distribution against magnitude [17]. Completeness in magnitude reporting varies systematically as a function of space and time, and particularly the temporal changes can potentially produce erroneous estimates of seismicity parameters, especially in  $b$ -value. Since a part of this study deals with the seismicity rate change, the magnitude of completeness of the catalog used to detect the quiescence is an important parameter.

#### 3.2. Fractal Dimension, $D_c$

Fractal distributions imply that the number of objects larger than a specified size has a power law dependence on the size. Spatial patterns of earthquake distribution and temporal patterns of occurrence are demonstrated to be fractal using the two-point correlation dimension  $D_c$ . The correlation integral method was developed by Grassberger and Procaccia [18] and correlation dimension  $D_c$  is obtained from following equations:

$$Dc = \lim_{r \rightarrow 0} [\log C(r) / \log r], \quad (3)$$

$$C(r) = 2N_{R < r} / N(N-1), \quad (4)$$

where  $C(r)$  is the correlation function,  $r$  is the distance between two epicenters or hypocenters and  $N$  is the number of events pairs separated by a distance  $R < r$ . Fractal dimension is defined by fitting a straight line to a plot of  $\log C(r)$  against  $\log r$ . The nature of temporal-spatial fractal properties of the earthquake epicenters is characterized by fractal, in particular by the correlation dimension [19]. For the hypocenter distribution (3-D space), the uniform distribution equals the Eq. 4 and it decreases with an increase in the clustering of events [20]. It is reasonable to assume that the higher  $Dc$  and lower  $b$ -values are the dominant structural feature in the study area and may arise due to clusters.

### 3.3. Seismic quiescence Z-value and declustering of the catalogues

For the quantitative analysis of seismicity rate changes, it is necessary to eliminate the dependent events from the catalog. To separate the dependent events from the independent ones the earthquake catalog is declustered using the Reasenber [21] algorithm. The cluster analysis algorithm of Reasenber [21] “declusters” or decomposes a regional earthquake catalogue into main and secondary events. It removes all the dependent events from each cluster, and substitutes them with a unique event, equivalent in energy to that of the whole cluster. *ZMAP* software in Wiemer [22] is used for the declustering method. It is only changed epicenter and depth error values. Other standard parameters are defined as given in the software.

There are 9884 events in region 1 with magnitudes greater than or equal to 1.4.  $Mc$  value is 2.7 for region 1 and the number of earthquakes exceeding this magnitude threshold is 6514. The declustering procedure took away 258 (about 4%) events and 37% of the events in total were removed from whole catalogue of region 1. Thus, the number of events for Z-value analysis was reduced to 6256 for the Marmara part of the North Anatolian Fault Zone. There are 4669 events in region 2 with magnitudes greater than or equal to 1.4.  $Mc$  value for this region is 2.9 and the number of earthquakes exceeding this magnitude threshold is 3224. The declustering algorithm took away 267 (about 8%) events and 37% of the events were totally removed from whole catalogue of region 2. As a result, the number of events for Z-value analysis was reduced to 2957 for the Anatolian part of the North Anatolian Fault Zone. In region 3, there are 2645 earthquakes with magnitudes greater than or equal to 2.0. The  $Mc$  value for region 3 is 2.9 and the number of earthquakes exceeding this magnitude threshold is 1980. The declustering process took away 417 (about 21%) events and thus 41% of the events were totally removed from whole catalogue of region 3. Consequently, the number of events for Z-value analysis was reduced to 1563 for the Eastern part of the North Anatolian Fault Zone and after completing the declustering processes, a more reliable, homogeneous and robust seismicity data has been obtained.

The standard normal deviate Z-test is one of the statistical methods frequently used for analyzing seismic quiescence. A continuous image of space and time rate changes in seismicity is produced by *ZMAP*, creating a grid of geographical co-ordinates, and associating to each grid node a selected number of nearest events. It is applied the *ZMAP* method for imaging the areas exhibiting a seismic quiescence. In order to rank the significance of quiescence, it is used the standard deviate Z-test [23,24], generating the LTA (Log Term Average) function for the statistical evaluation of the confidence level in units of standard deviations:

$$Z = (R_1 - R_2) / (S_1^2 / N_1 + S_2^2 / N_2)^{1/2} \quad (5)$$

where  $R_2$  is the mean seismicity rate in the foreground window,  $R_1$  is the average number of events in the whole background period,  $S$  and  $N$  are the standard deviations and the number of samples, within and outside the window. The Z-value computed as a function of time, letting the foreground window slide along the time duration of catalogue, is called LTA.

## 4. SEISMICITY PROPERTIES OF THE NORTH ANATOLIAN FAULT ZONE

Many statistical analysis techniques of *ZMAP* software package have been used for the 3 data set of seismicity catalogues of the NAFZ. The  $b$ -value in Gutenberg-Richter relationship is calculated by the maximum likelihood method, because it yields a more robust estimate than the least-square regression method [25]. Figure 3 shows the Gutenberg-Richter relations for all parts of the NAFZ. The  $b$ -values are calculated as  $1.13 \pm 0.01$  with  $Mc=2.7$  for region 1 (Figure 3a),  $1.02 \pm 0.02$  with  $Mc=2.9$  for region 2 (Figure 3b), and  $1.01 \pm 0.02$  with  $Mc=2.9$  for region 3 (Figure 3c). It is clearly seen that magnitude-frequency distributions of the earthquakes are well represented by the Gutenberg-Richter law with the  $b$ -value typically close to 1.



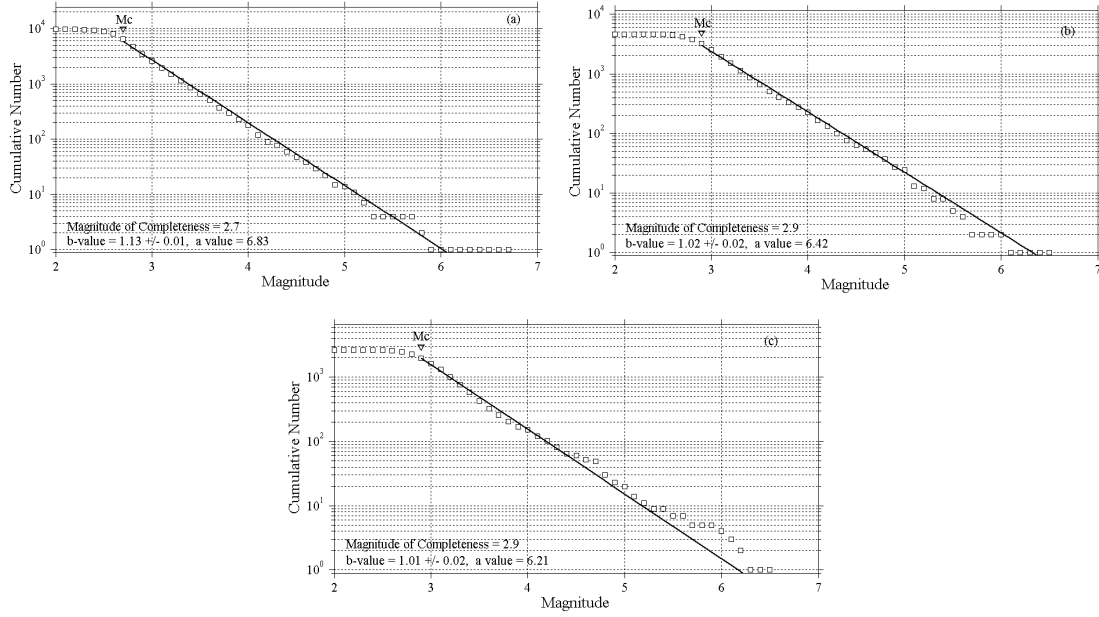


Figure 3. The  $b$ -value of the frequency-magnitude relationships for (a) region 1, (b) region 2 and (c) region 3.

The  $b$ -value and its standard deviation, as well as the  $a$ -value in the Gutenberg-Richter relation are given.

Correlation dimension  $D_c$  is estimated by fitting a straight (solid) line to the curve of mean correlation integral against the event distance,  $R$  (km).  $D_c$ -values for all parts of the study area are obtained with 95% confidence limits by linear regression (Figure 4). The earthquake distribution of 9884 earthquakes in the MNAFZ is shown in Figure 4a.  $D_c$  is calculated as  $2.20 \pm 0.03$  and this log-log correlation function exhibits a clear linear range and scale invariance in the cumulative statistics between 0.50 and 32.15 km (indicated in Figure 4a). The earthquake distribution of 4669 events in the ANAFZ is shown in Figure 4b.  $D_c$  is computed as  $2.40 \pm 0.03$  and this log-log correlation function exhibits a clear linear range and scale invariance in the cumulative statistics between 0.63 and 24.26 km (indicated in Figure 4b). The earthquake distribution of 2645 earthquakes in the ENAFZ is shown in Figure 4c.  $D_c$  is calculated as  $2.37 \pm 0.04$  and this log-log correlation function exhibits a clear linear range and scale invariance in the cumulative statistics between 1.19 and 11.32 km (indicated in Figure 4c).  $D_c$  and standard error in Figure 4 are also determined within these distances.

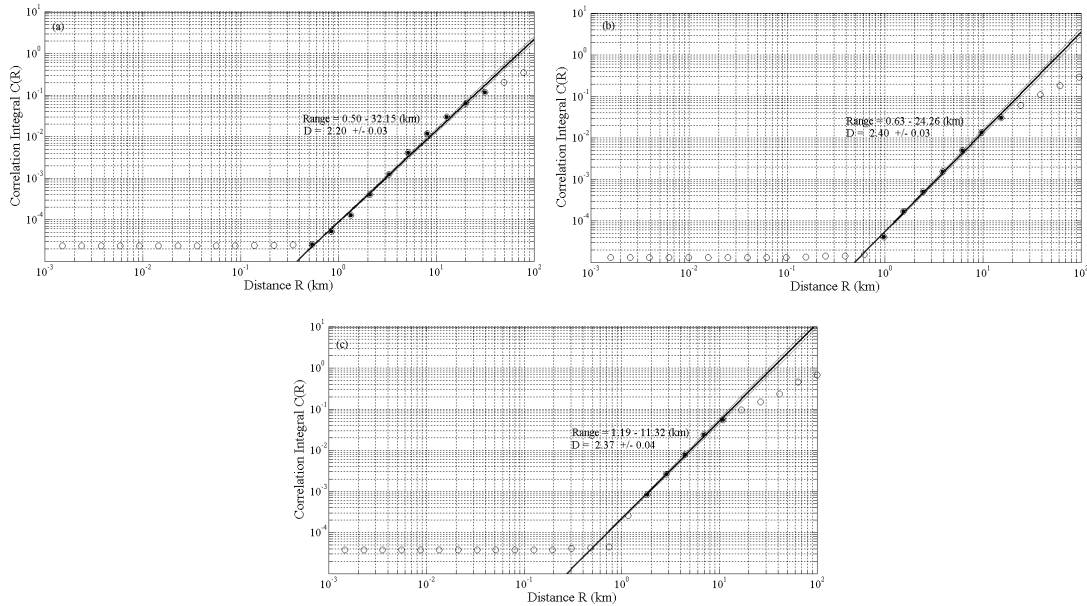


Figure 4. Fractal dimension for (a) region 1, (b) region 2 and (c) region 3. The slope of the black line corresponds to the  $D_c$  value and the gray lines illustrate the standard errors.

The variation of the  $b$ -value as a function of time in different parts of the NAFZ is also analyzed (Figure 5). Temporal changes of  $b$ -value are calculated for sample size of 1000 earthquakes for region 1, 250 earthquakes for regions 2 and 3. A systematic increase in  $b$ -value can be observed until 1996 with  $b > 1.5$  in region 1.  $b$ -value shows a great decrease with  $b \approx 0.9$  before the occurrence of 1999 Izmit earthquake and a clear increase after the main shock (Figure 5a). Such kind of behaviors is also observed for some great earthquakes in regions 2 and 3. In region 2, there is a clear tendency of decrease with  $b \approx 0.7$  before the 1999 Duzce earthquake and an increase with  $b > 1.0$  after the main shock (Figure 5b). In region 3, the same properties of  $b$ -values showing a decrease are observed before the three great earthquakes.  $b$ -values shows a decrease before the occurrence of 2003 Tunceli, 2003 Bingol and 2005 Bingol earthquake sequences and a clear increase after the main shocks (Figure 5c). The  $b$ -value for a region does not reflect only the relative proportion of the number of large and small earthquakes in the region, but is also related to the stress condition over the region [14]. Therefore, it is interpreted that the anomalies of decreases in  $b$ -value before the main shocks may be due to an increase in effective stress and can be used as an indicator of the future earthquake by observing the changes in  $b$ -value with time in all parts of the NAFZ. Also, the step increase in  $b$ -value is related to the reduced stress in these times after the main shocks.

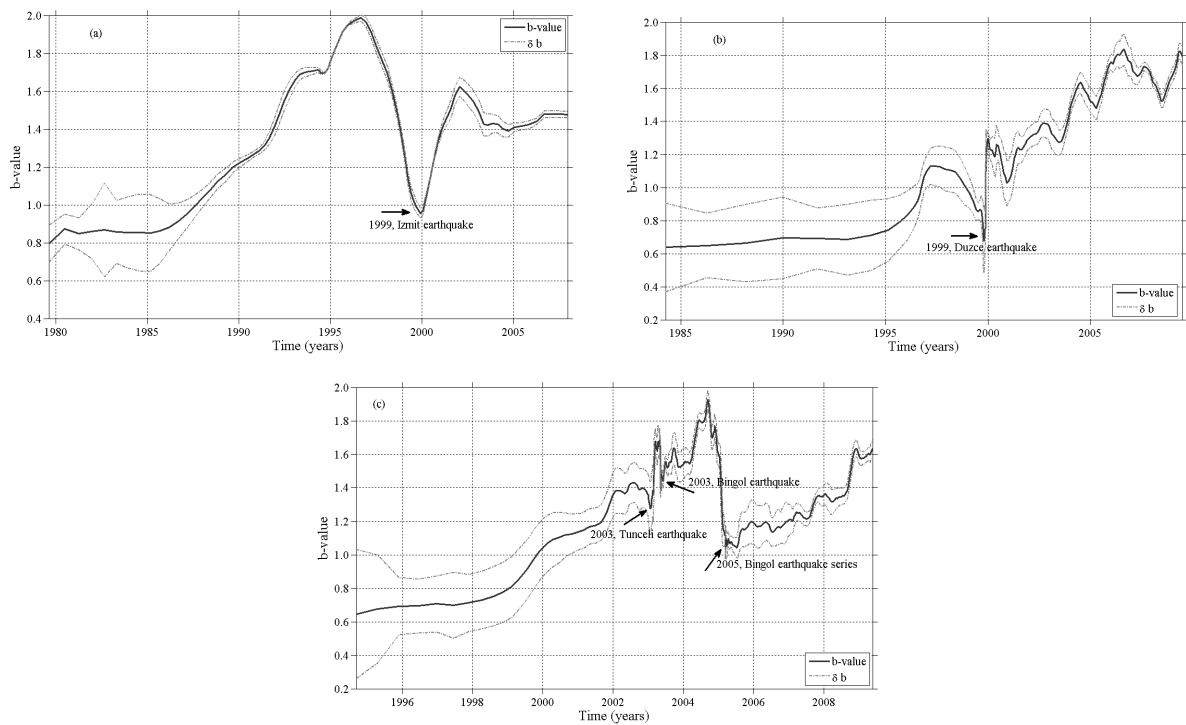


Figure 5. The  $b$ -value as a function of time for (a) region 1, (b) region 2 and (c) region 3. Standard deviation ( $\delta b$ ) (dashed lines) is also given. Arrows show the great decrease in  $b$ -values before the large earthquakes.

Regional distribution of the standard deviate Z-value for all parts of the NAFZ is presented for the beginning of 2010 (Figure 6). To establish the regional distribution of the seismic quiescence, it is applied the Reasenber [21] algorithm to decluster data. The areas under analysis were divided into rectangular cells spacing  $0.02^\circ$  in longitude and latitude. The nearest earthquakes,  $N$ , at each node are taken as 50 events for all regions and the seismicity rate changes are searched by a moving time window  $T_w = 5.5$  years. For each grid point we binned the earthquake population into many binning spans of 28 days for all regions in order to have a continuous and dense coverage in time. Eight significant quiescence anomalies were identified in the study regions. In region 1 covering the MNAFZ, the first significant anomaly is found centered at  $41.08^\circ\text{N}-28.58^\circ\text{E}$  (region A, around Silivri) and the second one is found centered at  $41.47^\circ\text{N}-29.51^\circ\text{E}$  (region B, in the Black Sea). The third significant quiescence is observed centered at  $40.69^\circ\text{N}-29.78^\circ\text{E}$  (region C, including Izmit) and the fourth significant anomaly is found centered at  $40.26^\circ\text{N}-26.46^\circ\text{E}$  (region D, around Gelibolu, Canakkale). In region 2 including the ANAFZ, the first significant anomaly is found centered at  $40.59^\circ\text{N}-31.03^\circ\text{E}$  (region E, including Duzce fault) and the second quiescence area is found centered at  $40.86^\circ\text{N}-35.30^\circ\text{E}$  (region F, around Amasya). In region 3 covering the ENAFZ, the first significant anomaly is found centered at  $39.48^\circ\text{N}-39.74^\circ\text{E}$  (region G, around Erzincan) and the second anomaly is found centered at  $39.06^\circ\text{N}-40.50^\circ\text{E}$  (region H, around Bingol).

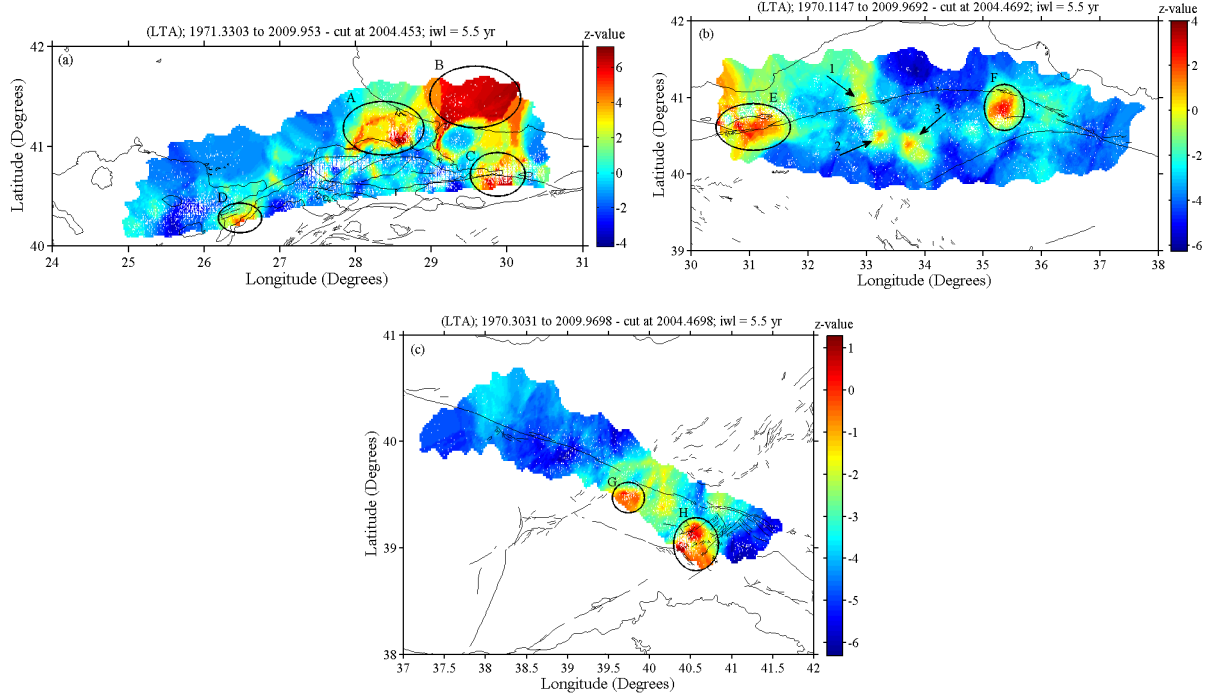


Figure 6. Z-value distributions in the beginning of 2010 with  $T_w = 5.5$  years for (a) region 1, (b) region 2 and (c) region 3. White dots show the declustered earthquakes with  $M_D \geq 2.7$  for region 1,  $M_D \geq 2.9$  for regions 2 and 3.

## 5. CONCLUSIONS

Spatial and temporal properties of the seismic activity from 1970 to 2010 in the North Anatolian Fault Zone are investigated in order to characterize the seismic behaviors. For this purpose a number of statistical parameters are used; namely size-scaling parameters (such as slope of recurrence curve  $b$ -value), seismic quiescence Z-value, temporal and spatial distribution of earthquakes with characteristic of fractal correlation dimension,  $D_c$ , as well as the histograms of temporal, spatial and magnitude distribution. For this purpose, statistical analysis techniques based on the seismic tool ZMAP are applied. The instrumental earthquake catalog of the Bogazici University, Kandilli Observatory and Earthquake Research Institute between 1970 and 2010, for 17198 crustal earthquakes of magnitude equal and greater than 1.4, with depths less than 70 km is used. The catalogue is homogeneous and complete for duration magnitude.

Magnitude completeness analyses present a value between 2.7 and 2.9 for all parts of the NAFZ. The  $b$ -values for all regions are close to 1 and typical for earthquake catalogs. Temporal distributions of  $b$ -values show a strong tendency of decreases before the great main shocks and this behavior can be used as an indicator of the next earthquake. Correlation dimension values are greater than 2.20 for all parts of the NAFZ. This suggests that seismic activity is more clustered at larger scales (or in smaller areas) in the North Anatolian Fault Zone.

There are eight regions exhibiting significant seismic quiescence on the North Anatolian Fault Zone in the beginning of 2010. On the Marmara part of the North Anatolian Fault Zone, four anomalies are found centered at 41.08°N-28.58°E (around Silivri), 41.47°N-29.51°E (in the Black Sea), 40.69°N-29.78°E (including Izmit) and 40.26°N-26.46°E (around Gelibolu, Canakkale). The other two quiescence areas are found centered at 40.59°N-31.03°E (including Duzce fault) and 40.86°N-35.30°E (around Amasya) on the Anatolian part of the North Anatolian Fault Zone. The rest of the quiescence anomalies are found centered at 39.48°N-39.74°E (around Erzincan) and 39.06°N-40.50°E (around Bingol) on the Eastern part of the North Anatolian Fault Zone.

The North Anatolian Fault Zone was struck with devastating earthquakes in recent years. Therefore, prediction of the future large earthquake on the NAFZ would be useful. Such a prediction must be relied on the observation of phenomena related to precursory quiescence. Previous studies for the North Anatolian Fault zone show that the return periods of  $M_D \geq 5.5$  have been exceeded in the Anatolian part of the North Anatolian Fault Zone. However, the return periods of  $M_D \geq 5.5$  for the Marmara and the Eastern part and the return period of  $M_D \geq 6.0$  for the Anatolian part of the North Anatolian Fault Zone will be exceeded between 2010 and 2012. For this reason, special attention should be given to these regions where the seismic quiescence is observed.

## 6. REFERENCES

- [1] Q. Huang, A.O. Öncel and G.A. Sobolev, Precursory seismicity changes associated with the  $M_w=7.4$  1999 August 17 Izmit (Turkey) earthquake, *J. Geophys. Int.*, 151, 235-242 (2002).
- [2] V. Yılmaz, M. Erisoglu and H.E. Çelik, Probabilistic prediction of the next earthquake in the NAFZ (North Anatolian Fault Zone), Turkey, *Doğuş Üniversitesi Dergisi*, 5(2), 243-250 (in English with Turkish abstract) (2004).
- [3] H.S. Kutoglu and H. Akcin, Determination of the 30-year creep trend on the Ismetpasa segment of the North Anatolian Fault using an old geodetic network, *Earth Planets Space*, 58, 937-942 (2006).
- [4] H.S. Kutoglu, H. Akcin, H. Kemaldere and K.S. Gormus, Triggered creep rate on the Ismetpasa segment of the North Anatolian Fault, *Natural Hazards and Earth System Sciences*, 8, 1369-1373 (2008).
- [5] S. Öztürk, Y. Bayrak, H. Çinar, G.Ch. Koravos and T.M. Tsapanos, A quantitative appraisal of earthquake hazard parameters computed from Gumbel I method for different regions in and around Turkey, *Nat. Haz.*, 47, 471-495 (2008).
- [6] M.N. Toksöz, A.F. Shakal and A.J. Michael, Space-time migration of earthquakes along the North Anatolian Fault Zone and seismic gaps, *Pure and Applied Geophysics*, 117, 1258-1270 (1979).
- [7] A. Barka, Slip distribution along the North Anatolian Fault associated with the large earthquakes of the period 1939 to 1967, *Bull. Seism. Soc. Am.*, 86(5), 1238-1254 (1996).
- [8] S. Özalaybey, M. Ergin, M. Aktar, C. Tapırdamaz, F. Biçmen and A. Yörük, The 1999 Izmit Earthquake Sequence in Turkey: Seismological and Tectonic Aspects, *Bull. Seism. Soc. Am.*, 92, 376-386 (2002).
- [9] S. Öztürk, *Deprem Tehlikesi ve Artçı şok Olasılığı Değerlendirme Yöntemlerinin Türkiye'deki depremlere Bir Uygulaması (An Application of the Earthquake Hazard and Aftershock Probability Evaluation methods to Turkey Earthquakes)*. PhD Thesis, Karadeniz Technical University, Trabzon, Turkey (in Turkish with English abstract, unpublished) (2009).
- [10] F. Şaroğlu, O. Emre and I. Kuşcu, *Active fault map of Turkey*, General Directorate of Mineral Research and Exploration, Ankara, Turkey (1992).
- [11] E. Bozkurt, Neotectonics of Turkey-a synthesis, *Geodinamica Acta*, 14, 3-30 (2001).
- [12] R.E. Reilinger, S.C. McClusky, M.B. Oral, W. King and M.N. Toksöz, Global Positioning System measurements of present-day crustal movements in the Arabian-Africa-Eurasia plate collision zone, *J. Geophys. Res.*, 102, 9983-9999 (1997).
- [13] R. Gutenberg, and C.F. Richter, Frequency of earthquakes in California, *Bull. Seism. Soc. Am.*, 34, 185-188 (1944).
- [14] T. Utsu, Aftershock and earthquake statistic (III): Analyses of the distribution of earthquakes in magnitude, time and space with special consideration to clustering characteristics of earthquake occurrence (1), *J. Faculty Sci., Hokkaido University, Ser. VII (Geophys.)*, 3, 379-441 (1971).
- [15] C. Frohlich and S. Davis, Teleseismic  $b$ -values: Or, much ado about 1.0, *J. Geophys. Res.*, 98, 631-644 (1993).
- [16] K. Aki, Maximum likelihood estimate of  $b$  in the formula  $\log N = a - bM$  and its confidence limits, *Bull. Earthquake Res. Inst., Tokyo Univ.*, 43, 237-239 (1965).
- [17] S. Wiemer, and M. Wyss, Minimum magnitude of completeness in earthquake catalogs: Examples from Alaska, the Western United States, and Japan, *Bull. Seismol. Soc. Am.*, 90, 859-869 (2000).
- [18] P. Grassberger and I. Procaccia, Measuring the strangeness of strange attractors, *Physica* 9(D), 189-208 (1983).
- [19] Y.Y. Kagan, Earthquake spatial distribution: the correlation dimension, *J. Geophys. Int.*, 168, 1175-1194. (2007).
- [20] H. Awad, M. Mekkavi, G. Hassib and M. Elbohuty, Temporal and three dimensional spatial analysis of seismicity in the Lake Aswan area, Egypt, *Acta Geophysica Polonica* 53, (2), 152-166 (2005).
- [21] P.A. Reasenbergs Second-order moment of Central California Seismicity, 1969-1982, *J. Geophys. Res.*, 90, 5479-5495 (1985).
- [22] S. Wimer, A software package to analyze seismicity: ZMAP, *Seismological Research Letters*, 72(2), 373-382 (2001).
- [23] R.E. Habermann, Teleseismic detection in the Aleutian Island arc, *J. Geophys. Res.*, 88, 5056-5064 (1983).
- [24] S. Wiemer and M. Wyss, Seismic quiescence before the Landers ( $M=7.5$ ) and Big Bear (6.5) 1992 earthquakes, *Bull. Seismol. Soc. Am.*, 84, 900-916 (1994).

# Estimating the Nonlinear Behavior of Mitral Valve Doppler Signals

Fatma Latifoğlu<sup>1</sup>, Esma Uzunhisarcıklı<sup>2</sup>, Türker Koza<sup>3</sup>

October 20, 2009

In the present study, Nonlinear analysis techniques were realized on mitral valve Doppler signals from patient with stenosis and healthy subjects. The maximum Lyapunov exponent and correlation dimension variant representing nonlinear behavior has been showed the unpredictability and complexity levels of the mitral valve Doppler signals, respectively. As a result our data suggests that useful tool to describe complexity of cardiovascular auto regulation.

## 1 Introduction

The ends Mitral valve stenosis is a serious disorder among the heart disease and characterized by the narrowing of the orifice of the mitral valve of the heart. When the orifice narrows, the blood can only be carried from the left atrium to the left ventricle by an abnormally increased from atrial to ventricular pressure gradient. Therefore, early diagnosis of mitral valve stenosis has been an important aspect for the relevant medical research [1]. A kind of diagnostic tools can be utilized diagnose of mitral valve stenosis. These techniques are electrocardiography, chest X-rays, heart sounds murmur from stethoscope, Doppler ultrasound imaging and an invasive technique angiography and transoesophageal echocardiography [2]. Today, color Doppler is the most widely used diagnostic tool for assessing intracardiac blood flow, although most cardiac valve diseases produce geometrically complex flows [3]. Doppler ultrasound has been widely used in noninvasive assessment of cardiovascular disease. In ultrasound Doppler systems, an ultrasonic signal is transmitted through the body

---

<sup>1</sup> Erciyes University, Faculty of Engineering, Department of Biomedical Engineering, 38039, Kayseri, Turkey

flatifoglu@erciyes.edu.tr

<sup>2</sup> Erciyes University, Kayseri Vocational College, Biomedical Programme, 38039, Kayseri, Turkey

uzunhise@erciyes.edu.tr

<sup>3</sup> Bozok University, Vocational College, Electronic Programme, 66100, Yozgat, Turkey

turker.koza@bozok.edu.tr

and an echo signal is backscattered from the red blood cells is received. Under these condition, The Doppler shift frequency is given by,

$$f_d^{\rightarrow} = f_t - f_r = (2f_t v \cos \Theta) / C \quad (1)$$

In the equation above,  $f_t$  and  $f_r$  are the transmitted and received ultrasound frequencies, respectively,  $v$  is the velocity of the blood flow,  $C$  is the velocity of the sound in the **environment** and  $\Theta$  is the angle between ultrasound beam and the direction of motion of the target [4].

A number of analysis methods are available for the obtaining a pictorial view of the Doppler signal of which the best and most commonly used method is spectral analysis. Spectral analysis of the Doppler signals produces information about the blood flow in the arteries. Traditional spectral analysis techniques have been used to extract information about the Doppler signals over the last two decades. Doppler signals are nonstationary, **although** traditional spectral analysis techniques are assumed to be the signal as stationary. Therefore, the Doppler signals can be considered as a chaotic signals because of complex nonlinear characteristics arising from deterministic physical processes [5,6]. The nonlinear analysis is a mathematical method applied to describe shapes and numerical time-varying processes.

In our study, chaos analysis was performed on the mitral valve Doppler signals to extract information about mitral valve stenosis.

The aim of this study is to characterize the usefulness of nonlinear analysis in mitral valve autoregulation.

## 2 Materials and Methodds

### 2.1. Patients and Measurements

In this study, The Doppler ultrasound signals were acquired from Erciyes University Cardiology Hospital, mitral valve of 12 patients with mitral valve stenosis with mild level and 13 healthy volunteers. The healthy subjects had no clinical and echocardiographic evidence of valvular disease or heart failure. The patient group is diagnosed of mitral stenosis through cardiac angiographies. Healthy volunteers were young non-smokers who seem to not bear any risk of stenosis.

Doppler echocardiographic examinations were performed with GE Vivid7 ultrasound device in the cardiology departments of Erciyes university hospital. The system hardware was composed of Digital Doppler ultrasound unit that can work in the pulsed mode, linear ultrasound probe, input– output card and a personal computer. All examinations were recorded on PC and calculations were made MATLAB software.

A linear ultrasound probe of 5 MHz was used to transmit pulsed ultrasound signals to the mitral valve. In all recording performed on the patients and healthy

subjects, the **probe application** angle and the presettings of the ultrasound were kept constant. The **probe application** angle was adjusted via electronic steering methods. The sampling volume was placed within the center of the mitral valve. The amplification gain was carefully set to obtain a clean spectral output with minimized background noise on the spectral display. The audio output of ultrasound unit was sampled at 44100 Hz [7].

The Doppler sonograms belonging to healthy and patient subject is plotted with the frequency components and power spectral density values sequenced on the timeline as seen figure 1 and 2 respectively.

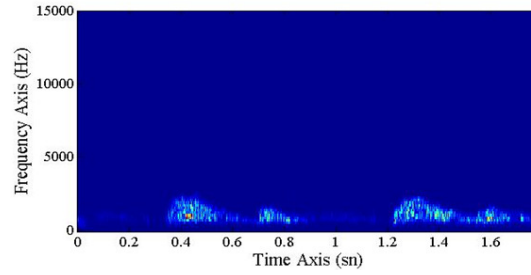


Fig.1. Mitral valve Doppler sonogram derived from healthy subject

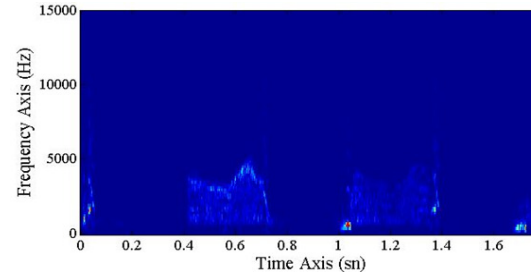


Fig. 2. Mitral valve Doppler sonogram derived from patient subject

## 2.2. Nonlinear Analysis of Mitral Valve Doppler Signals

Nonlinear analysis techniques such as Lyapunov exponents and fractal dimension were applied to mitral valve Doppler signals so as to determine variability of these signals.

### 2.2.1. Phase Space Reconstruction

Doppler ultrasound signals have time series and nonlinear characteristics. Analysis with nonlinear methods for a time series, we need phase space reconstruction with time delay samples [8]. Two parameters need to be given: the embedding dimension and time delay [9-12].

$$\vec{X}_i = (y_i, y_{i+\tau}, y_{i+2\tau}, \dots, y_{i+(m-1)\tau}) \quad (2)$$

In this equation,  $\tau$  is delay time and  $m$  is the embedding dimension. Different  $\tau$  and  $m$  choices reconstructs different trajectories.

### 2.2.2. Time Delay

Taken's time delay expression theorem is available to obtain the requested information from the time series [8]. If  $\tau$  is chosen smaller, data points cannot be distinguished from each other. If  $\tau$  is chosen higher, data points are totally independent from each other statistically sense. In the nonlinear systems average mutual function is used for selecting the  $\tau$  [12]. This function is applied to measurements obtained from physical systems;  $s(n)$  is a set of measured values. Measurements are considered as a set of  $s(n+T)$  after  $T$  time delay. The average mutual function information between  $n$  and  $n+T$  is average value of  $s(n+T)$  which obtained by values of  $s(n)$ ;

$$I(T) = \sum_{n=1}^N P(s(n), s(n+T)) \log_2 \left[ \frac{P(s(n), s(n+T))}{P(s(n))P(s(n+T))} \right], \quad I(T) \geq 0 \quad (3)$$

The best estimation for  $\tau$ , proposed by Fraser and Swinney, is the first local minimum value of the mutual information. The mutual information is a measure of how much information can be predicted about one time series point included all the necessary about others [11,13]. In our study, time delay value has been found as 12 time point, as seen Figure 3.

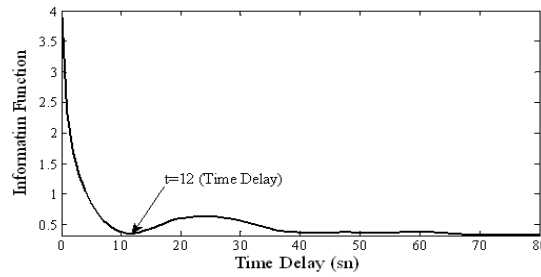


Fig. 3. Time Delay values for mitral valve Doppler signals from healthy subject



### 2.2.3. Determining Embedded Dimension

The aim of the phase space reconstruction is to provide a large enough Euclidian space ( $Rm$ ). This process supports system's attractor without any ambiguity. The higher values of  $m$ , two nearest point can be seen in  $m$  dimension [12]. In  $Rm$  space all the ambiguities can be solve. We can use Cao's method [14] to determine the embedded dimension. According to this method, the difference between the nearest neighborhood pairs in the  $y_i(m)$  where  $m$  is the embedded dimension and  $y_i(m+1)$  where  $m+1$  is the embedded dimension.

$T$  is the time delay of phase space,  $\|\cdot\|$  shows the Euclidian difference, It is given that;

$$a(i, m) = \frac{\|y_i(m+1) - y_{n(i, m)}(m+1)\|}{\|y_i(m) - y_{n(i, m)}(m)\|}$$

$$i = 1, 2, \dots, N - mT \quad (4)$$

$$\|y_k(d) - y_l(d)\| = \max_{0 \leq j \leq d-1} \|x_{k+jT} - x_{l+jT}\| \quad (5)$$

If  $m$  value is determined successfully, any two points are close to each other in  $m$  dimension, It has been close in the constructed phase space of  $m+1$  dimension too [14]. This type of couple of points are called right neighbors, otherwise they are called wrong neighbors. If there is a wrong neighborhood,  $a(i, m)$  value is too different from calculated threshold value. Threshold value  $E(m)$  can be obtained with average of all the  $a(i, m)$ .

$$E(m) = \frac{1}{N - mT} \sum_{i=1}^{N-mT} a(i, m) \quad (6)$$

Where,  $E(m)$  value depends on  $m$  dimension and  $T$  time delay.

In our study Cao's method has been applied to Doppler signal to find embedding dimension. The embedding dimension values have been determined as  $m=8$ . We can see the minimum embedding dimension curve from Doppler signals in the Figure 4.

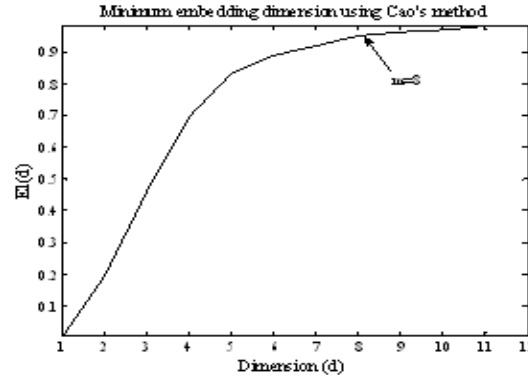


Fig. 4. The minimum embedding dimension curve

#### 2.2.4. Lyapunov Exponentials

For a time series, two important indexes to identify the chaotic behavior are its mutual dimension and maximum Lyapunov exponents [9]. Lyapunov exponents determine the nearby phase space trajectories between average exponential separation. The generic mechanism to compose deterministic randomness and unpredictability is the exponential divergence of initially nearby trajectories in phase space coupled with folding trajectories. [10,15].

For a small dimensional deterministic process, the Lyapunov exponents should be a positive finite number. For a linear process, it should be zero and for a stochastic process it should be infinite [15]. In an chaotic attractor, the maximal Lyapunov exponent must be greater than zero which means that the neighboring trajectories of the attractor are locally diverging in at least one direction of the phase space [16].

Rosenstein et al. [17] proposed a method to calculate the largest Lyapunov exponent from an observed time series. In this method, following  $S$  value is computed for different  $N$  values:

$$S(t) = \frac{1}{N} \sum_{n=0}^{N-1} \left( \ln \frac{1}{|v_n|} \sum |s_{n+t} - s'_{n+1}| \right) \quad (7)$$

If  $S$  exhibits a linear increase with an identical slope, this slope can be taken as an estimate of the maximal Lyapunov exponent [16].

The maximum Lyapunov exponent curves belonging to patient and healthy subject are seen in Figure 5.

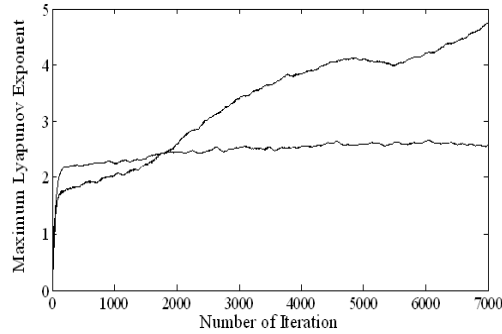


Fig. 5. The maximum Lyapunov exponent curve for the patient and healthy subject

### 3. Results and Discussion

In our study, It was determined that, nonlinear behaviors of mitral valve Doppler ultrasound signals. In reconstructed eight dimension phase space the time delay and embedded dimension have been derived also, correlation dimension and Lyapunov exponents have been calculated from time series Doppler signals. Maximum Lyapunov exponent values and the maximum correlation dimension values are given in Table 1.

Table 1. Maximum Lyapunov Exponent and Correlation Dimension Values

	Healthy Subject	Patient Subject
	Mean $\pm$ std	Mean $\pm$ std
Max. Lyap. Exponent	2.6175 $\pm$ 0.2319	5.6860 $\pm$ 0.6922
Max. Fractal Dimension	2.0433 $\pm$ 0.1936	0.8911 $\pm$ 0.08640

The maximum values of Lyapunov exponent for the Doppler signals from mitral valve stenosis patient subjects have been obtained as 5.6860 $\pm$ 0.6922 and for the Doppler signals from mitral valve healthy subjects have been obtained as 2.6175 $\pm$  0.2319. The increment in maximum Lyapunov exponent derived from patient subjects indicates the increasing of the chaotic behavior than maximum Lyapunov exponent derived from healthy subjects .The higher value of maximum Lyapunov exponent imply randomness and unpredictability in the long term which can also be observed from the sonogram in Fig. 2. On the other side, the lower values of the maximum Lyapunov exponent from healthy subjects imply more considerable periodicity which can also be detected from the sonograms in Figure 1. According to our nonlinear analysis, it has been shown that all the Doppler time series signals are not only nonlinear, but also it can be supposed as stationary in certain time interval. This means that the nonlinear methods have been applied to estimate the invariant measures like correlation dimension and maximum Lyapunov exponent.

The correlation dimension values have been calculated as  $2.0433 \pm 0.1936$  for healthy subject and  $0.8911 \pm 0.08640$  for the patient with mitral valve stenosis. This paper indicated that the two chaotic invariant measures, maximum Lyapunov exponent and correlation dimension have been pointed out the unpredictability and complexity levels of the mitral valve Doppler signals, respectively. The chaotic measures of the Doppler signals are useful to describe cardiovascular regulation. Ongoing trials the classification studies can be made using more subjects.

#### 4. References

- [1] W.C. Wu, G.F.Aziz, "The use of stres echocardiography in the assessment of mitral valvular diseases" *Echocardiography: A Journal of Cardiovascular Ultrasound and Allied Techniques*, vol. 21(5), 2004.
- [2] Nanda, N. C. "Doppler echocardiography", (2nd ed.). London:Lea & Febiger, 1993.
- [3] De Simone, R., Glombitza, G., Vahl, C. F., Meinzer, H. P., & Hagl, S. "Three-dimensional color Doppler reconstruction of intracardiac blood flow in patients with different heart valve diseases", *The American Journal of Cardiology*, vol. 86(12), pp. 1343–1348, 2000.
- [4] Evans DH, McDicken WN, Skidmore R, Woodcock JP. "Doppler ultrasound: physics, instrumentation and clinical applications", Chichester: Wiley; 1989.
- [5] El-Brawany MA, Nassiri DK. "New approach for modeling ultrasound blood backscatter signal", *Ultrasound in Medicine and Biology*, vol 28(4), pp. 527–34, 2002.
- [6] El-Brawany MA, Nassiri DK., "Microemboli detection using ultrasound backscatter." *Ultrasound in Medicine and Biology*, vol. 28(11/12), pp. 1439–46, 2002.
- [7] Attkson, P. "Doppler ultrasound and its use in clinical measurement". Prentice-Hall, 1982.
- [8] Takens F., "Detecting Strange Attractors in Turbulance", *Lecture Notes in Mathematics, Phys. Rev.*, vol. 898, pp. , 366-3881, 1981.
- [9] Xu P., "Differential Phase Space Reconstructed for Chaotic Time Series", *Applied Mathematical Modelling*, vol. 33, pp. 999-1013, 2009.
- [10] Akay M., Nonlinear Biomedical Signal Processing, IEE Press, 18, 2000
- [11] Yılmaz D., Musapaşaoğlu H., Kırbaş İ., Güler N.F., "Karotid Atardamar Doppler Sinyalleri Üzerinde En Büyük Lyapunov Üsteli ve İlinti Boyutu Hesabı", *Journal of İstanbul Kültür Universty*, pp. 61-72, 2006
- [12] Abarbanel, H.D.I., Brown R., Sidorowich J.J. ve Tsimring L.S., "The Analysis of Observed Chaotic Data in Physical Systems", *Reviews of Modern Physics*, vol. 65(4), pp. 1331, 1993.
- [13] Fraser A.M., Swinney H. L., "Independent Coordinates for Strange Attractors from Mutual Information", *Phys. Rev. A*, vol. 33, pp. 1134, 1986.
- [14] Cao, L., "Practical Method for Determining the Minimum Embedding Dimension of a Scalar Time Series", *Physica D*, vol. 110(1), pp. 43-50, 1997.

- [15] Shang P., Li X., Kamae S., “Chaotic analysis of traffic time series”, *Chaos, Solitons and Fractals*, vol. 25, pp. 121-128, 2005
- [16] Öztürk A., Arslan A., “Classification of Transcranial Doppler Signals Using Their Chaotic Invariant Measures”, *Computer Methods and Programs In Biomedicine*, vol. 86, pp. 171-180, 2007.
- [17] M.T. Rosenstein, J.J. Collins, C.J. De Luca, “A practical method for calculating largest Lyapunov exponents from small data sets”, *Phys. D.*, vol. 65, pp. 117–134, 1993.

# Phase diagrams of an Ising System with Competing binary, prolonged ternary and next-nearest interactions on a Cayley Tree

Nasir Ganikhodjaev,<sup>\*</sup> Hasan Akin,<sup>†</sup> Selman Uguz,<sup>‡</sup> Seyit Temir<sup>§</sup>

July 10, 2010

## Abstract

In this paper we consider the Ising model with spin values in  $\Phi = \{-1, 1\}$ , the relevant Hamiltonian with competing binary nearest-neighbor, prolonged ternary and prolonged next-nearest neighbors interactions has the form

$$H(\sigma) = -J_p \sum_{\langle x, y \rangle} \sigma(x)\sigma(y) - J_t \sum_{\langle x, y, z \rangle} \sigma(x)\sigma(y)\sigma(z) - J_1 \sum_{\langle x, y \rangle} \sigma(x)\sigma(y),$$

where  $J_p, J_t, J_1 \in \mathbb{R}$  are coupling constants. We study the phase diagram of this model. To perform this study, an iterative scheme similar to that appearing in real space renormalization group frameworks is established. At vanishing temperature, the phase diagram is fully determined for all values and signs of  $J_1, J_t$  and  $J_p$ . At finite temperatures several interesting features are exhibited for typical values of  $-J_t/J_1$  and  $J_p/J_1$ .

**PACS:** 05.50.+q, 64.60.-i, 64.60.De, 75.10.Hk

**Keywords:** Ising model, Cayley tree, phase diagram, ternary neighbors, modulated phase, Lifshitz point.

## 1 Introduction

Complex phase diagrams with a variety of transition lines and modulated phases are obtained via the presence of competing interactions in magnetic and ferroelectric systems. The ANNNI (Axial Next-Nearest-Neighbor Ising) model, which consists of an Ising spin Hamiltonian on a Cayley tree, with ferromagnetic interactions on the planes, and competing ferromagnetic and antiferromagnetic interactions between nearest and next-nearest neighbors along an axial direction, is known to reproduce some features of these complex phase diagrams [1]. The Ising model on a Cayley tree of order  $k$  with competing interactions has recently been studied extensively because of the appearance of nontrivial magnetic orderings [2] (see also references in [2]). Also, the Ising model has found some applications physical, chemical and biological systems, and even in sociology. The Cayley tree is not a realistic lattice; however, its amazing topology makes the exact calculation of various quantities possible. For many problems the solution on a tree is much simpler than on a regular lattice and is equivalent to the standard Bethe-Peierls theory [5]. In the literature, it has been working many different lattice types similar to Cayley trees [6, 7, 13, 14, 15, 16, 17]. As initiated by Vannimenus [2], a Cayley tree is a counterpart of the ANNNI (Axial Next-Nearest-Neighbor Ising) model, which is used to provide an approximate description of some materials, such as CESb [8] and ferroelectric  $\text{NaNO}_2$  [9]. In recent years, investigation of phase diagrams of the Ising model has attracted increased attention [10, 11, 12].

---

<sup>\*</sup>Department of Computational and Theoretical Sciences, Faculty of Science, IIUM, 25200 Kuantan, Malaysia, nasir-gani@hotmail.com

<sup>†</sup>Department of Mathematics, Faculty of Education, Zirve University, 27260, Gaziantep, Turkey, hasanakin69@gmail.com

<sup>‡</sup>Department of Mathematics, Arts and Science Faculty, Harran University, Sanliurfa, 63120, Turkey, selmanuguz@gmail.com

<sup>§</sup>Department of Mathematics, Arts and Science Faculty, Harran University, Sanliurfa, 63120, Turkey, temirseyt@harran.edu.tr

On the Cayley tree one can consider two type of next-nearest-neighbors: prolonged and one-level next-nearest-neighbors. In the case of the Ising model on the Cayley tree with competing nearest-neighbor interactions  $J_1$  and prolonged next-nearest-neighbor interactions  $J_p$ , Vannimenus [2] was able to find new modulated (**M**) phases, in addition to the expected paramagnetic (**P**) and ferromagnetic (**F**) ones. From this result follows that Ising model with competing interactions on a Cayley tree is real interest since it has many similarities with models on periodic lattices. In fact, it has many common features with them, in particular the existence of a **M** phase, and shows no sign of pathological behavior at least no more than mean-field theories of similar systems [2]. Inawashiro *et al* [18, 19] independently of Vannimenus investigated the Ising model with nearest-neighbors and prolonged next-nearest-neighbors interactions on a Cayley tree, but they allowed  $J_p = J_o$ , where  $J_o$  is the one-level next-nearest-neighbor interaction on Cayley tree. Mariz *et al* [20] extended this results assuming existence also binary interaction  $J_o$  on Cayley tree of order 2. Later da Silva *et al* [25] investigated the Ising model on the Cayley tree of general connectivity with competing interactions between the first-,second-, and third-neighbor spin generation.

The aim of this paper is to extend Ganikhodjaev and Akin [4] results on Cayley tree by adding prolonged next-nearest-neighbor interactions. By changing  $J_p$  (prolonged next-nearest-neighbor interactions) and  $J_t$  (prolonged ternary interactions) values, a new model is obtained. We combine the parameters in [2] and [4]. Here by using the similar computational techniques as in [2, 20, 27], we describe the phase diagrams of an Ising model on a Cayley tree with competing nearest-neighbor  $J_1$ , prolonged ternary  $J_t$  and prolonged next-nearest-neighbor interactions  $J_p$ .

The outline of this paper is given as follows: we set up the basic definitions of our model in Section 2 and the recurrence relations are obtained in Section 3. Section 4 is devoted to the analysis of the phase diagrams. Finally, the conclusions are presented in Section 5.

## 2 Definitions

### 2.1 Cayley tree

A Cayley tree  $\Gamma^k$  of order  $k \geq 1$  is an infinite tree, i.e., a graph without cycles with exactly  $k+1$  edges issuing from each vertex. Let denote the Cayley tree as  $\Gamma^k = (V, \Lambda)$ , where  $V$  is the set of vertices of  $\Gamma^k$ ,  $\Lambda$  is the set of edges of  $\Gamma^k$ . The distance  $d(x, y)$ ,  $x, y \in V$ , on the Cayley tree  $\Gamma^k$ , is the number of edges in the shortest path from  $x$  to  $y$ . For a fixed  $x_0 \in V$  we set  $W_n = \{x \in V | d(x, x_0) = n\}$ ,  $V_n = \{x \in V | d(x, x_0) \leq n\} = \bigcup_{i=0}^n W_i$ , and  $L_n$  denotes the set of edges in  $V_n$ . The fixed vertex  $x_0$  is called the 0-th level and the vertices in  $W_n$  are called the  $n$ -th level. For the sake of simplicity we put  $|x| = d(x, x_0)$ ,  $x \in V$ .

Two vertices  $x$  and  $y$ ,  $x, y \in V$  are called *nearest-neighbors* if there exists an edge  $l \in \Lambda$  connecting them, which is denoted by  $l = \langle x, y \rangle$ . Two vertices  $x, y \in V$  are called *the next-nearest-neighbors* if  $d(x, y) = 2$ . The next-nearest-neighbor vertices  $x$  and  $y$  are called *prolonged next-nearest-neighbors* if  $|x| \neq |y|$  and is denoted by  $\langle \widetilde{x, y} \rangle$  (see [2]). Three vertices  $x, y$  and  $z$  are called a triple of neighbors and they are denoted by  $\langle x, y, z \rangle$ , if  $\langle x, y \rangle, \langle y, z \rangle$  are nearest neighbors. The triple of vertices  $x, y, z$  is called *prolonged* if  $x \in W_n, y \in W_{n+1}$  and  $z \in W_{n+2}$  for some nonnegative integer  $n$  and is denoted by  $\langle \widetilde{x, y, z} \rangle$  (see [4]).

### 2.2 Ising model

For the Ising model with spin values in  $\Phi = \{-1, 1\}$ , the relevant Hamiltonian with competing nearest-neighbor  $J_1$ , prolonged next-nearest-neighbor binary interactions  $J_p$ , one-level next-nearest-neighbor binary interactions  $J_o$ , and one-level next-nearest-neighbor quadruple interactions  $J_{l_1}$  has the form

$$\begin{aligned} H(\sigma) = & -J_1 \sum_{\langle x, y \rangle} \sigma(x)\sigma(y) - J_p \sum_{\langle \widetilde{x, y} \rangle} \sigma(x)\sigma(y) - J_o \sum_{\langle x, y \rangle} \sigma(x)\sigma(y) \\ & - J_t \sum_{\langle \widetilde{x, y, z} \rangle} \sigma(x)\sigma(y)\sigma(z) - J_{l_1} \sum_{\langle x, y, z, t \rangle} \sigma(x)\sigma(y)\sigma(z)\sigma(t) \end{aligned} \quad (1)$$

where  $J_1, J_p, J_o, J_t, J_{l_1} \in \mathbb{R}$  are coupling constants.

In the case of  $J_p = J_t = J_{l_1} = 0$ , Ising model (1) is exactly solvable [21] and its phase diagram consists of ferromagnetic and antiferromagnetic phases only. In the presence of  $J_p$  with  $J_o = J_t = J_{l_1} = 0$  this

model was considered by Vannimenus [2]. He proved that phase diagram contains new modulated phase with the expected paramagnetic and ferromagnetic ones. The case  $J_t = J_{l_1} = 0$  with binary interaction of  $J_o$  on Cayley tree of order 2 was considered in [20] and the case  $J_p = J_{l_1} = J_o = 0$ , the Ising model (1) was studied in [4].

Below we consider model (1) with  $J_o = J_{l_1} = 0$  on a Cayley tree of second order and clarify the role of prolonged triple interaction  $J_t \neq 0$ .

### 3 Basic Equations

In order to produce the recurrent equations, we consider the relation of the partition function on  $V_n$  to the partition function on subsets of  $V_{n-1}$ . Given the initial conditions on  $V_1$ , the recurrence equations indicate how their influence propagates down the triangular chandelier. Let

$$Z^{(n)} \left( \begin{array}{c} i_0 \\ i_1, i_2 \end{array} \right) \quad (2)$$

be the partition function on  $V_n$  where the spin in the root  $x_0$  is  $i_0$  and the 2 spins in the proceeding ones are  $i_1, i_2$ .

There are 6 different partition functions of such form. We define for convenience the following variables:

$$\begin{aligned} z_1 &= Z^{(n)} \left( \begin{array}{c} + \\ +, + \end{array} \right), z_2 = Z^{(n)} \left( \begin{array}{c} + \\ +, - \end{array} \right), z_3 = Z^{(n)} \left( \begin{array}{c} + \\ -, - \end{array} \right) \\ z_4 &= Z^{(n)} \left( \begin{array}{c} - \\ +, + \end{array} \right), z_5 = Z^{(n)} \left( \begin{array}{c} - \\ +, - \end{array} \right), z_6 = Z^{(n)} \left( \begin{array}{c} - \\ -, - \end{array} \right) \end{aligned} \quad (3)$$

One gets through a direct enumeration:

$$\begin{aligned} z'_1 &= a^2(b^2c^2z_1 + 2z_2 + b^{-2}c^{-2}z_3)^2 \\ z'_2 &= (b^2c^2z_1 + 2z_2 + b^{-2}c^{-2}z_3)(b^2c^{-2}z_4 + 2z_5 + b^{-2}c^2z_6) \\ z'_3 &= a^{-2}(b^2c^{-2}z_4 + 2z_5 + b^{-2}c^2z_6)^2 \\ z'_4 &= a^{-2}(b^{-2}c^{-2}z_1 + 2z_2 + b^2c^2z_3)^2 \\ z'_5 &= (b^{-2}c^{-2}z_1 + 2z_2 + b^2c^2z_3)(b^{-2}c^2z_4 + 2z_5 + b^2c^{-2}z_6) \\ z'_6 &= a^2(b^{-2}c^2z_4 + 2z_5 + b^2c^{-2}z_6)^2, \end{aligned}$$

where primed variables ( $z'_1, z'_2, \dots$ ) correspond to the partition functions (2) on  $V_{(n+1)}$ , and the interactions appear through the parameters

$$a = \exp(J_1/T), \quad b = \exp(J_p/T), \quad c = \exp(J_t/T). \quad (4)$$

Note that  $z'^2_2 = z'_1z'_3$ , and  $z'^2_5 = z'_4z'_6$ , only four independent variables remain, and through the introduction of the new variables  $u_i = \sqrt{z'_i}$ , we produce the following recurrence system:

$$\begin{aligned} u'_1 &= a(b^2c^2u_1^2 + 2u_1u_3 + b^{-2}c^{-2}u_3^2) \\ u'_3 &= a^{-1}(b^2c^{-2}u_4^2 + 2u_4u_6 + b^{-2}c^2u_6^2) \\ u'_4 &= a^{-1}(b^{-2}c^{-2}u_1^2 + 2u_1u_3 + b^2c^2u_3^2) \\ u'_6 &= a(b^{-2}c^2u_4^2 + 2u_4u_6 + b^2c^{-2}u_6^2). \end{aligned}$$

The total partition function is given in terms of  $(u_i)$  by  $Z^{(n)} = (u_1 + u_3)^2 + (u_4 + u_6)^2$ . For discussing the phase diagram, the following choice of reduced variables is convenient:

$$x = \frac{u_3 + u_4}{u_1 + u_6}, \quad y_1 = \frac{u_1 - u_6}{u_1 + u_6}, \quad y_2 = \frac{u_3 - u_4}{u_1 + u_6}.$$

The variable  $x$  is just a measure of the frustration of the nearest-neighbor bonds and is not an order parameter like  $y_1, y_2$ .



The relations now have following form:

$$\begin{aligned} x' &= \frac{1}{a^2 D} [A_1(x, y_1, y_2) + A_2(x, y_1, y_2)] \\ y_1' &= \frac{1}{D} [A_3(x, y_1, y_2) - A_4(x, y_1, y_2)] \\ y_2' &= \frac{1}{a^2 D} [A_1(x, y_1, y_2) - A_2(x, y_1, y_2)] \end{aligned} \quad (5)$$

where

$$\begin{aligned} A_1(x, y_1, y_2) &= b^2 c^{-2} (x - y_2)^2 + 2(x - y_2)(1 - y_1) + b^{-2} c^2 (1 - y_1)^2 \\ A_2(x, y_1, y_2) &= b^{-2} c^{-2} (1 + y_1)^2 + 2(1 + y_1)(x + y_2) + b^2 c^2 (x + y_2)^2 \\ A_3(x, y_1, y_2) &= b^2 c^2 (1 + y_1)^2 + 2(1 + y_1)(x + y_2) + b^{-2} c^{-2} (x + y_2)^2 \\ A_4(x, y_1, y_2) &= b^{-2} c^2 (x - y_2)^2 + 2(x - y_2)(1 - y_1) + b^2 c^{-2} (1 - y_1)^2 \\ D(x, y_1, y_2) &= A_3(x, y_1, y_2) + A_4(x, y_1, y_2). \end{aligned}$$

The average magnetization  $m$  for the  $n$ th generation are defined by

$$m = \frac{(1 + x + y_1 + y_2)^2 - (1 + x - y_1 - y_2)^2}{(1 + x + y_1 + y_2)^2 + (1 + x - y_1 - y_2)^2} = 2 \frac{(1 + x)(y_1 + y_2)}{(1 + x)^2 + (y_1 + y_2)^2}.$$

## 4 Analysis of the phase diagrams

In this section we present a qualitative study of the exact phase diagrams of the model (1) in the space  $(\alpha, \beta, \gamma)$  space for given some fixed  $\beta$  and  $\gamma$ , where  $T/J_1 = \alpha$ ,  $-J_p/J_1 = \beta$ ,  $J_t/J_1 = \gamma$  and respectively  $a = \exp(\alpha^{-1})$ ,  $b = \exp(-\alpha^{-1}\beta)$  and  $c = \exp(\alpha^{-1}\gamma)$ . A phase diagram of a model describes a morphology of phases, transitions from one phase to another, stability of phases and corresponding transitions line. It is convenient to know the broad features of the phase diagram before discussing the different transitions in more detail. This can be achieved numerically in a straightforward fashion. The recursion relations (5) provide us the numerically exact phase diagrams in  $(T/J_1, -J_p/J_1, J_t/J_1)$  space. Starting from initial conditions

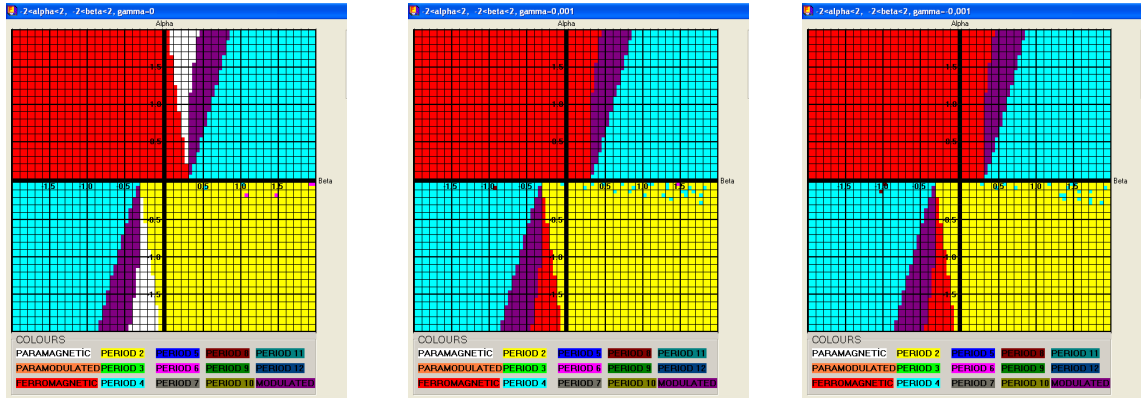


Figure 1: Phase diagrams of the model for  $\gamma = 0$ ,  $\gamma = 0.001$  and  $\gamma = -0.001$ .

$$x^{(1)} = \frac{1}{a^2 c^4}, \quad y_1^{(1)} = \frac{b^4 - 1}{b^4 + 1}, \quad y_2^{(1)} = \frac{1}{a^2 c^4} \left( \frac{b^4 - 1}{b^4 + 1} \right), \quad (6)$$

that corresponds to positive boundary condition  $\bar{\sigma}^{(n)}(V \setminus V_n) \equiv 1$ , one iterates the recurrence relations (5) and observes their behavior after a large number of iterations. In the simplest situation a fixed point

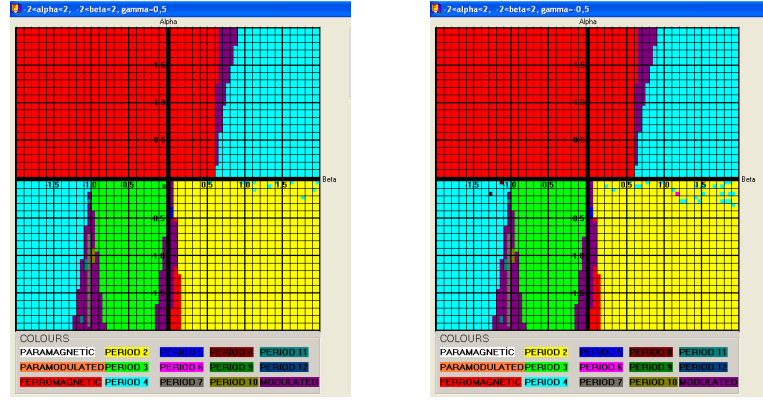


Figure 2: Phase diagrams of the model for  $\gamma = 0.5$  and  $\gamma = -0.5$ .

$(x^*, y_1^*, y_2^*)$  is reached. It corresponds to a *paramagnetic* phase if  $y_1^* = 0, y_2^* = 0$  or to a *ferromagnetic* phase if  $y_1^*, y_2^* \neq 0$ . The system may be periodic with period  $p$ , where case  $p = 2$  corresponds to *antiferromagnetic* (**AF**) phase and case  $p = 4$  corresponds to so-called *antiphase*, that denoted  $< 2 >$  for compactness. Finally, the system may remain aperiodic. The distinction between a truly aperiodic case and one with a very long period is difficult to make numerically. Detailed information about the phases and the relation with partition functions, we mainly refer to works given by Vannimenus [2] and Mariz *et al* [20]. Below we consider periodic phases with period  $p$  (briefly **P2-P12**) where  $p \leq 12$ . We will consider all periodic phases with period  $p > 12$  and aperiodic phase as modulated **M** phase.

Below we clarify the role of the parameters  $\gamma = J_t/J_1$  and  $\beta = -J_p/J_1$ . The resultant phase diagrams for some values of  $\gamma$  are shown in Fig. 1-4 with  $-2 \leq \alpha, \beta \leq 2$ . In Fig. 1 the case  $\gamma = 0$  corresponds to the Vannimenus's phase diagram [2]. For  $\gamma \neq 0$  (see Figures 1-4) one can see that corresponding phase diagram does not contain **P** phase. For the values  $|\gamma| = 0.001$  and  $|\gamma| = 0.5$  given in Fig. 1 and Fig. 2 respectively, the **P** phase disappears suddenly. For the case  $|\gamma| = 0.001$ , in the third quadrant, instead of **P** phase, the **F** phase appears. That is, **P** region is replaced by the **F** region.

Here we have three multicritical points (**LP**):  $(T = 0; -J_p/J_1 = 0.3)$ ,  $(T/J_1 = -0.04; -J_p/J_1 = -0.3)$  and  $(T/J_1 = -0.2; -J_p/J_1 = -0.25)$ .

In Fig. 2 for  $|\gamma| = 0.5$ , in the first quadrant, while region **M** is narrowed, in the third quadrant the region **P3** is extended. In first quadrant ( $J_t < 0; J_1 > 0$ ), the diagram consists of three phases: **F**, **P4** and **M**, three of them meeting at the multicritical point  $(T = 0; -J_p/J_1 = 0.6)$ . In second quadrant ( $J_t > 0; J_1 > 0$ ), the diagram consists of **F** phase only.

In third and fourth quadrants, phase diagram consists of mainly **F**, **AF**, **P3** and **M** phases. Also, we have **P7** as an island in third quadrant. Here we have many multicritical points, some of these multicritical **LPs** occur at non-zero temperature  $(T/J_1 = -0.15; -J_p/J_1 = -1)$ ,  $(T/J_1 = -1.1; -J_p/J_1 = 0.1)$  and  $(T/J_1 = -0.5; -J_p/J_1 = 0.1)$ .

In Fig. 3, for values  $\gamma = 0.8$  and  $\gamma = -0.8$  the figures are changed considerable. For  $\gamma = 0.8$ , we have many multicritical points, six of these multicritical **LPs** occur at zero temperature  $(T/J_1 = 0; -J_p/J_1 = 0.8)$ ,  $(T/J_1 = 0; -J_p/J_1 = 0.5)$ ,  $(T/J_1 = 0; -J_p/J_1 = 0.2)$ ,  $(T/J_1 = 0; -J_p/J_1 = -0.45)$ ,  $(T/J_1 = 0; -J_p/J_1 = -1.26)$  and  $(T/J_1 = 0; -J_p/J_1 = -1.4)$ , some **LPs** occur at non-zero temperature. For  $\gamma = -0.8$ , the phase diagram has similar properties. In Fig. 4, for values  $\gamma = 1$  and  $\gamma = -1$  the figures are changed completely. For  $\gamma = 1$ , we have many multicritical points, three of these multicritical **LPs** occur at zero temperature  $(T/J_1 = 0; -J_p/J_1 = 0.2)$ ,  $(T/J_1 = 0; -J_p/J_1 = -0.65)$  and  $(T/J_1 = 0; -J_p/J_1 = -1.3)$ , **LPs**  $(T/J_1 = 0.2; -J_p/J_1 = 1)$ ,  $(T/J_1 = 0.2; -J_p/J_1 = -0.7)$ ,  $(T/J_1 = -1.7; -J_p/J_1 = 0.2)$  occur at non-zero temperature. For  $\gamma = -1$ , the phase diagram has similar properties.

The resultant phase diagrams for some values of  $\beta$  are shown in Fig. 5-8 with  $-2 \leq \alpha, \gamma \leq 2$ . In Fig. 5 for  $\beta = 0$ , we obtain the phase diagram of our model which is given also in [4]. Here we have four phases: **F**, **P2**, **P4** and **M** phases.

Consider the case  $|\beta| = 0.3$  (Fig. 5). For  $\beta = 0.3$  we have six multicritical **LPs**, two of them is at zero temperature:  $(T/J_1 = 0, J_t/J_1 = 0.72)$  and  $(T/J_1 = 0, J_t/J_1 = -0.72)$ . The other **LPs** are at nonzero

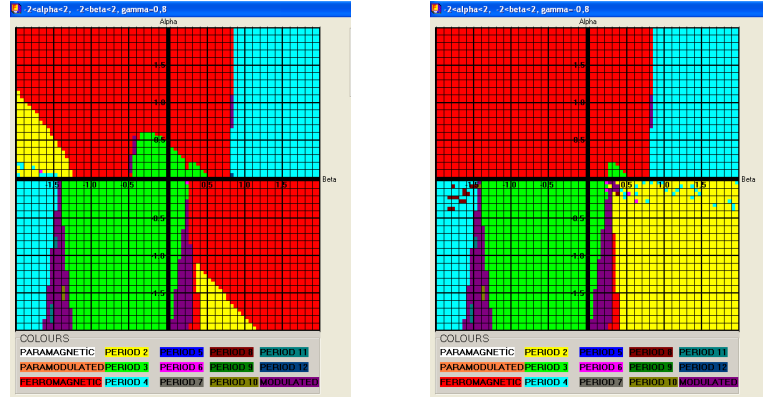


Figure 3: Phase diagrams of the model for  $\gamma = 0.8$  and  $\gamma = -0.8$ .

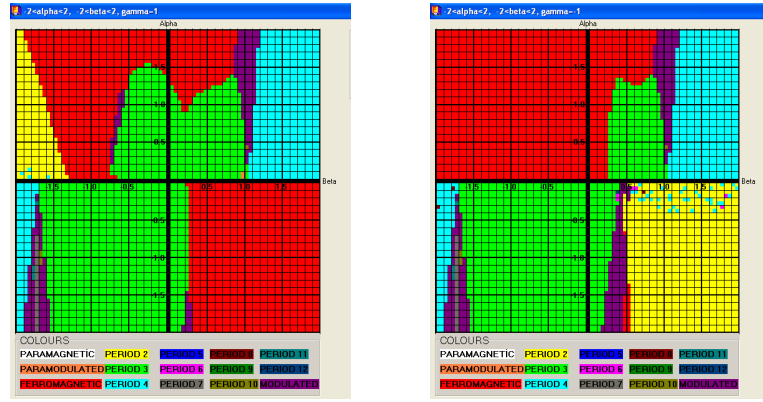


Figure 4: Phase diagrams of the model for  $\gamma = 1$  and  $\gamma = -1$ .

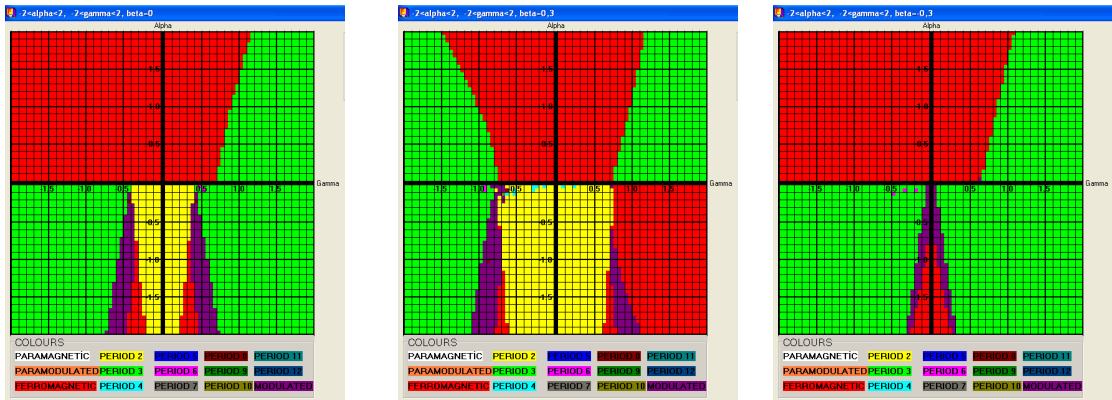


Figure 5: Phase diagram of the model for  $\beta = 0$ ,  $\beta = 0.3$  and  $\beta = -0.3$ .

temperature:  $(T/J_1 = -0.1, J_t/J_1 = -0.72)$ ,  $(T/J_1 = -1.15, J_t/J_1 = -0.65)$ ,  $(T/J_1 = -0.42, J_t/J_1 = 0.72)$  and  $(T/J_1 = -1.15, J_t/J_1 = 0.95)$ . For  $\beta = -0.3$ , the **P2** phase disappears suddenly, a new figure of phases appears as a tower in the third and fourth quadrants.

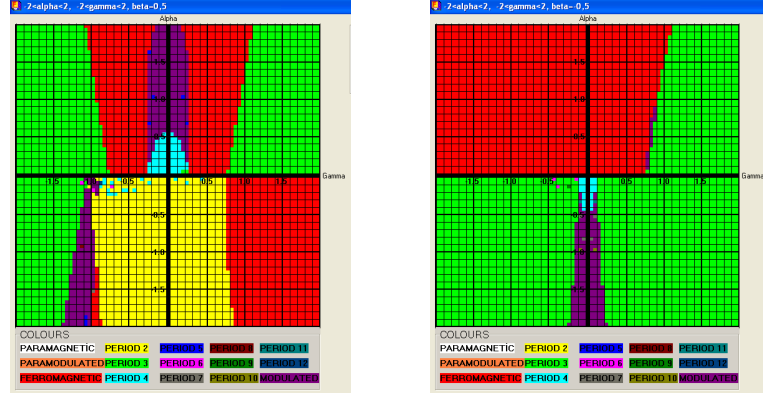


Figure 6: Phase diagrams of the model for  $\beta = 0.5$  and  $\beta = -0.5$ .

In Fig. 6, the **P4** phase appears. For  $\beta = 0.5$ , the phase diagram is changed in the first and second quadrants. Also, we have many multicritical **LPs**. In the fourth quadrant, the **M** phase disappears completely.

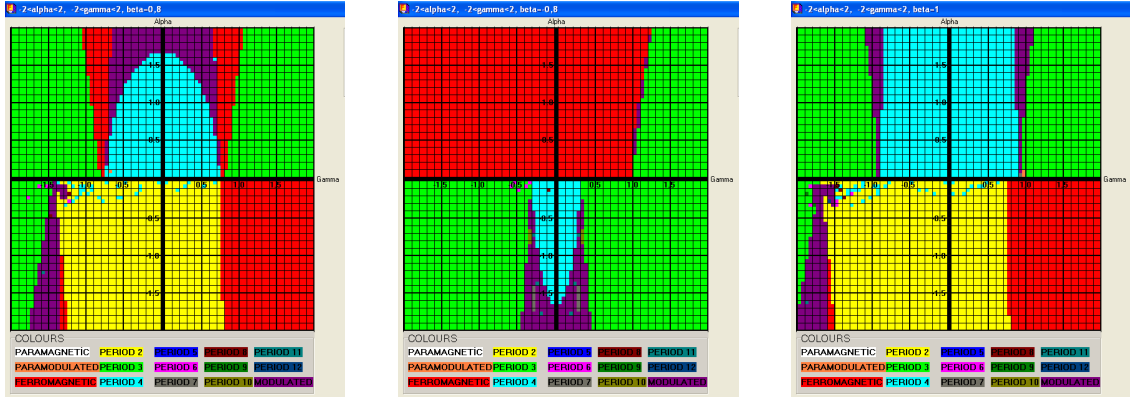


Figure 7: Phase diagrams of the model for  $\beta = 0.8$ ,  $\beta = -0.8$  and  $\beta = 1$ .

In Fig. 7, for  $\beta = 0.8$ , in the first and second quadrants the **P4** phase region is expanded. Similarly, for  $\beta = -0.8$  the **P4** phase region is expanded in the third and fourth quadrants. Also, we have many multicritical **LPs** and the phase diagrams consist of a some numbers of islands with different phases inside the **M** phase region.

In Fig. 7 and Fig. 8, one can observe that the phase diagrams are changed considerable; the **P4** phase region is expanded. For  $|\beta| = 1.5$ , one can see a new phase: the **P6** phase emerges as small islands. Analytical investigation on the stability of fixed points (paramagnetic, ferromagnetic and modulated) given in equations (5) left to another publication. The transition lines between the phases will also be considered later on.

## 5 Conclusions

We have found exact phase diagrams of the Ising model with competing prolonged and ternary next nearest-neighbor and nearest-neighbor on the Cayley tree of order 2. The basic equations produced for Ising model with competing interactions mentioned above are essentially complete than similar equations produced in

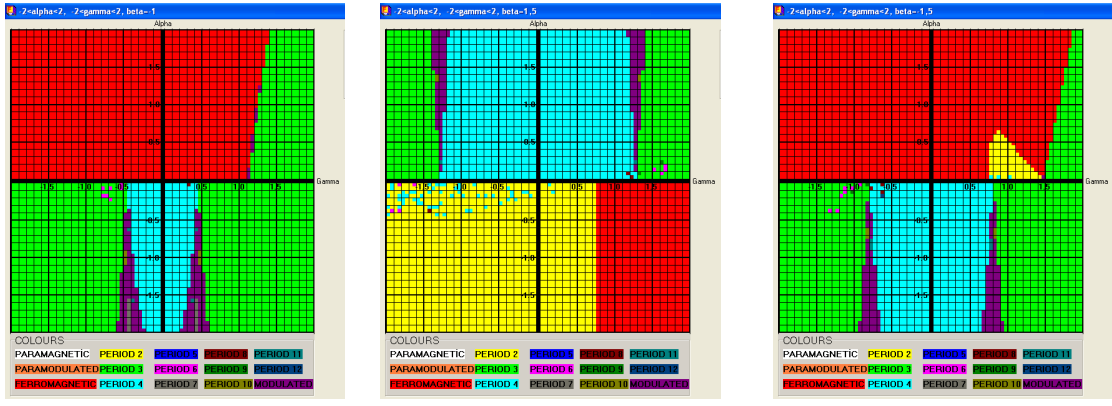


Figure 8: Phase diagrams of the model for  $\beta = -1$ ,  $\beta = 1.5$  and  $\beta = -1.5$ .

[2], [18] and [20]. In [2], there are four phases **P**, **F**, **P4** and **M**. In [4], there are also four phases **F**, **P2**, **P4** and **M** only. One can find the multicritical Lifshitz points [24] that are at nonzero temperature. It appears to shift the multicritical Lifshitz to finite temperature, while it was stuck at zero temperature  $T$  for all systems with competing interactions, studied on the Cayley tree previously [2] and [20]. Finally the study of additional aspects [24, 26] of this and related models is planned to be the subject of forthcoming publications.

### Acknowledgments

The work is supported by The Scientific and Technological Research Council of Turkey-TUBITAK (Project No: 109T678).

## References

- [1] R.F.S. Andrade and S.R. Salinas, *Phys. Rev. E* **56** (1997) 14291436
- [2] J. Vannimenus, *Z. Phys. B* **43** (1981) 141-148.
- [3] S. Uğuz, H. Akın, *Physica A*, **389**, 9, (2010) 1839-1848.
- [4] N.N. Ganikhodjaev, H. Akın, Modulated phase of an Ising model with competing binary and ternary interactions on a Cayley Tree, submitted for publication (2010).
- [5] S. Katsura, M. Takizawa, *Prog. Theor. Phys.* **51** (1974) 82-98.
- [6] T. Hasegawa, K. Nemoto, *Physica A*, **387** (2008) 1404-1410.
- [7] T. Hasegawa, K. Nemoto, *Physical Review E*, **75** (2007) 026105.
- [8] J. Rossat-Mignod, P. Burlet, H. Bartholin, O., Vogt and R. Lagnier, *J. Phys. C: Solid State Phys.* **13** (1980) 6381.
- [9] Y. Yamada, I. Shibuya, S. Hoshino, *Phys. Soc. Japan* **18** (1963) 1594
- [10] H. Ez-Zahraouy, A. Kassou-Ou-Ali, *J. Magn. Magn. Mat.* **299** (2006) 12713.
- [11] C. Ekiz, *Physics Letters A* **327** (2004) 374-379.
- [12] Y. Muraoka, K. Oda, T. Idogaki, *J. Magn. Magn. Mat.* **195** (1999) 156-167.
- [13] A. Maritan, A.L. Stella, *J. Phys. A: Math. Gen.*, **16** (1983) L157-L162.
- [14] H. Moraal, *Physica A*, **92**, 1-2, (1978) 305-314.
- [15] R. Lyons, *Commun. in Math. Phys.*, **125**, 2 (1989) 337-353.

- [16] M. Knezevic, S. Elezovic-Hadzic, *J. Phys. A: Math. Gen.*, **30** (1997) 2103-2107.
- [17] M. Mezard, A. Montanari, *Jour. Stat. Phys.*, **124**, 6 (2006) 2103-2107.
- [18] S. Inawashiro, C.J. Thompson, *Physics Letters*, **97A** (1983) 245-248.
- [19] S. Inawashiro, C.J. Thompson and G. Honda, *Jour. Stat. Phys.*, **33**, 2 (1983) 419.
- [20] M. Mariz, C. Tsallis, A.L. Albuquerque, 1985 *Jour. Stat. Phys.* **40**, 577-592.
- [21] R.J. Baxter, *Exactly Solved Models in Statistical Mechanics*, Academic Press, London/New York (1982).
- [22] J.L. Monroe, *Jour. Stat. Phys.* **67** (1992) 1185-2000.
- [23] J.L. Monroe, *Phys. Lett. A* **188** (1994) 80-84.
- [24] J.G. Moreira, S.R. Salinas, *J. Phys. A: Math. Gen.*, **20** (1987) 1621-1625.
- [25] C.R. da Silva, S.Coutinho, *Physical Review B*, **34** (1986) 7975-7985
- [26] C.S.O. Yokoi, M.J. Oliveira, S.R. Salinas, *Phys. Rev. Lett.*, **54**, 3 (1985) 163-166.
- [27] N.N Ganikhodjaev, S. Temir, H. Akin, *Jour. Stat. Phys.* **137** ( 2009) 701-715.
- [28] N.N Ganikhodjaev, F.M. Mukhamedov, C.H. Pah, *Phys. Lett. A* **373** (2008) 33-38.
- [29] N.N Ganikhodjaev, H. Akin, S. Temir, *Turk. J. Math.* **31** (2007) 229-238.

# Localization of unstable periodical solutions in chaotic systems

Dubrovskiy Alexey

*Faculty of Computational Mathematics and Cybernetics, Moscow State University,  
Moscow, Russia*

*BE, European Organization for Nuclear Research (CERN), Geneva, Switzerland*

*✉alex@solf.ru, ✉Alexey.Dubrovskiy@cern.ch*

February 15, 2010

## Abstract

In order to decode a chaotic attractor of an autonomous dynamical system, it's necessary to find as many periodic solutions as possible. Usually all periodic solutions are unstable and all together they form a fractal structure in multi-dimensional space. To localize solutions many methods require a lot of calculations. The following approach is based on the clusterization of non-invariant manifold on the Poincaré section, which all periodic solutions pass through. Such approach not only faster, but also the process can be parallelized.

*Keywords:* unstable, periodic, cluster, localization, chaos

In this article there will be described an approach to localize periodical solutions in a chaotic or a high-order periodical attractor of an autonomous dynamical system. For clearness we will conceder the approach on the example of the Rössler system:

$$\begin{aligned}x'_t &= -y - z, \\y'_t &= x + ay, \\z'_t &= b + z(x - \mu),\end{aligned}\tag{1}$$

where the system parameters are chosen as  $a = \frac{1}{2}$ ,  $b = \frac{3}{4}$  and  $c = 2.375$ . In this system the chaotic motion is present and it's widely studied [1, 2, 3]. There exists a supposition that states that all unstable periodical solutions giving birth to the chaotic attractor passes though one-dimensional non-invariant manifold. This condition is not obligatory, but it's significantly reduce the time of computation. In the Rössler system there exists a Poincaré section such that points of intersection of unstable periodic solutions with the section form one dimensional

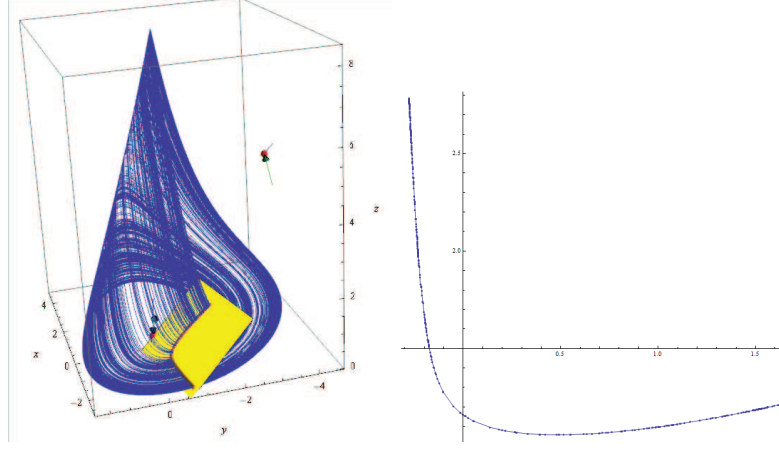


Figure 1: Rössler chaotic attractor, the Poincaré section and the non-invariant one dimensional manifold.

manifold. The chosen Poincaré section contains two equilibria points of the system. The set of points of intersection of the Rössler chaotic attractor with the section lies on one dimensional smooth curve (fig. 1). Starting from any point on the curve after one turn the Rössler dynamical system brings it back on the curve when it crosses the Poincaré section. That allows us to consider the Poincaré map  $P\mathbf{u}$ , where  $\mathbf{u} = (x, y, z)$  is a point, as one dimensional map on the tree dimensional curve. And the Poincaré map  $P\mathbf{u}$  defines connections between points  $\mathbf{u}$  on the curve.

The chosen Poincaré section simplifies the problem from unbounded tree dimensional to bounded one dimensional search. It's well known that unstable periodic solutions of Rössler attractor organize a fractal structure on the non-invariant curve. Thus in order to find periodical solutions the clusterization method is appropriate. Let's take  $N$  equally spaced points  $\mathbf{u}_1, \dots, \mathbf{u}_N$  on the curve. And each point has its Poincaré map  $P\mathbf{u}_i$ . All pairs  $(\mathbf{u}_i, P\mathbf{u}_i)$  are unique. Using the Euclidean distance between pairs the set of pairs can be clusterized in such a way that in one cluster there were only pairs with near start points  $\mathbf{u}_i$  and near its Poincaré map points  $P\mathbf{u}_i$  [4, 5]. Start points from one cluster can have its Poincaré map near start points of the other clusters. This relation between clusters gives an oriented graph. One cluster of points  $C_1$  has oriented connection with another cluster  $C_1 \rightarrow C_2$ , if they fulfill the following condition:

$$\min_{\mathbf{u}_i \in C_1, \mathbf{u}_j \in C_2} \|P\mathbf{u}_i - \mathbf{u}_j\| < \delta, \quad (2)$$

where  $C_1$  is a set of starts points from one cluster and  $C_2$  - starts points from the related cluster. The parameter  $\delta$  should be as small as distance between start points:  $\delta \approx \|\mathbf{u}_i - \mathbf{u}_j\|, i \neq j$ .

In the Rössler case taking only 200 start points and corresponding its Poincaré



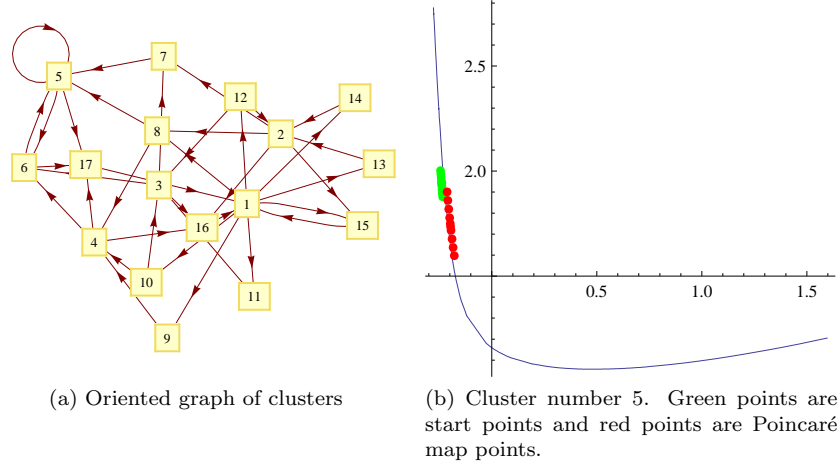


Figure 2: Clusters of the non-invariant curve of a chaotic attractor of the Rössler system.

map points one can divide them by 17 clusters and using the relation condition Eqs.2 draw connections between clusters (fig. 2a). The derived graph is fully connected and there are 62 simple cycles. We'll search periodic solutions of the Rössler system in subgraphs connected in cycles. In other words a periodical solution can pass many times any simple cycle of connected clusters in the graph. The simplest case is the self connected cycle  $\{5\}$  of the length 1 (fig. 2b). After the filtering points which are not connected to the cluster 5 there are left only 4 points, which potentially can represent a periodic solution. These 4 points are corresponded to a small range on the curve. In order to increase precision one can chose new discretization of the new range with a smaller step between points, for example, up to 200 points. With the new set of start points and its Poincaré map points we repeat again the clusterization and we draw a new graph, and so on. In the chosen cycle  $\{5\}$  of the original graph this process will lead to a self connected subgraph corresponding to a range on the curve, which tends to zero by norm. It means that the periodic solution of period one is localized (fig. 3a).

In case if there are more than one cluster in a cycle, for example,  $\{1, 15\}$  of the graph (fig. 2), after the filtering and the extension of start points each of clusters can be subclusterized separately or united and then reclusterized. Using reclusterization approach there were found another periodic solutions of period 4, 6, 8 etc (fig. 3).

In many systems there exists more than one dimensional non-invariant manifold on the Poincaré section. This approach to search of unstable periodic solutions is still valid. The only difference is that start points  $\{\mathbf{u}\}$  should be taken inside the attractor bonding tori on a Poincaré section. All points from the invariant manifold will be rejected at the filtering stage.

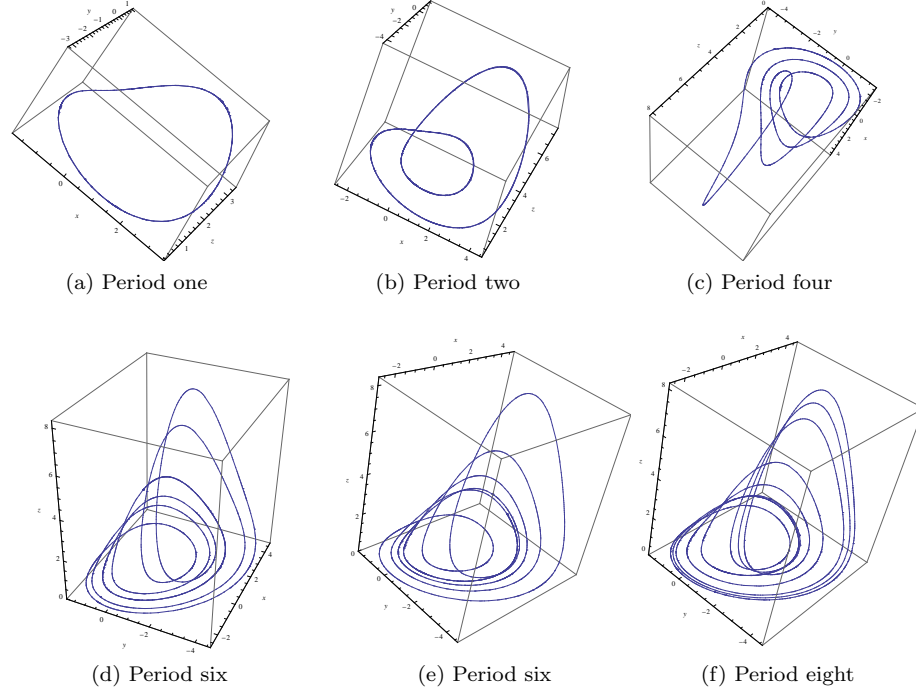


Figure 3: Periodical solution in the Rössler chaotic system. (a):  $x \approx -1.71327$ ,  $y \approx -0.55776$  and  $z \approx 0.187936$ ; (b):  $x \approx -2.42754$ ,  $y \approx -0.669782$  and  $z \approx 0.156963$ ; (c):  $x \approx -0.767252$ ,  $y \approx -1.6213$  and  $z \approx 1.32838$ ; (d):  $x \approx -1.82617$ ,  $y \approx -0.573996$  and  $z \approx 0.181707$ ; (e):  $x \approx -1.55795$ ,  $y \approx -0.538524$  and  $z \approx 0.199319$ ; (f):  $x \approx -1.32721$ ,  $y \approx -0.51608$  and  $z \approx 0.221794$ .

I acknowledge valuable conversations with Ninkolai Alexandrovich Magnitskii and Andrey Tsyganov.

## References

- [1] C. Letellier, P. Dutertre, and B. Maheu. Unstable periodic orbits and templates of the rossler system: Toward a systematic topological characterization. *Chaos*, 5:271–282, 1995.
- [2] N. A. Magnitskii. Hopf bifurcation in the rössler system. 31(3):538–541, 1995.
- [3] N. A. Magnitskii and S. V. Sidorov. *New methods for chaotic dynamics*, volume 58 of *A. World scientific*, 2006.

- [4] Pavel Berkhin. Survey of clustering data mining techniques. Technical report, 2002.
- [5] A. K. Jain, M. N. Murty, and P. J. Flynn. Data clustering: A review, 1999.

# Configuring Time-Lagged Recurrent Neural Network using Strange Attractor's Topological Properties

M.P. Hantias<sup>1</sup>, H.E. Nistazakis<sup>2\*</sup> and G.S. Tombras<sup>2</sup>

<sup>1</sup> Automation Department, Chalkis Institute of Technology, Psachna,  
Evia 34400, Greece, e-mail: mhanias@hol.gr

<sup>2</sup> Division of Electronics, Computers, Telecommunications and Control, Department of Physics,  
University of Athens, Athens, 15784, Greece, e-mails: {enistaz; gtombras}@phys.uoa.gr

\*Corresponding author, enistaz@phys.uoa.gr

## Abstract

In this work, we investigate how a focused time-lagged recurrent neural network topology can be efficiently configured based on the complexity of the underlying dynamics reflected by the observed chaotic time series of a Chua's electronic circuit. In particular, we examine the possibility to partition the input space by the number of near neighbours of the chaotic time series being modelled. By determining the number of near neighbours, the number of hidden units can then be specified. The validity of such an approach is examined by changing the number of neurons in the hidden layer.

*Keywords:* Chaos, Chua's Circuit, Neural Networks, Time Series Analysis.

## 1. Introduction

It is well known that neural networks are used for time series prediction problems. Many architecture schemes have been considered for such predictions, but in general time lagged recurrent neural networks give better results. Despite the neural network architecture, the definition of number of hidden units as well as the number of input variables remains as an open problem. In this work, we examine how we can specify the number of hidden units by the number of near neighbours. In other words, we investigate how a focused time-lagged recurrent neural network (FTLRNN) can be efficiently determined based on the complexity of the underlying dynamics reflected by an observed chaotic time series, and for this, we have chosen to use the output voltage of a Chua's electronic circuit.

Chaotic electronic circuits [1]-[4] have been widely studied during the last few decades due to their easy implementation, robustness, reproducibility of results, and also as a test platform for synchronization, chaos control, signal encryption and secure communications [5]-[11]. The Chua's circuit [12], [13] is one of the most famous circuits in this research area's literature. Here, we consider a typical implementation of the Chua's circuit and examine its operation in the MultiSim circuit simulation environment, as illustrated in Fig.1, by monitoring the voltage,  $v$ , across the resistor  $R_7$  of the circuit. As shown in Fig.2, the so obtained voltage  $v=v(t)$  time series clearly reveals the presence of chaos.

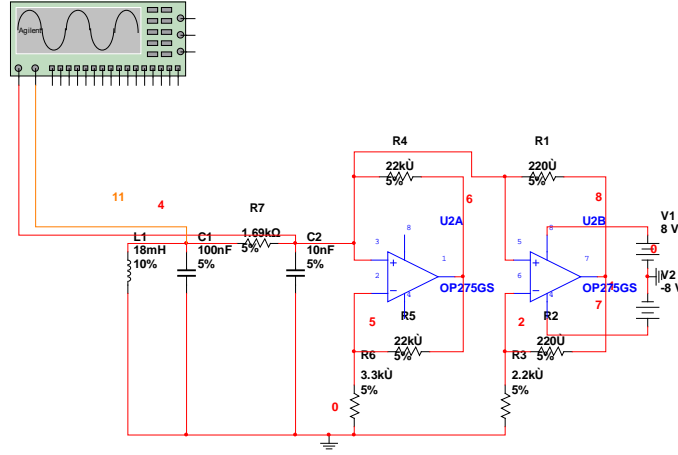
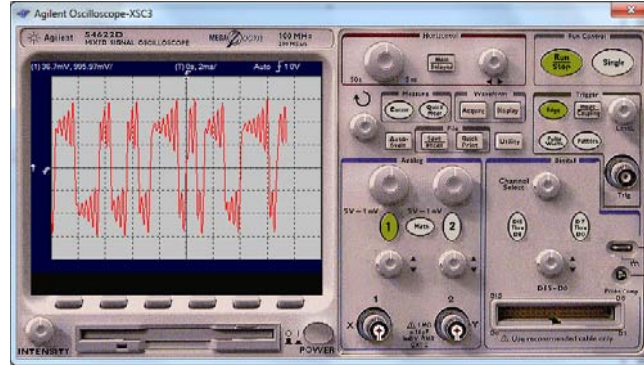


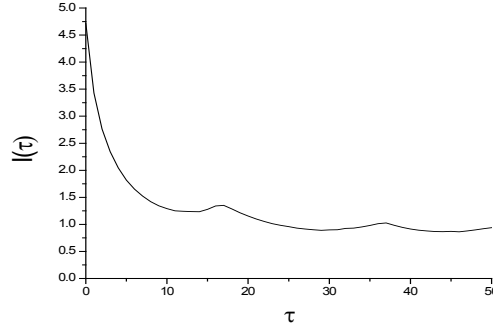
Figure 1: MultiSim simulation environment for the considered Chua circuit.


 Figure 2: The simulation obtained chaotic signal  $v=v(t)$  across the resistor  $R_7$  of the Chua circuit of Figure 1.

Using the recorded data, we now construct a vector  $\vec{X}_i$ ,  $i=1, \dots, N$ , where  $N=2870$  data values in the  $m$  dimensional phase space, given in the form, [14]:

$$\vec{X}_i = \{v_i, v_{i-\tau}, v_{i-2\tau}, \dots, v_{i+(m-1)\tau}\} \quad (1)$$

This vector represents a point in the  $m$  dimensional phase space, the attractor of which is embedded each time, where  $\tau$  is the time delay  $\tau=i\Delta t$  and  $\Delta t=9.76\mu s$  is the sample rate. The element  $v_i$  represents a value of the examined scalar time series in time, i.e. the voltage  $v$  across the resistor  $R_7$  corresponding to the  $i$ -th component of the time series. Use of this method reduces the problem of phase space reconstruction to that of proper determining suitable values of  $m$  and  $\tau$ . The choice of these values is not always simple, especially when we do not have any additional information about the original system and the only source of data is a simple sequence of scalar values, acquired from the original system. The dimension for which a time delay reconstruction of the phase space provides the necessary number of coordinates to unfold the dynamics from overlapping on itself as caused by projection, is called embedding dimension  $m$ . Using the average mutual information we can obtain  $\tau$ , being less associated with a linear point of view, and thus, more suitable for dealing with nonlinear problems. Following that, the average mutual information,  $I(\tau)$ , [14], expresses the amount of information (in bits) which can be extracted from the value in time  $v_i$  about the value in time  $v_{i+\tau}$ . Usually, the value of  $\tau$  suitable for the phase space reconstruction chosen is equal to the position of the first minimum of  $I(\tau)$ , [14]. Here,  $\tau=14$  time steps, as shown in Fig. 3.


 Figure 3: Mutual information  $I$  versus the time delay  $\tau$ .

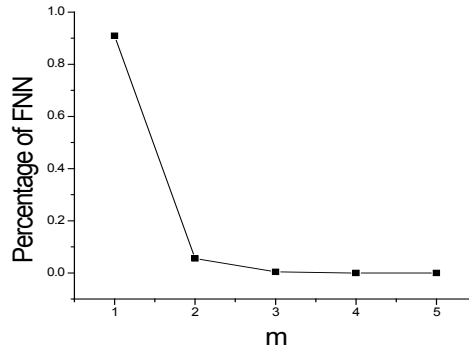
Next, we use the method of False Nearest Neighbours (FNN), [14], [15], in order to estimate the minimum embedding dimension. This method is based on the fact that when embedding dimension is too low, the trajectory in the phase space will cross itself. If we are able to detect these crossings, we may decide whether the used  $m$  is large enough for proper reconstruction of the original phase space, i.e. when no intersections occur, or not. When intersections are present for a given  $m$ , the embedding dimension is considered too low and we have to increase it at least by one. Then, we test the eventual presence of self-crossings again.

The practical realization of the described method is based on testing the neighbouring points in the  $m$ -dimensional phase space. Typically, we take a certain amount of points in the phase space and find the nearest neighbour to each of them. Then, we compute distances for all these pairs and also their distances in an  $(m+1)$ -dimensional phase space. The rate of those distances is

$$P = \frac{\|\bar{X}_i(m+1) - \bar{X}_{n(i)}(m+1)\|}{\|\bar{X}_i(m) - \bar{X}_{n(i)}(m)\|} \quad (2)$$

where  $\bar{X}_i(m)$  represents the reconstructed vector as described in (1), belonging to the  $i$ -th point in the  $m$ -dimensional phase space and index  $n(i)$  denotes the nearest neighbour to the  $i$ -th point. If  $P$  is greater than some value  $P_{\max}$ , we call this pair of points false nearest neighbours, i.e. neighbours which arise from trajectory self-intersection and not from the closeness in the original phase space. The dimension  $m$  is considered found only when the false nearest neighbours percentage falls below some limit, typically set to 1%, [16]. Hence, choosing an implicit value  $P_{\max}=10$ , we can finally calculate the quantity  $P$ .

The considered Chua's circuit is a 3-variable system and this means that the false nearest neighbour number should indicate the minimum embedding dimension to be equal to  $m=3$ , [13]. This is shown in Fig.4, where the obtained results indicate that application of FNN yields  $m=3$ , confirming that Chua's circuit is a 3-variable system.


 Figure 4: False nearest neighbour ratio as a function of the embedding dimension: false nearest neighbours become negligible after  $m = 3$ .

## 2. Time-lagged recurrent neural network structure

Time-lagged recurrent networks (TLRNs), [17], [18] are multilayer perception (MLP) neural networks extended with short-term memory structures, [19], [20], since most chaotic data contain valuable information in their time structure, i.e. how data change with time. Hence, TLRNs can capture the dynamics of chaotic data. Recurrent networks are neural networks with one or more feedback loops, while the memory structure is simply a cascade either of ideal delays, i.e. a delay of one sample, or of leaky integrators, called in this case gamma memory. When an input processing element (PE) of an MLP neural network is replaced by a tapped delay line, the neural network is characterized as focused and the topology is called focused because memory elements are present only at the input layer, [21], while it is clear that such a delay line holds or stores the past input samples. Following that, the combination of tap delay lines and the weights that connect the taps to the PEs of the first hidden layer can be seen as simple linear combiners followed by a static nonlinearity. Hence, the first layer of a neural network may act as a filtering layer with as many adaptive filters as PEs in the first hidden layer. The samples' depth parameter ( $D$ ) is used to compute the number of taps ( $T$ ) contained within the memory structure of the network. A typical time-lagged neural network structure is shown in Fig. 5.

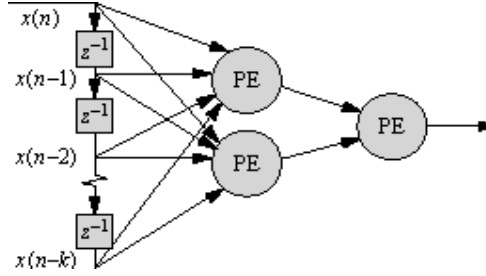


Figure 5: A time-lagged neural network with one hidden layer where  $z$  is the operator (linear system) that delays the input by one sample without distorting it.

In order to forecast the chaotic time series obtained from the Chua circuit, we construct a focused time-lagged (delay) neural network with one hidden layer. The number of inputs is set equal to the embedding dimension  $m=3$ , while the number of hidden layer neurons is obtained by specifying the number of near neighbours of each order. Furthermore, in order to examine the influence of this number into the prediction of the chaotic time series, we need to find the corresponding number. Thus, by applying the method proposed by [14] and [16] for a minimum embedding dimension  $m=3$  and a delay time  $\tau=14$  of the considered circuit, it is found that:

- for radius  $\varepsilon = 0.0216$ , the number of first order nearest neighbours is 41,
- for radius  $\varepsilon = 0.03068$ , the number of second order nearest neighbours is 119,
- for radius  $\varepsilon = 0.0433$ , the number of third order nearest neighbours is 283,
- for radius  $\varepsilon = 0.0612$ , the number of forth order nearest neighbours is 683.

In this respect, we now test the efficiency of the network with number of hidden layer neurons equal to the minimum embedding dimension, i.e. being equal to 3. In addition, we apply the Kolmogorov theorem, [22], according to which the number of hidden layer neurons is equal to  $2m+1=2 \times 3+1=7$ . We choose the transfer function to be the  $\tanh(\cdot)$  and we consider gamma memory, i.e. leaky integrators in the delay line. The depth in samples  $D$  that is used to compute the number of taps contained within the memory structure of the network is set equal to the embedding minimum dimension  $m$ , i.e.  $D=3$ , while the trajectory length  $T$  that corresponds to the samples/exemplar setting within the dynamic controller and specifies how many samples to read, i.e. steps in time to move forward, before back propagation occurs, is chosen to be  $2m$ , i.e.  $T=6$ . The efficiency of the network is then measured by applying mean square error (MSE) for training [23], and normalized mean square error (NMSE) [23] for testing set. For learning purposes we use 65% percent of our data, 15% for cross validation and 25% for testing. In all cases the learning process stopped at 10000 epochs with a learning rate equal to 0.1 and momentum equal to 0.7.

### 3. Time series prediction

The network is trained to predict the values of the signal at times  $(t+3)$ ,  $(t+4)$ ,  $(t+5)$ ,  $(t+6)$ ,  $(t+7)$  by using the values at time  $(t+2)$ ,  $(t+1)$ ,  $t$ . After the first prediction, these samples are used to feed the network's input in order to predict the future samples, recursively (iterative prediction) so that the forecasting horizon to be 5 steps ahead. Table 1 shows the performance of the proposed neural network scheme on the modelling of Chua's map for different values of hidden units for training set.

The results of Chua's voltage prediction are shown in Figs 6 and 7. In particular, Fig.6 shows that for training set MSE is decreased as the number of hidden units is increased, while there is a significant difference in the quality of the models when the number of hidden units is chosen to be equal to the number of third order nearest neighbours. Similarly, Fig.7 shows that for testing set NMSE is decreased as the number of hidden units is increased, while there is again a significant difference in the quality of the models when the number of hidden units is chosen to be equal to the number of third order nearest neighbours. The obtained results are shown in Fig.8, where it can readily be seen that using as number of hidden units the number of near neighbours of order 3, we achieve multistep prediction with a five step forecasting horizon.

Table 1: Neural net performance

Parameters	Minimum Embedding Dimension	Kolmogorov Theorem	First order NN	Second order NN	Third order NN	Fourth order NN
No. of hidden units	3	7	41	119	283	683
Training Set (MSE) $\times 10^{-3}$	7.64	7.23	4.12	1.80	1.46	1.42
Testing Set (NMSE) $\times 10^{-3}$ V(1)	22	34.4	4.05	5.49	2.38	2.77
Testing Set (NMSE) $\times 10^{-3}$ V(2)	44.2	38.7	23	11.9	5.34	4.14
Testing Set (NMSE) $\times 10^{-3}$ V(3)	46.3	48.6	55.3	12.5	9.76	8.74
Testing Set (NMSE) $\times 10^{-3}$ V(4)	70.6	88.5	34.3	20.1	18.1	16.9
Testing Set (NMSE) $\times 10^{-3}$ V(5)	90.1	121	70.2	33.1	27.6	27.6



Figure 6: Mean-square error of the Chua circuit's time series prediction for different values of hidden units (training set).



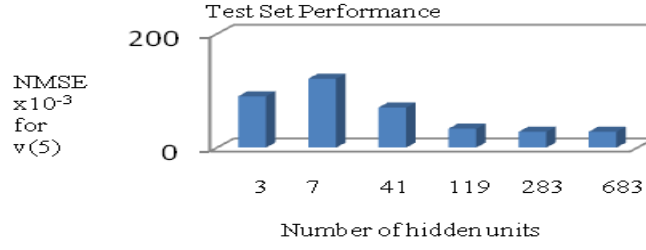


Figure 7: Normalized mean-square error of the Chua circuit's time series prediction for different values of hidden units (testing set)

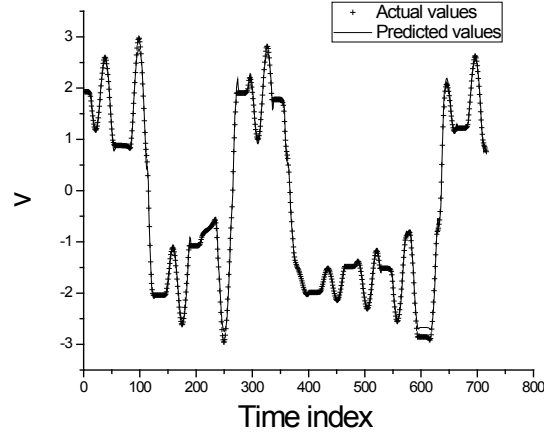


Figure 8: Actual (crosses) and predicted (black line) values of Chua's chaotic signal.

#### 4. Conclusions

It has been shown that focused time-lagged recurrent neural networks are capable to identify chaotic systems. However, when we deal with the observable results as obtained from some process, the mathematical formulation of which, as well as the total number of variables may not be known exactly, structure construction and adjustment of the artificial neural network remain an open problem. In this work, the chaotic analysis of the time series being modelled is used for the structure construction of a focused time-lagged recurrent neural network. In this respect, the number of hidden units is determined by the topological properties of the corresponding strange attractor. From the obtained results it is clear that the quality of prediction depends on the number of near neighbours that has been used as the number of hidden layer's neurons. According to the MSE of the training set as well as the NMSE of the testing set it has been found that the third order number of near neighbours give smaller error than the other parameters.

## References

- [1] M.P. Haniyas and G.S. Tombras, Time series analysis in single transistor chaotic circuit, *Chaos, Solitons and Fractals*, 40, 246–256, (2009).
- [2] M.P. Haniyas and G.S. Tombras, Time series crossprediction in single transistor chaotic circuit, *Chaos, Solitons and Fractals*, 41, 1167–1173, (2009).
- [3] S.G. Stavrinides, N.C. Deliolanis, Th. Laopoulos, I.M. Kyprianidis, A.N. Miliou and A.N. Anagnostopoulos, The intermitten behavior of a second - order non-linear nonautonomous oscillator, *Chaos, Solitons and Fractals*, 36, 1191–1199, (2008).
- [4] S.G. Stavrinides, A.N. Miliou, Th. Laopoulos, and A.N. Anagnostopoulos, The intermittency route to chaos of a second order non-linear non-autonomous oscillator, *Int. J. on Bifurcation & Chaos*, 18, 5, 1561–1566, (2008).
- [5] A. Bogris, P. Rizomiliotis, K.E. Chlouverakis, A. Argyris, and D. Syvridis, Feedback phase in optically generated chaos: a secret key for cryptographic applications, *IEEE Journal of Quantum Electronics*, 44, 2, 119–124, (2008).
- [6] G.P. Jiang, W.K.S. Tang and G. Chen, A simple global synchronization criterion for coupled chaotic systems, *Chaos, Solitons and Fractals*, 15, 5, 925–935, (2003).
- [7] J. Zhang, C. Li, H. Zhang and J. Yu, Chaos synchronization using single variable feedback based on back stepping method, *Chaos, Solitons and Fractals*, 21, 5, 1183–1193, (2004).
- [8] M.T. Yassen, Adaptive control and synchronization of a modified Chua's circuit system, *Applied Mathematics and Computation*, 135, 1, 113–128, (2003).
- [9] T. Wu and M.-S. Chen, Chaos control of the modified Chua's circuit system, *Physica D: Nonlinear Phenomena*, 164, 1-2, 53- 58, (2002).
- [10] C.C. Hwang, H.-Y. Chow and Y. K.Wang, A new feedback control of a modified Chua's circuit system, *Physica D: Nonlinear Phenomena*, 92, 1-2, 95–100, (1996).
- [11] K. Li, Y.C. Soh, and Z.G. Li, Chaotic cryptosystem with high sensitivity to parameter mismatch, *IEEE Trans. on Circuits and Systems I*, 50, 4, 579–583, (2003).
- [12] L.O. Chua, Chua's circuit: an overview ten years later, *Journal of Circuits Systems and Computers*, 4, 2, 117–159, (1994).
- [13] R.M. Rubinger, A.W.M. Nascimento, L.F. Mello, C.P.L. Rubinger, N. Manzanares Filho, and H.A. Albuquerque, Inductorless Chua's Circuit: Experimental Time Series Analysis, *Hindawi Publishing Corporation Mathematical Problems in Engineering*, 2007, Article ID 83893, 16 pages doi:10.1155/2007/83893 (2007).
- [14] H. Kantz and T. Schreiber, Nonlinear Time Series Analysis, *Cambridge University Press, Cambridge*, 1997.
- [15] K.E. Lonngren, Notes to accompany a student laboratory experiment on chaos, *IEEE Transactions on Education*, 34, 1, (1991).
- [16] M.B. Kennel, R. Brown, H.D.I. Abarbanel, Determining embedding dimension for phase-space reconstruction using a geometrical construction, *Phys. Rev. A*, 45, 3403, (1992).
- [17] A.W. Waibel., Phoneme recognition using time delay neural networks, *IEEE Proc.*, ASSP-37, 328–339, (1989).
- [18] S.N. Kale and S.V. Dudul, Intelligent Noise Removal from EMG Signal Using Focused Time-Lagged Recurrent Neural Network, *Hindawi Publishing Corporation Applied Computational Intelligence and Soft Computing*, 2009, Article ID 129761, 12 pages doi:10.1155/2009/129761, (2009).
- [19] H. Demuth and M. Beale, Neural Network Toolbox: User'Guide, *Version 3.0, The MathWorks, Natick, Mass, USA*, 1998.
- [20] G. Cybenko, Approximation by superpositions of a sigmoidal function, *Mathematics of Control, Signals, and Systems*, 2, 4, 303–314, (1989).
- [21] S.-Z. Qin, H.-T. Su, and T.J. McAvoy, Comparison of four neural net learning methods for dynamic system identification, *IEEE Transactions on Neural Networks*, 3, 1, 122–130, (1992).
- [22] V. Kiirkov, Kolmogorov's Theorem and Multilayer Neural Networks, *Neural Networks*, 5, 501–506, (1992).
- [23] Abbas Erfanian Omidvar, Configuring radial basis function network using fractal scaling process with application to chaotic time series prediction, *Chaos, Solitons and Fractals*, 22, 757–766, (2004).

# Strange attractor in the Potts model on a Cayley tree in the presence of competing interactions.

N.N. GANIKHODJAEV

*Department of Computational and Theoretical Sciences, Faculty of Science, International Islamic University Malaysia, 25200, Kuantan, Malaysia  
e-mail: nasirgani@hotmail.com*

## Abstract

For Potts model on a Cayley tree we produce recursive relations that provide us the numerically exact phase diagram of the model. Each phase is characterized by a particular attractor and the phase diagram is obtained by following the evolution and detecting the qualitative changes of these attractors. These changes can be either continuous or abrupt, respectively characterizing second- or first- order phase transitions. We present a few typical attractors and at finite temperatures, several interesting features (evolution of reentrances, separation of the modulated region into few disconnected pieces, etc) are exhibited for typical values of parameters.

**Keywords:** Potts model, recursive equations, attractor, phase diagram, phase transition.

## 1 Introduction

Consideration of spin models with multispin interactions has proved to be fruitful in many fields of physics, ranging from the determination of phase diagrams in metallic alloys and exhibition of new types of phase transition, to site percolation. The Potts model on the Cayley tree is one of these infinite dimensionality models that has received widespread attention by many authors recently since the appearance of the Vannimenus model [1],[2],[3],[5]. The Cayley tree, that is, an infinite connected tree whose sites have the same coordination number, has a thin structure without closed paths but with infinite dimensionality. By introducing competing interactions between Ising or Potts spin variables, assigned to each site, we enable the system to present a very rich phase diagram with many modulated phases. The Vannimenus model, that is, the Ising model on a Cayley tree of coordination number  $p = 3$ ,

with ferromagnetic nearest-neighbor interaction and with an antiferromagnetic next-nearest-neighbor interaction (then latter restricted to the sites belonging to the same branch) is the counterpart of the anisotropic next-nearest-neighbor Ising model (ANNNI) model defined on regular lattices. In the ANNNI model the competing interactions are restricted to a single direction, while in the Vannimenus model there is no preferential direction at all, that is, the competing interactions act between the ring generations in all directions. The phase diagram of the Vannimenus model shows in addition to the paramagnetic and the ferromagnetic phases a  $++--$  periodic antiphase  $<2>$  and a modulated phase, all of which meet at a multicritical point at zero temperature. From this result follows that the Ising model with competing interactions on a Cayley tree is of real interest since it has many similarities with models on periodic lattices. This suggests that more complicated models should be studied on trees, with the hope to discover new phases or unusual types of behavior. This important point is that statistical mechanics on trees involve nonlinear recursion equations and are naturally connected to the rich world of dynamical systems, a world under intense investigation.

In the present paper we have generalized for Potts model with competing binary interactions the approach used by Thompson [4] for the Ising model on the Cayley tree with only nearest-neighbor interactions and an external magnetic field. We were able to calculate exactly the partition function, the local magnetization, and the pair correlation function, by solving numerically a system of high-order coupled recursion equations for partial effective fields. The phase diagrams of our model can be obtained by studying the behavior of local magnetization and of the pair correlation function versus the generating number, and by looking at the fixed points of the coupled recursion relations for the partial effective fields. These diagrams have particularly distinct features depending on the range of competing parameters.

## 2 The Potts Model and Effective Fields

We consider a semi-infinite Cayley tree  $\Gamma_+^2 = (V, L)$  of order 2, i.e., an infinite graph without cycles with 3 edges issuing from each vertex except for  $x^0$  which has only 2 edges, where  $V$  is the set of vertices and  $L$  is the set of edges. Two vertices  $x$  and  $y$  are called nearest -neighbors if there exists an edge connecting them. The distance  $d(x, y)$  on the Cayley tree is the number of edges in the shortest path from  $x$  to  $y$ . For a fixed  $x^0$  we set  $W_n = \{x \in V : d(x, x^0) = n\}$  and  $V_n = \cup_{i=0}^n W_i$ . Two vertices  $x$  and  $y$  are called the second neighbors if  $d(x, y) = 2$ . The second neighbor vertices  $x$  and  $y$  are called one level second neighbors if  $x, y \in W_n$  for some  $n$ , and the second neighbor vertices  $x, y$  that are not one level are called prolonged second neighbors (see Fig.1).

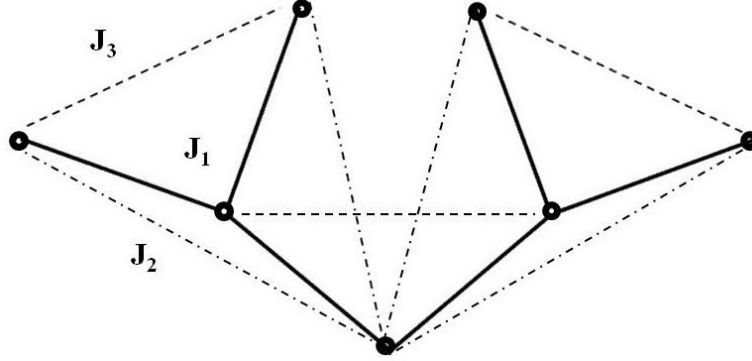


Fig.1 Three successive generations of a Cayley tree (solid line: nearest neighbor interactions; dot-dashed line: prolonged second neighbor interactions; dashed line: one-level second neighbor interactions).

Let us consider a Potts model on a Cayley tree with competing nearest-neighbor interaction  $J_1$ , prolonged and one level second neighbors interactions  $J_2$  and  $J_3$  respectively. For the three-state Potts model with spin values in  $\{1, 2, 3\}$ , the relevant Hamiltonian has the form

$$H(\sigma) = -\beta J_3 \sum \delta_{\sigma(x)\sigma(y)} - \beta J_2 \sum \delta_{\sigma(x)\sigma(y)} - \beta J_1 \sum \delta_{\sigma(x)\sigma(y)}, \quad (1)$$

where  $\sigma : V \rightarrow \{1, 2, 3\}$  is a configuration on  $V$  and  $\beta = \frac{1}{T}$  is the inverse temperature. Here first summation is over one-level second neighbors, second is over prolonged second neighbors, third is over nearest neighbors,  $J_1, J_2, J_3 \in R$  and  $\delta$  is the Kronecker symbol. Below we produce recursive relations obtained following the lines of Inawashiro et al. Firstly we slightly modify Hamiltonian (1). Suppose the set of values of the spin variables  $\sigma(x), x \in V$  consists of vectors  $\sigma_i \in R^2, i = 1, 2, 3$  such that  $|\sigma_i| = 1$  for all  $i$  with dot products  $\sigma_1\sigma_2 = \sigma_2\sigma_3 = \sigma_3\sigma_1 = -\frac{1}{2}$ . Since for all  $x, y \in V$

$$\frac{2}{3}(\sigma(x)\sigma(y) + \frac{1}{2}) = \delta_{\sigma(x)\sigma(y)},$$

the Hamiltonian (1) reduces to

$$H(\sigma) = -J_3 \sum \sigma(x)\sigma(y) - J_2 \sum \sigma(x)\sigma(y) - J_1 \sum \sigma(x)\sigma(y), \quad (2)$$

where first summation is over one-level second neighbors, second is over prolonged second neighbors and last is over nearest neighbors. On the plane  $R^2$  fix a basis  $e_1, e_2$ , setting

$e_1 = \sigma_1$  and  $e_2 = \sigma_2$ . Since  $\sigma_3 = -\sigma_1 - \sigma_2$ , for any vector  $h = (h_1, h_2) \in R^2$  we obviously have

$$h\sigma_1 = h_1 - h_2/2, h\sigma_2 = h_2 - h_1/2, h\sigma_3 = -h_1/2 - h_2/2. \quad (3)$$

The iterative scheme can be set up by summing successively spins as can be seen in Fig.2.

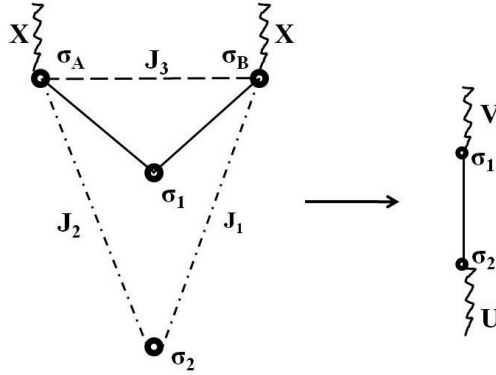


Fig.2 Schematic diagram to illustrate the summation used in Eq.(4).

Simple but tedious algebra gives

$$\sum_{\sigma(A), \sigma(B) \in \{\sigma_1, \sigma_2, \sigma_3\}} \exp[ K_1 \sigma(x)(\sigma(A) + \sigma(B)) + K_2 \sigma(y)(\sigma(A) + \sigma(B)) + K_3 \sigma(A)\sigma(B) + X(\sigma(A) + \sigma(B))] = C \exp[W\sigma(x)\sigma(y) + U\sigma(y) + V\sigma(x)], \quad (4)$$

where  $K_i = J_i/T$  ( $i = 1, 2, 3$ ),  $X = (X_1, X_2)$ ,  $U = (U_1, U_2)$ ,  $V = (V_1, V_2)$ , and

$$U_1 \equiv U_1(X, K_1, K_2, K_3) = \frac{2}{9} \ln \frac{\omega(1, 1)\omega(2, 1)\omega(3, 1)}{\omega(1, 3)\omega(2, 3)\omega(3, 3)} \quad (5)$$

$$U_2 \equiv U_2(X, K_1, K_2, K_3) = \frac{2}{9} \ln \frac{\omega(1, 2)\omega(2, 2)\omega(3, 2)}{\omega(1, 3)\omega(2, 3)\omega(3, 3)} \quad (6)$$

$$V_1 \equiv V_1(X, K_1, K_2, K_3) = \frac{2}{9} \ln \frac{\omega(1, 1)\omega(1, 2)\omega(1, 3)}{\omega(3, 1)\omega(3, 2)\omega(3, 3)} \quad (7)$$

$$V_2 \equiv V_2(X, K_1, K_2, K_3) = \frac{2}{9} \ln \frac{\omega(2, 1)\omega(2, 2)\omega(2, 3)}{\omega(3, 1)\omega(3, 2)\omega(3, 3)} \quad (8)$$

$$W \equiv W(X, K_1, K_2, K_3) = \frac{1}{9} \ln \frac{\omega^2(1, 1)\omega^2(2, 2)\omega^2(3, 3)}{\omega(1, 2)\omega(2, 1)\omega(1, 3)\omega(3, 1)\omega(2, 3)\omega(3, 2)} \quad (9)$$

$$C \equiv C(X, K_1, K_2, K_3) = [\omega(1, 1)\omega(1, 2)\omega(1, 3)\omega(2, 1)\omega(2, 2)\omega(2, 3)\omega(3, 1)\omega(3, 2)\omega(3, 3)]^{1/9} \quad (10)$$

with

$$\omega(\sigma, \sigma') = e^{K_3[a^2(\sigma, \sigma') + b^2(\sigma, \sigma') + c^2(\sigma, \sigma')]} + 2e^{-\frac{1}{2}K_3} \left[ \frac{1}{a(\sigma, \sigma')} + \frac{1}{b(\sigma, \sigma')} + \frac{1}{c(\sigma, \sigma')} \right] \quad (11)$$

where

$$a(\sigma, \sigma') = \exp(K_1\sigma_1\sigma + K_2\sigma_1\sigma' + X_1 - \frac{1}{2}X_2) \quad (12)$$

$$b(\sigma, \sigma') = \exp(K_1\sigma_2\sigma + K_2\sigma_2\sigma' + X_2 - \frac{1}{2}X_1) \quad (13)$$

$$c(\sigma, \sigma') = \exp(K_1\sigma_3\sigma + K_2\sigma_3\sigma' - \frac{1}{2}X_1 - \frac{1}{2}X_2). \quad (14)$$

Beginning with  $X^{(1)} = (0, 0)$  and  $K_1^{(1)} = K_1 = J_1/T$  with  $J_1$  the initial nearest-neighbor coupling, we obtain from the above results the iteration scheme, for  $r = 2, 3, \dots, N$ ,

$$X_1^{(r)} = 2U_1(X^{(r-2)}, K_1^{(r-2)}, K_2, K_3) + V_1(X^{(r-1)}, K_1^{(r-1)}, K_2, K_3) \quad (15)$$

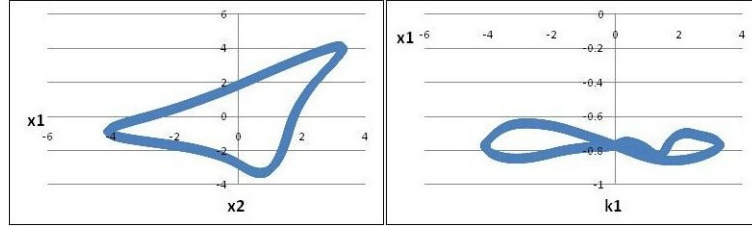
$$X_2^{(r)} = 2U_2(X^{(r-2)}, K_1^{(r-2)}, K_2, K_3) + V_2(X^{(r-1)}, K_1^{(r-1)}, K_2, K_3) \quad (16)$$

and

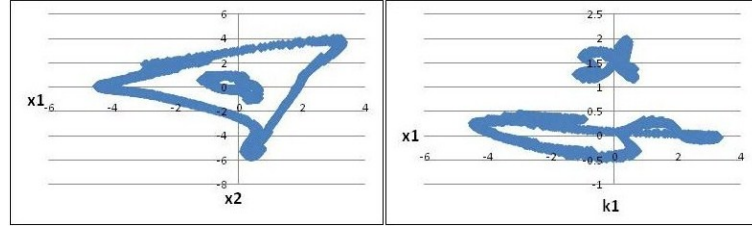
$$K_1^{(r)} = K_1 + W(X^{(r-1)}, K_1^{(r-1)}, K_2, K_3), \quad (17)$$

where  $X^{(0)} = (0, 0)$ ,  $K_1^{(0)} = 0$  and  $K_2 = J_2/T$ ,  $K_3 = J_3/T$  with  $J_2, J_3$  the initial prolonged and one-level second neighbors couplings respectively. Here vector  $X^{(r)}$  plays the role of an effective field, thus characterizing the  $r$ th shell mean magnetization. These recursion relations provide us the (numerically) exact phase diagram of the model. The equilibrium configuration for given values of  $T$  and  $J_1, J_2, J_3$  is found by repeated iterations of recursion relations (15)-(17). The magnetization vector  $(X_1, X_2)$  flows to one of the following attractors: (i) a trivial fixed point  $(X_1^*, X_2^*) = (0, 0)$  (which corresponds to the paramagnetic phase); (ii) a nontrivial fixed point  $(X_1^*, X_2^*) \neq (0, 0)$  (the ferromagnetic phase); (iii) a well defined periodic cycle (which corresponds to a commensurate phase with a given period); (iv) a one-dimensional orbit (associated with an incommensurate phase); and (v) a strange attractor with a fractal character. Each phase is characterized by a particular attractor in the  $(X_1^{(r)} - X_2^{(r)})$  and  $(X_1^{(r)} - K_1^{(r)})$  spaces and the phase diagram is obtained by following the evolution and detecting the qualitative changements of these attractors. These changements

can be either continuous or abrupt, respectively, characterizing second- or first-order phase transitions. Let us introduce  $a \equiv T/J_1$ ,  $b \equiv -J_2/J_1$  and  $c \equiv J_3/J_1$ . Below we consider a strange attractors in the planes  $(X_1 - X_2)$  and  $(X_1 - K_1)$  for selected values of  $a, b$  and  $c$ . A few typical strange attractors are presented in Figs. 3-6.



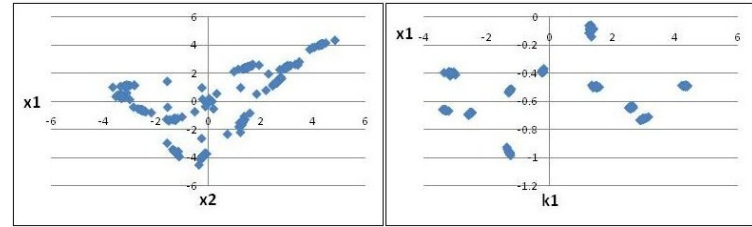
(i)  $a = -0.8; b = -1.2$



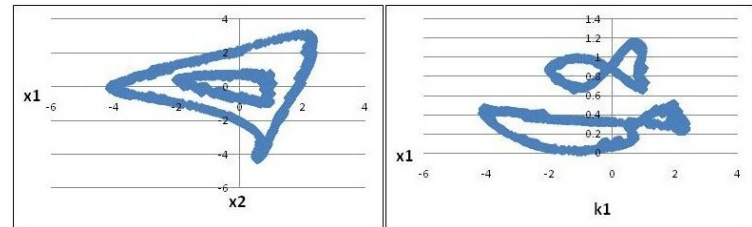
(ii)  $a = 0.7; b = 0.9$

Fig.3. Examples of attractors in the  $X_1 - X_2$  and  $X_1 - K_1$  spaces with  $c = 0$ .

Interesting feature is that fact that, for second case the modulated phase appears in two disconnected pieces.



(i)  $a = -1.0; b = -1.7$

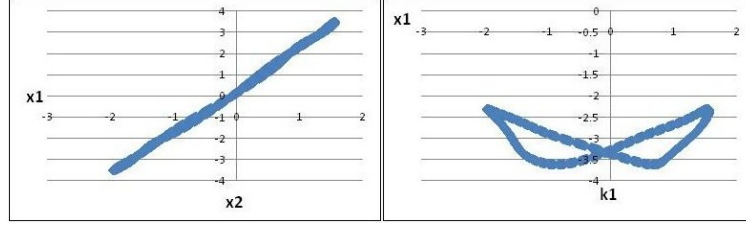




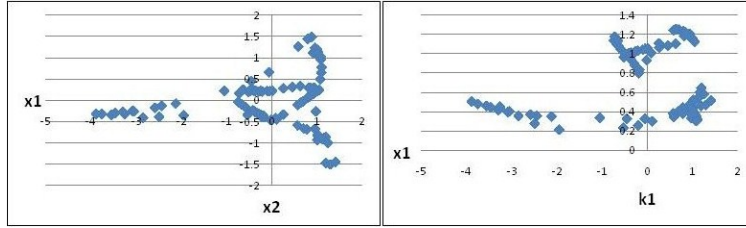
$$(ii) a = 1.0; b = 1.2$$

Fig.4. Examples of attractors in the  $X_1 - X_2$  and  $X_1 - K_1$  spaces with  $c = \pm 0.001$ .

Here for small  $c$  appear both commensurate and modulated phase with two disconnected pieces.

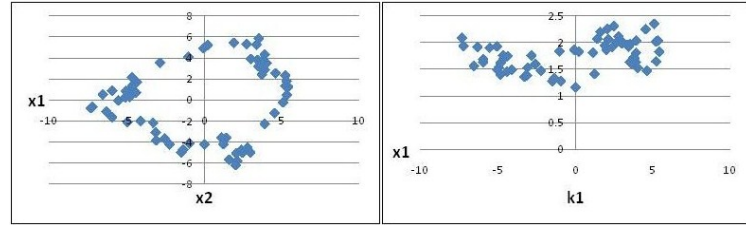


$$(i) a = -0.2; b = -0.6$$

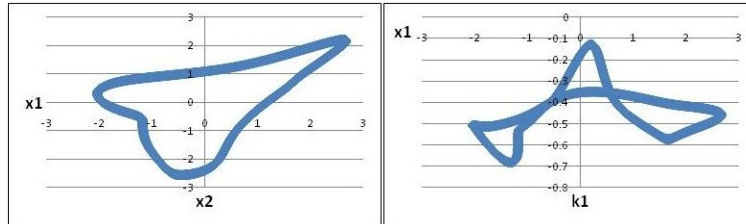


$$(ii) a = 0.75; b = 0.6$$

Fig.5. Examples of attractors in the  $X_1 - X_2$  and  $X_1 - K_1$  spaces with  $c = 1$ .



$$(i) a = 0.4; b = 1.0$$



$$(ii) a = -1.3; b = -1.3$$

Fig.6. Examples of attractors in the  $X_1 - X_2$  and  $X_1 - K_1$  spaces with  $c = -1$ .  
Attractors in last two figures correspond general modulated phases.

### 3 Conclusions

The numerical investigations of the mapping established the existence of a complete devil's staircase at low temperatures, and the appearance of chaotic phases, in the core of the tree, for a given set of boundary conditions. The study of additional aspects of this and related models is planned to be the subject of forthcoming publications.

### 4 Acknowledgements

The author is indebted to student of Faculty of Science International Islamic University Malaysia Ashraf Mohamed Nawi for computational assistance. This work was partially supported by The Scientific and Technological Research Council of Turkey-TUBITAK (Project No: 109T678) and Research Endowment Fund EDW B 0902-199.

### References

- [1] J. Vannimenus, Modulated Phase of an Ising System with Competing Interactions on a Cayley Tree. *Z. Phys. B* **43**, 141–148 (1981).
- [2] M. Mariz, C.Tsalis, A.L.Albuquerque.: Phase Diagram of the Ising Model on a Cayley tree in the Presence of competing Interactions and Magnetic Field, *Jour. Stat. Phys.* **40**, 577–592 (1985).
- [3] N.N. Ganikhodjaev, F.M. Mukhamedov, C.H.Pah, Phase Diagram of the Three States Potts Model with Next Nearest Neighbour Interactions on the Bethe Lattice, *Physics Letters A* **373**, 33–38 (2008).
- [4] C.J.Thompson, *J.Stat.Phys.* **27**, 441- (1982)
- [5] S.Inawashiro, C.J.Thompson, *Physics Letters* 97 A, 245-248 (1983)

# On Non-Associativity of Rhesus Factor Transmission.

N.N. GANIKHODJAEV, M.D.USMANOVA

*Kulliyyah of Science, International Islamic University Malaysia, Kuantan , Malaysia*  
*e-mails: nasirgani@hotmail.com; mahsuma2002@hotmail.com*

## Abstract

The Rhesus system is the second most significant blood group system in human blood transfusion. Individuals either have, or do not have, the Rhesus factor (or Rh D antigen) on the surface of their red blood cells. A child inherits two rhesus genes, one from each parent, where gene  $D$  correspond to positive rhesus factor and gene  $d$  correspond to negative rhesus factor. The transmission of rhesus from parents to their offspring are random and events that contradict Mendel laws increase this randomness. To study this transmission we apply theory of quadratic stochastic operators and show that corresponding genetic algebra is non-associative.

**Keywords:** Rhesus factor; quadratic stochastic operator; genetic algebra; divisible algebra.

## 1 Introduction

The theories of heredity attributed to Gregor Mendel (1822-1884), were based on his work with pea plants. The short monograph, *Experiments with Plant Hybrids*, in which Mendel described how traits were inherited, has become one of the most enduring and influential publications in the history of science. He saw that the traits were inherited in certain numerical ratios. From his studies, Mendel derived certain basic laws of heredity; hereditary factors do not combine, but are passed intact; each member of the parental generation transmits only half of its hereditary factors to each offspring; and different offspring of the same parents receive different sets of hereditary factors. Mendel's work became the foundation for modern genetics.

Mendel, in his first paper exploited some symbolism, which is quite algebraically suggestive, to express his genetic laws. In fact, it was later termed "Mendelian algebras" by several authors. General genetic algebras indeed are the product of interaction between biology and mathematics. The study of these algebras reveals the algebraic structure of Mendelian genetics, which always simplifies and shortens the way to understand the genetic and evolutionary phenomena in the real world.

Before we discuss the genetic from a mathematical perspective, it is useful to know some of the basic language from biology. A gene is a unit of hereditary information. The genetic code of an organism is carried on chromosomes. In addition, each gene on a chromosome can take different forms that are called alleles. For example, the gene that determines Rhesus system in humans has two different alleles, that are  $D$  and  $d$ . Recall that the Rhesus system is the second most significant blood group system in human blood transfusion. Individuals either have, or do not have, the Rhesus factor (or  $RhD$  antigen) on the surface of their red blood cells. This is usually indicated by  $Rh^+$  (does have the  $RhD$  antigen) or  $Rh^-$  (does not have the antigen) suffix to the  $ABO$  blood type. Rhesus factor for human are determined by two alleles since humans are diploid organisms. a child inherits two rhesus genes, one from each parent, where gene  $D$  correspond to positive rhesus factor and gene  $d$  correspond to negative rhesus factor. Offspring is rhesus negative if they have inherited a gene  $d$  from each parent ( $d, d$ ) and offspring is rhesus positive if they inherited a  $D$  gene from both parents. If

offspring have inherited a rhesus positive gene  $D$  and a rhesus negative gene  $d$ , they are most likely to be rhesus positive as the  $D$  gene is more dominant as compared to the  $d$  gene. Hence it is possible to have a rhesus negative child and a rhesus positive father. Thus rhesus of parents do not determine unambiguously their offspring's rhesus. The transmission of rhesus from parents to their offspring are random and events that contradict Mendel laws increase this randomness. To study this transmission we apply quadratic stochastic operators.

## 2 Quadratic Stochastic Operator

Quadratic stochastic operator was first introduced in [1]. Such operator frequently arises in many models of mathematical genetics [1], [2], [3]. Consider a biological population, that is a community of organisms closed with respect to reproduction. Assume that each individual in this population belongs to precisely one species  $1, 2, \dots, m$ . The scale of species is such that the species of the parents  $i$  and  $j$  unambiguously determines the probability of every species  $k$  for the first generation of direct descendants. We denote this probability, that is to be called the heredity coefficient, by  $p_{ij,k}$ . It is then obvious that  $p_{ij,k} \geq 0$  for all  $i, j, k$  and that

$$\sum_{k=1}^m p_{ij,k} = 1, \quad (i, j, k = 1, \dots, m). \quad (1)$$

Assume that the population is so large that frequency fluctuations can be neglected. Then the state of the population can be described by the tuple  $(x_1, x_2, \dots, x_m)$  of species probabilities, that is  $x_k$  is the fraction of the species  $k$  in the total population. In the case of panmixia (random interbreeding) the parent pairs  $i$  and  $j$  arise for a fixed state  $\mathbf{x} = (x_1, x_2, \dots, x_m)$  with probability  $x_i x_j$ . Hence

$$x'_k = \sum_{i,j=1}^m p_{ij,k} x_i x_j, \quad (k = 1, \dots, m), \quad (2)$$

is the total probability of the species  $k$  in the first generation of direct descendants.

Let

$$S^{m-1} = \{\mathbf{x} = (x_1, \dots, x_m) \in R^m : x_i \geq 0, \sum_{i=1}^m x_i = 1\} \quad (3)$$

is the  $(m-1)$ -dimensional simplex in  $R^m$ . The transformation  $V : S^{m-1} \rightarrow S^{m-1}$  is called a quadratic stochastic operator (q.s.o.) if

$$V : (V\mathbf{x})_k = \sum_{i,j=1}^m p_{ij,k} x_i x_j, \quad (k = 1, \dots, m), \quad (4)$$

where

$$a) p_{ij,k} \geq 0; \quad b) p_{ij,k} = p_{ji,k}; \quad \text{and} \quad c) \sum_{k=1}^m p_{ij,k} = 1$$

for arbitrary  $i, j, k = 1, \dots, m$ . Note that the condition  $p_{ij,k} = p_{ji,k}$  is not overloaded, since otherwise one can determine new heredity coefficient

$$q_{ij,k} = \frac{p_{ij,k} + p_{ji,k}}{2}$$

with preserving operator  $V$ .

We shall call a quadratic stochastic operator  $V$  a genetic realization of some model of heredity.

### 3 Algebra with genetic realization

Mathematically, the algebras that arise in genetics are very interesting structures. Many of the algebraic properties of these structures have genetic significance. Indeed, the interplay between the purely mathematical structure and the corresponding genetic properties makes this subject so fascinating.

The most general definition of an algebra  $\mathbb{R}$  which could have genetic significance is that of algebra with genetic realization.

Let a quadratic stochastic operator  $V : S^{n-1} \rightarrow S^{n-1}$  be a genetic realization, where  $V$  is defined by cubic matrix  $\{p_{ij,k} : i, j, k = 1, \dots, n\}$  such that

$$a) p_{ij,k} \geq 0; \quad b) p_{ij,k} = p_{ji,k}; \quad \text{and} \quad c) \sum_{k=1}^m p_{ij,k} = 1.$$

An algebra  $\mathbb{R}$  with genetic realization  $V$  is an algebra over the real numbers  $R$  which has a basis  $\{a_1, \dots, a_n\}$  and a multiplication table

$$a_i a_j = \sum_{k=1}^n p_{ij,k} a_k.$$

Here  $p_{ik,j}$  is a frequency that the next generation reproduced by two gametes carrying  $a_i$  and  $a_j$  will inherit  $a_k$ ,  $k = 1, 2, \dots, n$ .

Below we will consider case  $n = 2$  and let  $a_1 = A, a_2 = a$ . Then a general element  $\alpha A + \beta a$  of genetic algebra which satisfies  $\alpha, \beta \in R$  with  $0 \leq \alpha, \beta \leq 1$  and  $\alpha + \beta = 1$  can represent a population or a single individual of a population. In each case, the coefficients  $\alpha$  and  $\beta$  signify the percentage of frequency of the associated allele. I.e., if the element represents a population, then  $\alpha$  is the percentage of the population which carries the allele  $A$  on the gene under consideration. Likewise,  $\beta$  is the percentage of the population which has the allele  $a$ .

For those elements of the genetic algebra which represent populations, multiplication of two such elements represents random mating between the two populations. In general, the algebras which arise in genetics are commutative but non-associative. In [5] proved following Theorem.

**Theorem 1** The two-dimensional algebra with the standard basis  $\{A, a\}$  and with genetic realization

$$P_{AA,A} = z, P_{Aa,A} = y, P_{aa,A} = x$$

and

$$P_{AA,a} = 1 - z, P_{Aa,a} = 1 - y, P_{aa,a} = 1 - x,$$

is associative algebra if and only if the coefficients  $x, y, z$  satisfy the following equation

$$xz + y - y^2 - x = 0 \quad (5)$$

It is proved that arbitrary  $x \in [0, 1], y \in [x - x^2, 1]$ , and  $z = \frac{x^2 - x + y}{y}$  satisfy equation (5) with  $0 \leq x, y, z \leq 1$ .

## 4 Division Algebra

An algebra  $\mathbb{R}$  is called a division algebra if for any element  $f$  in  $\mathbb{R}$  and any non-zero element  $g$  in  $\mathbb{R}$  there exists precisely one element  $h$  in  $\mathbb{R}$  with  $f = gh$  and precisely one element  $d$  in  $\mathbb{R}$  such that  $f = dg$ . For associative algebras, the definition can be simplified as follows: an associative algebra  $\mathbb{R}$  over a field  $R$  is a division algebra iff it has a multiplicative identity element  $e \neq 0$  and every non-zero element  $f$  has a multiplicative inverse, i.e. an element  $h$  with  $fh = hf = e$ . We show that two-dimensional associative genetic algebra  $\mathbb{R}$  considered above is not the division algebra and describe non-invertible elements. It is easy to show that the element

$$e = \frac{y}{y-x}A + \frac{x}{x-y}a$$

is the multiplicative identity of  $\mathbb{R}$ . For arbitrary element  $f = \gamma A + \delta a$  in  $\mathbb{R}$  the element

$$\begin{aligned} & \frac{y[\gamma(y - xy + y^2) + \delta(y + xy - y^2)]}{(y-x)^2(\gamma + \delta)[\gamma(1-x) - \delta y]}A \\ & + \frac{\gamma x(x - 2y + 2xy - x^2 - y^2) - \delta y(2y^2 - 3xy + x^2 - y)}{(y-x)^2(\gamma + \delta)[\gamma(1-x) - \delta y]}a \end{aligned}$$

is a multiplicative inverse of  $f$  if  $\gamma + \delta \neq 0$  and  $\gamma(1-x) - \delta y \neq 0$ . Let

$$\mathbb{R}_{-1} = \{f = \gamma A + \delta a : \gamma + \delta = 0\} \quad (6)$$

and

$$\mathbb{R}_{\frac{1-x}{y}} = \{f = \gamma A + \delta a : \gamma(1-x) - \delta y = 0\}. \quad (7)$$

Thus  $f = \gamma A + \delta a \in \mathbb{R}_{\frac{1-x}{y}}$  is not invertible population if  $0 \leq \gamma, \delta \leq 1$  with  $\gamma + \delta = 1$ , i.e., for given  $x, y, z$  that satisfy (5), exist unique non-invertible population.

## 5 Genetic Algebra Generated by Transmission of Factor Rhesus

To describe the transmission of factor rhesus from parents to their offspring we need to find the probability  $P_{XY,Z}$  that from a father with factor rhesus  $X$  and a mother with factor rhesus  $Y$  their child receives factor rhesus  $Z$ , with  $X, Y, Z \in \{1, 2\}$ , where for brevity 1 denote positive rhesus and 2 denote negative rhesus. Let  $N(F_X, M_Y)$  be the number of offspring of fathers with rhesus factor  $4X4$  and mothers with rhesus factor  $Y$  and  $N^Z(F_X, M_Y)$  be the number of offspring with factor rhesus  $Z$ . Then the transmission probability  $P_{XY,Z}$  is defined as

$$P_{XY,Z} = \frac{N^Z(F_X, M_Y)}{N(F_X, M_Y)}. \quad (8)$$

For collected data according (8) we have following:

$$P_{11,1} = 0.985, P_{12,1} = 0.647, P_{21,1} = 0.657, P_{22,1} = 0.092.$$

One can see that the condition  $b$ ) in (3) is broken. Let consider new heredity coefficients

$$q_{ij,k} = \frac{P_{ij,k} + P_{ji,k}}{2},$$

where

$$q_{11,1} = 0.985, q_{12,1} = 0.652, q_{22,1} = 0.092.$$

Then

$$z = 0.985, y = 0.652, x = 0.092$$

that do not satisfy equation (5). Thus the genetic algebra generated by quadratic stochastic operator of rhesus factor transmission is non-associative algebra.

## Acknowledgement

This work was partially supported by Research Endowment Fund IIUM EDW B 0801-59.

## References

- [1] Bernstein S.N. Solution of a mathematical problem connected with the theory of heredity. *Ann.Sci. de l'Ukraine* **1**, 83–114 (1924).
- [2] Elson R.C., Stewart J., A general model for the genetic analysis of pedigree data, *Hum.Hered.* **21**, 523–542 (1971).
- [3] Kesten H., Quadratic transformations: a model for population growth. I,II, *Adv. Appl. Prob.*, **2**, 1–82, 179–228(1970)
- [4] Reed M.L. Algebraic structure of genetic inheritance. *Bulletin of AMS*, **34**, 107–130 (1997).
- [5] GanikhodjaevN.N., Haziana Hartini Binti Hisamuddin, Associativity in inheritance or are there associative populations? *Malaysian Journal of Science* **27**,131–136 ( 2008)

## Fractal analysis of macroradiographic images: Legg-Calvé-Perthes disease

*Nebojša T. Milošević*

Department of Biophysics, Medical School, University of  
Belgrade, Serbia; [mtn@med.bg.ac.rs](mailto:mtn@med.bg.ac.rs)

*Dušan Marić*

University Clinic for Pediatric Surgery, Medical School, University  
of Novi Sad, Serbia; [dmarić@sbb.rs](mailto:dmarić@sbb.rs)

*Herbert F. Jelinek*

School of Community Health, Centre for Research in Complex  
Systems, Charles Sturt University, Albury, Australia;  
[hjelinek@csu.edu.au](mailto:hjelinek@csu.edu.au)

### **Abstract**

A sample of sixty one two dimensional radiographic images of the lateral pillar of the femoral head were subjected to fractal analysis in order to investigate its ability to discriminate two groups of images - femoral heads with Legg-Calvé-Perthes disease and normal femoral heads. Skeletonized images of the femoral head contours were successfully quantified by the box counting method, showing significant difference in contours of the affected femoral heads than those of normal femoral heads. Further investigation in application of the fractal analysis to the current classification scheme of radiographs of the affected femoral heads is also discussed.

### **Keywords**

Box-counting method; Femoral head; Fractals; Hip; Lateral pillar; Radiograph



## 1. INTRODUCTION

Joint cartilage is in close contact with the underlying subchondral bone. Both the joint cartilage and the subchondral bone take part in transmission of the force in the craniocaudal direction and adjust themselves to mechanical load to the extent necessary to prevent any damage to their structure. The cause of Legg-Calvé-Perthes (LCP) disease has not been clearly defined yet, so that the very onset of the disease – infarct of the subchondral bone, remains unknown. For that reason, there is a wide span of accepted clinical and radiographic presentations of Legg-Calvé-Perthes disease [1,2]. It covers the cases from the minimum or no change in the contour of the femoral head to its massive destruction. As the disease develops in four stages (infarction, resorption, revascularization and remodeling), it is desirable that it is diagnosed and treated as early as possible [3]. Younger children have far better chances for a successful final outcome, but it depends on the stage of the disease at the moment of its identification and the beginning of the treatment [4].

Modern radiographic classification to assess the severity of LCP disease began with Catterall (1982), who defined 4 types of the disease, the first two associated with a good while the third and the forth type are associated with a poorer prognosis [1]. Salter and Thomson (1984) classified the severity of the disease on the basis of the extent and location of the subchondral fracture that appears early in the course of the disease [5]. The most recent radiographic classification is also classified into four groups but based on the degree of lateral pillar damage [6].

The aim of this study was to check the possibility of application of the fractal analysis to the radiographic image of the lateral pillar of normal femoral head and to the same image showing synovial fluid secretion in patients suspected of having LCP disease. Also, the study investigates the use of fractal dimension as a parameter, which quantifies the contour of the femoral head in patients with LCP disease and discriminates this group of patients from patients with normal femoral heads.

## 2. MATERIALS AND METHODS

### 2.1. Image acquisition

A sample of sixty one 2D radiographic images of hips, taken from children from 7 to 11 years, was used in this study. The group of thirty one images belonged to children with diagnosed LCP disease. Radiographic images were analyzed according to modified lateral pillar classification GBK [6], when changes in femoral heads have been confirmed. Thirty images, with no changes in femoral heads, were used as controls.

Radiographic images were digitized using a digital camera (Olympus 560 UZ, Japan) at a maximal camera resolution (8 MPix), imported into a PC computer and processed further by *Image J* software (NIH Image, [www.rsb.info.nih.gov/ij/](http://www.rsb.info.nih.gov/ij/)). Using the *Image J* program tools, a rectangular region of interest was selected from the digitalized femoral head image within the lateral pillar (Fig. 1.A, white rectangle), and saved as a new file in grayscale format (Fig. 1.B).

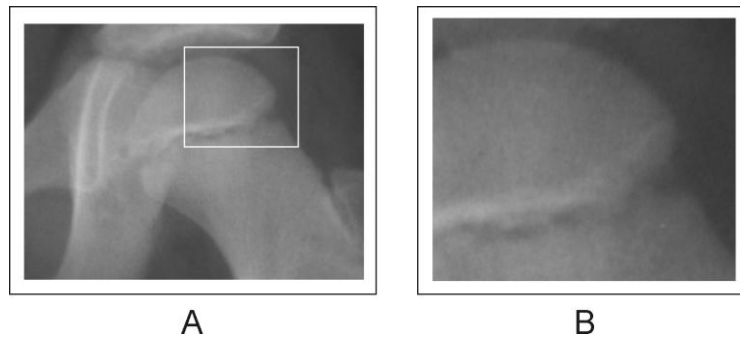


Figure 1. A) Radiographic image of the femoral head with region of interest (white rectangle) used for further analysis. B) Zoomed in region of interest of the femoral head within the lateral pillar.

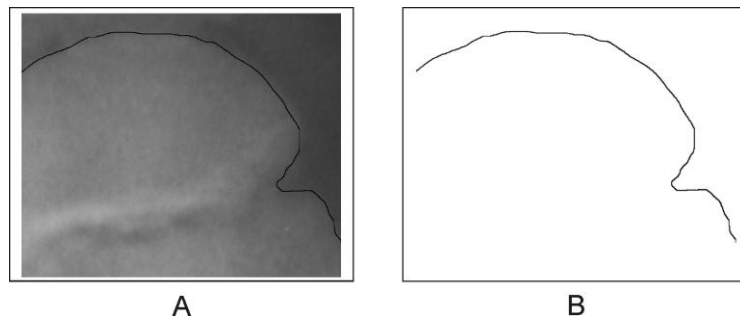


Figure 2. Image of the studied region of the femoral head with drawn contour (A) and a binary image of the femoral head contour (B).

Then, a line along the boundary of the selected lateral pillar region, from the lateral edge of the lateral pillar to the lateral aspect of the medial pillar of the head epiphysis, was drawn (Fig. 2.A). In the next step, all unnecessary points from the digitized image above and below the head contour were digitally

removed (Fig. 2.B). The obtained grayscale image contour of the head was converted to a binary image, skeletonized to a one pixel thick line and subjected to the fractal analysis.

## 2.2. Image analysis

Skeletonized images of the femoral head contours were examined quantitatively by fractal analysis, using its best-known technique, the box counting method [7,8]. The method is based on covering the object image with sets of square boxes of known box side size and on counting the boxes covering (or contiguous to) the image. The number of boxes covering the image increases with decreasing box size, with a correlation between the number of boxes  $N$  and the box side length  $r$  described by

$$N(r) = B \cdot r^{-D}, \quad (1)$$

where  $B$  is a constant and  $D$  is the fractal dimension. Taking the logarithm of the left and right side of Eq. (1), the equation of a straight line is obtained

$$\log N(r) = -D \cdot \log r + \log B. \quad (2)$$

The fractal dimension of the analyzed object is calculated by Eq. (2), as a positive value of the slope of the straight line plotted using the least squares method.

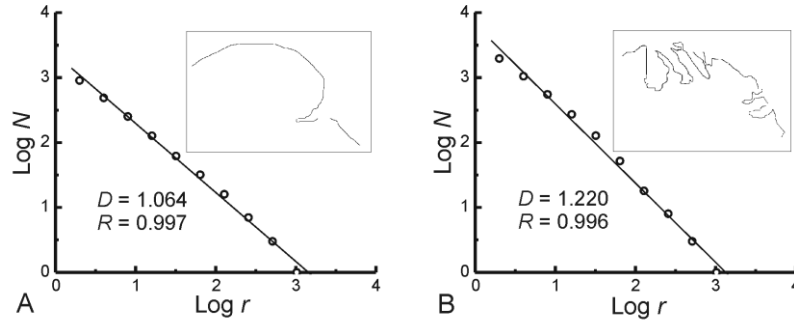


Figure 3. Log-log relationship between the number of boxes ( $N$ ) and the box side length ( $r$ ) of the control (A) and the patient group (B). Values of the fractal dimension  $D$  and the correlation coefficient  $R$  of the fitted straight lines are given on the graph (bottom left).

Box counting was performed using the *Fractal Box Count* program implemented in *Image J*. A series of measurements of the total number of boxes for box side length from  $2^1$  to  $2^k$  pixels was made, where  $k$  is the number for which the number of boxes is equal to one, i.e. when one box covers the whole image. Figure 3 shows the log of the number of boxes plotted against the log of the box side length for two skeletonized images of the femoral head contour of the control (Fig. 3.A) and the patient group (Fig. 3.B). The correlation coefficient ( $R$ ) for both straight lines (Fig. 3), obtained by fitted sets of ten points, is statistically different from zero ( $p < 0.001$ ), indicating linear dependence of the number of boxes on box side length over two or more decades.

### 2.3. Statistics

Statistical analysis of the calculated fractal dimension of the skeletonized images depends on whether the fractal dimension distribution is normal or not. In the case when the calculated fractal dimension follows a normal distribution, each group is described by the corresponding mean value and standard deviation (or standard error). Further analysis is performed according to the methods and tests of parametric statistics. Alternatively, when the calculated values do not follow a normal distribution, the groups are described by the medians, and value range, and further analysis proceeds according to non-parametric statistics laws.

It is known that the testing whether the data is distributed normally is performed by a chi-square test if the studied population consists of a large number of samples (more than 50). If the sample is small then testing of the distribution character is based on the calculation of two statistical parameters: skewness and excess of distribution. The interval of skewness and excess values, which define the normal distribution, is estimated when these two parameter are divided by the corresponding mean square errors ( $\sigma_3$  and  $\sigma_4$ ). If the absolute value of the quotients  $a_3/\sigma_3$  and  $a_4/\sigma_4$  is less than or equal to 2, then the data distribution is normal. Otherwise, the distribution in a sample (or population) has no characteristics of a normal distribution. For further explanation of this procedure, the reader is referred to [8].

## 3. RESULTS

Table 1 shows the values of the parameters used to assess the nature of the distribution of the fractal dimension of femoral head contours of the control and patient group. Also, the values of quotients  $|a_3/\sigma_3|$  and  $|e/\sigma_4|$  are given. As the values of these quotients do not exceed the critical value, i.e., 2, it means that the fractal dimension values for both groups are normally distributed. Therefore further statistical analysis of the fractal dimensions was performed according to the parametric statistics laws.

Table 1. The values of the third ( $m_3$ ) and the fourth moment ( $m_4$ ), skewness ( $a_3$ ), excess ( $e$ ), and the mean square errors ( $\sigma_3$  and  $\sigma_4$ ) in distribution of fractal dimensions of femoral head contours of the control and patient group.

Parameters	Control	Patients
$m_3$	$5.62 \cdot 10^{-6}$	$1.27 \cdot 10^{-5}$
$m_4$	$3.29 \cdot 10^{-6}$	$4.01 \cdot 10^{-5}$
$a_3$	0.15	0.05
$e$	-0.40	-0.28
$\sigma_3$	0.41	0.41
$\sigma_4$	0.74	0.74
$ a_3/\sigma_3 $	0.37	0.13
$ e/\sigma_4 $	0.53	0.37

Table 2. The values of the parameters used in statistical analysis of fractal dimensions of femoral head contours of the reference and patient group. Symbol  $p$  represents the level of confidence.

Fractal dimension	Control	Patients
Range	1.004 – 1.131	1.021 – 1.262
Mean value	1.058	1.121***
Standard deviation	0.034	0.062
Standard error	0.006	0.011
Sample size	30	31

\*\*\* -  $p < 0.001$

The results of calculated mean values of fractal dimensions of the femoral head contours, standard deviations and standard errors for the control and the patient group, as well as the statistical analysis of the obtained values are presented in Tab. 2. It can be seen from Tab. 2 that the intervals of the calculated fractal dimensions of the control and the patient group partially overlap. The mean values of fractal dimensions are different; the mean value of the fractal dimensions of the patient group is higher than that of the control group. The  $t$ -

test applied to the mean values of the fractal dimensions revealed a statistically significant difference of a high confidence level ( $p < 0.001$ ).

## 4. DISCUSSION

Fractal analysis is a set of mathematical techniques used to quantify complex structures. Namely, the fractal dimension of a structure expresses numerically the degree of geometrical complexity of that structure [7]. Quantitative analysis of the bone structure can be successfully made by applying the concept of fractal geometry, as the bone is known to have a complex and irregular structure. In past years, the fractal analysis of radiographic images of bones was applied to study the structure of normal bone [9], as well as that affected by osteoporosis [10-13] and osteoarthritis [14]. To the best of our knowledge, fractal analysis of the bone contour has not attracted researchers' attention, contrary to other scientific fields where the fractal analysis of the object's contour has been studied extensively [7,15,16].

In this study, using fractal analysis we examined the contour of the lateral pillar of the femoral bone in healthy children and children with diagnosed LCP disease. The fractal dimension of femoral head contours in children with LCP disease are higher than the fractal dimension of the contours in healthy children, which indicates that the contours of the affected femoral heads are more complex and irregular in shape than those of normal femoral heads. This result quantitatively confirms that the degree of damage to the femoral head affected by LCP disease can clearly be defined and quantified by fractal analysis. Having objective quantitative results allows for a stratification of treatment that best suits the stage of disease progression.

This study can be considered as a good start in further investigation of the quantification of macroradiographic images in patients with developed LCP disease. These images are classified with respect to the degree of damage of the femoral head, it would be interesting to test whether the fractal dimension can discriminate between the existing categories of disease. We believe that such analysis of macroradiographic images can lead to a more reliable interpretation of the stages of the disease in interobserver trials.

## REFERENCES

1. A. Catterall, *Legg-Calvé-Perthes' disease*, Churchill-Livingstone, New York, 1982.
2. J.R. Bowen, F.C. Schreiber, B.K. Foster, B.K. Wein, Premature femoral neck physeal closure in Perthes' disease, *Clin. Orthop.* 171,24-29(1982).

3. C.F. Bos, J.L. Bloem, R.M. Bloem, Sequential magnetic resonance imaging in Perthes' disease, *J. Bone Joint Surg. Br.* 73,219 -224 (1991).
4. P.L. Schoenecker, J.W. Stone, A.M. Capelli. Legg-Perthes disease in children under 6 years old, *Orthop. Rev.* 22:201-208(1993).
5. R.B. Salter, G.H. Thompson. Legg-Calvé-Perthes disease: The prognostic significance of the subchondral fracture and a two-group classification of the femoral head involvement, *J. Bone Joint Surg. Am.* 66:479-489(1984).
6. J.A. Herring, H.T. Kim, R. Browne, Legg-Calve-Perthes Disease Part I: Classification of radiographs with use of modified lateral pillar and Stulberg Classification, *J Bone Joint Surg. Am* 86,2103-2120(2004).
7. H.F. Jelinek, G.N. Elston, B. Zietsch, Fractal analysis: pitfalls and revelations in neuroscience. In: *Fractals in Biology and Medicine IV* (G.A. Losa, D. Merlini, T.F. Nonnenmacher and E.R. Weibel, eds.), Birkhäuser Verlag, Basel, Boston, Berlin, 2005, pp. 85–94.
8. N.T. Milošević, D. Ristanović, J.B. Stanković, R. Gudović, Fractal analysis of dendritic arborisation patterns of stalked and islet neurons in substantia gelatinosa of different species, *Fractals* 15,1-7(2007).
9. W.G. Geraets, P.F. van der Stelt, Fractal properties of bone, *Dentomaxillofac. Radiol.* 29,144-153(2000).
10. J.A. Lynch, D.J. Hawkes, J.C. Buckland-Wright, Analysis of texture in macroradiographs of osteoarthritic knees using the fractal signature, *Phys. Med. Biol.* 36,709-722(1991).
11. L. Pothuau, E. Lespessailles, R. Harba, R. Jennane, V. Royant, E. Eynard, C.L. Benhamou, Fractal analysis of trabecular bone texture on radiographs: discriminant value in postmenopausal osteoporosis, *Osteoporos. Int.* 8,618-625(1998).
12. S. Mishra, M.L. Knothe Tate, 2003 Effect of lacunocanalicular architecture on hydraulic conductance in bone tissue: implications for bone health and evolution, *Anat. Rec. A Discov. Mol. Cell. Evol. Biol.* 273,752-762(2003).
13. I. Stefan, C. Vertan, H.F. Jelinek, R. Badea, A. Prie, (2008) Classification of calcaneus X-rays using multifractal analysis, *Clujul Medical* 81,363-367(2008).
14. J.C. Buckland-Wright, J.A. Lynch, J. Rymer, I. Fogelman, Fractal signature analysis of macroradiographs measures trabecular organization in lumbar vertebrae of postmenopausal women, *Calcif. Tissue. Int.* 54,106-112(1994).
15. M. Tanaka, A. Kayama, R. Kato, Y. Ito, Estimation of the fractal dimension of fracture surface patterns by box-counting method, *Fractals* 7, 335-340(1999).
16. M. Tambasco, A. Kouznesov, A.M. Magliocco, Quantifying local variations in the architectural complexity of histology specimens, *Riv. Biol.* 101,155-158(2008).

## Predicting the Onset of Spontaneous Oscillations Using Impedance Method

Pototskaya V. V.<sup>a</sup>, Gichan O. I.<sup>b</sup>, Omel'chuk A. A.<sup>a</sup>

<sup>a</sup> V.I. Vernadskii Institute of General & Inorganic Chemistry, Ukrainian National Academy of Sciences, prospekt Palladina 32-34, 03680 Kyiv 142, Ukraine, e-mail: pototskaya@ionc.kiev.ua, omelchuk@ionc.kiev.ua

<sup>b</sup> O.O. Chuiko Institute of Surface Chemistry, Ukrainian National Academy of Sciences, vul. Henerala Naumova 17, 03164 Kyiv 164, Ukraine, e-mail: gichan@isc.gov.ua

The impedance method is applied for the identification of Hopf instability in a model electrochemical system with N-shaped voltammetric curve. The system displays a threshold response. At low and medium values of bifurcation parameter (the preceding chemical reaction rate) the system can have two and one Hopf bifurcation point, respectively, whereas at high values of this parameter the system remains stable to Hopf instability.

**Keywords:** Hopf bifurcation, Negative differential resistance (NDR), N-shaped current-potential curve, Impedance spectroscopy, Kinetics.

### 1. INTRODUCTION

Electrochemical systems are complex dynamical systems [1-15]. The frequent appearance of oscillations and pattern formation in electrochemistry can be explained by the inherently nonlinear electrochemical kinetics and far from equilibrium performance of electrochemical experiments. Based on the principles of nonlinear dynamics and characteristics of electrochemical systems, there are mainly two types of electrochemical oscillators: N-shaped current – potential (N-NDR) and S-shaped current – potential (S-NDR) characteristics [6, 7, 14]. In both cases voltammetric curve has a potential region with a negative slope (NDR). Most of the electrochemical oscillators (for example, electrodisolution of metals, electrocatalytic oxidation of small organic molecules such as formaldehyde, formic acid, methanol and hydrogen oxidation) belong to N-NDR type. In S-NDR systems (for example, electrodeposition of Zn, CO electrooxidation on Pt) electrochemical Turing structures can be observed.

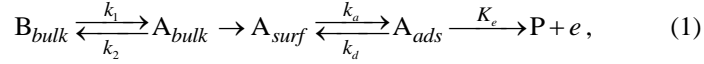
Electrochemical impedance spectroscopy (EIS) is an effective method for analyzing the dynamical properties of electrochemical processes over a large range of frequencies [1, 8]. In this method, a small amplitude electric modulation (either of potential or current) is applied near a stationary reference state and the linear response of the system is measured over a wide frequency range. As is known this method is useful for the identification of Hopf instability in the electrochemical systems, which is hard to realize by other methods [5].



In the paper, we focus on the detection of Hopf instability in a model system with electrocatalytic mechanism [5] on a flat electrode and a preceding homogeneous chemical reaction in bulk solution under potentiostatic conditions.

## 2. MODEL

The model process can be schematically written as



where  $k_1, k_2$  are the rate constants of chemical reaction in the bulk solution, and  $k_a, k_d, K_e$  are the rate constants of adsorption, desorption, and electron transfer, respectively. The last step of the reaction is considered to be irreversible.

The electroactive species of one sort, which are produced by preceding chemical reaction, diffuse from the diffusion layer to the flat electrode surface, where they are adsorbed and electrochemically oxidized. Neglecting the Ohmic losses and double layer influence, we can write the rates of adsorption-desorption and electron transfer as follows:

$$v_1(t) = \Gamma k_a \exp(\gamma\theta(t)/2) c(0,t) (1 - \theta(t)) - \Gamma k_d \exp(-\gamma\theta(t)/2) \theta(t), \quad (2)$$

$$v_2(t) = \Gamma K_e(t) \theta(t) = \Gamma k_e \exp(\alpha f E(t)) \theta(t). \quad (3)$$

Here,  $c(0,t)$  is concentration of electroactive species at the electrode surface,  $\theta(t)$  is the coverage of the electrode surface with the adsorbate,  $\gamma$  is an interaction parameter (the attraction constant),  $\Gamma$  is the maximum surface concentration,  $F$  is the Faraday's number,  $R$  is the gas constant,  $T$  is the absolute temperature,  $\alpha$  is the symmetry factor of electron transfer in the direction of oxidation,  $E$  is the electrode potential,  $f = F/RT$ . According to Eq. (2) the adsorption-desorption of species A on the electrode surface under steady-state conditions is described by the Frumkin isotherm.

The changes in the electrode surface coverage  $\theta$  with adsorbate and in the concentration  $c(x,t) = c_0 + u$  ( $u$  is a deviation of concentration from equilibrium concentration  $c_0$ ) satisfy the following equations:

$$\Gamma \frac{d\theta}{dt} = v_1(t) - v_2(t), \quad (4)$$

$$\frac{\partial u}{\partial t} = D \frac{\partial^2 u}{\partial x^2} - ku \quad (5)$$

with boundary conditions

$$J_c(x=0,t) = -D \frac{\partial u(x,t)}{\partial x} \Big|_{x=0} = -v_1(t), \quad u(d,t) = 0, \quad (6)$$

where  $k$  is the effective rate of preceding homogeneous chemical reaction,  $D$  is the diffusion coefficient,  $d$  is the Nernst diffusion layer thickness. The origin of coordinates coincides with the electrode plane.

The faradaic current density is determined by the following equation:

$$i_f(t) = F v_2(t) = F \Gamma k_e \exp[\alpha f E(t)] \theta(t). \quad (7)$$

### 2.1. Steady-State Conditions

The solution of the diffusion equation under steady-state conditions yields the following expressions for the steady-state electrode potential  $E_s$  and the steady-state concentration at the electrode surface  $c_{st}(x=0)$

$$E_s = (\alpha f)^{-1} \ln \left[ \frac{m_c(c_0 - c_{st}(0))}{\Gamma k_e \theta_s G_0} \right], \quad (8)$$

$$c_{st}(0) = \frac{m_c c_0 + \Gamma k_d \theta_s G_0 e^{-\gamma \theta_s / 2}}{m_c + (1 - \theta_s) \Gamma k_a e^{\gamma \theta_s / 2} G_0}, \quad (9)$$

where  $m_c = D/d$ ,  $G_0 = th\sqrt{\tau_d k} / \sqrt{\tau_d k}$ ,  $\tau_d = d^2/D$  ( $\tau_d$  is diffusion time of relaxation).

The steady-state faradaic current density is given as:

$$i_{fs} = F m_c (c_0 - c_{st}(0)). \quad (10)$$

To study the linear stability of a nonlinear system near its steady state, a well-known procedure is usually used, which consists in finding Jacobian matrix eigenvalues for equations of state. Recently it was shown that for an electrochemical system its complex impedance zeros are the eigenvalues of Jacobian under potentiostatic control (fixed applied potential) [9]. The sign of the real part of impedance zero indicates the stability region of the stationary state. As was shown, a Hopf bifurcation can realize when complex impedance of electrochemical system is equal to zero at nonzero frequency,  $Z(\omega) = 0$  at  $\omega = \omega_H \neq 0$  ( $\omega = 2\pi f$ ,  $f$  – frequency) [2, 5, 6, 13]. At Hopf bifurcation the system produces its own undamped periodic oscillations with frequency  $\omega_H$ , so in the case of influence on the system of an external signal with a frequency exactly coinciding with this value, the external signal will pass through the system without resistance.

In our calculations we neglected the electrolyte resistance and did not take into account the double layer impedance. In this case, the impedance of the considered model system is equal to the faradaic impedance.

### 2.2. Hopf bifurcation and impedance spectra

To calculate the faradaic impedance of this system we consider its dynamic behavior when a low periodical signal is applied to the steady-state polarization potential

$$E(t) = E_s + \Delta E_0 e^{j\omega t}, \quad (11)$$

where  $j = \sqrt{-1}$ .

In response to this excitation the electrode surface coverage  $\theta(t)$  oscillates near steady-state value as the faradaic current  $i_f(t)$  and concentration  $c(x,t)$  do.

$$\theta(t) = \theta_s + \Delta \theta_0 e^{j\omega t}, i_f(t) = i_{fs} + \Delta i_f(E, \theta), c(0,t) = c_{st}(0) + \Delta c(0, \theta). \quad (12)$$

The faradaic impedance in the Laplace image space  $\bar{F}(s) = \int_0^{\infty} f(t)e^{-st} dt$  is expressed as a function of complex frequency:

$$\bar{Z}(s) = \frac{\Delta \bar{E}(s)}{\Delta \bar{i}_f(s)}. \quad (13)$$

Omitting some mathematical computations the resultant expression for the faradaic impedance in the Laplace space can be written as:

$$Z(s, k) = R_{ct} \left\{ 1 + \frac{\partial_{\theta} v_2 [1 + \partial_c v_1 G(k, s)]}{\Gamma s [1 + \partial_c v_1 G(k, s)] - \partial_{\theta} v_1} \right\}, \quad (14)$$

where

$$R_{ct} = \frac{1}{\frac{\partial i_{fs}}{\partial E_s}} = \frac{1}{F \Gamma \alpha f k_e \exp(\alpha f E_s) \theta_s} \quad (\text{charge transfer resistance}), \quad (15)$$

$$G(k, s) = \frac{1}{m_c} \frac{th \sqrt{\tau_d(k+s)}}{\sqrt{\tau_d(k+s)}} \quad (\text{finite length Gerischer impedance}), \quad (16)$$

$$\partial_{\theta} v_1 = \Gamma \{ k_d \exp(-\gamma \theta_s / 2) [\gamma \theta_s / 2 - 1] + k_a \exp(\gamma \theta_s / 2) c_s(0) [\gamma (1 - \theta_s) / 2 - 1] \}, \quad (17)$$

$$\partial_c v_1 = \Gamma k_a (1 - \theta_s) \exp(\gamma \theta_s / 2), \quad (18)$$

$$\partial_{\theta} v_2 = \Gamma k_e \exp(\alpha f E_s), \quad (19)$$

$$\partial_E v_2 = \alpha f \Gamma k_e \exp(\alpha f E_{st}) \theta_s. \quad (20)$$

For the sake of convenience, the partial derivatives are designated here as  $\partial_x u = \partial u / \partial x$ .

Thus, to find the Hopf bifurcation points of the system, the zeros of impedance  $\bar{Z}_f(s)$  depending on electrode potential must be studied.

In our case, the impedance zeroes can be found from the following equation:

$$\Gamma s [1 + \partial_c v_1 G(k, s)] - \partial_{\theta} v_1 + \partial_{\theta} v_2 [1 + \partial_c v_1 G(k, s)] = 0. \quad (21)$$

This is the equality to zero of the numerator of Eq. (14).

Eq. (21) can be presented as

$$\Psi(s, \theta, k) = 0. \quad (22)$$

To satisfy the condition (22), it is necessary that

$$\begin{cases} \text{Re}[\Psi(s, \theta, k)] = 0 \\ \text{Im}[\Psi(s, \theta, k)] = 0 \end{cases} \quad (23)$$

Eq. (23) can be solved only numerically.

In order to pass from the Laplace space to the Fourier space, it is necessary to perform a substitution  $s = j\omega$ .

In the model calculations, the following values of the system parameters were taken:

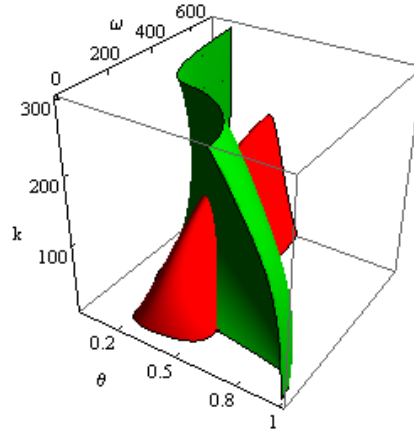
$\Gamma = 10^{-9} \text{ mol cm}^{-2}$ ;  $\gamma=8$ ;  $\Gamma k_a = 0.1 \text{ cm s}^{-1}$ ;  $\Gamma k_d = 10^{-5} \text{ mol /cm}^2 \text{ s}$ ;  $k_e=10 \text{ s}^{-1}$ ;  $D = 10^{-5} \text{ cm}^2/\text{s}$ ;  $d = 10^{-3} \text{ cm}$ ;  $\alpha = 0.5$ ;  $c_0 = 10^{-5} \text{ mol/cm}^3$ ;  $F = 96484 \text{ C/mol}$ ;  $R = 8,314 \text{ J/mol K}$ ;  $T = 295 \text{ K}$ ;  $f = F/RT = 38,7 \text{ V}^{-1}$ .

Numerical calculations were performed on the basis of the Matematica 6 mathematical package.

### 3. RESULTS AND DISCUSSION

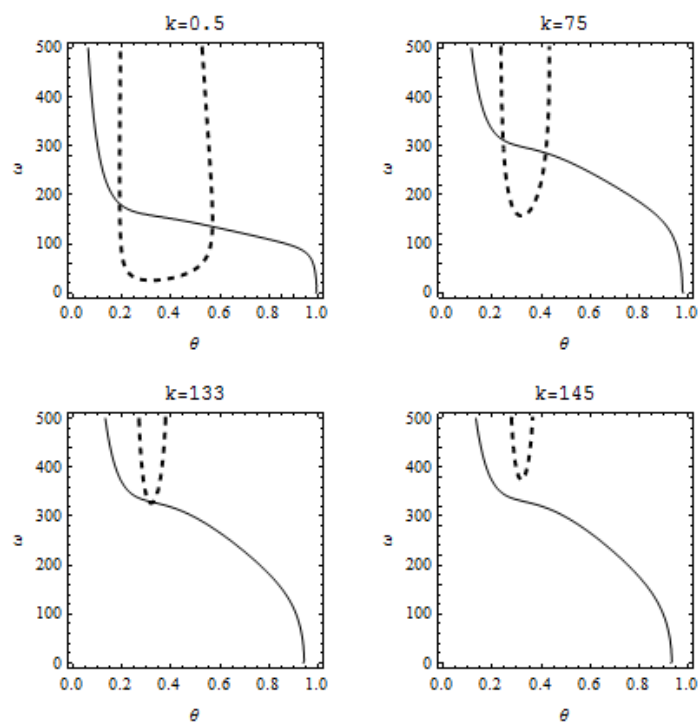
The steady-state curves  $i_{fs}$  vs.  $E_s$  of model process are N-shaped with a region of negative differential resistance (NDR) in which the Hopf instability occurs.

Fig. 1 shows the surfaces of zeros of functions  $\text{Re}[\Psi(s, \theta, k)]$  and  $\text{Im}[\Psi(s, \theta, k)]$ . The line of their intersection is the solution of Eq. (23). It consists of the Hopf bifurcation points, i.e. the bifurcation values of frequency, coverage of electrode with adsorbate and preceding chemical reaction rate.



**Fig. 1.** Surfaces  $\text{Re}[\Psi(s, \theta, k)] = 0$  and  $\text{Im}[\Psi(s, \theta, k)] = 0$ .

As is seen from Fig. 1, there are two types of dynamical behavior of the electrochemical system depending on the reaction rate as a bifurcation parameter. At low and medium values of  $k$  ( $k < 133 \text{ s}^{-1}$ ) the system has two Hopf bifurcation points, where the real and imaginary parts of faradaic impedance are equal to zero at nonzero angular frequency. The mentioned critical value of  $k$  and bifurcation values of frequency and coverage can be observed in Fig. 2 presenting the cuts of surfaces of impedance zeros. At the value  $k_{th} = 133 \text{ s}^{-1}$  one can find only one bifurcation point where spontaneous oscillations can set up. For the values of  $k$  higher than this threshold value  $k_{th}$  the system remains stable to Hopf bifurcation, and oscillations are absent.



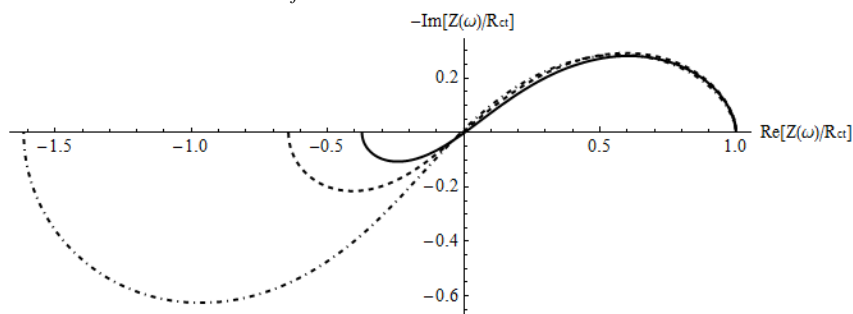
**Fig. 2.** Cuts of surfaces  $\text{Re}[\Psi(s, \theta, k)] = 0$  (bold line) and  $\text{Im}[\Psi(s, \theta, k)] = 0$  (dashed line) at fixed values of  $k$ .

Table 1 shows the bifurcation values of electrochemical parameters for the reaction rates  $k$  from the described above regions.

**Table 1.** Values of electrochemical system parameters at Hopf bifurcation points

$k, \text{s}^{-1}$	Point #	$\omega_H, \text{Hz}$	$\theta_H$	$i_{fH}, \text{A cm}^{-2}$	$E_H, \text{V}$
0.5	1	135.44	0.570	0.0081	0.139
	2	182.39	0.190	0.0044	0.166
75	3	286.39	0.420	0.0066	0.197
	4	313.34	0.243	0.0046	0.206
133	5	329.01	0.320	0.0053	0.214

Fig. 3 presents Nyquist faradaic impedance diagrams in the complex plane at bifurcation points 1, 3 and 5. Here one can see a decrease of the inductive loop, where the faradaic-impedance real part is negative, with an increase of  $k$ . The negative faradaic-impedance real part determines the instability existence in the system. For  $\omega \rightarrow \infty$ ,  $Z_f(\omega) = R_{ct}$ , all curves converge in one point.



**Fig. 3.** Nyquist impedance diagrams at Hopf bifurcation points (see text) for:

$k = 0.5$  - dotdashed line;  $k = 75$  - dashed line;  $k = 133$  - bold line.

An increase of  $k$  leads to a decrease of the impedance modulus. It turns to zero at  $\omega = \omega_H$  (Fig. 4). An increase of  $k$  shifts the bifurcation frequency to the region of higher values. The functional dependence of the impedance phase angle on the frequency  $\omega$  is changed in the Hopf bifurcation point.

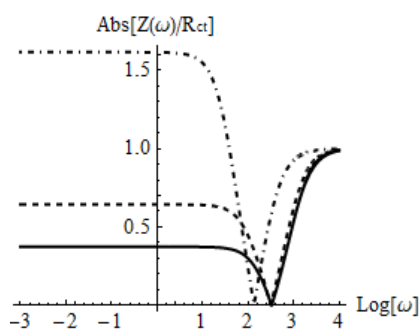


**Fig. 4.** Impedance modulus at

Hopf bifurcation points (see text)

for:  $k = 0.5$  - dotdashed line;

$k = 75$  - dashed line;  $k = 133$  -

bold line.

#### 4. CONCLUSION

On the basis of the theory of electrochemical impedance spectroscopy an effort was made to determine the origin of Hopf instability in a model system with a preceding homogeneous chemical reaction occurring in the bulk solution and a charge transfer reaction followed the potential-dependent adsorption-desorption process on a flat electrode. It was shown that the stability of the system can be influenced by the rate of such chemical reaction. The obtained results indicated the possibility of the instability control.

## REFERENCES

1. E. Barsoukov and J.R. Macdonald, *Impedance Spectroscopy: Theory, Experiment, and Applications* (2nd ed.), Wiley Interscience, New York, 2005.
2. F. Berthier, J. -P. Diard and C. Montella, Hopf bifurcation and sign of the transfer resistance, *Electrochim. Acta*, 44, 2397-2404 (1999).
3. A. Bonnefont, R. Morschl, P. Bauer, K. Krischer, Electrochemical impedance spectroscopy of patterned steady states on electrode surfaces, *Electrochim. Acta*, 55, 410-415 (2009).
4. J. Christoph and M. Eiswirth, Theory of electrochemical formation, *Chaos*, 12, 215-230 (2002).
5. M.T.M. Koper, Stability study and categorization of electrochemical oscillations by impedance spectroscopy, *J. Electroanal. Chem.*, 409, 175-182 (1996).
6. M.T.M. Koper, Non-linear phenomena in electrochemical systems, *J. Chem. Soc. Faraday Trans.*, 94, 1369-1378 (1998).
7. K. Krischer, Principles of temporal and spatial pattern formation in electrochemical systems, in *Modern Aspects of Electrochemistry* (B.E. Conway, J.O.M. Bockris and R.E. White, eds.), vol. 32, Kluwer Academic/Plenum Publishers, New York 1999, pp. 1-142.
8. A. Lasia, Electrochemical impedance spectroscopy and its application, in *Modern Aspects of Electrochemistry* (B. E. Conway, J. O. M. Bockris and R. E. White, eds.), vol. 32, Kluwer Academic/Plenum Publishers, New York 1999, pp. 143-248.
9. M. Naito, N. Tanaka, H. Okamoto, General relation between complex impedance and linear stability in electrochemical systems, *J. Chem. Phys.*, 111, 9908-9917 (1999).
10. R. Jurczakowski, M. Orlik, Experimental and theoretical impedance studies of oscillations and bistability in the Ni(II)–SCN electroreduction at the streaming mercury electrode, *J. Electroanal. Chem.*, 605, 41–52 (2007).
11. L. Pospíšil, M. Hromadová, M. Gál, M. Valášek, N. Fanelli and V. Kolivoška, Irregular polarographic currents obey Feigenbaum universality route from order to chaos, *Collect. Czech. Chem. Commun.*, 74, 1559-1570 (2009).
12. V.V. Pototskaya, O.I. Gichan, A.A. Omelchuk, S.V. Volkov, Specific features of the behavior of an electrochemical system in the case of the Hopf instability for a spherical electrode, *Russ. J. Electrochem.*, 44, 594-601 (2008).
13. A. Sadkowsky, Small signal (local) analysis of electrocatalytic reaction. Pole-zero approach, *J. Electroanal. Chem.*, 485 119-128 (1999).
14. P. Strasser, M. Eiswirth and M.T.M. Koper, Mechanistic classification of electrochemical oscillators - an operational experimental strategy, *J. Electroanal. Chem.*, 478, 50-66 (1999).
15. F. Seland, R. Tunold, D.A. Harrington, Impedance study of formic acid oxidation on platinum electrodes, *Electrochim. Acta*, 53, 6851-6864 (2008).

---

**Instructions to Contributors**  
**Journal of Concrete and Applicable Mathematics**  
A quarterly international publication of Eudoxus Press, LLC, of TN.

**Editor in Chief: George Anastassiou**  
Department of Mathematical Sciences  
University of Memphis  
Memphis, TN 38152-3240, U.S.A.

**1. Manuscripts hard copies in triplicate, and in English, should be submitted to the Editor-in-Chief:**

**Prof. George A. Anastassiou**  
Department of Mathematical Sciences  
The University of Memphis  
Memphis, TN 38152, USA.  
Tel. 901.678.3144  
e-mail: [ganastss@memphis.edu](mailto:ganastss@memphis.edu)

**Authors may want to recommend an associate editor the most related to the submission to possibly handle it.**

**Also authors may want to submit a list of six possible referees, to be used in case we cannot find related referees by ourselves.**

**2. Manuscripts should be typed using any of TEX, LaTeX, AMS-TEX, or AMS-LaTeX and according to EUDOXUS PRESS, LLC. LATEX STYLE FILE. (Click [HERE](#) to save a copy of the style file.) They should be carefully prepared in all respects. Submitted copies should be brightly printed (not dot-matrix), double spaced, in ten point type size, on one side high quality paper 8(1/2)x11 inch. Manuscripts should have generous margins on all sides and should not exceed 24 pages.**

**3. Submission is a representation that the manuscript has not been published previously in this or any other similar form and is not currently under consideration for publication elsewhere. A statement transferring from the authors (or their employers, if they hold the copyright) to Eudoxus Press, LLC, will be required before the manuscript can be accepted for publication. The Editor-in-Chief will supply the necessary forms for this transfer. Such a written transfer of copyright, which previously was assumed to be implicit in the act of submitting a manuscript, is necessary under the U.S. Copyright Law in order for the publisher to carry through the dissemination of research results and reviews as widely and effectively as possible.**



**4. The paper starts with the title of the article, author's name(s) (no titles or degrees), author's affiliation(s) and e-mail addresses. The affiliation should comprise the department, institution (usually university or company), city, state (and/or nation) and mail code.**

**The following items, 5 and 6, should be on page no. 1 of the paper.**

**5. An abstract is to be provided, preferably no longer than 150 words.**

**6. A list of 5 key words is to be provided directly below the abstract. Key words should express the precise content of the manuscript, as they are used for indexing purposes.**

**The main body of the paper should begin on page no. 1, if possible.**

**7. All sections should be numbered with Arabic numerals (such as: 1. INTRODUCTION) .**

**Subsections should be identified with section and subsection numbers (such as 6.1. Second-Value Subheading).**

**If applicable, an independent single-number system (one for each category) should be used to label all theorems, lemmas, propositions, corollaries, definitions, remarks, examples, etc. The label (such as Lemma 7) should be typed with paragraph indentation, followed by a period and the lemma itself.**

**8. Mathematical notation must be typeset. Equations should be numbered consecutively with Arabic numerals in parentheses placed flush right, and should be thusly referred to in the text [such as Eqs.(2) and (5)]. The running title must be placed at the top of even numbered pages and the first author's name, et al., must be placed at the top of the odd numbered pages.**

**9. Illustrations (photographs, drawings, diagrams, and charts) are to be numbered in one consecutive series of Arabic numerals. The captions for illustrations should be typed double space. All illustrations, charts, tables, etc., must be embedded in the body of the manuscript in proper, final, print position. In particular, manuscript, source, and PDF file version must be at camera ready stage for publication or they cannot be considered.**

**Tables are to be numbered (with Roman numerals) and referred to by number in the text. Center the title above the table, and type explanatory footnotes (indicated by superscript lowercase letters) below the table.**

**10. List references alphabetically at the end of the paper and number them consecutively. Each must be cited in the text by the appropriate Arabic numeral in square brackets on the baseline.**

**References should include (in the following order):  
initials of first and middle name, last name of author(s)  
title of article,**

name of publication, volume number, inclusive pages, and year of publication.

Authors should follow these examples:

### **Journal Article**

1. H.H.Gonska, Degree of simultaneous approximation of bivariate functions by Gordon operators, (journal name in italics) *J. Approx. Theory*, 62,170-191(1990).

### **Book**

2. G.G.Lorentz, (title of book in italics) *Bernstein Polynomials* (2nd ed.), Chelsea, New York, 1986.

### **Contribution to a Book**

3. M.K.Khan, Approximation properties of beta operators, in (title of book in italics) *Progress in Approximation Theory* (P.Nevai and A.Pinkus, eds.), Academic Press, New York, 1991, pp.483-495.

11. All acknowledgements (including those for a grant and financial support) should occur in one paragraph that directly precedes the References section.

12. Footnotes should be avoided. When their use is absolutely necessary, footnotes should be numbered consecutively using Arabic numerals and should be typed at the bottom of the page to which they refer. Place a line above the footnote, so that it is set off from the text. Use the appropriate superscript numeral for citation in the text.

13. After each revision is made please again submit three hard copies of the revised manuscript, including in the final one. And after a manuscript has been accepted for publication and with all revisions incorporated, manuscripts, including the TEX/LaTeX source file and the PDF file, are to be submitted to the Editor's Office on a personal-computer disk, 3.5 inch size. Label the disk with clearly written identifying information and properly ship, such as:

Your name, title of article, kind of computer used, kind of software and version number, disk format and files names of article, as well as abbreviated journal name.

Package the disk in a disk mailer or protective cardboard. Make sure contents of disks are identical with the ones of final hard copies submitted!

Note: The Editor's Office cannot accept the disk without the accompanying matching hard copies of manuscript. No e-mail final submissions are allowed! The disk submission must be used.

14. Effective 1 Nov. 2009 for current journal page charges, contact the Editor in Chief. Upon acceptance of the paper an invoice will be sent to the contact author. The fee payment will be due one month from the invoice date. The article will proceed to publication only after the fee is paid. The charges are to be sent, by money order or certified check, in US dollars, payable to Eudoxus Press, LLC, to the address shown on

the Eudoxus [homepage](#).

No galley proofs will be sent and the contact author will receive one(1) electronic copy of the journal issue in which the article appears.

15. This journal will consider for publication only papers that contain proofs for their listed results.

# **TABLE OF CONTENTS, JOURNAL OF CONCRETE AND APPLICABLE MATHEMATICS, VOL. 9, NO. 1, 2011**

Temporal and three dimensional spatial analysis of Earthquake activity between 1970 and 2010 along the North Anatolian fault zone, Turkey, Serkan Oztürk,.....9

Estimating the Nonlinear Behavior of Mitral Valve Doppler Signals, Fatma Latifoglu, Esma Uzunhisarc kl , Türker Koza,.....17

Phase diagrams of an Ising System with Competing binary,prolonged ternary and next-nearest interactions on a Cayley Tree,Nasir Ganikhodjaev, Hasan Ak n, Selman Uguz, Seyit Temir,.....26

Localization of unstable periodical solutions in chaotic systems, Dubrovskiy Alexey,.....35

Configuring Time-Lagged Recurrent Neural Network using Strange Attractor's Topological Properties, M.P. Hantias, H.E. Nistazakis and G.S. Tombras,.....40

Strange attractor in the Potts model on a Cayley tree in the presence of competing interactions, N.N.GANIKHODJAEV,.....47

On Non-Associativity of Rhesus Factor Transmission, N.N. GANIKHODJAEV, M.D.USMANOVA,.....55

Fractal analysis of macroradiographic images: Legg-Calvé-Perthes disease, Nebojša T. Milošević, Dušan Marić, .....60

Predicting the Onset of Spontaneous Oscillations Using Impedance Method, Pototskaya V. V., Gichan O. I., Omel'chuk A.A.,.....68

**VOLUME 9, NUMBER 2      APRIL 2011**

**ISSN:1548-5390 PRINT,1559-176X ONLINE**



**JOURNAL  
OF CONCRETE  
AND APPLICABLE  
MATHEMATICS  
EUDOXUS PRESS,LLC**

**GUEST EDITORS: HIKMET CAGLAR, LEVENT CUHACI,  
GURSEL HACIBEKIROGLU and MEHMET OZER  
SPECIAL ISSUE V: “CHAOS and COMPLEX SYSTEMS 2010”**

**SCOPE AND PRICES OF THE JOURNAL**  
**Journal of Concrete and Applicable Mathematics**

A quartely international publication of **Eudoxus Press,LLC**

**Editor in Chief: George Anastassiou**  
Department of Mathematical Sciences,  
University of Memphis  
Memphis, TN 38152, U.S.A.  
ganastss@memphis.edu

The main purpose of the "Journal of Concrete and Applicable Mathematics" is to publish high quality original research articles from all subareas of Non-Pure and/or Applicable Mathematics and its many real life applications, as well connections to other areas of Mathematical Sciences, as long as they are presented in a Concrete way. It welcomes also related research survey articles and book reviews. A sample list of connected mathematical areas with this publication includes and is not restricted to: Applied Analysis, Applied Functional Analysis, Probability theory, Stochastic Processes, Approximation Theory, O.D.E, P.D.E, Wavelet, Neural Networks, Difference Equations, Summability, Fractals, Special Functions, Splines, Asymptotic Analysis, Fractional Analysis, Inequalities, Moment Theory, Numerical Functional Analysis, Tomography, Asymptotic Expansions, Fourier Analysis, Applied Harmonic Analysis, Integral Equations, Signal Analysis, Numerical Analysis, Optimization, Operations Research, Linear Programming, Fuzzyness, Mathematical Finance, Stochastic Analysis, Game Theory, Math. Physics aspects, Applied Real and Complex Analysis, Computational Number Theory, Graph Theory, Combinatorics, Computer Science Math. related topics, combinations of the above, etc. In general any kind of Concretely presented Mathematics which is Applicable fits to the scope of this journal. Working Concretely and in Applicable Mathematics has become a main trend in many recent years, so we can understand better and deeper and solve the important problems of our real and scientific world. "Journal of Concrete and Applicable Mathematics" is a peer-reviewed International Quarterly Journal. We are calling for papers for possible publication. The contributor should send three copies of the contribution to the editor in-Chief typed in TEX, LATEX double spaced. [ See: Instructions to Contributors]

**Journal of Concrete and Applicable Mathematics(JCAAM)**  
**ISSN:1548-5390 PRINT, 1559-176X ONLINE.**

is published in January, April, July and October of each year by

**EUDOXUS PRESS,LLC,**  
1424 Beaver Trail Drive, Cordova, TN38016, USA,  
Tel.001-901-751-3553  
anastassioug@yahoo.com  
<http://www.EudoxusPress.com>.

**Visit also [www.msci.memphis.edu/~ganastss/jcaam](http://www.msci.memphis.edu/~ganastss/jcaam).**

**Webmaster: Ray Clapsadle**

**Annual Subscription Current Prices:** For USA and Canada, Institutional: Print \$400, Electronic \$250, Print and Electronic \$450. Individual: Print \$150, Electronic

\$80,Print &Electronic \$200.For any other part of the world add \$50 more to the above prices for Print.

Single article PDF file for individual \$15.Single issue in PDF form for individual \$60.

No credit card payments.Only certified check,money order or international check in US dollars are acceptable.

Combination orders of any two from JoCAAA,JCAAM,JAFA receive 25% discount,all three receive 30% discount.

**Copyright**©2011 by Eudoxus Press,LLC all rights reserved.JCAAM is printed in USA.

**JCAAM is reviewed and abstracted by AMS Mathematical Reviews,MATHSCI,and Zentralblatt MATH.**

It is strictly prohibited the reproduction and transmission of any part of JCAAM and in any form and by any means without the written permission of the publisher.It is only allowed to educators to Xerox articles for educational purposes.The publisher assumes no responsibility for the content of published papers.

***JCAAM IS A JOURNAL OF RAPID PUBLICATION***

---

## Editorial Board

### Associate Editors

---

#### Editor in -Chief:

George Anastassiou  
 Department of Mathematical Sciences  
 The University Of Memphis  
 Memphis, TN 38152, USA  
 tel. 901-678-3144, fax 901-678-2480  
 e-mail ganastss@memphis.edu  
[www.msci.memphis.edu/~anastasg/anlyjour.htm](http://www.msci.memphis.edu/~anastasg/anlyjour.htm)  
 Areas: Approximation Theory,  
 Probability, Moments, Wavelet,  
 Neural Networks, Inequalities, Fuzzyness.

#### Associate Editors:

1) Ravi Agarwal  
 Florida Institute of Technology  
 Applied Mathematics Program  
 150 W. University Blvd.  
 Melbourne, FL 32901, USA  
[agarwal@fit.edu](mailto:agarwal@fit.edu)  
 Differential Equations, Difference  
 Equations,  
 Inequalities

2) Drumi D. Bainov  
 Medical University of Sofia  
 P.O. Box 45, 1504 Sofia, Bulgaria  
[drumibainov@yahoo.com](mailto:drumibainov@yahoo.com)  
 Differential Equations, Optimal Control,  
 Numerical Analysis, Approximation Theory

3) Carlo Bardaro  
 Dipartimento di Matematica & Informatica  
 Università di Perugia  
 Via Vanvitelli 1  
 06123 Perugia, ITALY  
 tel. +390755855034, +390755853822,  
 fax +390755855024  
[bardaro@unipg.it](mailto:bardaro@unipg.it) ,  
[bardaro@dipmat.unipg.it](mailto:bardaro@dipmat.unipg.it)  
 Functional Analysis and Approximation Th.,  
 Summability, Signal Analysis, Integral  
 Equations,  
 Measure Th., Real Analysis

4) Francoise Bastin  
 Institute of Mathematics  
 University of Liege  
 4000 Liege

21) Gustavo Alberto Perla Menzala  
 National Laboratory of Scientific Computation  
 LNCC/MCT  
 Av. Getulio Vargas 333  
 25651-075 Petropolis, RJ  
 Caixa Postal 95113, Brasil  
 and

Federal University of Rio de Janeiro  
 Institute of Mathematics  
 RJ, P.O. Box 68530 Rio de Janeiro, Brasil  
[perla@lncc.br](mailto:perla@lncc.br) and [perla@im.ufrj.br](mailto:perla@im.ufrj.br)  
 Phone 55-24-22336068, 55-21-25627513 Ext 224  
 FAX 55-24-22315595  
 Hyperbolic and Parabolic Partial Differential  
 Equations,  
 Exact controllability, Nonlinear Lattices and  
 Global  
 Attractors, Smart Materials

22) Ram N. Mohapatra  
 Department of Mathematics  
 University of Central Florida  
 Orlando, FL 32816-1364  
 tel. 407-823-5080  
[ramm@pegasus.cc.ucf.edu](mailto:ramm@pegasus.cc.ucf.edu)  
 Real and Complex analysis, Approximation Th.,  
 Fourier Analysis, Fuzzy Sets and Systems

23) Rainer Nagel  
 Arbeitsbereich Funktionalanalysis  
 Mathematisches Institut  
 Auf der Morgenstelle 10  
 D-72076 Tuebingen  
 Germany  
 tel. 49-7071-2973242  
 fax 49-7071-294322  
[rana@fa.uni-tuebingen.de](mailto:rana@fa.uni-tuebingen.de)  
 evolution equations, semigroups, spectral th.,  
 positivity

24) Panos M. Pardalos  
 Center for Appl. Optimization  
 University of Florida  
 303 Weil Hall  
 P.O. Box 116595  
 Gainesville, FL 32611-6595  
 tel. 352-392-9011  
[pardalos@ufl.edu](mailto:pardalos@ufl.edu)  
 Optimization, Operations Research



BELGIUM

f.bastin@ulg.ac.be  
Functional Analysis,Wavelets

5) Yeol Je Cho  
Department of Mathematics Education  
College of Education  
Gyeongsang National University  
Chinju 660-701

KOREA

tel.055-751-5673 Office,  
055-755-3644 home,  
fax 055-751-6117  
yjcho@nongae.gsnu.ac.kr  
Nonlinear operator Th.,Inequalities,  
Geometry of Banach Spaces

6) Sever S.Dragomir  
School of Communications and Informatics  
Victoria University of Technology  
PO Box 14428  
Melbourne City M.C  
Victoria 8001,Australia  
tel 61 3 9688 4437,fax 61 3 9688 4050  
sever.dragomir@vu.edu.au,  
sever@sci.vu.edu.au  
Math.Analysis,Inequalities,Approximation  
Th.,  
Numerical Analysis, Geometry of Banach  
Spaces,  
Information Th. and Coding

7) Angelo Favini  
Università di Bologna  
Dipartimento di Matematica  
Piazza di Porta San Donato 5  
40126 Bologna, ITALY  
tel.++39 051 2094451  
fax.++39 051 2094490  
favini@dm.unibo.it  
Partial Differential Equations, Control  
Theory,  
Differential Equations in Banach Spaces

8) Claudio A. Fernandez  
Facultad de Matematicas  
Pontificia Universidad Católica de Chile  
Vicuna Mackenna 4860  
Santiago, Chile  
tel.++56 2 354 5922  
fax.++56 2 552 5916  
cfernand@mat.puc.cl  
Partial Differential Equations,  
Mathematical Physics,  
Scattering and Spectral Theory

25) Svetlozar T.Rachev  
Dept.of Statistics and Applied Probability  
Program

University of California,Santa Barbara  
CA 93106-3110,USA  
tel.805-893-4869  
rachev@pstat.ucsb.edu

AND

Chair of Econometrics and Statistics  
School of Economics and Business Engineering  
University of Karlsruhe  
Kollegium am Schloss,Bau II,20.12,R210  
Postfach 6980,D-76128,Karlsruhe,Germany  
tel.011-49-721-608-7535  
rachev@lsoe.uni-karlsruhe.de  
Mathematical and Empirical Finance,  
Applied Probability, Statistics and Econometrics

26) John Michael Rassias  
University of Athens  
Pedagogical Department  
Section of Mathematics and Infomatics  
20, Hippocratous Str., Athens, 106 80, Greece

Address for Correspondence

4, Agamemnonos Str.  
Aghia Paraskevi, Athens, Attikis 15342 Greece  
jrassias@primedu.uoa.gr  
jrassias@tellas.gr  
Approximation Theory,Functional Equations,  
Inequalities, PDE

27) Paolo Emilio Ricci  
Universita' degli Studi di Roma "La Sapienza"  
Dipartimento di Matematica-Istituto  
"G.Castelnuovo"  
P.le A.Moro,2-00185 Roma,ITALY  
tel.++39 0649913201,fax ++39 0644701007  
riccip@uniroma1.it,Paoloemilio.Ricci@uniroma1.it  
Orthogonal Polynomials and Special functions,  
Numerical Analysis, Transforms,Operational  
Calculus,  
Differential and Difference equations

28) Cecil C.Rousseau  
Department of Mathematical Sciences  
The University of Memphis  
Memphis,TN 38152,USA  
tel.901-678-2490,fax 901-678-2480  
ccrousse@memphis.edu  
Combinatorics,Graph Th.,  
Asymptotic Approximations,  
Applications to Physics

29) Tomasz Rychlik

- 9) A.M.Fink  
Department of Mathematics  
Iowa State University  
Ames, IA 50011-0001, USA  
tel.515-294-8150  
fink@math.iastate.edu  
Inequalities, Ordinary Differential Equations
- 10) Sorin Gal  
Department of Mathematics  
University of Oradea  
Str.Armatei Romane 5  
3700 Oradea, Romania  
galso@uoradea.ro  
Approximation Th., Fuzzyness, Complex Analysis
- 11) Jerome A. Goldstein  
Department of Mathematical Sciences  
The University of Memphis,  
Memphis, TN 38152, USA  
tel.901-678-2484  
jgoldste@memphis.edu  
Partial Differential Equations, Semigroups of Operators
- 12) Heiner H. Gonska  
Department of Mathematics  
University of Duisburg  
Duisburg, D-47048  
Germany  
tel.0049-203-379-3542 office  
gonska@informatik.uni-duisburg.de  
Approximation Th., Computer Aided Geometric Design
- 13) Dmitry Khavinson  
Department of Mathematical Sciences  
University of Arkansas  
Fayetteville, AR 72701, USA  
tel.(479)575-6331, fax(479)575-8630  
dmitry@uark.edu  
Potential Th., Complex Analysis, Holomorphic PDE,  
Approximation Th., Function Th.
- 14) Virginia S. Kiryakova  
Institute of Mathematics and Informatics  
Bulgarian Academy of Sciences  
Sofia 1090, Bulgaria  
virginia@diogenes.bg  
Special Functions, Integral Transforms, Fractional Calculus
- 15) Hans-Bernd Knoop  
Institute of Mathematics  
Polish Academy of Sciences  
Chopina 12, 87100 Torun, Poland  
T.Rychlik@impan.gov.pl  
Mathematical Statistics, Probabilistic Inequalities
- 30) Bl. Sendov  
Institute of Mathematics and Informatics  
Bulgarian Academy of Sciences  
Sofia 1090, Bulgaria  
bsendov@bas.bg  
Approximation Th., Geometry of Polynomials, Image Compression
- 31) Igor Shevchuk  
Faculty of Mathematics and Mechanics  
National Taras Shevchenko  
University of Kyiv  
252017 Kyiv  
UKRAINE  
shevchuk@univ.kiev.ua  
Approximation Theory
- 32) H.M. Srivastava  
Department of Mathematics and Statistics  
University of Victoria  
Victoria, British Columbia V8W 3P4  
Canada  
tel.250-721-7455 office, 250-477-6960 home,  
fax 250-721-8962  
harimsri@math.uvic.ca  
Real and Complex Analysis, Fractional Calculus and Appl.,  
Integral Equations and Transforms, Higher Transcendental Functions and Appl., q-Series and q-Polynomials, Analytic Number Th.
- 33) Stevo Stevic  
Mathematical Institute of the Serbian Acad. of Science  
Knez Mihailova 35/I  
11000 Beograd, Serbia  
sstevic@ptt.yu; sstevo@matf.bg.ac.yu  
Complex Variables, Difference Equations, Approximation Th., Inequalities
- 34) Ferenc Szidarovszky  
Dept. Systems and Industrial Engineering  
The University of Arizona  
Engineering Building, 111  
PO.Box 210020  
Tucson, AZ 85721-0020, USA  
szidar@sie.arizona.edu  
Numerical Methods, Game Th., Dynamic Systems,

Institute of Mathematics  
 Gerhard Mercator University  
 D-47048 Duisburg  
 Germany  
 tel.0049-203-379-2676  
 knoop@math.uni-duisburg.de  
 Approximation Theory, Interpolation

16) Jerry Koliha  
 Dept. of Mathematics & Statistics  
 University of Melbourne  
 VIC 3010, Melbourne  
 Australia  
 koliha@unimelb.edu.au  
 Inequalities, Operator Theory,  
 Matrix Analysis, Generalized Inverses

17) Mustafa Kulenovic  
 Department of Mathematics  
 University of Rhode Island  
 Kingston, RI 02881, USA  
 kulenm@math.uri.edu  
 Differential and Difference Equations

18) Gerassimos Ladas  
 Department of Mathematics  
 University of Rhode Island  
 Kingston, RI 02881, USA  
 gladas@math.uri.edu  
 Differential and Difference Equations

19) V. Lakshmikantham  
 Department of Mathematical Sciences  
 Florida Institute of Technology  
 Melbourne, FL 32901  
 e-mail: lakshmik@fit.edu  
 Ordinary and Partial Differential  
 Equations,  
 Hybrid Systems, Nonlinear Analysis

20) Rupert Lasser  
 Institut für Biomathematik & Biomertie, GSF  
 -National Research Center for environment  
 and health  
 Ingolstaedter landstr.1  
 D-85764 Neuherberg, Germany  
 lasser@gsf.de  
 Orthogonal Polynomials, Fourier Analysis,  
 Mathematical Biology

Multicriteria Decision making,  
 Conflict Resolution, Applications  
 in Economics and Natural Resources  
 Management

35) Gancho Tachev  
 Dept. of Mathematics  
 Univ. of Architecture, Civil Eng. and Geodesy  
 1 Hr. Smirnenski blvd  
 BG-1421 Sofia, Bulgaria  
 gtt\_fte@uacg.bg  
 Approximation Theory

36) Manfred Tasche  
 Department of Mathematics  
 University of Rostock  
 D-18051 Rostock  
 Germany  
 manfred.tasche@mathematik.uni-rostock.de  
 Approximation Th., Wavelet, Fourier Analysis,  
 Numerical Methods, Signal Processing,  
 Image Processing, Harmonic Analysis

37) Chris P. Tsokos  
 Department of Mathematics  
 University of South Florida  
 4202 E. Fowler Ave., PHY 114  
 Tampa, FL 33620-5700, USA  
 profcpt@math.usf.edu, profcpt@chumal.cas.usf.edu  
 Stochastic Systems, Biomathematics,  
 Environmental Systems, Reliability Th.

38) Lutz Volkmann  
 Lehrstuhl II für Mathematik  
 RWTH-Aachen  
 Templergraben 55  
 D-52062 Aachen  
 Germany  
 volkm@math2.rwth-aachen.de  
 Complex Analysis, Combinatorics, Graph Theory

## Preface

These six special issues, which constitute the proceedings of the symposium 3rd International Interdisciplinary Chaos Symposium on CHAOS and COMPLEX SYSTEMS - CCS2010 (21-24 May 2010), have tried to create a forum for the exchange of information and experience in the exciting interdisciplinary field of chaos. However the conference was more in the Applied Mathematics, Social Sciences and Physics direction centered.

The view of the organizers concerning international resonance of the conference has been fulfilled: approximately 200 scientists from 21 different countries (Algeria, Bulgaria, Croatia, Denmark, France, Germany, Greece, Iran, Italy, Jordan, Lebanon, Malaysia, Pakistan, Republic of Serbia, Russia, Sultanate of Oman, Tunisia, Turkey, Ukraine, United Kingdom and United States of America) have participated. Good relations to research institutes of these countries might be of great importance for science and applications in different fields of Chaos.

On behalf of the Organizing Committee we would like to express our thanks to the Scientific Committee, the Program Committee and to all who have contributed to this conference for their support and advice. We are also grateful to the invited lecturers Prof. Henry D.I. Abarbanel, Prof. David S. Byrne, Prof. George Anastassiou, Prof. Zidong Wang, Prof. Turgut Ozis and Prof. Markus J. Aschwenden.

Special thanks are due to Rector Prof. Dursun Kocer and Vice Rector Prof. Cetin Bolcal for their close support, advice and incentive encouraging.

Our thanks are also due to the Istanbul Kultur University, which was hosting this symposium and provided all of its facilities.

Finally, we are grateful to the Editor-in-Chief, Prof. George Anastassiou for accepting this volume for publication.

Hikmet Caglar, PhD in Mathematics, [s.caglar@iku.edu.tr](mailto:s.caglar@iku.edu.tr)  
Levent Cuhaci, PhD in Computer Science, [l.cuhaci@iku.edu.tr](mailto:l.cuhaci@iku.edu.tr)  
Gursel Hacibekiroglu, PhD in Physics, [g.hacibekiroglu@iku.edu.tr](mailto:g.hacibekiroglu@iku.edu.tr)  
Mehmet Ozer, PhD in Physics, [m.ozar@iku.edu.tr](mailto:m.ozar@iku.edu.tr)

Istanbul Kultur University, Faculty of Science and Letters, Istanbul, Turkey

## Computing the approximate frequency for nonlinear oscillators with discontinuities by He's bookkeeping parameter method

Canan Köroğlu<sup>a</sup> Turgut Öziş<sup>b</sup>

<sup>a</sup> *Department of Mathematics, Faculty of Science, Hacettepe University, Campus, 06800, Beytepe-Ankara, Turkey, Email: [ckoroglu@hacettepe.edu.tr](mailto:ckoroglu@hacettepe.edu.tr)*

<sup>b</sup> *Department of Mathematics, Faculty of Science, Ege University, Campus, 35100, Bornova-İzmir, Turkey, Email: [turgut.ozis@ege.edu.tr](mailto:turgut.ozis@ege.edu.tr)*

**Abstract:** In this paper, we have considered two examples of nonlinear oscillators with discontinuities by using Ji-Huan He's parameter-expanding method with an adjustment of restoring forces in terms of Chebyshev's series. The results found using this procedure are more accurate than those found using other approximate methods.

**Keywords:** Parameter-expanding method, Nonlinear oscillator

PACS numbers: 02.30.Jr, 02.30.Lt, 02.30.-f

### 1. Introduction

Nonlinear oscillations in engineering, physics, applied mathematics and in many real world applications has been a topic to intensive research for many years and several methods have been used to find approximate solutions to nonlinear oscillators [1-4]. In general, given the nature of a nonlinear phenomenon, the approximate methods can only be applied within certain ranges of the physical parameters and to certain classes of problems. However, the use of perturbation theory in many significant practical problems is invalid, or it simply breaks down for parameters beyond a certain specified range. Therefore, new analytical/approximate methods should be developed to beat these weaknesses.

Such a new method should labor over a large range of parameters and give accurate analytical approximate solutions beyond the coverage and ability of the classical perturbation methods.

For nonlinear oscillators, some of these methods include harmonic balance method [5-10], variational iteration method [11-16], homotopy perturbation method [17-23]. Also there are some other method surveys of the literature with numerous references and useful bibliography and a review of these methods can be found in detail in [24-26].

In this paper, we adapted He's bookkeeping parameter method [27] with an adjustment of restoring forces in terms of Chebyshev's series for nonlinear oscillators with discontinuities.

## 2. Parameter-expanding methods

In case no small parameter exists in a nonlinear equation, traditional perturbation methods cannot be directly applied. For this type of problem Ji Huan He [27] developed a technique where a bookkeeping parameter is introduced to the original differential equation. Recently parameter-expanding methods [28-35] including bookkeeping parameter method [27] and modified Lindstedt-Poincare methods [36-43] have been caught much attention; the parameter expansion can also be applied to homotopy perturbation method [44-45].

We, now, consider the following two examples for nonlinear oscillators with discontinuities.

**Example 1:** Ramos [54] has recently analyzed the nonlinear differential equation

$$u'' = -\text{sign}(u), u(0) = A, u'(0) = 0 \quad (1)$$

$$\text{where } \text{sign}(u) = \begin{cases} 1, u > 0 \\ -1, u < 0 \\ 0, u = 0 \end{cases}$$

Re-written Eq. (1) in the form

$$u'' + 0.u + 1.\text{sign}(u) = 0, u(0) = A, u'(0) = 0 \quad (2)$$

Suppose that the solution can be expressed as a power series in p:

$$u = u_0 + pu_1 + p^2u_2 + \dots \quad (3)$$

where p is a bookkeeping parameter.

We also suppose that the coefficients 0 and 1 in the left side of Eq.(2) can be, respectively, expanded into a series in p:

$$0 = w^2 + pw_1 + p^2w_2 + \dots \quad (4)$$

$$1 = a_1p + a_2p^2 + \dots \quad (5)$$

Substituting Eqs.(4) and (5) into Eq.(2) and equating the terms with the identical powers of p, we have

$$p^0: u_0'' + w^2 u_0 = 0, u_0(0) = A, u_0'(0) = 0 \quad (6)$$

$$p^1: u_1'' + w_1 u_0 + w^2 u_1 + a_1 \text{sign}(u_0) = 0 \quad (7)$$

The solution of (6) is  $u_0 = A \cos(wt)$ . Substituting  $u_0$  into Eq.(7) results into

$$u_1'' + w^2 u_1 + w_1 A \cos(wt) + a_1 \text{sign}(A \cos(wt)) = 0. \quad (8)$$

From Chebyshev series expansion, we have

$$f(x) = \sum_{n=0}^{\infty} c_{2n+1} T_{2n+1}(x),$$

where  $x = \cos(wt)$ ,  $T_{2n+1}(x) = \cos[(2n+1)wt]$  and the coefficients:

$$c_{2n+1} = \frac{2}{\pi} \int_{-1}^1 (1-x^2)^{-1/2} f(x) T_{2n+1}(x) dx$$

Through  $f(x) = \text{sign}(A \cos \theta)$ , (for  $A > 0$ ) coefficients form:

$$c_{2n+1} = \frac{2}{\pi} \int_0^{\pi} \text{sign}(\cos \theta) \cos[(2n+1)\theta] d\theta$$

And for  $n=0$  gives ( $\theta = wt$ )

$$c_1 = \frac{2}{\pi} \int_0^{\pi} \text{sign}(\cos \theta) \cos \theta d\theta \quad (9)$$

Noting that  $\text{sign}(\cos \theta) = 1$  when  $0 < \theta < \frac{\pi}{2}$ , and  $\text{sign}(\cos \theta) = -1$  when  $\frac{\pi}{2} < \theta < \pi$ , so we write Eq.(9) in the form

$$c_1 = \frac{2}{\pi} \left[ \int_0^{\pi/2} \text{sign}(\cos \theta) \cos \theta d\theta + \int_{\pi/2}^{\pi} \text{sign}(\cos \theta) \cos \theta d\theta \right]$$

$$c_1 = \frac{2}{\pi} \left[ \int_0^{\pi/2} \cos \theta d\theta - \int_{\pi/2}^{\pi} \cos \theta d\theta \right] = \frac{2}{\pi} [\sin \theta]_0^{\pi/2} - \sin \theta \Big|_{\pi/2}^{\pi}$$

$$c_1 = \frac{2}{\pi} (1 + 1) = \frac{4}{\pi}$$

No secular terms in  $u_1$  requires  $w_1 = -w^2$ ,  $a_1 = 1$

and

$$w_1 A + a_1 \frac{4}{\pi} = 0.$$

Thus, the first order approximation found as

$$w^2 = \frac{4}{\pi A} \quad (10)$$

Eq. (10) is the same result as Ramos' solution [54] using the method of variation of parameters and Liu' solution [55] which according to the modified Lindstedt-Poincare method.

**Example 2:** We, now, view the following nonlinear oscillator with discontinuity [56]:

$$u'' + u|u| = 0, u(0) = A, u'(0) = 0. \quad (11)$$

Eq. (11) was studied Wang and He [56].

We re-write Eq. (11) in the following form:

$$u'' + 0.u + 1.u|u| = 0 \quad (12)$$

We expand the solution,  $u$ , the constant, zero, and the coefficient of  $u|u|$ , 1, in series of  $p$ :

$$u = u_0 + pu_1 + p^2u_2 + \dots \quad (13)$$

$$0 = w^2 + pw_1 + p^2w_2 + \dots \quad (14)$$

$$1 = a_1p + a_2p^2 + \dots \quad (15)$$

Substituting Eqs.(14) and (15) into Eq.(12) and equating the terms with the identical powers of  $p$ , we have

$$p^0: u_0'' + w^2u_0 = 0, u_0(0) = A, u_0'(0) = 0 \quad (16)$$

$$p^1: u_1'' + w_1u_0 + w^2u_1 + a_1\text{sign}(u_0) = 0 \quad (17)$$

The solution of (16) is  $u_0 = A\cos(wt)$ . Substituting  $u_0$  into Eq.(17) results into

$$u_1'' + w^2u_1 + w_1A\cos(wt) + a_1A^2\cos(wt)|\cos(wt)| = 0. \quad (18)$$

From Chebyshev series expansion, we have

$$f(x) = \sum_{n=0}^{\infty} c_{2n+1}T_{2n+1}(x),$$

where  $x=\cos(wt)$ ,  $T_{2n+1}(x) = \cos[(2n+1)wt]$  and the coefficients:

$$c_{2n+1} = \frac{2}{\pi} \int_{-1}^1 (1-x^2)^{-1/2} f(x) T_{2n+1}(x) dx.$$

Through  $f(x) = \cos\theta|\cos\theta|$ , coefficients form:

$$c_{2n+1} = \frac{2}{\pi} \int_0^\pi (\cos\theta)|\cos\theta| \cos[(2n+1)\theta] d\theta$$

And for  $n=0$  gives  $(\theta=wt)$



$$c_1 = \frac{2}{\pi} \int_0^\pi \cos^2 \theta |\cos \theta| d\theta = \frac{2}{\pi} \left( \int_0^{\pi/2} \cos^3 \theta d\theta - \int_{\pi/2}^\pi \cos^3 \theta d\theta \right) = \frac{8}{3\pi}$$

No secular terms in  $u_1$  requires

$$a_1 A \frac{8}{3\pi} + w_1 = 0 \text{ and } w_1 = -w^2, a_1 = 1$$

Thus, the first order approximation found as

$$w = \sqrt{\frac{8A}{3\pi}} \approx 2.6667 \sqrt{\frac{A}{\pi}} \quad (19)$$

Above the obtained frequency is valid for  $0 < A < \infty$ . This result same as Wang and He's solution [56].

### 3. Conclusion

In this paper, we have represented Ji-Huan He's parameter-expanding method with two examples. The parameter-expanding method with an adjustment of restoring forces in terms of Chebyshev's series for nonlinear oscillators with discontinuities proved to be a powerful mathematical tool to nonlinear oscillators. The technology can be easily extended to any nonlinear oscillators, and the present short note can be used as prototype for many other applications in searching for period or frequency of various nonlinear oscillators.

### 4. References

- [1] Nayfeh, A. H., *Perturbation Methods*, Wiley-Interscience, New York ,1973
- [2] Mickens, R.E., *Oscillations in Planar Dynamics Systems*, World Scientific, Singapore, 1996
- [3] Jordan, D.W. and Smith, P., *Nonlinear Ordinary differential Equations*, Clarendon Press, Oxford, 1987
- [4] Hagedorn, P., *Nonlinear Oscillations*(translated by Wolfram Stadler), Clarendon Press, Oxford,1981
- [5] B.S. Wu, W.P. Sun, C.W. Lim, An analytical approximate technique for a class of strongly non-linear oscillators, *Int. J. Non-linear Mech.* 41 (2006) 766–774.
- [6] B.S. Wu, W.P. Sun, C.W. Lim, An analytical approximate technique for a class of strongly non-linear oscillators, *Int. J. Non-linear Mech.* 41 (2006) 766–774.

- [7] B.S. Wu, C.W. Lim, Y.F. Ma, Analytical approximation to large-amplitude oscillation of a non-linear conservative system, *Int. J. Non-linear Mech.* 38 (2003) 1037–1043.
- [8] B.S. Wu, C.W. Lim, Large amplitude non-linear oscillations of a general conservative system, *Int. J. Non-linear Mech.* 39 (2004) 859– 870.
- [9] B. Wu, P. Li, A method for obtaining approximate analytic periods for a class of nonlinear oscillators, *Meccanica* 36 (2001) 167–176.
- [10] A. Belendez, E. Gimeno, M.L.Alvarez, M. S.Yebra, D. I. Mendez, Analytical approximate solutions for conservative nonlinear oscillators by modified rational harmonic balance method, *International Journal of Computer Mathematics*, DOI: 10.1080/00207160802380942 (in press)
- [11] Ji-H. He, A new approach to nonlinear partial differential equations, *Commun. Nonlinear Sci. Numer. Simul.* 2 (1997) 230–235.
- [12] Ji-H. He, Variational iteration method – a kind of non-linear analytical technique: some examples, *Int. J. Non-Linear Mech.* 34 (1999) 699–708.
- [13] Ji-H. He, Some asymptotic methods for strongly nonlinear equations, *Int. J. Modern Phys.* 20 (2006) 1141–1199.
- [14] M. Rafei, D.D. Ganji\_, H. Daniali, H. Pashaei, The variational iteration method for nonlinear oscillators with discontinuities, *Journal of Sound and Vibration* 305 (2007) 614–620
- [15] J.I. Ramos, On the variational iteration method and other iterative techniques for nonlinear differential equations, *Appl. Math. Comput.*, 199 (2008) 39–69
- [16] Özis T, Yıldırım A (2007) A study of nonlinear oscillators with  $u^{1/3}$  force by He's variational iteration method., *J Sound Vib* 306:372–376
- [17] J.H. He, The homotopy perturbation method for nonlinear oscillators with discontinuities, *Applied Mathematics and Computation*, 151 (1) (2004) 287–292.

- [18]A. Belendez, C. Pascual, S. Gallego, M. Ortuno, C. Neipp, Application of a modified He's homotopy perturbation method to obtain higher order approximations of a  $x^{1/3}$  force nonlinear oscillator, Phys. Lett. A 371 (2007) 421-426.
- [19]A. Belendez, M. L. Alvarez, D. I. Mendez, E. Fernandez, M. S. Yebra, T. Belendez, Approximate Solutions for Conservative Nonlinear Oscillators by He's Homotopy Method, Z. Naturforsch. 63a (2008) 529-537
- [20]A. Belendez, C. Pascual, T. Belendez, A. Hernandez, Solution for an anti-symmetric quadratic nonlinear oscillator by a modified He's homotopy perturbation method, Nonlinear Analysis: Real World Applications 10 (2009) 416-427.
- [21]J.H. He, A coupling method of a homotopy technique and a perturbation technique for non-linear problems, International Journal of Non-linear Mechanics 35 (1) (2000) 37–43.
- [22]T. Öziş, A. Yildirim, A comparative study of He' homotopy perturbation method for determining frequency–amplitude relation of a nonlinear oscillator with discontinuities, International Journal of Nonlinear Sciences and Numerical Simulation 8 (2) (2007) 243–248.
- [23]Özis T, Yıldırım A (2007) A note on He's homotopy perturbation method for van der Pol oscillator with very strong nonlinearity. Chaos Solitons Fractals 34:989–991
- [24]Ji-H. He, Some asymptotic methods for strongly nonlinear equations, Int. J. Modern Phys. 20 (2006) 1141–1199.
- [25]He, JH, *Non-Perturbative Methods for Strongly nonlinear Problems*, dissertation.de-verlag im Internet GmbH, Berlin, 2006
- [26]He, J.H., An elementary introduction to recently developed asymptotic methods and nanomechanics in textile engineering, INTERNATIONAL JOURNAL OF MODERN PHYSICS B 22 ( 21) (2008) 3487-3578

- [27]He JH. Bookkeeping parameter in perturbation methods, International Journal of Nonlinear Sciences & Numerical Simulation 2 (3)(2001) 257-264
- [28] Xu, L., He's parameter-expanding methods for strongly nonlinear oscillators, Journal of Computational and Applied Mathematics, 207(2007)148-154
- [29]Da-Hua Shou , Ji-Huan He, Application of Parameter-expanding Method to Strongly Nonlinear Oscillators, International Journal of Nonlinear Sciences and Numerical Simulation, 8 (1) (2007) 121-124
- [30]S.T. Mohyud-Din,M.A.Noor, K.I. Noor, Parameter-expansion Techniques for Strongly Nonlinear Oscillators , International Journal of Nonlinear Sciences and Numerical Simulation,10 (5) (2009) 581-583
- [31]B.C.Shin,M.T.Darvishi, A.Karami, Application of He's Parameter-expansion Method to a Nonlinear Self-excited Oscillator System, International Journal of Nonlinear Sciences and Numerical Simulation 10(1)(2009) 137-143
- [32]Sweilam, NH; Al-Bar, RF Implementation of the Parameter-expansion Method for the Coupled Van der Pol Oscillators , International Journal of Nonlinear Sciences and Numerical Simulation,10 (2) (2009) 259-264
- [33]F. Özen Zengin, M.O. Kaya, S. Altay Demirbag, Approximate period calculation for some strongly nonlinear oscillation by He's parameter-expanding methods, Nonlinear Analysis: Real World Applications 10 (2009) 2177–2182
- [34] Zengin, FO; Kaya, MO; Demirbag, SA : Application of parameter-expansion method to nonlinear oscillators with discontinuities: International Journal of Nonlinear Sciences and Numerical Simulation, 9 (3) (2008) 267-270
- [35]Zhang, LN; Xu, L. Determination of the limit cycle by He's parameter-expansion for oscillators

- in a  $u(3)/(1+u(2))$  potential , Zeitschrift Fur Naturforschung Section A: 62( 7-8)(2007) 396-398
- [36]J.-H. He, Modified Linstedt–Poincare methods for some non-linear oscillations. Part I: expansion of constant, J. Non-linear Mech. 37 (2002) 309–314.
- [37]He, J.H., Modified Lindstedt-Poincare methods for some strongly non-linear oscillations Part II: a new transformation, International Journal of Non-Linear Mechanics, 37 (2): 315-320, 2002
- [38]He, J. H., Modified Lindsted-Poincare methods for some strongly nonlinear oscillations Part III: Double series expansion, International Journal of Nonlinear Sciences & Numerical Simulation 2 (4): 317-320 2001
- [39]Liu, H.M., Approximate period of nonlinear oscillators with discontinuities by modified Lindstedt-Poincare method, Chaos, Solitons & Fractals, 23(2) (2005) 577-579.
- [40]T. Öziş, A. Yıldırım, Determination of periodic solution of a  $u^{1/3}$  force by He's modified Linstedt–Poincare' method, J. Sound Vibr. 301 (2007) 415–419.
- [41]H.-M. Liu, Approximate period of nonlinear oscillators with discontinuities by modified Lindstedt–Poincare method, Chaos, Solitons and Fractals 23 (2005) 577–579.
- [42]A. Yıldırım, Determination of periodic solutions for nonlinear oscillators with fractional powers by He's modified Lindstedt-Poincaré method, Meccanica, DOI 10.1007/s11012-009-9212-4
- [43]J.I. Ramos, On Linstedt–Poincare' techniques for the quintic Duffing equation, Appl. Math. Comput.,193(2007)303-310
- [44]He, J.H., New interpretation of homotopy perturbation method, International Journal of Modern Physics B, 20(18)82006)2561-2568

- [45]C. Akçi, T. Öziş, Periodic solutions for certain non-smooth oscillators by iterated homotopy perturbation method combined with modified Lindstedt-Poincare technique, *Meccanica* (2009) (submitted)
- [46]Mickens, R. E., *Oscillations in Planar Dynamics Systems*, Singapore: World Scientific, (1996)
- [47]Mickens, R. E. 2007 Harmonic balance and iteration calculations of periodic solutions to  $\ddot{y} + y - 1 = 0$  *J. Sound Vib.* **306** 968–72
- [48]Beléndez A, Méndez, D. I., Beléndez T., Hernández, A. and Alvarez, M. L., Harmonic balance approaches to the nonlinear oscillators in which the restoring force is inversely proportional to the dependent variable *J. Sound Vib.* **314** (2008) 775–82
- [49]A. Beléndez, E. Gimeno, E. Fernández, D. I. Méndez and M. L. Alvarez, Accurate approximate solution to nonlinear oscillators in which the restoring force is inversely proportional to the dependent variable, *Phys. Scr.* **77** (2008) 065004 (7pp)
- [50]C.W. Lim, B.S. Wu, A new analytical approach to the Duffing-harmonic oscillator, *Physics Letters A* 311 (2003) 365–373.
- [51]R.E. Mickens, Mathematical and numerical study of the Duffing- harmonic, *Journal of Sound and Vibration* 244 (3) (2001) 563–567.
- [52]Belendez, A. Hernandez, T. Belendez, E. Fernandez, M.L. Alvarez, C. Neipp, Application of He's homotopy perturbation method to the Duffing-Harmonic oscillator, *International Journal of Nonlinear Mechanics* 8 (1) (2007) 79–88.
- [53]A. Belendez, C. Pascual, E. Fernandez, C. Neipp, T. Belendez, Higher-order approximate solutions to the relativistic and Duffing-harmonic oscillators by modified He's homotopy methods, *Physics Scripta* 77 (2) (2008). *Scr.* **77** 025004
- [54]J.I. Ramos On the variational iteration method and other iterative techniques for nonlinear

differential equations, *Applied Mathematics and Computation* 199 (2008) 39–69

[55] H-M Liu, Approximate period of nonlinear oscillators with discontinuities by modified Lindstedt–Poincare method, *Chaos, Solitons and Fractals* 23 (2005) 577–579

[56] S-Q. Wang, J-H. He, Nonlinear oscillator with discontinuity by parameter-expansion method, *Chaos, Solitons and Fractals* 35 (2008) 688–691

# Self-Organized Criticality in Solar Physics and Astrophysics

Markus J. Aschwanden

July 14, 2010

## Abstract

The concept of “self-organized criticality” (SOC) has been introduced by Bak, Tang, and Wiesenfeld (1987) to describe the statistics of avalanches on the surface of a sandpile with a critical slope, which produces a scale-free powerlaw size distribution of avalanches. In the meantime, SOC behavior has been identified in many nonlinear dissipative systems that are driven to a critical state. On a most general level, SOC is the statistics of coherent nonlinear processes, in contrast to the Poisson statistics of incoherent random processes. The SOC concept has been applied to laboratory experiments (of rice or sand piles), to human activities (population growth, language, economy, traffic jams, wars), to biophysics, geophysics (earthquakes, landslides, forest fires), magnetospheric physics, solar physics (flares), stellar physics (flares, cataclysmic variables, accretion disks, black holes, pulsar glitches, gamma ray bursts), and to galactic physics and cosmology.

*Keywords:* astrophysics - nonlinear dynamics - statistics - selforganized criticality - solar flares

## 1 Introduction

Physical processes in our universe can be subdivided into incoherent and coherent processes. Examples of incoherent processes are fractional Brownian motion, diffusion, collisional plasma processes, plasma heating, which all are governed by random processes and thus can be described by binomial and Poissonian statistics, which exhibit exponential-like or Gaussian-like distributions. In contrast, coherent processes overcome the threshold of the random noise background and grow in a multiplicative way, such as avalanches, chain reactions, or catastrophes, which all exhibit powerlaw-like size distributions. The dichotomy of incoherent and coherent processes is also reflected in the two types of linear and nonlinear processes. Linear systems are characterized by a proportionality between the input and output (Fig. 1, left). Small disturbances cause small effects, and large disturbances are required to produce a large effect. A hydropower plant, for instance, produces electric energy that is proportional to the



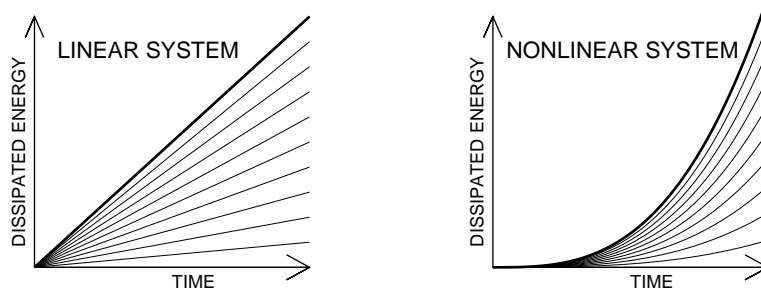


Figure 1: The output or dissipated energy in a linear system grows linearly with time, for a constant input rate (left), while the output is highly unpredictable and not correlated with the input rate in a nonlinear dissipative system (right).

water inflow rate and gravitational or kinetic energy of the water that is feeding the turbine. Nonlinear processes, in contrast, are governed by a multiplicative or amplification factor (Fig. 1, right), that leads to outputs of unpredictable magnitude, unlike linear systems. Small disturbances can cause both small or large avalanches. Classical examples are snow avalanches, landslides, floodings, forest fires, or earthquakes.

A conceptual model to understand the basic nature of nonlinear processes was introduced by Bak, Tang, and Wiesenfeld (1987) in terms of sandpile avalanches. We can build a sandpile by dripping sand grains randomly with a more or less steady rate, until it forms a cone. Once the sandpile reaches a critical slope (typically at an angle of repose of  $\approx 34^\circ - 37^\circ$ ), avalanches occur in an unpredictable way, even when the input of dripped sand grains is steady. Bak called this driven state “*self-organized criticality*” (SOC), which has become a paramount characteristic of many nonlinear systems (Aschwanden 2010). A sand beach, in contrast, would be in a sub-critical state without avalanches. The key features of nonlinear systems are powerlaw-like size distributions, which indicate scale-free parameter distributions, such as the size, time scale, or energy of an avalanche. The occurrence frequency distribution  $N(x)$  of a parameter  $x$  is defined as a powerlaw function when

$$N(x) \propto x^{-\alpha} . \quad (1)$$

The mathematical nature of such powerlaw distributions can easily be understood in terms of a coherent, exponential growth process as described in the following section.

## 2 Analytical Model of SOC Avalanches

Avalanches occurring in the state of self-organized criticality represent local instabilities that grow explosively for some time interval. The released energy

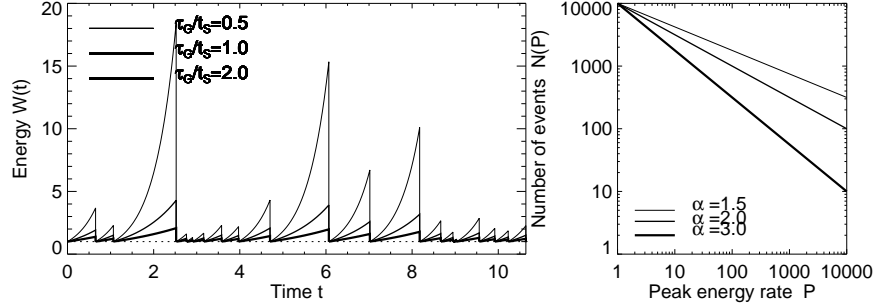


Figure 2: Time evolution of energy release rate  $W(t)$  for 3 different ratios of growth times to saturation times,  $\tau_G/t_S = (0.5, 1.0, 2.0)$  (left) and the corresponding powerlaw distributions of the peak energy release rate  $P$ . Note that the event set with the shortest growth time ( $\tau_G/t_S = 0.5$ ) reaches the highest energies and thus produces the flattest powerlaw slope ( $\alpha = 1 + \tau_G/t_S = 1.5$ ).

grows in a nonlinear way above some energy threshold, which can be parameterized by some nonlinear function, for instance by an exponential growth function. We define the time evolution of the energy release rate  $W(t)$  of a nonlinear process that starts at a threshold energy of  $W_0$  by

$$W(t) = W_0 \exp\left(\frac{t}{\tau_G}\right), \quad 0 \leq t \leq \tau, \quad (2)$$

where  $\tau_G$  represents the exponential growth time. The process grows exponentially until it saturates at time  $t = \tau$  with a saturation energy  $W_S$ ,

$$W_S = W(t = \tau) = W_0 \exp\left(\frac{\tau}{\tau_G}\right). \quad (3)$$

We define a peak energy release rate  $P$  that represents the maximum energy release rate  $W_S$ , after subtraction of the threshold energy  $W_0$ , that corresponds to the steady-state energy level before the nonlinear growth phase,

$$P = W_S - W_0 = W_0 \left[ \exp\left(\frac{\tau}{\tau_G}\right) - 1 \right]. \quad (4)$$

In the following, we will refer to the peak energy release rate  $P$  also briefly as “peak energy”. For the saturation times  $\tau$ , which we also call “rise times”, we assume a random probability distribution, approximated by an exponential function  $N(\tau)$  with e-folding time constant  $t_S$ ,

$$N(\tau)d\tau = \frac{N_0}{t_S} \exp\left(-\frac{\tau}{t_S}\right)d\tau. \quad (5)$$

This probability distribution is normalized to the total number of  $N_0$  events,

$$\int_0^\infty N(\tau)d\tau = N_0. \quad (6)$$

In order to derive the probability distribution  $N(P)$  of peak energy release rates  $P$ , we have to substitute the variable of the peak energy,  $P$ , into the function of the rise time  $\tau(P)$ ,

$$N(P)dP = N(\tau)d\tau = N[\tau(P)] \left| \frac{d\tau}{dP} \right| dP . \quad (7)$$

This requires the inversion of the evolution function  $P(\tau)$  (Eq. 4),

$$\tau(P) = \tau_G \ln \left( \frac{P}{W_0} + 1 \right) , \quad (8)$$

and the calculation of its derivative  $d\tau/dP$ , which is

$$\frac{d\tau}{dP} = \frac{\tau_G}{W_0} \left( \frac{P}{W_0} + 1 \right)^{-1} . \quad (9)$$

Inserting the probability distribution of saturation times  $N(\tau)$  (Eq. 5), the inverted evolution function  $\tau(P)$  (Eq. 8) and its time derivative  $(d\tau/dP)$  from Eq. (9) into the frequency distribution  $N(P)$  in Eq. (7) yields then,

$$N(P)dP = \frac{N_0(\alpha - 1)}{W_0} \left( \frac{P}{W_0} + 1 \right)^{-\alpha} dP , \quad (10)$$

which is an exact powerlaw distribution for large peak energies ( $P \gg W_0$ ) with a powerlaw slope  $\alpha$  of

$$\alpha = \left( 1 + \frac{\tau_G}{t_S} \right) . \quad (11)$$

The same mathematical result was derived in Rosner and Vaiana (1978), but the exponential growth was attributed to energy storage therein, rather than to the nonlinear growth phase of the instability here. The powerlaw slope thus depends on the ratio of the growth time to the e-folding saturation time, which is essentially the average number of growth times. Examples of time series with avalanches of different growth times ( $\tau_G/t_S = 0.5, 1.0, 2.0$ ) are shown in Fig. 2, along with the corresponding powerlaw distributions of peak energies  $P$ . Note that the fastest growing events produce the flattest powerlaw distribution of peak energies.

This simple model explains the powerlaw distribution of peak energies in nonlinear processes that have an exponential-like growth, which is the key characteristic of coherent processes. In incoherent processes, the growth time would be much larger than the average saturation time ( $\tau_G \gg t_S$ ), in which case the time evolution (Eq. 3) can be linearized, leading to  $P \propto \tau$  (Eq. 4), and the distribution of peak energies would be identical to that of the saturation times  $\tau$ , which is a Poissonian (exponential) distribution (Eq. 5) with a characteristic scale  $P \approx W_0$ . So, incoherent processes would have the same exponential distribution of peak fluxes  $P$  as their random durations  $\tau$ ,

$$N^{inc}(P)dP = \frac{N_0}{W_0} \exp \left( -\frac{P}{W_0} \right) dP . \quad (12)$$

Therefore, we can use the functional shape of the occurrence frequency distribution of event sizes as a diagnostic of linear or nonlinear processes: exponential distribution functions indicate an incoherent random process, while powerlaw distribution functions indicate a coherent growth process.

The exponential-growth model represents just the mathematically simplest function to produce a powerlaw distribution of peak energies. It corresponds to a multiplicative process where the number of avalanche elements doubles every time step until it saturates (Fig. 3, left). The saturation phase, however, abruptly ends with a discontinuity. A more natural model is the logistic equation (discovered by Pierre François Verhulst in 1845), which is a first-order differential equation that approaches the saturation limit asymptotically,

$$\frac{dE(t)}{dt} = \frac{E(t)}{\tau_G} \cdot \left[ 1 - \frac{E(t)}{E_\infty} \right] \quad (13)$$

as shown in Fig. 3 (right). The time derivative, which mimics the energy release rate, has a maximum when the total energy has the steepest slope. The avalanche grows first exponentially and dies out gradually after the peak time of the fastest growth. It can be shown mathematically that the frequency distribution of the peak energies is also a powerlaw (Aschwanden et al. 1998), and thus this more physical description of a *logistic avalanche* with a continuous time evolution shares the same characteristic as an exponentially-growing avalanche, and thus both models can be used to describe SOC processes.

### 3 Solar Observations of SOC Phenomena

Solar flares are probably the best-studied datasets regarding SOC statistics in astrophysics. Solar flares are catastrophic events in the solar corona, most likely caused by a magnetic instability that triggers a magnetic reconnection process, producing emission in almost all wavelengths, such as in gamma-rays, hard X-rays, soft X-rays, extreme ultraviolet (EUV), H $\alpha$  emission, radio wavelengths, and sometimes even in white light. EUV images of solar flares display a complex topology of the magnetic field produced by a magnetic reconnection process. Since the emission mechanisms are all different in each wavelength, such as nonthermal bremsstrahlung (in hard X-rays), thermal bremsstrahlung (in soft X-rays and EUV), gyrosynchrotron emission (in microwaves), plasma emission (in metric and decimetric waves), etc., we expect that the calculation of energies contained in each event strongly depends on the emission mechanism, and thus on the wavelength. It is therefore advisable to investigate the statistics of SOC events in each wavelength domain separately. The most unambiguous SOC parameters to report are the peak flux  $P$ , the total flux or fluence  $E$ , defined as the time-integrated flux over the entire event, and the total time duration  $T$  of the event. Conversions of fluxes and fluences into energy release rates and total energies require physical models.

Statistics of the peak count rates  $P$  of over 20,000 solar flares observed in hard X-rays during three different space missions (SMM 1980-1989; CGRO

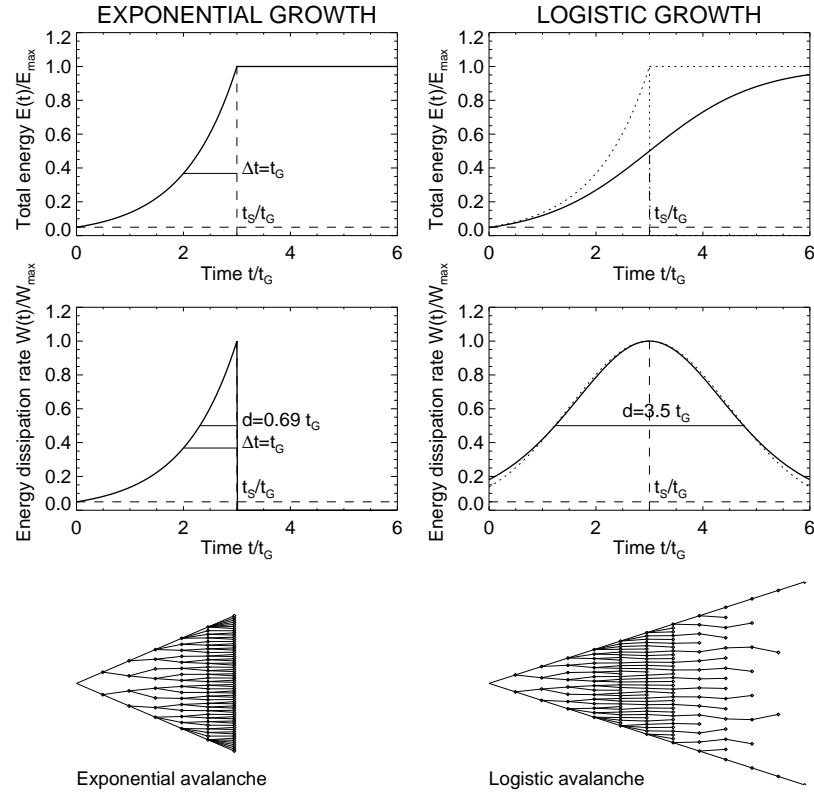


Figure 3: Time evolution of total released energy  $e(t)$  (top panels), the energy release rate  $W(t) = de(t)/dt$  (middle panels), and binary representation of avalanche growth rate (bottom panels), for both the exponential (left panels) and the logistic growth model (right panels). An exponential curve (right top) and a Gaussian curve (right middle) are drawn (with dotted lines) onto the logistic curves for comparison (Aschwanden et al. 1998).

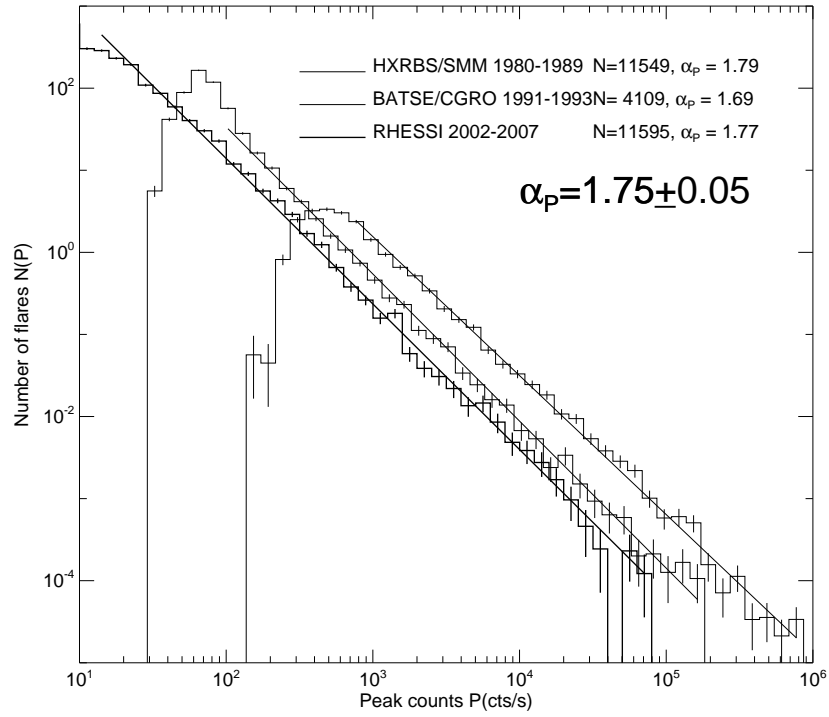


Figure 4: Occurrence frequency distributions of hard X-ray peak count rates  $P(\text{cts/s})$  observed with HXRBS/SMM (1980-1989), BATSE (1991-1993), and RHESSI (2002-2007), with powerlaw fits. Note that BATSE/CGRO has larger detector areas, and thus records higher count rates.

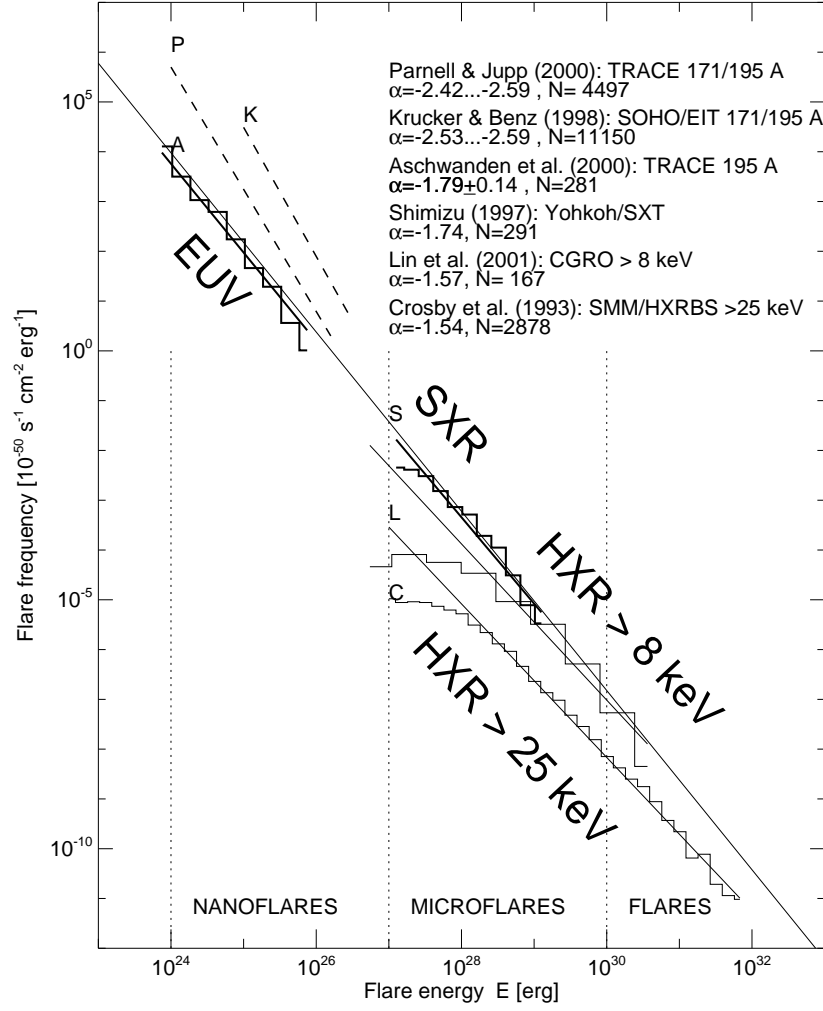


Figure 5: Composite flare frequency distribution in a normalized scale in units of  $10^{-50}$  flares per time unit ( $s^{-1}$ ), area unit ( $cm^{-2}$ ), and energy unit ( $erg^{-1}$ ). The energy is defined in terms of thermal energy  $E_{th} = 3n_e k_B T_e V$  for EUV and SXR, and in terms of non-thermal energy in > 25 keV (Crosby et al. 1993) or > 8 keV electrons (Lin et al. 2001). The slope of  $-1.8$  is extended over the entire energy domain of  $10^{24} - 10^{32}$  erg. The offset between the two HXR datasets is attributed to different lower energy cutoffs as well as different levels of flare activity during the observed time intervals [adapted from Aschwanden et al. 2000 and Lin et al. 2001].

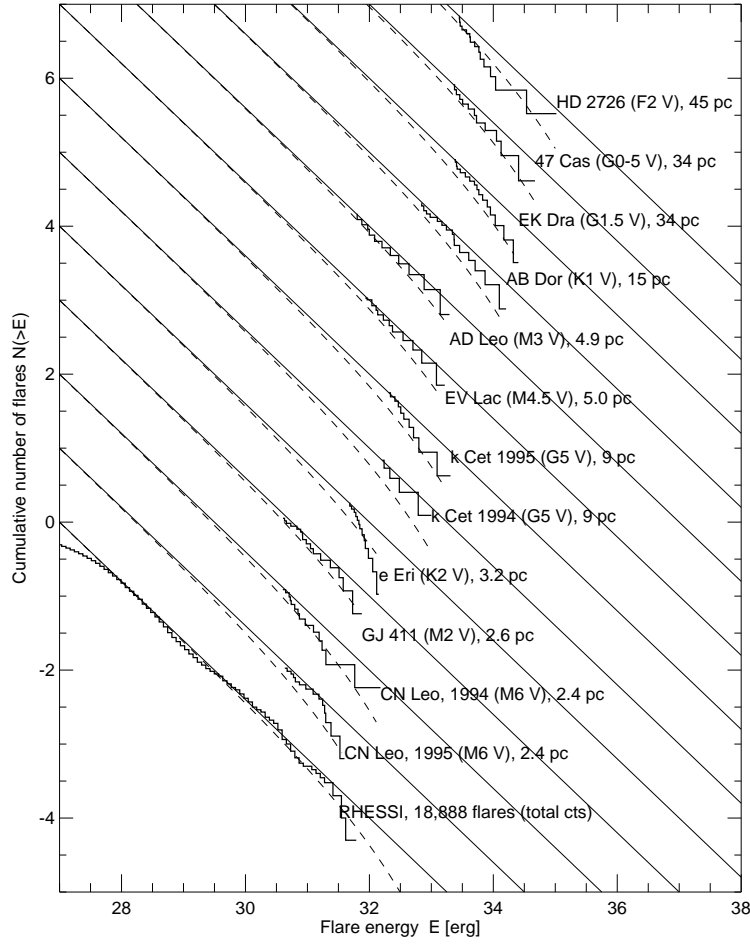


Figure 6: Cumulative occurrence frequency distributions  $N(>E)$  of stellar flares (vertically shifted for each star, in order of stellar distance) are shown as a function of the flare energy  $E$ , observed from 12 different stars by Audard et al. (2000). For comparison we show also the statistics of total hard X-ray emission of 18,888 solar flares observed with RHESSI, which covers an energy range of  $E \approx 10^{27.0} - 10^{31.7}$  ergs, while stellar flares have an energy range of  $E \approx 10^{30.7} - 10^{35.0}$  ergs. Note that most distributions show a (cumulative) powerlaw part with a slope of  $\alpha \approx 0.8$  (diagonal lines) at the low end and an exponential high-energy drop-off.



1991-1993; RHESSI 2002-2010) and during three different solar cycles have been gathered and their occurrence frequency distributions (or  $\log N - \log S$  distributions) are shown in Fig. 4. All three datasets show a near-perfect powerlaw distribution function with a mean slope of  $\alpha_P = 1.75 \pm 0.05$ . According to our model this value corresponds to a ratio of  $\tau_G/t_S = 0.75$  (Eq. 11) or a mean saturation time  $t_S/\tau_G = 1.33$  growth times. The distributions shown in Fig. 4 span together over 5 orders of magnitude, which means that the largest flare had a maximum saturation time of  $\ln(10^5) = 11.5$  growth times, which corresponds to an extremely coherent process that could never be explained by random probability.

Similar powerlaw-like occurrence frequency distributions have also been found for other flare parameters, such as the fluence, the flare duration, or flare energy (calculated from the thermal energy or energy in nonthermal hard X-ray producing electrons). Based on this fact of scale-free powerlaw distributions, Lu and Hamilton (1991) were the first to apply the concept of self-organized criticality (SOC) to solar flares. With a cellular automaton model that mimics sandpile avalanches, they were able to simulate the size frequency distribution with a powerlaw slope of  $\alpha_P = 1.67 \pm 0.02$ , which is close to the observed value of  $\alpha_P = 1.75 \pm 0.05$  shown in Fig. 4.

The statistics of peak energies in solar flares has been extended to other wavelengths, from hard X-rays to soft X-rays and EUV and the powerlaw-like size distribution has been found to extend over 8 orders of magnitude (Fig. 5). The events observed in soft X-rays have been called “*active region transients*”, having about 3-5 orders of magnitude less energy than the largest solar flare. The events observed in EUV have energies about 6-9 orders of magnitude less than the largest flare, and thus are called “*nanoflares*”. The self-similarity of flare parameters observed over this wide wavelength range, which implies also a large temperature range of  $T \approx (1-35) \times 10^6$  K, constitutes a powerful argument that the solar corona is in a state of self-organized criticality.

## 4 Astrophysical Observations of SOC Phenomena

Size distributions have also been sampled for stellar flares, although with much smaller statistics, typically  $\lesssim 15$  flare events per star. A comparison of size distributions from 12 flare stars (type F to M) observed by Audard et al. (2000) is shown in Fig. 6. Because of the smallness of the samples, the cumulative frequency distributions are shown, which have slope that is flatter by one compared with the differential frequency distribution ( $\alpha_P^{cum} = \alpha_P - 1$ ). The comparison in Fig. 6 demonstrates two important aspects: (1) stellar flares are up to two orders of magnitude more energetic ( $E \approx 10^{32} - 10^{34}$ ) than solar flares (see RHESSI comparison at bottom of Fig. 6), although the small sample implies common and relatively weak events, and (2) the drop-off at the upper bound of the cumulative frequency distribution yields a steeper slope than the powerlaw

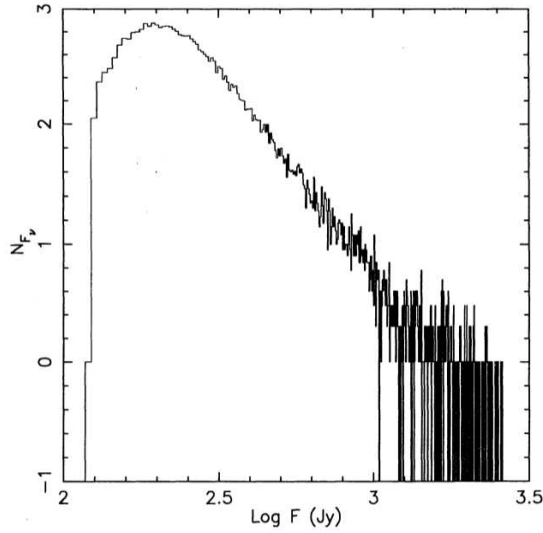


Figure 7: Frequency distribution of giant-pulse flux densities measured from the Crab pulsar, observed during 15-27 May 1991 with the Green Bank 43-m telescope at 1330, 800, and 812.5 MHz. The tail can be represented by a powerlaw distribution  $N_F \propto F^{-\alpha}$  with  $\alpha = 3.46 \pm 0.04$  for fluxes  $F > 200$  Jy (Lundgren et al. 1995).

slope obtained from more complete frequency distributions. Correcting for the latter effect, stellar flares seem to have a similar powerlaw distribution as solar flares, and thus may be governed by the same SOC process.

Other size distributions with powerlaw shape have been observed in astrophysical data for pulsar glitches (e.g., Lundgren et al. 1995; shown in Fig. 7), for soft gamma-ray repeaters (e.g., Gogus et al. 1999), accretion disk objects around black hole candidates, such as Cygnus X-1 (e.g., Negoro et al. 1995), or for blazars (e.g., Ciprini et al. 2003). These astrophysical objects display size distributions with different powerlaw values, and thus can be explained by different physical processes, but the distribution type of a powerlaw function constitutes a powerful argument that the underlying system is driven into the critical state of self-organized criticality, which is common to earthquakes, sunquakes (occurring during large flares), and neutron star quakes (pulsar glitches).

*Acknowledgements:* This work is partially supported by NASA contract NAS5-98033 of the RHESSI mission through University of California, Berkeley (subcontract SA2241-26308PG) and NASA grant NNX08AJ18G. We acknowledge access to solar mission data and flare catalogs from the Solar Data Analysis Center (SDAC) at the NASA Goddard Space Flight Center (GSFC).

## References

- Aschwanden, M.J., Dennis, B.R., and Benz, A.O. 1998, *Logistic avalanche processes, elementary time structures, and frequency distributions of flares*, *Astrophys. J.* **497**, 972-993.
- Aschwanden, M.J., Tarbell, T., Nightingale, R., Schrijver, C.J., Title, A., Kankelborg, C.C., Martens, P.C.H., and Warren, H.P. 2000, *Time variability of the quiet Sun observed with TRACE: II. Physical parameters, temperature evolution, and energetics of EUV nanoflares*, *Astrophys. J.* **535**, 1047-1065.
- Aschwanden, M.J. 2010, *Self-Organized Criticality in Astrophysics*, Springer/Praxis: Heidelberg, New York.
- Audard, M., Guedel, M., Drake, J.J., and Kashyap, V.L. 2000, *Extreme-ultraviolet flare activity in late-type stars* *Astrophys. J.* **541**, 396-409.
- Bak, P., Tang, C., & Wiesenfeld, K. 1987, *Self-organized criticality - An explanation of 1/f noise*, *Physical Review Lett.* **59/27**, 381-384.
- Ciprini, S., Fiorucci, M., Tosti, G., and Marchili, N. 2003, *The optical variability of the blazar GV 0109+224. Hints of self-organized criticality*, in *High energy blazar astronomy*, ASP Conf. Proc. **229**, (eds. L.O. Takalo and E. Valtaoja), ASP: San Francisco, p.265.
- Crosby, N.B., Aschwanden, M.J., and Dennis, B.R. 1993, *Frequency distributions and correlations of solar hard X-ray flare parameters*, *Solar Phys.* **143**, 275-299.
- Gogus, E., Woods, P.M., Kouveliotou, C., van Paradijs, J., Briggs, M.S., Duncan, R.C., and Thompson, C. 1999, *Statistical properties of SGR 1900+14 bursts*, *Astrophys. J.* **526**, L93-L96.
- Krucker, S. and Benz, A.O. 1998, *Energy distribution of heating processes in the quiet solar corona*, *Astrophys. J.* **501**, L213-L216.
- Lin, R.P., Feffer, P.T., and Schwartz, R.A. 2001, *Solar Hard X-Ray Bursts and Electron Acceleration Down to 8 keV*, *Astrophys. J.* **557**, L125-L128.
- Lu, E.T. and Hamilton, R.J. 1991, *Avalanches and the distribution of solar flares*, *Astrophys. J.* **380**, L89-L92.
- Lundgren, S.C., Cordes, J.M., Ulmer, M., Matz, S.M., Lomatch, S., Foster, R.S., and Hankins, T. 1995, *Giant pulses from the Crab pulsar: A joint radio and gamma-ray study*, *Astrophys. J.* **453**, 433-445.
- Negoro, H., Kitamoto, S., Takeuchi, M., and Mineshige, S. 1995, *Statistics of X-ray fluctuations from Cygnus X-1: Reservoirs in the disk ?*, *Astrophys. J.* **452**, L49-L52.
- Parnell, C.E. and Jupp, P.E. 2000, *Statistical analysis of the energy distribution of nanoflares in the quiet Sun*, *Astrophys. J.* **529**, 554-569.
- Rosner, R., and Vaiana, G.S. 1978, *Cosmic flare transients: constraints upon models for energy storage and release derived from the event frequency distribution*, *Astrophys. J.* **222**, 1104-1108.
- Shimizu, T. and Tsuneta, S. 1997, *Deep survey of solar nano-flares with Yohkoh*, *Astrophys. J.* **486**, 1045-1057.

# Applications and Lipschitz results of Approximation by Smooth Poisson-Cauchy Type Singular Integrals

George A. Anastassiou & Razvan A. Mezei

Department of Mathematical Sciences  
The University of Memphis  
Memphis, TN 38152, U.S.A.  
[ganastss@memphis.edu](mailto:ganastss@memphis.edu)  
[rmezei@memphis.edu](mailto:rmezei@memphis.edu)

**AMS 2000 Mathematics Subject Classification:**

*Primary:* 26A15, 26D15, 41A17, 41A35, 41A60, 41A80,

*Secondary:* 41A25

**Key Words and Phrases:** Simultaneous global smoothness, simultaneous approximation, Smooth Poisson-Cauchy Type singular integral, modulus of smoothness, Voronovskaya Type Theorem, rate of convergence,  $L_p$  convergence, Best constant, sharp inequality, Lipschitz functions.

**Abstract.** In this article we continue the study of  $L_p$  approximation,  $1 \leq p \leq \infty$ , by the smooth Poisson-Cauchy Type singular integral operators with their applications. We establish here also Lipschitz type results of approximation for these operators. Furthermore we produce some particular Voronovskaya type results.

## 1 Introduction

We are motivated by [5], [6].

We denote by  $L_p$ ,  $1 \leq p < \infty$ , the classes of functions  $f(x)$ , integrable in  $-\infty < x < \infty$  with the norm

$$\|f\|_p = \left[ \int_{-\infty}^{\infty} |f(u)|^p du \right]^{\frac{1}{p}}. \quad (1)$$

The *Poisson-Cauchy singular integral*  $M_\xi(f; x)$  corresponding to the function  $f(x)$ , is defined as follows

$$M_\xi(f, x) := W \int_{-\infty}^{\infty} f(x+y) \frac{1}{(y^{2\alpha} + \xi^{2\alpha})^\beta} dy, \quad \text{for all } x \in \mathbb{R}, \xi > 0, \quad (2)$$

where

$$W = \frac{\Gamma(\beta) \alpha \xi^{2\alpha\beta-1}}{\Gamma(\frac{1}{2\alpha}) \Gamma(\beta - \frac{1}{2\alpha})}, \quad (3)$$

and  $\alpha \in \mathbb{N}, \beta > \frac{1}{2\alpha}$ . We assume that  $f$  is such that  $M_\xi(f; x) \in \mathbb{R}, \forall x \in \mathbb{R}, \forall \xi > 0$ .

For suitable choices of  $\alpha, \beta$  (see [5], for  $\alpha = 1, \beta = 1$ ) we have, for  $f \in L_p, 1 \leq p < \infty$ , that the integral (2) exists for all  $x \in (-\infty, \infty)$  and  $\xi > 0$ , and for functions  $f(x)$  from the class  $L_p \cap C^\infty$ , it satisfies the following expressions

$$\|M_\xi(f, \cdot)\|_p \leq \|f\|_p, \xi > 0, \quad \lim_{\xi \rightarrow 0^+} \|M_\xi(f, \cdot) - f(\cdot)\|_p = 0. \quad (4)$$

The Poisson-Cauchy singular integral plays an important role in the theory of second-order partial differential equations. It can be shown to be the solution of the Dirichlet problem for Laplace's equation in the upper half-plane with boundary function  $f(x) \in L_p, 1 \leq p < \infty$ .

Here we give important applications of the main results from [1], [2], [3] and [4].

## 2 Uniform Convergence

Let  $f: \mathbb{R} \rightarrow \mathbb{R}$  be a Lebesgue measurable function. Next we define and study the smooth Poisson-Cauchy singular integral type operators  $M_{r,\xi}(f; x)$ .

For  $r \in \mathbb{N}$  and  $n \in \mathbb{Z}_+$  we set

$$\alpha_j := \begin{cases} (-1)^{r-j} \binom{r}{j} j^{-n}, & j = 1, \dots, r, \\ 1 - \sum_{j=1}^r (-1)^{r-j} \binom{r}{j} j^{-n}, & j = 0, \end{cases} \quad (5)$$

that is  $\sum_{j=0}^r \alpha_j = 1$ .

Let  $\xi > 0, \alpha \in \mathbb{N}, \beta > \frac{1}{2\alpha}$  and  $x \in \mathbb{R}$ . We consider the Lebesgue integral,

$$M_{r,\xi}(f; x) := W \int_{-\infty}^{\infty} \frac{\sum_{j=0}^r \alpha_j f(x+jt)}{(t^{2\alpha} + \xi^{2\alpha})^\beta} dt, \quad (6)$$

where the constant  $W$  is given by (3).

**Note 1.** The operators  $M_{r,\xi}$  are not in general positive, see [1].

**Note 2.** In particular we have  $M_{1,\xi} = M_\xi$ .

Here let  $f \in C^n(\mathbb{R})$  with  $\omega_1(f^{(n)}, h) < \infty$ ,  $h > 0$ ,  $n \in \mathbb{N}$ . Assume  $M_{j\xi}(f; x) \in \mathbb{R}$  for  $j = 1, \dots, r \in \mathbb{N}$ ,  $\xi > 0$ , all  $x \in \mathbb{R}$ . Also suppose that  $\beta > \frac{n+2}{2\alpha}$ .

We call also

$$\delta_{2m} := \sum_{j=1}^r \alpha_j j^{2m}, \quad (7)$$

and

$$E_{r,\xi}(f; x) := M_{r,\xi}(f; x) - f(x) - \sum_{m=1}^{\lfloor n/2 \rfloor} \frac{f^{(2m)}(x)}{(2m)!} \frac{\Gamma(\frac{2m+1}{2\alpha}) \Gamma(\beta - \frac{2m+1}{2\alpha})}{\Gamma(\frac{1}{2\alpha}) \Gamma(\beta - \frac{1}{2\alpha})} \delta_{2m} \xi^{2m}, \quad (8)$$

$x \in \mathbb{R}$ .  $\lfloor \cdot \rfloor$  denotes the integral part, the sum collapses for  $n = 1$ .

We study here the convergence of operators  $M_{r,\xi}$  to the unit operator  $I$  with rates,  $r \in \mathbb{N}$ .

For  $n = 1$ ,

$$E_{r,\xi}(f; x) = M_{r,\xi}(f; x) - f(x).$$

We give

**Theorem 3.** Let  $n = 1$ . Then

(i) for  $\alpha = 1$  and  $\beta = \frac{5}{2}$

$$\|M_{r,\xi}(f; \cdot) - f\|_\infty \leq \left[ \frac{1}{4} \sum_{j=1}^r \binom{r}{j} \left[ j + 1 + \frac{1}{2j} \right] \right] \xi \omega_1(f', \xi), \quad \xi > 0, \quad (9)$$

(ii) for  $\alpha = 2$  and  $\beta = 1$

$$\|M_{r,\xi}(f; \cdot) - f\|_\infty \leq \left[ \frac{1}{2} \sum_{j=1}^r \binom{r}{j} \left( j + \frac{1}{\sqrt{2}} + \frac{1}{4j} \right) \right] \xi \omega_1(f', \xi), \quad \xi > 0, \quad (10)$$

(iii) for  $\alpha = 2$  and  $\beta = \frac{5}{4}$

$$\|M_{r,\xi}(f; \cdot) - f\|_\infty \leq \left[ \frac{1}{2} \sum_{j=1}^r \binom{r}{j} \left[ (j+1) \frac{\pi \sqrt{2\pi}}{\Gamma^2(\frac{1}{4})} + \frac{1}{4j} \right] \right] \xi \omega_1(f', \xi), \quad \xi > 0, \quad (11)$$

(iv) for  $\alpha = 3$  and  $\beta = 1$

$$\|M_{r,\xi}(f; \cdot) - f\|_\infty \leq \left[ \sum_{j=1}^r \binom{r}{j} \left[ \frac{j}{4} + \frac{1}{2\sqrt{3}} + \frac{1}{8j} \right] \right] \xi \omega_1(f', \xi), \quad \xi > 0, \quad (12)$$

(v) for  $\alpha = 3$  and  $\beta = \frac{2}{3}$

$$\|M_{r,\xi}(f; \cdot) - f\|_\infty \leq \left[ \frac{1}{2} \sum_{j=1}^r \binom{r}{j} \left[ j + \frac{2^{\frac{1}{3}}}{\sqrt{3}} + \frac{1}{4j} \right] \right] \xi \omega_1(f', \xi), \quad \xi > 0, \quad (13)$$

(vi) for  $\alpha = 3$  and  $\beta = \frac{7}{6}$

$$\|M_{r,\xi}(f; \cdot) - f\|_\infty \leq \left[ \sum_{j=1}^r \binom{r}{j} \left[ \frac{j}{2} \sqrt{\pi} \frac{\Gamma(\frac{2}{3})}{\Gamma(\frac{1}{6})} + \frac{\sqrt{\pi} \Gamma(\frac{2}{3})}{2^{\frac{2}{3}} \Gamma(\frac{1}{6})} + \frac{1}{8j} \right] \right] \xi \omega_1(f', \xi), \quad \xi > 0, \quad (14)$$

(vii) for  $\alpha = 4$  and  $\beta = \frac{1}{2}$

$$\|M_{r,\xi}(f; \cdot) - f\|_\infty \leq \left[ \sum_{j=1}^r \binom{r}{j} \left[ \frac{j}{2} + \frac{1}{2} \frac{[\Gamma(\frac{1}{4})]^2}{\Gamma(\frac{1}{8}) \Gamma(\frac{3}{8})} + \frac{1}{8j} \right] \right] \xi \omega_1(f', \xi), \quad \xi > 0, \quad (15)$$

(viii) for  $\alpha = 4$  and  $\beta = \frac{9}{8}$

$$\|M_{r,\xi}(f; \cdot) - f\|_\infty \leq \left[ \sum_{j=1}^r \binom{r}{j} \left[ \frac{j}{2} \frac{\Gamma(\frac{3}{8}) \Gamma(\frac{3}{4})}{\Gamma(\frac{1}{8})} + \frac{1}{2} \frac{\Gamma(\frac{1}{4}) \Gamma(\frac{7}{8})}{\Gamma(\frac{1}{8})} + \frac{1}{8j} \right] \right] \xi \omega_1(f', \xi), \quad \xi > 0, \quad (16)$$

(ix) for  $\alpha = 4$  and  $\beta = 1$

$$\|M_{r,\xi}(f; \cdot) - f\|_\infty \leq \left[ \sum_{j=1}^r \binom{r}{j} \left[ \frac{1}{2} \sin \frac{7\pi}{8} \left( j \csc \frac{5\pi}{8} + \sqrt{2} \right) + \frac{1}{8j} \right] \right] \xi \omega_1(f', \xi), \quad \xi > 0, \quad (17)$$

(x) for  $\alpha = 4$  and  $\beta = \frac{3}{2}$

$$\|M_{r,\xi}(f; \cdot) - f\|_\infty \leq \left[ \sum_{j=1}^r \binom{r}{j} \left[ \frac{j}{6} + \frac{1}{3} \frac{[\Gamma(\frac{1}{4})]^2}{\Gamma(\frac{1}{8}) \Gamma(\frac{3}{8})} + \frac{1}{8j} \right] \right] \xi \omega_1(f', \xi), \quad \xi > 0, \quad (18)$$

(xi) for  $\alpha = 5$  and  $\beta = \frac{2}{5}$

$$\|M_{r,\xi}(f; \cdot) - f\|_\infty \leq \left[ \sum_{j=1}^r \binom{r}{j} \left[ \frac{j}{2} + \frac{1}{2^{\frac{7}{10}} \sqrt{5 - \sqrt{5}}} + \frac{1}{8j} \right] \right] \xi \omega_1(f', \xi), \quad \xi > 0, \quad (19)$$

(xii) for  $\alpha = 5$  and  $\beta = \frac{1}{2}$

$$\|M_{r,\xi}(f; \cdot) - f\|_\infty \leq \left[ \sum_{j=1}^r \binom{r}{j} \left[ \left( \frac{j+1}{2} \right) \frac{\Gamma(\frac{3}{10}) \Gamma(\frac{1}{5})}{\Gamma(\frac{1}{10}) \Gamma(\frac{2}{5})} + \frac{1}{8j} \right] \right] \xi \omega_1(f', \xi), \quad \xi > 0, \quad (20)$$

(xiii) for  $\alpha = 5$  and  $\beta = \frac{6}{5}$

$$\|M_{r,\xi}(f; \cdot) - f\|_\infty \leq \left[ \sum_{j=1}^r \binom{r}{j} \left[ \frac{5j \Gamma(\frac{3}{10}) \Gamma(\frac{9}{10})}{[\Gamma(\frac{1}{10})]^2} + \frac{5\Gamma(\frac{1}{5})}{[\Gamma(\frac{1}{10})]^2} + \frac{1}{8j} \right] \right] \xi \omega_1(f', \xi), \quad \xi > 0, \quad (21)$$

(xiv) for  $\alpha = 5$  and  $\beta = \frac{11}{10}$

$$\|M_{r,\xi}(f; \cdot) - f\|_\infty \leq \left[ \sum_{j=1}^r \binom{r}{j} \left[ \frac{j}{2} \frac{\Gamma(\frac{3}{10}) \Gamma(\frac{4}{5})}{\Gamma(\frac{1}{10})} + \frac{\Gamma(\frac{1}{5}) \Gamma(\frac{9}{10})}{2\Gamma(\frac{1}{10})} + \frac{1}{8j} \right] \right] \xi \omega_1(f', \xi), \quad \xi > 0, \quad (22)$$

(xv) for  $\alpha = 5$  and  $\beta = 1$

$$\|M_{r,\xi}(f; \cdot) - f\|_\infty \leq \left[ \sum_{j=1}^r \binom{r}{j} \left[ \frac{j}{4} (3 - \sqrt{5}) + \frac{1}{\sqrt{10 + 2\sqrt{5}}} + \frac{1}{8j} \right] \right] \xi \omega_1(f', \xi), \quad \xi > 0, \quad (23)$$

(xvi) for  $\alpha = 5$  and  $\beta = 2$

$$\|M_{r,\xi}(f; \cdot) - f\|_\infty \leq \left[ \sum_{j=1}^r \binom{r}{j} \left[ \frac{14j}{72} (3 - \sqrt{5}) + \frac{4}{9} \frac{\Gamma(\frac{1}{5}) \Gamma(\frac{4}{5})}{\Gamma(\frac{1}{10}) \Gamma(\frac{9}{10})} + \frac{1}{8j} \right] \right] \xi \omega_1(f', \xi), \quad \xi > 0. \quad (24)$$

**Proof.** We used [1], Theorem 9, (59). ■

We present

**Theorem 4.** Let  $n = 2$  and  $\alpha = 2$ . Here

$$E_{r,\xi}(f; x) = M_{r,\xi}(f; x) - f(x) - \frac{f''(x)}{2} \frac{\Gamma(\frac{3}{2\alpha}) \Gamma(\beta - \frac{3}{2\alpha})}{\Gamma(\frac{1}{2\alpha}) \Gamma(\beta - \frac{1}{2\alpha})} \left( \sum_{j=1}^r \alpha_j j^2 \right) \xi^2.$$

Then

(i) for  $\beta = \frac{3}{2}$

$$\|E_{r,\xi} f\|_\infty \leq \left[ \sum_{j=1}^r \binom{r}{j} \frac{1}{[\Gamma(\frac{1}{4})]^2} \left[ \frac{2j\sqrt{\pi}}{3} + \left[ \Gamma\left(\frac{3}{4}\right) \right]^2 + \frac{\sqrt{\pi}}{2j} \right] \right] \xi^2 \omega_1(f'', \xi), \quad \xi > 0, \quad (25)$$

(ii) for  $\beta = \frac{5}{2}$

$$\|E_{r,\xi} f\|_\infty \leq \left[ \sum_{j=1}^r \binom{r}{j} \left[ \frac{2\sqrt{\pi}}{5j [\Gamma(\frac{1}{4})]^2} + \frac{4j\sqrt{\pi}}{15 [\Gamma(\frac{1}{4})]^2} + \frac{3 [\Gamma(\frac{3}{4})]^2}{5 [\Gamma(\frac{1}{4})]^2} \right] \right] \xi^2 \omega_1(f'', \xi), \quad \xi > 0, \quad (26)$$



(iii) for  $\beta = 2$

$$\|E_{r,\xi}f\|_\infty \leq \left[ \sum_{j=1}^r \binom{r}{j} \frac{1}{72} \left[ 6 + \frac{3\sqrt{2}}{j} + \frac{8\sqrt{2}j}{\pi} \right] \right] \xi^2 \omega_1(f'', \xi), \xi > 0, \quad (27)$$

(iv) for  $\beta = 3$

$$\|E_{r,\xi}f\|_\infty \leq \left[ \sum_{j=1}^r \binom{r}{j} \frac{1}{252} \left[ 15 + \frac{9\sqrt{2}}{j} + \frac{16\sqrt{2}j}{\pi} \right] \right] \xi^2 \omega_1(f'', \xi), \xi > 0, \quad (28)$$

(v) for  $\beta = \frac{5}{4}$

$$\|E_{r,\xi}f\|_\infty \leq \left[ \sum_{j=1}^r \binom{r}{j} \left[ \frac{j}{6} + \frac{\sqrt{\pi}}{8j} \frac{\Gamma(\frac{3}{4})}{\Gamma(\frac{1}{4})} + \frac{\sqrt{\pi}}{4} \frac{\Gamma(\frac{3}{4})}{\Gamma(\frac{1}{4})} \right] \right] \xi^2 \omega_1(f'', \xi), \xi > 0. \quad (29)$$

**Proof.** We used [1], Theorem 9, (59). ■

We give

**Theorem 5.** Let  $n = 3$  and  $\alpha = 3$ . Here

$$E_{r,\xi}(f; x) = M_{r,\xi}(f; x) - f(x) - \frac{f''(x)}{2} \frac{\Gamma(\frac{3}{2\alpha}) \Gamma(\beta - \frac{3}{2\alpha})}{\Gamma(\frac{1}{2\alpha}) \Gamma(\beta - \frac{1}{2\alpha})} \left( \sum_{j=1}^r \alpha_j j^2 \right) \xi^2.$$

Then

(i) for  $\beta = 1$

$$\|E_{r,\xi}f\|_\infty \leq \left[ \sum_{j=1}^r \binom{r}{j} \left( \frac{3 + \frac{8j}{\sqrt{3}} + 4j^2}{96j} \right) \right] \xi^3 \omega_1(f''', \xi), \xi > 0, \quad (30)$$

(ii) for  $\beta = \frac{3}{2}$

$$\|E_{r,\xi}f\|_\infty \leq \left[ \sum_{j=1}^r \binom{r}{j} \left[ \frac{3\sqrt{\pi} + 2j(2+j) \Gamma(\frac{2}{3}) \Gamma(\frac{5}{6})}{16j \Gamma(\frac{1}{6}) \Gamma(\frac{1}{3})} \right] \right] \xi^3 \omega_1(f''', \xi), \xi > 0, \quad (31)$$

(iii) for  $\beta = \frac{5}{2}$

$$\|E_{r,\xi}f\|_\infty \leq \left[ \sum_{j=1}^r \binom{r}{j} \left[ \frac{9\sqrt{\pi} + 2j(2j+5) \Gamma(\frac{2}{3}) \Gamma(\frac{5}{6})}{64j \Gamma(\frac{1}{6}) \Gamma(\frac{1}{3})} \right] \right] \xi^3 \omega_1(f''', \xi), \xi > 0, \quad (32)$$

(iv) for  $\beta = \frac{7}{6}$

$$\|E_{r,\xi}f\|_\infty \leq \left[ \sum_{j=1}^r \binom{r}{j} \left[ \frac{(3+4j) \sqrt{\pi} \Gamma\left(\frac{2}{3}\right) + 2j^2 \Gamma\left(\frac{1}{3}\right) \Gamma\left(\frac{5}{6}\right)}{48j \Gamma\left(\frac{1}{6}\right)} \right] \right] \xi^3 \omega_1(f''', \xi), \xi > 0, \quad (33)$$

(v) for  $\beta = 2$

$$\|E_{r,\xi}f\|_\infty \leq \left[ \sum_{j=1}^r \binom{r}{j} \left[ \frac{16\sqrt{3} + \frac{27}{j} + 12j}{1440} \right] \right] \xi^3 \omega_1(f''', \xi), \xi > 0. \quad (34)$$

**Proof.** We used Theorem 9 of [1], (59). ■

We also have

**Theorem 6.** Let  $n = 4$  and  $\alpha = 4$ . Then

(i) for  $\beta = 1$

$$\|E_{r,\xi}f\|_\infty \leq \left[ \sum_{j=1}^r \binom{r}{j} \left[ \frac{(5 + 2\sqrt{2}j^2 + 5j \csc\left(\frac{5\pi}{8}\right)) \sin \frac{7\pi}{8}}{240j} \right] \right] \xi^4 \omega_1(f^{(4)}, \xi), \xi > 0, \quad (35)$$

(ii) for  $\beta = \frac{7}{8}$

$$\|E_{r,\xi}f\|_\infty \leq \left[ \sum_{j=1}^r \binom{r}{j} \frac{1}{480} \left[ 4j + 5\sqrt[4]{2} \left( \frac{[\Gamma\left(\frac{5}{8}\right)]^2}{\sqrt{\pi} \Gamma\left(\frac{3}{4}\right)} + \frac{2 \sin\left(\frac{7\pi}{8}\right)}{j} \right) \right] \right] \xi^4 \omega_1(f^{(4)}, \xi), \xi > 0, \quad (36)$$

(iii) for  $\beta = 2$

$$\|E_{r,\xi}f\|_\infty \leq \left[ \sum_{j=1}^r \binom{r}{j} \left[ \frac{(5 + \sqrt{2}j^2 + \frac{15}{4}j \csc\left(\frac{5\pi}{8}\right)) \sin \frac{\pi}{8}}{420j} \right] \right] \xi^4 \omega_1(f^{(4)}, \xi), \xi > 0, \quad (37)$$

(iv) for  $\beta = \frac{3}{2}$

$$\|E_{r,\xi}f\|_\infty \leq \left[ \sum_{j=1}^r \binom{r}{j} \left[ \frac{(5\sqrt{\pi} + 2j^2 (\Gamma\left(\frac{3}{4}\right))^2 + 5j \Gamma\left(\frac{5}{8}\right) \Gamma\left(\frac{7}{8}\right))}{90j \Gamma\left(\frac{1}{8}\right) \Gamma\left(\frac{3}{8}\right)} \right] \right] \xi^4 \omega_1(f^{(4)}, \xi), \xi > 0, \quad (38)$$

(v) for  $\beta = \frac{4}{3}$

$$\|E_{r,\xi}f\|_\infty \leq \left[ \sum_{j=1}^r \binom{r}{j} \left[ \frac{5j\Gamma\left(\frac{5}{8}\right)\Gamma\left(\frac{17}{24}\right) + 2j^2\Gamma\left(\frac{7}{12}\right)\Gamma\left(\frac{3}{4}\right) + 5\sqrt{\pi}\Gamma\left(\frac{5}{6}\right)}{50j\Gamma\left(\frac{1}{8}\right)\Gamma\left(\frac{5}{24}\right)} \right] \right] \xi^4 \omega_1(f^{(4)}, \xi), \xi > 0. \quad (39)$$

**Proof.** We used [1], Theorem 9, (59). ■

We also have

**Theorem 7.** Let  $n = 5$  and  $\alpha = 5$ . Then

(i) for  $\beta = 1$

$$\|E_{r,\xi}f\|_\infty \leq \left[ \sum_{j=1}^r \binom{r}{j} \left[ \frac{\sin \frac{\pi}{10} \left( 15 + 4j \left( \frac{3}{\sin \frac{2\pi}{5}} + \frac{j}{\sin \frac{3\pi}{10}} \right) \right)}{2880j} \right] \right] \xi^5 \omega_1(f^{(5)}, \xi), \xi > 0, \quad (40)$$

(ii) for  $\beta = 2$

$$\|E_{r,\xi}f\|_\infty \leq \left[ \sum_{j=1}^r \binom{r}{j} \left[ \frac{25 + 4j \left( 8\sqrt{\frac{2}{5+\sqrt{5}}} + (\sqrt{5}-1)j \right)}{8640(\sqrt{5}+1)j} \right] \right] \xi^5 \omega_1(f^{(5)}, \xi), \xi > 0, \quad (41)$$

(iii) for  $\beta = \frac{3}{2}$

$$\|E_{r,\xi}f\|_\infty \leq \left[ \sum_{j=1}^r \binom{r}{j} \left[ \frac{15\sqrt{\pi} + 4j \left( j\Gamma\left(\frac{7}{10}\right)\Gamma\left(\frac{4}{5}\right) + 3\Gamma\left(\frac{3}{5}\right)\Gamma\left(\frac{9}{10}\right) \right)}{1152j\Gamma\left(\frac{1}{10}\right)\Gamma\left(\frac{2}{5}\right)} \right] \right] \xi^5 \omega_1(f^{(5)}, \xi), \xi > 0, \quad (42)$$

(iv) for  $\beta = \frac{4}{3}$

$$\|E_{r,\xi}f\|_\infty \leq \left[ \sum_{j=1}^r \binom{r}{j} \left[ \frac{4j \left( j\Gamma\left(\frac{19}{30}\right)\Gamma\left(\frac{7}{10}\right) + 3\Gamma\left(\frac{3}{5}\right)\Gamma\left(\frac{11}{15}\right) \right) + 15\sqrt{\pi}\Gamma\left(\frac{5}{6}\right)}{672j\Gamma\left(\frac{1}{10}\right)\Gamma\left(\frac{7}{30}\right)} \right] \right] \xi^5 \omega_1(f^{(5)}, \xi), \xi > 0, \quad (43)$$

(v) for  $\beta = \frac{4}{5}$

$$\|E_{r,\xi}f\|_\infty \leq \left[ \sum_{j=1}^r \binom{r}{j} \left[ \frac{j}{720} + \frac{5\sqrt{\pi}\Gamma\left(\frac{3}{10}\right) + 4j\Gamma\left(\frac{1}{5}\right)\Gamma\left(\frac{3}{5}\right)}{960j\Gamma\left(\frac{1}{10}\right)\Gamma\left(\frac{7}{10}\right)} \right] \right] \xi^5 \omega_1(f^{(5)}, \xi), \xi > 0, \quad (44)$$

(vi) for  $\beta = \frac{5}{2}$

$$\|E_{r,\xi}f\|_\infty \leq \left[ \sum_{j=1}^r \binom{r}{j} \left[ \frac{15\sqrt{\pi} + 4j \left( j\Gamma\left(\frac{7}{10}\right)\Gamma\left(\frac{9}{5}\right) + 3\Gamma\left(\frac{3}{5}\right)\Gamma\left(\frac{19}{10}\right) \right)}{2880j\Gamma\left(\frac{1}{10}\right)\Gamma\left(\frac{12}{5}\right)} \right] \right] \xi^5 \omega_1(f^{(5)}, \xi), \xi > 0. \quad (45)$$

**Proof.** We used [1], Theorem 9, (59). ■

We further add

**Theorem 8.** Let  $n = 1$ . Then

(i) for  $\alpha = 1$  and  $\beta = 2$

$$\|M_{r,\xi}f - f\|_\infty \leq \left[ \sum_{j=1}^r \binom{r}{j} \left( \frac{j}{2} + \frac{1}{\pi} + \frac{1}{8j} \right) \right] \xi \omega_1(f', \xi), \xi > 0, \quad (46)$$

(ii) for  $\alpha = 2$  and  $\beta = 2$

$$\|M_{r,\xi}f - f\|_\infty \leq \left[ \sum_{j=1}^r \binom{r}{j} \left( \frac{3 + 4j(\sqrt{2} + j)}{24j} \right) \right] \xi \omega_1(f', \xi), \xi > 0, \quad (47)$$

(iii) for  $\alpha = 2$  and  $\beta = \frac{5}{2}$

$$\|M_{r,\xi}f - f\|_\infty \leq \left[ \sum_{j=1}^r \binom{r}{j} \left( \frac{1}{8j} + \frac{\sqrt{\pi} + \frac{3j}{4} \left[ \Gamma\left(\frac{3}{4}\right) \right]^2}{\frac{5}{8} \left[ \Gamma\left(\frac{1}{4}\right) \right]^2} \right) \right] \xi \omega_1(f', \xi), \xi > 0, \quad (48)$$

(iv) for  $\alpha = 2$  and  $\beta = \frac{3}{2}$

$$\|M_{r,\xi}f - f\|_\infty \leq \left[ \sum_{j=1}^r \binom{r}{j} \left( \frac{1}{8j} + \frac{2\sqrt{\pi}}{\left[ \Gamma\left(\frac{1}{4}\right) \right]^2} + 2j \frac{\left[ \Gamma\left(\frac{3}{4}\right) \right]^2}{\left[ \Gamma\left(\frac{1}{4}\right) \right]^2} \right) \right] \xi \omega_1(f', \xi), \xi > 0. \quad (49)$$

**Proof.** We used [1], Corollary 4. ■

### 3 A Voronovskaya Type Theorem

Let  $\alpha_j$  as in (5).

Let  $f : \mathbb{R} \rightarrow \mathbb{R}$  be such that  $f^{(n)}$  exists and it is bounded and Lebesgue measurable. Also for  $x \in \mathbb{R}$ ,  $\xi > 0$  and  $\alpha \in \mathbb{N}$ ,  $\beta > \frac{1}{2\alpha}$  the Lebesgue singular integrals  $M_{r,\xi}(f; x)$  as in (6).

Next we present some Voronovskaya type results.

**Theorem 9.** Let  $f : \mathbb{R} \rightarrow \mathbb{R}$  be such that  $f^{(5)}$  exists, and is bounded and Lebesgue measurable on  $\mathbb{R}$ , and let  $\xi \rightarrow 0+$ ,  $0 < \gamma \leq 1$ . Then

(i) for  $\alpha = 1, \beta = 6$ , we have

$$M_{r,\xi}(f; x) - f(x) = f''(x) \left( \sum_{j=1}^r \alpha_j j^2 \right) \frac{\xi^2}{18} + f^{(4)}(x) \left( \sum_{j=1}^r \alpha_j j^4 \right) \frac{\xi^4}{504} + o(\xi^{5-\gamma}),$$

(ii) for  $\alpha = 2, \beta = 3$ , we have

$$M_{r,\xi}(f; x) - f(x) = f''(x) \left( \sum_{j=1}^r \alpha_j j^2 \right) \frac{5}{42} \xi^2 + f^{(4)}(x) \left( \sum_{j=1}^r \alpha_j j^4 \right) \frac{\xi^4}{168} + o(\xi^{5-\gamma}),$$

(iii) for  $\alpha = 3, \beta = 2$ , we have

$$M_{r,\xi}(f; x) - f(x) = f''(x) \frac{3\xi^2}{20} \left( \sum_{j=1}^r \alpha_j j^2 \right) + f^{(4)}(x) \frac{\xi^4}{120} \left( \sum_{j=1}^r \alpha_j j^4 \right) + o(\xi^{5-\gamma}).$$

**Proof.** We used Theorem 4 in [2], with  $n = 5$ . ■

**Corollary 10.(n=3 case)** Let  $f$  such that  $f^{(3)}$  exists and is bounded and Lebesgue measurable on  $\mathbb{R}$ . Let  $\xi \rightarrow 0+$ ,  $0 < \gamma \leq 1$ . Then

i) for  $\alpha = 1, \beta = 4$  we obtain

$$M_{r,\xi}(f; x) - f(x) = \frac{\xi^2 f''(x)}{10} \left( \sum_{j=1}^r \alpha_j j^2 \right) + o(\xi^{3-\gamma}), \quad (50)$$

ii) for  $\alpha = 2, \beta = 2$  we obtain

$$M_{r,\xi}(f; x) - f(x) = \frac{\xi^2 f''(x)}{6} \left( \sum_{j=1}^r \alpha_j j^2 \right) + o(\xi^{3-\gamma}), \quad (51)$$

iii) for  $\alpha = 3, \beta = 2$  we obtain

$$M_{r,\xi}(f; x) - f(x) = \frac{3}{20} \xi^2 f''(x) \left( \sum_{j=1}^r \alpha_j j^2 \right) + o(\xi^{3-\gamma}). \quad (52)$$

**Proof.** In Theorem 4 of [2] we place  $n = 3$ , and the corresponding values for  $\alpha$  and  $\beta$ . ■

**Corollary 11.(n=4 case)** Let  $f$  such that  $f^{(4)}$  exists and is bounded and Lebesgue measurable on  $\mathbb{R}$ . Let  $\xi \rightarrow 0+$ ,  $0 < \gamma \leq 1$ . Then

i) for  $\alpha = 1, \beta = 5$  we obtain

$$M_{r,\xi}(f; x) - f(x) = \frac{1}{14}\xi^2 f''(x) \left( \sum_{j=1}^r \alpha_j j^2 \right) + o(\xi^{4-\gamma}), \quad (53)$$

ii) for  $\alpha = 2, \beta = 3$  we obtain

$$M_{r,\xi}(f; x) - f(x) = \frac{5}{42}\xi^2 f''(x) \left( \sum_{j=1}^r \alpha_j j^2 \right) + o(\xi^{4-\gamma}), \quad (54)$$

iii) for  $\alpha = 3, \beta = 2$  we obtain

$$M_{r,\xi}(f; x) - f(x) = \frac{3}{20}\xi^2 f''(x) \left( \sum_{j=1}^r \alpha_j j^2 \right) + o(\xi^{4-\gamma}). \quad (55)$$

**Proof.** In Theorem 4 of [2] we place  $n = 4$ , and the corresponding values for  $\alpha$  and  $\beta$ . ■

## 4 Higher Order Uniform Convergence with Rates

Let  $\alpha \in \mathbb{N}, \beta > \frac{1}{2\alpha}$ , and  $f: \mathbb{R} \rightarrow \mathbb{R}$  be Lebesgue measurable. We define for  $x \in \mathbb{R}$ ,  $\xi > 0$  the Lebesgue integral  $M_{r,\xi}(f; x)$  as in (6) and assume that  $M_{r,\xi}(f; x) \in \mathbb{R}$  for all  $x \in \mathbb{R}$ .

Let  $f \in C^n(\mathbb{R})$ ,  $n \in \mathbb{Z}^+$  with the  $r$ th modulus of smoothness finite, i.e.

$$\omega_r(f^{(n)}, h) := \sup_{|t| \leq h} \|\Delta_t^r f^{(n)}(x)\|_{\infty, x} < \infty, \quad h > 0, \quad (56)$$

where

$$\Delta_t^r f^{(n)}(x) := \sum_{j=0}^r (-1)^{r-j} \binom{r}{j} f^{(n)}(x + jt). \quad (57)$$

We need to introduce

$$\delta_k := \sum_{j=1}^r \alpha_j j^k, \quad k = 1, \dots, n \in \mathbb{N}. \quad (58)$$

Denote by  $\lfloor \cdot \rfloor$  the integral part.

We present the Lipschitz type result corresponding to the Theorem 1 of [4].

**Theorem 12.** Let  $f$  be defined as above in this section, with  $n \in \mathbb{N}$ . Furthermore we assume the following Lipschitz condition:  $\omega_r(f^{(n)}, \delta) \leq K\delta^{r-1+\gamma}$ ,

$K > 0$ ,  $0 < \gamma \leq 1$ , for any  $\delta > 0$ . For  $\alpha \in \mathbb{N}$ ,  $\beta > \frac{n+r+\gamma}{2\alpha}$ , it holds that

$$\begin{aligned} & \left| M_{r,\xi}(f; x) - f(x) - \sum_{m=1}^{\lfloor n/2 \rfloor} \left[ \frac{f^{(2m)}(x)}{(2m)!} \delta_{2m} \xi^{2m} \left( \frac{\Gamma\left(\frac{2m+1}{2\alpha}\right) \Gamma\left(\beta - \frac{2m+1}{2\alpha}\right)}{\Gamma\left(\frac{1}{2\alpha}\right) \Gamma\left(\beta - \frac{1}{2\alpha}\right)} \right) \right] \right| \\ & \leq \frac{K \Gamma(\gamma+r) \Gamma\left(\frac{n+r+\gamma}{2\alpha}\right) \Gamma\left(\beta - \frac{n+r+\gamma}{2\alpha}\right)}{\Gamma(n+\gamma+r) \Gamma\left(\frac{1}{2\alpha}\right) \Gamma\left(\beta - \frac{1}{2\alpha}\right)} \xi^{n+r+\gamma-1}. \end{aligned} \quad (59)$$

In L.H.S.(59) the sum collapses when  $n = 1$ .

**Proof.** As in the proof of Theorem 1, of [4], we get again that

$$M_{r,\xi}(f; x) - f(x) = \sum_{k=1}^n \frac{f^{(k)}(x)}{k!} \delta_k W \left( \int_{-\infty}^{\infty} \frac{t^k}{(t^{2\alpha} + \xi^{2\alpha})^\beta} dt \right) + \mathcal{R}_n^*, \quad (60)$$

where

$$\mathcal{R}_n^* := W \int_{-\infty}^{\infty} \mathcal{R}_n(0, t) \frac{1}{(t^{2\alpha} + \xi^{2\alpha})^\beta} dt. \quad (61)$$

and

$$\mathcal{R}_n(0, t) := \int_0^t \frac{(t-w)^{n-1}}{(n-1)!} \left( \sum_{j=0}^r \alpha_j j^n f^{(n)}(x+jw) - \delta_n f^{(n)}(x) \right) dw. \quad (62)$$

Also we get

$$|\mathcal{R}_n(0, t)| \leq \int_0^{|t|} \frac{(|t|-w)^{n-1}}{(n-1)!} \omega_r(f^{(n)}, w) dw. \quad (63)$$

Using the Lipschitz type condition we obtain

$$\begin{aligned} |\mathcal{R}_n(0, t)| & \leq \int_0^{|t|} \frac{(|t|-w)^{n-1}}{(n-1)!} K w^{r-1+\gamma} dw \\ & = \frac{K |t|^{n+r+\gamma-2}}{(n-1)!} \int_0^{|t|} \left(1 - \frac{w}{|t|}\right)^{n-1} \left(\frac{w}{|t|}\right)^{r-1+\gamma} dw \\ & = \frac{K |t|^{n+r+\gamma-1}}{(n-1)!} \int_0^1 (1-y)^{n-1} y^{r-1+\gamma} dy \\ & = \frac{K |t|^{n+r+\gamma-1}}{(n-1)!} \frac{\Gamma(n) \Gamma(\gamma+r)}{\Gamma(n+\gamma+r)}. \end{aligned} \quad (64)$$

and

$$\begin{aligned}
|\mathcal{R}_n^*| &\leq W \int_{-\infty}^{\infty} \frac{K|t|^{n+r+\gamma-1}}{(n-1)!} \frac{\Gamma(n)\Gamma(\gamma+r)}{\Gamma(n+\gamma+r)} \frac{1}{(t^{2\alpha} + \xi^{2\alpha})^\beta} dt \\
&= \frac{WK\Gamma(\gamma+r)}{\Gamma(n+\gamma+r)} \int_{-\infty}^{\infty} \frac{|t|^{n+r+\gamma-1}}{(t^{2\alpha} + \xi^{2\alpha})^\beta} dt \\
&= \frac{2WK\Gamma(\gamma+r)}{\Gamma(n+\gamma+r)} \int_0^{\infty} \frac{t^{n+r+\gamma-1}}{(t^{2\alpha} + \xi^{2\alpha})^\beta} dt \\
&= \frac{WK\Gamma(\gamma+r)\Gamma\left(\frac{n+r+\gamma}{2\alpha}\right)\Gamma\left(\beta - \frac{n+r+\gamma}{2\alpha}\right)}{\xi^{2\alpha\beta-(n+r+\gamma)}\alpha\Gamma(n+\gamma+r)\Gamma(\beta)} \\
&= \frac{K\Gamma(\gamma+r)\Gamma\left(\frac{n+r+\gamma}{2\alpha}\right)\Gamma\left(\beta - \frac{n+r+\gamma}{2\alpha}\right)}{\Gamma(n+\gamma+r)\Gamma\left(\frac{1}{2\alpha}\right)\Gamma\left(\beta - \frac{1}{2\alpha}\right)} \xi^{n+r+\gamma-1}. \tag{65}
\end{aligned}$$

We notice also that

$$\begin{aligned}
M_{r,\xi}(f; x) - f(x) - \sum_{m=1}^{\lfloor n/2 \rfloor} \frac{f^{(2m)}(x)}{(2m)!} \delta_{2m} W \left( \int_{-\infty}^{\infty} \frac{t^{2m}}{(t^{2\alpha} + \xi^{2\alpha})^\beta} dt \right) = \\
M_{r,\xi}(f; x) - f(x) - \sum_{m=1}^{\lfloor n/2 \rfloor} \left[ \frac{f^{(2m)}(x)}{(2m)!} \delta_{2m} \xi^{2m} \left( \frac{\Gamma\left(\frac{2m+1}{2\alpha}\right)\Gamma\left(\beta - \frac{2m+1}{2\alpha}\right)}{\Gamma\left(\frac{1}{2\alpha}\right)\Gamma\left(\beta - \frac{1}{2\alpha}\right)} \right) \right] = \mathcal{R}_n^*. \tag{66}
\end{aligned}$$

By (65) and (66) we complete the proof of the theorem.  $\blacksquare$

We give

**Corollary 13.** Let  $f$  be defined as above in this section. Furthermore we assume the following Lipschitz condition:  $\omega_2(f', \delta) \leq K\delta^{1+\gamma}$ ,  $K > 0$ ,  $0 < \gamma \leq 1$ , for any  $\delta > 0$ . Then

$$|M_{2,\xi}(f; x) - f(x)| \leq \frac{K}{2(\gamma+2) \sin\left(\frac{(3+\gamma)\pi}{6}\right)} \xi^{2+\gamma}. \tag{67}$$

**Proof.** In Theorem 12 we used  $n = 1$ ,  $\alpha = 3$ ,  $\beta = 1$  and  $r = 2$ .  $\blacksquare$

For the case  $n = 0$  we have

**Theorem 14.** Let  $f$  be defined as above in this section, with  $n = 0$ . Furthermore we assume the following Lipschitz condition:  $\omega_r(f, \delta) \leq K\delta^{r-1+\gamma}$ ,  $K > 0$ ,  $0 < \gamma \leq 1$ , for any  $\delta > 0$ . For  $\alpha \in \mathbb{N}$ ,  $\beta > \frac{r+\gamma}{2\alpha}$ , it holds that

$$|M_{r,\xi}(f; x) - f(x)| \leq \frac{K\Gamma\left(\frac{r+\gamma}{2\alpha}\right)\Gamma\left(\beta - \frac{r+\gamma}{2\alpha}\right)}{\Gamma\left(\frac{1}{2\alpha}\right)\Gamma\left(\beta - \frac{1}{2\alpha}\right)} \xi^{r+\gamma-1}. \tag{68}$$



**Proof.** As in the proof of Corollary 1, of [4], with  $n = 0$ , using the Lipschitz type condition, we get that

$$\begin{aligned}
|M_{r,\xi}(f; x) - f(x)| &\leq 2W \int_0^\infty \omega_r(f, t) \frac{1}{(t^{2\alpha} + \xi^{2\alpha})^\beta} dt \\
&\leq 2W \int_0^\infty K t^{r-1+\gamma} \frac{1}{(t^{2\alpha} + \xi^{2\alpha})^\beta} dt \\
&= 2KW \int_0^\infty \frac{t^{r-1+\gamma}}{(t^{2\alpha} + \xi^{2\alpha})^\beta} dt \\
&= \frac{K\Gamma\left(\frac{r+\gamma}{2\alpha}\right)\Gamma\left(\beta - \frac{r+\gamma}{2\alpha}\right)}{\Gamma\left(\frac{1}{2\alpha}\right)\Gamma\left(\beta - \frac{1}{2\alpha}\right)} \xi^{r+\gamma-1}.
\end{aligned}$$

This completes the proof of Theorem 14.  $\blacksquare$

**Corollary 15.** Let  $f$  be defined as above in this section, with  $n = 0$ . Furthermore we assume the following Lipschitz condition:  $\omega_r(f, \delta) \leq K\delta^{1+\gamma}$ ,  $K > 0$ ,  $0 < \gamma \leq 1$ , for any  $\delta > 0$ . Then

$$|M_{2,\xi}(f; x) - f(x)| \leq \frac{K}{2 \sin\left[\left(\frac{2+\gamma}{6}\right)\pi\right]} \xi^{\gamma+1}. \quad (69)$$

**Proof.** In Theorem 14 we used  $\alpha = 3, \beta = 1$  and  $r = 2$ .  $\blacksquare$

In the next we consider  $f \in C^n(\mathbb{R})$ ,  $n \geq 2$  even,  $\alpha \in \mathbb{N}, \beta > \frac{1}{2\alpha}$  and the simple smooth singular operator of symmetric convolution type

$$M_\xi(f, x_0) := W \int_{-\infty}^\infty f(x_0 + y) \frac{1}{(y^{2\alpha} + \xi^{2\alpha})^\beta} dy, \quad \text{for all } x_0 \in \mathbb{R}, \xi > 0. \quad (70)$$

That is

$$M_\xi(f; x_0) = W \int_0^\infty (f(x_0 + y) + f(x_0 - y)) \frac{1}{(y^{2\alpha} + \xi^{2\alpha})^\beta} dy, \quad \text{for all } x_0 \in \mathbb{R}, \xi > 0. \quad (71)$$

We assume that  $f$  is such that

$$M_\xi(f; x_0) \in \mathbb{R}, \quad \forall x_0 \in \mathbb{R}, \forall \xi > 0 \quad \text{and} \quad \omega_2(f^{(n)}, h) < \infty, \quad h > 0.$$

Note that  $M_{1,\xi} = M_\xi$  and if  $M_\xi(f; x_0) \in \mathbb{R}$  then  $M_{r,\xi}(f; x_0) \in \mathbb{R}$ .

**Proposition 16.** Assume  $\omega_2(f, h) < \infty$ ,  $h > 0$ ,  $\alpha \in \mathbb{N}, \beta > \frac{2+\gamma}{2\alpha}$ . Furthermore we assume the following Lipschitz condition:  $\omega_2(f, \delta) \leq K\delta^{1+\gamma}$ ,  $K > 0$ ,  $0 < \gamma \leq 1$ , for any  $\delta > 0$ . Then

$$\|M_\xi(f) - f\|_\infty \leq \frac{K\Gamma\left(\frac{2+\gamma}{2\alpha}\right)\Gamma\left(\beta - \frac{2+\gamma}{2\alpha}\right)\xi^{\gamma+1}}{2\Gamma\left(\frac{1}{2\alpha}\right)\Gamma\left(\beta - \frac{1}{2\alpha}\right)}. \quad (72)$$

**Proof.** Using Proposition 1 of [4] we obtain

$$\begin{aligned}
|M_\xi(f; x_0) - f(x_0)| &\leq W \int_0^\infty \omega_2(f, y) \frac{1}{(y^{2\alpha} + \xi^{2\alpha})^\beta} dy \\
&\leq W \int_0^\infty \frac{K y^{1+\gamma}}{(y^{2\alpha} + \xi^{2\alpha})^\beta} dy \\
&= \frac{K \Gamma\left(\frac{2+\gamma}{2\alpha}\right) \Gamma\left(\beta - \frac{2+\gamma}{2\alpha}\right) \xi^{\gamma+1}}{2\Gamma\left(\frac{1}{2\alpha}\right) \Gamma\left(\beta - \frac{1}{2\alpha}\right)}, \tag{73}
\end{aligned}$$

proving the claim of the proposition.  $\blacksquare$

In particular we have

**Corollary 17.** Assume  $\omega_2(f, h) < \infty$ ,  $h > 0$ . Furthermore we assume the following Lipschitz condition:  $\omega_2(f, \delta) \leq K\delta^{1+\gamma}$ ,  $K > 0$ ,  $0 < \gamma \leq 1$ , for any  $\delta > 0$ . Then

$$\|M_\xi(f) - f\|_\infty \leq \frac{K\sqrt{2}}{4 \sin\left[\left(\frac{2+\gamma}{4}\right)\pi\right]} \xi^{\gamma+1}. \tag{74}$$

**Proof.** In Proposition 16 we used  $\alpha = 2, \beta = 1$ .  $\blacksquare$

Let

$$\begin{aligned}
K_2(x_0) &:= M_\xi(f; x_0) - f(x_0) \\
&= -\frac{1}{\Gamma\left(\frac{1}{2\alpha}\right) \Gamma\left(\beta - \frac{1}{2\alpha}\right)} \sum_{\rho=1}^{n/2} \left[ \frac{f^{(2\rho)}(x_0)}{(2\rho)!} \xi^{2\rho} \Gamma\left(\frac{2\rho+1}{2\alpha}\right) \Gamma\left(\beta - \frac{2\rho+1}{2\alpha}\right) \right]
\end{aligned} \tag{75}$$

We give

**Theorem 18.** Let  $f \in C^n(\mathbb{R})$ ,  $n$  even,  $M_\xi(f)$  real valued and  $\alpha \in \mathbb{N}$ ,  $\beta > \frac{\gamma+n+2}{2\alpha}$ . Furthermore we assume the following Lipschitz condition:  $\omega_2(f^{(n)}, \delta) \leq K\delta^{1+\gamma}$ ,  $K > 0$ ,  $0 < \gamma \leq 1$ , for any  $\delta > 0$ . Then

$$|K_2(x_0)| \leq \frac{K \Gamma\left(\frac{\gamma+n+2}{2\alpha}\right) \Gamma\left(\beta - \frac{\gamma+n+2}{2\alpha}\right)}{n! 2\Gamma\left(\frac{1}{2\alpha}\right) \Gamma\left(\beta - \frac{1}{2\alpha}\right)} \xi^{n+\gamma+1}. \tag{76}$$

**Proof.** Using Theorem 6 of [4] we obtain

$$\begin{aligned}
|K_2(x_0)| &\leq \frac{1}{n!} W \int_0^\infty \omega_2(f^{(n)}, y) \frac{y^n}{(y^{2\alpha} + \xi^{2\alpha})^\beta} dy \\
&\leq \frac{1}{n!} \frac{\Gamma(\beta) \alpha \xi^{2\alpha\beta-1}}{\Gamma\left(\frac{1}{2\alpha}\right) \Gamma\left(\beta - \frac{1}{2\alpha}\right)} \int_0^\infty K y^{1+\gamma} \frac{y^n}{(y^{2\alpha} + \xi^{2\alpha})^\beta} dy \\
&= \frac{K \Gamma\left(\frac{\gamma+n+2}{2\alpha}\right) \Gamma\left(\beta - \frac{\gamma+n+2}{2\alpha}\right)}{n! 2\Gamma\left(\frac{1}{2\alpha}\right) \Gamma\left(\beta - \frac{1}{2\alpha}\right)} \xi^{n+\gamma+1}, \tag{77}
\end{aligned}$$

proving the claim of the theorem. ■

In particular we have

**Corollary 19.** *Let  $f \in C^4(\mathbb{R})$  such that  $M_\xi(f)$  is real valued. Furthermore we assume the following Lipschitz condition:  $\omega_2(f^{(4)}, \delta) \leq K\delta^{1+\gamma}$ ,  $K > 0$ ,  $0 < \gamma \leq 1$ , for any  $\delta > 0$ . Then*

$$|K_2(x_0)| \leq \frac{(\gamma + 2) \sqrt{2} K}{288 \sin \left[ \left( \frac{\gamma+2}{4} \right) \pi \right]} \xi^{\gamma+5}. \quad (78)$$

**Proof.** In Theorem 18 we used  $\alpha = 2, \beta = 2$  and  $n = 4$ . ■

We also give

**Corollary 20.** *Let  $f \in C^2(\mathbb{R})$ , such that*

$$\omega_2(f'', |y|) \leq 2A|y|^\gamma, \quad 0 < \gamma \leq 2, \quad A > 0.$$

*Then for  $x_0 \in \mathbb{R}$  we have*

$$\left| M_\xi(f; x_0) - f(x_0) - \frac{f''(x_0)}{6} \xi^2 \right| \leq \frac{2\sqrt{2}A\Gamma\left(\frac{\gamma+3}{4}\right)\Gamma\left(\frac{5-\gamma}{4}\right)}{3\pi(\gamma+1)(\gamma+2)} \xi^{\gamma+2}. \quad (79)$$

*Inequality (79) is sharp, namely it is attained at  $x_0 = 0$  by*

$$f_*(y) = \frac{A|y|^{\gamma+2}}{(\gamma+1)(\gamma+2)}.$$

**Proof.** In Theorem 7 of [4] we used  $\alpha = \beta = 2$  and  $n = 2$ . ■

We also give

**Corollary 21.** *Assume that  $\omega_2(f, \xi) < \infty$  and  $n = 0$ . Then*

$$\|M_{2,\xi}(f) - f\|_\infty \leq (2 + \sqrt{2}) \omega_2(f, \xi), \quad (80)$$

and as  $\xi \rightarrow 0$ ,

$$M_{2,\xi} \xrightarrow{u} I \text{ with rates.}$$

**Proof.** By formula (37) of [4] with  $\alpha = 2, \beta = 1$  and  $r = 2$ . ■

Let

$$K_1 := \left\| M_{r,\xi}(f; x) - f(x) - \sum_{m=1}^{\lfloor n/2 \rfloor} \left[ \frac{f^{(2m)}(x)}{(2m)!} \delta_{2m} \xi^{2m} \left( \frac{\Gamma\left(\frac{2m+1}{2\alpha}\right) \Gamma\left(\beta - \frac{2m+1}{2\alpha}\right)}{\Gamma\left(\frac{1}{2\alpha}\right) \Gamma\left(\beta - \frac{1}{2\alpha}\right)} \right) \right] \right\|_{\infty, x} \quad (81)$$

We present

**Corollary 22.** *Assuming  $f \in C^2(\mathbb{R})$  and  $\omega_2(f'', \xi) < \infty$ ,  $\xi > 0$  we have*

$$\begin{aligned} K_1 &= \left\| M_{2,\xi}(f; x) - f(x) - \frac{f''(x)}{4} \delta_2 \xi^2 \right\|_{\infty, x} \\ &\leq \frac{1}{3} \left( 1 + \frac{1}{\sqrt{3}} \right) \xi^2 \omega_2(f'', \xi). \end{aligned} \quad (82)$$

That is as  $\xi \rightarrow 0$  we get  $M_{2,\xi} \rightarrow I$ , pointwise with rates, given that  $\|f''\|_\infty < \infty$ .

**Proof.** In Theorem 11 of [4] we used  $\alpha = 3, \beta = 1$  and  $r = n = 2$ . ■

We also present

**Corollary 23.** *Assuming  $f \in C^2(\mathbb{R})$  and  $\omega_2(f'', \xi) < \infty$ ,  $\xi > 0$  we have*

$$\begin{aligned} \|K_2(x)\|_{\infty, x} &= \left\| M_\xi(f; x_0) - f(x_0) - \frac{f''(x_0)}{4} \xi^2 \right\|_{\infty, x} \\ &\leq \frac{1}{6} \left( 1 + \frac{1}{\sqrt{3}} \right) \xi^2 \omega_2(f'', \xi). \end{aligned} \quad (83)$$

That is as  $\xi \rightarrow 0$  we get  $M_\xi \rightarrow I$ , pointwise with rates, given that  $\|f''\|_\infty < \infty$ .

**Proof.** In Theorem 12 of [4] we used  $\alpha = 3, \beta = 1$  and  $n = 2$ . ■

## 5 $L_p$ Convergence with Rates

For  $r \in \mathbb{N}$  and  $n \in \mathbb{Z}_+$  we let  $\alpha_j$  as in (5).

Let  $f \in C^n(\mathbb{R})$  and  $f^{(n)} \in L_p(\mathbb{R})$ ,  $1 \leq p < \infty$ ,  $\alpha \in \mathbb{N}$ ,  $\beta > \frac{1}{2\alpha}$ , we define for  $x \in \mathbb{R}$ ,  $\xi > 0$  the Lebesgue integral

$$M_{r,\xi}(f; x) = W \int_{-\infty}^{\infty} \frac{\sum_{j=0}^r \alpha_j f(x + jt)}{(t^{2\alpha} + \xi^{2\alpha})^\beta} dt, \quad (84)$$

where the constant  $W$  is defined as in (3).

We need the  $r$ th  $L_p$ -modulus of smoothness

$$\omega_r(f^{(n)}, h)_p := \sup_{|t| \leq h} \|\Delta_t^r f^{(n)}(x)\|_{p,x}, \quad h > 0, \quad (85)$$

where

$$\Delta_t^r f^{(n)}(x) := \sum_{j=0}^r (-1)^{r-j} \binom{r}{j} f^{(n)}(x + jt), \quad (86)$$

Here we have that  $\omega_r(f^{(n)}, h)_p < \infty$ ,  $h > 0$ .

We need to introduce

$$\delta_k := \sum_{j=1}^r \alpha_j j^k, \quad k = 1, \dots, n \in \mathbb{N}. \quad (87)$$

We define

$$\Delta(x) := M_{r,\xi}(f; x) - f(x) - \sum_{m=1}^{\lfloor n/2 \rfloor} \frac{f^{(2m)}(x) \delta_{2m}}{(2m)!} \frac{\Gamma\left(\frac{2m+1}{2\alpha}\right) \Gamma\left(\beta - \frac{2m+1}{2\alpha}\right)}{\Gamma\left(\frac{1}{2\alpha}\right) \Gamma\left(\beta - \frac{1}{2\alpha}\right)} \xi^{2m}, \quad (88)$$

the sum collapses for  $n = 0, 1$ .

We have the following results.

**Theorem 24.** *Let  $n \in \mathbb{N}$ ,  $\alpha \in \mathbb{N}$ ,  $\beta > \frac{1}{\alpha} \left(\frac{1}{2} + n + r\right)$  and the rest as above. Then*

$$\|\Delta(x)\|_2 \leq \frac{(2\alpha)^{\frac{1}{2}} \Gamma(\beta)^{\frac{1}{2}} \xi^n \tau^{\frac{1}{2}}}{\Gamma\left(\frac{1}{2\alpha}\right)^{\frac{1}{2}} \Gamma\left(\beta - \frac{1}{2\alpha}\right)^{\frac{1}{2}} (2r+1)^{\frac{1}{2}} [(n-1)!] (2n-1)^{1/2}} \omega_r(f^{(n)}, \xi)_2, \quad (89)$$

where

$$0 < \tau := \left[ \int_0^\infty (1+u)^{2r+1} \frac{u^{2n-1}}{(u^{2\alpha} + 1)^\beta} du - \int_0^\infty \frac{u^{2n-1}}{(u^{2\alpha} + 1)^\beta} du \right] < \infty. \quad (90)$$

Hence as  $\xi \rightarrow 0$  we obtain  $\|\Delta(x)\|_2 \rightarrow 0$ .

If additionally  $f^{(2m)} \in L_2(\mathbb{R})$ ,  $m = 1, 2, \dots, \lfloor \frac{n}{2} \rfloor$  then  $\|M_{r,\xi}(f) - f\|_2 \rightarrow 0$ , as  $\xi \rightarrow 0$ .

**Proof.** In Theorem 1 of [3], we place  $p = q = 2$ . ■

**Corollary 25.** *Let  $\beta > \left(\frac{3}{2} + r\right)$  and the rest as above. Then*

$$\|M_{r,\xi}(f; \cdot) - f\|_2 \leq \frac{\xi \sqrt{2\Gamma(\beta)} \tau}{\sqrt[4]{\pi} \sqrt{(2r+1) \Gamma\left(\beta - \frac{1}{2}\right)}} \omega_r(f', \xi)_2, \quad (91)$$

where

$$0 < \tau := \left[ \int_0^\infty (1+u)^{2r+1} \frac{u}{(u^2 + 1)^\beta} du - \int_0^\infty \frac{u}{(u^2 + 1)^\beta} du \right] < \infty. \quad (92)$$

Hence as  $\xi \rightarrow 0$  we obtain  $\|M_{r,\xi}(f; \cdot) - f\|_2 \rightarrow 0$ .

**Proof.** In Theorem 1 of [3], we place  $p = q = 2$ ,  $n = 1$ ,  $\alpha = 1$ . ■

**Corollary 26.** *Let  $f$  be as above in this section. Then*

$$\|M_{3,\xi}(f; \cdot) - f\|_2 \leq \frac{16\sqrt{\tau}}{7\sqrt{5\pi}} \xi \omega_3(f', \xi)_2, \quad (93)$$

where

$$0 < \tau := \left[ \int_0^\infty (1+u)^7 \frac{u}{(u^2 + 1)^5} du - \int_0^\infty \frac{u}{(u^2 + 1)^5} du \right] < \infty. \quad (94)$$

Hence as  $\xi \rightarrow 0$  we obtain  $\|M_{3,\xi}(f; \cdot) - f\|_2 \rightarrow 0$ .

**Proof.** In Theorem 1 of [3], we place  $p = q = 2$ ,  $n = 1$ ,  $\alpha = 1$ ,  $\beta = 5$  and  $r = 3$ . ■

**Corollary 27.** Let  $\beta > \frac{1}{2}(\frac{5}{2} + r)$  and the rest as above. Then

$$\|\Delta(x)\|_2 \leq \sqrt{\frac{\Gamma(\beta) \tau}{3\Gamma(\frac{1}{4}) \Gamma(\beta - \frac{1}{4})}} \frac{2\xi^2}{\sqrt{2r+1}} \omega_r(f'', \xi)_2, \quad (95)$$

where

$$0 < \tau := \left[ \int_0^\infty (1+u)^{2r+1} \frac{u^3}{(u^4+1)^\beta} du - \int_0^\infty \frac{u^3}{(u^4+1)^\beta} du \right] < \infty. \quad (96)$$

Hence as  $\xi \rightarrow 0$  we obtain  $\|\Delta(x)\|_2 \rightarrow 0$ .

If additionally  $f'' \in L_2(\mathbb{R})$  then  $\|M_{r,\xi}(f) - f\|_2 \rightarrow 0$ , as  $\xi \rightarrow 0$ .

**Proof.** In Theorem 1 of [3], we place  $p = q = 2$ ,  $n = 2$ ,  $\alpha = 2$ . ■

**Corollary 28.** Let  $f$  be as above in this section. Then

$$\|M_{4,\xi}(f; x) - f(x) - \frac{f''(x)\delta_2}{2} \frac{\Gamma(\frac{3}{2\alpha}) \Gamma(\beta - \frac{3}{2\alpha})}{\Gamma(\frac{1}{2\alpha}) \Gamma(\beta - \frac{1}{2\alpha})} \xi^2\|_2 \leq \sqrt{\frac{65\tau}{2}} \frac{\xi^2}{24} \omega_4(f'', \xi)_2, \quad (97)$$

where

$$0 < \tau := \left[ \int_0^\infty (1+u)^9 \frac{u^3}{(u^4+1)^{4.25}} du - \int_0^\infty \frac{u^3}{(u^4+1)^{4.25}} du \right] < \infty. \quad (98)$$

Hence as  $\xi \rightarrow 0$  we obtain  $\|\Delta(x)\|_2 \rightarrow 0$ .

If additionally  $f'' \in L_2(\mathbb{R})$  then  $\|M_{4,\xi}(f) - f\|_2 \rightarrow 0$ , as  $\xi \rightarrow 0$ .

**Proof.** In Theorem 1 of [3], we place  $p = q = 2$ ,  $n = 2$ ,  $\alpha = 2$ ,  $\beta = 4.25$  and  $r = 4$ . ■

**Corollary 29.** Let  $\beta > \frac{1}{3}(\frac{7}{2} + r)$  and the rest as above. Then

$$\|\Delta(x)\|_2 \leq \sqrt{\frac{6\tau\Gamma(\beta)}{5(2r+1)\Gamma(\frac{1}{6})\Gamma(\beta - \frac{1}{6})}} \frac{\xi^3}{2} \omega_r(f''', \xi)_2, \quad (99)$$

where

$$0 < \tau := \left[ \int_0^\infty (1+u)^{2r+1} \frac{u^5}{(u^6+1)^\beta} du - \int_0^\infty \frac{u^5}{(u^6+1)^\beta} du \right] < \infty. \quad (100)$$

Hence as  $\xi \rightarrow 0$  we obtain  $\|\Delta(x)\|_2 \rightarrow 0$ .

If additionally  $f'' \in L_2(\mathbb{R})$  then  $\|M_{r,\xi}(f) - f\|_2 \rightarrow 0$ , as  $\xi \rightarrow 0$ .

**Proof.** In Theorem 1 of [3], we place  $p = q = 2$ ,  $n = 3$ ,  $\alpha = 3$ . ■

**Corollary 30.** *Let  $f$  be as above in this section. Then*

$$\|M_{5,\xi}(f; x) - f(x) - f''(x)\delta_2 \frac{\Gamma(\frac{8}{3})\sqrt{\pi}}{4\Gamma(\frac{1}{6})}\xi^2\|_2 \leq \left(\sqrt{\frac{91\tau}{110}}\right) \frac{\xi^3}{12}\omega_5(f''', \xi)_2, \quad (101)$$

where

$$0 < \tau := \left[ \int_0^\infty (1+u)^{11} \frac{u^5}{(u^6+1)^{\frac{19}{6}}} du - \int_0^\infty \frac{u^5}{(u^6+1)^{\frac{19}{6}}} du \right] < \infty. \quad (102)$$

Hence as  $\xi \rightarrow 0$  we obtain  $\|\Delta(x)\|_2 \rightarrow 0$ .

If additionally  $f'' \in L_2(\mathbb{R})$  then  $\|M_{5,\xi}(f) - f\|_2 \rightarrow 0$ , as  $\xi \rightarrow 0$ .

**Proof.** In Theorem 1 of [3], we place  $p = q = 2$ ,  $n = 3$ ,  $\alpha = 3$ ,  $\beta = \frac{19}{6}$  and  $r = 5$ .

**Corollary 31.**  $\alpha \in \mathbb{N}$ ,  $\beta > \frac{1}{\alpha}(\frac{9}{2} + r)$  and the rest as above. Then

$$\|\Delta(x)\|_2 \leq \sqrt{\frac{2\alpha\tau\Gamma(\beta)}{7(2r+1)\Gamma(\frac{1}{2\alpha})\Gamma(\beta - \frac{1}{2\alpha})}} \frac{\xi^4}{6}\omega_r(f^{(4)}, \xi)_2, \quad (103)$$

where

$$0 < \tau := \left[ \int_0^\infty (1+u)^{2r+1} \frac{u^7}{(u^{2\alpha}+1)^\beta} du - \int_0^\infty \frac{u^7}{(u^{2\alpha}+1)^\beta} du \right] < \infty. \quad (104)$$

Hence as  $\xi \rightarrow 0$  we obtain  $\|\Delta(x)\|_2 \rightarrow 0$ .

If additionally  $f^{(2m)} \in L_2(\mathbb{R})$ ,  $m = 1, 2$  then  $\|M_{r,\xi}(f) - f\|_2 \rightarrow 0$ , as  $\xi \rightarrow 0$ .

**Proof.** In Theorem 1 of [3], we place  $p = q = 2$ ,  $n = 4$ . ■

**Corollary 32.** *Let  $f$  be as above in this section. Then*

$$\|\Delta(x)\|_2 \leq \frac{5\sqrt{10634129\tau}}{786432}\xi^4\omega_6(f^{(4)}, \xi)_2, \quad (105)$$

where

$$0 < \tau := \left[ \int_0^\infty (1+u)^{13} \frac{u^7}{(u^8+1)^{\frac{81}{8}}} du - \int_0^\infty \frac{u^7}{(u^8+1)^{\frac{81}{8}}} du \right] < \infty. \quad (106)$$

Hence as  $\xi \rightarrow 0$  we obtain  $\|\Delta(x)\|_2 \rightarrow 0$ .

If additionally  $f^{(2m)} \in L_2(\mathbb{R})$ ,  $m = 1, 2$  then  $\|M_{6,\xi}(f) - f\|_2 \rightarrow 0$ , as  $\xi \rightarrow 0$ .

**Proof.** In Theorem 1 of [3], we place  $p = q = 2$ ,  $n = 4$ ,  $\alpha = 4$ ,  $\beta = \frac{81}{8}$  and  $r = 6$ . ■

**Corollary 33.** *Let  $f$  be as above in this section. Then*

$$\|\Delta(x)\|_2 \leq \left( \sqrt{\frac{11\tau}{10}} \right) \frac{\xi^4}{60} \omega_7(f^{(4)}, \xi)_2, \quad (107)$$

where

$$0 < \tau := \left[ \int_0^\infty (1+u)^{15} \frac{u^7}{(u^{10}+1)^{\frac{31}{10}}} du - \int_0^\infty \frac{u^7}{(u^{10}+1)^{\frac{31}{10}}} du \right] < \infty. \quad (108)$$

Hence as  $\xi \rightarrow 0$  we obtain  $\|\Delta(x)\|_2 \rightarrow 0$ .

If additionally  $f^{(2m)} \in L_2(\mathbb{R})$ ,  $m = 1, 2$  then  $\|M_{7,\xi}(f) - f\|_2 \rightarrow 0$ , as  $\xi \rightarrow 0$ .

**Proof.** In Theorem 1 of [3], we place  $p = q = 2$ ,  $n = 4$ ,  $\alpha = 5$ ,  $\beta = \frac{31}{10}$  and  $r = 7$ . ■

Next we present the Lipschitz type result corresponding to Theorem 1 of [3].

**Theorem 34.** *Let  $p, q > 1$  such that  $\frac{1}{p} + \frac{1}{q} = 1$ ,  $n \in \mathbb{N}$ ,  $\alpha \in \mathbb{N}$ ,  $\beta > \max \left\{ \frac{1}{q\alpha}, \frac{1}{2\alpha}, \frac{n+\gamma+r-1}{\alpha} + \frac{1}{p\alpha} \right\}$ , and the rest as above. Furthermore we assume the following Lipschitz condition:  $\omega_r(f^{(n)}, \delta)_p \leq K\delta^{r-1+\gamma}$ ,  $K > 0$ ,  $0 < \gamma \leq 1$ , for any  $\delta > 0$ . Then*

$$\begin{aligned} \|\Delta(x)\|_p &\leq \frac{[\Gamma(\beta)] \Gamma\left(\frac{q\beta}{2} - \frac{1}{2\alpha}\right)^{\frac{1}{q}} \Gamma\left(\frac{p(r-1+\gamma+n)+1}{2\alpha}\right)^{\frac{1}{p}}}{\Gamma\left(\frac{q\beta}{2}\right) \Gamma\left(\frac{1}{2\alpha}\right)^{\frac{1}{p}} \Gamma\left(\beta - \frac{1}{2\alpha}\right) ((n-1)!)} \\ &\quad \cdot \frac{\Gamma\left(\frac{p\beta}{2} - \frac{p(r-1+\gamma+n)+1}{2\alpha}\right)^{\frac{1}{p}} K}{(q(n-1)+1)^{\frac{1}{q}} [p(r-1+\gamma)+1]^{\frac{1}{p}}} \xi^{r-1+\gamma+n}. \end{aligned} \quad (109)$$

Hence as  $\xi \rightarrow 0$  we obtain  $\|\Delta(x)\|_p \rightarrow 0$ .

If additionally  $f^{(2m)} \in L_p(\mathbb{R})$ ,  $m = 1, 2, \dots, \lfloor \frac{n}{2} \rfloor$  then  $\|M_{r,\xi}(f) - f\|_p \rightarrow 0$ , as  $\xi \rightarrow 0$ .

**Proof.** As in the proof of Theorem 1, [3], we get again

$$I := \int_{-\infty}^\infty |\Delta(x)|^p dx \leq c_1 \left( \int_{-\infty}^\infty \left( \int_0^{|t|} \omega_r(f^{(n)}, w)_p^p dw \right) |t|^{np-1} \frac{1}{(t^{2\alpha} + \xi^{2\alpha})^{p\beta/2}} dt \right), \quad (110)$$

where

$$c_1 := \frac{\xi^{p\alpha\beta-1} \alpha [\Gamma(\beta)]^p \Gamma\left(\frac{q\beta}{2} - \frac{1}{2\alpha}\right)^{\frac{p}{q}}}{\Gamma\left(\frac{q\beta}{2}\right)^{\frac{p}{q}} \Gamma\left(\frac{1}{2\alpha}\right) \Gamma\left(\beta - \frac{1}{2\alpha}\right)^p ((n-1)!)^p (q(n-1)+1)^{p/q}}. \quad (111)$$



Using the Lipschitz condition, we obtain

$$\begin{aligned}
 I &\leq c_1 \left( \int_{-\infty}^{\infty} \left( \int_0^{|t|} (K w^{r-1+\gamma})^p dw \right) |t|^{np-1} \frac{1}{(t^{2\alpha} + \xi^{2\alpha})^{p\beta/2}} dt \right) \\
 &= \frac{c_1 K^p}{(p(r-1+\gamma)+1)} \left( \int_{-\infty}^{\infty} \frac{|t|^{p(r-1+\gamma+n)}}{(t^{2\alpha} + \xi^{2\alpha})^{p\beta/2}} dt \right) \\
 &= \frac{2c_1 K^p}{(p(r-1+\gamma)+1)} \left( \int_0^{\infty} \frac{t^{p(r-1+\gamma+n)}}{(t^{2\alpha} + \xi^{2\alpha})^{p\beta/2}} dt \right) \\
 &= \frac{2c_1 K^p \xi^{p(r-1+\gamma+n-\alpha\beta)+1}}{(p(r-1+\gamma)+1)} \left( \int_0^{\infty} \frac{u^{p(r-1+\gamma+n)}}{(u^{2\alpha} + 1)^{p\beta/2}} du \right)
 \end{aligned}$$

$$\left( \text{it holds for } k > -1, \alpha > 0, \lambda > \frac{k+1}{2\alpha} \text{ that } \int_0^{\infty} \frac{u^k}{(u^{2\alpha} + 1)^\lambda} du = \frac{\Gamma\left(\frac{k+1}{2\alpha}\right) \Gamma\left(\lambda - \frac{k+1}{2\alpha}\right)}{2\alpha \Gamma(\lambda)} \right) \quad (112)$$

$$\begin{aligned}
 &= \frac{[\Gamma(\beta)]^p \Gamma\left(\frac{q\beta}{2} - \frac{1}{2\alpha}\right)^{\frac{p}{q}} \Gamma\left(\frac{p(r-1+\gamma+n)+1}{2\alpha}\right) \Gamma\left(\frac{p\beta}{2} - \frac{p(r-1+\gamma+n)+1}{2\alpha}\right) K^p \xi^{p(r-1+\gamma+n)}}{\Gamma\left(\frac{q\beta}{2}\right)^{1+\frac{p}{q}} \Gamma\left(\frac{1}{2\alpha}\right) \Gamma\left(\beta - \frac{1}{2\alpha}\right)^p ((n-1)!)^p (q(n-1)+1)^{p/q} [p(r-1+\gamma)+1]}.
 \end{aligned}$$

Thus we obtain

$$\begin{aligned}
 I &\leq \frac{[\Gamma(\beta)]^p \Gamma\left(\frac{q\beta}{2} - \frac{1}{2\alpha}\right)^{\frac{p}{q}} \Gamma\left(\frac{p(r-1+\gamma+n)+1}{2\alpha}\right)}{\Gamma\left(\frac{q\beta}{2}\right)^{1+\frac{p}{q}} \Gamma\left(\frac{1}{2\alpha}\right) \Gamma\left(\beta - \frac{1}{2\alpha}\right)^p ((n-1)!)^p} \\
 &\quad \cdot \frac{\Gamma\left(\frac{p\beta}{2} - \frac{p(r-1+\gamma+n)+1}{2\alpha}\right) K^p \xi^{p(r-1+\gamma+n)}}{(q(n-1)+1)^{p/q} [p(r-1+\gamma)+1]}. \quad (113)
 \end{aligned}$$

That is finishing the proof of the theorem. ■

In particular we have

**Corollary 35.** *Let  $f$  such that the following Lipschitz condition holds:  $\omega_7(f^{(4)}, \delta)_2 \leq K\delta^{6+\gamma}$ ,  $K > 0$ ,  $0 < \gamma \leq 1$ , for any  $\delta > 0$ , and the rest as above in this section. Then*

$$\|\Delta(x)\|_2 \leq \frac{K}{6} \sqrt{\frac{\Gamma\left(\frac{2\gamma+21}{10}\right) \Gamma\left(1 - \frac{\gamma}{5}\right)}{14(13+2\gamma) \Gamma\left(\frac{1}{10}\right)}} \xi^{\gamma+10}. \quad (114)$$

Hence as  $\xi \rightarrow 0$  we obtain  $\|\Delta(x)\|_2 \rightarrow 0$ .

If additionally  $f^{(2m)} \in L_2(\mathbb{R})$ ,  $m = 1, 2$ , then  $\|M_{7,\xi}(f) - f\|_2 \rightarrow 0$ , as  $\xi \rightarrow 0$ .

**Proof.** In Theorem 34 we placed  $p = q = 2$ ,  $n = 4$ ,  $\alpha = 5$ ,  $\beta = \frac{31}{10}$  and  $r = 7$ .  $\blacksquare$

**Corollary 36.** Let  $f$  such that the following Lipschitz condition holds:  $\omega_6(f^{(4)}, \delta)_2 \leq K\delta^{5+\gamma}$ ,  $K > 0$ ,  $0 < \gamma \leq 1$ , for any  $\delta > 0$ , and the rest as above in this section. Then

$$\|\Delta(x)\|_2 \leq \frac{K}{6} \sqrt{\frac{\Gamma(\frac{31-\gamma}{4}) \Gamma(\frac{2\gamma+19}{8})}{7(11+2\gamma) \Gamma(\frac{1}{8}) 9!}} \xi^{\gamma+9}. \quad (115)$$

Hence as  $\xi \rightarrow 0$  we obtain  $\|\Delta(x)\|_2 \rightarrow 0$ .

If additionally  $f^{(2m)} \in L_2(\mathbb{R})$ ,  $m = 1, 2$ , then  $\|M_{6,\xi}(f) - f\|_2 \rightarrow 0$ , as  $\xi \rightarrow 0$ .

**Proof.** In Theorem 34 we placed  $p = q = 2$ ,  $n = 4$ ,  $\alpha = 4$ ,  $\beta = \frac{81}{8}$  and  $r = 6$ .  $\blacksquare$

**Theorem 37.** Let  $f \in C^n(\mathbb{R})$  and  $f^{(n)} \in L_1(\mathbb{R})$ ,  $n \in \mathbb{N}$ ,  $\alpha \in \mathbb{N}$ ,  $\beta > \frac{n+r+\gamma}{2\alpha}$ . Furthermore we assume the following Lipschitz condition:  $\omega_r(f^{(n)}, \delta)_1 \leq K\delta^{r-1+\gamma}$ ,  $K > 0$ ,  $0 < \gamma \leq 1$ , for any  $\delta > 0$ . Then

$$\|\Delta(x)\|_1 \leq \frac{K\Gamma(\frac{n+r+\gamma}{2\alpha}) \Gamma(\beta - \frac{n+r+\gamma}{2\alpha})}{(r+\gamma)(n-1)! \Gamma(\frac{1}{2\alpha}) \Gamma(\beta - \frac{1}{2\alpha})} \xi^{n+r+\gamma-1}. \quad (116)$$

Hence as  $\xi \rightarrow 0$  we obtain  $\|\Delta(x)\|_1 \rightarrow 0$ .

If additionally  $f^{(2m)} \in L_1(\mathbb{R})$ ,  $m = 1, 2, \dots, \lfloor \frac{n}{2} \rfloor$  then  $\|M_{r,\xi}(f) - f\|_1 \rightarrow 0$ , as  $\xi \rightarrow 0$ .

**Proof.** As in the proof of Theorem 2, [3] we get

$$\|\Delta(x)\|_1 \leq \frac{W}{(n-1)!} \left( \int_{-\infty}^{\infty} \left( \int_0^{|t|} \omega_r(f^{(n)}, w)_1 dw \right) \frac{|t|^{n-1}}{(t^{2\alpha} + \xi^{2\alpha})^\beta} dt \right). \quad (117)$$

Consequently we have

$$\begin{aligned} \|\Delta(x)\|_1 &\leq \frac{W}{(n-1)!} \left( \int_{-\infty}^{\infty} \left( \int_0^{|t|} (Kw^{r-1+\gamma}) dw \right) \frac{|t|^{n-1}}{(t^{2\alpha} + \xi^{2\alpha})^\beta} dt \right) \\ &= \frac{KW}{(n-1)!} \left( \int_{-\infty}^{\infty} \left( \frac{|t|^{r+\gamma}}{r+\gamma} \right) \frac{|t|^{n-1}}{(t^{2\alpha} + \xi^{2\alpha})^\beta} dt \right) \\ &= \frac{KW}{(r+\gamma)(n-1)!} \left( \int_{-\infty}^{\infty} \frac{|t|^{n+r+\gamma-1}}{(t^{2\alpha} + \xi^{2\alpha})^\beta} dt \right) \\ &= \frac{2KW}{(r+\gamma)(n-1)!} \left( \int_0^{\infty} \frac{t^{n+r+\gamma-1}}{(t^{2\alpha} + \xi^{2\alpha})^\beta} dt \right). \end{aligned} \quad (118)$$

We have gotten so far

$$\|\Delta(x)\|_1 \leq \frac{2KW\lambda}{(r+\gamma)(n-1)!}, \quad (119)$$

where

$$\begin{aligned} \lambda &:= \int_0^\infty \frac{t^{n+r+\gamma-1}}{(t^{2\alpha} + \xi^{2\alpha})^\beta} dt \\ &= \xi^{n+r+\gamma-2\alpha\beta} \int_0^\infty \frac{T^{n+r+\gamma-1}}{(T^{2\alpha} + 1)^\beta} dT \\ &= \xi^{n+r+\gamma-2\alpha\beta} \frac{\Gamma\left(\frac{n+r+\gamma}{2\alpha}\right) \Gamma\left(\beta - \frac{n+r+\gamma}{2\alpha}\right)}{\Gamma(\beta) 2\alpha}. \end{aligned} \quad (120)$$

Hence the validity of (116). ■

**Corollary 38.** *Let  $f \in C^2(\mathbb{R})$  and  $f'' \in L_1(\mathbb{R})$ . Furthermore we assume the following Lipschitz condition:  $\omega_2(f'', \delta)_1 \leq K\delta^{1+\gamma}$ ,  $K > 0$ ,  $0 < \gamma \leq 1$ , for any  $\delta > 0$ . Then*

$$\|\Delta(x)\|_1 \leq \frac{\gamma K \Gamma\left(\frac{\gamma}{4}\right) \Gamma\left(\frac{2-\gamma}{4}\right)}{(2+\gamma) \Gamma\left(\frac{1}{4}\right)^2} \xi^{\gamma+3}. \quad (121)$$

Hence as  $\xi \rightarrow 0$  we obtain  $\|\Delta(x)\|_1 \rightarrow 0$ .

If additionally  $f'' \in L_1(\mathbb{R})$ , then  $\|M_{2,\xi}(f) - f\|_1 \rightarrow 0$ , as  $\xi \rightarrow 0$ .

**Proof.** In Theorem 37 we placed  $n = 2$ ,  $\alpha = 2$ ,  $\beta = \frac{3}{2}$  and  $r = 2$ . ■

**Corollary 39.** *Let  $f \in C^4(\mathbb{R})$  and  $f^{(4)} \in L_1(\mathbb{R})$ . Furthermore we assume the following Lipschitz condition:  $\omega_4(f^{(4)}, \delta)_1 \leq K\delta^{3+\gamma}$ ,  $K > 0$ ,  $0 < \gamma \leq 1$ , for any  $\delta > 0$ . Then*

$$\|\Delta(x)\|_1 \leq \frac{K \Gamma\left(\frac{8+\gamma}{10}\right) \Gamma\left(\frac{3-\gamma}{10}\right)}{(4+\gamma) 6 \Gamma\left(\frac{1}{10}\right)} \xi^{\gamma+7}. \quad (122)$$

Hence as  $\xi \rightarrow 0$  we obtain  $\|\Delta(x)\|_1 \rightarrow 0$ .

If additionally  $f^{(2m)} \in L_1(\mathbb{R})$ ,  $m = 1, 2$ , then  $\|M_{4,\xi}(f) - f\|_1 \rightarrow 0$ , as  $\xi \rightarrow 0$ .

**Proof.** In Theorem 37 we placed  $n = 4$ ,  $\alpha = 5$ ,  $\beta = \frac{11}{10}$  and  $r = 4$ . ■

In general, when  $n = 0$  we get

**Proposition 40.** *Let  $r \in \{1, 2\}$  and the rest as above. Then*

$$\|M_{r,\xi}(f) - f\|_2 \leq \frac{2\sqrt[4]{4\pi}}{\Gamma\left(\frac{1}{4}\right)} \theta^{\frac{1}{2}} \omega_r(f, \xi)_2, \quad (123)$$

where

$$0 < \theta := \int_0^\infty (1+t)^{2r} \frac{1}{(t^4+1)^{3/2}} dt < \infty. \quad (124)$$

Hence as  $\xi \rightarrow 0$  we obtain  $M_{r,\xi} \rightarrow$  unit operator  $I$  in the  $L_2$  norm.

**Proof.** In the proof of Proposition 1 of [3] we used  $p = 2, q = 2, \alpha = 2, \beta = \frac{3}{2}$ .  
 ■

We also have

**Proposition 41.** *Let  $r \in \{1, 2, \dots, 9\}$  and the rest as above. Then*

$$\|M_{r,\xi}(f) - f\|_4 \leq \frac{13}{2} \left[ \frac{\Gamma\left(\frac{35}{18}\right)}{6\Gamma\left(\frac{19}{9}\right)} \right]^{\frac{3}{4}} \left[ \Gamma\left(\frac{1}{6}\right) \right]^{-\frac{1}{4}} \left[ \Gamma\left(\frac{13}{6}\right) \right] \theta^{\frac{1}{4}} \omega_r(f, \xi)_4, \quad (125)$$

where

$$0 < \theta := \int_0^\infty (1+t)^{4r} \frac{1}{(t^6+1)^{19/3}} dt < \infty. \quad (126)$$

Hence as  $\xi \rightarrow 0$  we obtain  $M_{r,\xi} \rightarrow$  unit operator  $I$  in the  $L_4$  norm.

**Proof.** In the proof of Proposition 1 of [3] we used  $p = 4, q = \frac{4}{3}, \alpha = 3, \beta = \frac{19}{6}, r \in \{1, 2, \dots, 9\}$ .  
 ■

We continue with

**Proposition 42.** *Let  $p, q > 1$  such that  $\frac{1}{p} + \frac{1}{q} = 1, \alpha \in \mathbb{N}, \beta > \max \left\{ \frac{1}{q\alpha}, \frac{1}{2\alpha}, \frac{r+\gamma-1}{\alpha} + \frac{1}{p\alpha} \right\}$  and the rest as above. Furthermore we assume the following Lipschitz condition:  $\omega_r(f, \delta)_p \leq K\delta^{r-1+\gamma}, K > 0, 0 < \gamma \leq 1$ , for any  $\delta > 0$ . Then*

$$\|M_{r,\xi}(f) - f\|_p \leq \frac{K\Gamma(\beta)\Gamma\left(\frac{q\beta}{2} - \frac{1}{2\alpha}\right)^{\frac{1}{q}}\Gamma\left(\frac{(r-1+\gamma)p+1}{2\alpha}\right)^{\frac{1}{p}}\Gamma\left(\frac{p\beta}{2} - \frac{(r-1+\gamma)p+1}{2\alpha}\right)^{\frac{1}{p}}}{\Gamma\left(\frac{1}{2\alpha}\right)^{\frac{1}{p}}\Gamma\left(\beta - \frac{1}{2\alpha}\right)\Gamma\left(\frac{q\beta}{2}\right)^{\frac{1}{q}}\Gamma\left(\frac{p\beta}{2}\right)^{\frac{1}{p}}}\xi^{(r-1+\gamma)}. \quad (127)$$

Hence as  $\xi \rightarrow 0$  we obtain  $M_{r,\xi} \rightarrow$  unit operator  $I$  in the  $L_p$  norm,  $p > 1$ .

**Proof.** As in the proof of Proposition 1 of [3] we find

$$\int_{-\infty}^{\infty} |M_{r,\xi}(f; x) - f(x)|^p dx$$

$$\begin{aligned}
&\leq \frac{2\alpha\xi^{\alpha\beta p-1} [\Gamma(\beta)]^p \Gamma\left(\frac{q\beta}{2} - \frac{1}{2\alpha}\right)^{\frac{p}{q}}}{\Gamma\left(\frac{1}{2\alpha}\right) \Gamma\left(\beta - \frac{1}{2\alpha}\right)^p \Gamma\left(\frac{q\beta}{2}\right)^{\frac{p}{q}}} \int_0^\infty \omega_r(f, t)_p^p \frac{1}{(t^{2\alpha} + \xi^{2\alpha})^{p\beta/2}} dt \\
&\leq \frac{2\alpha\xi^{\alpha\beta p-1} [\Gamma(\beta)]^p \Gamma\left(\frac{q\beta}{2} - \frac{1}{2\alpha}\right)^{\frac{p}{q}}}{\Gamma\left(\frac{1}{2\alpha}\right) \Gamma\left(\beta - \frac{1}{2\alpha}\right)^p \Gamma\left(\frac{q\beta}{2}\right)^{\frac{p}{q}}} \int_0^\infty (Kt^{r-1+\gamma})^p \frac{1}{(t^{2\alpha} + \xi^{2\alpha})^{p\beta/2}} dt \quad (128)
\end{aligned}$$

$$\begin{aligned}
&= \frac{K^p 2\alpha [\Gamma(\beta)]^p \xi^{(r-1+\gamma)p} \Gamma\left(\frac{q\beta}{2} - \frac{1}{2\alpha}\right)^{\frac{p}{q}}}{\Gamma\left(\frac{1}{2\alpha}\right) \Gamma\left(\beta - \frac{1}{2\alpha}\right)^p \Gamma\left(\frac{q\beta}{2}\right)^{\frac{p}{q}}} \int_0^\infty \frac{T^{(r-1+\gamma)p}}{(T^{2\alpha} + 1)^{p\beta/2}} dT \quad (129) \\
&= \frac{K^p [\Gamma(\beta)]^p \Gamma\left(\frac{q\beta}{2} - \frac{1}{2\alpha}\right)^{\frac{p}{q}} \Gamma\left(\frac{(r-1+\gamma)p+1}{2\alpha}\right) \Gamma\left(\frac{p\beta}{2} - \frac{(r-1+\gamma)p+1}{2\alpha}\right)}{\Gamma\left(\frac{1}{2\alpha}\right) \Gamma\left(\beta - \frac{1}{2\alpha}\right)^p \Gamma\left(\frac{q\beta}{2}\right)^{\frac{p}{q}} \Gamma\left(\frac{p\beta}{2}\right)} \xi^{(r-1+\gamma)p}
\end{aligned}$$

We have established the claim of the Proposition.  $\blacksquare$

**Corollary 43.** *Let  $f$  such that the following Lipschitz condition holds:  $\omega_4(f, \delta)_2 \leq K\delta^{3+\gamma}$ ,  $K > 0$ ,  $0 < \gamma \leq 1$ , for any  $\delta > 0$ , and the rest as above in this section. Then*

$$\|M_{4,\xi}(f) - f\|_2 \leq \sqrt{\frac{\Gamma\left(\frac{7+2\gamma}{8}\right) \Gamma\left(\frac{5-2\gamma}{8}\right)}{\Gamma\left(\frac{1}{8}\right) \Gamma\left(\frac{11}{8}\right)}} K \xi^{3+\gamma}. \quad (130)$$

Hence as  $\xi \rightarrow 0$  we obtain  $M_{4,\xi} \rightarrow$  unit operator  $I$  in the  $L_2$  norm.

**Proof.** In Proposition 42 we place  $p = 2$ ,  $q = 2$ ,  $\alpha = 4$ ,  $\beta = \frac{3}{2}$  and  $r = 4$ .  $\blacksquare$

**Corollary 44.** *Let  $f$  such that the following Lipschitz condition holds:  $\omega_2(f, \delta)_4 \leq K\delta^{1+\gamma}$ ,  $K > 0$ ,  $0 < \gamma \leq 1$ , for any  $\delta > 0$ , and the rest as above in this section. Then*

$$\|M_{2,\xi}(f) - f\|_4 \leq \sqrt[4]{\frac{\Gamma\left(\frac{3}{4}\right)^3 \Gamma\left(\frac{5+4\gamma}{4}\right) \Gamma\left(\frac{7-4\gamma}{4}\right)}{\Gamma\left(\frac{1}{4}\right)^5 2}} 2K\sqrt{\pi}\xi^{1+\gamma}. \quad (131)$$

Hence as  $\xi \rightarrow 0$  we obtain  $M_{2,\xi} \rightarrow$  unit operator  $I$  in the  $L_4$  norm.

**Proof.** In Proposition 42 we place  $p = 4$ ,  $q = 4/3$ ,  $\alpha = 2$ ,  $\beta = \frac{3}{2}$  and  $r = 2$ .  $\blacksquare$

In general, in  $L_1$  case,  $n = 0$  we have

**Proposition 45.** For  $r \in \{1, 2, 3\}$  it holds

$$\|M_{r,\xi}f - f\|_1 \leq \left( \int_0^\infty (1+t)^r \frac{1}{(t^4 + 1)^{\frac{5}{4}}} dt \right) \omega_r(f, \xi)_1. \quad (132)$$

Hence as  $\xi \rightarrow 0$  we get  $M_{r,\xi} \rightarrow I$  in the  $L_1$  norm.

**Proof.** In the proof of Proposition 2 of [3] we used  $\alpha = 2, \beta = \frac{5}{4}$ . ■

**Proposition 46.** For  $r \in \{1, 2, \dots, 5\}$  it holds

$$\|M_{r,\xi}f - f\|_1 \leq \left( \int_0^\infty (1+t)^r \frac{1}{(t^6+1)^{\frac{7}{6}}} dt \right) \omega_r(f, \xi)_1. \quad (133)$$

Hence as  $\xi \rightarrow 0$  we get  $M_{r,\xi} \rightarrow I$  in the  $L_1$  norm.

**Proof.** In the proof of Proposition 2 of [3] we used  $\alpha = 3, \beta = \frac{7}{6}$ . ■

**Proposition 47.** Assume  $\beta > \frac{r+\gamma}{2\alpha}$ . Furthermore we suppose the following Lipschitz condition:  $\omega_r(f, \delta)_1 \leq K\delta^{r-1+\gamma}$ ,  $K > 0$ ,  $0 < \gamma \leq 1$ , for any  $\delta > 0$ . Then

$$\|M_{r,\xi}f - f\|_1 \leq \frac{K\Gamma\left(\frac{r+\gamma}{2\alpha}\right)\Gamma\left(\beta - \frac{r+\gamma}{2\alpha}\right)}{\Gamma\left(\frac{1}{2\alpha}\right)\Gamma\left(\beta - \frac{1}{2\alpha}\right)} \xi^{r-1+\gamma}. \quad (134)$$

Hence as  $\xi \rightarrow 0$  we get  $M_{r,\xi} \rightarrow I$  in the  $L_1$  norm.

**Proof.** As in the proof of Proposition 2 of [3] we get

$$\begin{aligned} \int_{-\infty}^\infty |M_{r,\xi}(f; x) - f(x)| dx &\leq W \int_{-\infty}^\infty \omega_r(f, |t|)_1 \frac{1}{(t^{2\alpha} + \xi^{2\alpha})^\beta} dt \\ &\leq W \int_{-\infty}^\infty K|t|^{r-1+\gamma} \frac{1}{(t^{2\alpha} + \xi^{2\alpha})^\beta} dt \\ &= 2KW \int_0^\infty \frac{t^{r-1+\gamma}}{(t^{2\alpha} + \xi^{2\alpha})^\beta} dt \\ &= K \frac{\Gamma(\beta) 2\alpha \xi^{r-1+\gamma}}{\Gamma\left(\frac{1}{2\alpha}\right)\Gamma\left(\beta - \frac{1}{2\alpha}\right)} \int_0^\infty \frac{T^{r-1+\gamma}}{(T^{2\alpha} + 1)^\beta} dT \\ &= \frac{K\Gamma\left(\frac{r+\gamma}{2\alpha}\right)\Gamma\left(\beta - \frac{r+\gamma}{2\alpha}\right)}{\Gamma\left(\frac{1}{2\alpha}\right)\Gamma\left(\beta - \frac{1}{2\alpha}\right)} \xi^{r-1+\gamma}. \end{aligned} \quad (135)$$

We have proved the claim of the proposition. ■

**Corollary 48.** Assume the following Lipschitz condition:  $\omega_2(f, \delta)_1 \leq K\delta^{1+\gamma}$ ,  $K > 0$ ,  $0 < \gamma \leq 1$ , for any  $\delta > 0$ . Then

$$\|M_{2,\xi}f - f\|_1 \leq \frac{K}{2 \sin\left(\frac{(2+\gamma)\pi}{6}\right)} \xi^{1+\gamma}. \quad (136)$$

Hence as  $\xi \rightarrow 0$  we get  $M_{2,\xi} \rightarrow I$  in the  $L_1$  norm.

**Proof.** In Proposition 47 we place  $\alpha = 3, \beta = 1$  and  $r = 2$ . ■

In the next we consider  $f \in C^n(\mathbb{R})$  and  $f^{(n)} \in L_p(\mathbb{R})$ ,  $n = 0$  or  $n \geq 2$  even,  $1 \leq p < \infty$  and the similar *smooth singular operator of symmetric convolution type*

$$M_\xi(f; x) = W \int_{-\infty}^{\infty} f(x+y) \frac{1}{(y^{2\alpha} + \xi^{2\alpha})^\beta} dy, \quad \text{for all } x \in \mathbb{R}, \xi > 0. \quad (137)$$

Denote

$$K(x) := M_\xi(f; x) - f(x) - \sum_{\rho=1}^{n/2} \frac{f^{(2\rho)}(x)}{(2\rho)!} \frac{\Gamma(\frac{2\rho+1}{2\alpha})}{\Gamma(\frac{1}{2\alpha})} \frac{\Gamma(\beta - \frac{2\rho+1}{2\alpha})}{\Gamma(\beta - \frac{1}{2\alpha})} \xi^{2\rho}, \quad (138)$$

the sum collapses for  $n = 0$ .

We give

**Theorem 49.** *Let  $n \in \{2, 4, 6\}$  and the rest as above. Then*

$$\|K(x)\|_2 \leq \left[ \sqrt{\frac{663}{2(2n-1)}} \frac{1}{64(n-1)!} \right] \tilde{\tau}^{1/2} \xi^n \omega_2(f^{(n)}, \xi)_2, \quad (139)$$

where

$$0 < \tilde{\tau} = \int_0^\infty \left( (1+u)^5 - 1 \right) u^{2n-1} \frac{1}{(1+u^4)^{\frac{21}{4}}} du < \infty. \quad (140)$$

Hence as  $\xi \rightarrow 0$  we get  $\|K(x)\|_2 \rightarrow 0$ .

If additionally  $f^{(2m)} \in L_2(\mathbb{R})$ ,  $m = 1, 2, \dots, \frac{n}{2}$  then  $\|M_\xi(f) - f\|_2 \rightarrow 0$ , as  $\xi \rightarrow 0$ .

**Proof.** In the proof of Theorem 3 of [3] we used  $\alpha = 2, \beta = \frac{21}{4}, p = 2, q = 2$ . ■

**Theorem 50.** *Let  $n \in \{2, 4, 6, 8, 10\}$  and the rest as above. Then*

$$\|K(x)\|_4 \leq \left[ \left( \frac{\Gamma(\frac{47}{18})}{2\Gamma(\frac{25}{9})} \right)^{\frac{3}{4}} \frac{\Gamma(\frac{25}{6})}{2\sqrt{3}(4n-1)^{\frac{3}{4}} \Gamma(\frac{1}{6})^{\frac{1}{4}} (n-1)!} \right] \tilde{\tau}^{1/4} \xi^n \omega_2(f^{(n)}, \xi)_4, \quad (141)$$

where

$$0 < \tilde{\tau} = \int_0^\infty \left( (1+u)^9 - 1 \right) u^{4n-1} \frac{1}{(1+u^6)^{25/3}} du < \infty. \quad (142)$$

Hence as  $\xi \rightarrow 0$  we get  $\|K(x)\|_4 \rightarrow 0$ .

If additionally  $f^{(2m)} \in L_4(\mathbb{R})$ ,  $m = 1, 2, \dots, \frac{n}{2}$  then  $\|M_\xi(f) - f\|_4 \rightarrow 0$ , as  $\xi \rightarrow 0$ .

**Proof.** In the proof of Theorem 3 of [3] we used  $\alpha = 3, \beta = \frac{25}{6}, p = 4, q = 4/3$ . ■

It follows a Lipschitz type approximation result.

**Theorem 51.** *Let  $p, q > 1$  such that  $\frac{1}{p} + \frac{1}{q} = 1$ ,  $n \geq 2$  even,  $\alpha \in \mathbb{N}$ ,  $\beta > \frac{n+\gamma+1}{\alpha} + \frac{1}{p\alpha}$  and the rest as above. Furthermore we assume the following Lipschitz condition:  $\omega_2(f^{(n)}, \delta)_p \leq K\delta^{\gamma+1}$ ,  $K > 0$ ,  $0 < \gamma \leq 1$ , for any  $\delta > 0$ . Then*

$$\|K(x)\|_p \leq \frac{K [\Gamma(\beta)] \Gamma\left(\frac{q\beta}{2} - \frac{1}{2\alpha}\right)^{\frac{1}{q}} \Gamma\left(\frac{(\gamma+1+n)p+1}{2\alpha}\right)^{\frac{1}{p}} \Gamma\left(\frac{p\beta}{2} - \frac{(\gamma+1+n)p+1}{2\alpha}\right)^{\frac{1}{p}} \xi^{\gamma+1+n}}{[(\gamma+1)p+1]^{\frac{1}{p}} 2[(n-1)!] \Gamma\left(\frac{1}{2\alpha}\right)^{\frac{1}{p}} \Gamma\left(\beta - \frac{1}{2\alpha}\right) \Gamma\left(\frac{q\beta}{2}\right)^{\frac{1}{q}} \Gamma\left(\frac{p\beta}{2}\right)^{\frac{1}{p}} (q(n-1)+1)^{\frac{1}{q}}}. \quad (143)$$

Hence as  $\xi \rightarrow 0$  we get  $\|K(x)\|_p \rightarrow 0$ .

If additionally  $f^{(2m)} \in L_p(\mathbb{R})$ ,  $m = 1, 2, \dots, \frac{n}{2}$  then  $\|M_\xi(f) - f\|_p \rightarrow 0$ , as  $\xi \rightarrow 0$ .

**Proof.** As in the proof of Theorem 3, of [3] we find

$$\begin{aligned} \int_{-\infty}^{\infty} |K(x)|^p dx &\leq c_2 \left( \int_0^{\infty} \left( \int_0^y \omega_2(f^{(n)}, t)_p^p dt \right) y^{pn-1} \frac{1}{(y^{2\alpha} + \xi^{2\alpha})^{p\beta/2}} dy \right) \\ &\leq K^p c_2 \left( \int_0^{\infty} \left( \frac{y^{(\gamma+1)p+1}}{(\gamma+1)p+1} \right) y^{pn-1} \frac{1}{(y^{2\alpha} + \xi^{2\alpha})^{p\beta/2}} dy \right) \\ &= \frac{K^p c_2}{(\gamma+1)p+1} \left( \int_0^{\infty} \frac{y^{(\gamma+1+n)p}}{(y^{2\alpha} + \xi^{2\alpha})^{p\beta/2}} dy \right) \\ &= \frac{K^p c_2 \xi^{(\gamma+1+n)p+1}}{[(\gamma+1)p+1] \xi^{\alpha p \beta}} \left( \int_0^{\infty} \frac{T^{(\gamma+1+n)p}}{(T^{2\alpha} + 1)^{p\beta/2}} dT \right) \\ &= \frac{K^p c_2 \xi^{(\gamma+1+n)p+1}}{[(\gamma+1)p+1] \xi^{\alpha p \beta}} \frac{1}{2\alpha} \frac{\Gamma\left(\frac{(\gamma+1+n)p+1}{2\alpha}\right) \Gamma\left(\frac{p\beta}{2} - \frac{(\gamma+1+n)p+1}{2\alpha}\right)}{\Gamma\left(\frac{p\beta}{2}\right)} \\ &= \frac{K^p [\Gamma(\beta)]^p \Gamma\left(\frac{q\beta}{2} - \frac{1}{2\alpha}\right)^{p/q} \Gamma\left(\frac{(\gamma+1+n)p+1}{2\alpha}\right) \Gamma\left(\frac{p\beta}{2} - \frac{(\gamma+1+n)p+1}{2\alpha}\right) \xi^{(\gamma+1+n)p}}{[(\gamma+1)p+1] 2^{\frac{p}{q}+1} \Gamma\left(\frac{1}{2\alpha}\right)^p \Gamma\left(\beta - \frac{1}{2\alpha}\right)^p \Gamma\left(\frac{q\beta}{2}\right)^{p/q} \Gamma\left(\frac{p\beta}{2}\right)^p [(n-1)!]^p (q(n-1)+1)^{p/q}}, \quad (144) \end{aligned}$$

where here we denoted

$$c_2 := \frac{[\Gamma(\beta)]^p \alpha \xi^{\alpha \beta p - 1} \Gamma\left(\frac{q\beta}{2} - \frac{1}{2\alpha}\right)^{p/q}}{2^{\frac{p}{q}} \Gamma\left(\frac{1}{2\alpha}\right)^p \Gamma\left(\beta - \frac{1}{2\alpha}\right)^p \Gamma\left(\frac{q\beta}{2}\right)^{p/q} [(n-1)!]^p (q(n-1)+1)^{p/q}}. \quad (145)$$

We have established the claim of the theorem. ■



**Corollary 52.** Assume the following Lipschitz condition:  $\omega_2(f'', \delta)_2 \leq K\delta^{\gamma+1}$ ,  $K > 0$ ,  $0 < \gamma \leq 1$ , for any  $\delta > 0$ , and the rest as above in this section. Then

$$\|K(x)\|_2 \leq \sqrt{\frac{\Gamma\left(\frac{5-2\gamma}{6}\right) \Gamma\left(\frac{2\gamma+7}{6}\right)}{5(2\gamma+3)\pi}} \frac{K}{2} \xi^{\gamma+3}. \quad (146)$$

Hence as  $\xi \rightarrow 0$  we get  $\|K(x)\|_2 \rightarrow 0$ .

If additionally  $f'' \in L_2(\mathbb{R})$ , then  $\|M_\xi(f) - f\|_2 \rightarrow 0$ , as  $\xi \rightarrow 0$ .

**Proof.** In Theorem 51 we place  $p = 2, q = 2, \alpha = 3, \beta = 2$ , and  $n = 2$ . ■

**Corollary 53.** Assume the following Lipschitz condition:  $\omega_2(f^{(4)}, \delta)_4 \leq K\delta^{\gamma+1}$ ,  $K > 0$ ,  $0 < \gamma \leq 1$ , for any  $\delta > 0$ , and the rest as above in this section. Then

$$\|K(x)\|_4 \leq \sqrt[4]{\frac{\Gamma\left(\frac{21+4\gamma}{6}\right) \Gamma\left(\frac{15-4\gamma}{6}\right)}{40\pi(4\gamma+5)}} \frac{K}{55} \xi^{\gamma+5}. \quad (147)$$

Hence as  $\xi \rightarrow 0$  we get  $\|K(x)\|_4 \rightarrow 0$ .

If additionally  $f^{(2m)} \in L_4(\mathbb{R}), m = 1, 2$  then  $\|M_\xi(f) - f\|_4 \rightarrow 0$ , as  $\xi \rightarrow 0$ .

**Proof.** In Theorem 51 we place  $p = 4, q = \frac{4}{3}, \alpha = 3, \beta = 3$ , and  $n = 4$ . ■

**Theorem 54.** Let  $f \in C^2(\mathbb{R})$  and  $f'' \in L_1(\mathbb{R})$ . Here  $K(x) = M_\xi(f; x) - f(x) - 2f''(x) \left[ \frac{\Gamma(\frac{3}{4})}{\Gamma(\frac{1}{4})} \right]^2 \xi^2$ . Then

$$\|K(x)\|_1 \leq \frac{1}{6\left(\Gamma\left(\frac{1}{4}\right)\right)^2} \left[ 12 \left( \Gamma\left(\frac{3}{4}\right) \right)^2 + 12\sqrt{\pi} + \left( \Gamma\left(\frac{1}{4}\right) \right)^2 \right] \omega_2(f'', \xi)_1 \xi^2. \quad (148)$$

Hence as  $\xi \rightarrow 0$  we obtain  $\|K(x)\|_1 \rightarrow 0$ .

Also  $\|M_\xi(f) - f\|_1 \rightarrow 0$ , as  $\xi \rightarrow 0$ .

**Proof.** In the proof of Theorem 4 of [3] we used  $\alpha = 2, \beta = \frac{3}{2}, n = 2$ . ■

**Theorem 55.** Let  $f \in C^6(\mathbb{R})$  and  $f^{(6)} \in L_1(\mathbb{R})$ . Then

$$\|K(x)\|_1 \leq \frac{4\sqrt{3}+9}{7200} \omega_2(f^{(6)}, \xi)_1 \xi^6. \quad (149)$$

Hence as  $\xi \rightarrow 0$  we obtain  $\|K(x)\|_1 \rightarrow 0$ .

If additionally  $f^{(2m)} \in L_1(\mathbb{R}), m = 1, 2, 3$  then  $\|M_\xi(f) - f\|_1 \rightarrow 0$ , as  $\xi \rightarrow 0$ .

**Proof.** In the proof of Theorem 4 of [3] we used  $\alpha = 3, \beta = 2, n = 6$ . ■

The Lipschitz case of  $p = 1$  follows.

**Theorem 56.** Let  $f \in C^n(\mathbb{R})$  and  $f^{(n)} \in L_1(\mathbb{R}), n \geq 2$  even,  $\alpha \in \mathbb{N}, \beta > \frac{n+\gamma+2}{2\alpha}$ . Furthermore we assume the following Lipschitz condition:  $\omega_2(f^{(n)}, \delta)_1 \leq K\delta^{\gamma+1}$ ,  $K > 0$ ,  $0 < \gamma \leq 1$ , for any  $\delta > 0$ . Then

$$\|K(x)\|_1 \leq \frac{K\Gamma\left(\frac{\gamma+n+2}{2\alpha}\right) \Gamma\left(\beta - \frac{\gamma+n+2}{2\alpha}\right) \xi^{\gamma+n+1}}{(n-1)!2(\gamma+2) \Gamma\left(\frac{1}{2\alpha}\right) \Gamma\left(\beta - \frac{1}{2\alpha}\right)}. \quad (150)$$

Hence as  $\xi \rightarrow 0$  we obtain  $\|K(x)\|_1 \rightarrow 0$ .

If additionally  $f^{(2m)} \in L_1(\mathbb{R})$ ,  $m = 1, 2, \dots, \frac{n}{2}$  then  $\|M_\xi(f) - f\|_1 \rightarrow 0$ , as  $\xi \rightarrow 0$ .

**Proof.** As in the proof of Theorem 4 of [3] we have

$$\begin{aligned}
 \|K(x)\|_1 &\leq W \int_0^\infty \left( \left( \int_0^y \omega_2(f^{(n)}, t)_1 dt \right) \frac{y^{n-1}}{(n-1)!} \frac{1}{(y^{2\alpha} + \xi^{2\alpha})^\beta} \right) dy \\
 &\leq W \int_0^\infty \left( \left( \int_0^y (Kt^{\gamma+1}) dt \right) \frac{y^{n-1}}{(n-1)!} \frac{1}{(y^{2\alpha} + \xi^{2\alpha})^\beta} \right) dy \\
 &= \frac{KW\xi^{\gamma+n+2-2\alpha\beta}}{(n-1)!(\gamma+2)} \int_0^\infty \frac{x^{\gamma+n+1}}{(x^{2\alpha} + 1)^\beta} dx \\
 &= \frac{KW\xi^{\gamma+n+2-2\alpha\beta}}{(n-1)!(\gamma+2)} \frac{1}{2\alpha} \frac{\Gamma\left(\frac{\gamma+n+2}{2\alpha}\right) \Gamma\left(\beta - \frac{\gamma+n+2}{2\alpha}\right)}{\Gamma(\beta)} \\
 &= \frac{K\Gamma\left(\frac{\gamma+n+2}{2\alpha}\right) \Gamma\left(\beta - \frac{\gamma+n+2}{2\alpha}\right) \xi^{\gamma+n+1}}{(n-1)!2(\gamma+2) \Gamma\left(\frac{1}{2\alpha}\right) \Gamma\left(\beta - \frac{1}{2\alpha}\right)}. \tag{151}
 \end{aligned}$$

We have proved the claim of the theorem.  $\blacksquare$

**Corollary 57.** Let  $f \in C^6(\mathbb{R})$  and  $f^{(6)} \in L_1(\mathbb{R})$ . Furthermore we assume the following Lipschitz condition:  $\omega_2(f^{(6)}, \delta)_1 \leq K\delta^{\gamma+1}$ ,  $K > 0$ ,  $0 < \gamma \leq 1$ , for any  $\delta > 0$ . Then

$$\|K(x)\|_1 \leq \frac{K(\gamma+4)\gamma\sqrt{2}}{10080(\gamma+2)\sin\frac{\pi}{4}} \xi^{\gamma+7}. \tag{152}$$

Hence as  $\xi \rightarrow 0$  we obtain  $\|K(x)\|_1 \rightarrow 0$ .

If additionally  $f^{(2m)} \in L_1(\mathbb{R})$ ,  $m = 1, 2, 3$  then  $\|M_\xi(f) - f\|_1 \rightarrow 0$ , as  $\xi \rightarrow 0$ .

**Proof.** In Theorem 56 we place  $\alpha = 2$ ,  $\beta = 3$ , and  $n = 6$ .  $\blacksquare$

The case of  $n = 0$  follows.

**Proposition 58.** Let  $f$  as above in this section. Then

$$\|M_\xi(f) - f\|_2 \leq \frac{\sqrt{15+8\sqrt{3}}}{2\sqrt{3}} \omega_2(f, \xi)_2. \tag{153}$$

Hence as  $\xi \rightarrow 0$  we obtain  $M_\xi \rightarrow I$  in the  $L_2$  norm.

**Proof.** In the proof of Proposition 3 of [3] we used  $p = 2, q = 2, \alpha = 3, \beta = 1$ .  $\blacksquare$

The related Lipschitz case for  $n = 0$  comes next.

**Proposition 59.** Let  $p, q > 1$  such that  $\frac{1}{p} + \frac{1}{q} = 1$ ,  $\alpha \in \mathbb{N}$ ,  $\beta > \max\left\{\frac{1}{q\alpha}, \frac{1+\gamma}{\alpha} + \frac{1}{p\alpha}\right\}$  and the rest as above. Furthermore we assume the following Lipschitz condition:

$\omega_2(f, \delta)_p \leq K\delta^{1+\gamma}$ ,  $K > 0$ ,  $0 < \gamma \leq 1$ , for any  $\delta > 0$ . Then

$$\|M_\xi(f) - f\|_p \leq \frac{K [\Gamma(\beta)] \Gamma\left(\frac{q\beta}{2} - \frac{1}{2\alpha}\right)^{\frac{1}{q}} \Gamma\left(\frac{(1+\gamma)p+1}{2\alpha}\right)^{\frac{1}{p}} \Gamma\left(\frac{\beta p}{2} - \frac{(1+\gamma)p+1}{2\alpha}\right)^{\frac{1}{p}} \xi^{1+\gamma}}{2\Gamma\left(\frac{1}{2\alpha}\right)^{\frac{1}{p}} \Gamma\left(\beta - \frac{1}{2\alpha}\right) \Gamma\left(\frac{q\beta}{2}\right)^{\frac{1}{q}} \Gamma\left(\frac{\beta p}{2}\right)^{\frac{1}{p}}}. \quad (154)$$

Hence as  $\xi \rightarrow 0$  we obtain  $M_\xi \rightarrow I$  in the  $L_p$  norm,  $p > 1$ .

**Proof.** As in the proof of Proposition 3 of [3] we get

$$\begin{aligned} \int_{-\infty}^{\infty} |M_\xi(f; x) - f(x)|^p dx &\leq \frac{[\Gamma(\beta)]^p \alpha \xi^{\alpha\beta p-1} \Gamma\left(\frac{q\beta}{2} - \frac{1}{2\alpha}\right)^{p/q}}{2^{\frac{p}{q}} \Gamma\left(\frac{1}{2\alpha}\right) \Gamma\left(\beta - \frac{1}{2\alpha}\right)^p \Gamma\left(\frac{q\beta}{2}\right)^{p/q}} \int_0^\infty \omega_2(f, y)_p^p \frac{1}{(y^{2\alpha} + \xi^{2\alpha})^{\beta p/2}} dy \\ &\leq \frac{K^p [\Gamma(\beta)]^p \alpha \xi^{\alpha\beta p-1} \Gamma\left(\frac{q\beta}{2} - \frac{1}{2\alpha}\right)^{p/q}}{2^{\frac{p}{q}} \Gamma\left(\frac{1}{2\alpha}\right) \Gamma\left(\beta - \frac{1}{2\alpha}\right)^p \Gamma\left(\frac{q\beta}{2}\right)^{p/q}} \int_0^\infty \frac{y^{(1+\gamma)p}}{(y^{2\alpha} + \xi^{2\alpha})^{\beta p/2}} dy \\ &= \frac{K^p [\Gamma(\beta)]^p \alpha \Gamma\left(\frac{q\beta}{2} - \frac{1}{2\alpha}\right)^{p/q} \xi^{(1+\gamma)p}}{2^{\frac{p}{q}} \Gamma\left(\frac{1}{2\alpha}\right) \Gamma\left(\beta - \frac{1}{2\alpha}\right)^p \Gamma\left(\frac{q\beta}{2}\right)^{p/q}} \int_0^\infty \frac{t^{(1+\gamma)p}}{(t^{2\alpha} + 1)^{\beta p/2}} dt \\ &= \frac{K^p [\Gamma(\beta)]^p \Gamma\left(\frac{q\beta}{2} - \frac{1}{2\alpha}\right)^{p/q} \Gamma\left(\frac{(1+\gamma)p+1}{2\alpha}\right) \Gamma\left(\frac{\beta p}{2} - \frac{(1+\gamma)p+1}{2\alpha}\right) \xi^{(1+\gamma)p}}{2^{\frac{p}{q}+1} \Gamma\left(\frac{1}{2\alpha}\right) \Gamma\left(\beta - \frac{1}{2\alpha}\right)^p \Gamma\left(\frac{q\beta}{2}\right)^{p/q} \Gamma\left(\frac{\beta p}{2}\right)}. \quad (155) \end{aligned}$$

The proof of the claim is now completed.  $\blacksquare$

A particular example follows

**Corollary 60.** Let  $f$  as above in this section. Furthermore we assume the following Lipschitz condition:  $\omega_2(f, \delta)_2 \leq K\delta^{1+\gamma}$ ,  $K > 0$ ,  $0 < \gamma \leq 1$ , for any  $\delta > 0$ . Then

$$\|M_\xi(f) - f\|_2 \leq K \sqrt{\frac{\Gamma\left(\frac{3+2\gamma}{4}\right) \Gamma\left(\frac{5-2\gamma}{4}\right)}{3\pi\sqrt{2}}} \xi^{1+\gamma}. \quad (156)$$

Hence as  $\xi \rightarrow 0$  we obtain  $M_\xi \rightarrow I$  in the  $L_2$  norm.

**Proof.** In Proposition 59 we place  $p = q = \alpha = \beta = 2$ .  $\blacksquare$

Also we give

**Proposition 61.** It holds

$$\|M_\xi f - f\|_1 \leq \frac{4\sqrt{3}+9}{12} \omega_2(f, \xi)_1. \quad (157)$$

Hence as  $\xi \rightarrow 0$  we get  $M_\xi \rightarrow I$  in the  $L_1$  norm.

**Proof.** In the proof of Proposition 4 of [3] we used  $\alpha = 3, \beta = 1$ .  $\blacksquare$

It follows the Lipschitz type result

**Proposition 62.** *Assume the following Lipschitz condition:  $\omega_2(f, \delta)_1 \leq K\delta^{\gamma+1}$ ,  $K > 0$ ,  $0 < \gamma \leq 1$ , for any  $\delta > 0$ . For  $\alpha \in \mathbb{N}$ ,  $\beta > \frac{\gamma+2}{2\alpha}$ , it holds,*

$$\|M_\xi f - f\|_1 \leq \frac{K\Gamma\left(\frac{\gamma+2}{2\alpha}\right)\Gamma\left(\beta - \frac{\gamma+2}{2\alpha}\right)}{2\Gamma\left(\frac{1}{2\alpha}\right)\Gamma\left(\beta - \frac{1}{2\alpha}\right)}\xi^{\gamma+1}. \quad (158)$$

Hence as  $\xi \rightarrow 0$  we get  $M_\xi \rightarrow I$  in the  $L_1$  norm.

**Proof.** As in the proof of Proposition 4 of [3] we derive

$$\begin{aligned} \int_{-\infty}^{\infty} |M_\xi(f; x) - f(x)| dx &\leq W \int_0^{\infty} \omega_2(f, y)_1 \frac{1}{(y^{2\alpha} + \xi^{2\alpha})^\beta} dy \\ &\leq W \int_0^{\infty} Ky^{\gamma+1} \frac{1}{(y^{2\alpha} + \xi^{2\alpha})^\beta} dy \\ &= \frac{\Gamma(\beta) \alpha K \xi^{\gamma+1}}{\Gamma\left(\frac{1}{2\alpha}\right) \Gamma\left(\beta - \frac{1}{2\alpha}\right)} \int_0^{\infty} \frac{t^{\gamma+1}}{(t^{2\alpha} + 1)^\beta} dt \\ &= \frac{K\Gamma\left(\frac{\gamma+2}{2\alpha}\right)\Gamma\left(\beta - \frac{\gamma+2}{2\alpha}\right)}{2\Gamma\left(\frac{1}{2\alpha}\right)\Gamma\left(\beta - \frac{1}{2\alpha}\right)}\xi^{\gamma+1}. \end{aligned} \quad (159)$$

We have established the claim. ■

In particular, we have

**Corollary 63.** *Assume the following Lipschitz condition:  $\omega_2(f, \delta)_1 \leq K\delta^{\gamma+1}$ ,  $K > 0$ ,  $0 < \gamma \leq 1$ , for any  $\delta > 0$ . It holds*

$$\|M_\xi f - f\|_1 \leq \frac{K}{4} \left( \csc \frac{(\gamma+2)\pi}{6} \right) \xi^{\gamma+1}. \quad (160)$$

Hence as  $\xi \rightarrow 0$  we get  $M_\xi \rightarrow I$  in the  $L_1$  norm.

**Proof.** In Proposition 62 we place  $\alpha = 3, \beta = 1$ . ■

## References

- [1] G.A. Anastassiou and R. A. Mezei, *Global Smoothness and Uniform Convergence of Smooth Poisson-Cauchy Type Singular Operators*, Applied Mathematics and Computation, 215 (2009), 1718-1731.
- [2] G.A. Anastassiou and R. A. Mezei, *A Voronovskaya Type Theorem for Poisson-Cauchy Type Singular Operators*, submitted 2009.
- [3] G.A. Anastassiou and R. A. Mezei, *Lp Convergence with Rates of Smooth Poisson-Cauchy Type Singular Operators*, submitted 2009.

- [4] G.A. Anastassiou and R. A. Mezei, *Uniform Convergence with Rates of Smooth Poisson-Cauchy Type Singular Integral Operators*, Mathematical and Computer Modelling 50 (2009), 1553-1570.
- [5] V. I. Gorbaichuk, *Direct and inverse theorem for approximation by solutions of boundary- value problems for certain elliptic equations*, in: Theory of the approximation of functions, Proc. Internat. Conf., Kaluga, 1975 (Russian), pp. 126-128, "Nauka", Moscow, 1977.
- [6] V. I. Gorbaichuk, *Some properties of the Cauchy-Poisson Singular Integral*, Ukrainian Mathematical Journal, Vol. 28, No. 1, 1976, 61-63.

## Analysis of snore sounds by using the largest Lyapunov exponent

Derya Yılmaz\*, Haydar Ankişhan\*

\*Department of Biomedical Equipment Technology, Vocational School of Technology, Başkent University, Ankara, Turkey.  
e-mail: derya@baskent.edu.tr, hankishan@baskent.edu.tr

### Abstract

In recent years, chaotic analysis methods have been used for studying the physiological systems and developing contributions for making a medical decision. In this study, snore sounds have been analyzed using chaotic methods, such as embedding dimension, average mutual information (AMI) and the largest Lyapunov exponent (LLE). The LLE calculation as an indicator of chaos is performed to investigate the disturbance of snore sound in normal and apnea/hypopnea diseases. The results show that the LLE of normal snore group have been found significantly higher than apnea/hypopnea group ( $P < 0.05$ ). It is concluded from experimental results that the LLE, as a chaotic analysis method, is a useful tool for determining the chaotic behaviour of snore sounds and can be used for diagnosis of these diseases.

Keywords: Nonlinear analysis, OSAH, Snore analysis

### 1. Introduction

Obstructive sleep apnea/hypopnea (OSAH) is characterized by repetitive obstruction of the upper airways during sleep. OSAH is general example of a treatable disease, which is not suddenly life threatening. However, it may cause a range of complications such as a reduction in cognitive function, cardiovascular disease and fatigue [1, 2]. Many researchers have studied to analyze snoring

sounds associated with OSAH using different techniques such as sound intensity calculations, power spectrum estimation and counting of snores in a related time interval [1, 3-5]. These studies showed that snoring carries information on obstructive sleep apnea (OSA). In recent years, three studies have been published to classify snore sounds into snore/non-snore [6-8]. Duckitt *et al* [2006] presented a method which allows the automatic monitoring of snoring characteristic, depending on intensity and frequency of data [6]. They used Mel frequency cepstral coefficients (MFCCs) as the features in a hidden Markov model (HMM) based classification. Cavusoglu *et al* [2007] estimated sound energy, zero crossing and using linear regression for classification [7]. The other method used feature of sounds such as number of zero-crossings, energy, normalized autocorrelation coefficients, and first predictor coefficient of linear predictive coding (LPC) analysis for classification of snore sounds [8].

Recently, there are many studies which applied chaotic methods to the physiological signal for detecting some diseases [9-11]. The snore sounds have time varying characteristics, did not be analyzed by chaotic analysis methods in the previous studies. Differently from these studies, we have investigated the chaotic dynamics of snore related sound, using chaotic measures such as embedding dimension, average mutual information (AMI) and the largest Lyapunov exponent (LLE). The LLE is the most commonly used method in nonlinear analysis of physiological signals as a chaotic indicator. In this study, the sounds have been reconstructed in the phase space after determining the embedding dimension and time delay, and then the LLE calculations have been performed for normal and apnea/hypopnea cases. The student's t test has been applied to the results obtained from these analyses.

## 2. Material and Methods

### 2.1. Snore data and segmentation

In this study, we used the same data which is [7], obtained from Gulhane Military Medical Science Sleep Laboratory. The database contains 20 patients, 12 OSAH patients, age is between 44 and 62, 8 normal snores, age is between 40 and 54. The details about this database are referred to [7]. While working these data, 34 segments were chosen for feature extraction and analyzing illnesses. These segments consist of 17 normal sleep states, and 17 apnea/hypopnea problems' states.

Snore sounds are segmented as described in [12] and shown in Fig.1. Abeyratne *et al* [2007] classified raw data into three classes such as silence, unvoiced non-silence and voiced non-silence [12]. Fig. 1 shows how snore sound segments belonging to these classes are combined to form snoring and breathing episodes. Voiced and unvoiced segments were used in our study.

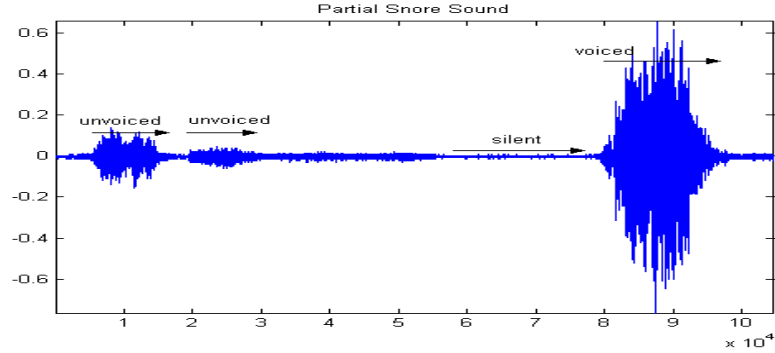


Figure 1. Segmentation of a snore sound

## 2.2. Methods

### 2.2.1. Nonlinear analysis

There are many methods such as Lyapunov exponents, correlation dimension, poincaré plots, Kolmogorov entropy etc. used as chaotic measures [13, 14]. To estimate the chaotic measures of a system, the phase space of system has to be reconstructed from the time series data [13]. The nonlinear measures of the system are calculated from this reconstructed attractor [13]. In this work, snore related sounds were reconstructed by using Takens' embedding theorem in the  $m$ -dimensional phase space with delay  $\tau$  as [15]:

$$X_i = (x_i, x_{i+\tau}, x_{i+2\tau}, x_{i+3\tau}, \dots, x_{i+(m-1)\tau}) \quad (1)$$

where,  $X_i$  is the  $i$ th point on the attractor ( $i = N-(m-1)\tau$ ),  $x(i)$  is the  $i$ th value of snore data,  $m$  is phase space dimension,  $\tau$  is time delay. We used AMI function for  $\tau$  selection. The proper  $\tau$  is the first minimum value of AMI function according to [16]. The phase space dimension, is called as embedding dimension ( $m$ ), has to be  $m \geq 2D+1$  ( $D$  is the attractor's dimension), but attractor dimension is not known in advance [13]. There are several methods for choosing the embedding dimension [13, 17, 18]. We used  $m$  chosen from false nearest neighborhood (FNN) method [17].

### 2.2.2. The largest Lyapunov exponent (LLE)

The Lyapunov exponent is defined as a quantitative measure of the sensitive dependence to the initial conditions. The value of Lyapunov exponent increases with the degree of chaos. In the system embedded in the  $m$  dimensional phase space, the number of Lyapunov exponents is equal to the number of phase space dimension. Each exponent gives the long-term average divergence ( $\lambda_i > 0$ ) or



convergence ( $\lambda_i < 0$ ) rate along the related axis in the phase space [13, 19]. Hence, Lyapunov spectrum will be arranged such that  $\lambda_1 \geq \lambda_2 \geq \dots \geq \lambda_m$ , the largest value ( $\lambda_1$ ) is called as LLE. Since a positive Lyapunov exponent indicates chaos, if the LLE of the system is positive ( $\lambda_1 > 0$ ), the system is chaotic [13, 19]. Therefore, the estimation of the LLE is sufficient and a common technique to determine the presence of chaotic behavior. There are several algorithms for calculating of the LLE from time series signal [19-22]. In this study, Rosenstein *et al* [22]'s algorithm has been used. This method is based on estimating the average local divergence rate, can work short and noisily time series.

According to Rosenstein *et al* [22], after reconstructing the system's attractor and the lyapunov exponents are given as

$$\lambda_{1(i)} = \frac{1}{i \Delta t} \frac{1}{M-i} \sum_{j=1}^{M-i} \ln \frac{d_j(i)}{d_j(0)} \quad (2)$$

where  $\Delta t$  is the sampling period of the time series, and  $d_j(i)$  is the distance between the  $j^{\text{th}}$  pair of nearest neighbors after  $i$  discrete-time steps,  $M$  is the number of reconstructed points, and  $d_j(i) \approx C_j e^{\lambda_1(i \Delta t)}$ .  $C_j$  is initial separation. By taking the logarithm of both sides of this equation,  $\ln d_j(i) \approx \ln C_j + \lambda_1(i \Delta t)$  is obtained. It represents a set of approximately parallel lines (for  $j = 1, 2, \dots, M$ ), each with a slope roughly proportional to  $\lambda_1$ . The largest Lyapunov exponent is easily and accurately calculated using a least-squares fit to the "average" line defined by

$$y(i) = \frac{1}{\Delta t} \langle \ln d_j(i) \rangle \quad (3)$$

where,  $\langle \dots \rangle$  denotes the average over all values of  $j$  [22].

### 2.2.3. Statistical analysis

Statistical analysis was performed by using the unpaired student-t test. The normality tests were applied to the data groups prior to statistical tests and it was seen that they had normal distribution. The level of significance was selected as  $P < 0.05$ .

## 3. Results and Discussion

The time delay ( $\tau$ ) and embedding dimension ( $m$ ) were determined for reconstruction of the snore segments.  $\tau$  measured as the number of samples was

found as first minimum of AMI function [13, 16]. The AMI function of a normal snore segment (SN: 2) is shown in Figure 2a. The optimal  $\tau$  was chosen as 6 for this segment. The  $\tau$  values obtained from normal and apnea/hypopnea segments were not statistically different (normal snore segments:  $7.18 \pm 1.85$ , apnea/hypopnea segments:  $7.88 \pm 2.52$  ( $P=0.375$ )). The optimal embedding dimension was found to be 5 according to FNN method [17] for the same segment, is given in Figure 2b. The embedding dimensions of normal and apnea/hypopnea segments have commonly found to be close to 5 in experiments (normal group:  $4.12 \pm 0.33$ , apnea/hypopnea group:  $4.06 \pm 0.56$  ( $P=0.71$ )). Therefore, for the LLE calculation, embedding dimension was set to 5 for all segments.

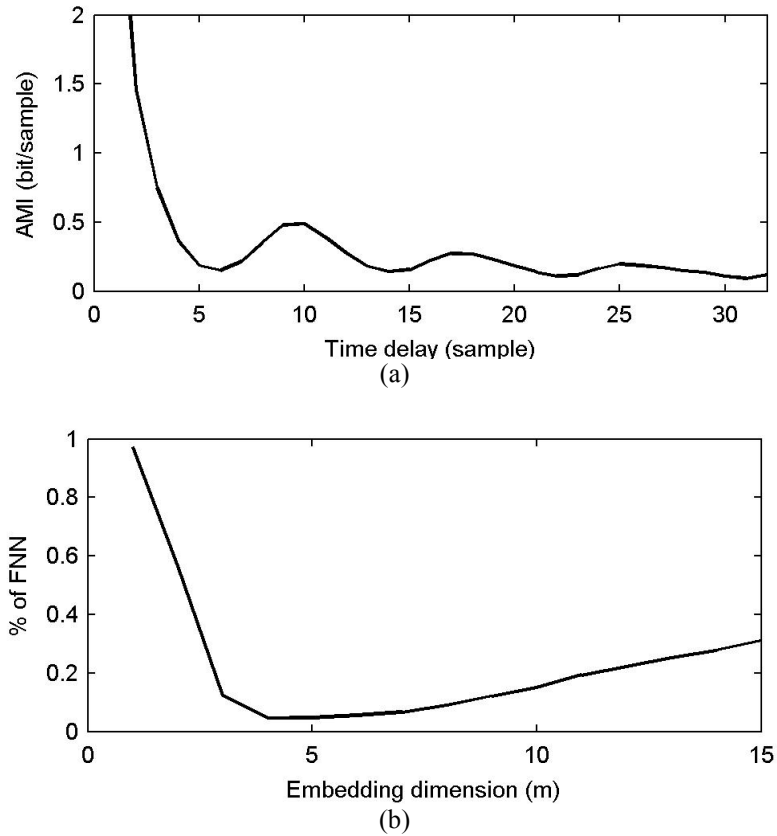


Figure 2. Determination of time delay (a) and embedding dimension (b) for a normal snore segment

The results obtained from LLE analysis for each normal and apnea/hypopnea segments are given in Table 1. According to unpaired student-t test result and Table 1, mean LLE value of normal group is higher than apnea/hypopnea group, significantly ( $P=0.0071$ ). If the results taking into account, we can say that,

unlike the embedding dimension and time delay measures, the LLE measures are successful for classifying these segments.

Table 1. The estimated LLE values for normal and apnea/hypopnea snore segments

Segment No	Normal snore group	Segment No	Apnea/hypopnea group
1	0.0862	18	0.0690
2	0.0593	19	0.0659
3	0.0429	20	0.0479
4	0.0405	21	0.0362
5	0.0283	22	0.0171
6	0.0211	23	0.0609
7	0.1618	24	0.0115
8	0.0643	25	0.0295
9	0.1855	26	0.0347
10	0.0395	27	0.0433
11	0.0932	28	0.0268
12	0.0718	29	0.0115
13	0.0690	30	0.0122
14	0.0853	31	0.0106
15	0.0343	32	0.0311
16	0.0225	33	0.0473
17	0.0343	34	0.0271
Mean±SD	0.0671±0.046*		0.0343±0.019*

\*P=0.0071

#### 4. Conclusions

In this study, LLE analysis of snore related sounds which are obtained from normal and apnea/hypopnea snore segments have been performed by using the algorithm of Rosenstein *et al* [22]. The results have shown that LLE is significantly lower for apnea/hypopnea group than normal. Namely, the LLE decreases with the apnea/hypopnea disorders. This decrement of the LLE in the cases of apnea/hypopnea indicate that dynamics of snore sound have low level chaotic behaviour with respect to normal case.

Consequently, LLE calculation gives useful information for diagnosing the apnea/hypopnea diseases. In future, snore sounds may be analyzed by using other chaotic measures. These analysis results can be used in classification studies for apnea detection.

## Acknowledgement

We thank to Tolga Çiloğlu for snore data.

## References

- [1] T.H. Lee, U.R. Abeyratne, K. Puvanendran, K.L. Goh, *Formant structure and phase-coupling analysis of human snoring sounds for detection of obstructive sleep apnea*. In: Middleton J, Jones ML, Pande GN (eds) Computer methods in biomechanics and biomedical engineering-3. Gordon& Breach Science Publishers Amsterdam, 2000.
- [2] W.W. Flemons, M.R. Littner, J.A. Rowley, P. Gay, W.M. Anderson, D.W. Hudgel, R.D. McEvo, D.I. Loube, Home diagnosis of sleep apnea: a systematic review of the literature, *Chest* 124 1543–79(2003).
- [3] U.R. Abeyratne, C.K.K. Patabandi, K. Puvanendran, Pitch–Jitter analysis snoring signals in the diagnosis of obstructive sleep apnea *23-rd annual international conference of the IEEE Engineering in Medicine and Biology Society*, (2001).
- [4] J.A. Fiz, J. Abad, R. Jane, M. Riera, M.A. Mananas, P. Caminal, D. Rodenstein, J. Morera, Acoustic analysis of snoring in patients with simple snoring and obstructive sleep apnea, *Eur Resp J*, 9(11):2365–2370(1996).
- [5] T.H. Lee, U.R. Abeyratne, Analysis of snoring sounds for the detection of obstructive sleep apnea. *Med Biol Eng Comput.* 37(2):538–539(1999).
- [6] W.D. Duckitt, S.K. Tuomi, Automatic detection, segmentation and assessment of snoring ambient acoustic data, *Physiological Meas.*, 27:1047-1056(2006).
- [7] M. Cavusoglu, M. Kamasak, O. Erogul, T. Ciloglu, Y. Serinagaoglu, T. Akcam, An Efficient method for snore/nonsnore classification of sleep sounds, *Physiol. Meas.*, 28:1-13(2007).
- [8] A.S. Karunajeewa, U.R. Abeyratne, Silence-breathing-snore classification from Snore-Related Sounds, *Physiological Meas.*, 29:227-243(2008).
- [9] A. Stefanovska, M. Bracic, Reconstructing Cardiovascular Dynamics, *Cont. Eng. Prac.*, 7: 161 (1999).
- [10] R.U. Acharya, A. Kumar, P.S. Bhat, C.M. Lim, S.S. Iyengar, N. Kannathal, S. M. Krishnan, Classification of cardiac abnormalities using heart rate signals, *Medical and Biological Eng. and Compt.*, 42:288-293(2004).
- [11] D. Yılmaz, N.F. Güler, Analysis of the Doppler signals using largest Lyapunov exponent and correlation dimension in healthy and stenosed internal carotid artery patients, *Digital Signal Processing*, 20(2):401-409(2010).
- [12] U.R. Abeyrathne, A.S. Karunajeewa, Mixed-phase modelling in snore sound analysis, *Med. Bio. Eng. Comput.* 45:791-806(2007).
- [13] H.D.I. Abarbanel, R. Brown, J.J. Sidorowich, L.S Tsimring., The analysis of observed chaotic data in physical systems, *Reviews of Modern Physics*, 65(4):1331(1993).

- [14] D. Yılmaz, N.F. Güler, A study on the chaotic time series analysis, *J. Fac. Eng. Arch. Gazi Univ.*, 21(4):759(2006).
- [15] F. Takens, Detecting strange attractors in turbulence, *Lecture Notes in Mathematics*, 898, 366(1981).
- [16] A.M. Fraser, H.L. Swinney, Independent coordinates for strange attractors from mutual information”, *Phys. Rev. A*, 33:1134(1986).
- [17] M.B. Kennel, R. Brown, H.D.I. Abarbanel., Determining embedding dimension for phase-space reconstruction using a geometrical construction, *Phys. Rev. A*, 45:3403-3411(1992).
- [18] L. Cao, Practical method for determinig the minimum embedding dimension of a scalar time series, *Physica D* 110:43-50(1997).
- [19] A. Wolf, J.B. Swift, H.L. Swinney, J.A. Vastano, Determining Lyapunov exponents from a time series, *Physica D*, 16:285-317(1985).
- [20] K. Briggs, An improved method for estimating Liapunov exponents of chaotic time series, *Physics Letters A*, 151:27-32(1990).
- [21] R. Brown, Calculating Lyapunov exponents for short and/or noisy data set, *Phys. Rev. E*, 47: 3962-3969(1993).
- [22] M.T. Rosenstein, J.J. Collins, C.J. De Luca, A practical method for calculating largest Lyapunov exponents from small data sets, *Physica D*, 65: 117(1993).

## Chaotic analysis of penicillin induced epileptiform activity rats

Sinan Canan<sup>1</sup>, Derya Yılmaz<sup>2</sup>

<sup>1</sup>Department of Physiology, Faculty of Medicine, Turgut Ozal University, Ankara, Turkey. e-mail: [sinancanan@gmail.com](mailto:sinancanan@gmail.com)

<sup>2</sup>Department of Biomedical Equipment Technology, Başkent University, Ankara, Turkey. e-mail: [derya@baskent.edu.tr](mailto:derya@baskent.edu.tr)

### Abstract

In this study, the chaotic indicators of penicillin-induced epileptiform activity in comparison with basal brain activity were calculated in anesthetized Wistar rats. Male Wistar rats were anesthetized with i.p. urethane and connected to an electrocorticogram setup. After a short period of basal activity recording, epileptic focus was induced by injecting 400 IU/2 µl penicillin-G potassium into the left lateral ventricle while the cortical activity was continuously recorded. Basal activity, latent period and the penicillin-induced epileptiform activity periods were selected and analyzed using both the largest Lyapunov exponent (LLE) and correlation dimension (CD) techniques. Results suggest a marked decrease in signal predictability and increased chaotic behavior during the generation of epileptiform spikes, which is generally in accordance with various human studies performed previously. Those preliminary results may be interpreted as a proof for the similar dynamics of experimental and clinical epilepsy.

Keywords: Electrocorticogram, Penicillin-induced epileptiform activity, Chaos, Nonlinear analysis, Time series analysis

### 1. Introduction

Chaotic analysis techniques have been frequently used in the analysis of non-stationary physiological signals [1]. There are some studies which are analyzed epileptic brain signals by using chaotic analysis methods [2-6]. The correlation dimension (CD), autocorrelation and largest Lyapunov exponent (LLE)

calculations were performed on the human EEG and it is found that epileptic EEG has a low dimensional chaotic behavior [2]. In the study made for children subjects with epilepsy and epilepticus during slow-wave sleep, the evidence of nonlinear dynamics was found for all EEG signals [3]. The predictive power of Lyapunov exponent was studied and it is said that usage of Lyapunov exponents practically impossible to predict epileptic seizures and EcoG signals more chaotic than low dimensional chaotic systems [4]. Despite of this result, Yambe *et al* [2005] stated that epileptic seizures can be predicted by using chaotic analysis methods. Kannathal *et al* [2005] examined the epileptic human EEG using the LLE, CD, Hurst exponent and entropy measures and found that LLE of epileptic group was higher and CD of epileptic group was lower than control.

Such analysis may also provide important insights about the nature of complex physiological phenomena, such as the generation of epileptic syndromes. Signal complexity and predictability measurements may show some different aspects of electrophysiological signals compared to traditional analysis methods. In the present study we analyzed penicillin-induced epileptiform activity recorded from rat brain after intracortical penicillin injection.

## 2. Material and Methods

### Animals and experimental procedure

Four months old male Wistar rats weighing  $198 \pm 13.05$  g were used in this study. Animals were kept in heat-regulated rooms, on a 12-h day/12-h night cycle, and given as much food and water as needed. All experimental procedures were carried out according to the guidelines of European Community Council for experimental animal care.

Animals were anesthetized with urethane (1.2 g/kg; i.p.) and the scalp covering the skull has been cut with a rostro-caudal incision of 3—4 cm long. Skull bone covering the left upper surface of the brain was removed by gradual thinning with a dental drill. After complete removal of the left side of the skull, dura mater was removed using micro scissors and the animal was fixed on a stereotaxic instrument (Harvard, USA). Body temperatures of the animals were continuously monitored and kept constant at a temperature of  $37 \pm 0.5$  °C using a homoeothermic blanket system throughout the study (Harvard Homoeothermic Blanket System).

Two Ag—AgCl ball electrodes were placed over the left somatomotor cortex (electrode coordinates: first electrode; 2mm lateral to sagittal suture and 1mm anterior to bregma; second electrode; 2mm lateral to sagittal suture 5mm posterior to bregma). Electrodes were connected to a digital data-acquisition system (Powerlab/4SP, AD Instruments, Australia) and electrocorticograms (ECoGs) were recorded digitally to a computer hard drive using 1 kHz sampling resolution and 0.1—100 Hz filter. In order to induce an epileptic focus, each animal was received an intracerebroventricular (i.c.v.) injection of crystallized penicillin-G potassium (400 IU/2\_1) using a Hamilton microinjector through an injection point located 1.5mm anterior, 2mm lateral to the Bregma, with a depth of 4.2mm located on the left somatomotor cortex [7]. This injection causes

generalized epileptiform activity characterized by large amplitude, spike, spike-wave and burst-like discharges in the recorded EEG or ECoG [8, 9].

### Recording data

All ECoG data were continuously recorded (by 200 Hz sampling rate) on a personal computer's hard drive through a data acquisition software (Chart 4.0.1, AD Instruments) and subsequent analysis of the ECoG data were performed offline. Online calculation channel recordings (including the spike amplitude and frequency calculations) were also performed during the experiments to monitor the severity of the epileptiform waves. At the end of the experiments, the position of the cannula was visually confirmed by 2% methylene blue infusion through the i.c.v. cannula after the animals sacrificed by cervical dislocation under anesthesia. Recorded ECoG data were visually assessed offline. Three distinct episodes were analyzed for each subject using nonlinear analysis methods and for analysis, three minutes of continuous and noise-free segments of each episode were selected.

1. Basal brain activity under urethane anesthesia (Fig. 1a).
2. Latent (silent) period which immediately follows the i.c.v. penicillin-G injection (the period in which the large amplitude ECoG components were significantly reduced; Fig. 1b).
3. Episode of mature epileptiform spikes (generally begins 15—30 min after the penicillin-G injection; Fig. 1c).

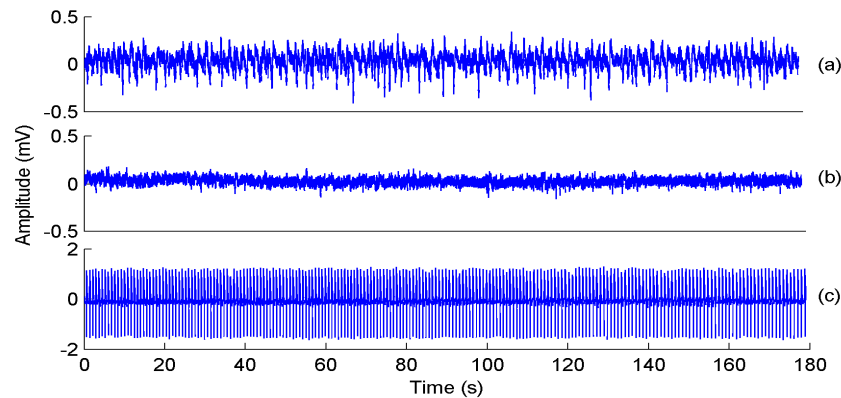


Figure 1. The ECoG signals obtained from a intracotically anesthetized rat for basal activity (a), latent period (b) and epileptic activity (c) (subject no:1).

### Nonlinear analysis

For estimating the chaotic indicators of a system, the phase space of the system has to be reconstructed from the variable [10]. An attractor is a set of states to which a dynamical system converges. The nonlinear measures of the system are calculated on this attractor [10, 11]. The Lyapunov exponent is a quantitative measure of the sensitive dependence to the initial conditions and a positive



Lyapunov exponent is accepted as an indicator of the chaos [10-12]. Another property of chaotic systems is that their attractor has fractal dimension. The CD is a measure of the complexity of a system [10].

In this work time-delay embedding method is used for reconstruction of brain signals [13]. The ECoG signal is reconstructed in the m dimensional phase space with delay coordinate T by using Takens' embedding theorem as:

$$X_i = (x_i, x_{iT}, x_{i+2T}, x_{i+3T}, \dots, x_{i+(m-1)T}) \quad (1)$$

where,  $X_i$  is the ith point on the attractor ( $i = N-(m-1)T$ ),  $x(i)$  is the ith value of the time series, m is the phase space dimension, T is the time delay. In this study, T is selected as the first minimum value of the average mutual information [10, 11, 14].

### **Largest Lyapunov exponent (LLE)**

The Lyapunov exponent  $\lambda$  gives predictability of system. The number of Lyapunov exponents is equal to the number of dimension of the phase space. Each exponent gives the long-term average divergence ( $\lambda_i > 0$ ) or convergence ( $\lambda_i < 0$ ) rate along the related axis in the phase space. Since a chaotic system has at least one positive Lyapunov exponent, if the largest Lyapunov exponent (LLE) of the system is positive, the system is chaotic [10].

In this study, the Wolf's method was applied to the epileptic brain signals to estimate the LLE [13]. This algorithm is based on the direct calculation of divergence or convergence of the trajectories on the attractor. There is an Euclidean distance,  $\delta x(0)$ , at the  $t_0$ , between the two nearest points on the reconstructed attractor. At a later time t,  $\delta x(0)$  initial distance will be evolved to distance  $\delta x(t)$ . The ratio of these two distances gives the evolution of these two points on the attractor for this time interval ( $t-t_0$ ) as given in Eqs. (3). This procedure is repeated by selecting the new data points on the attractor until the end of data. The LLE is defined as the average growth rate [13].

$$\lambda(i) = \lim_{t \rightarrow \infty} \frac{1}{t} \log \frac{\|\delta x_i(t)\|}{\|\delta x_i(0)\|} \quad (3)$$

### **Correlation dimension (CD)**

In this study, The CD was examined to characterize the system's complex behaviour. The CD gives the minimum number of independent variables necessary to generate the dynamics of a dynamic system [10, 15]. The CD was estimated using the Grassberger-Procaccia algorithm [15] and given as:

$$C(r) = \lim_{N \rightarrow \infty} \frac{1}{N^2} \sum_{i,j}^N \Theta(r - \|X_i - X_j\|) \quad (4)$$

Where,  $\|X_i - X_j\|$  is calculated as Euclidean norm and  $\Theta(\bullet)$  is the Heaviside function. The correlation integral  $C(r)$  is estimated for the range of  $r$ . The CD is the slope of the linear scaling region of the plot of  $\ln C(r)$  versus  $\ln(r)$  and is defined as:

$$D_2 = \lim_{r \rightarrow 0} \frac{\ln C(r)}{\ln r} \quad (5)$$

The slopes (D2) are calculated by using the least squares fit and plotted as a function of  $m$ . These D2 values go to saturation for as increasing  $m$  and this value was taken as the CD of the system. In the CD calculation, the embedding dimension was set to 20 for all signals.

### Statistical analysis

The results obtained from LLE and CD analysis for control, basal activity, latent period and epileptic activity of brain signals were expressed as mean $\pm$ SD. The paired and unpaired student-t tests were used for statistical analysis after normality test.  $p < 0.05$  was accepted as statistically significant.

## 3. Results

The time delay and embedding dimension are determined for reconstruction of the ECoG signals. The time delay has been estimated using the average mutual information function. The embedding dimension is set to 5 for LLE calculation

The 36,000 data points which are equal to 3-minute time window were used to reconstruct the dynamics of ECoG signals for each activity. In Fig. 2, reconstructed ECoG signals obtained from a intracotically anesthetized rats for basal, latent period and epileptic brain activities were shown in a, b, c respectively (Subject No:1 (left column) and Subject No:2 (right column)). In Fig. 2, the embedding dimension was selected as 3. The attractor of epileptic brain activity was different others as seen in below.

In the LLE analysis, the exponential evolution of the phase space trajectories has been found by calculating the differences between the point pairs. Fig. 3 shows the LLE computed for three different activities ECoG signals recorded from a intracotically anesthetized rat (Subject No:1).

The brain signals have also been processed for the CD analysis. The D2 values were plotted as a function of embedding dimension and go to saturation for as increasing embedding dimension  $m$  from 1 to 20. As shown in Fig. 4, the CD of basal activity, latent period and epileptic activity was obtained as 11.280, 9.806, 7.515 respectively.

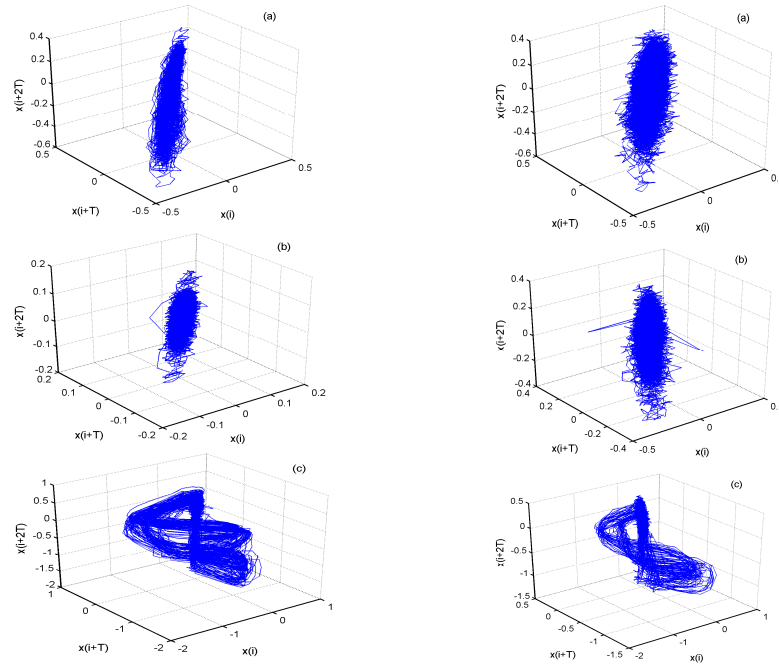


Figure 2 The attractors in the three dimensional phase space for (a) basal activity (b) latent period (c) epileptic activity.

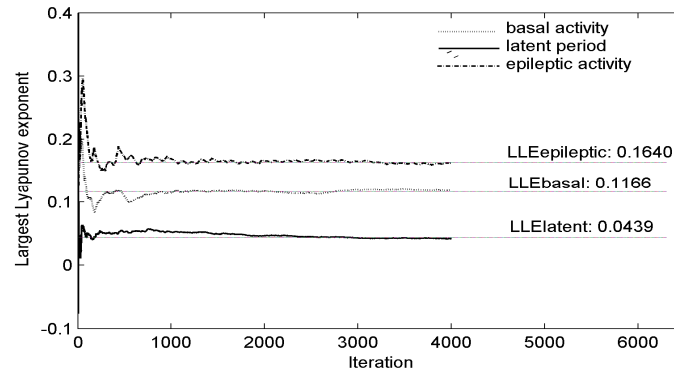


Figure 3 Time evolution of the LLE estimated from basal activity, latent period and epileptic activity signals.

The results obtained from LLE and CD calculations for control, basal activity, latent period and epileptic activity were expressed as means $\pm$ SD in Table 1. After the normality tests, the paired student-t test was applied to compare the chaotic measures of these different groups. For comparing control and basal activity data, unpaired student-t test was used.

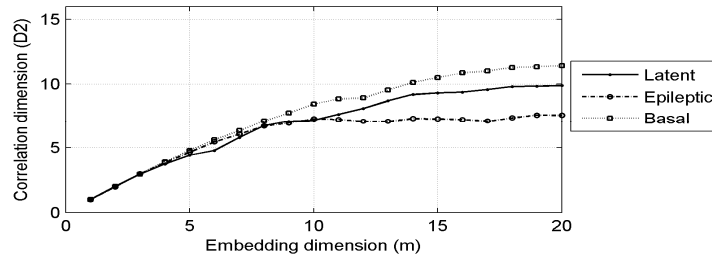


Figure 4 The CD estimation for three different activities (subject no:1).

Table 1 The LLE and CD values (mean±standart deviation) of ECoG signals.

	Control Group	Basal Activity	Latent Period	Epileptic Activity
LLE	0.0023±0.00083	0.088±0.041	0.034±0.038	0.177±0.047
<b>P=0.001<sup>a</sup> P=0.007<sup>b</sup> P=0.012<sup>c</sup> P=0.00017<sup>d</sup></b>				
CD	9.003±1.950	11.43±1.673	10.684±1.090	7.167±1.014
<b>P=0.053<sup>a</sup> P=0.48<sup>b</sup> P=0.001<sup>c</sup> P=0.0003<sup>d</sup></b>				

Student-t test P value between a: control group and basal activity, b: latent period and basal activity, c: epileptic activity and basal activity, d: epileptic activity and latent period.

According to results given in Table 1, the LLE for three groups were found statistically higher than control. The LLE of ECoG signals significantly increased in basal period compared to control. In the epileptic case, increment of the LLE is found quite high. The CD values for control, basal and latent periods were found higher than epilepsy, significantly. CD increased in basal activity by reason of anaesthesia and decreased in latent period if it is compared to basal activity, by induced penicillin.

## 4. Discussion

Penicillin-induced epileptiform activity is a widely used experimental model. This model is also suitable for analysis of spread of seizure activity and accepted as a model of simple aptrial (focal) seizures [16]. Thus, investigating the results of such a model with new approaches may provide new insights, especially by comparing new results with the previous findings on this particular model. This study has been designed as an introductory attempt for such a comparison.

Some previous studies have provided evidence that epileptic seizures are nonlinear chaotic processes [17]. The most prominent result among our findings is the increased LLE through the epileptiform spike generation during the penicillin-induced epilepsy. The increase in LLE represents a more chaotic behavior in epileptiform activity compared to basal brain activity and the silent

period just before the spike onset. Increased chaotic behavior or decreased predictability of the signal suggest that there are more neural driving forces generating epileptiform activity than the ones which drive normal basal brain activity. Although the apparent shape and the rhythm of the epileptiform spikes seem rather regular, there is an increased complexity and unpredictability during the epileptiform area, as suggested by LLE estimations. The reason and the mechanism of this behavioral change should be investigated further. The LLE values obtained from silent period appears to be significantly lower than the epileptiform period, suggesting that this period is more predictable and less chaotic. It is however unclear from our findings that how this predictable activity becomes more and more chaotic when the epileptiform spikes begin.

There is also a marked difference in CD values between different episodes. Through the generation of epileptiform spikes, CD values decreasing and reach their lowest value when the epileptiform activity begins. This finding, together with the LLE values, suggests a lower dimensional chaotic activity when compared to basal and silent brain activity episodes.

There is some evidence on the increased chaotic behavior during the epileptogenesis obtained from human studies (REF) although some other studies indicate otherwise [17]. In the light of such previous findings, our results also suggest that the nature of penicillin-induced epileptiform activity might be similar to some epileptic disorders in humans. After further investigations, such analysis may also help to justify such pharmacologically-induced epilepsy models as a tool for the study of clinical epileptic disorders. A common ground between different findings on the chaotic behavior during epileptogenesis is the fact that the epilepsy, or epileptiform activity possess different dynamical properties compared to normal or interictal electrophysiological behavior [17].

In the current literature, analysis of penicillin-induced epileptiform activity was carried out mostly with conventional signal analysis approaches, primarily by spike-counting or spectral measurements [*as an example, see ref.* 18]. Analysis used in our study lead us to think that such nonlinear analysis methods can be used in the analysis of such signals obtained from conventional experimental methods in order to gain a better understanding of the underlying mechanism of electrophysiological phenomena. Among those parameters, especially LLE can be used as an indicator of chaotic behavior.

## References

- [1] M. Akay, *Nonlinear Biomedical Signal Processing. Volume 2: Dynamic Analysis and Modelling*, IEEE Press Series on Biomedical Engineering, NewYork (2000).
- [2] A. Babloyantz, A. Destexhe, Low-dimensional chaos in an instance of epilepsy, *Proc. Natl. Acad. Sci. USA, Neurobiology*, 83:3513-3517 (1986).
- [3] R. Feri, E. Maurizio, A.M. Sebastiano, C.J. Stam, Non-linear EEG analysis in children with epilepsy and electrical status epilepticus during slow-wave sleep (ESES), *Clinical Neurophysiology*, 112:2274-2280 (2001).

- [4] Y.C. Lai, M.A.F. Harrison, G.F. Mark, I. Osorio, Controlled test for predictive power of Lyapunov exponents: Their inability to predict epileptic seizures, *Chaos*, 14(3):630-642 (2004).
- [5] T. Yambe, E. Asano, S. Mauyama, Y. Shiraishi, M. Shibata, K. Sekine, M. Watanabe, T. Yamaguchi, T. Kuwayama, S. Konno, S. Nitta, Chaos analysis of electro encephalography and control of seizure attack of epilepsy patients, *Biomedecine& Pharmacotherapy*, 59(1):236-238 (2005).
- [6] N. Kannathal, U.R. Acharya, C.M. Lim, P.K. Sadasivan, Characterization of EEG-a coparative study, *Comp. Meth. Prog. in Biomed.*, 80:17-23 (2005).
- [7] G. Paxinos, C. Watson, The rat brain in the stereotaxic coordinates. Academic Press, Sydney/New York/London (1982).
- [8] F. Bagirici, F.M. Gokce, S. Demir, C. Marangoz, Calcium channel blocker flunarizine suppresses epileptiform activity induced by penicillin in rats. *Neurosci. Res. Commun.* 28:135-140 (2001).
- [9] F. Bagirici, F.M. Gokce, C. Marangoz Depressive effect of nicardipine on penicillin induced epileptiform activity in rats. *Neurosci. Res. Commun.* 24:149-154(1999).
- [10] H.D.I. Abarbanel, R. Brown, J.J. Sidorowich, L.S Tsimring., The analysis of observed chaotic data in physical systems, *Reviews of Modern Physics*, 65(4):1331 (1993).
- [11] D. Yılmaz, N.F. Güler, A study on the chaotic time series analysis, *J. Fac. Eng. Arch. Gazi Univ.*, 21(4):759 (2006).
- [12] A. Wolf, J.B. Swift, H.L. Swinney, J.A. Vastano, Determining Lyapunov exponents from a time series, *Physica D*, 16:285-317 (1985).
- [13] F. Takens, Detecting strange attractors in turbulence, *Lecture Notes in Mathematics*, 898, 366 (1981).
- [14] A.M. Fraser, H.L. Swinney, Independent coordinates for strange attractors from mutual information, *Phys. Rev. A*, 33:1134 (1986).
- [15] P. Grassberger, I. Procaccia, Measuring the strangeness of strange attractors. *Physica D9*, 189-208 (1983).
- [16] R.S. Fisher, Animal models of epilepsy. *Brain Research Reviews*, 14: 245-278 (1989).
- [17] L.D. Iasemidis, J.C. Sackellares, Chaos Theory and Epilepsy. *The Neuroscientist* 2:118-126 (1996).
- [18] M. Yildirim, M. Ayyildiz, E. Agar, Endothelial nitric oxide synthase activity involves in the protective effect of ascorbic acid against penicillin-induced epileptiform activity. *Seizure* 19(2):102-108(2010).

# A Simulation Study of a Simple Optoelectronic Chaotic Circuit

M.P. Hantias<sup>1</sup>, H.E. Nistazakis<sup>2\*</sup> and G.S. Tombras<sup>2</sup>

<sup>1</sup> Department of Automation, Chalkis Institute of Technology,  
Psachna, Evia 34400, Greece, e-mail: mhanias@hol.gr

<sup>2</sup> Division of Electronics, Computers, Telecommunications and Control, Department of Physics,  
University of Athens, Athens 15784, Greece, e-mails: {enistaz; gtombras}@phys.uoa.gr

\*Corresponding author, enistaz@phys.uoa.gr

## Abstract

In this paper, we examine the chaotic operation of an optoelectronic circuit based on a single optocoupling device. The complete circuit is very simple and its software simulated operation demonstrates how chaos can be generated through external triggering at first, and then, how this chaos can be controlled by varying specific circuit parameters. The analysis of the obtained chaotic time series includes calculation of the optimal delay time as well as estimation of the minimum embedding dimension with the method of False Nearest Neighbors.

**Keywords:** Chaos, Optoelectronic Circuit, Time Series Analysis.

## 1. Description of the circuit

There is a growing interest for non-autonomous chaotic signal generation circuits. Such a circuit may be externally driven and it can typically consist of only one active and a few passive components. Here, we consider a particularly simple circuit based on a single optocoupling device. Its complete layout is shown in Fig.1 and it consists of a 4N25 optocoupler in a typical common emitter configuration along with an emitter degeneration resistor  $R_2=3.3\text{K}\Omega$ , a collector resistor  $R=33\Omega$ , and a DC power supply  $V_{SS}=12\text{V}$ .

The circuit is driven by an input sinusoidal voltage  $v_{IN}(t)$  with amplitude  $V_{in}=13\text{V}$  and frequency  $f=800\text{ Hz}$ , which is applied through an inductor  $L=1\text{mH}$  connected in series to the driver LED and a resistor  $R_1$ , the value of which, as we will see, plays a crucial role in the circuit's operation and the generation of chaotic voltage time series across  $R_1$  and  $R_2$ . In this respect, we use the MultiSim circuit simulation software in order to examine the complete circuit operation by monitoring the voltages  $v_D(t)$  and  $v_E(t)$  across  $R_1$  and  $R_2$ , respectively.

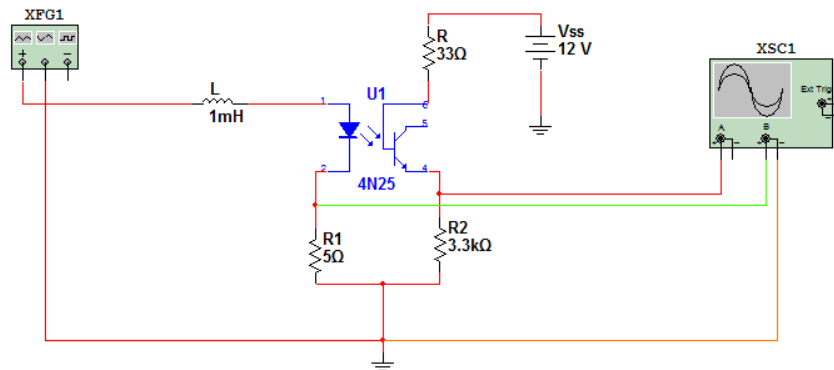


Figure 1: The considered optocoupling circuit and its MultiSim simulation environment.

At this point, we must note that the considered circuit layout resembles the resistor-inductor-diode (RLD) and the resistor-inductor-transistor (RLT) circuits, whose chaotic operation details

have been presented and discussed in [1]-[5]. More specifically, following the conclusions derived in [1]-[3], we use various values for  $R_1$  in order to achieve chaotic operation in both - if possible - the input LED loop and the emitter output loop, i.e. across  $R_1$  and  $R_2$ , respectively. Then, as already mentioned, the simulated circuit operation is monitored by checking the voltages  $v_D(t)$ , across  $R_1$ , and  $v_E(t)$ , across  $R_2$ , since both of these voltage signals depend on the chosen value of the LED resistor  $R_D$ .

## 2. Simulation results

For the considered circuit operation simulation, we use  $v_{IN}(t)=V_{in}\sin(2\pi ft)$  with  $V_{in}=13$  volts and  $f=800$  Hz. It is known that, chaotic operation may be generated under various operation conditions and parameters' values. In this work, we choose to keep  $V_{in}$  and  $f$  constant, while varying the value of  $R_1$ . Our goal is to first examine whether chaos can be achieved for a specific  $R_1$  value and then to examine whether variation of that value  $R_1$  may strengthen, weaken, or even destroy the achieved chaos, by returning the circuit to its typically expected operation.

Under these conditions and after some try-and-error selections for the value of  $R_1$ , we conclude that if  $R_1$  is set equal to  $5\Omega$  then the circuit will exhibit a fully chaotic operation, meaning that both voltage signals  $v_D(t)$  across  $R_1$ , and  $v_E(t)$  across  $R_2$ , are chaotic. This is readily shown in Fig.2. Then, using this as a starting point, we see that an increase of  $R_1$  weakens the already obtained chaotic signals, and this continues up to a value of  $R_1=500\Omega$ , for which a weak chaotic signal can still be seen across  $R_1$ , but not across  $R_2$ . This is shown in Fig.3. Finally, further increase of  $R_1$  leads to the total destruction of the remaining chaotic signal across  $R_1$ . This is shown in Fig.4 in which, for  $R_1=1K\Omega$ , both voltage signals  $v_D(t)$  and  $v_E(t)$ .

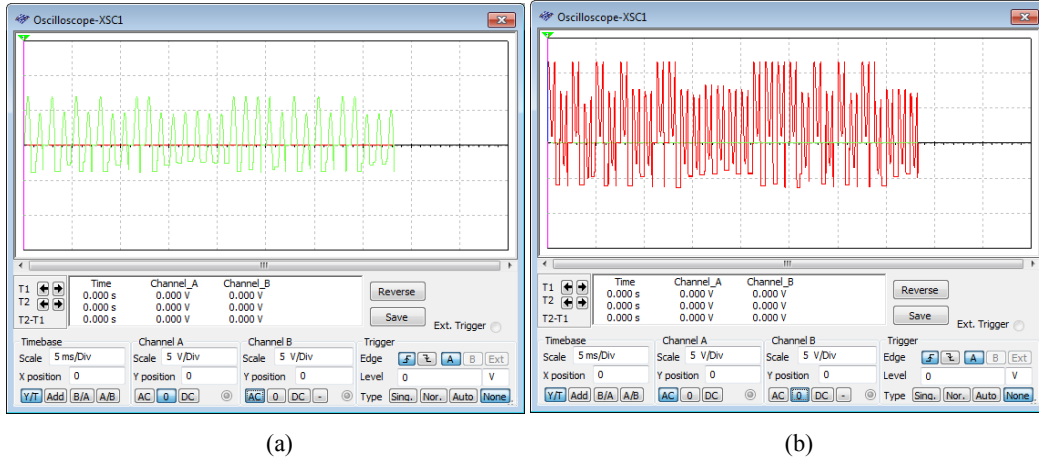


Figure 2: For  $R_1=5\Omega$ : both voltage signals (a),  $v_D(t)$  across  $R_1$ , and (b),  $v_E(t)$  across  $R_2$ , are chaotic.

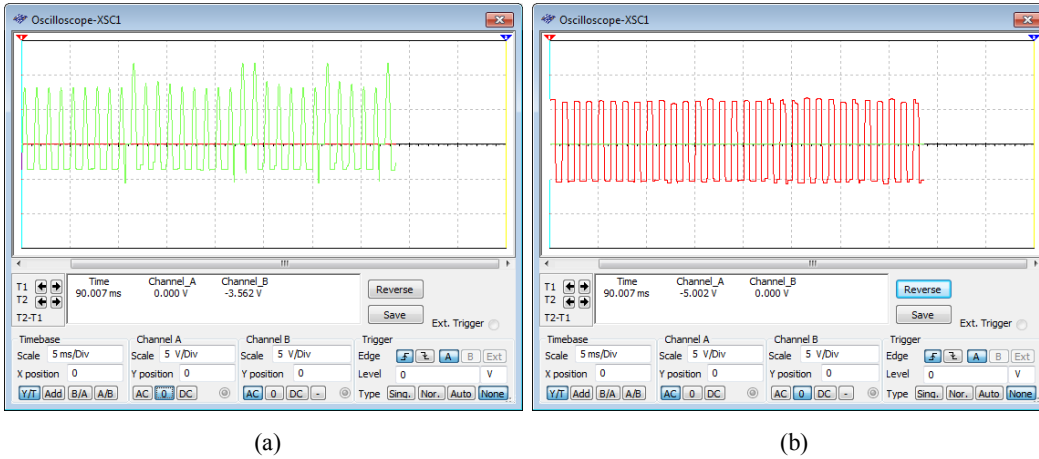


Figure 3: For  $R_1=500\Omega$ : (a)  $v_D(t)$  is a weak chaotic signal across  $R_1$ , and (b),  $v_E(t)$  across  $R_2$  is non chaotic.



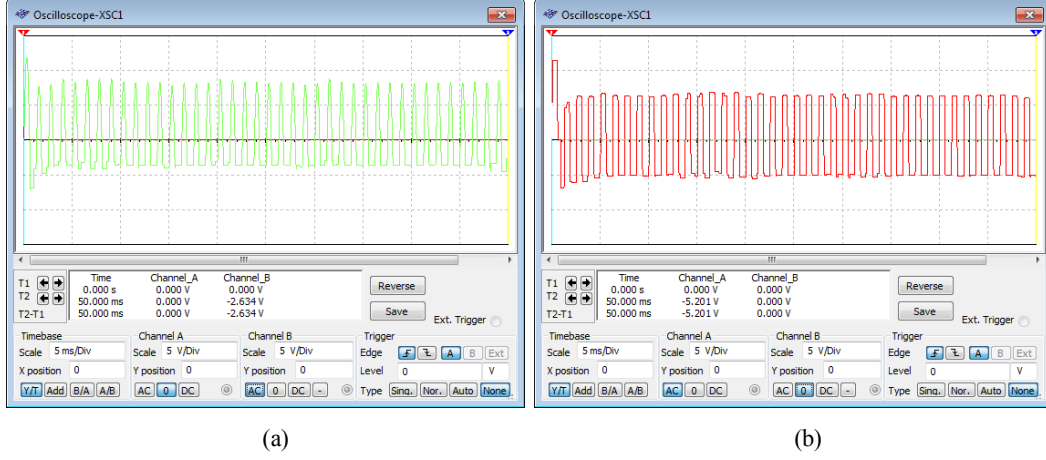


Figure 4: For  $R_1=1\text{ K}\Omega$ : both voltage signals (a),  $v_D(t)$  across  $R_1$ , and (b),  $v_E(t)$  across  $R_2$ , are non chaotic.

### 3. Nonlinear analysis

In this section, we proceed to the analysis of the obtained chaotic signals time series when  $R_1=5\Omega$ . Using our data, with value of  $R_1=5\Omega$  we construct a vector  $\vec{X}_i$ ,  $i=1..N$ , where  $N=5000$  data values in the  $m$  dimensional phase space given in the following form, [4]:

$$\vec{X}_i = \{v_i, v_{i-\tau}, v_{i-2\tau}, \dots, v_{i+(m-1)\tau}\} \quad (1)$$

This vector, represents a point of the  $m$  dimensional phase space in which the attractor is embedded each time, where  $\tau$  is the time delay  $\tau=i\Delta t$  and  $\Delta t=0.1\mu s$  is the sample rate. The element  $v_i$  represents a value of the examined scalar time series in time, i.e. here a voltage value  $v$ , across  $R_1$  or  $R_2$ , corresponding to the  $i$ -th component of the time series. The use of this method reduces phase space reconstruction to a problem of proper determination of suitable values of  $m$  and  $\tau$ . The choice of these values is not always simple, especially when there is no additional information about the original system and the only source of data is a simple sequence of scalar values as acquired from that system.

The dimension, where a time delay reconstruction of the phase space provides for the necessary number of coordinates to unfold the dynamics from overlaps on itself caused by projection is called embedding dimension  $m$ . Using the average mutual information, we can then obtain  $\tau$  as being less associated with a linear point of view, and, thus, more suitable for dealing with nonlinear problems. The average mutual information  $I(\tau)$ , [6], expresses the amount of information (in bits), which may be extracted from the value in time  $v_i$  about the value in time  $v_{i+\tau}$ . As  $\tau$ , suitable for the phase space reconstruction, the position of the first minimum of  $I(\tau)$  is usually used [6]. In this case  $\tau=77$  time steps for chaotic signal across emitter resistor  $R_2$  and  $\tau=38$  steps for chaotic signal across LED resistor  $R_1$  as shown in Fig. 5.

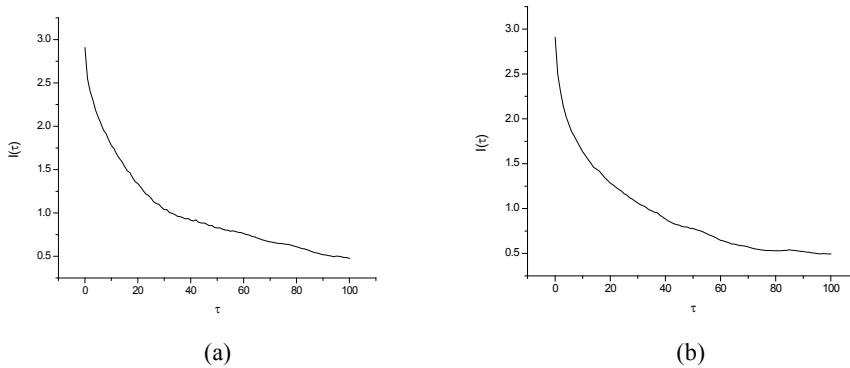


Figure 5: Mutual information  $I$  versus time delay  $\tau$  for both chaotic signals across  $R_1=5\Omega$  (a) and  $R_2$  (b).

Next, we use the method of False Nearest Neighbors (FNN), [6]-[7], in order to estimate the minimum embedding dimension. This method is based on the fact that when the embedding dimension is too small, the trajectory in the phase space will cross itself. Hence, if we are in position to detect these crossings, we may decide whether the used  $m$  is large enough for correct reconstruction of the original phase space (i.e. when no intersections occur) or not. If, however, intersections are present for a given  $m$ , then the embedding dimension must be considered too small and it must be increased by one at least. Then, again, we test the eventual presence of self-crossings.

The practical realization of the described method is based on testing the neighboring points in the  $m$ -dimensional phase space. Typically, we take a certain amount of points in the phase space and find the nearest neighbor to each of them. Then we compute distances for all these pairs and also their distances in  $(m+1)$ -dimensional phase space. The rate of these distances is given by

$$P = \frac{\|\bar{X}_i(m+1) - \bar{X}_{n(i)}(m+1)\|}{\|\bar{X}_i(m) - \bar{X}_{n(i)}(m)\|} \quad (2)$$

where  $\bar{X}_i(m)$  represents the reconstructed vector as described in (1), belonging to the  $i$ -th point in the  $m$ -dimensional phase space and index  $n(i)$  denotes the nearest neighbor to the  $i$ -th point. If  $P$  is greater than some value  $P_{\max}$ , we call this pair of points false nearest neighbors (i.e. neighbors, which arise from trajectory self-intersection and not from the closeness in the original phase space). The dimension  $m$  will then be found when the false nearest neighbors percentage falls below some limit, typically set to 1%, [8]. Thus, by choosing  $P_{\max}=10$ , we finally calculate the quantity  $m$ . The so obtained results are shown in Fig. 6 indicating that the application of the FNN method yields a minimum embedding equal to value 5 for both chaotic signals.

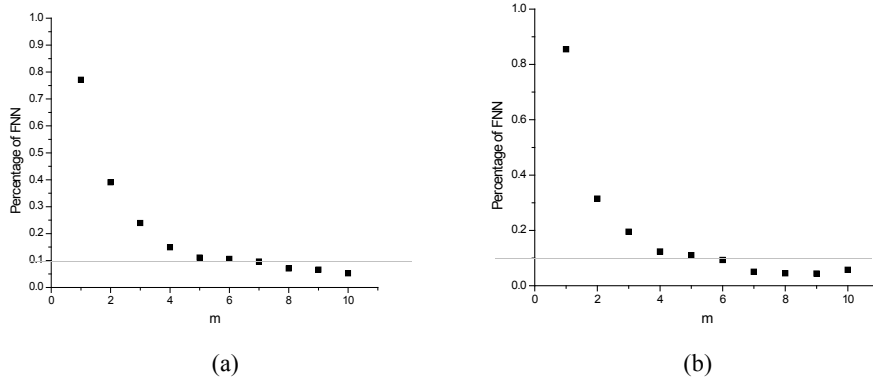


Figure 6: False nearest neighbor ratio as a function of the embedding dimension. The false nearest neighbors become negligible after  $m = 5$  for the chaotic signals (a) across LED resistor  $R_1=5\Omega$  and (b) across emitter resistor  $R_2$ .

#### 4. Conclusion

In this work, the obtained simulation results indicate that a simple externally triggered optoelectronic circuit can be used in order first to generate chaotic voltage signals and then to control the obtained chaotic signals by varying specific circuit parameters, for example, the value of a specific component. In the considered optoelectronic circuit, the crucial parameter is the input loop resistor  $R_1$ , the value of which leads to the generation of a chaotic voltage signal  $v_D(t)$  across the resistor  $R_1$ . However, this chaotic voltage reflects a chaotic current through  $R_1$  and, thus, through the optocoupler's input driving LED. Hence, the so driven phototransistor will generate a chaotic voltage signal  $v_E(t)$  across emitter resistor  $R_2$ , according to the strength of the driving chaotic light signal as controlled by the value of the input loop resistor  $R_1$ .

## References

- [1] M.P. Halias, Z. Augerinos, and G.S. Tombras, Period doubling, Feigenbaum constant and time series prediction in an experimental chaotic RLD circuit, *Chaos, Solitons and Fractals*, 40, 1050–1059, (2009).
- [2] M.P. Halias and G.S. Tombras, Time series analysis in single transistor chaotic circuit, *Chaos, Solitons and Fractals*, 40, 246–256, (2009).
- [3] M.P. Halias and G.S. Tombras, Time series crossprediction in single transistor chaotic circuit, *Chaos, Solitons and Fractals*, 41, 1167-1173, (2009).
- [4] S.G. Stavrinos, N.C. Deliolanis, Th. Laopoulos, I.M. Kyprianidis, A.N. Miliou and A.N. Anagnostopoulos, The intermitten behavior of a second - order non-linear nonautonomous oscillator, *Chaos, Solitons and Fractals*, 36, 1191-1199, (2008).
- [5] S.G. Stavrinos, A.N. Miliou, Th. Laopoulos, and A.N. Anagnostopoulos, The intermittency route to chaos of a second order non-linear non-autonomous oscillator, *Int. J. on Bifurcation & Chaos*, 18, 5, 1561-1566, (2008).
- [6] H. Kantz and T. Schreiber, *Nonlinear Time Series Analysis*, Cambridge University Press, Cambridge, 1997.
- [7] K.E. Lonngren, Notes to accompany a student laboratory experiment on chaos, *IEEE Transactions on Education*, 34, 1, (1991).
- [8] M.B. Kennel, R. Brown, H.D.I. Abarbanel, Determining embedding dimension for phase-space reconstruction using a geometrical construction, *Phys. Rev. A*, 45, 3403, (1992).

## Classes of Special Solutions of the Maxwell Bloch System and its Generalization

A. Hacınlıyan <sup>†</sup>

Department of Information Systems and Technologies  
Department of Physics, Yeditepe University  
Department of Mathematics, Gebze Institute of Technology  
Department of Physics, Bogazici University  
*ahacinliyan@yeditepe.edu.tr*

I. Kusbeyzi <sup>‡</sup>

Department of Information Systems and Technologies  
Yeditepe University  
Department of Mathematics, Gebze Institute of Technology  
*ikusbeyzi@yeditepe.edu.tr*

O. O. Aybar <sup>§</sup>

Department of Information Systems and Technologies  
Yeditepe University  
Department of Mathematics, Gebze Institute of Technology  
*oaybar@yeditepe.edu.tr*

March 7, 2010

Specialized solutions of the Maxwell Bloch equations using subsidiary conditions are known to give predator prey like systems [1]. It is also known that the Maxwell Bloch system can be related to the Lorenz system. Both the predator prey system and specialized integrals of the Lorenz system can give solutions that can describe the relatively stable operation of lasers. We also investigate the consequences of modifying the self coupling in the resulting equations to a logistic map type self coupling and the interaction coupling to the form  $x^k y$  [1, 2, 3]. Both generalizations lack structural stability, but have locally stable structures. Results of the linearized stability analysis are given for both generalizations [4, 5, 6].

## 1 Introduction

The Maxwell Bloch model (henceforth referred to as MB) is an interesting system that models the operation of an atomic system resonantly coupled to the laser field. There have been several attempts to relate laser dynamical models to predator prey models of the Lotka Volterra type, (henceforth referred to as LV), since predator models have oscillatory solutions that explain vertical Hopf bifurcation in laser models. The MB model under study involves  $E$  as the field amplitude coupling to the collective atomic polarization  $P$ .  $\Delta$  represents population inversion with its initial value  $\Delta_0$ . The model is described by the following equations [7, 9, 12].

$$\dot{E} = -kE + gP \quad (1)$$

$$\dot{P} = -\gamma_{\perp}P + gE\Delta \quad (2)$$

$$\dot{\Delta} = -\gamma_{\parallel}(\Delta - \Delta_0) - 4gPE. \quad (3)$$

Special solutions to the MB system that make either of the two nonlinear terms proportional to the third have been studied [7, 8, 9]. They are suitable candidates for stable behavior, since the third variable gets an exponentially decaying solution.

The MB equations can be transformed into the system proposed by [9, 10, 11], that resembles the LV problem with  $I$  representing the intensity of the laser field and  $N$  denoting population density. The dimensionless rate equations of  $I$  and  $N$  are obtained by assuming  $I = E^2$  and multiplying the first MB equation (1) by  $E$  which gives

$$E\dot{E} = -kE^2 + gPE.$$

Using the subsidiary condition  $gP = kE\Delta$ , the second MB equation (2) is obtained as follows

$$\dot{P} = -\gamma_{\perp}P + \frac{g^2P}{k}.$$

The subsidiary condition for the Polarization equation enables decoupling and solving for the polarization as

$$P = P_0 \exp \left[ -\left( \gamma_{\perp} - \frac{g^2}{k} \right) t \right].$$

Finally we transform the MB equation (3) into

$$\dot{\Delta} = -\gamma_{\parallel}(\Delta - \Delta_0) - 4kE^2\Delta.$$

The MB model given above can be cast into the form of a predator prey equation by defining the intensity and population density as  $\Delta = N$ ,  $2kt = \tau$  and  $\tilde{I} = 2I\gamma$  [7, 8, 9, 10].

$$\begin{aligned}\dot{\tilde{I}} &= (-1 + N)\tilde{I} \\ \dot{N} &= \gamma(\Delta_0 - N - N\tilde{I}).\end{aligned}\tag{4}$$

We have successfully transformed the MB system into a new form that resemble the LV equations by assuming  $\Delta_0 = 0$  and  $\gamma \leq 0$  in the physical region [7, 8, 9, 11]. Thus the population fluctuations in the laser system can emulate a predator prey system governed by the pumping and lasing actions when the coupling  $\gamma$  is negative where we get a pair of purely imaginary eigenvalues. Here equilibrium points are  $(0, 0)$ ,  $(1, -1)$  and linearized eigenvalues are  $\{-1, -\gamma\}$ ,  $\{\sqrt{\gamma}, -\sqrt{\gamma}\}$ . We see that these type of lasers naturally exhibit damped intensity oscillations that satisfy a degenerate form of the LV equations [8, 10, 11]. LV equations appear as an underlying problem and allow us to describe the bifurcation type that has been also analytically verified in the original system [8, 10, 12].

For the special case  $\Delta_0 = 0$  of equation (4), which physically means an initially empty population inversion, the system has the following LV like integral:

$$\log N - N - \gamma \log \tilde{I} - \gamma \tilde{I} = \text{constant}$$

Furthermore, if  $\gamma = -1$  then eigenvalues of this system become  $\{-i, i\}$  where the system resembles the LV model with Hopf bifurcation [8, 9, 10, 12]. Two generalizations of this model will be investigated here. One involves the simplest polynomial generalization by the addition of a quadratic term (6) to the self coupling which changes it from a Malthus like unstable term to a logistic map like term. The other involves generalizing the coupling from a simple product form,  $xy$  to the more general  $x^k y$  form [10]. The comparison to the Lorenz model is also of interest, since under special conditions, it possesses first integrals that point to conditions under which chaotic behavior is absent.

## 2 Connection with the Lorenz Model and Its Integrable Cases

The relation between this model and the Lorenz model:

$$\begin{aligned}\dot{x} &= \sigma(y - x) \\ \dot{y} &= -rx - y - xz \\ \dot{z} &= xy - \beta z\end{aligned}\tag{5}$$

was first given by Khanin[6]. For  $k = \sigma$ ,  $\gamma_{\perp} = \frac{g^2}{k} = 1$ ,  $g^2 \frac{\Delta_0}{k} = r$ ,  $\gamma_{\parallel} = \beta$ , the system can be transformed into the Lorenz system about the equilibrium point  $\Delta = \Delta_0$  by setting  $x = E$ ,  $y = \frac{gP}{k}$ ,  $z = \Delta_0 - \Delta$ . Here,  $\sigma, r, \beta$  are the Lorenz parameters. Since the MB equations have more parameters than the Lorenz system, some ambiguities do occur, for example the condition  $4k = 1$

$(\beta, \sigma, r)$	<i>First Integrals</i>
$(2k, k, \Delta_0)$	$I_1 = (E^2 - 2k(\Delta - \Delta_0)) \exp(2kt)$
$(1, k, 0)$	$I_2 = (E^2 + (\frac{g^P}{k})^2) \exp(2t)$
$(1, 1, \Delta_0)$	$I_3 = (-\Delta_0 E^2 + (\frac{g^P}{k})^2 + (\Delta - \Delta_0)^2) \exp(2t)$
$(6k - 2, k, 2k - 1)$	$I_4 = (\frac{(2k-1)^2}{k} E^2 + k(\frac{g^P}{k})^2 - (4k - 2)E(\frac{g^P}{k}) - \frac{1}{4k} + E^2(\Delta - \Delta_0)) \exp(4kt)$
$(0, \frac{1}{3}, \Delta_0)$	$I_5 = (\Delta_0 E^2 + \frac{1}{3}(\frac{g^P}{k})^2 + \frac{2}{3}E\frac{g^P}{k} + E^2(\Delta - \Delta_0) - \frac{3}{4}E^4) \exp(\frac{4}{3}t)$
$(4, 1, \Delta_0)$	$I_6 = (4(\Delta_0 - 1)(\Delta - \Delta_0) - \Delta_0 E^2 - (\frac{g^P}{k})^2 + 2E(\frac{g^P}{k}) - E^2(\Delta - \Delta_0) + \frac{1}{4}E^4) \exp(4t)$

Table 1: Integrals of MB System related to Lorenz system

can be used instead of  $k = \sigma$ , for physical reasons we will use the first set of conditions. Under these circumstances the known first integrals of the Lorenz system [7, 8, 9, 13] for special cases gives the first integrals in the Table (1) for the MB system [12, 13]. Parameter requirements for the first three integrals and the sixth integral are moderately reasonable.

### 3 Adding quadratic term to the LV model related to the MB system

Models such as Malthus and Verhulst are single species models. Many of the most interesting dynamical systems have complex interactions between species. Hence mathematical models that include both these single species coupling and coupling interactions are required to simulate these dynamics. The addition of a quadratic self coupling suggested by the Verhulst model produces the simplest polynomial generalization depending on the coefficient between the linear and quadratic term. Rescaling the variables and the parameters enables us to make the coefficient of the quadratic term unity without loss of generality. This generalization can introduce one or two stable equilibrium points for appropriate values of the modified parameters that belong to the following system where  $x$  plays the role of  $I = E^2$  and  $y$  plays the role of  $N$ :

$$\begin{aligned}\dot{x} &= a(x - x^2) - bxy \\ \dot{y} &= -c(y + y^2) + dxy.\end{aligned}\tag{6}$$

For  $c = a + b + d$ , this system has the following integral:

$$x^{c_1} y^{c_2} (1 - x + y)\tag{7}$$

where  $c_1, c_2$  are given expressions involving the equation parameters and provided that  $ac + bd \neq 0$ .

Two additional equilibrium points are introduced into the system where the predator species consume one type of prey species represented by equation (6). The equilibrium points are  $(0, 0)$ ,  $(1, 0)$ ,  $(\frac{(a+b)c}{ac+bd}, \frac{-a(c-d)}{ac+bd})$  and  $(0, -1)$ . The linearized eigenvalues associated with the equilibrium point  $(0, 0)$  are  $\{a, -c\}$  that becomes a saddle node, the eigenvalues associated with the equilibrium point  $(1, 0)$  are  $\{-a, -c + d\}$ . If  $d \geq c$  this equilibrium becomes a saddle node or a stable equilibrium, the eigenvalues associated with the equilibrium point  $(\frac{(a+b)c}{ac+bd}, \frac{-a(c-d)}{ac+bd})$  are a complex conjugates pair with complex conjugates eigenvectors. If

$$\frac{a^2c + abc - ac^2 + acd}{-2(ac + bd)} \leq 0$$

then the equilibrium becomes stable and finally the eigenvalues associated with the equilibrium point  $(0, -1)$  are  $\{a + b, c\}$ . This equilibrium is unstable. Hence, this generalization can introduce one or two stable equilibrium points in the linearized approximation for appropriate values of the parameters.

## 4 Generalization involving $x^k y$ coupling

A different generalization can be obtained by introducing the nonlinearity  $x^k y$  in the prey equation together with a quadratic term. The predator equation is LV. For a given value of the number  $k$  we define the following family of systems of differential equations. The specialized choice of parameters is dictated by the requirement that the system be compatible with a resonant normal form for integer values of the folding parameter  $a$ . The system is

$$\begin{aligned} \dot{x} &= (a - 1)x - x^2 - xy - a^{-k+1}x^k y \\ \dot{y} &= -y + xy \end{aligned} \quad (8)$$

and the following Lemmas apply. **3.1, 3.2** are obtained;

**Lemma 3.1:** The general form of equilibrium points of the system given above are  $(a - 1, 0)$  and  $(1, \frac{a-2}{1+a^{-k+1}})$  for all  $k$ . In addition to these points the system acquires one more equilibrium point at the origin if  $k \geq 2$ .

**Lemma 3.2:** The system in concern has three saddle points whose linearized eigenvalues are  $\{-1, a - 1\}$ ,  $\{1 - a, a - 2\}$  and a third set of eigenvalues which start out as a saddle point for  $a \leq 2$ , degenerate into a sink and eventually into a stable focus for values of  $a \sim 2.3$ , the value is relatively insensitive to the value of  $k$  as long as  $k > 2$ .

The general form of equilibrium points of the system (8) are  $(0, 0)$  for  $k \geq 2$ ,  $(a - 1, 0)$  and  $(1, \frac{a-2}{1+a^{-k+1}})$  for all  $k$ . Two of these are saddle points whose linearized eigenvalues are  $\{-1, a - 1\}$ ,  $\{1 - a, a - 2\}$ . If  $\frac{-3a+a^2-a^k-2ak+a^2k}{2(a+a^k)}$  is defined as  $\Delta$  then the eigenvalues of the  $k$  dependent equilibrium point are



$$\Delta \pm \frac{\sqrt{-4(-2+a)(a+a^k)^2 + (a^k + a(3-2k) + a^2(-1+k))^2}}{2(a+a^k)}.$$

They imply that the equilibrium point starts out as a saddle point for  $a \leq 2$ , degenerate into a sink and eventually into a stable focus for values of  $a \sim 2.3$ , the value is relatively insensitive to the value of  $k$  as long as  $k > 2$ .

By the change of variables  $x = r \cos \theta$  and  $y = r \sin \theta$  the following result which shows that there exists an infinite a family of periodic orbits near the parameter value  $a = 2$  due to the crudity of the approximation independently of  $k$  [7, 8, 9, 13] .

$$x\dot{x} + y\dot{y} = (a-1)x^2 - x^3 - x^2y - a^{-k+1}x^{k+1}y - y^2 + xy^2 \quad (9)$$

$$\frac{d\rho^2}{dt} = (a/2 - 1)\rho^2. \quad (10)$$

In order to understand this behavior, we pass to a rotating frame using  $x = u(t) \cos \omega t + v(t) \sin \omega t$  and  $y = -u(t) \sin \omega t + v(t) \cos \omega t$ , where  $u(t)$  and  $v(t)$  are slowly varying functions. We can then average the system over a full period  $0 \leq t \leq \frac{2\pi}{\omega}$ . For  $k = 2$  this yields the following system

$$\begin{aligned} \dot{u} &= \left(\frac{a}{2} - 1\right)u - \omega v - \frac{u^2v}{8a} - \frac{v^3}{8a} \\ \dot{v} &= \left(\frac{a}{2} - 1\right)v + \omega u + \frac{uv^2}{8a} + \frac{u^3}{8a}. \end{aligned} \quad (11)$$

It is clear that for  $a = 2$ , the quadratic nonlinearity is the predominant one. In particular, if  $k = 2$ , a family of periodic solutions are available, nonlinear terms persist. If  $k = 3$  the same behavior occurs, but nonlinear terms do not persist. This explains both the behavior at  $a = 2$  and the insensitivity of the results to the value of  $k$  [7, 8, 9, 13] .

## 5 Conclusion

The MB model exhibits chaotic behavior in a wide range of its parameter space [7, 8, 9]. For realistic models of lasers, chaotic behavior is undesirable. The aim of this work is to look at these cases. One possibility is the relation of the MB model to the Lorenz model, that has isolating integrals for specialized values of its parameters. Another possibility is relating the model to a predator prey type model. A special solution related to the predator prey system and a class of Predator - Prey Models that generalize this model by couplings of the form  $x^k y$  in the prey equation or  $xy^k$  in the predator equation are studied. Stability properties of these models are examined. It is also shown that they have limit cycles irrespective of the detailed form of the coupling [7, 8, 9, 12, 13] .

## References

- [1] F. T. Arecchi, Chaos and Generalized Multistability in Quantum Optics, *Physica Scripta*, 85-92 (1985).
- [2] R. Rand, A. Verdugo, Hopf bifurcation formula for first order differential-delay equations, *Communications in Nonlinear Science and Numerical Simulation*, 12, 859864 (2007).
- [3] W. Ruiping Wang, X. Dongmei, Bifurcations and chaotic dynamics in a 4-dimensional competitive LotkaVolterra system, *Nonlinear Dynamcics*, DOI 10.1007/s11071-009-9547-3 (2009).
- [4] X. K. Sun, Xiao-Ke, Huo, Hai-F., H. Xiang, Bifurcation and stability analysis in predatorprey model with a stage-structure for predator, *Nonlinear Dynamics*, DOI 10.1007/s11071-009-9495-y (2009).
- [5] H. Haken, Laser Light Dynamics, *North Holland*, 2, (1985)
- [6] Y. I. Khanin, *Dynamics of Lasers*, Soviet Radio, Moscow (1975).
- [7] A. Hacinliyan, I. Kusbeyzi, Bifurcation Scenarios of Some modified PredatorPrey Nonlinear Systems, *Journal of Applied Functional Analysis*, Vol.4, No.3, 519-527, (2009) Eudoxus Press.
- [8] A. Hacinliyan, I. Kusbeyzi, O. O. Aybar, Maxwell-Bloch Equations as Predator-Prey System, *Chaotic Systems Theory and Applications Selected Papers from the 2nd Chaotic Modeling and Simulation International Conference*, ISBN:978-981-4299-71-8, (2010).
- [9] A. Hacinliyan, I. Kusbeyzi, O. O. Aybar, Approximate Solutions of Maxwell Bloch Equations and Possible Lotka Volterra Type Behavior, *submitted to Nonlinear Dynamics*(2009).
- [10] Erneux, T., Kozyreff G., Nearly Vertical Hopf Bifurcation for a Passively Q-Switched Microchip Laser, *Journal of Statistical Physics*, Springer, 1-2, 101, (2000).
- [11] Wiggins, S., Introduction to Applied Nonlinear Dynamical Systems and Chaos, *Springer, Verlag, NY*, (ISBN 0387970037), (1996).
- [12] Clarici, G., Griesse, E., Analytical Laser Model for Optical Signal Integrity Analysis, *International Students and Young Scientists Workshop "Photonics and Microsystems"*, (2005).
- [13] A. Goriely, Integrability and Nonintegrability of Dynamical Systems, *World Scientific Publishing Company*, (ISBN-10: 981023533X ), (2001).

# Semi-analytical Solutions of Integral and Integro-differential Equations

Emine Mısırlı , Meryem Odabaşı <sup>1</sup>

*Department of Mathematics, Ege University, 35100 Bornova, İzmir, Turkey*

March 7, 2010

## Abstract

In this letter, the variational iteration method is applied to solve integral and integro-differential equations. Some examples are given to investigate the capacity of the method. The results show that the method provides a straightforward and powerful mathematical tool for solving various integral and integro-differential equations. The considered examples reveal that the method is very effective and simple compared with the homotopy perturbation method.

**Keywords:** Integral and integro-differential equations

## 1. Introduction

Mathematical modeling of real-life, physics and engineering problems usually results in functional equations, e.g. partial differential equations, integral and integro-differential equations, stochastic equations and others. Many mathematical formulation of physical phenomena contain integral and integro-differential equations, these equations arise in fluid dynamics, biological models and chemical kinetics; for more details see [1,2] and the references cited therein. Integro-differential equations are usually difficult to solve analytically so it is required to obtain an efficient approximate solution. Therefore, they have been of great interest by several authors. In literature, there exist numerical techniques such as Wavelet-Galerkin method (WGM) [3], CAS wavelet approximating method [4], Lagrange interpolation method [5] and Tau method [6] and semi analytical-numerical techniques such as Adomian's decomposition method [7], Taylor polynomials [8], rationalized Haar functions method [9], differential transform method [10] and homotopy perturbation method [11]. However, none of them propose a methodical way to solve these equations.

---

<sup>1</sup> E-mail addresses : emine.misirli@gmail.com (E. Mısırlı), meryemodabasi@gmail.com (M. Odabaşı)

In recent years, variational iteration method has been used in obtaining approximate solutions of a wide class of differential, integral and integro-differential equations. The method can solve various different nonlinear equations [12-14]. In this work, the variational iteration method has been applied to the several integral and integro-differential equations and exact solutions have been obtained.

## 2. Variational Iteration Method

Variational iteration method was first proposed by He [15-17] and has been successfully used by many researchers to solve various linear and nonlinear models [18-21]. The idea of the method is based on constructing a correction functional by a general Lagrange multiplier and the multiplier is chosen in such a way that its correction solution is improved with respect to the initial approximation or to the trial function.

Now, to illustrate the basic concept of the method, we consider the following general nonlinear system

$$L[u(t)] + N[u(t)] = g(t) \quad (1)$$

where  $L$  is a linear operator,  $N$  is a nonlinear operator and  $g(x)$  is a known analytical function. According to the variational iteration methodology we can construct the correction functional as:

$$u_{n+1}(t) = u_n(t) + \int_0^t \lambda(s) [Lu_n(s) + N\tilde{u}_n(s) - g(s)] ds, \quad (2)$$

where  $\lambda$  is a general Lagrange multiplier, which can be identified optimally via variational theory, the subscript  $n$  denotes the  $n$ th approximation, and  $\tilde{u}_n$  is considered as a restricted variation, namely  $\delta\tilde{u}_n = 0$ . Successive approximations will be obtained by applying the obtained Lagrange multiplier and a properly chosen initial approximation  $u_0(t)$ .

## 3. Applications

**Example 1.** We first consider the integro-differential equation

$$u'(x) = (x+1)e^x - x + \int_0^1 xu(t)dt, \quad u(0) = 0, \quad (3)$$

with the exact solution  $u(x) = xe^x$  (see [4] and [22]).

Approximate solution of this problem obtained by homotopy perturbation method [23] with four terms has the following form :

$$u(x) = xe^x - \frac{1}{432}x^2 \quad (4)$$

We applied the variational iteration method (VIM) to obtain the solution of the Equation (3).

Eq. (3) is equivalent to

$$u'(x) = (x+1)e^x + \int_0^1 (xu(t) - x)dt \quad , \quad (5)$$

and its iteration formula reads

$$u_{n+1}(x) = u_n(x) + \int_0^x \lambda(s) \left\{ u_n'(s) - (s+1)e^s - \int_0^1 (su_n(p) - s)dp \right\} ds . \quad (6)$$

By via variational theory Lagrange multiplier can be find as

$$\lambda = -1 . \quad (7)$$

Substituting the identified multiplier into Eq. (6), we have the following iteration formula

$$u_{n+1}(x) = (x+1)e^x - \int_0^x \left\{ u_n'(s) - (s+1)e^s - \int_0^1 (su_n(p) - s)dp \right\} ds . \quad (8)$$

By variational iteration,

$$L(u) = u'(x) - f(x) = 0 \quad (9)$$

$$L(u_0) = u_0'(x) - (x+1)e^x = 0 \quad (10)$$

So, we can take  $u_0(x)$  as

$$u_0(x) = xe^x \quad (11)$$

Substituting (11) into Eq. (8), we have

$$\begin{aligned} u_1(x) &= (x+1)e^x - \int_0^x \left\{ u_0'(s) - (s+1)e^s - \int_0^1 (su_0(p) - s)dp \right\} ds \Rightarrow u_1(x) = xe^x \\ u_2(x) &= (x+1)e^x - \int_0^x \left\{ u_1'(s) - (s+1)e^s - \int_0^1 (su_1(p) - s)dp \right\} ds \Rightarrow u_2(x) = xe^x \end{aligned} \quad (12)$$

Similarly

$$\begin{aligned} u_3(x) &= xe^x \\ u_4(x) &= xe^x \\ &\vdots \end{aligned} \quad (13)$$

Thus, we obtain

$$u(x) = xe^x \quad (14)$$

which is the exact solution of Equation (3).

In the Table 1, we list the results obtained by variational iteration method and gived the errors for CAS wavelet approximating method [4] , differential transform method [22] and homotopy perturbation method [23].

**Example 2 .** We next consider the integro-differential equation

$$u'(x) = 3e^{3x} - \frac{1}{3}(2e^3 + 1)x + \int_0^1 3xtu(t)dt \quad , \quad (15)$$

with condition

$$u(0) = 1 . \quad (16)$$

Table I- Numerical results for Example 1

$x$	Error (DTM)	Error (CAS wavelet )	Error (HPM)	$u$ (exact-VIM)
0.1	1.00118319e-02	1.34917637e_03	0.2314814815e_05	0.110517091
0.2	2.78651355e-02	1.15960044e_03	0.9259259259e_05	0.244280551
0.3	5.08730892e-02	5.67152531e_03	0.2083333333e_04	0.404957642
0.4	7.55356316e-02	5.93105645e_02	0.3703703704e_04	0.596729879
0.5	9.71888592e-02	1.32330751e_02	0.5787037037e_04	0.824360635
0.6	1.09551714e-01	4.39287720e_02	0.8333333333e_04	1.093271280
0.7	1.04133232e-01	1.41201624e_02	0.1134259259e_03	1.409626895
0.8	0.94512700e-02	1.34514117e_02	0.1481481481e_03	1.780432742
0.9	1.00034260e-02	1.32045209e_02	0.1875000000e_03	2.213642800

By homotopy perturbation method (HPM), Kajani et al. [24] obtained the approximate solution of Eq. (15-16) in the form

$$u_{appr}(x) = e^{3x} - \frac{1}{6}(2e^3 + 1)x^2 + \left(\frac{5}{24}e^3 + \frac{5}{48}\right)x^2 \left\{1 + \frac{3}{8} + \frac{9}{64} + \frac{27}{512} + \dots\right\}. \quad (17)$$

In order to solve Eq. (15-16) we applied the variational iteration method (VIM). First, we rewrite the Eq. (15) as

$$u'(x) = 3e^{3x} + \int_0^1 \left( 3xtu(t) - \frac{1}{3}(2e^3 + 1)x \right) dt, \quad (18)$$

and according to via variational theory its iteration formula reads

$$u_{n+1}(x) = u_n(x) - \int_0^x \left\{ u_n'(s) - 3e^{3x} - \int_0^1 \left( 3spu_n(p) - \frac{1}{3}(2e^3 + 1)s \right) dp \right\} ds \quad (19)$$

By variational iteration,

$$L(u) = u'(x) - f(x) = 0 \quad (20)$$

$$L(u_0) = u_0'(x) - 3e^{3x} = 0 \quad (21)$$

So, we can take  $u_0(x)$  as

$$u_0(x) = e^{3x} \quad (22)$$

Substituting (22) into Eq. (19), we have

$$u_1(x) = e^{3x} - \int_0^x \left\{ 3e^{3x} - 3e^{3x} - \int_0^1 \left( 3spe^{3p} - \frac{1}{3}(2e^3 + 1)s \right) dp \right\} ds \quad (23)$$

$$u_1(x) = e^{3x}$$

Similarly,

$$u_2(x) = e^{3x}$$

$$u_3(x) = e^{3x} \quad (24)$$

$\vdots$

Thus, we obtain

$$u(x) = e^{3x} \quad (25)$$

which is the exact solution of Eq. (15-16).

**Example 3.** Consider the second order integro-differential equation

$$u''(x) = e^x - x + \int_0^1 xtu(t)dt \quad (26)$$

with initial conditions

$$u(0) = 1, \quad u'(0) = 1. \quad (27)$$

Golbabai and Javidi [11] obtained the approximate solution of Eq. (26-27) by using homotopy perturbation method.

Darania and Ebadian [22] obtained the approximate solution by differential transform method (DTM).

In order to solve this equation we applied the variational iteration method.

Equation (26) is equivalent to

$$u''(x) = e^x + \int_0^1 (-x + xtu(t))dt, \quad (28)$$

and its iteration formula reads

$$u_{n+1}(x) = u_n(x) + \int_0^x \lambda(s) \left\{ u_n''(s) - e^s - \int_0^1 (-s + spu_n(p))dp \right\} ds. \quad (29)$$

By via variational theory Lagrange multiplier can be find as

$$\lambda(s) = s - x \quad (30)$$

So, the iteration formula becomes

$$u_{n+1}(x) = u_n(x) + \int_0^x (s - x) \left\{ u_n''(s) - e^s - \int_0^1 (-s + spu_n(p))dp \right\} ds \quad (31)$$

By variational iteration method, we have

$$L(u) = u''(x) - f(x) = 0 \quad (32)$$

$$L(u_0) = u_0''(x) - e^x = 0 \quad (33)$$

We now obtain

$$u_0''(x) = e^x. \quad (34)$$

So, we can take  $u_0(x)$  as

$$u_0(x) = e^x + ax + b \quad (35)$$

By using initial conditions, we obtain

$$u_0(0) = 1 + b = 1 \Rightarrow b = 0 \quad (36)$$

$$u_0'(0) = 1 + a = 1 \Rightarrow a = 0$$

So, we can select

$$u_0(x) = e^x \quad (37)$$

We now successively obtain

$$\begin{aligned} u_1(x) &= u_0(x) + \int_0^x (s-x) \left\{ u_0''(s) - e^s - \int_0^1 (-s + spu_0(p)) dp \right\} ds \\ u_1(x) &= e^x \\ u_2(x) &= e^x \\ u_3(x) &= e^x \\ &\vdots \end{aligned} \quad (38)$$

Thus we obtain

$$u(x) = e^x \quad (39)$$

which is the exact solution of Eq. (26-27).

In Table II, we list the results obtained by variational iteration method compaired with differential method (DTM) results given in [22] and homotpoy perturbation method (HPM) results given in [11] at  $x = 0.2(0.2)1$ .

**Example 4 .** Consider the nonlinear Volterra integral equation

$$u(x) = 2x - \frac{1}{2}x^4 + \int_0^x \frac{1}{4}(u(t))^3 dt \quad (40)$$

Javidi et al. [25] applied the Adomian method and obtained the approximate solution of Eq. (40).

In order to solve this equation we applied the VIM and obtained the exact solution. We can rewrite the Eq. (40) as

$$u(x) = 2x + \int_0^x \frac{1}{4}(u^3(t) - 8t^3) dt . \quad (41)$$

According to the via variational theory, its iterative formula reads

$$u_{n+1}(x) = 2x + \int_0^x \frac{1}{4}(u_n^3(t) - 8t^3) dt , \quad (42)$$

and

$$u_0(x) = 2x \quad (43)$$

Substituting (43) into Eq. (42) gives

$$\begin{aligned} u_1(x) &= 2x + \int_0^x \frac{1}{4}(u_0^3(t) - 8t^3) dt \Rightarrow u_1(x) = 2x \\ u_2(x) &= 2x + \int_0^x \frac{1}{4}(u_1^3(t) - 8t^3) dt \Rightarrow u_2(x) = 2x \\ &\vdots \end{aligned} \quad (44)$$

Thus, we obtain  $u(x) = 2x$  which is the exact solution of Eq. (40).



Table II - Numerical results for Example 3

$x$	Error(DTM)	Error (HPM, N=5)	Error (HPM, N=10)	$u$ (Exact- VIM)
0.2	4.6310e_4	7.7074e_6	8.2305e_10	1.2214
0.4	2.9438e_3	5.9259e_5	6.5844e_9	1.4928
0.6	7.8064e_3	2.0000e_4	2.2222e_8	1.8221
0.8	1.5474e_2	4.7407e_4	5.2674e_8	2.2255
1.0	2.6436e_2	9.2593e_4	1.0288e_7	2.7183

**Example 5.** Consider the integro-differential equation

$$u'(x) = 1 - \frac{1}{3}x + \int_0^1 xt u(t) dt, \quad (45)$$

with initial condition

$$u(0) = 0. \quad (46)$$

Golbabai and Javidi [11] obtained the approximate solution of Eq. (45-46) by using homotopy perturbation method as

$$u_{approx}^4(x) = x - \frac{1}{24576}x^2, \quad (47)$$

$$u_{approx}^9(x) = x - \frac{1}{805306368}x^2.$$

In order to solve this equation we applied the variational iteration method. We can rewrite the equation as

$$u'(x) = 1 + \int_0^1 \left( -\frac{1}{3}x + xt u(t) \right) dt, \quad (48)$$

its iteration formula reads

$$u_{n+1}(x) = u_n(x) - \int_0^x \left\{ u_n'(s) - 1 - \int_0^1 \left( -\frac{1}{3}s + sp u_n(p) \right) dp \right\} ds, \quad (49)$$

and

$$u_0(x) = x \quad (50)$$

Substituting (50) into Eq. (45), we have the following results

$$\begin{aligned} u_1(x) &= x \\ u_2(x) &= x \\ &\vdots \end{aligned} \quad (51)$$

So, we obtain

$$u(x) = x \quad (52)$$

which is the exact solution of Eq. (45-46).

## 4. Conclusion

In this work, He's variational iteration method (VIM) is applied for solving integral and integro-differential equations. Comparison of the result obtained by the VIM with that obtained by homotopy perturbation method (HPM) and differential transform method (DTM) reveals that the variational iteration method is very effective and convenient.

## Acknowledgement

Authors thank to TÜBİTAK (The Scientific and Technological Research Council of Turkey) for their financial support.

## References

- [1] P.K. Kythe, P. Puri, *Computational methods for linear integral equations*, University of New Orleans, New Orleans, 1992.
- [2] A.M. Wazwaz, A comparison study between the modified decomposition method and the traditional methods, *Applied Mathematics and Computation* ,181 , 1703\_1712 (2006).
- [3] A. Avudainayagam, C. Vani, Wavelet-Galerkin method for integro-differential equations, *Applied Numerical Mathematics*, 32 ,247\_254 (2000).
- [4] H. Danfu, S. Xufeng, Numerical solution of integro-differential equations by using CAS wavelet operational matrix of integration ,*Applied Mathematics and Computation*, 194, 460-466 (2007).
- [5] M.T. Rashed, Lagrange interpolation to compute the numerical solutions of differential, integral and integro-differential equations, *Applied Mathematics and Computation*, 151 , 869\_878(2004).
- [6] S.M. Hosseini, S. Shahmorad, Tau numerical solution of Fredholm integro-differential equations with arbitrary polynomial bases, *Applied Mathematical Modeling*, 27 , 145-154(2003).
- [7] A.M. Wazwaz, A reliable algorithm for solving boundary value problems for higher-order integro-differential equations, *Applied Mathematics and Computation* 118 , 327\_342(2001).
- [8] K. Maleknejad, Y. Mahmoudi, Taylor polynomial solution of high-order nonlinear Volterra-Fredholm integro-differential equations, *Applied Mathematics and Computation* 145 , 641-653(2003).
- [9] K. Maleknejad, F. Mirzaee, S. Abbasbandy, Solving linear integro-differential equations system by using rationalized Haar function method, *Applied Mathematics and Computation* 155, 317-328(2005).
- [10] A. Arikoglu, I. Ozkol, Solution of boundary value problems for integro-differential equations by using differential transform method, *Applied Mathematics and Computation* 168, 1145\_1158(2005).

- [11] A. Golbabai, M. Javidi, Application of He's homotopy perturbation method for  $n$ th-order integro-differential equations, *Applied Mathematics and Computation*, 190, 1409-1416 (2007).
- [12] J.H. He, Variational iteration method - a kind of non-linear analytical technique: Some examples, *Int. J. Nonlinear Mech.* 34 (4) ,699-708 (1999).
- [13] N.H. Sweilam, M.M. Khader, Variational iteration method for one dimensional nonlinear thermoelasticity, *Chaos Solitons Fractals* ,32, 145-149(2007).
- [14] J. Biazar, H. Aminikhah, Exact and numerical solutions for non-linear Burger's equation by VIM , *Mathematical and Computer Modelling*, 49, 1394-1400 (2009).
- [15] J. H. He, Variational iteration method for autonomous ordinary differential systems, *Applied Mathematics and Computation* , 114,115-123(2000).
- [16] J.H. He, A.M. Wazwaz, L. Xu, The variational iteration method: Reliable, efficient, and promising ,*Computers & Mathematics with Applications*, 54, 879-880(2007).
- [17] J.H. He, X.H. Wu, Variational iteration method: New development and applications, *Computers & Mathematics with Applications*, 54, 881-894 (2007).
- [18] J.H. He, X.H. Wu, Construction of solitary solution and Compton-like solution by variational iteration method, *Chaos Solitons Fractals*, 29, 108-113(2006).
- [19] Z.M. Odibat, S. Momani, Application of variational iteration method to nonlinear differential equations of fractional order, *Int. J. Nonlinear Sci. Numer. Simul.*, 7 , 27-34(2006).
- [20] S. Momani, S. Abuasad, Application of He's variational iteration method to Helmutz equation, *Chaos Solitons Fractals*, 27, 1119-1123 (2006).
- [21] T. Öziş, A. Yıldırım , A study of nonlinear oscillators with  $u^{1/3}$  force by He's variational iteration method, *Journal of Sound and Vibration*, 306, 372-376 (2007).
- [22] P. Darania, A. Ebadian, A method for the numerical solution of the integro-differential equations , *Applied Mathematics and Computation*, 188, 657-668(2007).
- [23] E. Yusufoglu (Adagjanov) , Improved homotopy perturbation method for solving Fredholm type integro-differential equations, *Chaos, Solitons & Fractals*, 41, 28-37 (2009).
- [24] M.T. Kajani, M. Ghasemi, E. Babolian, Comparison between the homotopy perturbation method and the sine-cosine wavelet method for solving linear integro-differential equations, *Comput Math Appl* , 54, 1162-6(2007).
- [25] S.H. Javadi, A. Davari and E. Babolian, Numerical implementation of the Adomian decomposition method for nonlinear Volterra integral equations of the second kind, *International Journal of Computer Mathematics*, 84, 75 - 79 (2007).

---

**Instructions to Contributors**  
**Journal of Concrete and Applicable Mathematics**  
A quarterly international publication of Eudoxus Press, LLC, of TN.

**Editor in Chief: George Anastassiou**  
Department of Mathematical Sciences  
University of Memphis  
Memphis, TN 38152-3240, U.S.A.

**1. Manuscripts hard copies in triplicate, and in English, should be submitted to the Editor-in-Chief:**

**Prof. George A. Anastassiou**  
Department of Mathematical Sciences  
The University of Memphis  
Memphis, TN 38152, USA.  
Tel. 901.678.3144  
e-mail: [ganastss@memphis.edu](mailto:ganastss@memphis.edu)

**Authors may want to recommend an associate editor the most related to the submission to possibly handle it.**

**Also authors may want to submit a list of six possible referees, to be used in case we cannot find related referees by ourselves.**

**2. Manuscripts should be typed using any of TEX, LaTeX, AMS-TEX, or AMS-LaTeX and according to EUDOXUS PRESS, LLC. LATEX STYLE FILE. (Click [HERE](#) to save a copy of the style file.) They should be carefully prepared in all respects. Submitted copies should be brightly printed (not dot-matrix), double spaced, in ten point type size, on one side high quality paper 8(1/2)x11 inch. Manuscripts should have generous margins on all sides and should not exceed 24 pages.**

**3. Submission is a representation that the manuscript has not been published previously in this or any other similar form and is not currently under consideration for publication elsewhere. A statement transferring from the authors (or their employers, if they hold the copyright) to Eudoxus Press, LLC, will be required before the manuscript can be accepted for publication. The Editor-in-Chief will supply the necessary forms for this transfer. Such a written transfer of copyright, which previously was assumed to be implicit in the act of submitting a manuscript, is necessary under the U.S. Copyright Law in order for the publisher to carry through the dissemination of research results and reviews as widely and effectively as possible.**

**4. The paper starts with the title of the article, author's name(s) (no titles or degrees), author's affiliation(s) and e-mail addresses. The affiliation should comprise the department, institution (usually university or company), city, state (and/or nation) and mail code.**

**The following items, 5 and 6, should be on page no. 1 of the paper.**

**5. An abstract is to be provided, preferably no longer than 150 words.**

**6. A list of 5 key words is to be provided directly below the abstract. Key words should express the precise content of the manuscript, as they are used for indexing purposes.**

**The main body of the paper should begin on page no. 1, if possible.**

**7. All sections should be numbered with Arabic numerals (such as: 1. INTRODUCTION) .**

**Subsections should be identified with section and subsection numbers (such as 6.1. Second-Value Subheading).**

**If applicable, an independent single-number system (one for each category) should be used to label all theorems, lemmas, propositions, corrolaries, definitions, remarks, examples, etc. The label (such as Lemma 7) should be typed with paragraph indentation, followed by a period and the lemma itself.**

**8. Mathematical notation must be typeset. Equations should be numbered consecutively with Arabic numerals in parentheses placed flush right, and should be thusly referred to in the text [such as Eqs.(2) and (5)]. The running title must be placed at the top of even numbered pages and the first author's name, et al., must be placed at the top of the odd numbed pages.**

**9. Illustrations (photographs, drawings, diagrams, and charts) are to be numbered in one consecutive series of Arabic numerals. The captions for illustrations should be typed double space. All illustrations, charts, tables, etc., must be embedded in the body of the manuscript in proper, final, print position. In particular, manuscript, source, and PDF file version must be at camera ready stage for publication or they cannot be considered.**

**Tables are to be numbered (with Roman numerals) and referred to by number in the text. Center the title above the table, and type explanatory footnotes (indicated by superscript lowercase letters) below the table.**

**10. List references alphabetically at the end of the paper and number them consecutively. Each must be cited in the text by the appropriate Arabic numeral in square brackets on the baseline.**

**References should include (in the following order):  
initials of first and middle name, last name of author(s)  
title of article,**

name of publication, volume number, inclusive pages, and year of publication.

Authors should follow these examples:

### **Journal Article**

1. H.H.Gonska, Degree of simultaneous approximation of bivariate functions by Gordon operators, (journal name in italics) *J. Approx. Theory*, 62,170-191(1990).

### **Book**

2. G.G.Lorentz, (title of book in italics) *Bernstein Polynomials* (2nd ed.), Chelsea, New York, 1986.

### **Contribution to a Book**

3. M.K.Khan, Approximation properties of beta operators, in (title of book in italics) *Progress in Approximation Theory* (P.Nevai and A.Pinkus, eds.), Academic Press, New York, 1991, pp.483-495.

11. All acknowledgements (including those for a grant and financial support) should occur in one paragraph that directly precedes the References section.

12. Footnotes should be avoided. When their use is absolutely necessary, footnotes should be numbered consecutively using Arabic numerals and should be typed at the bottom of the page to which they refer. Place a line above the footnote, so that it is set off from the text. Use the appropriate superscript numeral for citation in the text.

13. After each revision is made please again submit three hard copies of the revised manuscript, including in the final one. And after a manuscript has been accepted for publication and with all revisions incorporated, manuscripts, including the TEX/LaTeX source file and the PDF file, are to be submitted to the Editor's Office on a personal-computer disk, 3.5 inch size. Label the disk with clearly written identifying information and properly ship, such as:

Your name, title of article, kind of computer used, kind of software and version number, disk format and files names of article, as well as abbreviated journal name.

Package the disk in a disk mailer or protective cardboard. Make sure contents of disks are identical with the ones of final hard copies submitted!

Note: The Editor's Office cannot accept the disk without the accompanying matching hard copies of manuscript. No e-mail final submissions are allowed! The disk submission must be used.

14. Effective 1 Nov. 2009 for current journal page charges, contact the Editor in Chief. Upon acceptance of the paper an invoice will be sent to the contact author. The fee payment will be due one month from the invoice date. The article will proceed to publication only after the fee is paid. The charges are to be sent, by money order or certified check, in US dollars, payable to Eudoxus Press, LLC, to the address shown on

the Eudoxus [homepage](#).

No galley proofs will be sent and the contact author will receive one(1) electronic copy of the journal issue in which the article appears.

15. This journal will consider for publication only papers that contain proofs for their listed results.

## **TABLE OF CONTENTS, JOURNAL OF CONCRETE AND APPLICABLE MATHEMATICS, VOL. 9, NO. 2, 2011**

Computing the approximate frequency for nonlinear oscillators with discontinuities by He's bookkeeping parameter method, Canan Köroğlu, Turgut Özis, .....89

Self-Organized Criticality in Solar Physics and Astrophysics,  
Markus J. Aschwanden, .....100

Applications and Lipschitz results of Approximation by Smooth Poisson-Cauchy Type Singular Integrals,  
George A. Anastassiou & Razvan A. Mezei, .....112

Analysis of snore sounds by using the largest Lyapunov exponent,  
Derya Yılmaz, Haydar Ankişhan, .....146

Chaotic analysis of penicillin induced epileptiform activity rats  
Sinan Canan, Derya Yılmaz, .....154

A Simulation Study of a Simple Optoelectronic Chaotic Circuit,  
M.P. Haniyas, H.E. Nistazakis and G.S. Tombras, .....163

Classes of Special Solutions of the Maxwell Bloch System and its Generalization,  
A. Hacınlıyan et al, .....168

Semi-analytical Solutions of Integral and Integro-differential Equations,  
Emine Mısırlı , Meryem Odabası, .....175



**VOLUME 9, NUMBER 3      JULY 2011**

**ISSN:1548-5390 PRINT,1559-176X ONLINE**



**JOURNAL  
OF CONCRETE  
AND APPLICABLE  
MATHEMATICS  
EUDOXUS PRESS,LLC**

**GUEST EDITORS: HIKMET CAGLAR, LEVENT CUHACI,  
GURSEL HACIBEKIROGLU and MEHMET OZER  
SPECIAL ISSUE VI: “CHAOS and COMPLEX SYSTEMS 2010”**

**SCOPE AND PRICES OF THE JOURNAL**  
**Journal of Concrete and Applicable Mathematics**

A quartely international publication of **Eudoxus Press,LLC**

**Editor in Chief: George Anastassiou**

Department of Mathematical Sciences,  
University of Memphis  
Memphis, TN 38152, U.S.A.  
ganastss@memphis.edu

The main purpose of the "Journal of Concrete and Applicable Mathematics" is to publish high quality original research articles from all subareas of Non-Pure and/or Applicable Mathematics and its many real life applications, as well connections to other areas of Mathematical Sciences, as long as they are presented in a Concrete way. It welcomes also related research survey articles and book reviews. A sample list of connected mathematical areas with this publication includes and is not restricted to: Applied Analysis, Applied Functional Analysis, Probability theory, Stochastic Processes, Approximation Theory, O.D.E, P.D.E, Wavelet, Neural Networks, Difference Equations, Summability, Fractals, Special Functions, Splines, Asymptotic Analysis, Fractional Analysis, Inequalities, Moment Theory, Numerical Functional Analysis, Tomography, Asymptotic Expansions, Fourier Analysis, Applied Harmonic Analysis, Integral Equations, Signal Analysis, Numerical Analysis, Optimization, Operations Research, Linear Programming, Fuzzyness, Mathematical Finance, Stochastic Analysis, Game Theory, Math. Physics aspects, Applied Real and Complex Analysis, Computational Number Theory, Graph Theory, Combinatorics, Computer Science Math. related topics, combinations of the above, etc. In general any kind of Concretely presented Mathematics which is Applicable fits to the scope of this journal.

Working Concretely and in Applicable Mathematics has become a main trend in many recent years, so we can understand better and deeper and solve the important problems of our real and scientific world.

"Journal of Concrete and Applicable Mathematics" is a peer-reviewed International Quarterly Journal.

We are calling for papers for possible publication. The contributor should send three copies of the contribution to the editor in-Chief typed in TEX, LATEX double spaced. [ See: Instructions to Contributors]

**Journal of Concrete and Applicable Mathematics(JCAAM)**

**ISSN:1548-5390 PRINT, 1559-176X ONLINE.**

is published in January, April, July and October of each year by

**EUDOXUS PRESS,LLC,**

1424 Beaver Trail Drive, Cordova, TN38016, USA,

Tel.001-901-751-3553

anastassioug@yahoo.com

<http://www.EudoxusPress.com>.

**Visit also [www.msci.memphis.edu/~ganastss/jcaam](http://www.msci.memphis.edu/~ganastss/jcaam).**

**Webmaster: Ray Clapsadle**

**Annual Subscription Current Prices:** For USA and Canada, Institutional: Print \$400, Electronic \$250, Print and Electronic \$450. Individual: Print \$150, Electronic

\$80,Print &Electronic \$200.For any other part of the world add \$50 more to the above prices for Print.

Single article PDF file for individual \$15.Single issue in PDF form for individual \$60.

No credit card payments.Only certified check,money order or international check in US dollars are acceptable.

Combination orders of any two from JoCAAA,JCAAM,JAFA receive 25% discount,all three receive 30% discount.

**Copyright**©2011 by Eudoxus Press,LLC all rights reserved.JCAAM is printed in USA.

**JCAAM is reviewed and abstracted by AMS Mathematical Reviews,MATHSCI,and Zentralblatt MATH.**

It is strictly prohibited the reproduction and transmission of any part of JCAAM and in any form and by any means without the written permission of the publisher.It is only allowed to educators to Xerox articles for educational purposes.The publisher assumes no responsibility for the content of published papers.

***JCAAM IS A JOURNAL OF RAPID PUBLICATION***

---

## Editorial Board

### Associate Editors

---

#### Editor in -Chief:

George Anastassiou  
 Department of Mathematical Sciences  
 The University Of Memphis  
 Memphis, TN 38152, USA  
 tel. 901-678-3144, fax 901-678-2480  
 e-mail ganastss@memphis.edu  
[www.msci.memphis.edu/~anastasg/anlyjour.htm](http://www.msci.memphis.edu/~anastasg/anlyjour.htm)  
 Areas: Approximation Theory,  
 Probability, Moments, Wavelet,  
 Neural Networks, Inequalities, Fuzzyness.

#### Associate Editors:

1) Ravi Agarwal  
 Florida Institute of Technology  
 Applied Mathematics Program  
 150 W. University Blvd.  
 Melbourne, FL 32901, USA  
[agarwal@fit.edu](mailto:agarwal@fit.edu)  
 Differential Equations, Difference  
 Equations,  
 Inequalities

2) Drumi D. Bainov  
 Medical University of Sofia  
 P.O. Box 45, 1504 Sofia, Bulgaria  
[drumibainov@yahoo.com](mailto:drumibainov@yahoo.com)  
 Differential Equations, Optimal Control,  
 Numerical Analysis, Approximation Theory

3) Carlo Bardaro  
 Dipartimento di Matematica & Informatica  
 Università di Perugia  
 Via Vanvitelli 1  
 06123 Perugia, ITALY  
 tel. +390755855034, +390755853822,  
 fax +390755855024  
[bardaro@unipg.it](mailto:bardaro@unipg.it) ,  
[bardaro@dipmat.unipg.it](mailto:bardaro@dipmat.unipg.it)  
 Functional Analysis and Approximation Th.,  
 Summability, Signal Analysis, Integral  
 Equations,  
 Measure Th., Real Analysis

4) Francoise Bastin  
 Institute of Mathematics  
 University of Liege  
 4000 Liege

21) Gustavo Alberto Perla Menzala  
 National Laboratory of Scientific Computation  
 LNCC/MCT  
 Av. Getulio Vargas 333  
 25651-075 Petropolis, RJ  
 Caixa Postal 95113, Brasil  
 and

Federal University of Rio de Janeiro  
 Institute of Mathematics  
 RJ, P.O. Box 68530 Rio de Janeiro, Brasil  
[perla@lncc.br](mailto:perla@lncc.br) and [perla@im.ufrj.br](mailto:perla@im.ufrj.br)  
 Phone 55-24-22336068, 55-21-25627513 Ext 224  
 FAX 55-24-22315595  
 Hyperbolic and Parabolic Partial Differential  
 Equations,  
 Exact controllability, Nonlinear Lattices and  
 Global  
 Attractors, Smart Materials

22) Ram N. Mohapatra  
 Department of Mathematics  
 University of Central Florida  
 Orlando, FL 32816-1364  
 tel. 407-823-5080  
[ramm@pegasus.cc.ucf.edu](mailto:ramm@pegasus.cc.ucf.edu)  
 Real and Complex analysis, Approximation Th.,  
 Fourier Analysis, Fuzzy Sets and Systems

23) Rainer Nagel  
 Arbeitsbereich Funktionalanalysis  
 Mathematisches Institut  
 Auf der Morgenstelle 10  
 D-72076 Tuebingen  
 Germany  
 tel. 49-7071-2973242  
 fax 49-7071-294322  
[rana@fa.uni-tuebingen.de](mailto:rana@fa.uni-tuebingen.de)  
 evolution equations, semigroups, spectral th.,  
 positivity

24) Panos M. Pardalos  
 Center for Appl. Optimization  
 University of Florida  
 303 Weil Hall  
 P.O. Box 116595  
 Gainesville, FL 32611-6595  
 tel. 352-392-9011  
[pardalos@ufl.edu](mailto:pardalos@ufl.edu)  
 Optimization, Operations Research

BELGIUM

f.bastin@ulg.ac.be  
Functional Analysis,Wavelets

5) Yeol Je Cho  
Department of Mathematics Education  
College of Education  
Gyeongsang National University  
Chinju 660-701

KOREA

tel.055-751-5673 Office,  
055-755-3644 home,  
fax 055-751-6117  
yjcho@nongae.gsnu.ac.kr  
Nonlinear operator Th.,Inequalities,  
Geometry of Banach Spaces

6) Sever S.Dragomir  
School of Communications and Informatics  
Victoria University of Technology  
PO Box 14428  
Melbourne City M.C  
Victoria 8001,Australia  
tel 61 3 9688 4437,fax 61 3 9688 4050  
sever.dragomir@vu.edu.au,  
sever@sci.vu.edu.au  
Math.Analysis,Inequalities,Approximation  
Th.,  
Numerical Analysis, Geometry of Banach  
Spaces,  
Information Th. and Coding

7) Angelo Favini  
Università di Bologna  
Dipartimento di Matematica  
Piazza di Porta San Donato 5  
40126 Bologna, ITALY  
tel.++39 051 2094451  
fax.++39 051 2094490  
favini@dm.unibo.it  
Partial Differential Equations, Control  
Theory,  
Differential Equations in Banach Spaces

8) Claudio A. Fernandez  
Facultad de Matematicas  
Pontificia Universidad Católica de Chile  
Vicuna Mackenna 4860  
Santiago, Chile  
tel.++56 2 354 5922  
fax.++56 2 552 5916  
cfernand@mat.puc.cl  
Partial Differential Equations,  
Mathematical Physics,  
Scattering and Spectral Theory

25) Svetlozar T.Rachev  
Dept.of Statistics and Applied Probability  
Program

University of California,Santa Barbara  
CA 93106-3110,USA  
tel.805-893-4869  
rachev@pstat.ucsb.edu

AND

Chair of Econometrics and Statistics  
School of Economics and Business Engineering  
University of Karlsruhe  
Kollegium am Schloss,Bau II,20.12,R210  
Postfach 6980,D-76128,Karlsruhe,Germany  
tel.011-49-721-608-7535  
rachev@lsoe.uni-karlsruhe.de  
Mathematical and Empirical Finance,  
Applied Probability, Statistics and Econometrics

26) John Michael Rassias  
University of Athens  
Pedagogical Department  
Section of Mathematics and Infomatics  
20, Hippocratous Str., Athens, 106 80, Greece

Address for Correspondence

4, Agamemnonos Str.  
Aghia Paraskevi, Athens, Attikis 15342 Greece  
jrassias@primedu.uoa.gr  
jrassias@tellas.gr  
Approximation Theory,Functional Equations,  
Inequalities, PDE

27) Paolo Emilio Ricci  
Universita' degli Studi di Roma "La Sapienza"  
Dipartimento di Matematica-Istituto  
"G.Castelnuovo"  
P.le A.Moro,2-00185 Roma,ITALY  
tel.++39 0649913201,fax ++39 0644701007  
riccip@uniroma1.it,Paoloemilio.Ricci@uniroma1.it  
Orthogonal Polynomials and Special functions,  
Numerical Analysis, Transforms,Operational  
Calculus,  
Differential and Difference equations

28) Cecil C.Rousseau  
Department of Mathematical Sciences  
The University of Memphis  
Memphis,TN 38152,USA  
tel.901-678-2490,fax 901-678-2480  
ccrousse@memphis.edu  
Combinatorics,Graph Th.,  
Asymptotic Approximations,  
Applications to Physics

29) Tomasz Rychlik

- 9) A.M.Fink  
Department of Mathematics  
Iowa State University  
Ames, IA 50011-0001, USA  
tel.515-294-8150  
fink@math.iastate.edu  
Inequalities, Ordinary Differential Equations
- 10) Sorin Gal  
Department of Mathematics  
University of Oradea  
Str.Armatei Romane 5  
3700 Oradea, Romania  
galso@uoradea.ro  
Approximation Th., Fuzzyness, Complex Analysis
- 11) Jerome A. Goldstein  
Department of Mathematical Sciences  
The University of Memphis,  
Memphis, TN 38152, USA  
tel.901-678-2484  
jgoldste@memphis.edu  
Partial Differential Equations, Semigroups of Operators
- 12) Heiner H. Gonska  
Department of Mathematics  
University of Duisburg  
Duisburg, D-47048  
Germany  
tel.0049-203-379-3542 office  
gonska@informatik.uni-duisburg.de  
Approximation Th., Computer Aided Geometric Design
- 13) Dmitry Khavinson  
Department of Mathematical Sciences  
University of Arkansas  
Fayetteville, AR 72701, USA  
tel.(479)575-6331, fax(479)575-8630  
dmitry@uark.edu  
Potential Th., Complex Analysis, Holomorphic PDE,  
Approximation Th., Function Th.
- 14) Virginia S. Kiryakova  
Institute of Mathematics and Informatics  
Bulgarian Academy of Sciences  
Sofia 1090, Bulgaria  
virginia@diogenes.bg  
Special Functions, Integral Transforms, Fractional Calculus
- 15) Hans-Bernd Knoop  
Institute of Mathematics  
Polish Academy of Sciences  
Chopina 12, 87100 Torun, Poland  
T.Rychlik@impan.gov.pl  
Mathematical Statistics, Probabilistic Inequalities
- 30) Bl. Sendov  
Institute of Mathematics and Informatics  
Bulgarian Academy of Sciences  
Sofia 1090, Bulgaria  
bsendov@bas.bg  
Approximation Th., Geometry of Polynomials, Image Compression
- 31) Igor Shevchuk  
Faculty of Mathematics and Mechanics  
National Taras Shevchenko  
University of Kyiv  
252017 Kyiv  
UKRAINE  
shevchuk@univ.kiev.ua  
Approximation Theory
- 32) H.M. Srivastava  
Department of Mathematics and Statistics  
University of Victoria  
Victoria, British Columbia V8W 3P4  
Canada  
tel.250-721-7455 office, 250-477-6960 home,  
fax 250-721-8962  
harimsri@math.uvic.ca  
Real and Complex Analysis, Fractional Calculus and Appl.,  
Integral Equations and Transforms, Higher Transcendental Functions and Appl., q-Series and q-Polynomials, Analytic Number Th.
- 33) Stevo Stevic  
Mathematical Institute of the Serbian Acad. of Science  
Knez Mihailova 35/I  
11000 Beograd, Serbia  
sstevic@ptt.yu; sstevo@matf.bg.ac.yu  
Complex Variables, Difference Equations, Approximation Th., Inequalities
- 34) Ferenc Szidarovszky  
Dept. Systems and Industrial Engineering  
The University of Arizona  
Engineering Building, 111  
PO.Box 210020  
Tucson, AZ 85721-0020, USA  
szidar@sie.arizona.edu  
Numerical Methods, Game Th., Dynamic Systems,

Institute of Mathematics  
 Gerhard Mercator University  
 D-47048 Duisburg  
 Germany  
 tel.0049-203-379-2676  
 knoop@math.uni-duisburg.de  
 Approximation Theory, Interpolation

16) Jerry Koliha  
 Dept. of Mathematics & Statistics  
 University of Melbourne  
 VIC 3010, Melbourne  
 Australia  
 koliha@unimelb.edu.au  
 Inequalities, Operator Theory,  
 Matrix Analysis, Generalized Inverses

17) Mustafa Kulenovic  
 Department of Mathematics  
 University of Rhode Island  
 Kingston, RI 02881, USA  
 kulenm@math.uri.edu  
 Differential and Difference Equations

18) Gerassimos Ladas  
 Department of Mathematics  
 University of Rhode Island  
 Kingston, RI 02881, USA  
 gladas@math.uri.edu  
 Differential and Difference Equations

19) V. Lakshmikantham  
 Department of Mathematical Sciences  
 Florida Institute of Technology  
 Melbourne, FL 32901  
 e-mail: lakshmik@fit.edu  
 Ordinary and Partial Differential  
 Equations,  
 Hybrid Systems, Nonlinear Analysis

20) Rupert Lasser  
 Institut für Biomathematik & Biomertie, GSF  
 -National Research Center for environment  
 and health  
 Ingolstaedter landstr.1  
 D-85764 Neuherberg, Germany  
 lasser@gsf.de  
 Orthogonal Polynomials, Fourier Analysis,  
 Mathematical Biology

Multicriteria Decision making,  
 Conflict Resolution, Applications  
 in Economics and Natural Resources  
 Management

35) Gancho Tachev  
 Dept. of Mathematics  
 Univ. of Architecture, Civil Eng. and Geodesy  
 1 Hr. Smirnenski blvd  
 BG-1421 Sofia, Bulgaria  
 gtt\_fte@uacg.bg  
 Approximation Theory

36) Manfred Tasche  
 Department of Mathematics  
 University of Rostock  
 D-18051 Rostock  
 Germany  
 manfred.tasche@mathematik.uni-rostock.de  
 Approximation Th., Wavelet, Fourier Analysis,  
 Numerical Methods, Signal Processing,  
 Image Processing, Harmonic Analysis

37) Chris P. Tsokos  
 Department of Mathematics  
 University of South Florida  
 4202 E. Fowler Ave., PHY 114  
 Tampa, FL 33620-5700, USA  
 profcpt@math.usf.edu, profcpt@chumal.cas.usf.edu  
 Stochastic Systems, Biomathematics,  
 Environmental Systems, Reliability Th.

38) Lutz Volkmann  
 Lehrstuhl II für Mathematik  
 RWTH-Aachen  
 Templergraben 55  
 D-52062 Aachen  
 Germany  
 volkm@math2.rwth-aachen.de  
 Complex Analysis, Combinatorics, Graph Theory

## Preface

These six special issues, which constitute the proceedings of the symposium 3rd International Interdisciplinary Chaos Symposium on CHAOS and COMPLEX SYSTEMS - CCS2010 (21-24 May 2010), have tried to create a forum for the exchange of information and experience in the exciting interdisciplinary field of chaos. However the conference was more in the Applied Mathematics, Social Sciences and Physics direction centered.

The view of the organizers concerning international resonance of the conference has been fulfilled: approximately 200 scientists from 21 different countries (Algeria, Bulgaria, Croatia, Denmark, France, Germany, Greece, Iran, Italy, Jordan, Lebanon, Malaysia, Pakistan, Republic of Serbia, Russia, Sultanate of Oman, Tunisia, Turkey, Ukraine, United Kingdom and United States of America) have participated. Good relations to research institutes of these countries might be of great importance for science and applications in different fields of Chaos.

On behalf of the Organizing Committee we would like to express our thanks to the Scientific Committee, the Program Committee and to all who have contributed to this conference for their support and advice. We are also grateful to the invited lecturers Prof. Henry D.I. Abarbanel, Prof. David S. Byrne, Prof. George Anastassiou, Prof. Zidong Wang, Prof. Turgut Ozis and Prof. Markus J. Aschwanden.

Special thanks are due to Rector Prof. Dursun Kocer and Vice Rector Prof. Cetin Bolcal for their close support, advice and incentive encouraging.

Our thanks are also due to the Istanbul Kultur University, which was hosting this symposium and provided all of its facilities.

Finally, we are grateful to the Editor-in-Chief, Prof. George Anastassiou for accepting this volume for publication.

Hikmet Caglar, PhD in Mathematics, [s.caglar@iku.edu.tr](mailto:s.caglar@iku.edu.tr)  
Levent Cuhaci, PhD in Computer Science, [l.cuhaci@iku.edu.tr](mailto:l.cuhaci@iku.edu.tr)  
Gursel Hacibekiroglu, PhD in Physics, [g.hacibekiroglu@iku.edu.tr](mailto:g.hacibekiroglu@iku.edu.tr)  
Mehmet Ozer, PhD in Physics, [m.ozel@iku.edu.tr](mailto:m.ozel@iku.edu.tr)

Istanbul Kultur University, Faculty of Science and Letters, Istanbul, Turkey



# Applied Chaos: Linearizing Multibit $\Delta\Sigma$ Converters for Telecom Applications

K. Papathanasiou, L. Voudouris, S.G. Stavriniades, S. Nikolaidis  
Physics Dept., Aristotle University of Thessaloniki, GR-54124, Greece.

July 4, 2010

Chaotic system communication is mainstream application of nonlinear circuits. In this paper an alternative approach to multi-bit delta sigma linearization, utilizing the wideband non repetitive pattern properties of deterministic chaotic signals, is presented. In this fashion the chaotic transmitted signal can also be used for DAC linearization. The techniques, algorithms and associated signal conditioning for a multi-bit Delta Sigma DAC, suitable for wideband communications such as distributed sensor arrays are demonstrated<sup>1</sup>.

## 1 Introduction

The introduction of Chaos Theory in almost all areas of scientific research from physics and electronics to social sciences has provided a new perspective [1]-[2]. Over the last years the problem of controlling system chaotic behavior has become the main issue in all applied science fields [3], [4]. Any strongly nonlinear circuit or dynamical system tends to exhibit not only periodic behavior, but also more complicated behaviors, ranging from quasi-periodicity to chaotic behavior [5]. Potential applications of nonlinear chaotic circuits for secure [6], [7] or ultra-wideband data transmission [8], have raised the engineering society's interest and offers an alternative way to several new applications and performance enhancements to existing communication systems. Two key features of chaos are a noise-like time series and sensitive dependence on initial conditions and control parameters [9]. A chaotic generator can produce nonlinear and non-repeating sequences and it is very hard to predict chaotic

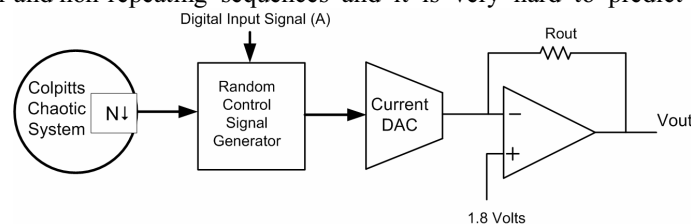


**Figure 1:** Overall System

<sup>1</sup> This work was partly presented at the “3<sup>rd</sup> International Interdisciplinary Symposium on Chaos and Complex Systems – CCS2010”

patterns and sequences even when the chaotic function is known.

Although communications is a concessive field for applied chaotic electronics, it is not the only one. Power electronics [10], as well as, neural computing [11] are examples of applications other than communications. In this paper a novel approach to multi-bit Delta-Sigma converter linearization is presented (Figure 1). A random control signal, derived from the input digital signal generator, drives the DAC control switches. The randomization, demanded for linearizing the DAC, is achieved by the digital words generated by sub-sampling the digital output of a Colpitts oscillator, to eliminate the main frequency component. Finally, the output current is converted to a voltage signal by the means of a current to voltage converter.

## 2 Multi-bit Oversampled Data Converters

Oversampled data converters, well known for their ability to offer the best resolution in accuracy, are of a significant importance [12]. Modern applications such as digital terrestrial television or ultra-wide-band communications demand high accuracy combined to high signal bandwidth [13], while power consumption is of increasingly significant importance. This led to the introduction of multi-bit- $\Delta\Sigma$  converters [14], which reduce the requirement for analog reconstruction filters, and can produce more aggressive noise transfer functions (for example a fifth order  $\Delta\Sigma$  modulator can produce 60dB or 10bit accuracy at an OSR of 16 while the same order  $\Delta\Sigma$  4-bit modulator can produce in theory 120dB SNR, or 20bits of accuracy).

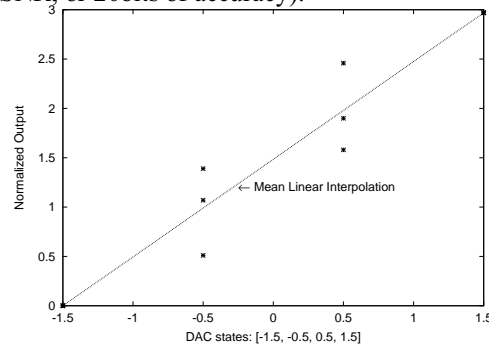


**Figure 2:** DAC nonlinearities in a 2bit DAC example

Albeit, the facts presented above lead to the introduction of multi-bit converters there is one implied shortcoming introduced in the complexity of the design of the associated multi-bit DAC in all  $\Delta\Sigma$  modulators corresponding to modulator accuracy. This is not a trivial task for analog design, since  $\Delta\Sigma$  modulators were introduced mainly to accommodate for accuracy shortcomings of analog circuits. The proposed solution utilize averaging in individual DAC element selection. This can be explained by the means of Figure 2, showing the response of a two bit DAC for demonstration purposes. The data of Figure 2 show a Monte-Carlo snapshot for a single variation matrix of the three normalized current sources which realize the two bit DAC. The left-most DAC value (-1.5, used for  $\Delta\Sigma$  modulators in order to provide a signal mean of zero for modulation mathematics

to be valid) is present when all elementary current sources  $I_1$ ,  $I_2$  and  $I_3$  are off and a robust «0» value is obtained; this needs to be offset by means of a constant current sink (or common mode feedback), in order for the DAC characteristic to be centered around «0,0». We also accept the full DAC range value  $I_{\max}=I_1 + I_2 + I_3$  being accurate (an assumption which if not valid will only yield gain and offset mismatches, easily corrected by the  $\Delta\Sigma$  digital loop). This also implies that the individual current source errors  $e(n)$ :  $\Delta I_1$ ,  $\Delta I_2$  and  $\Delta I_3$  give  $\Delta I_1 + \Delta I_2 + \Delta I_3 = 0$ , since the full scale DAC output is accurate. As a result, the average output value  $\Sigma y(n) = \Sigma f(n) + \Sigma e(n)$  becomes  $\Sigma f(n)$ , since  $\Sigma e(n) \rightarrow 0$  for a large number of samples; or in other words the DAC transfer function is the line connecting all mean values derived by  $I_1$ ,  $I_2$  and  $I_3$  combinations. In this way the DAC linearization is achieved by averaging.

### 3 Generation of Random Control Signals

The Random Control Signal Generator (RCSG) unit takes as an input a random digital word-level signal with an appropriate number of bits (e.g. 32) and creates an output of a set of  $2^N-1$  bits ( $N$  is the DAC accuracy) with programmable values of ones and zeros driving the DC switches. The number of 1s (and of course of 0s) in the output signal can be configured according to the value of a control input signal  $A$  (the digital input signal).

If  $A=k$  the number of 1s in the output signal should be  $k$  ( $k \leq 2^N-1$ ). These 1s should be distributed in a random way along with the bits of the output word. Instead of designing a specialized unit to achieve that, which is a rather difficult task, all the corresponding combinations were stored in a ROM and addressed by random values. In our case where  $N=3$ , there exist  $k$  1s and  $(7-k)$  0s, thus the total number of different output combinations is given by  $7!/k!(7-k)!$ . The number of these combinations is shown in Table 1.

**Table 1:** Combinations for different values of  $A$

A	0	1	2	3	4	5	6	7
Combinations	1	7	21	35	35	21	7	1

For  $A=k$  and  $A=7-k$  the same number of combinations is achieved. Also, each combination results from another, simply by inversion of bit values. For example, when  $A=3$  a possible combination is 0100110, and the corresponding combination for  $A=4$  results to 1011001. In this way, we can store only the combinations for half of the values of  $A$  (0, 1, 2 and 3) and the rest will be provided by the appropriate inversion.

The RCSG unit is shown in Figure 3. For convenience and in order to simplify the design, three different ROMs were used for storing the corresponding combinations for  $A=1, 2$  and 3. For  $A=0$  only one combination exists “0000000” and was set as a fixed value. The outputs of the ROMs (and the combination “0000000”) are fed to a multiplexer, which is controlled by the 3-bit input signal  $A$  (a2a1a0). The XOR gates in the control bits and the output bits are used to make the appropriate inversions, so that the circuit can provide the combinations for  $A=4, 5, 6$ , and 7. Addresses for the ROM are provided by the Random Address Generator (RAG) unit, which takes as input a number of groups (e.g. 5)

of bits (e.g. 5 bits) of the output of a sub-sampled chaotic digital system. Since the number of the words stored in the ROMs is not a power of 2, the creation of random addresses is not a straightforward procedure and appropriate circuits should be designed.

The RAG unit consists of three different circuits, each one responsible for providing random addresses to the corresponding ROM. Taking as input a number of bits with random values, each circuit has to provide to its output some numbers with random distribution. For example, RAG2, shown in Figure 4, provides addresses for ROM2 ( $A=2$ ) and has to create in its output 21 numbers (e.g. from 0 up to 20) uncorrelated and with similar probability to appear. Since 21 is not a power of 2, this makes things quite complicated.

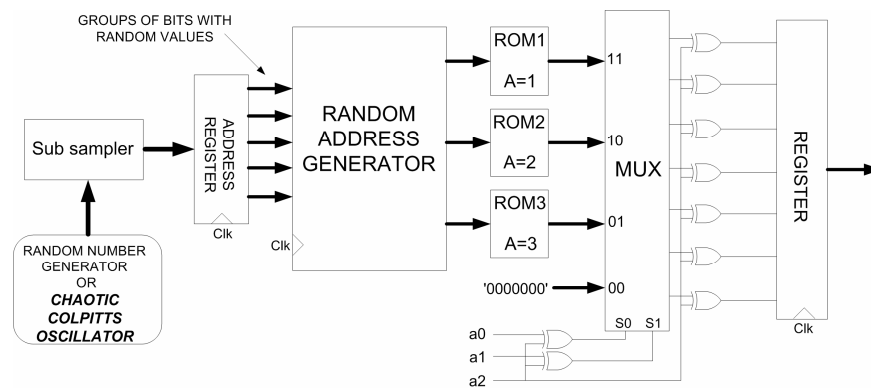


**Figure 3:** The Random Control Signal Generator

RAG2 takes as input groups of bits from an output of a digital chaotic system. Each group is compared to 20. The output of each comparator controls the selection in the corresponding multiplexer, as shown in Figure 4. If the binary value of Group1 is less than 21, then Group1 is an acceptable address (in the range 0 - 20) and is passed to the output, addressing ROM2. If Group1 is higher than 20, then Group1 is not a valid address and MUX2 takes the responsibility to provide the right address. This appears with a 34.44% probability. Group2 is

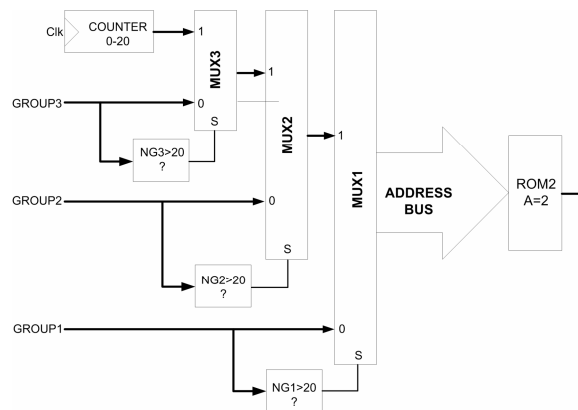


**Figure 4:** Random Address Generator

compared to 20. If  $\text{Group2} < 21$ , Group2 will be the valid address; otherwise, MUX3 takes the responsibility to provide the right address. This probability of is 11.82%. Group3 is compared to 20. If  $\text{Group3} < 21$ , Group3 will be the valid address; otherwise, *Counter* takes the responsibility to provide the valid address. Now this probability is 4.06%. Since the counter takes values from 0 to 20, the probability of a number to appear at its output in a random time instance is  $1/21$ , 4.76%. Therefore there is an equal probability (0.19%) for any number to appear, with the exception of 4 individual values (of a 0.39% probability). This probability mismatch is very small and does not affect the linearized DAC. Corresponding circuits, with similar structure, are used for RAG1 and RAG3 to address ROM1 ( $A=1$ ) and ROM3 ( $A=3$ ), respectively. In case of RAG1 addresses 0-6 are provided. Two Group inputs of 3 bits are compared to 6. Two multiplexers and a 0-6 counter are also needed. In case of RAG3 addresses 0-35 are provided. Five Group inputs of 6 bits are compared to 34. Consequently five multiplexers and a 0-34 counter are demanded.

#### 4 Colpitts Oscillator

A modified FET-based Colpitts oscillator implementation has been proposed and proven to exhibit a chaotic behaviour [15]. This oscillator is a three-dimensional nonlinear system and its dynamics are governed by the following (normalized)

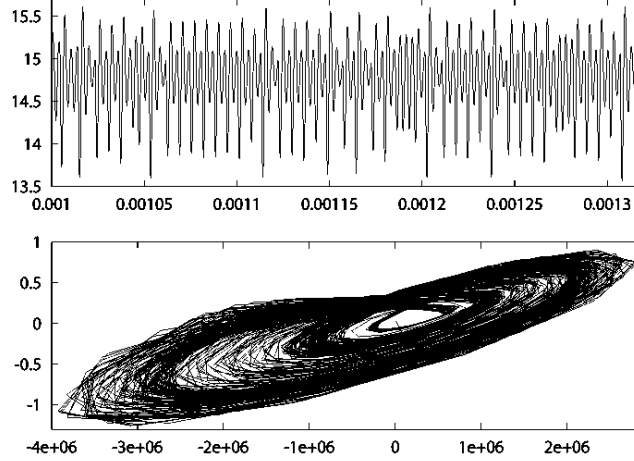


**Figure 5:** A typical chaotic time series and the associated phase portrait, produced by the Colpitts chaotic oscillator.

set of equations:

$$\begin{cases} \dot{x} = a \cdot z - f(y) \\ \dot{y} = -b \cdot y - a \cdot z + p \\ \dot{z} = -c \cdot x - d \cdot y - g \cdot z + q \end{cases} \quad (1)$$

The system state variables  $x$ ,  $y$ ,  $z$  correspond to the capacitor voltages and the inductor current, while parameter values are dependent on the circuit's elements and supply voltages. Function  $f(y)$  in the first of Eq. (1) is defined as follows:

$$f(y) \propto k(y - l)^2 \quad (2)$$

As already mentioned, for certain parameter values this Colpitts oscillator could operate in a chaotic mode [15]. A digitized implementation of the above described oscillator provided normalized time series and the associated phase portrait illuminated in Figure 5.

#### 4.1 Sub-sampling and randomization

When the above described Colpitts oscillator chaotic behaviour, it still demonstrates a strong sinusoidal component: its center frequency (in our case 31.4MHz). Due to this the resultant signal is deterministic and not suitable for acting as a stochastic random number. However, if this center frequency was to be rejected the wideband chaotic signal should exhibit frequency behaviour similar to that of white noise. This can be achieved by utilizing sub-sampling techniques.

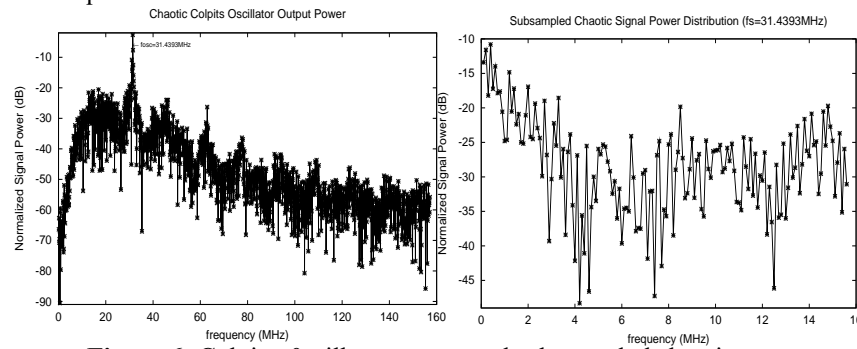


**Figure 6:** Colpitts Oscillator output and sub-sampled chaotic output

This in effect cancels the strong sinusoidal frequency component shown in Figure 6, while folds the entire spectrum over 31.4MHz down to the interval from DC to 31MHz. As a result, the sub-sampled signal spectrum becomes almost uniform with the exception of a limited area around the DC.

### 5. Analog Design of the Current DAC

The DAC circuit is shown in Figure 7. The right side is the elementary DAC block, this is repeated  $2^N-1$  times ( $N$  is the DAC resolution), to achieve the desired thermometer coded DAC circuit. Transistor  $M1$  gives the elementary tail current and is biased to the desired gate level which defines this appropriate current. The differential transistor pair  $M2$ ,  $M3$  is a current steering switch, driven by the input signal  $IN$  and its non-overlapping inverted version. In that

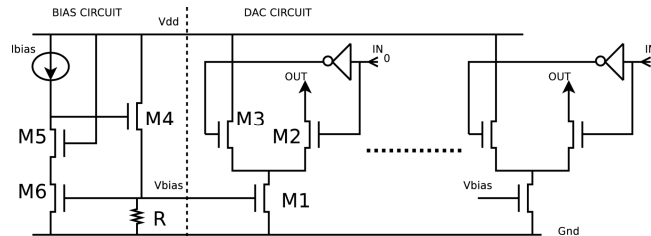


**Figure 7:** Elementary DAC Circuit and Bias Schematic

fashion the tail current is either driven to the output node (*OUT*) or to the power supply rail ( $V_{dd}=1.8V$ ). The length of *M1* is twice the minimum device geometry, to ensure some channel length modulation reduction, with the appropriate width for the given current is chosen. Transistors *M2*, *M3* are operating as switching devices and therefore require minimum length and half the width of *M1*, to realize similar bias conditions. This elementary cell needs to be repeated as desired to realize the appropriate current DAC accuracy.

The bias circuit is consisted of *M4*, *M5*, *M6* and *R*. *M6* is a diode connected replica version of *M1* and is biased by the reference current  $I_{bias}$ , the gate voltage ( $V_{bias}$ ) of this device will therefore raise to the appropriate level to ensure both *M6* and *M1* sink the same current  $I_{bias}$ . However, potentially different voltage levels on the drains of *M6* and *M1* will result in a different current on *M1*. To minimize this the transistor *M5* is used, which is the same size as *M2*, *M3* and connected to  $V_{dd}$ . This ensures that the voltage drain on *M5* is exactly the same as on *M1*, furthermore *M4* and *R* form a source follower and thus a unity gain buffer to ensure input isolation to the bias generating point.

To further enhance voltage stability the output signal is assumed to drive the high impedance input of an OPAMP as shown in Figure 1 with a common mode voltage of 1.8V and a supply level of 3.6V.

## 5.1 Simulation Results

A three bit DAC was realized on a 180nm process. The input was assumed to be a full range sinusoidal signal. The DAC was deliberately mismatched by modulating the width of the individual current sources (*M1* in Figure 7). The initial output current signal is observed in the left side of Figure 8 and appears to be a sampled sinusoid, while transient switching glitches are also noted with insignificant feed-through contribution. Those glitches are essentially the charge that needs to be injected on the drain of *M2* for every switching element. The output signal Fourier transform, without utilizing the techniques presented in this paper, is shown in the lower right side of Figure 8. It is clear that the sine wave is

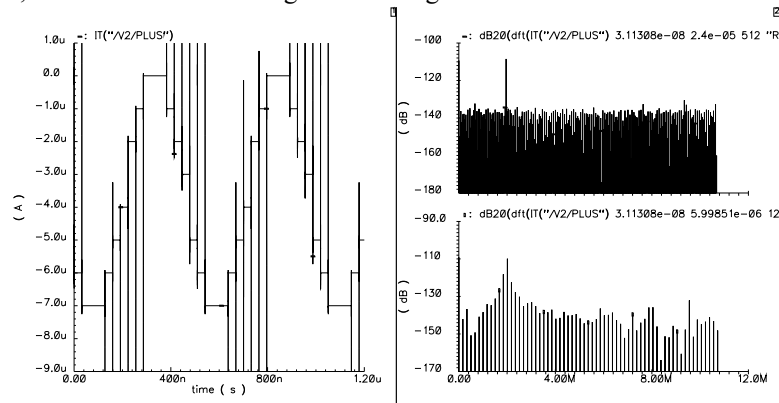


**Figure 8: DAC Simulation Results**

significantly distorted with power leaking and higher harmonics. Once the proposed system is in place the output signal FFT (upper right side in Figure 8)

is enhanced. Two observations are inevitable: the power leaking to neighboring frequencies and higher harmonics is diminished, while the overall Fourier noise is increased. In other words all this unwanted power in specific frequencies is appearing as flat noise spectral density in the observed spectrum.

## 7. Conclusions

In this paper a novel application for chaotic systems is demonstrated. This real-world circuit implementation diminishes the inherent analog nonlinearities of a multi-bit DAC. This was achieved by utilizing an already existent chaotic oscillator output signal, and applying common place signal conditioning to it. This wideband noise-like signal was fed to a digital block, in order to randomize the control of the switching arrangement of a current steering DAC.

Simulation results in the *Cadence DFII* environment, for a 180nm technology, of the overall system were presented, to signify the appropriate operation of the approach. It is approaches like this that can also demonstrate the applicability of chaotic signal conditioning to other novel areas of IC design.

## Acknowledgement

The authors would like to thank the referees for their valuable comments.

## References

- [1] R.C. Hillborn, *Chaos and Nonlinear Dynamics: An introduction for Scientist and Engineers*, 2<sup>nd</sup> edition, New York: Oxford University Press, 2000.
- [2] L.D. Kiel, E. Elliott, *Chaos Theory in Social Sciences: Foundations and Applications*, The University of Michigan Press, 2004.
- [3] E. Ott, C. Grebogi, J.A. Yorke, Controlling Chaos, *Phys. Rev. Lett.*, 64(11), 1196-1199 (1990).
- [4] E. Scholl and H.G. Schuster, *Handbook of Chaos Control*, 2nd ed., Weinheim: Wiley-VCH, 2008.
- [5] G. Chen, T. Ueta (eds), *Chaos in circuits and systems*, Nonlinear Science-Series B (vol.11), World Scientific, 2002.
- [6] A.N. Miliou, A.P. Valaristos, S.G. Stavriniades, K.G. Kyritsi and A.N. Anagnostopoulos, Characterization of a non-autonomous second order non-linear circuit for secure data transmission, *Chaos Sol. Fractals*, 33(4), 1248-1255 (2007).
- [7] S.G. Stavriniades, A.N. Anagnostopoulos, A.N. Miliou, A. Valaristos, L. Magafas, K. Kosmatopoulos, S. Papaioannou, A digital chaotic synchronized communication system, *J. of Eng Sci Rev*, 2(1), 82-86 (2009).
- [8] A.S. Dmitriev, A.V. Kletsov, A.M. Laktushkin, A.I. Panas, S.O. Starkov, Ultrawideband `wireless communications based on dynamic chaos, *Uspekhi sovremennoi radioelektroniki*, 1, 4-16 (2008).
- [9] H.G. Shuster, W. Just, *Deterministic Chaos: An Introduction*, 3<sup>rd</sup> extended edition, Weinheim: Wiley-VCH, 2005.
- [10] C.K. Tse, *Complex behaviour of switching power converters*, CRC Press, 2004.
- [11] M.P. Kennedy, R. Rovatti, G. Setti (eds), *Chaotic Electronics in Communications*, CRC Press, 2000.
- [12] S.R. Norsworthy, R. Schreier, G.C. Temes, *Delta-Sigma data converters*, IEEE Press, 1997.
- [13] L. Doerrer, P. Greco, M. Motz, P. Torta, United States Patent: 7432840 - Multi-bit sigma/delta converter, *U.S. Patent 7432840*, October 7, 2008.
- [14] Y. Geerts, M. Steyaert, W.M.C. Sansen, *Design of multi-bit delta-sigma A/D converters*, Springer, 2002.
- [15] A.S. Dmitriev, E.V. Efremova, L.V. Kuzmin, A.N. Miliou, S.G. Stavriniades, Generation of chaotic oscillations in dynamical system with field-effect transistor as an active element, *J. Applied Functional Analysis*, 4, 409-416 (2009).



## Chaos Synchronization and its Application to Secure Communication

M.S. Papadopoulou<sup>1</sup>, I.M. Kyprianidis<sup>2</sup>, I.N. Stouboulos<sup>3</sup>,  
A.N. Anagnostopoulos<sup>4</sup>

Physics Dept., Aristotle University of Thessaloniki, 54124 Thessaloniki, Greece  
<sup>1</sup>mpapa@physics.auth.gr, <sup>2</sup>imkypr@auth.gr, <sup>3</sup>stouboulos@physics.auth.gr ,  
<sup>4</sup>anagnost@physics.auth

March 07, 2010

In this paper, theoretical and experimental investigations of chaos synchronization and its application to chaotic data transmission in a communication scheme with two identical nonlinear circuits are presented. The conditions for chaos synchronization and its application as a secure communication system based on two 4<sup>th</sup> order non-autonomous chaotic circuits are studied. Information signal transmission and recovery are demonstrated. The information signal is embedded in a chaotic carrier by using the chaotic masking technique.<sup>1</sup>

**Keywords:** Non-autonomous circuit, unidirectional coupling, chaos synchronization, chaotic masking, secure communication.

### 1 Introduction

Chaotic systems are dynamical systems with long-term unpredictable behaviour. Two identical non-autonomous chaotic systems started at nearby initial conditions have trajectories that diverge exponentially. Although the systems could have identical attractors in state space, determining where on the attractor the system is at a distant, future time given its position in the past is a problem that becomes difficult to predict as time passes. One way to demonstrate this is to run two, identical chaotic systems side by side, starting both at close, but not exactly the same initial conditions. The systems soon diverge from each other, but both retain the same attractor pattern. The position of each system on its own attractor has no relation to where the other system is, thus would seem impossible to synchronize.

---

<sup>1</sup> This work was partly presented in the “3rd International Interdisciplinary Symposium on Chaos and Complex Systems – CCS2010”.

Since the first prediction of chaos synchronization by Pecora and Carroll [1], synchronization of chaotic oscillations between two nonlinear systems has been reported in various fields of science, such as electronics [2]-[5], optics [6]-[9], biomedicine [10]-[11], etc. To use a chaotic signal in communications a basic requirement must be satisfied: somehow the receiver must have a duplicate of the transmitter's chaotic signal or, better yet, the two systems must be synchronized. In fact, synchronization is a requirement of many types of communication systems, not only chaotic ones. Chaos synchronization and its application to communications have received a great deal of attention the last twenty years [1], [12]-[16]. Synchronization has opened the way to scientists to investigate an engineering application of chaos, to design secure communication systems [17]-[19]. Synchronization is a basic requirement for chaotic secure communications [1], [20].

In this paper, theoretical and experimental results of chaos synchronization of two identical, unidirectional coupled, non-autonomous circuits are presented. A chaotic secure communication system based on two 4<sup>th</sup> order non-autonomous chaotic circuits is proposed. The chaotic masking technique is used. In chaotic masking [16] the randomness of chaos is utilized to mask the information signal and the original signal is decoded (unmasking) from the received signal by a system (circuit) with an elaboration.

## 2 Circuit's Dynamics

The circuit, we have studied, is presented in Figure 1. It is a four-dimensional non-autonomous, non linear electronic circuit, with two active elements, a nonlinear resistor  $R_N$  and a linear negative conductance  $G_n$ . The circuit's parameters are considered unchangeable during our study. More particularly:  $L_1 = L_2 = 100\text{mH}$ ,  $C_1 = 33\text{nF}$ ,  $C_2 = 75\text{nF}$ ,  $R_1 = 1\text{K}\Omega$ . We consider a sinusoidal input signal  $v_s(t)$  with  $V_o = 0.75\text{V}$  and  $f = 35\text{Hz}$ . The theoretical v-i characteristics of the nonlinear element and negative conductance are seen in Figures 2(a) and 3(a), while in Figures 2(b) and 3(b) the experimental characteristics are presented, respectively. To compare directly theoretical and experimental results we must divide the values of experimental y-axis (voltage in mV) by 10 (current in mA).

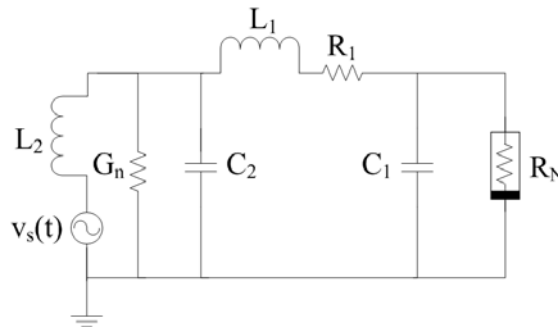


**Figure 1.** Non-autonomous circuit

Using Kirchhoff's circuit laws, the following state equations (Eqs. (1)-(4)) for the system have been derived.

$$\frac{dv_{C1}}{dt} = \frac{1}{C_1}(i_{L1} - i_{RN}) \quad (1)$$

$$\frac{dv_{C2}}{dt} = -\frac{1}{C_2}(G_n \cdot v_{C2} + i_{L1} + i_{L2}) \quad (2)$$

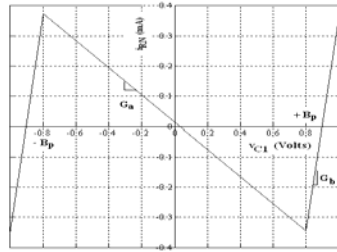
$$\frac{di_{L1}}{dt} = \frac{1}{L_1}(v_{C2} - v_{C1} - R_1 i_{L1}) \quad (3)$$

$$\frac{di_{L2}}{dt} = \frac{1}{L_2}[v_{C2} - R_2 i_{L2} - v_s(t)] \quad (4)$$

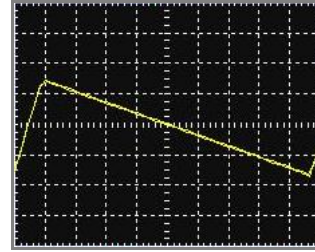
Where the current  $i_{RN}$  through the nonlinear element and input signal  $v_s(t)$  are given by Eqs. (5) and (6).

$$i_{RN} = g(v_{C1}) = G_b v_{C1} + 0.5(G_a - G_b)(|v_{C1} + B_p| - |v_{C1} - B_p|) \quad (5)$$

$$v_s(t) = V_o \cdot \cos(2\pi ft) \quad (6)$$

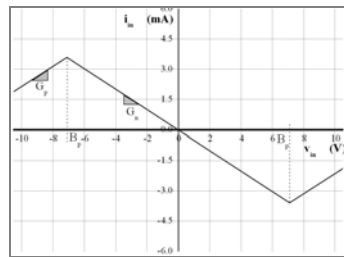


(a) theoretical

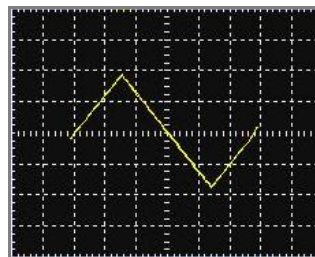


(b) experimental x: 200mV/div, y: 2mV/div

**Figure 2.** input characteristics of  $R_N$  with  $G_a = -0.35\text{mS}$ ,  $G_b = 5.0\text{mS}$  and  $B_p = 0.8\text{V}$



(a) theoretical



(b) experimental x: 5V/div, y: 20mV/div

**Figure 3.** input characteristics of  $G_n$  with  $G_n = 0.50\text{mS} = -G_p$  and  $B_p = 7.5\text{V}$

Circuit's dynamics in low frequency area has been extensively studied in the past [21]-[23]. Using the above parameters circuit exhibits chaotic behaviour. In

Figures 4(a), (b) and (c) the theoretical and experimental phase portraits, as well as the Poincare section are presented.

In Figures 5(a) and (b) theoretical and experimental diagrams  $v_{C22}$  vs.  $v_{C21}$  are presented, while the two systems are uncoupled. In Figures 5(c) and (d) theoretical and experimental diagrams  $v_{C22}(t) - v_{C21}(t)$  are presented. We can see that the two systems have the same pattern-attractor but they are not synchronized.

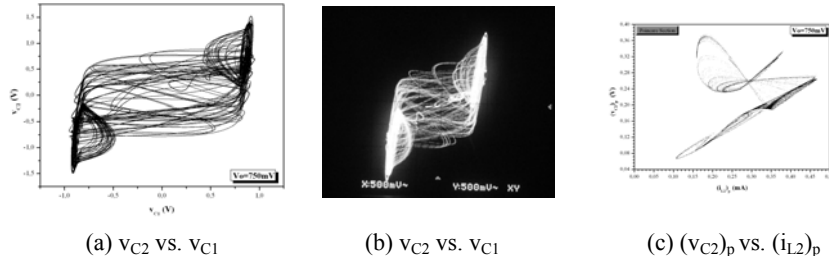


**Figure 4.** (a) theoretical (b) experimental (c) Poincare section

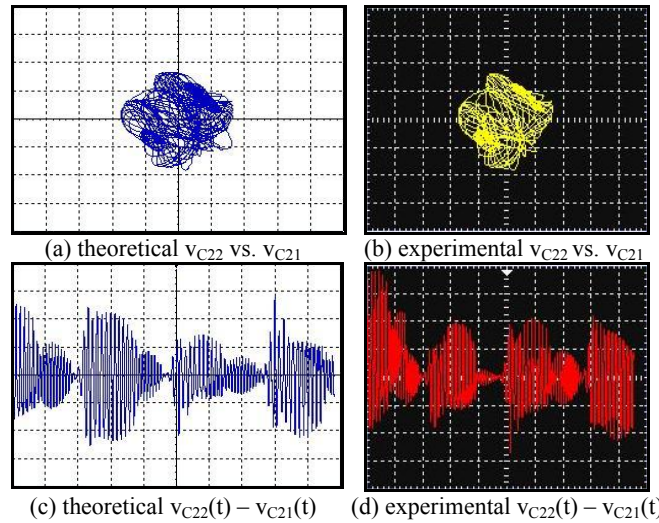


**Figure 5.** (a), (b) x: 1V/div, y: 1V/div (c), (d) x: 5ms/div, y: 1V/div

### 3 Unidirectional Coupling

First of all, chaotic communication requires that the two identical subsystems would be synchronized. Second, with no parameter mismatch, exact recovery is possible involving only some simple signal processing techniques, such as summation, subtraction and inversion. When two identical circuits are resistively coupled, complex dynamics can be observed, such as chaotic and hyperchaotic synchronization, as the coupling coefficient is varied. The two circuits can be

either  $v_{C1}$ -coupled or  $v_{C2}$ -coupled. The unidirectional  $v_{C2}$ -coupled system of two identical non-autonomous nonlinear circuits via a linear resistor  $R_C$  is illustrated in Figure 6.

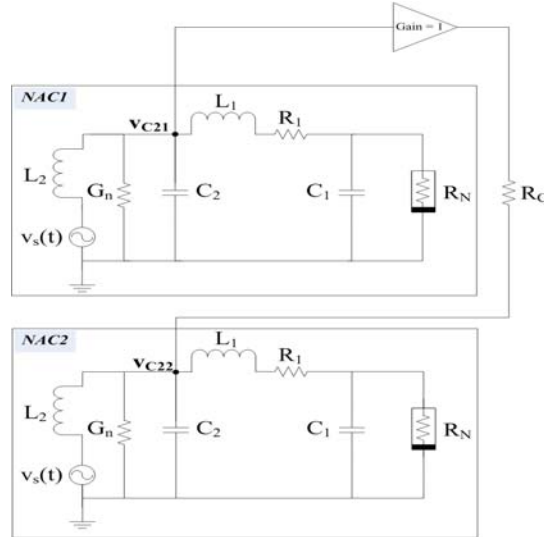


**Figure 6.** Unidirectional coupling of two non-autonomous circuits

The two circuits are synchronized for coupling resistance  $R_C < 3.0k\Omega$ . In Figures 7(a) and (b) the theoretical and experimental phase portraits  $v_{C21}v_{C22}$  are presented, while in Figures 7(c) and (d) we can see theoretical and experimental diagrams  $v_{C22}(t) - v_{C21}(t)$ .

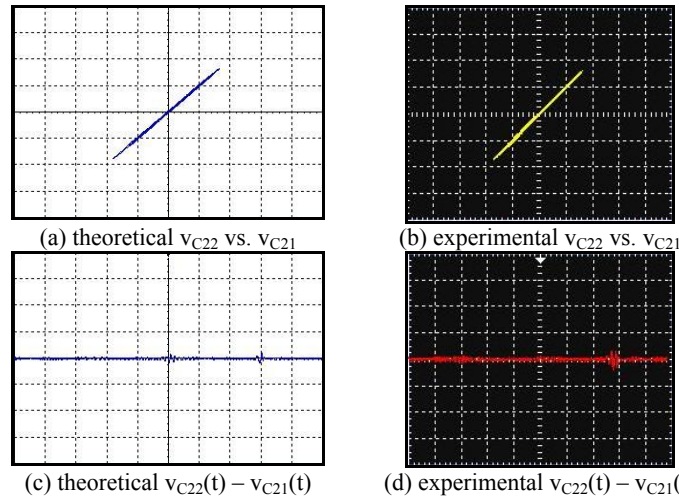


**Figure 7.** Chaotic synchronization for coupling resistance  $R_C = 3.0k\Omega$   
 (a), (b) x: 1V/div, y: 1V/div (c), (d) x: 5ms/div, y: 1V/div

## 4 Chaotic Communication

The proposed communication system is based on chaotic masking technique and presented in Figure 8.

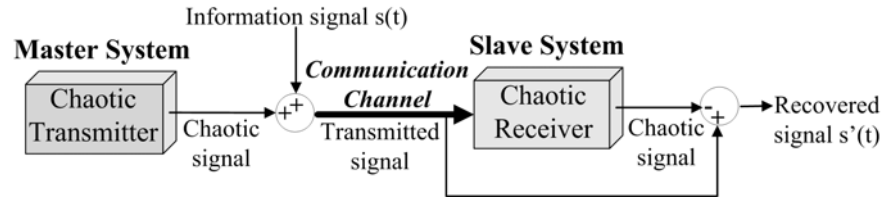


**Figure 8.** Chaotic communication system using masking technique

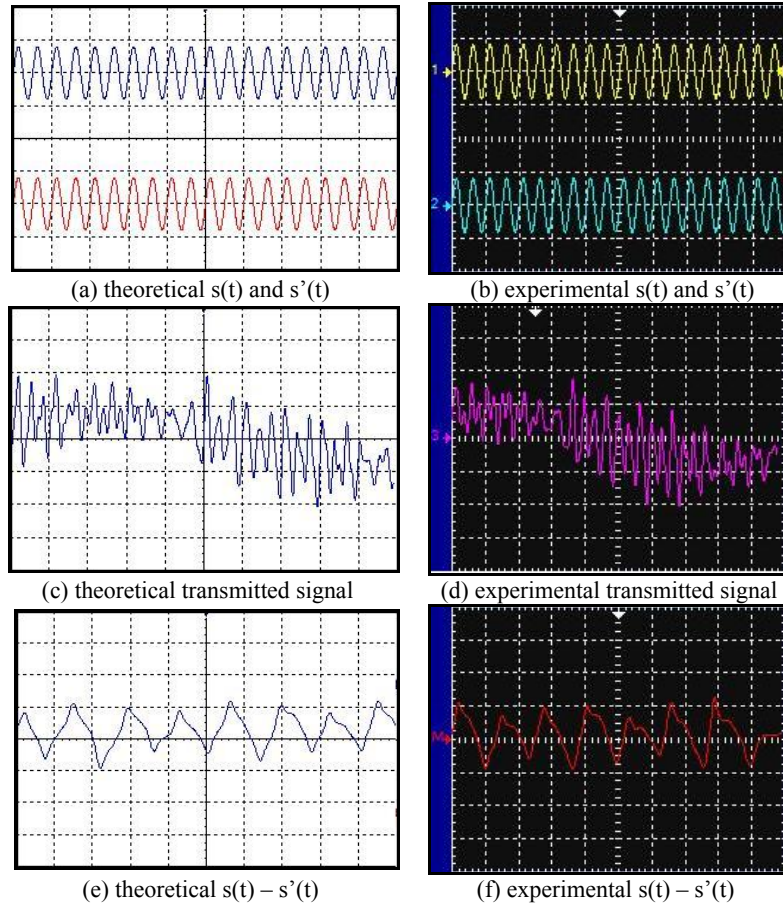


**Figure 9.** (a), (b) x: 2ms/div, y: 500mV/div (c), (d) x: 2ms/div, y: 1V/div (e), (f) x: 500us/div, y: 5mV/div

The information  $s(t)$  is a sinusoidal signal with  $V_{os}= 0.40V$  and  $f_s= 1kHz$  and is given by Eq. (7):

$$s(t)=V_{os} \cdot \cos(2\pi f_s t) \quad (7)$$

In Figure 9(a) the theoretical information  $s(t)$  (above) and recovered  $s'(t)$  (below) signals are presented, while in Figure 9(b) we can see the experimental ones. In Figure 9(c) and (d) the theoretical and experimental transmitted signals are displayed, while in Figures 9(e) and (f) the theoretical and experimental  $s(t)-s'(t)$  are presented.

## 5 Conclusions

In this paper, theoretical and experimental study of chaos synchronization of two identical, 4<sup>th</sup> order, unidirectionally coupled, non-autonomous circuits is presented. The two circuits are been synchronized for coupling resistance  $R_C < 3.0k\Omega$ . A chaotic secure communication system based on chaotic masking technique is proposed. Transmission and recovery of a sinusoidal input signal are demonstrated. Both, theoretical and experimental results verified the performance of proposed secure communication system and showed that the difference between transmitted information  $s(t)$  and recovered information  $s'(t)$  is less than 5mV. The investigation of communication scheme established that chaotic secure communication using the two non-autonomous 4<sup>th</sup> order circuits is feasible and efficient.

## Acknowledgements

The authors would like to thank the referees for their valuable comments.

## References

- [1] L. M. Pecora, T. L. Carroll, Synchronization in chaotic systems, *Phys. Rev. Lett.*, 64, 821-824, (1990).
- [2] M.S. Papadopoulou, I.N. Kyprianidis, I.N. Stouboulos, Dynamics of two coupled nonlinear autonomous 4<sup>th</sup> order circuits, *J. of Istanbul Kultur University*, 14, 55-64, (2006).
- [3] M.S. Papadopoulou, I.N. Kyprianidis, I.N. Stouboulos, Study of the behaviour of a 4<sup>th</sup> order non driven Circuit. Chaotic synchronization of two identical circuits, *WSEAS Trans. on Circuits Syst.*, 5, 993-1000, (2006).
- [4] M.S. Papadopoulou, I.N. Kyprianidis, I.N. Stouboulos, A.N. Anagnostopoulos, Study of the bidirectional synchronization of two identical four-dimensional nonlinear systems, *J. Appl. Funct. Anal.*, 4, 337-346, (2009).
- [5] A. Kittela, J. Parisia, K. Pyragas, Generalized synchronization of chaos in electronic circuit experiments, *Physica D*, 112, 459-471, (1998).
- [6] Z.C. Gao, Z.M. Wu, L.P. Cao, G.Q. Xia, Chaos synchronization of optoelectronic coupled semiconductor lasers ring, *Appl. Phys. B*, 97, 645-651, (2009).

- [7] Y. Imaia, H. Murakawab, T. Imotob, Chaos synchronization characteristics in erbium-doped fiber laser systems, *Optics Communications*, 217, 415-420, (2003).
- [8] D. Cheng, C. Huang, S. Cheng, J. Yan, Synchronization of optical chaos in vertical-cavity surface-emitting lasers via optimal PI controller, *Expert Syst. Appl.*, 36, 6854-6858, (2009).
- [9] A. Uchida, S. Kinugawaa, S. Yoshimoria, Synchronization of chaos in two microchip lasers by using incoherent feedback method, *Chaos, Solitons & Fractals*, 17, 363-368, (2003).
- [10] R.E. Mirollo, S.H. Strogatz, Synchronization of Pulse-Coupled Biological Oscillators, *SIAM J. on Appl. Mathematics*, 50, 1645-1662, (1990).
- [11] J. Lachaux, E. Rodriguez, M. Le Van Quyen, A. Lutz, J. Martinerie, F. Varela, Studying single trials of phase synchronization activity in the brain, *Int. J. Bif. Chaos*, 10, 2429-2439, (2000).
- [12] G. Kolumban, M.P. Kennedy, L.O. Chua, The role of synchronization in digital communications using chaos—Part I: Fundamentals of digital communications, *IEEE Trans. Circuits Syst. I*, 44, 927-936, (1997).
- [13] G. Kolumban, M.P. Kennedy, L.O. Chua, The role of synchronization in digital communications using chaos—Part II: Chaotic modulation and chaotic synchronization, *IEEE Trans. Circuits Syst. I*, 45, 1129-1140, (1998).
- [14] G. Kolumban and M.P. Kennedy, The role of synchronization in digital communications using chaos—Part III: Performance bounds for correlation receivers, *IEEE Trans. Circuits Syst. I*, 47, 1673-1683, (2000).
- [15] L.M. Pecora, T.L. Carroll, G.A. Johnson, D.J. Mar, Fundamentals of synchronization in chaotic systems, concepts, and applications, *American Institute of Physics-Chaos*, 7, 520-542, (1997).
- [16] K.M. Cuomo, A.V. Oppenheim, Circuit implementation of synchronized chaos with applications to communication, *Phys. Rev. Lett.*, 71, 65-68, (1993).
- [17] Y. Senlin, C. Zeying, C. Wenjian, Chaotic laser synchronization and its application in optical fiber secure communication, *Science in China Ser. F Information Sciences*, 47, 332-347, (2004).
- [18] L. Kocarev, U. Parlitz, General Approach for Chaotic Synchronization with Applications to Communication, *Phys. Rev. Lett.*, 74, 5028-5031, (1995).
- [19] F. Zhu, Observer-based synchronization of uncertain chaotic system and its application to secure communications, *Chaos, Solitons & Fractals*, 40, 2384-2391, (2009).
- [20] R.F. Douglas, Chaotic digital encoding: an approach to secure communication, *IEEE Trans. Circuits Syst. II*, 40, 660-666, (1994).
- [21] M.S. Papadopoulou, I.M. Kyprianidis, I.N. Stouboulos, Complex Chaotic Dynamics of the Double-Bell Attractor, *WSEAS Trans. Circuits Syst.*, 7, 13-21, (2008).
- [22] M.S. Papadopoulou, I.N. Stouboulos, I.M. Kyprianidis, Study of the Behavior of a 4<sup>th</sup> Order Non-Autonomous Circuit in Low Frequency Area, *Nonlinear Phenomena in Complex Systems*, 11, 193-197, (2008).
- [23] I.N. Stouboulos, I.M. Kyprianidis, M.S. Papadopoulou, Genesis and Catastrophe of the Chaotic Double-Bell Attractor, *Proc. of the 7<sup>th</sup> WSEAS Int. Conf. on Systems Theory and Scientific Computation*, 141-146, (2007).



# STRICT STABILITY CRITERIA OF UNPERTURBED SYSTEMS WITH INITIAL TIME DIFFERENCE

COŞKUN YAKAR and MUSTAFA BAYRAM GÜCEN

Gebze Institute of Technology  
Department of Mathematics, Faculty of Sciences  
Gebze, Kocaeli, TURKEY 141-41400  
E-mail: cyakar@penta.gyte.edu.tr

and  
Yıldız Technical University  
Department of Mathematics, Faculty of Sciences and Arts  
Davutpasa-Esenler, İstanbul, TURKEY 34210  
E-mail: mgucen@yildiz.edu.tr

**Summary:** In this paper we investigate the strict stability criteria of an unperturbed differential system with respect to an unperturbed differential system that have different initial conditions and an initial time difference.

**Key Words:** strict stability, initial time difference, unperturbed differential systems, Lyapunov's stability.

**AMS Mathematics Subject Classification (2000):** 34D10, 34D20, 34D99, 74H55.

## 1 Introduction

The method of Lyapunov's stability has been very useful and fruitful techniques in the qualitative theory of differential equations since it is a practical tool in the investigation of the behavior of solutions of differential equations. It has been applied to investigate the behavior of unperturbed and perturbed systems in nonlinear differential systems [2, 4, 5, 6, 7, 8] the boundedness, stability properties of unperturbed systems. Recently in [1, 5, 6, 7, 8], the study of initial value problems with an initial time difference has been initiated and the corresponding theory of differential inequalities has been investigated. As in all measurements, errors occur in measurements of starting time and the solutions of an unperturbed differential system may start at an initial time that is different than the starting time of the perturbed differential system. In real situations it may be impossible to have only a change in the space variable and not also in the initial time.

We investigate strict stability criteria of an unperturbed system with different initial conditions and unperturbed systems with different initial conditions. We are not only consider the change in initial position, but also an initial time difference. Previously, the investigation of initial value problems in differential equations has been restricted to a perturbation only in the space variable with the initial time unchanged.

## 2 Definition and Notation

Consider the differential systems

$$x' = f(t, x), x(t_0) = x_0 \text{ for } t \geq \tau_0 \geq t_0, t_0 \in \mathbb{R}_+ \quad (2.1)$$

where  $f \in C[\mathbb{R}_+ \times \mathbb{R}^n, \mathbb{R}^n]$  and  $\eta = \tau_0 - t_0 \geq 0$ . Assume that we have the sufficient conditions for the existence and uniqueness of the solutions  $x(t) = x(t, t_0, x_0)$  of (2.1) for  $t \geq t_0$  and  $y(t) = y(t, \tau_0, y_0)$  of (2.1) for  $t \geq \tau_0$ .

Let us give the definition of the strict stability criteria with initial time difference.

**Definition 2.1:** The solution  $y(t, \tau_0, y_0)$  of the system (2.1) through  $(\tau_0, y_0)$  is said to be initial time difference strict stable with respect to the solution  $x(t - \eta, t_0, x_0)$ , where  $x(t, t_0, x_0)$  is any solution of the system (2.1) for  $t \geq \tau_0 \geq 0, t_0 \in \mathbb{R}_+$  and  $\eta = \tau_0 - t_0$ . If given any  $\epsilon_1 > 0$  and  $\tau_0 \in \mathbb{R}_+$  there exist  $\delta_1 = \delta_1(\epsilon_1, \tau_0) > 0$  and  $\delta_2 = \delta_2(\epsilon_1, \tau_0) > 0$  such that

$$\|y(t, \tau_0, y_0) - x(t - \eta, t_0, x_0)\| < \epsilon_1 \text{ for } t \geq \tau_0$$

whenever  $\|y_0 - x_0\| < \delta_1$  and  $|\tau_0 - t_0| < \delta_2$  and, for  $\delta_1^* < \delta_1$  and  $\delta_2^* < \delta_2$  there exist  $\epsilon_2 < \min\{\delta_1^*, \delta_2^*\}$  such that

$$\|y(t, \tau_0, y_0) - x(t - \eta, t_0, x_0)\| > \epsilon_2 \text{ for } t \geq \tau_0$$

whenever  $\|y_0 - x_0\| > \delta_1^*$  and  $|\tau_0 - t_0| > \delta_2^*$ .

**Definition 2.2:** If  $\delta_1, \delta_2$  and  $\epsilon_2$  in Definition 2.1 are independent of  $\tau_0$ , then the solution  $y(t, \tau_0, y_0)$  of the system (2.1) is initial time difference uniformly strict stable with respect to the solution  $x(t - \eta, t_0, x_0)$  for  $t \geq \tau_0$ .

**Definition 2.3:** The solution  $y(t, \tau_0, y_0)$  of the system (2.1) through  $(\tau_0, y_0)$  is said to be initial time difference strictly attractive with respect to the solution  $x(t - \eta, t_0, x_0)$ , where  $x(t, t_0, x_0)$  is any solution of the system (2.1) for  $t \geq \tau_0 \geq 0, t_0 \in \mathbb{R}_+$  and  $\eta = \tau_0 - t_0$ . If given any  $\alpha_1 > 0, \gamma_1 > 0, \epsilon_1 > 0$  and  $\tau_0 \in \mathbb{R}_+$ , for every  $\alpha_2 < \alpha_1$  and  $\gamma_2 < \gamma_1$ , there exist  $\epsilon_2 < \epsilon_1, T_1 = T_1(\epsilon_1, \tau_0)$  and  $T_2 = T_2(\epsilon_1, \tau_0)$  such that

$$\|y(t, \tau_0, y_0) - x(t - \eta, t_0, x_0)\| < \epsilon_1 \text{ for } T_1 + \tau_0 \leq t \leq T_2 + \tau_0$$

whenever  $\|y_0 - x_0\| < \alpha_1$  and  $|\tau_0 - t_0| < \gamma_1$  and

$$\|y(t, \tau_0, y_0) - x(t - \eta, t_0, x_0)\| > \epsilon_2 \text{ for } T_2 + \tau_0 \geq t \geq T_1 + \tau_0$$

whenever  $\|y_0 - x_0\| > \alpha_2$  and  $|\tau_0 - t_0| > \gamma_2$ .

If  $T_1$  and  $T_2$  in Definition 2.3 are independent of  $\tau_0$ , then the solution  $y(t, \tau_0, y_0)$  of the system (2.1) is initial time difference uniformly strictly attractive stable with respect to the solution  $x(t - \eta, t_0, x_0)$  for  $t \geq \tau_0$ .

**Definition 2.4:** The solution  $y(t, \tau_0, y_0)$  of the system (2.1) through  $(\tau_0, y_0)$  is said to be initial time difference strictly asymptotically stable with respect to the solution  $x(t - \eta, t_0, x_0)$  if Definition 2.3 satisfies and the solution  $y(t, \tau_0, y_0)$  of the system (2.3) through  $(\tau_0, y_0)$  is initial time difference strictly stable with respect to the solution  $x(t - \eta, t_0, x_0)$ .

If  $T_1$  and  $T_2$  in Definition 2.3 are independent of  $\tau_0$ , then the solution  $y(t, \tau_0, y_0)$  of the system (2.1) is initial time difference uniformly strictly asymptotically stable with respect to the solution  $x(t - \eta, t_0, x_0)$  for  $t \geq \tau_0$ .

**Definition 2.5:** For any function  $V_n \in C[\mathbb{R}_+ \times \mathbb{R}^n, \mathbb{R}_+]$ , we define the Dini derivative of the function with respect to the solution of the system (2.1)

$$D^+V(t, y - x) = \lim_{h \rightarrow 0^+} \sup \frac{1}{h} [V(t + h, y - x + h(f(t, y) - f(t, x))) - V(t, y - x)]$$

and

$$D_-V(t, y - x) = \lim_{h \rightarrow 0^-} \inf \frac{1}{h} [V(t + h, y - x + h(f(t, y) - f(t, x))) - V(t, y - x)]$$

where  $y = y(t, \tau_0, y_0)$  and  $x = x(t, t_0, x_0)$  for  $(t, x)$  and  $(t, y) \in \mathbb{R}_+ \times \mathbb{R}^n$ .

**Definition 2.6:**  $\mathcal{K}$  is said to be the class  $\mathcal{K}$  set of functions such that

$\mathcal{K} := [a : a \in C([0, \rho], \mathbb{R}_+), a \text{ is strictly increasing and } a(0) = 0]$  and  $S_\rho = \{z \in \mathbb{R}^n : \|z\| \leq \rho\}$ .

### 3 Main Results

In this section we obtain the strict stability concepts with initial time difference parallel to the Lyapunov's results.

**Theorem 3.1:** Assume that

(A<sub>1</sub>) for each  $\mu, 0 < \mu < \rho, V_\mu \in C[\mathbb{R}_+ \times S_\rho, \mathbb{R}_+]$  and  $V_\mu$  is locally Lipschitzian in  $z$  and for  $(t, z) \in \mathbb{R}_+ \times S_\rho$  and  $\|z\| \geq \mu$ ,

$$b_1(\|z\|) \leq V_\mu(t, z) \leq a_1(\|z\|), a_1, b_1 \in \mathcal{K}$$

$$D^+V_\mu(t, z) \leq 0; \quad (3.1)$$

(A<sub>2</sub>) for each  $\theta, 0 < \theta < \rho, V_\theta \in C[\mathbb{R}_+ \times S_\rho, \mathbb{R}_+]$  and  $V_\theta$  is locally Lipschitzian in  $z$  and for  $(t, z) \in \mathbb{R}_+ \times S_\rho$  and  $\|z\| \leq \theta$ ,

$$b_2(\|z\|) \leq V_\theta(t, z) \leq a_2(\|z\|), a_2, b_2 \in \mathcal{K}$$

$$D^+V_\theta(t, z) \geq 0; \quad (3.2)$$

where  $z(t) = y(t, \tau_0, y_0) - x(t - \eta, t_0, x_0)$  for  $t \geq \tau_0, y(t, \tau_0, y_0)$  of the system (2.1) through  $(\tau_0, y_0)$  and  $x(t - \eta, t_0, x_0)$ , where  $x(t, t_0, x_0)$  is any solution of the system (2.1) for  $t \geq \tau_0 \geq 0, t_0 \in \mathbb{R}_+$  and  $\eta = \tau_0 - t_0$ .

Then the solution  $y(t, \tau_0, y_0)$  of the system (2.1) is the initial time difference strictly stable with respect to  $x(t - \eta, t_0, x_0)$  of the system (2.1) for  $t \geq \tau_0 \geq 0, t_0 \in \mathbb{R}_+$  and  $\eta = \tau_0 - t_0$ .

**Proof of Theorem 3.1:** Let  $0 < \epsilon_1 < \rho$  and  $\tau_0 \in \mathbb{R}_+$ . Let us choose  $\delta_1 = \delta_1(\epsilon_1, \tau_0) > 0$  such that

$$a_1(\delta_1) < b_1(\epsilon_1) \quad (3.3)$$

since we have  $b_1(\epsilon_1) \leq a_1(\delta_1)$  in (A<sub>1</sub>). Then we claim that

$$\|y(t, \tau_0, y_0) - x(t - \eta, t_0, x_0)\| < \epsilon_1 \text{ for } t \geq \tau_0 \quad (3.4)$$

whenever  $\|y_0 - x_0\| < \delta_1$  and  $|\tau_0 - t_0| < \delta_2$ .

If (3.4) is not true, then there exist  $t_1 > t_2 > \tau_0$  and the solution of (2.1) with  $\|y_0 - x_0\| < \delta_1, |\tau_0 - t_0| < \delta_2$  satisfying

$$\|y(t_1) - \tilde{x}(t_1)\| = \epsilon_1, \|y(t_2) - \tilde{x}(t_2)\| = \delta_1 \text{ and } \delta_1 \leq \|y(t) - \tilde{x}(t)\| \leq \epsilon_1 \text{ for } t \in [t_2, t_1].$$

Let us set  $\mu = \delta_1$ , and using  $(A_1)$  we can obtain

$$\begin{aligned} b_1(\epsilon_1) &= b_1(\|y(t_1) - \tilde{x}(t_1)\|) \leq V_\mu(t_1, y(t_1) - \tilde{x}(t_1)) \\ &\leq V_\mu(t_2, y(t_2) - \tilde{x}(t_2)) \leq a_1(\|y(t_2) - \tilde{x}(t_2)\|) = a_1(\delta_1) \end{aligned}$$

which contradicts with (3.3). Hence (3.4) is valid.

Now let  $0 < \delta_1^* < \delta_1, 0 < \delta_2^* < \delta_2$  and  $\epsilon_2 < \delta = \min\{\delta_1^*, \delta_2^*\}$  such that

$$a_2(\epsilon_2) < b_2(\delta) \quad (3.5)$$

since we have  $a_2(\epsilon_2) \geq b_2(\delta)$  in  $(A_2)$ . Then we can prove that

$$\epsilon_2 < \|y(t, \tau_0, y_0) - x(t - \eta, t_0, x_0)\| < \epsilon_1 \text{ for } t \geq \tau_0 \quad (3.6)$$

whenever  $\delta_1^* < \|y_0 - x_0\| < \delta_1$  and  $\delta_2^* < |\tau_0 - t_0| < \delta_2$ .

If (3.6) is not true, then there would exist  $t_1 > t_2 > \tau_0$  and the solution of (2.1) and (3.2) with  $\delta_1^* < \|y_0 - x_0\| < \delta_1, \delta_2^* < |\tau_0 - t_0| < \delta_2$  satisfying

$$\|y(t_1) - \tilde{x}(t_1)\| = \epsilon_2, \|y(t_2) - \tilde{x}(t_2)\| = \delta \text{ and } \|y(t) - \tilde{x}(t)\| \leq \delta \text{ for } t \in [t_2, t_1]. \quad (3.7)$$

Let us set  $\theta = \delta$  and using  $(A_2)$ , we get

$$\begin{aligned} a_2(\epsilon_2) &= a_2(\|y(t_1) - \tilde{x}(t_1)\|) \geq V_\theta(t_1, y(t_1) - \tilde{x}(t_1)) \\ &\geq V_\theta(t_2, y(t_2) - \tilde{x}(t_2)) \geq b_2(\|y(t_2) - \tilde{x}(t_2)\|) = b_2(\delta) \end{aligned}$$

which contradicts with (3.5). Thus (3.6) is valid. Then the solution  $y(t, \tau_0, y_0)$  of the system (2.1) through  $(\tau_0, y_0)$  is initial time difference strictly stable with respect to the solution  $x(t - \eta, t_0, x_0)$ .

This completes the proof of Theorem 3.1.

If  $\delta_1, \delta_2$  and  $\epsilon_2$  in Theorem 3.1 are independent of  $\tau_0$ , then the solution  $y(t, \tau_0, y_0)$  of the system (2.1) is initial time difference uniformly strict stable with respect to the solution  $x(t - \eta, t_0, x_0)$  for  $t \geq \tau_0$ .

**Theorem 3.2:** Assume that

$(A_1)$  for each  $\mu, 0 < \mu < \rho, V_\mu \in C[\mathbb{R}_+ \times S_\rho, \mathbb{R}_+]$  and  $V_\mu$  is locally Lipschitzian in  $z$  and for  $(t, z) \in \mathbb{R}_+ \times S_\rho$  and  $\|z\| \geq \mu$ ,

$$b_1(\|z\|) \leq V_\mu(t, z) \leq a_1(\|z\|), a_1, b_1 \in \mathcal{K},$$

$$D^+V_\mu(t, z) \leq -c_1(\|z\|) \quad c_1 \in \mathcal{K}; \quad (3.8)$$

$(A_2)$  for each  $\theta, 0 < \theta < \rho, V_\theta \in C[\mathbb{R}_+ \times S_\rho, \mathbb{R}_+]$  and  $V_\theta$  is locally Lipschitzian in  $z$  and for  $(t, z) \in \mathbb{R}_+ \times S_\rho$  and  $\|z\| \leq \theta$ ,

$$b_2(\|z\|) \leq V_\theta(t, z) \leq a_2(\|z\|), a_2, b_2 \in \mathcal{K},$$

$$D^+V_\theta(t, z) \geq -c_2(\|z\|) \quad c_2 \in \mathcal{K}; \quad (3.9)$$

where  $z(t) = y(t, \tau_0, y_0) - x(t - \eta, t_0, x_0)$  for  $t \geq \tau_0$ ,  $y(t, \tau_0, y_0)$  of the system (2.1) through  $(\tau_0, y_0)$  and  $x(t - \eta, t_0, x_0)$ , where  $x(t, t_0, x_0)$  is any solution of the system (2.1) for  $t \geq \tau_0 \geq 0, t_0 \in \mathbb{R}_+$  and  $\eta = \tau_0 - t_0$ .

Then the solution  $y(t, \tau_0, y_0)$  of the system (2.1) through  $(\tau_0, y_0)$  is the initial time difference strictly asymptotically stable with respect to  $x(t - \eta, t_0, x_0)$  of the solution of the system (2.1) for  $t \geq \tau_0 \geq 0, t_0 \in \mathbb{R}_+$  and  $\eta = \tau_0 - t_0$ .

**Proof of Theorem 3.2:** We note that (3.8) implies (3.1). However, (3.9) does not yield (3.2). As a result of these, we obtain because of (3.8) only stability of unperturbed systems with initial time difference with respect to  $x(t - \eta, t_0, x_0)$  that is for given any  $\epsilon_1 \leq \rho$  and  $\tau_0 \in \mathbb{R}_+$  there exist  $\delta_{10} = \delta_{10}(\epsilon_1, \tau_0) > 0$  and  $\delta_{20} = \delta_{20}(\epsilon_1, \tau_0) > 0$  such that

$$\|y(t, \tau_0, y_0) - x(t - \eta, t_0, x_0)\| < \epsilon_1 \text{ for } t \geq \tau_0 \text{ whenever } \|y_0 - x_0\| < \delta_{10} \text{ and } |\tau_0 - t_0| < \delta_{20}. \quad (3.10)$$

To prove the conclusion of Theorem 3.2 we need to show that the solution  $y(t, \tau_0, y_0)$  of the system (2.1) through  $(\tau_0, y_0)$  is strictly attractive with respect to  $x(t - \eta, t_0, x_0)$  for this purpose, let  $\epsilon_1 = \rho$  and set  $\delta_{10} = \delta_1(\rho, \tau_0)$  and  $\delta_{20} = \delta_2(\rho, \tau_0)$  so that (3.10) yields  $\|y(t, \tau_0, y_0) - x(t - \eta, t_0, x_0)\| < \rho$  for  $t \geq \tau_0$  whenever  $\|y_0 - x_0\| < \delta_1$  and  $|\tau_0 - t_0| < \delta_2$ .

Let  $\|y_0 - x_0\| < \delta_{10}$  and  $|\tau_0 - t_0| < \delta_{20}$ . We show, using standard argument, that there exists a  $t^* \in [\tau_0, \tau_0 + T]$ , where  $T = T(\epsilon, \tau_0) > \frac{a_1(\delta_{10}, \delta_{20})}{c_1(\delta_1, \delta_2)}$  where  $\delta_{10}$  and  $\delta_{20}$  are the numbers corresponding to  $\epsilon_1$  in (3.10) that is in stability of unperturbed systems with initial time difference with respect to  $x(t - \eta, t_0, x_0)$  such that  $\|y(t^*, \tau_0, y_0) - x(t^* - \eta, t_0, x_0)\| < \delta_1$  for any solutions of the system (2.1) with  $\|y_0 - x_0\| < \delta_{10}$  and  $|\tau_0 - t_0| < \delta_{20}$ . If this is not true, we will have  $\|y(t^*, \tau_0, y_0) - x(t^* - \eta, t_0, x_0)\| \geq \delta_1$  for  $t^* \in [\tau_0, \tau_0 + T]$ . Then,  $\mu = \delta_1$  and using  $(A_1)$  with (3.8), we have

$$\begin{aligned} b_1(\delta_1) &\leq b_1(\|y(\tau_0 + T) - \tilde{x}(\tau_0 + T)\|) \\ &\leq V_\mu(\tau_0 + T, y(\tau_0 + T) - \tilde{x}(\tau_0 + T)) \\ &\leq V_\mu(\tau_0, y_0 - x_0) - \int_{\tau_0}^{\tau_0 + T} c_1(\|y(s) - \tilde{x}(s)\|) ds \\ &\leq a_1(\delta_{10}, \delta_{20}) - c_1(\delta_1, \delta_2)T \\ &< b_1(\delta_1) \end{aligned}$$

in view of the choice of  $T$ . This contradiction implies that there exist a  $t^* \in [\tau_0, \tau_0 + T]$  satisfying  $\|y(t^*, \tau_0, y_0) - x(t^* - \eta, t_0, x_0)\| < \delta_1$ . Because of the stability  $y(t, \tau_0, y_0)$  of unperturbed systems with initial time difference with respect to  $x(t - \eta, t_0, x_0)$ , this yields that

$$\|y(t, \tau_0, y_0) - x(t - \eta, t_0, x_0)\| < \epsilon_1 \text{ for } t \geq \tau_0 + T \geq t^*$$

which implies that there exists a  $\tau_0 < T_1 < T$  such that

$$\|y(\tau_0 + T_1, \tau_0, y_0) - x(\tau_0 + T_1 - \eta, t_0, x_0)\| = \epsilon_1.$$

Now, for any  $\delta_{12}, 0 < \delta_{12} < \delta_{10}$  and  $0 < \delta_{12} < \delta_{20}$  we can choose  $\epsilon_2$  such that  $b_2(\epsilon_1) > a_2(\epsilon_2)$  and  $0 < \epsilon_2 < \epsilon_1 < \delta_{12}$ .

Suppose that  $\delta_{12} < \|y_0 - x_0\| < \min\{\delta_{10}, \delta_{20}\}$  and  $\delta_{12} < |\tau_0 - t_0| < \min\{\delta_{10}, \delta_{20}\}$ . Let us define  $\tau = \frac{b_2(\epsilon_1) - a_2(\epsilon_2)}{c_2(\epsilon_1)}$ , and  $T_2 = T_1 + \tau$ . Since  $\|y(t, \tau_0, y_0) - x(t - \eta, t_0, x_0)\| \leq \epsilon_1$  for  $t \geq \tau_0 + T_1$ , choosing  $\theta = \epsilon_1$  and using  $(A_2)$  with (3.9) we have for  $t \in [\tau_0 + T_1, \tau_0 + T_2]$ ,

$$\begin{aligned} a_2(\|y(t) - \tilde{x}(t)\|) &\geq V_\theta(t, y(t) - \tilde{x}(t)) \\ &\geq V_\theta(\tau_0 + T_1, y(\tau_0 + T_1) - \tilde{x}(\tau_0 + T_1)) - \int_{\tau_0 + T_1}^t c_2(\|y(s) - \tilde{x}(s)\|) ds \\ &\geq b_2(\epsilon_1) - \int_{\tau_0 + T_1}^t c_2(\|y(s) - \tilde{x}(s)\|) ds \\ &\geq b_2(\epsilon_1) - c_2(\epsilon_1)[t - (\tau_0 + T_1)]. \end{aligned}$$

Since,  $t - (\tau_0 + T_1) > \tau$ , it follows that

$$a_2(\|y(t) - \tilde{x}(t)\|) > b_2(\epsilon_1) - c_2(\epsilon_1)\left[\frac{b_2(\epsilon_1) - a_2(\epsilon_2)}{c_2(\epsilon_1)}\right] = a_2(\epsilon_2).$$

This yields that

$$\|y(t, \tau_0, y_0) - x(t - \eta, t_0, x_0)\| > \epsilon_2 \text{ for } t \in [\tau_0 + T_1, \tau_0 + T_2]$$

and therefore,

$$\epsilon_2 < \|y(t, \tau_0, y_0) - x(t - \eta, t_0, x_0)\| < \epsilon_1 \text{ for } t \in [\tau_0 + T_1, \tau_0 + T_2].$$

This completes the proof. Then the solution  $y(t, \tau_0, y_0)$  of the system (2.1) through  $(\tau_0, y_0)$  is initial time difference strictly asymptotically stable with respect to the solution  $x(t - \eta, t_0, x_0)$ , where  $x(t, t_0, x_0)$  is any solution of the system (2.1) for  $t \geq \tau_0 \geq 0, t_0 \in \mathbb{R}_+$  and  $\eta = \tau_0 - t_0$ .

If  $T_1$  and  $T_2$  in Theorem 3.2 are independent of  $\tau_0$ , then the solution  $y(t, \tau_0, y_0)$  of the system (2.1) is initial time difference uniformly strictly asymptotically stable with respect to the solution  $x(t - \eta, t_0, x_0)$  for  $t \geq \tau_0$ .

Before we prove the general result in terms of the comparison principle. Let us consider the uncoupled comparison differential systems,

$$\begin{cases} (i) & u'_1 = g_1(t, u_1), u_1(\tau_0) = u_{10} \geq 0 \\ (ii) & u'_2 = g_2(t, u_2), u_2(\tau_0) = u_{20} \geq 0 \end{cases} \quad \text{where } g_1, g_2 \in C[\mathbb{R}_+^2, \mathbb{R}] \quad (3.11)$$

The comparison system (3.11) is said to be strictly stable: If given any  $\epsilon_1 > 0$  and  $t \geq \tau_0, \tau_0 \in \mathbb{R}_+$ , there exist a  $\delta_1 > 0$  such that

$$u_{10} \leq \delta_1 \text{ implies } u_1(t) < \epsilon_1 \text{ for } t \geq \tau_0$$

and for every  $\delta_2 < \delta_1$  there exists an  $\epsilon_2 > 0, 0 < \epsilon_2 < \delta_2$  such that

$$u_{20} \geq \delta_2 \text{ implies } u_2(t) < \epsilon_2 \text{ for } t \geq \tau_0.$$

Here,  $u_1(t)$  and  $u_2(t)$  are any solutions of (i) in (3.11) and (ii) in (3.11); respectively.

Following main result based on this definition that result is formulated in terms of comparison principle.

**Theorem 3.3:** Assume that

(A<sub>1</sub>) for each  $\mu$ ,  $0 < \mu < \rho$ ,  $V_\mu \in C[\mathbb{R}_+ \times S_\rho, \mathbb{R}_+]$  and  $V_\mu$  is locally Lipschitzian in  $z$  and for  $(t, z) \in \mathbb{R}_+ \times S_\rho$  and  $\|z\| \geq \mu$ ,

$$b_1(\|z\|) \leq V_\mu(t, z) \leq a_1(\|z\|), a_1, b_1 \in \mathcal{K},$$

$$D^+V_\mu(t, z) \leq g_1(t, V_\mu(t, z)); \quad (3.12)$$

(A<sub>2</sub>) for each  $\theta$ ,  $0 < \theta < \rho$ ,  $V_\theta \in C[\mathbb{R}_+ \times S_\rho, \mathbb{R}_+]$  and  $V_\theta$  is locally Lipschitzian in  $z$  and for  $(t, z) \in \mathbb{R}_+ \times S_\rho$  and  $\|z\| \leq \theta$ ,

$$b_2(\|z\|) \leq V_\theta(t, z) \leq a_2(\|z\|), a_2, b_2 \in \mathcal{K},$$

$$D^+V_\theta(t, z) \geq g_2(t, V_\theta(t, z)); \quad (3.13)$$

where  $g_2(t, u) \leq g_1(t, u)$ ,  $g_1, g_2 \in C[\mathbb{R}_+^2, \mathbb{R}]$ ,  $g_1(t, 0) = g_2(t, 0) = 0$  and  $z(t) = y(t, \tau_0, y_0) - x(t - \eta, t_0, x_0)$  for  $t \geq \tau_0$ ,  $y(t, \tau_0, y_0)$  of the system (2.1) through  $(\tau_0, y_0)$  and  $x(t - \eta, t_0, x_0)$ , where  $x(t, t_0, x_0)$  is any solution of the system (2.1) for  $t \geq \tau_0 \geq 0$ ,  $t_0 \in \mathbb{R}_+$  and  $\eta = \tau_0 - t_0$ .

Then any strict stability concept of the comparison system implies the corresponding strict stability concept of the solution  $y(t, \tau_0, y_0)$  of the system (2.1) through  $(\tau_0, y_0)$  with respect to the solution  $x(t - \eta, t_0, x_0)$  of the system (2.1) with initial time difference where  $x(t, t_0, x_0)$  is any solution of the system (2.1) for  $t \geq \tau_0 \geq 0$ ,  $t_0 \in \mathbb{R}_+$ .

**Proof of Theorem 3.3:** We will only prove the case of strict uniformly asymptotically stability. Suppose that the comparison differential systems in (3.11) is strictly uniformly asymptotically stable, then for any given  $\epsilon_1$ ,  $0 < \epsilon_1 < \delta$ , there exist a  $\delta^* > 0$  such that  $u_{10} \leq \delta^*$  implies that  $u_1(t, \tau_0, u_{10}) < b_1(\epsilon_1)$  for  $t \geq \tau_0$ .

For this  $\epsilon_1$  we choose  $\delta_1$  and  $\delta_{11}$ , such that  $a_1(\delta_1^*) \leq \delta^*$  and  $\delta_1^* < \epsilon_1$  where  $\delta_1^* = \max\{\delta_1, \delta_{11}\}$ , then we claim that

$$\|y_0 - x_0\| < \delta_1, |\tau_0 - t_0| < \delta_{11} \text{ imply that } \|y(t, \tau_0, y_0) - x(t - \eta, t_0, x_0)\| < \epsilon_1 \text{ for } t \geq \tau_0. \quad (3.14)$$

If it is not true, then there exist  $t_1$  and  $t_2$ ,  $t_2 > t_1 > \tau_0$  and a solution  $z(t)$  of

$$z' = \tilde{f}(t, z), \quad z(\tau_0) = y_0 - x_0 \text{ for } t \geq \tau_0 \text{ with } |\tau_0 - t_0| < \delta_{11} \text{ and } \|y_0 - x_0\| < \delta_1$$

$$\|y(t, \tau_0, y_0) - x(t - \eta, t_0, x_0)\| < \delta_1^*, \quad \|y(t, \tau_0, y_0) - x(t - \eta, t_0, x_0)\| = \epsilon_1 \text{ and}$$

$$\delta_1^* \leq \|y(t, \tau_0, y_0) - x(t - \eta, t_0, x_0)\| < \epsilon_1 \text{ for } [t_1, t_2].$$

Choosing  $\mu = \delta_1^*$  and using the theory of differential inequalities we get

$$\begin{aligned}
b_1(\epsilon_1) &= b_1(\|y(t_2, \tau_0, y_0) - x(t_2 - \eta, t_0, x_0)\|) \\
&\leq V_\mu(t_2, y(t_2, \tau_0, y_0) - x(t_2 - \eta, t_0, x_0)) \\
&\leq r(t_2, t_1, V_\mu(t_1, y(t_1, \tau_0, y_0) - x(t_1 - \eta, t_0, x_0))) \\
&\leq r(t_2, t_1, a_1(\delta_1^*)) \\
&\leq r(t_2, t_1, \delta^*) \\
&< b_1(\epsilon_1)
\end{aligned}$$

which is a contradiction. Here  $r(t, \tau_0, u_{10})$  is the maximal solution of (3.11). Hence, (3.14) is true and we have uniformly stability with initial time difference. Now, we shall prove strictly uniformly attractive with initial time difference.

For any given  $\delta_2, \epsilon_2 > 0, \delta_2 < \delta^*$  we choose  $\bar{\delta}_2$  and  $\bar{\epsilon}_2$  such that  $a_1(\delta_2) < \bar{\delta}_2$  and  $b_1(\epsilon_2) \geq \bar{\epsilon}$ . For these  $\bar{\delta}_2$  and  $\bar{\epsilon}$ , since (2.11) is strictly uniformly attractive, for any  $\bar{\delta}_3 < \bar{\delta}_2$  there exist  $\bar{\epsilon}_3$  and  $T_1$  and  $T_2$  ( $T_2 < T_1$ ) such that  $\bar{\delta}_3 < u_{10} = u_{20} < \bar{\delta}_2$  implies

$$\begin{aligned}
r(t, \tau_0, u_{10}) &\leq r(t, \tau_0, \bar{\delta}_2) < \bar{\epsilon}_2 \\
\rho(t, \tau_0, u_{20}) &\geq \rho(t, \tau_0, \bar{\delta}_3) > \bar{\epsilon}_2
\end{aligned}$$

where  $r(t, \tau_0, u_{10})$  and  $\rho(t, \tau_0, u_{20})$  is the maximal solution and minimal solution of (3.11) (i) and (3.11) (ii); respectively.

Now, for any  $\delta_3$ , let  $b_2(\delta_3) \geq \bar{\delta}_3$ . We choose  $\epsilon_3$  such that  $a_2(\epsilon_3) < \bar{\epsilon}_3$ . Then by using comparison principle (3.11) (i) and  $(A_1)$ , we have

$$\begin{aligned}
b_1(\|y(t, \tau_0, y_0) - x(t - \eta, t_0, x_0)\|) &\leq V_\mu(t, y(t, \tau_0, y_0) - x(t - \eta, t_0, x_0)) \\
&\leq r(t, \tau_0, V_\mu(\tau_0, y_0 - x_0)) \\
&\leq r(t, \tau_0, a_1(\|y_0 - x_0\|)) \\
&\leq r(t, \tau_0, \bar{\delta}_2) \\
&< \bar{\epsilon}_2 \leq b_1(\epsilon_2)
\end{aligned}$$

which implies that  $\|y(t, \tau_0, y_0) - x(t - \eta, t_0, x_0)\| < \epsilon_2$  for  $t \in [\tau_0 + T_2, \tau_0 + T_1]$ . Similarly, by using comparison principle in (3.11) (ii) and  $(A_2)$  we get

$$\begin{aligned}
a_2(\|y(t, \tau_0, y_0) - x(t - \eta, t_0, x_0)\|) &\geq V_\theta(t, y(t, \tau_0, y_0) - x(t - \eta, t_0, x_0)) \\
&\geq \rho(t, \tau_0, V_\theta(\tau_0, y_0 - x_0)) \\
&\geq \rho(t, \tau_0, b_2(\delta_3)) \\
&\geq \rho(t, \tau_0, \bar{\delta}_3) \\
&> \bar{\epsilon}_3 \geq a_2(\epsilon_3)
\end{aligned}$$



which implies that for  $\|y(t, \tau_0, y_0) - x(t - \eta, t_0, x_0)\| > \epsilon_3$  for  $t \in [\tau_0 + T_2, \tau_0 + T_1]$ . Hence, the solution  $y(t, \tau_0, y_0)$  of the system (2.1) through  $(\tau_0, y_0)$  is strictly uniformly attractive with respect to the solution  $x(t - \eta, t_0, x_0)$  is any solution of the system (2.1) for  $t \geq \tau_0 \geq 0$ ,  $t_0 \in \mathbb{R}_+$ . The proof is complete.

## References

- [1] Köksal, S. and Yakar, C., Generalized Quasilinearization Method with Initial Time Difference.: Journal of Engineering Simulation **(2002)** 24 (5).
- [2] Lakshmikantham, V. and Leela, S. : Differential and Integral Inequalities Vol. 1, Academic Press, New York. **(1969)**
- [3] Lakshmikantham, V. and Mohapatra, R. N.: Strict Stability of Differential Equations, Nonlinear Analysis, Volume 46, Issue 7, **(2001)** Pages 915-921.
- [4] Rajalakshmi, S and Sivasundaram, S.: Variational Lyapunov Second Method, Dyn. Sys. and Appl. 2, **(1993)** 485-490.
- [5] Shaw, M.D. and Yakar, C., Generalized variation of parameters with initial time difference and a comparison result in term Lyapunov-like functions, International Journal of Nonlinear Differential Equations-Theory Methods and Applications **5**, **(1999)** 86-108.
- [6] Shaw, M.D. and Yakar, C., Stability criteria and slowly growing motions with initial time difference, Problems of Nonlinear Analysis in Engineering Systems **1**, **(2000)** 50-66.
- [7] Yakar, C. Boundedness Criteria in Terms of Two Measures with Initial Time Difference. Dynamics of Continuous, Discrete and Impulsive Systems. Series A: Mathematical Analysis. Watam Press. Waterloo. Page: 270-275. DCDIS 14 (S2) **(2007)** 1-305 .
- [8] Yakar C. Fractional Differential Equations in Terms of Comparison Results and Lyapunov Stability with Initial Time Difference. Journal of Abstract and Applied Analysis. (Accepted) AAA/762857. Vol 3. Article ID 762857, **(2010)** 16 pages doi:10.1155/2010/762857.
- [9] Yakar C., Strict Stability Criteria of Perturbed Systems with respect to Unperturbed Systems in term of Initial Time Difference. Proceedings of the Conference on Complex Analysis and Potential Theory. World Scientific Publishing. **(2007)** Page: 239-248 .
- [10] Yakar C., Keleş M. and S.G., Deo. Variation of Parameters Formulae for Nonlinear Integro-differential Equations with Initial Time Difference. Accepted in Journal of Nonlinear Studies. **(2009)**.
- [11] Yakar C. and Shaw, M.D., A Comparison Result and Lyapunov Stability Criteria with Initial Time Difference. Dynamics of Continuous, Discrete and Impulsive Systems. A: Mathematical Analysis. Volume 12, Number 6 **(2005)** (731-741).
- [12] Yakar C. and Shaw, M.D., Initial Time Difference Stability in Terms of Two Measures and Variational Comparison Result. Dynamics of Continuous, Discrete and Impulsive Systems. Series A: Mathematical Analysis 15 **(2008)** 417-425.

- [13] Yakar C. and Shaw M.D. Practical Stability in Terms of Two Measures with Initial Time Difference. Nonlinear Analysis: Theory, Methods & Applications. **(2009)**. Page: e781-e785 Vol. 71 .
- [14] Yakar, C. and Yakar, A. Further Generalization of Quasilinearization Method with Initial Time Difference. Journal of Applied Functional Analysis. Eudoxus Press, Llc. Issn: 1559-1948 (Print). 1559-1956 (Online). Vol. 4 No: 4, **(2009)**.Page 714-727.

# Boundedness and Lagrange Stability of Fractional Order Differential Equations in Caputo's Sense with Initial Time Difference

Coşkun YAKAR and Muhammed ÇİÇEK  
Gebze Institute of Technology, Department of Mathematics  
Gebze-Kocaeli 141-41400, TURKEY  
E-mail: cyakar@gyte.edu.tr and mcicek@gyte.edu.tr

## Abstract

In this paper we investigate that initial time difference boundedness criteria and Lagrange stability of Fractional order differential equations in Caputo's sense are unified with Lyapunov-like functions to establish comparison result. We present a comparison result which again gives the null solution a central role in the comparison fractional order differential equation when establishing initial time difference boundedness criteria and Lagrange stability of the unperturbed fractional order differential equation with respect to the unperturbed fractional order differential equation.

**Key Words:** boundedness and Lagrange stability, fractional order differential equation, comparison results, initial time difference.

**AMS(MOS) subject classification:** 34C11, 34D10, 34D99.

## 1 Introduction

We have investigated that the Boundedness and Lagrange stability of an unperturbed fractional order differential equation with respect to an unperturbed fractional order differential equation with initial time difference. The differential operators with the order  $q$  ( $0 < q < 1$ ) are considered in the Caputo's sense, we have the relations among the Caputo, Riemann-Liouville and Grünwald-Letnikov fractional derivatives, and the initial conditions are specified according to Caputo's suggestion [1], thus allowing for interpretation in a physically meaningful way [4, 7, 10].

The concept of a Lyapunov function has been employed with great success in a wide variety of investigations to understand qualitative and quantitative properties of dynamic systems for many years. Lyapunov's second method is a standard technique used in the study of the qualitative behavior of differential systems [2, 5, 6, 7] along with a comparison result [3, 12] that allows the prediction of behavior of a differential system when the behavior of the null solution of a comparison system is known. The application of Lyapunov's second method in boundedness theory [5, 6, 7, 14,] has the advantage of not requiring knowledge of solutions. However; there has been difficulty with this approach when trying to apply it to unperturbed fractional differential systems [4, 7, 10] and associated unperturbed fractional differential systems with different initial conditions and an initial time difference. . The difficulty arises because there is a significant difference between initial time difference (ITD) Boundedness and Lagrange stability [8,11-18] and the classical notion of Boundedness and Lagrange stability for fractional differential systems [4, 7]. The classical notions of Boundedness and Lagrange stability [2, 4, 5, 6, 9,10] are with respect to the null solution, but ITD Boundedness and Lagrange stability [8,11-18] is with respect to the unperturbed fractional order differential system where the unperturbed fractional order differential system and the unperturbed fractional order differential system differ both in initial position and initial time [8,11-18].

In this paper, we have dissipated this complexity and have a new comparison result which again gives the null solution a central role in the comparison fractional order differential system. This result creates many paths for continuing research by direct application and generalization [15, 17, 18, 19].

In section 2, we present the basic definitions, fundamental lemmata and necessary rudimentary material. In section 3, we have a comparison result in which the stability properties of the null solution of the comparison system imply the corresponding (ITD) Boundedness and Lagrange stability properties of the unperturbed fractional order differential system with respect to the unperturbed fractional order differential system.

## 2 Preliminaries

In this section we give relation among the fractional order derivatives; Caputo, Reimann-Liouville and Grünwald-Letnikov fractional order derivatives, necessary definition of initial value problems of fractional order differential equations with these sense and a comparison result for Lyapunov-like functions.

### 2.1 Fractional Order Derivatives: Caputo, Reimann-Liouville and Grünwald-Letnikov

Caputo's and Reimann-Liouville's definition of fractional derivatives, namely,

$${}^c D^q x = \frac{1}{\Gamma(1-q)} \int_{\tau_0}^t (t-s)^{-q} x'(s) ds, \quad \tau_0 \leq t \leq T \quad (2.1.1)$$

$$D^q x = \frac{1}{\Gamma(p)} \left( \frac{d}{dt} \int_{\tau_0}^t (t-s)^{p-1} x(s) ds \right), \quad \tau_0 \leq t \leq T \quad (2.1.2)$$

respectively order of  $0 < q < 1$ , and  $p + q = 1$  where  $\Gamma$  denotes the Gamma function.

Fractional derivatives and integrals play an important role in the development of theory of fractional dynamical systems [4, 7, 10] Using of half-order derivatives and integrals leads to a formulation of certain real world problems in different areas.[3, 11] Fractional derivatives and integrals are also useful in pure mathematics and in applications outside mathematics include such otherwise unrelated topics as: transmission line theory, chemical analysis of aqueous solutions, design of heat-flux meters, rheology of soils, growth of intergranular grooves at metal surfaces, quantum mechanical calculations, and dissemination of atmospheric pollutants.

The main advantage of Caputo's approach is that the initial conditions for fractional order differential equations with Caputo derivative take on the same form as that of ordinary differential equations with integer derivatives. Another difference is that the Caputo derivative for a constant  $C$  is zero, while the Riemann-Liouville fractional derivative for a constant  $C$  is not zero but equals to  $D^q C = \frac{C(t-\tau_0)^{-q}}{\Gamma(1-q)}$ . By using (2.1.1) and therefore,

$${}^c D^q x(t) = D^q [x(t) - x(\tau_0)] \quad (2.1.3)$$

and

$${}^c D^q x(t) = D^q x(t) - \frac{x(\tau_0)}{\Gamma(1-q)} (t - \tau_0)^{-q}. \quad (2.1.4)$$

In particular, if  $x(\tau_0) = 0$ , we obtain

$${}^c D^q x(t) = D^q x(t). \quad (2.1.5)$$

Hence, we can see that Caputo's derivative is defined for functions for which Riemann-Liouville fractional order derivative exists.

Let us write that Grünwald-Letnikov's notion of fractional order derivative in a convenient form

$$D_0^q x(t) = \lim_{\substack{h \rightarrow 0 \\ nh = t - \tau_0}} \frac{1}{h^q} [x(t) - S(x, h, r, q)] \quad (2.1.6)$$

where  $S(x, h, r, q) = \sum_{r=1}^n (-1)^{r+1} \binom{q}{r} x(t - rh)$ . If we know that  $x(t)$  is continuous and  $\frac{dx(t)}{dt}$  exist and integrable, then Riemann-Liouville and Grünwald-Letnikov fractional order derivatives are connected by the relation

$$D^q x(t) = D_0^q x(t) = \frac{x(\tau_0) (t - \tau_0)^{-q}}{\Gamma(1-q)} + \int_{\tau_0}^t \frac{(t-s)^{-q}}{\Gamma(1-q)} \frac{d}{ds} x(s) ds. \quad (2.1.7)$$

By using (2.3) implies that we have the relations among the Caputo, Riemann-Liouville and Grünwald-Letnikov fractional derivatives

$${}^c D^q x(t) = D^q [x(t) - x(\tau_0)] = D_0^q [x(t) - x(\tau_0)] = \frac{1}{\Gamma(1-q)} \int_{\tau_0}^t (t-s)^{-q} \frac{dx(s)}{ds} ds. \quad (2.1.8)$$

The foregoing equivalent expressions are very useful in the study of qualitative properties of solutions of fractional differential equations.

## 2.2 Fractional Order Differential Equations with Caputo's Derivative

The main advantage of Caputo's approach to fractional derivative is that the initial values and the notion of solution parallels the IVP of differential equations, where the derivative is of order one, that is the usual derivative. Since no known physical interpretation of initial conditions in Riemann-Liouville's sense [4, 7,10] was available, it was felt the solutions obtained are practically useless. Under natural conditions on  $x(t)$  as  $q \rightarrow n$ , the Caputo's derivative becomes the conventional  $n - th$  derivative of  $x(t)$ , for  $n - 1 < q < n$ .

Consider the initial value problems of the fractional order differential equations with Caputo derivative

$${}^c D^q x = f(t, x), x(t_0) = x_0 \text{ for } t \geq t_0, t_0 \in \mathbb{R}_+ \quad (2.2.1)$$

$${}^c D^q y = f(t, y), y(\tau_0) = y_0 \text{ for } t \geq \tau_0, \tau_0 \in \mathbb{R}_+ \quad (2.2.2)$$

$${}^c D^q \omega = H(t, \omega), \omega(\tau_0) = y_0 - x_0 \text{ for } t \geq \tau_0 \quad (2.2.3)$$

where  $x_0 = \lim_{t \rightarrow t_0} D^{q-1} x(t)$ ,  $y_0 = \lim_{t \rightarrow \tau_0} D^{q-1} y(t)$  and  $y_0 - x_0 = \lim_{t \rightarrow \tau_0} D^{q-1} \omega(t)$  exist and  $f, H \in C[[t_0, \tau_0 + T] \times \mathbb{R}^n, \mathbb{R}^n]$ ; satisfy a local Lipschitz condition on the set  $\mathbb{R}_+ \times S_\rho$ ,  $S_\rho = [x \in \mathbb{R}^n : \|x\| \leq \rho < \infty]$  and  $f(t, 0) = 0$  for  $t \geq 0$ .

We will only give the basic existence and uniqueness result with the Lipschitz condition by using contraction mapping theorem and a weighted norm with Mittag-Leffler function in [7].

**Theorem 2.3.1:** Assume that

- (i)  $f \in C[R, \mathbb{R}^n]$  and bounded by  $M$  on  $R$  where  $R = [(t, x) : t_0 \leq t \leq t_0 + T, \|x - x_0\| \leq b]$ ;
- (ii)  $\|f(t, x) - f(t, y)\| \leq L \|x - y\|$ ,  $L > 0$ ,  $(t, x) \in R$  where the inequalities are componentwise.

Then there exist a unique solution  $x(t) = x(t, t_0, x_0)$  on  $[t_0, t_0 + \alpha]$  for the initial value problem of the fractional order differential equation with Caputo's derivative of (2.2.1) where  $\alpha = \min \left[ T, \left( \frac{b\Gamma(q+1)}{M} \right)^{\frac{1}{q}} \right]$ .

Proof of Theorem 2.3.1, please see in [7].

**Corollary 2.3.1:** Let  $0 < q < 1$ , and  $f : (t_0, t_0 + T) \times S_\rho \rightarrow \mathbb{R}$  be a function such that  $f(t, x) \in L(t_0, t_0 + T)$  for any  $x \in S_\rho$ . If  $x(t) \in L(t_0, t_0 + T)$ , then  $x(t)$  satisfies a.e. the initial value problems of the fractional order differential equations with Caputo's derivative (2.2.1) if, and only if,  $x(t)$  satisfies a.e. the Volterra fractional order integral equation (2.2.4).

Proof of Corollary 2.3.1, please see in [4].

We assume that we have sufficient conditions to the existence and uniqueness of solutions through  $(t_0, x_0)$  and  $(\tau_0, y_0)$ . If  $f \in C[[t_0, t_0 + T] \times \mathbb{R}^n, \mathbb{R}^n]$  and  $x(t) \in C^q[[t_0, T], \mathbb{R}]$  is the solution of (2.2.1), then it also satisfies the Volterra fractional order integral equation

$$x(t) = x_0 + \frac{1}{\Gamma(q)} \int_{t_0}^t (t-s)^{q-1} f(s, x(s)) ds, t_0 \leq t \leq t_0 + T \quad (2.2.4)$$

and that is every solution of (2.2.1) is also a solution of (2.2.4), for detail please see [4].

## 2.3 ITD Boundedness Criteria and Lagrange Stability, Fundamental Lemmata and Lyapunov-like Function

Before we can establish our comparison theorem and Boundedness criteria and Lagrange stability for initial time difference we need to introduce the following definitions of ITD Boundedness and Lagrange stability and Lyapunov-like functions.

**Definition 2.3.1:** The solution  $y(t, \tau_0, y_0)$  of the initial value problems of fractional order differential equation with Caputo's derivative of (2.2.2) through  $(\tau_0, y_0)$  is said to be initial time difference equi-bounded with respect to the solution  $\tilde{x}(t, \tau_0, x_0) = x(t - \eta, t_0, x_0)$ , where  $x(t, t_0, x_0)$  is any solution of the initial value problems of fractional order differential equation with Caputo's derivative of (2.2.1) for  $t \geq \tau_0$ ,  $\tau_0 \in \mathbb{R}_+$  and  $\eta = \tau_0 - t_0 > 0$

if and only if for any  $\alpha > 0$  there exist positive functions  $\beta = \beta(\tau_0, \alpha)$  and  $\gamma = \gamma(\tau_0, \alpha)$  that is continuous in  $\tau_0$  for each  $\alpha$  such that

$$\|y_0 - x_0\| \leq \alpha \text{ and } |\tau_0 - t_0| \leq \gamma \text{ implies } \|y(t, \tau_0, y_0) - x(t - \eta, t_0, x_0)\| < \beta \text{ for } t \geq \tau_0. \quad (2.3.1)$$

If  $\beta$  and  $\gamma$  are independent of  $\tau_0$ , then the solution  $y(t, \tau_0, y_0)$  of the initial value problems of fractional order differential equation with Caputo's derivative of (2.2.2) is initial time difference uniformly equi-bounded with respect to the fractional solution  $x(t - \eta, t_0, x_0)$ .

**Definition 2.3.2:** The solution  $y(t, \tau_0, y_0)$  of the initial value problems of fractional order differential equation with Caputo's derivative of (2.2.2) through  $(\tau_0, y_0)$  is said to be initial time difference quasi-equi asymptotically stable(equi-attractive in the large) with respect to the solution  $\tilde{x}(t, \tau_0, x_0) = x(t - \eta, t_0, x_0)$ , where  $x(t, t_0, x_0)$  is any solution of the initial value problems of fractional order differential equation with Caputo's derivative of (2.2.1) for  $t \geq \tau_0$ ,  $\tau_0 \in \mathbb{R}_+$  and  $\eta = \tau_0 - t_0$  if for each  $\epsilon > 0$  and each  $\alpha > 0$  there exist a positive function  $\gamma = \gamma(\tau_0, \alpha)$  and  $T = T(\tau_0, \epsilon, \alpha) > 0$  a number such that

$$\|y_0 - x_0\| \leq \alpha \text{ and } |\tau_0 - t_0| \leq \gamma \text{ implies } \|y(t, \tau_0, y_0) - x(t - \eta, t_0, x_0)\| < \epsilon \text{ for } t \geq \tau_0 + T. \quad (2.3.2)$$

If  $T$  and  $\gamma$  are independent of  $\tau_0$ , then the solution  $y(t, \tau_0, y_0)$  of the initial value problems of fractional order differential equation with Caputo's derivative of (2.2.2) is initial time difference uniformly quasi-equi asymptotically stable(equi-attractive in the large) with respect to the fractional solution  $x(t - \eta, t_0, x_0)$ .

**Definition 2.3.3:** A function  $\phi(r)$  is said to belong to the class  $\mathcal{K}$  if  $\phi \in C[(0, \rho), \mathbb{R}_+]$ ,  $\phi(0) = 0$ , and  $\phi(r)$  is strictly monotone increasing in  $r$ . It is said to belong to class  $\mathcal{K}_\infty$  if  $\rho = \infty$  and  $\phi(r) \rightarrow \infty$  as  $r \rightarrow \infty$ .

**Definition 2.4.3:** For any Lyapunov-like function  $V(t, x) \in C[\mathbb{R}_+ \times \mathbb{R}^n, \mathbb{R}_+]$  we define the fractional order Dini derivatives in Caputo's sense  ${}^c D_+^q V(t, x)$  and  ${}^c D_-^q V(t, x)$  as follows

$${}^c D_+^q V(t, x) = \lim_{h \rightarrow 0^+} \sup \frac{1}{h^q} [V(t, x) - V(t - h, x - h^q f(t, x))] \quad (2.4.3)$$

$${}^c D_-^q V(t, x) = \lim_{h \rightarrow 0^-} \inf \frac{1}{h^q} [V(t, x) - V(t - h, x - h^q f(t, x))] \quad (2.4.4)$$

for  $(t, x) \in \mathbb{R}_+ \times \mathbb{R}^n$ .

**Definition 2.4.4:** For a real-valued function  $V(t, x) \in C[\mathbb{R}_+ \times \mathbb{R}^n, \mathbb{R}_+]$  we define the generalized fractional order derivatives (Dini-like derivatives) in Caputo's sense  ${}_s^c D_+^q V(t, y - \tilde{x})$  and  ${}_s^c D_-^q V(t, y - \tilde{x})$  as follows

$${}_s^c D_+^q V(t, y - \tilde{x}) = \lim_{h \rightarrow 0^+} \sup \frac{1}{h^q} [V(t, y - \tilde{x}) - V(t - h, y - \tilde{x} - h^q (f(t, y) - \tilde{f}(t, \tilde{x})))] \quad (2.4.5)$$

$${}_s^c D_-^q V(t, y - \tilde{x}) = \lim_{h \rightarrow 0^-} \inf \frac{1}{h^q} [V(t, y - \tilde{x}) - V(t - h, y - \tilde{x} - h^q (f(t, y) - \tilde{f}(t, \tilde{x})))] \quad (2.4.6)$$

for  $(t, x) \in \mathbb{R}_+ \times \mathbb{R}^n$ .

**Lemma 2.3.1:** (See [19]) Let  $f \in C[[t_0, T] \times \mathbb{R}^n, \mathbb{R}^n]$ , and let

$$G(t, r) = \max_{\tilde{x}, y \in \bar{B}(x_0; r)} \|f(t, y) - \tilde{f}(t, \tilde{x})\| \quad (2.3.7)$$

where  $G(t, r) \in C[\mathbb{R}_+ \times \mathbb{R}_+, \mathbb{R}_+]$  and  $\bar{B}$  is closed ball with center at  $x_0$  and radius  $r$ . Assume that  $r^*(t, \tau_0, \|y_0 - x_0\|)$  is the maximal solution of initial value problem of fractional order differential equation with Caputo's derivative  ${}^c D^q u = G(t, u)$ ,  $u(\tau_0) = \|y_0 - x_0\|$  through  $(\tau_0, \|y_0 - x_0\|)$ .  $\tilde{x}(t, \tau_0, x_0) = x(t - \eta, t_0, x_0)$  where  $x(t, t_0, x_0)$  is any solution of fractional order differential equation of (2.3.1) for  $t \geq \tau_0 \geq 0$ ,  $t_0 \in \mathbb{R}_+$  and  $\eta = \tau_0 - t_0$  and  $y(t, \tau_0, y_0)$  is the solution of fractional order differential equation (2.3.2) with Caputo's derivatives. Then

$$\|y(t, \tau_0, y_0) - x(t - \eta, t_0, x_0)\| \leq r^*(t, \tau_0, \|y_0 - x_0\|) \text{ for } t \geq \tau_0.$$

**Lemma 2.3.2:** (See [19]) Let  $V(t, z) \in C[\mathbb{R}_+ \times \mathbb{R}^n, \mathbb{R}_+]$  and  $V(t, z)$  be locally Lipschitzian in  $z$ . Assume that the generalized fractional order derivatives (Dini-like derivatives) in Caputo's sense

$${}_s^c D_+^q V(t, y - \tilde{x}) = \lim_{h \rightarrow 0^+} \sup \frac{1}{h^q} [V(t, y - \tilde{x}) - V(t - h, y - \tilde{x} - h^q (f(t, y) - \tilde{f}(t, \tilde{x})))] \quad (2.3.8)$$

satisfies  ${}^c D_+^q V(t, y - \tilde{x}) \leq G(t, V(t, y - \tilde{x}))$  with  $(t, \tilde{x}), (t, y) \in \mathbb{R}_+ \times \mathbb{R}^n$ , where  $G(t, u) \in C[\mathbb{R}_+ \times \mathbb{R}_+, \mathbb{R}]$ . Let  $r(t) = r(t, \tau_0, u_0)$  be the maximal solution of the fractional order differential equation  ${}^c D^q u = G(t, u), u(\tau_0) = u_0 \geq 0$ , for  $t \geq \tau_0$ . If  $\tilde{x}(t) = x(t - \eta, t_0, x_0)$  where  $x(t, t_0, x_0)$  is any solution of the system (2.2.1) for  $t \geq \tau_0 \geq 0$ ,  $t_0 \in \mathbb{R}_+$  and  $\eta = \tau_0 - t_0$  and  $y(t) = y(t, \tau_0, y_0)$  is any solution of (2.2.2) for  $t \geq \tau_0$  such that  $V(\tau_0, y_0 - x_0) \leq u_0$  then  $V(t, y(t) - \tilde{x}(t)) \leq r(t)$  for  $t \geq \tau_0$ .

### 3 Initial Time Difference Fractional Comparison Results

In order to have this result we need to use these two Lemmas in [19]

In this section, we have an other comparison result in which the boundedness and Lagrange Stability properties of the null solution of the comparison system imply the corresponding initial time difference boundedness and Lagrange Stability properties of the perturbed fractional order differential system in Caputo's sense with respect to the unperturbed fractional order differential system in Caputo's sense.

#### 3.1 ITD Boundedness Criteria and Lagrange Stability

**Theorem 3.1.1:** Assume that

(i) Let  $V(t, z) \in C[\mathbb{R}_+ \times \mathbb{R}^n, \mathbb{R}_+]$  be locally Lipschitzian in  $z$ , positive definite and decrescent where the fractional order Dini derivatives in Caputo's sense  ${}^c D_+^q m(t)$

$${}^c D_+^q m(t) \leq \lim_{h \rightarrow 0^+} \sup \frac{1}{h^q} [V(t, y - \tilde{x}) - V(t - h, (y - \tilde{x}) - h^q(f(t, y) - \tilde{f}(t, \tilde{x})))]$$

satisfies  ${}^c D_+^q V(t, y - \tilde{x}) \leq G(t, V(t, y - \tilde{x}))$  for  $(t, \tilde{x})$  and  $(t, y) \in \mathbb{R}_+ \times \mathbb{R}^n$ , where  $G(t, u) \in C[\mathbb{R}_+ \times \mathbb{R}_+, \mathbb{R}]$  and the generalized fractional order (Dini-like) derivatives in Caputo's sense  ${}^c D_+^q V(t, x)$ ,

(ii) Let  $V(t, x)$  be positivedefinite such that

$$b(\|x\|) \leq V(t, x) \text{ with } (t, x) \in \mathbb{R}_+ \times \mathbb{R}^n \quad (3.1.1)$$

and  $b \in \mathcal{K}$ .  $b(u) \rightarrow \infty$  as  $u \rightarrow \infty$  on the interval  $0 \leq u < \infty$ ;

(iii) Let  $r(t) = r(t, \tau_0, u_0)$  be the maximal solution of the fractional order differential equation with Caputo's derivative

$${}^c D^q u = G(t, u), \quad u(\tau_0) = u_0 \geq 0 \text{ for } t \geq \tau_0. \quad (3.1.2)$$

Then the initial time difference boundedness properties of the null solution of the fractional order differential system with Caputo's derivative (3.1.2) with  $G(t, 0) = 0$  imply the corresponding stability properties of  $y(t, \tau_0, y_0)$  any solution of fractional order differential system with Caputo's derivative (2.2.2) with respect to  $\tilde{x}(t, \tau_0, x_0) = x(t - \eta, t_0, x_0)$  where  $x(t, t_0, x_0)$  is any solution of fractional order differential system with Caputo's derivative of (2.2.1).

**Proof:** Let  $\alpha > 0$  and  $\tau_0 \in \mathbb{R}_+$  be given, and let  $\|y_0 - x_0\| \leq \alpha$  and  $|\tau_0 - t_0| \leq \gamma$  for  $\gamma(\tau_0, \alpha) > 0$ . In view of the hypotheses on  $V(t, x)$ , there exists a number  $\alpha_1 = \alpha_1(\tau_0, \alpha) > 0$  satisfying the inequalities

$$\|y_0 - x_0\| \leq \alpha \text{ and } |\tau_0 - t_0| \leq \gamma, \quad V(\tau_0, y_0 - x_0) \leq \alpha_1$$

together. Assume that comparison system (3.1.2) is equibounded. Then, given  $\alpha_1 > 0$  and  $\tau_0 \in \mathbb{R}_+$  there exist a  $\beta_1 = \beta_1(\tau_0, \alpha) > 0$  that is continues in  $\tau_0$  for each  $\alpha$  such that

$$r(t, \tau_0, u_0) < \beta_1 \text{ provided } u_0 \leq \alpha_1. \quad (3.1.3)$$

Moreover, as  $b(u) \rightarrow \infty$  as  $u \rightarrow \infty$ , we can choose a  $L = L(\tau_0, \alpha)$  verifying the relation

$$b(L) \geq \beta_1(\tau_0, \alpha) \quad (3.1.4)$$

now let  $u_0 = V(\tau_0, y_0 - x_0)$ . Then assumption (i) and Lemma 2.3.2 show that

$$V(t, y(t, \tau_0, y_0) - x(t - \eta, t_0, x_0)) \leq r(t, \tau_0, u_0), \quad t \geq \tau_0 \quad (3.1.5)$$

where  $r(t, \tau_0, u_0)$  is the maximal solution of comparison equation (3.1.2). Suppose, if possible, that there is a solution of system (2.2.3)  $\omega(t, \tau_0, w_0) = y(t, \tau_0, y_0) - x(t - \eta, t_0, x_0)$  for  $t \geq \tau_0$  with  $\|y_0 - x_0\| \leq \alpha$  and  $|\tau_0 - t_0| \leq \gamma$  having the property that, for some  $t_1 > \tau_0$ ,  $\|y(t_1, \tau_0, y_0) - \tilde{x}(t_1, \tau_0, x_0)\| = L$ . Then because of relations (3.1.1), (3.1.3), (3.1.4) and (3.1.5), there results oddity

$$b(L) \leq V(t_1, y(t_1, \tau_0, y_0) - x(t_1, \tau_0, x_0)) \leq r(t_1, \tau_0, u_0) < \beta_1(\tau_0, \alpha) \leq b(L)$$

then

$$\|y(t, \tau_0, y_0) - \tilde{x}(t, \tau_0, x_0)\| < L(\tau_0, \alpha) \text{ provided } \|y_0 - x_0\| \leq \alpha \text{ and } |\tau_0 - t_0| \leq \gamma.$$

These completes the proof.

**Theorem 3.1.2:** Let the assumption of Theorem 3.1.1 holds. Then the initial time difference quasi-equi asymptotically stable (equi-attractive in the large) properties of the null solution of the fractional order differential system with Caputo's derivative (3.1.2) with  $G(t, 0) = 0$  imply the corresponding initial time difference quasi-equi asymptotically stable properties of  $y(t, \tau_0, y_0)$  any solution of fractional order differential system with Caputo's derivative (2.2.2) with respect to  $\tilde{x}(t, \tau_0, x_0) = x(t - \eta, t_0, x_0)$  where  $x(t, t_0, x_0)$  is any solution of fractional order differential system with Caputo's derivative of (2.2.1).

**Proof:** We want to prove the theorem by considering Definition 2.3.2

Let  $\epsilon > 0, \alpha \geq 0$  and  $\tau_0 \in \mathbb{R}_+$  be given and let  $\|y_0 - x_0\| \leq \alpha$  and  $|\tau_0 - t_0| \leq \gamma$  for  $\gamma(\tau_0, \alpha) > 0$ . As in the proof in theorem (3.1.1), there exists a  $\alpha_1 = \alpha_1(\tau_0, \alpha)$  satisfying

$$\|y_0 - x_0\| \leq \alpha, V(\tau_0, y_0 - x_0) \leq \alpha_1$$

simultaneously. Since for comparison system (3.1.2) is quasi-equi asymptotically stable (equi-attractive in the large). Then, given  $\alpha_1 \geq 0, b(\epsilon)$  and  $\tau_0 \in \mathbb{R}_+$  there exist a  $T = T(\tau_0, \alpha, \epsilon)$  such that

$$\|u_0\| \leq \alpha_1 \text{ implies } r(t, \tau_0, u_0) < b(\epsilon), \text{ for } t \geq \tau_0 + T. \quad (3.1.6)$$

Choose  $u_0 = V(\tau_0, y_0 - x_0)$ . Then assumption (i) and Lemma 2.3.2 show that

$$V(t, y(t, \tau_0, y_0) - x(t - \eta, t_0, x_0)) \leq r(t, \tau_0, u_0), t \geq \tau_0. \quad (3.1.7)$$

If possible, let there exist a sequence  $\{t_k\}$ ,

$$t_k \geq \tau_0 + T, t_k \rightarrow \infty \text{ as } k \rightarrow \infty$$

such that, for some solution of system (2.2.3)  $\omega(t, \tau_0, w_0) = y(t, \tau_0, y_0) - x(t - \eta, t_0, x_0)$  for  $t \geq \tau_0$  with  $\|y_0 - x_0\| \leq \alpha$  and  $|\tau_0 - t_0| \leq \gamma$  for  $\gamma(\tau_0, \alpha) > 0$  we have

$$\|y(t, \tau_0, y_0) - \tilde{x}(t, \tau_0, x_0)\| \geq \epsilon$$

this implies, in view of the inequalities (3.1.1), (3.1.6) and (3.1.7)

$$b(\epsilon) \leq V(t_k, y(t_k, \tau_0, y_0) - x(t_k, \tau_0, x_0)) \leq r(t_k, \tau_0, u_0) < b(\epsilon)$$

which proves

$$\|y(t, \tau_0, y_0) - \tilde{x}(t, \tau_0, x_0)\| < \epsilon \text{ for } t \geq \tau_0 + T(\tau_0, \epsilon, \alpha) \text{ provided } \|y_0 - x_0\| \leq \alpha \text{ and } |\tau_0 - t_0| \leq \gamma \text{ for } \gamma(\tau_0, \alpha) > 0.$$

Therefore, these completes the proof.

**Theorem 3.1.3:** Let the assumption of Theorem 3.1.1 holds as

(i) Let  $V(t, z) \in C[\mathbb{R}_+ \times \mathbb{R}^n, \mathbb{R}_+]$  be locally Lipschitzian in  $z$ , positive definite and decrescent where the fractional order Dini derivatives in Caputo's sense  ${}^c D_+^q m(t)$

$${}^c D_+^q m(t) \leq \lim_{h \rightarrow 0^+} \sup \frac{1}{h^q} [V(t, y - \tilde{x}) - V(t - h, (y - \tilde{x}) - h^q(f(t, y) - \tilde{f}(t, \tilde{x})))]$$

satisfies  ${}^c D_+^q V(t, y - \tilde{x}) \leq G(t, V(t, y - \tilde{x}))$  for  $(t, \tilde{x})$  and  $(t, y) \in \mathbb{R}_+ \times \mathbb{R}^n$ , where  $G(t, u) \in C[\mathbb{R}_+ \times \mathbb{R}_+, \mathbb{R}]$  and the generalized fractional order (Dini-like) derivatives in Caputo's sense  ${}^c D_+^q V(t, x)$ ;



(ii) Let  $V(t, x)$  be positive definite such that

$$b(\|x\|) \leq V(t, x) \text{ with } (t, x) \in \mathbb{R}_+ \times \mathbb{R}^n$$

and  $b \in \mathcal{K}$ .  $b(u) \rightarrow \infty$  as  $u \rightarrow \infty$  on the interval  $0 \leq u < \infty$ ;

(iii) Let  $r(t) = r(t, \tau_0, u_0)$  be the maximal solution of the fractional order differential equation with Caputo's derivative

$${}^c D^q u = G(t, u), \quad u(\tau_0) = u_0 \geq 0 \text{ for } t \geq \tau_0.$$

Then the initial time difference Boundedness and Lagrange stability properties of the null solution of the fractional order differential system with Caputo's derivative (3.1.2) with  $G(t, 0) = 0$  imply the corresponding stability properties of  $y(t, \tau_0, y_0)$  any solution of fractional order differential system with Caputo's derivative (2.2.2) with respect to  $\tilde{x}(t, \tau_0, x_0) = x(t - \eta, t_0, x_0)$  where  $x(t, t_0, x_0)$  is any solution of fractional order differential system with Caputo's derivative of (2.2.1).

**Proof:** We know that equi-Lagrange stability requires the equi-boundedness and equi-attractive in the large. We proved in Theorem 3.1.1 and Theorem 3.1.2, respectively. Then the proof of Theorem 3.1.3 is complete.

### 3.2 ITD Uniformly Boundedness Criteria and Lagrange Stability

**Theorem 3.2.1:** Assume that the assumptions of Theorem 3.1.1 holds. In addition to hypotheses of Theorem 3.1.1, let  $V(t, x)$  verify the inequality

$$V(t, x) \leq a(\|x\|) \text{ with } (t, x) \in \mathbb{R}_+ \times \mathbb{R}^n \quad (3.2.1)$$

where,  $a \in \mathcal{K}$ .  $a(u) \rightarrow \infty$  as  $u \rightarrow \infty$  on the interval  $0 \leq u < \infty$ .

Then, if fractional order comparison system (3.1.2) is uniformly bounded, the solution  $y(t, \tau_0, y_0)$  of (2.2.2) through  $(\tau_0, y_0)$  is initial time difference uniformly bounded for  $t \geq \tau_0 \in \mathbb{R}_+$  with respect to the solution  $x(t - \eta, t_0, x_0)$  of (2.2.1) through  $(t_0, x_0)$  where  $x(t, t_0, x_0)$  is the solution of (2.2.1) through  $(t_0, x_0)$ .

**Proof:** Let  $\alpha > 0$  and  $\tau_0 \in \mathbb{R}_+$  be given, and let  $\|y_0 - x_0\| \leq \alpha$  and  $|\tau_0 - t_0| \leq \gamma$  for  $\gamma(\tau_0, \alpha) > 0$ . In view of the hypotheses on  $V(t, x)$ , there exists a number  $\alpha_1 = a(\alpha) > 0$  satisfying the inequalities

$$\|y_0 - x_0\| \leq \alpha, \quad V(\tau_0, y_0 - x_0) \leq \alpha_1 = a(\alpha)$$

together. Assume that fractional order comparison system (3.1.2) is uniformly equibounded. Then, given  $\alpha_1 > 0$  and  $\tau_0 \in \mathbb{R}_+$  there exist a  $\beta_1 = \beta_1(\alpha) > 0$  that is continues in  $\tau_0$  for each  $\alpha$  such that

$$r(t, \tau_0, u_0) < \beta_1 \text{ provided } u_0 \leq \alpha_1 \text{ (}\beta_1 \text{ and } \alpha_1 \text{ are independent of } \tau_0\text{)}. \quad (3.2.2)$$

Moreover,  $b(u) \rightarrow \infty$  as  $u \rightarrow \infty$ , we can choose a  $L = L(\alpha)$  verifying the relation

$$b(L) \geq \beta_1(\alpha) \quad (3.2.3)$$

now let  $u_0 = V(\tau_0, y_0 - x_0)$ . Then assumption (i) and Lemma 2.3.2 show that

$$V(t, y(t, \tau_0, y_0) - x(t - \eta, t_0, x_0)) \leq r(t, \tau_0, u_0), \quad t \geq \tau_0$$

where  $r(t, \tau_0, u_0)$  is the maximal solution of comparison equation (3.1.2). Suppose, if possible, that there is a solution of system (2.2.4)  $\omega(t, \tau_0, w_0) = y(t, \tau_0, y_0) - x(t - \eta, t_0, x_0)$  for  $t \geq \tau_0$  with  $\|y_0 - x_0\| \leq \alpha$  and  $|\tau_0 - t_0| \leq \gamma$  having the property that, for some  $t_1 > \tau_0$ ,

$$\|y(t, \tau_0, y_0) - \tilde{x}(t, \tau_0, x_0)\| = L$$

is independent of  $\tau_0$ . Then because of relations (3.1.1), (3.1.5), (3.2.2) and (3.2.3), there results contradiction

$$b(L) \leq V(t_1, y(t_1, \tau_0, y_0) - \tilde{x}(t_1, \tau_0, x_0)) \leq r(t_1, \tau_0, u_0) < \beta_1(\alpha) \leq b(L).$$

Therefore,

$$\|y(t, \tau_0, y_0) - \tilde{x}(t, \tau_0, x_0)\| < L(\alpha) \text{ provided } \|y_0 - x_0\| \leq \alpha \text{ and } |\tau_0 - t_0| \leq \gamma \text{ for } t \geq \tau_0.$$

These completes the proof.

**Theorem 3.2.2:** Assume that the assumptions of Theorem 3.2.1 holds. Then, if fractional order comparison system (3.1.2) is uniformly quasi-equi asymptotically stable (equi-attractive in the large), the solution  $y(t, \tau_0, y_0)$  of (2.2.3) through  $(\tau_0, y_0)$  is initial time difference uniformly quasi-equi asymptotically stable (equi-attractive in the large) for  $t \geq \tau_0 \in \mathbb{R}_+$  with respect to the solution  $x(t - \eta, t_0, x_0)$  of (2.2.1) through  $(t_0, x_0)$  where  $x(t, t_0, x_0)$  is the solution of (2.2.1) through  $(t_0, x_0)$ .

**Proof:** We want to prove the theorem by considering Definition 3.3.2 as independent of  $\tau_0$ . Let  $\epsilon > 0$ ,  $\alpha > 0$  and  $\tau_0 \in \mathbb{R}_+$  be given and let  $\|y_0 - x_0\| \leq \alpha$  and  $|\tau_0 - t_0| \leq \gamma$  for  $\gamma(\tau_0, \alpha) > 0$ . As in the preceding proof, there exists a  $\alpha_1 = a(\alpha)$  satisfying

$$\|y_0 - x_0\| \leq \alpha, \quad V(\tau_0, y_0 - x_0) \leq \alpha_1$$

simultaneously. Since for comparison system (3.1.2) is equi-attractive in the large. Then, given  $\alpha_1 > 0$ ,  $b(\epsilon) > 0$  and  $\tau_0 \in \mathbb{R}_+$  there exist a  $T = T(\alpha, \epsilon)$  such that

$$\|u_0\| \leq \alpha_1 \text{ implies } r(t, \tau_0, u_0) < b(\epsilon) \text{ for } t \geq \tau_0 + T. \quad (3.2.4)$$

Choose  $u_0 = V(\tau_0, y_0 - x_0)$ . Then assumption (i) and Lemma 2.3.2 show that

$$V(t, y(t, \tau_0, y_0) - x(t - \eta, t_0, x_0)) \leq r(t, \tau_0, u_0), \quad t \geq \tau_0.$$

If possible, let there exist a sequence  $\{t_k\}$ ,

$$t_k \geq \tau_0 + T, t_k \rightarrow \infty \text{ as } k \rightarrow \infty$$

such that, for some solution of system (2.2.3)  $\omega(t, \tau_0, w_0) = y(t, \tau_0, y_0) - x(t - \eta, t_0, x_0)$  for  $t \geq \tau_0$  with  $\|y_0 - x_0\| \leq \alpha$  we have

$$\|y(t, \tau_0, y_0) - \tilde{x}(t, \tau_0, x_0)\| \geq \epsilon$$

this implies, in view of the inequalities (3.1.1), (3.1.5) and (3.2.4), we obtain

$$b(\epsilon) \leq V(t_k, y(t_k, \tau_0, y_0) - x(t_k, \tau_0, x_0)) \leq r(t_k, \tau_0, u_0) < b(\epsilon)$$

which proves

$$\|y(t, \tau_0, y_0) - \tilde{x}(t, \tau_0, x_0)\| < \epsilon \text{ provided } \|y_0 - x_0\| \leq \alpha \text{ and } |\tau_0 - t_0| \leq \gamma \text{ for } t \geq \tau_0 + T(\epsilon, \alpha).$$

Therefore, these completes the proof.

**Theorem 3.2.3:** Assume that

(i) Let  $V(t, z) \in C[\mathbb{R}_+ \times \mathbb{R}^n, \mathbb{R}_+]$  be locally Lipschitzian in  $z$ , positive definite and decrescent where the fractional order Dini derivatives in Caputo's sense  ${}^c D_+^q m(t)$

$${}^c D_+^q m(t) \leq \lim_{h \rightarrow 0^+} \sup \frac{1}{h^q} [V(t, y - \tilde{x}) - V(t - h, (y - \tilde{x}) - h^q(f(t, y) - \tilde{f}(t, \tilde{x})))]$$

satisfies  ${}^c D_+^q V(t, y - \tilde{x}) \leq G(t, V(t, y - \tilde{x}))$  for  $(t, \tilde{x})$  and  $(t, y) \in \mathbb{R}_+ \times \mathbb{R}^n$ , where  $G(t, u) \in C[\mathbb{R}_+ \times \mathbb{R}_+, \mathbb{R}]$  and the generalized fractional order (Dini-like) derivatives in Caputo's sense  ${}^c D_+^q V(t, x)$ ;

(ii) Let  $V(t, x)$  be positive definite such that

$$b(\|x\|) \leq V(t, x) \leq a(\|x\|) \text{ with } (t, x) \in \mathbb{R}_+ \times \mathbb{R}^n \quad (3.2.5)$$

and  $a, b \in \mathcal{K}$ .  $b(u) \rightarrow \infty$  as  $u \rightarrow \infty$  on the interval  $0 \leq u < \infty$  and  $a(u) \rightarrow \infty$  as  $u \rightarrow \infty$  on the interval  $0 \leq u < \infty$ ;

(iii) Let  $r(t) = r(t, \tau_0, u_0)$  be the maximal solution of the fractional order differential equation with Caputo's derivative

$${}^c D^q u = G(t, u), \quad u(\tau_0) = u_0 \geq 0 \text{ for } t \geq \tau_0.$$

Then the uniform-Lagrange stability properties of the null solution of the fractional order differential system with Caputo's derivative (3.1.2) with  $G(t, 0) = 0$  imply the corresponding uniform-Lagrange properties of  $y(t, \tau_0, y_0)$  any solution of fractional order differential system with Caputo's derivative (2.2.2) with respect to

$\tilde{x}(t, \tau_0, x_0) = x(t - \eta, t_0, x_0)$  where  $x(t, t_0, x_0)$  is any solution of fractional order differential system with Caputo's derivative of (2.2.1).

**Proof:** By using the Theorem 3.2.1 and the Theorem 3.2.2 we have that the uniform boundedness and uniform attractive in the large of comparison system (3.1.2) imply the corresponding uniform boundedness and uniform attractive in the large of  $y(t, \tau_0, y_0)$  of perturbed differential system of (2.2.2) that differs in initial position and initial time with respect to the solution  $x(t - \eta, t_0, x_0)$ , where  $x(t, t_0, x_0)$  is any solution of the unperturbed differential system of (2.2.1). These completes the proof. ■

#### Acknowledgements

This work has been supported by The Scientific and Technological Research Council of Turkey and Yeditepe University Department of Mathematics.

## References

- [1] Caputo, M. , Linear models of dissipation whose Q is almost independent, II, Geophy. J. Roy. Astronom. **13** (1967) 529–539.
- [2] Brauer, F. and Nohel, J., *The Qualitative Theory of Ordinary Differential Equations*, W.A. Benjamin, Inc., New York **1969**.
- [3] Oldham, K. B. and Spanier, J., *The Fractional Calculus*, Academic Press, New York, 1974.
- [4] Kilbas, A. A., Srivastava, H. M., Trujillo, J. J. *Theory and Applications of Fractional Differential Equations*, Amsterdam, The Netherlands, **2006**.
- [5] Lakshmikantham, V. and Leela, S., *Differential and Integral Inequalities*, Vol. **1**, Academic Press, New York **1969**.
- [6] Lakshmikantham, V., Leela, S. and Martynyuk, A.A., *Stability Analysis of Nonlinear Systems*, Marcel Dekker, New York **1989**.
- [7] Lakshmikantham, V. Leela, S. and Vasundhara Devi, J. *Theory of Fractional Dynamical Systems*, Cambridge Scientific Publishers **2009**.
- [8] Lakshmikantham, V. and Vatsala, A.S., Differential inequalities with time difference and application, Journal of Inequalities and Applications **3**, (1999) 233-244.
- [9] Lakshmikanthama, V. and Vatsala, A.S. Basic theory of fractional differential equations. Nonlinear Analysis **69** (2008) 2677–2682
- [10] Podlubny, I., *Fractional Differential Equations*, Acad. Press, New York **1999**.
- [11] Samko, S., Kilbas, A. and Marichev, O. *Fractional Integrals and Derivatives : Theory and Applications*, Gordon and Breach, 1993, 1006 pages, ISBN 2881248640.
- [12] Shaw, M.D. and Yakar, C., Generalized variation of parameters with initial time difference and a comparison result in term Lyapunov-like functions, International Journal of Non-linear Differential Equations-Theory Methods and Applications **5**, (1999) 86-108.
- [13] Shaw, M.D. and Yakar, C., Stability criteria and slowly growing motions with initial time difference, Problems of Nonlinear Analysis in Engineering Systems **1**, (2000) 50-66.
- [14] Yakar, C. Boundedness Criteria in Terms of Two Measures with Initial Time Difference. Dynamics of Continuous, Discrete and Impulsive Systems. Series A: Mathematical Analysis. Watam Press. Waterloo. Page: 270-275. DCDIS 14 (S2) 1-305 (2007).
- [15] Yakar C., Strict Stability Criteria of Perturbed Systems with respect to Unperturbed Systems in term of Initial Time Difference. Proceedings of the Conference on Complex Analysis and Potential Theory. World Scientific Publishing. Page: 239-248 (2007).
- [16] Yakar C. and Shaw, M.D., A Comparison Result and Lyapunov Stability Criteria with Initial Time Difference. Dynamics of Continuous, Discrete and Impulsive Systems. A: Mathematical Analysis. Volume 12, Number 6 (2005) (731-741).
- [17] Yakar C. and Shaw, M.D., Initial Time Difference Stability in Terms of Two Measures and Variational Comparison Result. Dynamics of Continuous, Discrete and Impulsive Systems. Series A: Mathematical Analysis 15 (2008) 417-425.
- [18] Yakar C. and Shaw, M.D., Practical stability in terms of two measures with initial time difference. Nonlinear Analysis: Theory, Methods & Applications. Vol. 71 (2009) e781-e785.
- [19] Yakar C., Fractional Differential Equations in Terms of Comparison Results and Lyapunov Stability with Initial Time Difference. Abstract and Applied Analysis. Vol 3., Article ID 762857, 16 pages doi:10.1155/2010/762857. (2010)

# Monotone Technique in Terms of Two Monotone Functions in Finite System

Coşkun YAKAR, Bircan BAL and Ali YAKAR

Department of Mathematics, Gebze Institute of Technology

Gebze, KOCAELI 141-41400 TURKEY

E-mail: cyakar@gyte.edu.tr, bircanbal@hotmail.com, ali\_yakar@hotmail.com

**Abstract.** In this paper, we have investigated the monotone iterative technique that is used to obtain the minimal and maximal quasisolution for the first order initial value problem in finite systems assuming that right hand side of the equation is the sum of two distinct monotone functions.

**AMS (MOS) Mathematics Subject Classification Codes (2000).** 34A12, 34A25, 34A34, 34A45.

**Key Words and Phrases:** Coupled lower and upper quasisolution, coupled minimal and maximal quasisolution, coupled quasisolution, monotone functions.

## 1 Introduction

The original method of monotone iterative techniques provides an explicit analytic representation for the solution of nonlinear differential equations, which yields pointwise upper and lower estimates for the solution of the problem whenever the functions involved are monotone nondecreasing and nonincreasing [1, 3]. The most important applications of this method has been applied to obtain a sequence of lower bounds which are the solutions of linear differential equations that converge uniformly and monotonically [1, 3]. As a result, the method has been popular in applied areas [3, 4]. Recently [1], this method has been generalized, refined and extended in several directions so as to be applicable to a much larger class of nonlinear problems by demanding monotonicity property. Moreover, other possibilities have been explored which make the method of monotone iterative techniques universally useful and fruitful in applications [3].

In this paper, the monotone iterative technique is extended to finite systems assuming that right hand side is sum of two monotone functions. This technique used to obtain upper and lower sequences in terms of the solution of linear differential equations and bound the coupled quasisolutions of a given nonlinear differential equation. It is also shown that these sequences converge to the coupled quasisolution of the nonlinear equation uniformly and monotonically.

## 2 Basic Definitions and Theorems

In this section we will give some basic definition and Theorems which are very useful to use our future references.

We consider the differential system

$$u' = f(t, u), \quad u(t_0) = u_0 \quad (2.1)$$

where  $f \in C[J \times \mathbb{R}^n, \mathbb{R}^n]$  and  $J = [t_0, t_0 + T]$ .

**Definition 2.1:** A function  $f \in C[J \times \mathbb{R}^n, \mathbb{R}^n]$  is said to be quasimonotone nondecreasing (nonincreasing) if, for some  $i$  such that  $1 \leq i \leq n$ ,  $u \leq v$  and  $u_i = v_i$ ,  $f_i(t, u) \leq f_i(t, v)$ , ( $f_i(t, u) \geq f_i(t, v)$ ) for  $t \in J$ .

**Definition 2.2:** A function  $f \in C[J \times \mathbb{R}^n, \mathbb{R}^n]$  is said to possess mixed quasimonotone property if for each  $i$  such that  $1 \leq i \leq n$ ,  $f_i(t, u_i, [u]_{p_i}, [u]_{q_i})$  is monotone nondecreasing in  $[u]_{p_i}$  and monotone nonincreasing in  $[u]_{q_i}$  where  $p_i + q_i = n - 1$ .

Let us consider the initial value problem as follows

$$u' = f(t, u) + g(t, u), \quad u(t_0) = u_0 \quad (2.2)$$

where  $f, g \in C[J \times \mathbb{R}^n, \mathbb{R}^n]$ .

**Definition 2.3:** The functions  $\alpha, \beta \in C^1[J, \mathbb{R}^n]$ ,  $t_0, T > 0$  are said to be coupled lower and upper solutions of (2.2) if  $\alpha$  and  $\beta$  satisfy the differential inequalities

$$\alpha' \leq f(t, \beta(t)) + g(t, \alpha(t)), \alpha(t_0) \leq u_0 \quad (2.3)$$

$$\beta' \geq f(t, \alpha(t)) + g(t, \beta(t)), \beta(t_0) \geq u_0. \quad (2.4)$$

The following Theorem 2.1 is an extension of [3, Theorem 1.1.1] to systems. Please see [3] for the proof of the following Theorems.

**Theorem 2.1:** Let  $v, w \in C^1[J, \mathbb{R}^n]$  be lower and upper solutions of (2.1) respectively. Suppose that  $f$  is quasimonotone nondecreasing and for each  $i$

$$f_i(t, x_1, \dots, x_n) - f_i(t, y_1, \dots, y_n) \leq L_i \sum_{i=1}^n (x_i - y_i) \quad (2.5)$$

whenever  $x \geq y$  and  $L_i > 0$ ,  $t \in J$ . Then  $v(t_0) \leq w(t_0)$  implies  $v(t) \leq w(t)$  on  $J$ .

**Theorem 2.2:** Let  $v, w \in C^1[J, \mathbb{R}^n]$  be lower and upper solutions of (2.1) such that  $v(t) \leq w(t)$  on  $J$  and let  $f \in C[\Omega, \mathbb{R}^n]$  where

$$\Omega = \{(t, u) \in J \times \mathbb{R}^n : v(t) \leq u(t) \leq w(t)\}$$

then there exists a solution  $u$  of (2.1) such that  $v(t) \leq u(t) \leq w(t)$  on  $J$  provided  $v(t_0) \leq u(t_0) \leq w(t_0)$ .

**Theorem 2.3:** Let us consider the initial value problem as follows

$$u'_i = f_i(t, u_i, [u]_{p_i}, [u]_{q_i}), \quad u(t_0) = u_0 \quad (2.6)$$

$f \in C[J \times \mathbb{R}^n, \mathbb{R}^n]$  possess mixed quasimonotone property and let  $v_0, w_0$  be coupled lower and upper quasisolutions of system (2.6) such that  $v_0 \leq w_0$  on  $J$ . Suppose further that

$$f_i(t, u_i, [u]_{p_i}, [u]_{q_i}) - f_i(t, \bar{u}_i, [u]_{p_i}, [u]_{q_i}) \geq -M_i(t)(u_i - \bar{u}_i) \quad (2.7)$$

whenever  $v_0 \leq u \leq w_0$  and for each  $i = 1, 2, \dots, n$ ,  $v_{0i} \leq \bar{u}_i \leq u_i \leq w_{0i}$  and  $M_i \geq 0$ . Then there exist monotone sequences  $\{v_n\}$ ,  $\{w_n\}$  such that  $v_n \rightarrow v$ ,  $w_n \rightarrow w$  as  $n \rightarrow \infty$  uniformly and monotonically to coupled minimal and maximal quasisolutions of (2.6) on  $J$  provided  $v_0(t_0) \leq u_0 \leq w_0(t_0)$ . Further if  $u$  is any solution of (2.6) such that  $v_0 \leq u \leq w_0$  then  $v \leq u \leq w$  on  $J$ .

**Theorem 2.4:** Let  $\alpha, \beta \in C^1[J, \mathbb{R}^n]$  be coupled lower and upper solutions of (2.2) respectively. Suppose that  $f$  is quasimonotone nondecreasing and  $g$  is quasimonotone nonincreasing in  $x$  for each  $t$ , and for each  $i$

$$F_i(t, \tilde{x}(t), \tilde{y}(t)) - F_i(t, x(t), y(t)) \leq L_i \left[ \sum_{i=1}^n (\tilde{x}_i(t) - x_i(t)) + (\tilde{y}_i(t) - y_i(t)) \right] \quad (2.8)$$

whenever  $\tilde{x}(t) \geq x(t)$ ,  $\tilde{y}(t) \geq y(t)$  and where  $L_i > 0$  and  $F_i(t, x(t), y(t)) = f_i(t, (x_1, \dots, x_n)) + g_i(t, (y_1, \dots, y_n))$ .

Then  $\alpha(t_0) \leq \beta(t_0)$  implies that  $\alpha(t) \leq \beta(t)$  for  $t \in [t_0, t_0 + T]$ .

**Proof :** We first prove the theorem for strict inequalities. We suppose that

$$\beta' > f(t, \alpha) + g(t, \beta), \quad \alpha' \leq f(t, \beta) + g(t, \alpha), \quad t \in J$$

and  $\alpha(t_0) \leq \beta(t_0)$ .

We shall prove that  $\alpha(t) < \beta(t)$ ,  $t \in J$ . Suppose the conclusion is not true. Then the set

$$Z = \bigcup_{i=1}^n \{t \in J : \beta_i(t) \leq \alpha_i(t)\}$$

is nonempty.

Let  $t_1 = \inf Z$ . Certainly  $t_1 > 0$ . Since  $Z$  is closed,  $t_1 \in Z$  and consequently there exists a  $j$  such that  $\beta_j(t_1) = \alpha_j(t_1)$  and  $\alpha_j(t) \leq \beta_j(t)$  for  $t \in [t_0, t_1]$ . Moreover  $\alpha_i(t_1) \geq \beta_i(t_1)$  for  $i \neq j$ . Hence, we have for small  $h > 0$

$$\alpha_j(t_1 - h) - \alpha_j(t_1) \leq \beta_j(t_1 - h) - \beta_j(t_1).$$

That implies,  $\alpha'_j(t_1) \geq \beta'_j(t_1)$ . This, together with the quasimonotonicity of  $f$ , yields

$$\begin{aligned} & f_j(t_1, \beta_1(t_1), \beta_2(t_1), \dots, \beta_n(t_1)) + g_j(t_1, \alpha_1(t_1), \alpha_2(t_1), \dots, \alpha_n(t_1)) \\ & \geq \alpha'_j(t_1) \\ & \geq \beta'_j(t_1) \\ & > f_j(t_1, \alpha_1(t_1), \alpha_2(t_1), \dots, \alpha_n(t_1)) + g_j(t_1, \beta_1(t_1), \beta_2(t_1), \dots, \beta_n(t_1)) \\ & = f_j(t_1, \alpha_1(t_1), \alpha_2(t_1), \dots, \beta_j(t_1), \dots, \alpha_n(t_1)) \\ & \quad + g_j(t_1, \beta_1(t_1), \beta_2(t_1), \dots, \alpha_j(t_1), \dots, \beta_n(t_1)) \\ & \geq f_j(t_1, \beta_1(t_1), \beta_2(t_1), \dots, \beta_n(t_1)) + g_j(t_1, \alpha_1(t_1), \alpha_2(t_1), \dots, \alpha_n(t_1)) \end{aligned}$$

which leads to contradiction. Therefore, we have proved that  $\alpha(t) < \beta(t)$ ,  $t \in J$ .

In order to prove the case of nonstrict inequalities, consider functions for each  $i$  and  $\epsilon > 0$

$$\tilde{\alpha}_i(t) = \alpha_i(t) + \epsilon e^{(2n+1)Lt} \text{ and } \tilde{\beta}_i(t) = \beta_i(t) + \epsilon e^{(2n+1)Lt}$$

where  $L = \max\{L_i > 0 : i = 1, 2, \dots, n\}$ .

$$\begin{aligned} \tilde{\beta}'_i(t) &= \beta'_i(t) + \epsilon(2n+1)L e^{(2n+1)Lt} \\ &\geq f_j(t_1, \alpha_1(t_1), \alpha_2(t_1), \dots, \alpha_n(t_1)) \\ &\quad + g_j(t_1, \beta_1(t_1), \beta_2(t_1), \dots, \beta_n(t_1)) + \epsilon(2n+1)L e^{(2n+1)Lt} \\ &\geq F_i(t, \tilde{\alpha}(t), \tilde{\beta}(t)) - L_i \epsilon 2n L e^{(2n+1)Lt} + \epsilon L e^{(2n+1)Lt} + \epsilon 2n L e^{(2n+1)Lt} \\ &> F_i(t, \tilde{\alpha}(t), \tilde{\beta}(t)) \\ &= f_i(t, \tilde{\alpha}_1(t_1), \tilde{\alpha}_2(t_1), \dots, \tilde{\alpha}_n(t_1)) + g_j(t_1, \tilde{\beta}_1(t_1), \tilde{\beta}_2(t_1), \dots, \tilde{\beta}_n(t_1)). \end{aligned}$$

Also  $\alpha_i(t_0) \leq \beta_i(t_0) \leq \tilde{\beta}_i(t_0)$ . Now using the result corresponding to strict inequalities we get

$$\alpha_i(t) < \tilde{\beta}_i(t) = \beta_i(t) + \epsilon e^{(2n+1)Lt}$$

for  $t \in J$ .

Letting  $\epsilon \rightarrow 0$ , we now obtain the required result  $\alpha_i(t) \leq \beta_i(t)$  for  $t \in J$ . The proof is completed.

### 3 Main Results

In this section we will give necessary definitions and then the our main results.

For each fixed  $i$ ,  $1 \leq i \leq n$  let  $p_i, q_i$  be two nonnegative integers such that  $1 + p_i + q_i = n$  so that we can split the vector  $u$  into  $(u_i, [u]_{p_i}, [u]_{q_i})$ . Then the system (2.2) can be written as

$$u'_i = f_i(t, u_i, [u]_{p_i}, [u]_{q_i}) + g_i(t, u_i, [u]_{p_i}, [u]_{q_i}), \quad u(t_0) = u_0. \quad (3.1)$$

**Definition 3.1:** The functions  $\alpha_0, \beta_0 \in C^1[J, \mathbb{R}^n]$  and  $f, g \in C[J \times \mathbb{R}^n, \mathbb{R}^n]$ . Then  $\alpha_0, \beta_0$  are said to be coupled lower and upper quasisolutions of (3.1) if they satisfy

$$\alpha'_{0,i} \leq f_i(t, \alpha_{0,i}, [\alpha_0]_{p_i}, [\beta_0]_{q_i}) + g_i(t, \beta_{0,i}, [\beta_0]_{p_i}, [\alpha_0]_{q_i}), \quad \alpha_0(t_0) \leq u_0 \quad (3.2)$$

$$\beta'_{0,i} \geq f_i(t, \beta_{0,i}, [\beta_0]_{p_i}, [\alpha_0]_{q_i}) + g_i(t, \alpha_{0,i}, [\alpha_0]_{p_i}, [\beta_0]_{q_i}), \quad \beta_0(t_0) \geq u_0. \quad (3.3)$$

**Definition 3.2:** Let  $\alpha, \beta \in C^1[J, \mathbb{R}^n]$  and  $f, g \in C[J \times \mathbb{R}^n, \mathbb{R}^n]$ . Then  $\alpha$  and  $\beta$  are said to be coupled quasisolutions of (3.1) if

$$\alpha'_i = f_i(t, \alpha_i, [\alpha]_{p_i}, [\beta]_{q_i}) + g_i(t, \beta_i, [\beta]_{p_i}, [\alpha]_{q_i}), \quad \alpha(t_0) = u_0 \quad (3.4)$$

$$\beta'_i = f_i(t, \beta_i, [\beta]_{p_i}, [\alpha]_{q_i}) + g_i(t, \alpha_i, [\alpha]_{p_i}, [\beta]_{q_i}), \quad \beta(t_0) = u_0. \quad (3.5)$$

**Theorem 3.1:** Let  $\alpha_0$  and  $\beta_0$  be the coupled lower and upper quasisolutions of (3.1) such that  $\alpha_0(t) \leq \beta_0(t)$ ,  $t \in J$ . For each  $i$ ,  $f_i(t, u_i, [u]_{p_i}, [u]_{q_i})$  is nondecreasing in  $u_i$  and  $[u]_{p_i}$  and nonincreasing in  $[u]_{q_i}$  and  $g_i(t, u_i, [u]_{p_i}, [u]_{q_i})$  is nonincreasing in  $u_i$  and  $[u]_{p_i}$  and nondecreasing in  $[u]_{q_i}$ , then there exists monotone sequences  $\alpha_n \rightarrow \alpha$  and  $\beta_n \rightarrow \beta$  as  $n \rightarrow \infty$ , uniformly and monotonically to coupled quasisolutions of (3.1).

**Proof:** Let us consider the following linear system of differential equations

$$\alpha'_{k+1,i} = f_i(t, \alpha_{k,i}, [\alpha_k]_{p_i}, [\beta_k]_{q_i}) + g_i(t, \beta_{k,i}, [\beta_k]_{p_i}, [\alpha_k]_{q_i}), \quad \alpha_{k+1}(t_0) = u_0 \quad (3.6)$$

$$\beta'_{k+1,i} = f_i(t, \beta_{k,i}, [\beta_k]_{p_i}, [\alpha_k]_{q_i}) + g_i(t, \alpha_{k,i}, [\alpha_k]_{p_i}, [\beta_k]_{q_i}), \quad \beta_{k+1}(t_0) = u_0 \quad (3.7)$$

for  $i = 1, 2, \dots, n$  and  $k = 0, 1, 2, 3, \dots$ . The solutions of linear system (3.6) and (3.7) exist on  $J$ . To show that  $\alpha_1(t) \geq \alpha_0(t)$  we set  $p_i(t) = \alpha_{1,i}(t) - \alpha_{0,i}(t)$  for  $t \in J$ ,  $p_i(t_0) \geq 0$ . Then

$$\begin{aligned} p'_i(t) &= \alpha'_{1,i}(t) - \alpha'_{0,i}(t) \\ &\geq f_i(t, \alpha_{0,i}, [\alpha_0]_{p_i}, [\beta_0]_{q_i}) + g_i(t, \beta_{0,i}, [\beta_0]_{p_i}, [\alpha_0]_{q_i}) \\ &\quad - f_i(t, \alpha_{0,i}, [\alpha_0]_{p_i}, [\beta_0]_{q_i}) - g_i(t, \beta_{0,i}, [\beta_0]_{p_i}, [\alpha_0]_{q_i}) \\ &= 0 \end{aligned}$$

which implies  $p_i(t) \geq 0$  for  $i = 1, 2, \dots, n$  and hence  $\alpha_1(t) \geq \alpha_0(t)$  for  $t \in J$ . Similarly, we can show that  $\beta_1(t) \leq \beta_0(t)$  on  $J$ . To show  $\beta_1(t) \geq \alpha_1(t)$  we set  $p_i(t) = \beta_{1,i}(t) - \alpha_{1,i}(t)$ ,  $p_i(t_0) \geq 0$ . So that

$$\begin{aligned} p'_i(t) &= \beta'_{1,i}(t) - \alpha'_{1,i}(t) \\ &= f_i(t, \beta_{0,i}, [\beta_0]_{p_i}, [\alpha_0]_{q_i}) + g_i(t, \alpha_{0,i}, [\alpha_0]_{p_i}, [\beta_0]_{q_i}) \\ &\quad - f_i(t, \alpha_{0,i}, [\alpha_0]_{p_i}, [\beta_0]_{q_i}) - g_i(t, \beta_{0,i}, [\beta_0]_{p_i}, [\alpha_0]_{q_i}) \\ &\geq f_i(t, \alpha_{0,i}, [\alpha_0]_{p_i}, [\beta_0]_{q_i}) + g_i(t, \beta_{0,i}, [\beta_0]_{p_i}, [\alpha_0]_{q_i}) \\ &\quad - f_i(t, \alpha_{0,i}, [\alpha_0]_{p_i}, [\beta_0]_{q_i}) - g_i(t, \beta_{0,i}, [\beta_0]_{p_i}, [\alpha_0]_{q_i}) \\ p'_i(t) &\geq 0 \end{aligned}$$

since  $f$  is nondecreasing in  $u_i$  and  $[u]_{p_i}$  and nonincreasing in  $[u]_{q_i}$  and  $g$  is nonincreasing in  $u_i$  and  $[u]_{p_i}$  and nondecreasing in  $[u]_{q_i}$ . Then  $p_i(t) \geq 0$  for  $i = 1, 2, \dots, n$  and hence  $\beta_1(t) \geq \alpha_1(t)$  for  $t \in J$ . Hence we have

$$\alpha_0(t) \leq \alpha_1(t) \leq \beta_1(t) \leq \beta_0(t) \quad \text{on } J. \quad (3.8)$$



Now, assume that for some  $k > 1$

$$\alpha_0(t) \leq \alpha_{k-1}(t) \leq \alpha_k(t) \leq \beta_k(t) \leq \beta_{k-1}(t) \leq \beta_0(t) \text{ on } J \quad (3.9)$$

We want to show that

$$\alpha_k(t) \leq \alpha_{k+1}(t) \leq \beta_{k+1}(t) \leq \beta_k(t) \text{ on } J \quad (3.10)$$

To prove this, we let  $p_i(t) = \alpha_{k+1,i}(t) - \alpha_{k,i}(t)$  clearly that  $p_i(t_0) = 0$ . Thus we have

$$\begin{aligned} p_i'(t) &= \alpha'_{k+1,i}(t) - \alpha'_{k,i}(t) \\ &= f_i\left(t, \alpha_{k,i}, [\alpha_k]_{p_i}, [\beta_k]_{q_i}\right) + g_i\left(t, \beta_{k,i}, [\beta_k]_{p_i}, [\alpha_k]_{q_i}\right) \\ &\quad - f_i\left(t, \alpha_{k-1,i}, [\alpha_{k-1}]_{p_i}, [\beta_{k-1}]_{q_i}\right) - g_i\left(t, \beta_{k-1,i}, [\beta_{k-1}]_{p_i}, [\alpha_{k-1}]_{q_i}\right) \\ &\geq f_i\left(t, \alpha_{k-1,i}, [\alpha_{k-1}]_{p_i}, [\beta_{k-1}]_{q_i}\right) - g_i\left(t, \beta_{k-1,i}, [\beta_{k-1}]_{p_i}, [\alpha_{k-1}]_{q_i}\right) \\ &\quad - f_i\left(t, \alpha_{k-1,i}, [\alpha_{k-1}]_{p_i}, [\beta_{k-1}]_{q_i}\right) - g_i\left(t, \beta_{k-1,i}, [\beta_{k-1}]_{p_i}, [\alpha_{k-1}]_{q_i}\right) \\ p_i'(t) &\geq 0 \end{aligned}$$

since  $f$  is nondecreasing in  $u_i$  and  $[u]_{p_i}$  and nonincreasing in  $[u]_{q_i}$  and  $g$  is nonincreasing in  $u_i$  and  $[u]_{p_i}$  and nondecreasing in  $[u]_{q_i}$ . Then  $p_i(t) \geq 0$  for  $i = 1, 2, \dots, n$  and hence  $\alpha_{k+1}(t) \geq \alpha_k(t)$  for  $t \in J$ . To show that we set  $p_i(t) = \beta_{k+1}(t) - \beta_k(t)$  for  $t \in J$  and  $p_i(t_0) \leq 0$ .

$$\begin{aligned} p_i'(t) &= \beta'_{k+1}(t) - \beta'_k(t) \\ &= f_i\left(t, \beta_{k,i}, [\beta_k]_{p_i}, [\alpha_k]_{q_i}\right) + g_i\left(t, \alpha_{k,i}, [\alpha_k]_{p_i}, [\beta_k]_{q_i}\right) \\ &\quad - f_i\left(t, \beta_{k-1,i}, [\beta_{k-1}]_{p_i}, [\alpha_{k-1}]_{q_i}\right) - g_i\left(t, \alpha_{k-1,i}, [\alpha_{k-1}]_{p_i}, [\beta_{k-1}]_{q_i}\right) \\ &\leq f_i\left(t, \beta_{k-1,i}, [\beta_{k-1}]_{p_i}, [\alpha_{k-1}]_{q_i}\right) - g_i\left(t, \alpha_{k-1,i}, [\alpha_{k-1}]_{p_i}, [\beta_{k-1}]_{q_i}\right) \\ &\quad - f_i\left(t, \beta_{k-1,i}, [\beta_{k-1}]_{p_i}, [\alpha_{k-1}]_{q_i}\right) - g_i\left(t, \alpha_{k-1,i}, [\alpha_{k-1}]_{p_i}, [\beta_{k-1}]_{q_i}\right) \\ p_i'(t) &\leq 0 \end{aligned}$$

since  $f$  is nondecreasing in  $u_i$  and  $[u]_{p_i}$  and nonincreasing in  $[u]_{q_i}$  and  $g$  is nonincreasing in  $u_i$  and  $[u]_{p_i}$  and nondecreasing in  $[u]_{q_i}$ . Then  $p_i(t) \geq 0$  for  $i = 1, 2, \dots, n$  and hence  $\beta_{k+1}(t) \leq \beta_k(t)$  for  $t \in J$ .

To show that we set  $p_i(t) = \beta_{k+1,i}(t) - \alpha_{k+1,i}(t)$  for  $t \in J$  and  $p_i(t_0) \geq 0$ .

$$\begin{aligned} p_i'(t) &= \beta'_{k+1,i}(t) - \alpha'_{k+1,i}(t) \\ &= f_i\left(t, \beta_{k,i}, [\beta_k]_{p_i}, [\alpha_k]_{q_i}\right) + g_i\left(t, \alpha_{k,i}, [\alpha_k]_{p_i}, [\beta_k]_{q_i}\right) \\ &\quad - f_i\left(t, \alpha_{k,i}, [\alpha_k]_{p_i}, [\beta_k]_{q_i}\right) - g_i\left(t, \beta_{k,i}, [\beta_k]_{p_i}, [\alpha_k]_{q_i}\right) \\ &\geq f_i\left(t, \alpha_{k,i}, [\alpha_k]_{p_i}, [\beta_k]_{q_i}\right) + g_i\left(t, \beta_{k,i}, [\beta_k]_{p_i}, [\alpha_k]_{q_i}\right) \\ &\quad - f_i\left(t, \alpha_{k,i}, [\alpha_k]_{p_i}, [\beta_k]_{q_i}\right) - g_i\left(t, \beta_{k,i}, [\beta_k]_{p_i}, [\alpha_k]_{q_i}\right) \\ p_i'(t) &\geq 0 \end{aligned}$$

since  $f$  is nondecreasing in  $u_i$  and  $[u]_{p_i}$  and nonincreasing in  $[u]_{q_i}$  and  $g$  is nonincreasing in  $u_i$  and  $[u]_{p_i}$  and nondecreasing in  $[u]_{q_i}$ . Then  $p_i(t) \geq 0$  for  $i = 1, 2, \dots, n$  and hence  $\beta_{k+1}(t) \geq \alpha_{k+1}(t)$  for  $t \in J$ . Hence by induction (3.9) is valid for all  $n$ . Thus we have the monotone sequences such that

$$\alpha_0(t) \leq \alpha_1(t) \leq \alpha_2(t) \leq \dots \leq \alpha_n(t) \leq \beta_n(t) \leq \dots \leq \beta_2(t) \leq \beta_1(t) \leq \beta_0(t) \text{ for } t \in J. \quad (3.11)$$

By the standard argument [3], there exist monotone sequences  $\{\alpha_n(t)\}$  and  $\{\beta_n(t)\}$  such that  $\alpha_n \rightarrow \alpha$  and  $\beta_n \rightarrow \beta$  as  $n \rightarrow \infty$  uniformly and monotonically to coupled minimal and maximal quasisolutions of (3.1).

It is now easy to conclude that the sequences  $\{\alpha_k(t)\}$  and  $\{\beta_k(t)\}$  coupled minimal and maximal quasisolutions of (3.1).

$$\alpha'_{k+1,i} = f_i\left(t, \alpha_{k,i}, [\alpha_k]_{p_i}, [\beta_k]_{q_i}\right) + g_i\left(t, \beta_{k,i}, [\beta_k]_{p_i}, [\alpha_k]_{q_i}\right), \quad \alpha_{k+1}(t_0) = u_0 \quad (3.12)$$

then

$$\alpha_{k+1,i} = u_0 + \int_{t_0}^t \left\{ f_i\left(s, \alpha_{k,i}, [\alpha_k]_{p_i}, [\beta_k]_{q_i}\right) + g_i\left(s, \beta_{k,i}, [\beta_k]_{p_i}, [\alpha_k]_{q_i}\right) \right\} ds \quad (3.13)$$

and for  $k \rightarrow \infty$

$$\alpha_i(t) = u_0 + \int_{t_0}^t \left\{ f_i\left(s, \alpha_i, [\alpha]_{p_i}, [\beta]_{q_i}\right) + g_i\left(s, \beta_i, [\beta]_{p_i}, [\alpha]_{q_i}\right) \right\} ds \quad (3.14)$$

consequently,

$$\alpha'_i(t) = f_i\left(s, \alpha_i, [\alpha]_{p_i}, [\beta]_{q_i}\right) + g_i\left(s, \beta_i, [\beta]_{p_i}, [\alpha]_{q_i}\right), \quad \alpha(t_0) = u_0. \quad (3.15)$$

Similarly, we can show that

$$\beta'_i(t) = f_i\left(s, \beta_i, [\beta]_{p_i}, [\alpha]_{q_i}\right) + g_i\left(s, \alpha_i, [\alpha]_{p_i}, [\beta]_{q_i}\right), \quad \beta_{k+1}(t_0) = u_0 \quad (3.16)$$

then  $\alpha(t)$  and  $\beta(t)$  coupled quasisolutions of (3.1). This completes the proof.

**Corollary 3.1:** Let  $\alpha_0$  and  $\beta_0$  be the coupled lower and upper quasisolutions of (3.1) such that  $\alpha_0(t) \leq u(t) \leq \beta_0(t)$ ,  $t \in J$ .  $f$  is nondecreasing in  $u_i$  and  $[u]_{p_i}$  and nonincreasing in  $[u]_{q_i}$  and  $g$  is nonincreasing in  $u_i$  and  $[u]_{p_i}$  and nondecreasing in  $[u]_{q_i}$ , then there exists monotone sequences  $\alpha_n \rightarrow \alpha$  and  $\beta_n \rightarrow \beta$  as  $n \rightarrow \infty$ , uniformly and monotonically to coupled maximal and minimal quasisolutions of (3.1). Further if  $u$  is any solution of (3.1) such that  $\alpha_0(t) \leq u(t) \leq \beta_0(t)$  then  $\alpha(t) \leq u(t) \leq \beta(t)$  on  $J$ .

**Proof:** Let  $\{u_1(t), u_2(t)\}$  be any coupled quasisolution of (3.1). Let assume that for  $t \in J$  and  $k \in Z$ ,  $\alpha_{k-1}(t) \leq u_1(t)$  and  $\beta_{k-1}(t) \geq u_2(t)$ . Set

$$p_i(t) = \alpha_{k,i}(t) - u_{1,i}(t), \quad p_i(t_0) = 0.$$

$$\begin{aligned} p'_i(t) &= \alpha'_{k,i}(t) - u'_{1,i}(t) \\ &= f_i\left(t, \alpha_{k-1,i}, [\alpha_{k-1}]_{p_i}, [\beta_{k-1}]_{q_i}\right) + g_i\left(t, \beta_{k-1,i}, [\beta_{k-1}]_{p_i}, [\alpha_{k-1}]_{q_i}\right) \\ &\quad - f_i\left(t, u_{1,i}, [u_1]_{p_i}, [u_2]_{q_i}\right) - g_i\left(t, u_{2,i}, [u_2]_{p_i}, [u_1]_{q_i}\right) \\ &\leq f_i\left(t, u_{1,i}, [u_1]_{p_i}, [u_2]_{q_i}\right) + g_i\left(t, u_{2,i}, [u_2]_{p_i}, [u_1]_{q_i}\right) \\ &\quad - f_i\left(t, u_{1,i}, [u_1]_{p_i}, [u_2]_{q_i}\right) - g_i\left(t, u_{2,i}, [u_2]_{p_i}, [u_1]_{q_i}\right) \\ p'_i(t) &\leq 0 \end{aligned}$$

since  $f$  is nondecreasing in  $u_i$  and  $[u]_{p_i}$  and nonincreasing in  $[u]_{q_i}$  and  $g$  is nonincreasing in  $u_i$  and  $[u]_{p_i}$  and nondecreasing in  $[u]_{q_i}$ . Then  $p_i(t) \geq 0$  for  $i = 1, 2, \dots, n$  and hence  $\alpha_{k+1}(t) \geq \alpha_k(t)$  for  $t \in J$ . Similarly, the setting for  $t \in J$

$$p_i(t) = \beta_{k,i}(t) - u_{2,i}(t), \quad p_i(t_0) = 0.$$

$$\begin{aligned}
p'_i(t) &= \beta'_{k,i}(t) - u'_{2,i}(t) \\
&= f_i\left(t, \beta_{k-1,i}, [\beta_{k-1}]_{p_i}, [\alpha_{k-1}]_{q_i}\right) + g_i\left(t, \alpha_{k-1,i}, [\alpha_{k-1}]_{p_i}, [\beta_{k-1}]_{q_i}\right) \\
&\quad - f_i\left(t, u_{2,i}, [u_2]_{p_i}, [u_1]_{q_i}\right) - g_i\left(t, u_{1,i}, [u_1]_{p_i}, [u_2]_{q_i}\right) \\
&\geq f_i\left(t, u_{2,i}, [u_2]_{p_i}, [u_1]_{q_i}\right) + g_i\left(t, u_{1,i}, [u_1]_{p_i}, [u_2]_{q_i}\right) \\
&\quad - f_i\left(t, u_{2,i}, [u_2]_{p_i}, [u_1]_{q_i}\right) - g_i\left(t, u_{1,i}, [u_1]_{p_i}, [u_2]_{q_i}\right) \\
p'_i(t) &\geq 0
\end{aligned}$$

since  $f$  is nondecreasing in  $u_i$  and  $[u]_{p_i}$  and nonincreasing in  $[u]_{q_i}$  and  $g$  is nonincreasing in  $u_i$  and  $[u]_{p_i}$  and nondecreasing in  $[u]_{q_i}$ . Then  $p_i(t) \geq 0$  for  $i = 1, 2, \dots, n$  and hence  $\alpha_{k+1}(t) \geq \alpha_k(t)$  for  $t \in J$ . It follows by induction that  $\alpha_k(t) \leq u_1(t)$  and  $\beta_k(t) \geq u_2(t)$  on  $J$ . Then  $\alpha(t) \leq u_1(t)$  and  $\beta(t) \geq u_2(t)$  on  $J$  for  $k \rightarrow \infty$  proving  $\{u_1(t), u_2(t)\}$  are coupled minimal and maximal quasisolutions of (3.1). Since any solution  $u$  of (3.1) such that  $\alpha_0(t) \leq u(t) \leq \beta_0(t)$  can be considered as  $\{u(t), u(t)\}$  coupled quasisolutions of (3.1) we also have  $\alpha(t) \leq u(t) \leq \beta(t)$  for  $t \in J$ . This completes the proof.

**Definition 3.3:** Let  $\alpha, \beta \in C^1[J, \mathbb{R}^n]$  and  $f, g \in C[J \times \mathbb{R}^n, \mathbb{R}^n]$ . Then  $\alpha, \beta$ , are said to be coupled quasisolutions of (3.1) if they satisfy

$$\alpha'_i = f_i\left(t, \beta_i, [\beta]_{p_i}, [\alpha]_{q_i}\right) + g_i\left(t, \alpha_i, [\alpha]_{p_i}, [\beta]_{q_i}\right), \quad \alpha(t_0) = u_0 \quad (3.17)$$

$$\beta'_i = f_i\left(t, \alpha_i, [\alpha]_{p_i}, [\beta]_{q_i}\right) + g_i\left(t, \beta_i, [\beta]_{p_i}, [\alpha]_{q_i}\right), \quad \beta(t_0) = u_0 \quad (3.18)$$

**Remark 3.1:** Let  $\alpha_0$  and  $\beta_0$  be the coupled lower and upper quasisolutions of (3.1) such that  $\alpha_0(t) \leq \beta_0(t)$ ,  $t \in J$ .  $f$  is nonincreasing in  $u_i$  and  $[u]_{p_i}$  and nondecreasing in  $[u]_{q_i}$  and  $g$  is nondecreasing in  $u_i$  and  $[u]_{p_i}$  and nondecreasing in  $[u]_{q_i}$  then there exists monotone sequences such that  $\alpha_0 \leq \alpha_1$  and  $\beta_0 \geq \beta_1$ ,  $\alpha_n \rightarrow \alpha$  and  $\beta_n \rightarrow \beta$  as  $n \rightarrow \infty$ , uniformly and monotonically to coupled quasisolutions of (3.1).

**Proof:** Let us consider the following linear system of differential equations

$$\alpha'_{k+1,i} = f_i\left(t, \beta_{k,i}, [\beta_k]_{p_i}, [\alpha_k]_{q_i}\right) + g_i\left(t, \alpha_{k,i}, [\alpha_k]_{p_i}, [\beta_k]_{q_i}\right), \quad \alpha_{k+1}(t_0) = u_0 \quad (3.19)$$

$$\beta'_{k+1,i} = f_i\left(t, \alpha_{k,i}, [\alpha_k]_{p_i}, [\beta_k]_{q_i}\right) + g_i\left(t, \beta_{k,i}, [\beta_k]_{p_i}, [\alpha_k]_{q_i}\right), \quad \beta_{k+1}(t_0) = u_0 \quad (3.20)$$

for  $i = 1, 2, \dots, n$  and  $k = 0, 1, 2, 3, \dots$ . We proceed very much similar to Theorem 3.1, then we obtain to desire conclusion.

**Remark 3.1.2:** The main theorem may be applied to get monotone iterative techniques for nonlinear problems in term of two monotone functions. That is the generalization of [1].

## References

- [1] Bhaskar, T. G. and McRae, Farzana A., *Monotone iterative techniques for nonlinear problems involving the difference of two monotone functions*, Applied Mathematics and Computation, Volume 133, Issue 1, 25 November 2002, Pages 187-192.
- [2] Koksall, S. and Yakar, C., "Generalized quasilinearization method with initial time difference," Simulation, an International Journal of Electrical, Electronic and other Physical Systems, 24(5), 2002.
- [3] Ladde, G.S, Lakshmikantham, V., and Vatsala A.S., *Monotone Iterative Technique for Nonlinear Differential Equations*, Pitman Publishing Inc., Boston 1985.
- [4] Lakshmikantham, V. and Vatsala A.S., *Generalized Quasilinearization for Nonlinear Problems*, Kluwer Academic Publishers, The Netherlands 1998.

## **Dynamical Analysis and Electronic Implementation of A New Chaotic Attractor**

**İhsan Pehlivan<sup>1</sup>, Yılmaz Uyaroglu<sup>2</sup>, İhsan Bayır<sup>3</sup>, Serkan Akkaya<sup>4</sup>, Nazım İmal<sup>5</sup>**

<sup>1,2,3,4</sup> Sakarya University, Eng. Faculty, Electrical Electronics Engineering Department  
54187, Esentepe Campus, Sakarya, TURKEY.

<sup>5</sup> Bilecik University, Eng. Faculty, Computer Engineering Department

E-mails: <sup>1</sup>ipehlivan@sakarya.edu.tr, <sup>2</sup>uyaroglu@sakarya.edu.tr, <sup>3</sup>ibayir@sakarya.edu.tr

<sup>4</sup>serkanakkaya26@hotmail.com, <sup>5</sup>nazim.imal@bilecik.edu.tr

### **Abstract**

Dynamical behaviors of a new chaotic attractor is investigated in this paper. Basic dynamical properties of the new attractor system are analyzed by means of equilibrium points, eigenvalue structures, Lyapunov exponents and parameters regions. Chaotic electronic implementation of the new attractor were designed and simulated in OrCad-PSpice®. Finally, the chaos generators are experimentally confirmed via a novel circuit design.

**Indexing Terms:** Chaotic attractors, Chaotic systems, Chaotic circuits, Chaotic oscillators, Lyapunov Exponents

### **1. Introduction**

The first classical chaotic system is found by Lorenz when he studied the atmospheric convection in 1963[1]. Rossler carried out an important work, which rekindled the interest in low dimensional dissipative dynamical systems[2] in 1976. Rossler himself proposed an even simpler (algebraic) system[3] in 1979. Sprott embarked upon an extensive search[4] for autonomous three dimensional chaotic systems. Chen constructed another chaotic system[5], which nevertheless is not topologically equivalent to the Lorenz's[5, 6]. This system is the dual to the Lorenz system and similarly has a simple structure[6]. Lü and Chen found the critical new chaotic system [7], which represents the transition between the Lorenz and Chen attractors. It has been noticed that purposefully creating chaos can be a nontrivial task with interesting impact on both basic research and engineering applications. There has been increasing interest in exploiting chaotic dynamics in engineering applications, where some attention has been focused on effectively creating chaos via simple physical systems such as electronic circuits[8]-[11]. Lately,

the pursuit of designing circuits to produce chaotic attractors became a focal subject for electronic engineers, due not only to the theoretical interest but more importantly to their potential real-world applications[12] in various chaos-based technologies and information systems [12-18].

Motivated by these works, this paper introduces one more simple, interesting three-dimensional quadratic autonomous system which can depict complex 2-scroll chaotic attractors simultaneously. Section 2 introduces and analysis the new chaotic system. Analysis and simulation results of the new system (Fig. 1., 2.) are also obtained in section 2. Section 3 presents the designed electronic circuit schematic(Fig. 3.), the OrCad-PSpice® simulation results(Fig. 4.) and the real circuit implementation oscilloscope outputs(Fig. 5.) of the new attractor. Finally, conclusions and discussions are given.

## 2. Dynamical Analyses of A New Chaotic Attractor

Following nonlinear autonomous ordinary differential equations are the new chaotic system:

$$\begin{aligned}\dot{x} &= -a \cdot y \cdot z \\ \dot{y} &= -a \cdot x - y + y \cdot z \\ \dot{z} &= b + c \cdot x - d \cdot y^2\end{aligned}\tag{1}$$

Typical parameters are  $a=3$ ,  $b=12$ ,  $c=2$ , and  $d=6$ . The new system equations has two equilibrium

points as  $(x^*, y^*, z^*) = \left( \frac{c \pm \sqrt{c^2 + 4 \cdot a^2 \cdot b \cdot d}}{2 \cdot a^2 \cdot d}, -\frac{c \pm \sqrt{c^2 + 4 \cdot a^2 \cdot b \cdot d}}{2 \cdot a \cdot d}, 0 \right)$ .

As the variables  $x, y, z \in \mathcal{R}$ , this implies that fixed point to exist,  $\sqrt{c^2 + 4 \cdot d \cdot a^2 \cdot b} > 0$ . The equilibrium points of the new systems are  $(x^*, y^*, z^*) = (0.4903, -1.4709, 0)$  and  $(x^*, y^*, z^*) = (-0.4532, 1.3597, 0)$  for  $a=3$ , for  $b=12$ ,  $c=2$ , and  $d=6$  values. For the fixed

point\_1,  $(x^*, y^*, z^*) = \left( \frac{c + \sqrt{c^2 + 4 \cdot a^2 \cdot b \cdot d}}{2 \cdot a^2 \cdot d}, -\frac{c + \sqrt{c^2 + 4 \cdot a^2 \cdot b \cdot d}}{2 \cdot a \cdot d}, 0 \right)$ , by solving the

characteristic equation, the eigenvalues are found as follows;

$$\lambda_1 = -5.4422, \lambda_2 = 2.2211 - 6.0314 \cdot i, \lambda_3 = 2.2211 + 6.0314 \cdot i \text{ for } a=3, b=12, c=2, \text{ and } d=6.$$

For the fixed point\_2,  $(x^*, y^*, z^*) = \left( \frac{c - \sqrt{c^2 + 4 \cdot a^2 \cdot b \cdot d}}{2 \cdot a^2 \cdot d}, -\frac{c - \sqrt{c^2 + 4 \cdot a^2 \cdot b \cdot d}}{2 \cdot a \cdot d}, 0 \right)$ , by

solving the characteristic equation, the eigenvalues are found as follows;

$\lambda_1 = -4.5050$ ,  $\lambda_2 = 1.7525 - 6.5623 \cdot i$ ,  $\lambda_3 = 1.7525 + 6.5623 \cdot i$  for  $a=3$ ,  $b=12$ ,  $c=2$ , and  $d=6$ .

Note that the real parts of these eigenvalues are positive. Consequently the equilibrium points are unstable and this implies chaos. So, the system orbits around the two unstable equilibrium points. Interestingly, the origin(0,0,0) point is not equilibria for the new system. The equilibria and eigenvalues for certain chaotic systems are tabulated in Table I.

Table I. Equilibria and eigenvalues for certain chaotic systems

System	Parameters	Equilibria	Eigenvalues
Lorenz system	$a=10, b=8/3, c=28$	$\begin{cases} (0, 0, 0) \\ (\pm 6\sqrt{2}, \pm 6\sqrt{2}, 27) \end{cases}$	$\begin{cases} -22.8277, -2.6667, 11.8277 \\ -13.8546, 0.0940 \pm 0.1945 \cdot i \end{cases}$
Chen system	$a=35, b=3, c=28$	$\begin{cases} (0, 0, 0) \\ (\pm 3\sqrt{7}, \pm 3\sqrt{7}, 21) \end{cases}$	$\begin{cases} -30.8359, -3, 23.8359 \\ -18.4288, 4.2140 \pm 14.8846 \cdot i \end{cases}$
Lü system	$a=36, b=3, c=20$	$\begin{cases} (0, 0, 0) \\ (\pm 2\sqrt{15}, \pm 2\sqrt{15}, 20) \end{cases}$	$\begin{cases} -36, -3, 20 \\ -22.6516, 1.8258 \pm 13.6887 \cdot i \end{cases}$
The new system(1)	$a=3, b=12, c=2, d=6$	$\begin{cases} (0.4903, -1.4709, 0) \\ (-0.4532, 1.3597, 0) \end{cases}$	$\begin{cases} -5.4422, 2.2211 \pm 6.0314 \cdot i \\ -4.5050, 1.7525 \pm 6.5623 \cdot i \end{cases}$

Figure 1. shows the Lyapunov Spectrum of the new system for varying parameter  $a$ , and constant parameters  $b=12$ ,  $c=2$ , and  $d=6$ . As can be seen from the Lyapunov exponents spectrum, the new system is chaotic when a positive Lyapunov exponent.

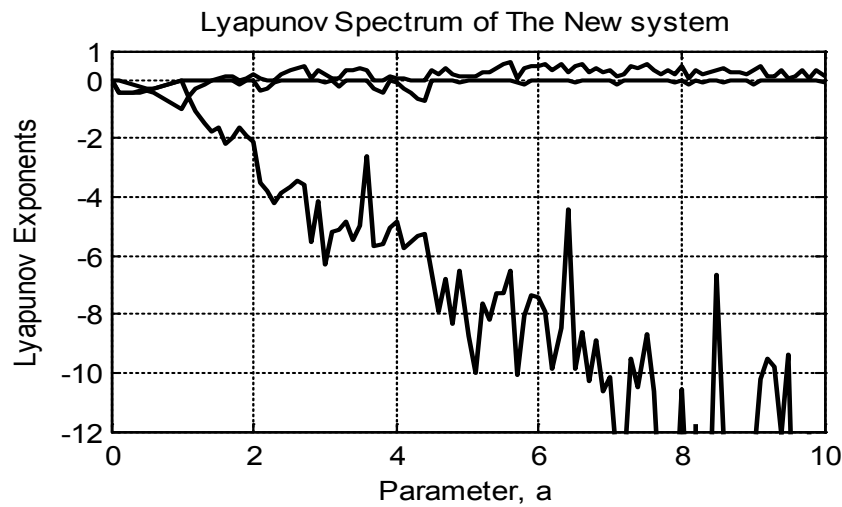


Figure 1. Lyapunov Spectrum of the new system for varying parameter  $b$ , and constant parameters  $b=12$ ,  $c=2$ , and  $d=6$ .

The Figure 2. shows the Matlab® simulation results of the new attractor.

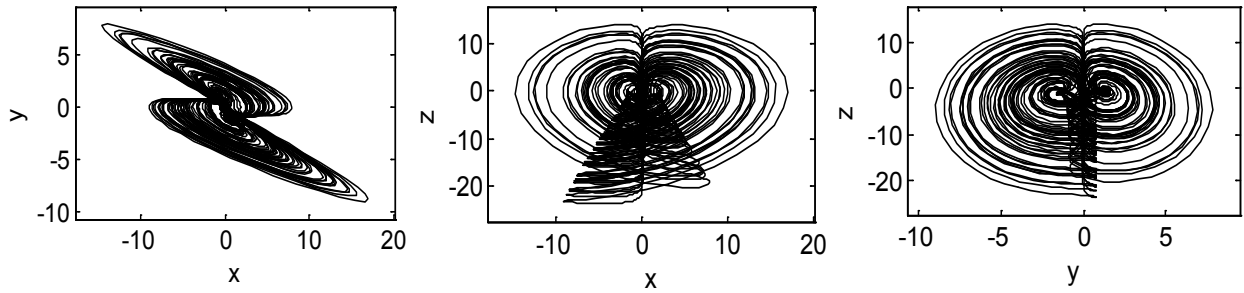


Figure 2. Phase portraits of the new attractor (  $a=3$ ,  $b=12$ ,  $c=2$ ,  $d=6$  )

### 3. Electronic Circuit Design and Implementation of The New Attractor

Figure 3. shows the designed circuit schematic for the new chaotic system(1). The circuit employs simple electronic elements such as resistors, and operational amplifiers, and is easy to construct. Despite the fact that origin(0,0,0) point is equilibria for the Lorenz, Chen, and Lü systems, it's not equilibria for the new system. Because of the fact that origin(0,0,0) point is not equilibria for the new system, it's not require the initial condition voltages for executing the circuit. Consequently realization of the new circuit is very easy.

We use UA741 opamps, the Analog Devices AD633JN multipliers, appropriate valued resistors and capacitors for pspice simulations and real circuit implementation. The circuit is supplied  $\pm 15V$  power supplies. Acceptable inputs to the AD633 multiplier IC are  $-10$  to  $+10$  V. The resistors R1 – R10, are all shown with nominal values in Figure 3.

The OrCad-PSpice® simulation results of the new attractor (x-y, x-z, y-z attractors respectively ) is shown in Figure 4. The real circuit implementation oscilloscope outputs(x-y, x-z, y-z attractors respectively) of the new chaotic system also shown in Figure 5. The parameters are taken as  $a=3$ ,  $b=12$ ,  $c=2$ ,  $d=6$  and the all initial conditions as zero on both the OrCad-PSpice® simulation and the real circuit implementation.

As can be seen the related figures, the Matlab® and the OrCad-PSpice® simulation results(Fig.2,4) and also the real circuit implementation oscilloscope outputs(Fig. 5) give the same conclusions.

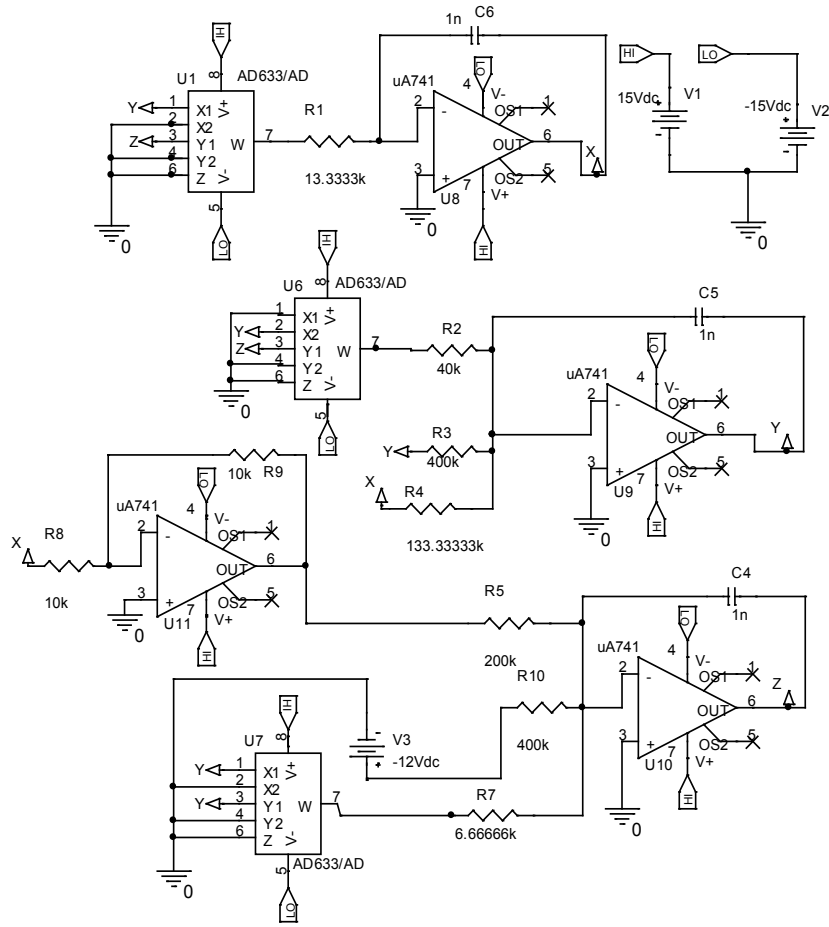


Figure 3. Designed Electronic Circuit Schematic of the New Chaotic Attractor

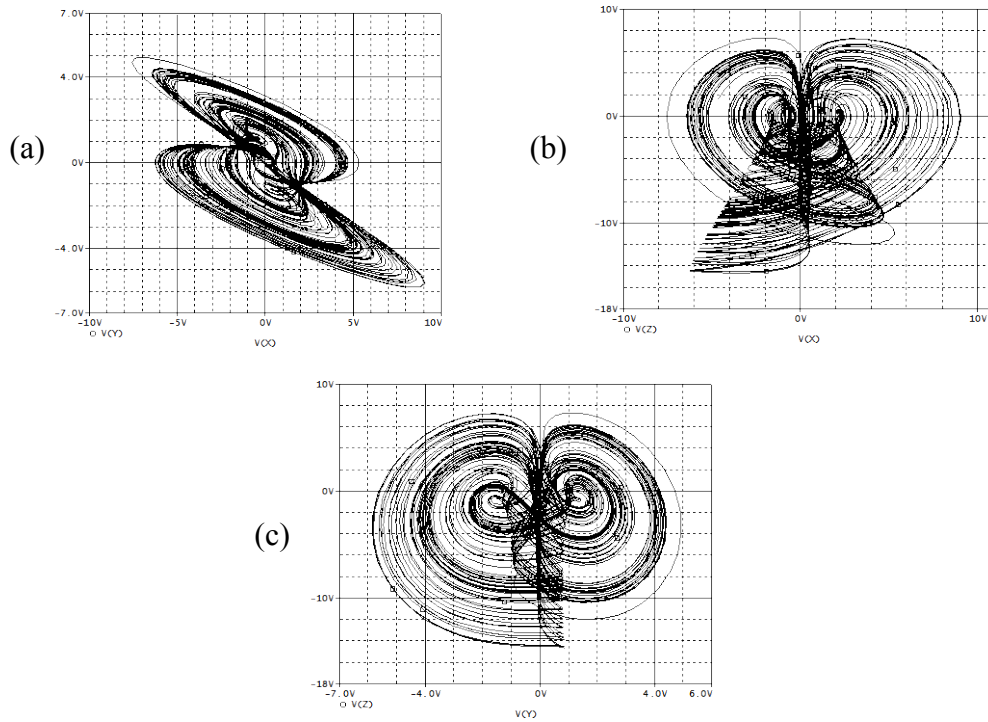


Figure 4. The Pspice simulation results of the New Chaotic Electronic Circuit. (a) x-y phase portrait, (b) x-z phase portrait, (c) y-z phase portrait



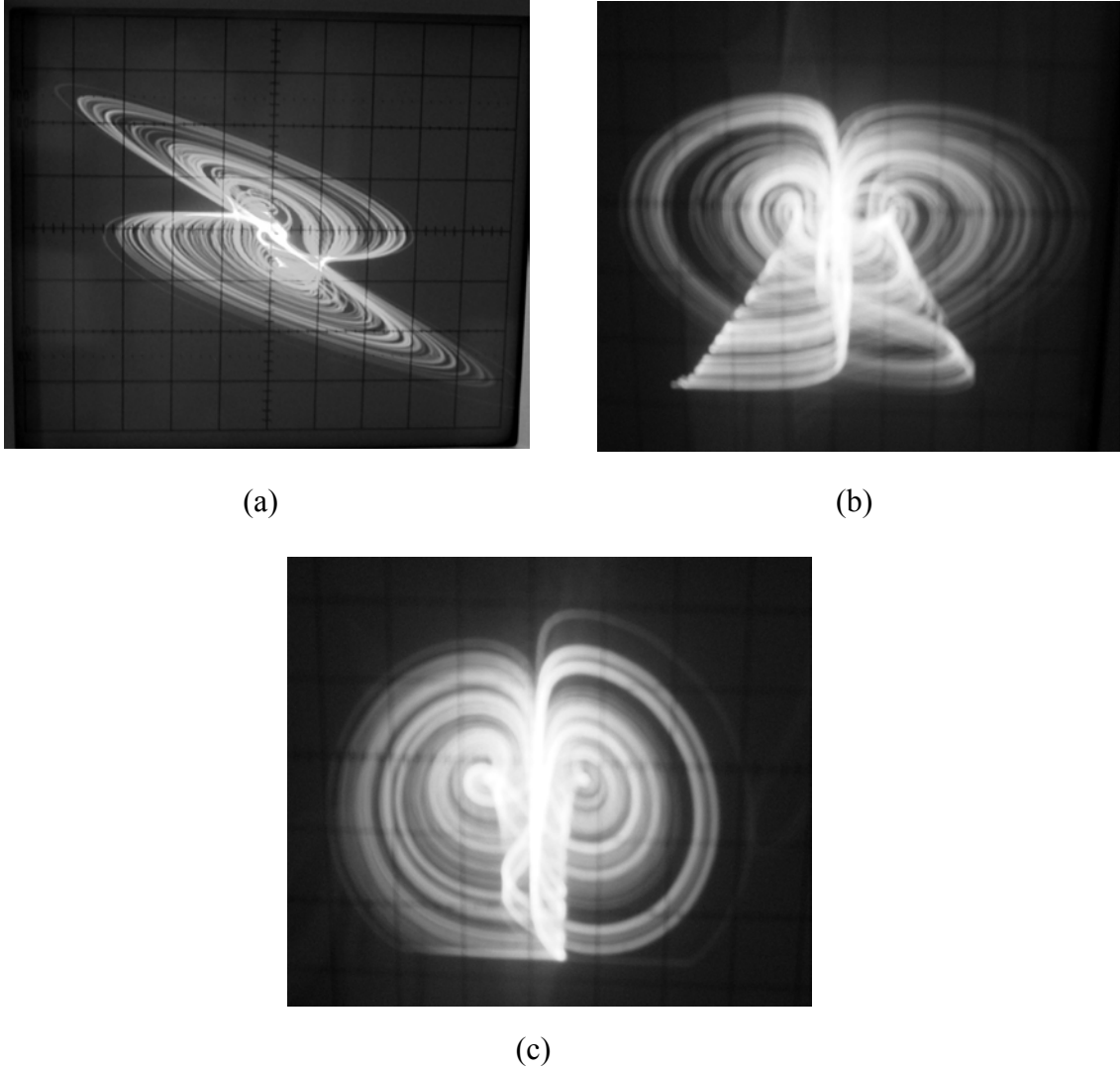


Figure 5. Oscilloscope outputs of the real circuit implementation of the new attractor (xy, xz, yz attractors respectively)

#### 4. Conclusions

The aim of this article is to present and further study a simple, interesting, and yet complex three-dimensional quadratic autonomous chaotic system which can generate complex 2-scroll chaotic attractors simultaneously. Our investigation was completed using a combination of theoretical analysis, simulations and real experimental implementation. Electronic circuitry of the new chaotic system is very simple. The simulation results were produced using Orcad-PSpice® program. As can be seen the related figures(Fig. 2,4), the Matlab® and the OrCad-PSpice® simulation results and also the real circuit implementation oscilloscope outputs(Fig. 5) give the same conclusions. To implement as electronics of this new chaotic system is very easy due to having zero initial conditions.

## References

- [1] E.N.Lorenz, Deterministic nonperiodic flow, *J.Atmos. Sci.*, 20:130-141(1963).
- [2] O.E.Rossler, An equation for continuous chaos, *Physics Letters A*, 57, 397-398(1976).
- [3] O.E.Rossler, Continuous chaos;four prototype equations, *Ann.(N.Y.) A. Sci.*, 316, 376-392(1979).
- [4] J.C. Sprott, Some simple chaotic flows, *Phys. Rev. E*, 50, R647-R650(1994).
- [5] G.Chen and T.Ueta, Yet another chaotic attractor, *Int. J. Bifurcation and Chaos*, Vol. 9,1465-1466(1999).
- [6] T.Ueta and G.Chen, Bifurcation analysis of Chen's attractor, *Int. J. Bifurcation and Chaos*, Vol 10(8), pp. 1917-1931(2000).
- [7] J.Lü and G.Chen, A new chaotic attractor coined, *Int. J. Bifurcation and Chaos*, Vol. 12(3), 659-661(2002).
- [8] A.Vanecek and S.Celikovsky, *Control Systems:From Linear Analysis to Synthesis of Chaos*, Prentice-Hall, London, 1996.
- [9] K.M.Cuomo and A.V. Oppenheim, Circuit Implementation of Synchronized Chaos with Applications to Communications, *Physical Review Letters*, vol. 71, 65(1993).
- [10] J.C. Sprott, A new class of chaotic circuit, *Physics Letters A*, 266,19-23.(2000).
- [11] S.Özoğuz, A.Elwakil and M.Kennedy, Experimental verification of the butterfly attractor in a modified Lorenz system, *IEEE Trans. Circuits Syst. I*, (2001).
- [12] A.Elwakil, M.Kennedy, Construction of classes of circuit-independent chaotic oscillators using passive-only nonlinear devices, *IEEE Trans. Circuits Syst. I*, 48,289-307(2001).
- [13] S.Yu, J.Lü, W.Tang and G.Chen, A general multiscroll Lorenz system family and its realization via digital signal processors, *Chaos*, 16,033126(2006).
- [14] M.E.Yalcin, J.A. K.Suykens, J.Vandewalle, and S.Ozoguz, Families of Scroll Grid Attractors, *Int. J. Bifurcation Chaos*, 12(1), pp. 23-41(2002).
- [15] M.E.Yalcin, J.A. K.Suykens, and J.P.L.Vandewalle, *Cellular Neural Networks, Multi-Scroll Chaos and Synchronization*, World Scientific, Singapore, 2005.
- [16] J.Lü and G.Chen, Generating Multiscroll Chaotic Attractors: Theories, Methods and Applications, *Int. J. Bifurcation Chaos*, 16,775-858(2006).
- [17] İ.Pehlivan, Y.Uyaroglu, Rikitake Attractor and its Synchronization Application for Secure Communication Systems, *Journal of Applied Sciences*, 7(2):232-236(2007).
- [18] İ.Pehlivan, Y.Uyaroglu, Simplified Chaotic Diffusionless Lorenz Attractor and its Application to Secure Communication Systems, *IET Communications*, 1(5),1015-1022(2007)

## TESTING STABILITY AND ROBUSTNESS IN THREE CRYPTOGRAPHIC CHAOTIC SYSTEMS

N. A. Anagnostopoulos<sup>a</sup>, K. Konstantinidis<sup>a</sup>, A. N. Miliou<sup>a,\*</sup>  
and S. G. Stavrinos<sup>b</sup>

<sup>a</sup> Department of Informatics, Aristotle University of Thessaloniki, GR 54124, Thessaloniki, Greece

<sup>b</sup> Physics Department, Aristotle University of Thessaloniki, GR 54124, Thessaloniki, Greece

March 5, 2010

In practical applications it is crucial that the drive-response systems, although identical in all respects, are synchronized at all times even if there is noise present. In this work we are testing the stability and robustness of three distinct and well-known cryptographic chaotic systems and compare the results in relation to the desired security.

**Keywords:** Chaos, chaotic signal, nonlinear circuits, synchronization, communication system security

### 1 Introduction

The use of synchronized chaotic systems for communications usually relies on the robustness of the synchronization within the transmitter and receiver pair [1-7]. However, if the communication channel is noisy and/or there is internal noise at the electronic circuitry, the distorted signal at the receiver input might cause considerable synchronization mismatch between the transmitter-receiver pair [8-12].

In this paper, we consider three dynamical systems; the first one is presented in [13], the second one is a Chua-like dynamical system [14] and the third one is a Lorenz-like system presented in [15] and we compare the effect of noise on the synchronization of the systems with different noise levels.

The paper is organized as follows: the circuits' descriptions and the synchronization properties are presented in Section 2. The simulation results obtained are shown in Section 3. Finally, concluding remarks are given in Section 4.

---

\* Corresponding author. Tel.: +30 2310 998407; fax: +30 2310 998419.  
E-mail address: amiliou@csd.auth.gr (A.N. Miliou)

## 2 Description of Circuits

We present three non-linear cryptographic chaotic circuits and investigate their synchronization's stability and robustness to external noise.

### 2.1 Non-autonomous, non-linear electronic circuit

The first circuit [13] is a combination of two stages (both for the transmitter and the receiver). The first stage is a linear periodic oscillator consisting of an inverting amplifier and two integrators. The second stage that acts as nonlinear feedback consists of a comparator, a sub-stage that adjusts voltage levels from  $\pm V_{\text{sat}}$  Volts to 0 and 5 Volts respectively, a XOR gate and a buffer with a voltage divider as input. This stage is used to externally trigger the oscillator. The entire circuit produces chaotic oscillations under certain triggering conditions. All amplifiers, integrators, the comparator and the buffer were implemented with operational amplifiers.

The chaotic voltage across the last of the two integrators is selected and compared with a certain dc voltage level. The result of the comparison is a voltage signal switching between  $\pm V_{\text{sat}}$  voltage levels, where  $\pm V_{\text{sat}}$  are the positive and negative saturation levels of the operational amplifier. This signal, after being normalized to 0 and 5 Volts, is multiplexed at the transmitter's XOR gate with the message and transmitted to the receiver. The transmitted signal is used at the receiver to drive the receiver's XOR gate, which decrypts the original message, Fig.1. The transmitter-receiver system is governed by the following set of equations:

$$H^S = \begin{cases} -V_{\text{sat}}, & V_2 > V_o \\ +V_{\text{sat}}, & V_2 < V_o \end{cases} \Leftrightarrow H^S = \begin{cases} 0, & \left(\frac{V_2}{V_o}\right) > 1 \\ 1, & \left(\frac{V_2}{V_o}\right) < 1 \end{cases} \quad (1)$$

$$RC \frac{dV_2}{dt} = -V_1 - \frac{R}{R_s} V_2 \quad (2)$$

$$RC \frac{dV_1}{dt} = -V - \frac{R}{R_s} V_1 \quad (3)$$

$$\text{Where } V = -\frac{R}{R_f} V_{\text{out}} - V_2, V_{\text{out}} = U^* \cdot F, F = M \oplus H^S \text{ and } U^* = \kappa \cdot 5 \text{ V},$$

where  $\kappa$  is the ratio of potentiometer  $R_2$ . When we are adding the filter after  $V_{\text{out}2}$

$$V_C = \frac{1}{\sqrt{1 + \omega^2 R_e^2 C_e^2}} V_{\text{out}2} \quad (4)$$

$$V_M = \begin{cases} 0 \text{ V}, & V_C \leq 2.5 \text{ V} \\ 5 \text{ V}, & V_C > 2.5 \text{ V} \end{cases} \Leftrightarrow V_M = \begin{cases} 0, & V_C \leq 2.5 \text{ V} \\ 1, & V_C > 2.5 \text{ V} \end{cases} \quad (5)$$

The values of the parameters used in circuit A are given in Table 1.

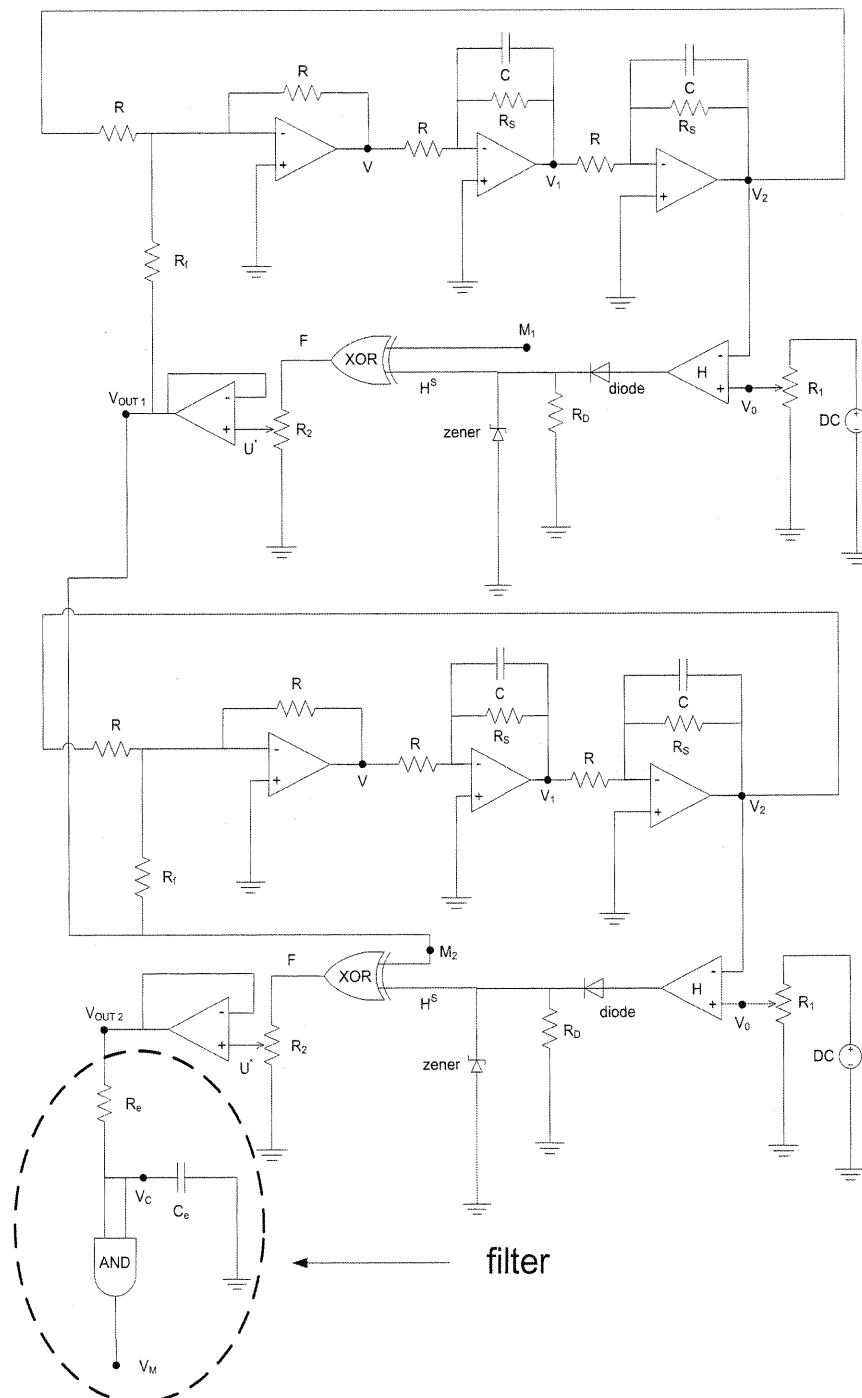


Fig.1 Schematic diagram of the transmitter-receiver system (circuitA).

R	10 k $\Omega$
R <sub>s</sub>	510 k $\Omega$
R <sub>f</sub>	18 k $\Omega$
R <sub>1</sub>	10 k $\Omega$ (potentiometer at 50%)
R <sub>2</sub>	10 k $\Omega$ (potentiometer at 100%)
R <sub>D</sub>	1 k $\Omega$
DC voltage	2 V
C	1 nF
diode	1N4001
zener	1N4733A
AND gate	74ALS08M
XOR gate	74ALS86M
op amp's	TL084CD

Table 1 Parameters values and types of the elements used in the circuit A

## 2.2 Chua-like non-linear electronic circuit

The second circuit is a combination of two stages (both for the transmitter and the receiver). The first stage is a Chua-like chaotic oscillator [14] where the nonlinear resistor (Chua's diode) is implemented with two negative resistors connected in parallel, using two operational amplifiers and six resistors. The circuit has the same functionality with the original Chua's circuit and with appropriate values of the variable resistor produces chaotic oscillations.

The second stage consists of a comparator, a sub-stage that adjusts voltage levels from  $\pm V_{\text{sat}}$  Volts to 0 and 5 Volts respectively, a XOR gate and a buffer with a voltage divider as input. Both the comparator and the buffer were implemented with operational amplifiers. The receiver is identical to the transmitter except that a low-pass filter is added at the buffer's output, followed by an AND gate.

The chaotic voltage across one of the two capacitors is selected and compared with a certain dc voltage level. The result of the comparison is a voltage signal switching between  $\pm V_{\text{sat}}$  voltage levels, where  $\pm V_{\text{sat}}$  are the positive and negative saturation levels of the operational amplifier. This signal, after being normalized to 0 and 5 Volts, is multiplexed at the transmitter's XOR gate with the message and transmitted to the receiver. The transmitted signal is used at the receiver to drive the receiver's XOR gate, which decrypts the original message. There is no feedback, so we use the voltage across the other capacitor as the synchronization signal between transmitter and receiver, Fig.2. The transmitter-receiver system is governed by the following set of equations:

$$C_1 \frac{dV_{C1}}{dt} = G(V_{C2} - V_{C1}) - g(V_{C1}) \quad (6)$$

$$C_2 \frac{dV_{C2}}{dt} = G(V_{C1} - V_{C2}) + i_L \quad (7)$$

$$L \frac{di_L}{dt} = -V_{C2} \quad (8)$$

$$\text{Where } g(V_{C1}) = m_0 V_{C1} + \frac{1}{2}(m_1 - m_0) (|V_{C1} + B_p| - |V_{C1} - B_p|), \quad G = \frac{1}{R_C},$$

$$m_0 = m_{11} + m_{02} = \frac{1}{R_B} - \frac{1}{R_{g1}}, \quad m_1 = m_{11} + m_{12} = -\left(\frac{1}{R_{g1}} + \frac{1}{R_{g2}}\right) \quad \text{and}$$

$$B_p = \frac{R_{g2}}{R_B + R_{g2}} E_{sat}.$$

$$V_{out} = U^* \cdot F \quad (9)$$

$$\text{Where } F = M \oplus H^S, \quad H^S = \begin{cases} -V_{saturation}, & V_{C1} > V_o \\ +V_{saturation}, & V_{C1} < V_o \end{cases} \Leftrightarrow H^S = \begin{cases} 0, & \left(\frac{V_{C1}}{V_o}\right) > 1 \\ 1, & \left(\frac{V_{C1}}{V_o}\right) < 1 \end{cases}$$

and  $U^* = \kappa \cdot 5 \text{ V}$ , where  $\kappa$  is the ratio of potentiometer  $R_2$ .

While when we are adding the filter after  $V_{out2}$

$$V_C = \frac{1}{\sqrt{1 + \omega^2 R_e^2 C_e^2}} V_{out2} \quad (10)$$

$$V_M = \begin{cases} 0 \text{ V}, & V_C \leq 2.5 \text{ V} \\ 5 \text{ V}, & V_C > 2.5 \text{ V} \end{cases} \Leftrightarrow V_M = \begin{cases} 0, & V_C \leq 2.5 \text{ V} \\ 1, & V_C > 2.5 \text{ V} \end{cases} \quad (11)$$

The values of the parameters used in circuit B are given in Table 2.

$R_A$	220 $\Omega$
$R_B$	22 k $\Omega$
$R_C$	2 k $\Omega$ (potentiometer at 50% [chaotic region ranging from ~20% to ~90%])
$R_{g1}$	2.2 k $\Omega$
$R_{g2}$	3.3 k $\Omega$
$R_D$	1 k $\Omega$
$R_1$	10 k $\Omega$ (potentiometer at 50%)
$R_2$	10 k $\Omega$ (potentiometer at 100%)
$C_1$	10 nF
$C_2$	100 nF
$L$	18 mH
DC voltage	2 V
diode	1N4001
zener	1N4733A
AND gate	74ALS08M
XOR gate	74ALS86M
op amp's	TL084CD ( $E_{sat} \approx 7.5 \text{ V}$ for 9V feed)

Table 2 Parameters values and types of the elements used in the circuit B

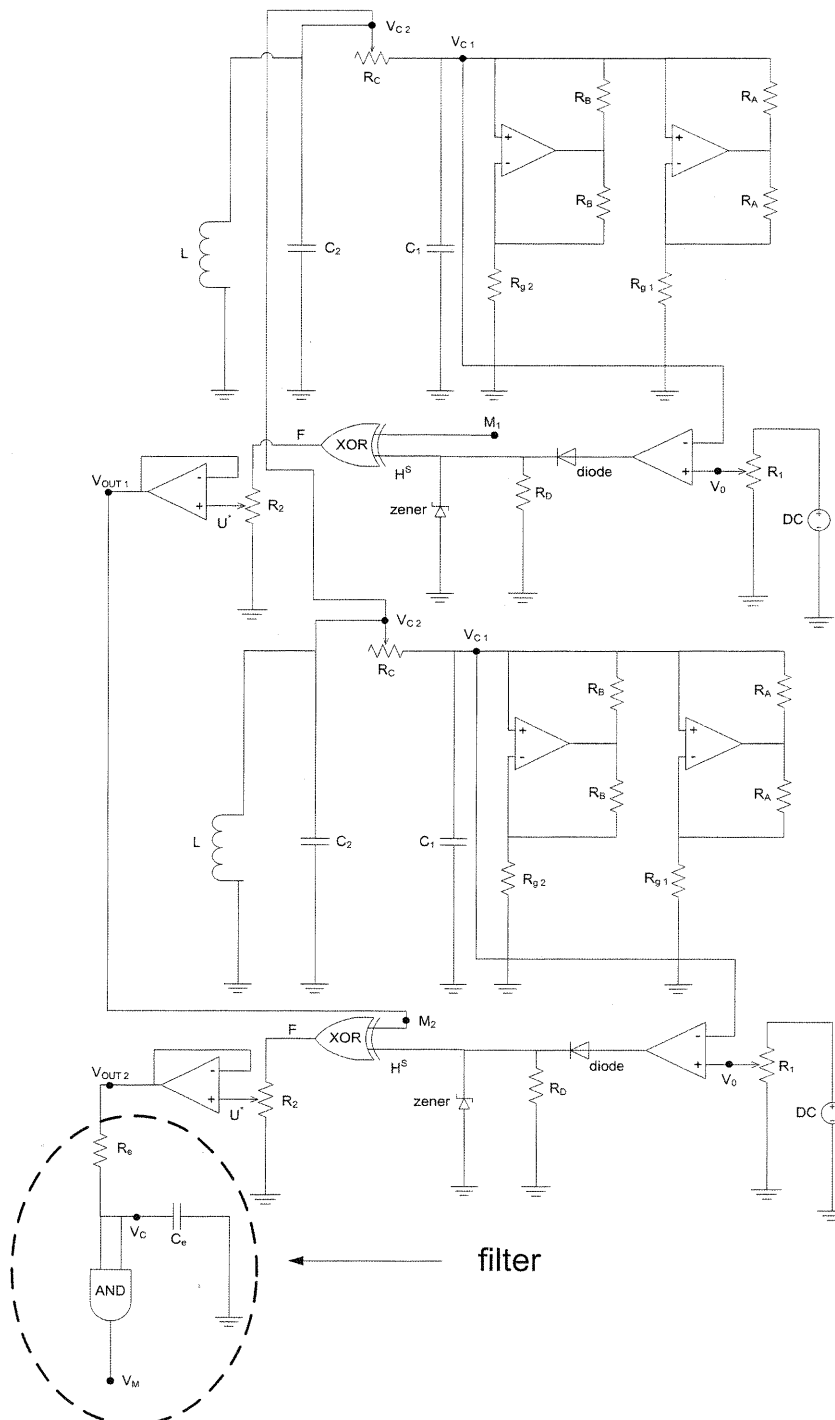


Fig.2 Schematic diagram of the Chua-like transmitter-receiver system (circuit B).



### 2.3 Lorenz-like non-linear electronic circuit

The third circuit is a combination of two stages (both for the transmitter and the receiver). The first stage is a Lorenz-like chaotic oscillator [15]. It consists of three integrators, four summing amplifiers (having two inputs each), three inverting amplifiers (having one input each), a non-inverting amplifier (with one input) and two multipliers.

The second stage consists of a comparator, a sub-stage that adjusts voltage levels from  $\pm V_{\text{sat}}$  Volts to 0 and 5 Volts respectively, a XOR gate and a buffer with a voltage divider as input. All amplifiers, integrators, the comparator and the buffer were implemented with operational amplifiers. The receiver is identical to the transmitter except that a low-pass filter is added at the buffer's output, followed by an AND gate.

The chaotic voltage across one of the three capacitors is selected and compared with a certain dc voltage level. The result of the comparison is a voltage signal switching between  $\pm V_{\text{sat}}$  voltage levels, where  $\pm V_{\text{sat}}$  are the positive and negative saturation levels of the operational amplifier. This signal, after being normalized to 0 and 5 Volts, is multiplexed at the transmitter's XOR gate with the message and transmitted to the receiver. The transmitted signal is used at the receiver to drive the receiver's XOR gate, which decrypts the original message. Again, there is no feedback, so we use the voltage across one of the other two capacitors as the synchronization signal between transmitter and receiver, Fig.3. The transmitter-receiver system is governed by the following set of equations:

$$\frac{dV_1}{dt} = -\frac{R_{s0}}{R_x CR} V_1 - \frac{1}{R_x CR} V_3 \quad (12)$$

$$\frac{dV_3}{dt} = -\frac{R_{200}}{R_x CR} V_1 - \frac{1}{R_x CR_{200}} \left(1 + \frac{R_{30}}{R_x}\right) V_1 V_2 \quad (13)$$

$$\frac{dV_2}{dt} = -\frac{R_6}{R_x CR_3} V_2 + \frac{1}{R_x C} \left(1 + \frac{R_{30}}{R_x}\right) V_1 V_3 \quad (14)$$

$$V_{\text{out}} = U^* \cdot F \quad (15)$$

$$\text{where } F = M \oplus H^S, \quad H^S = \begin{cases} -V_{\text{saturation}}, & V_3 > V_o \\ +V_{\text{saturation}}, & V_3 < V_o \end{cases} \Leftrightarrow H^S = \begin{cases} 0, & \left(\frac{V_3}{V_o}\right) > 1 \\ 1, & \left(\frac{V_3}{V_o}\right) < 1 \end{cases}$$

and  $U^* = \kappa \cdot 5 \text{ V}$ , where  $\kappa$  is the ratio of potentiometer  $R_2$ .

While when we are adding the filter after  $V_{\text{out} 2}$

$$V_C = \frac{1}{\sqrt{1 + \omega^2 R_e^2 C_e^2}} V_{\text{out} 2} \quad (16)$$

$$V_M = \begin{cases} 0 \text{ V}, & V_C \leq 2.5 \text{ V} \\ 5 \text{ V}, & V_C > 2.5 \text{ V} \end{cases} \Leftrightarrow V_M = \begin{cases} 0, & V_C \leq 2.5 \text{ V} \\ 1, & V_C > 2.5 \text{ V} \end{cases} \quad (17)$$

The values of the parameters used in circuit C are given in Table 3.



R	10 k $\Omega$
R <sub>50</sub>	50 k $\Omega$
R <sub>x</sub>	1 k $\Omega$
R <sub>200</sub>	200 k $\Omega$
R <sub>v</sub>	2 k $\Omega$
R <sub>30</sub>	30 k $\Omega$
R <sub>3</sub>	3 k $\Omega$
R <sub>6</sub>	6 k $\Omega$
R <sub>100M</sub>	100 M $\Omega$
R <sub>1</sub>	10 k $\Omega$ (potentiometer at 50%)
R <sub>2</sub>	10 k $\Omega$ (potentiometer at 100%)
R <sub>D</sub>	1 k $\Omega$
C	100 nF
DC1 voltage	2 V
DC2 voltage	-20 mV
diode	1N4001
zener	1N4733A
AND gate	74ALS08M
XOR gate	74ALS86M
op amp's	TL084CD

Table 3 Parameters values and types of the elements used in the circuit C

### 3. Simulation results

We have selected Multisim to simulate the three chaotic systems, since it provides an interface similar to the real implementation environment. External noise is applied on the communication channel, while different noise amplitudes  $A$  have been utilized ranging from 0.01% to 50% of the mean signal amplitude. As the noise amplitude  $A$  is increased, the synchronization of the system continuously deteriorates and is practically destroyed in all cases above a certain noise level.

A thermal noise generator connected at the communication channel provided artificial external noise added at the simulation. The information added is a square pulse with a frequency of 6.222 KHz ranging from 0 to 5 V connected at the XOR gate of each circuit's transmitter. Both the transmitter and the receiver are identical circuits. The filters used in the simulations are presented in Table 4.

R <sub>e</sub>	Filter 1 R <sub>e</sub> =40 $\Omega$ Filter 2 R <sub>e</sub> =1 k $\Omega$ Filter 3 R <sub>e</sub> =1 k $\Omega$
C <sub>e</sub>	Filter 1 C <sub>e</sub> =7 nF Filter 2 C <sub>e</sub> =2.5 nF Filter 3 C <sub>e</sub> =7 nF

Table 4 Filter parameters

### 3.1 Circuit A

Fig. 4 and 5 show the response of circuit A, without noise and with the application of 10% noise on the communication channel, which also acts as the synchronization channel. Different noise amplitudes  $A$  have been utilized and the synchronization of the system deteriorates severely above 10% noise level.

It is apparent that the signal at the receiver without filtering shows some glitches due to the response of the circuit's elements, which disappear when a filter is added at the receiver's output. In Fig. 5, filter 2 eliminates the glitches completely compared to filter 1 although both filters introduced a slight time shift in the response signal.

However, the synchronization is good (up to 10% noise level) and the transmitted information is received and reconstructed (decoded) at the output with good quality.

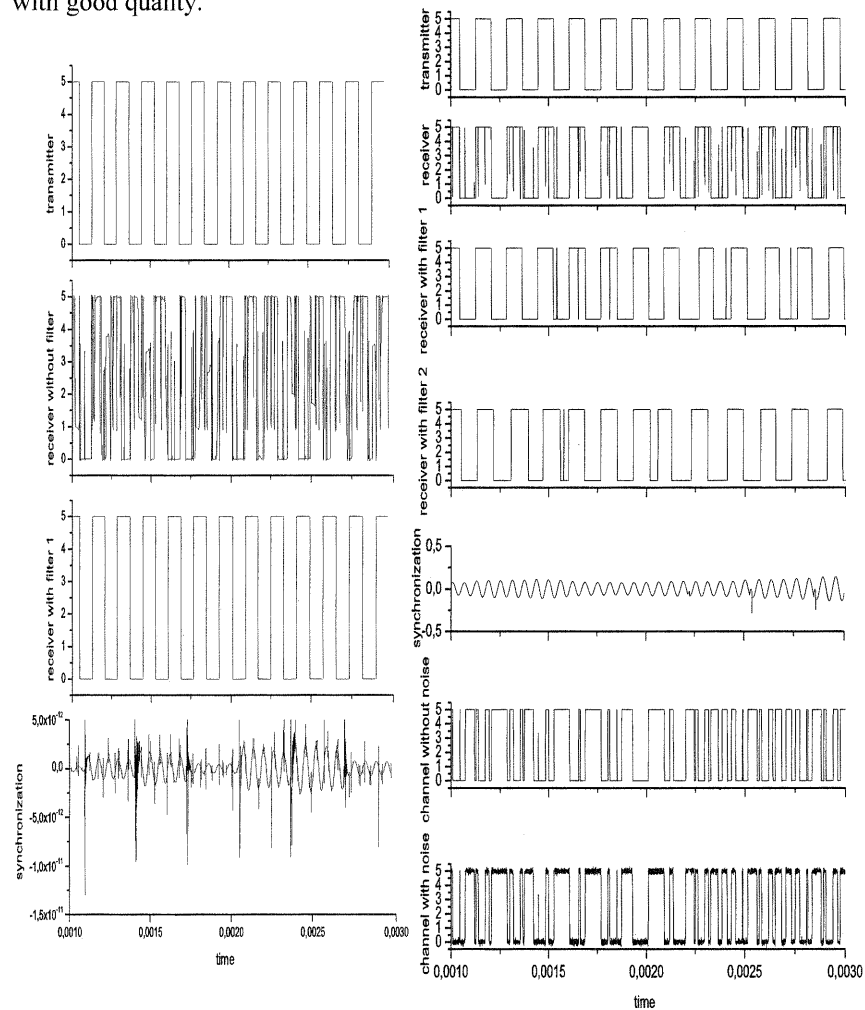


Fig.4 Response of circuit A without noise

Fig.5 Response of circuit A with 10% noise

### 3.2 Circuit B (Chua-like)

In circuit B we used two communication channels, one for the synchronization and one for the information transmittance. All simulations of circuit B at the receiver are performed with the usage of filter 1.

Similarly with the previous circuit, we experimented with different noise levels and the synchronization is very good up to 10% noise level, Fig. 6 and 7. The noise was added either to synchronization channel only or to information channel only or to both channels. However, one could observe that in the third case, at the receiver with noise in both channels, the response signal demonstrates a transient behavior before perfect synchronization is achieved, Fig. 7.

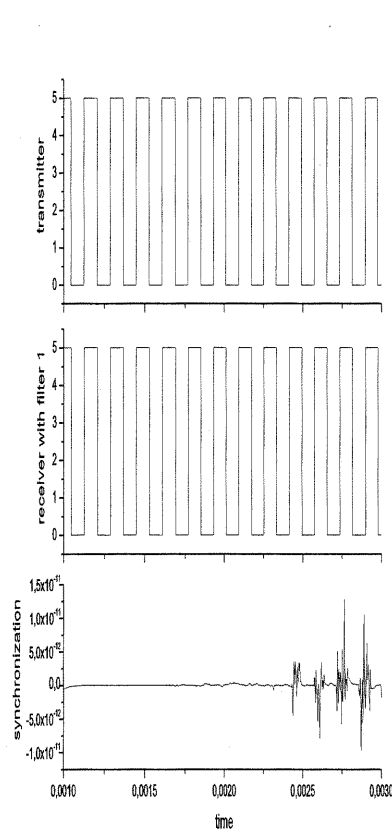


Fig.6 Response of circuit B without noise

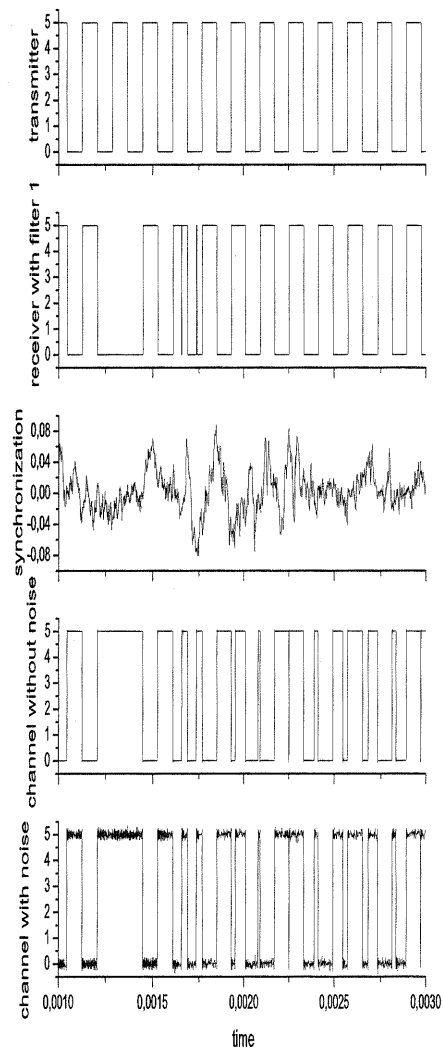


Fig.7 Response of circuit B with 10% noise

### 3.3 Circuit C (Lorenz-like)

In circuit C, as in B, we used two communication channels, one for the synchronization and one for the information transmittance, while filter 3 is used at the receiver.

Additionally, in this system we can distinguish two separate cases (Ca and Cb); the first one where we use  $V_1$  as the synchronization voltage and  $V_3$  is the voltage that goes to the comparator (Fig. 8 and 9). The schematic diagram in Fig. 3 is corresponding to this case. In the second case we are using  $V_3$  as the synchronization voltage and  $V_1$  as the voltage that goes to the comparator (Fig. 10 and 11).

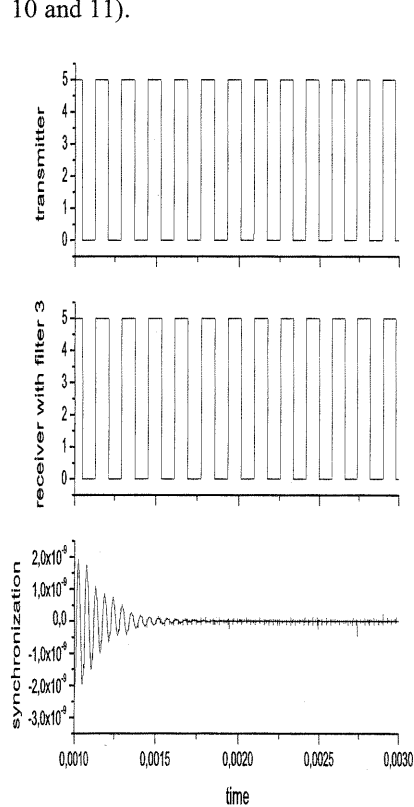


Fig.8 Response of circuit Ca without noise

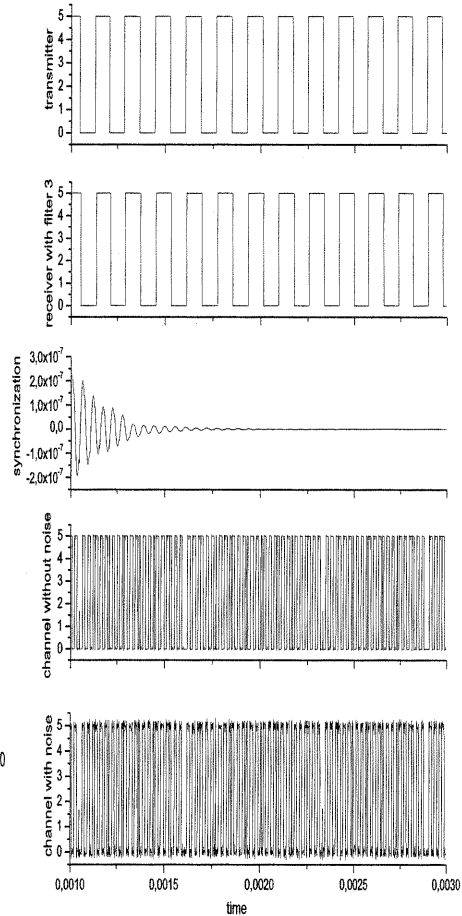


Fig.9 Response of circuit Ca with 1% noise

Fig. 8 and 9 show the response of circuit Ca without noise and with the application of 1% noise on the communication (synchronization and information) channels. Different noise amplitudes  $A$  have been utilized and the synchronization of the system deteriorates severely above 1% noise level.

However, it is apparent that the signal at the receiver with noise in both the information and the synchronization channel is decoded with no impairment at the present level of noise. The synchronization of the transmitter –receiver system is very good up to 1% noise level.

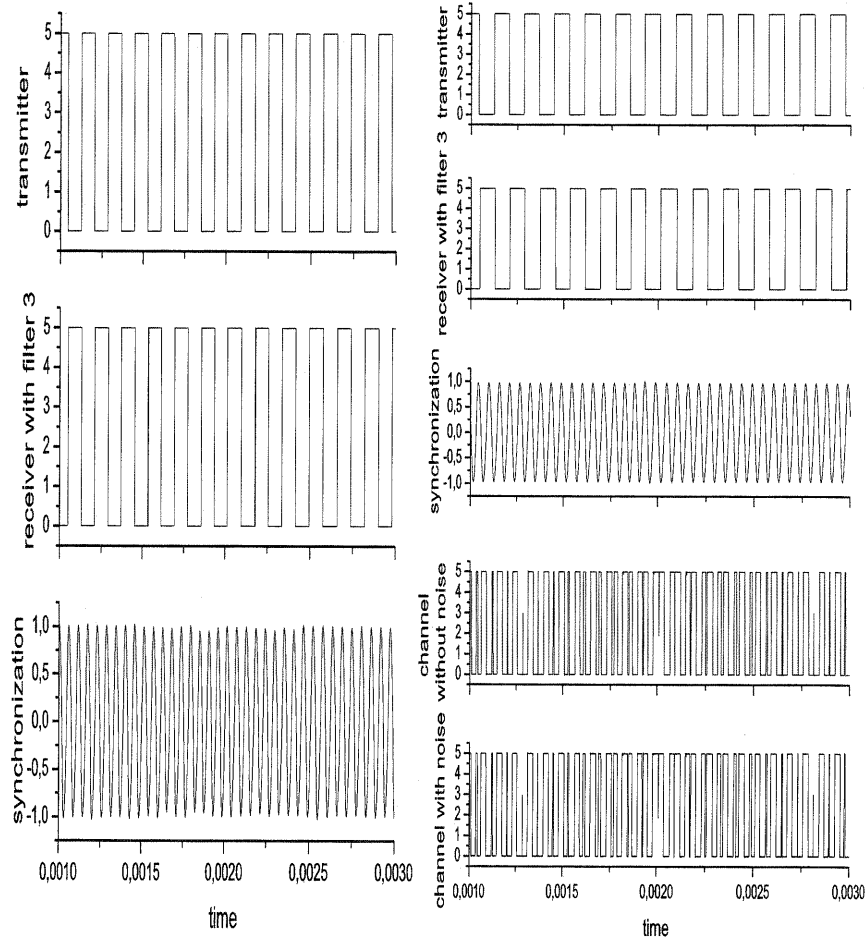


Fig.10 Response of circuit Cb without noise Fig.11 Response of circuit Cb with 1% noise

Fig. 10 and 11 depict the response of circuit Cb without and with noise. In this case we observed anti-synchronization (AS) phenomenon in the coupled Lorenz-like chaotic oscillators depending on the initial conditions [16]. AS has potential application in practical fields such as secure communications and digital communication. As in circuit Ca the system is robust up to 1% noise level and the received signal although anti-synchronized is decoded with no impairments.

#### 4. Concluding remarks

The use of synchronized chaotic systems for communications relies on the robustness of the synchronization to perturbations in the drive signal.

In this work we have studied the influence of noise on the synchronization of the transmitter–receiver pair presented in [13, 14, 15] by simulating the behavior of the systems in Multisim. The results have shown the robustness of the systems on the synchronization for similar levels of noise amplitudes. Specifically, circuits A and B are withstanding higher amplitude noise perturbations comparing to circuit C. Among circuits A and B, the latter one uses a filter with a lower cut-off frequency in order to eliminate the glitches appearing at the receiver and, even though it shows some transient behavior, the output is of better quality than A. Although circuit C uses the filter with the lowest cut-off frequency, it decodes the signal without flaws even in the anti-synchronization case.

Concluding our experimental study, we could state that there is no doubt that robustness to noise is very advantageous for the synchronization of a system, especially when the system is realized with off-the-shelf electronics.

#### Acknowledgements

This work was supported by NATO ICS.EAP.CLG 983334.



## References

1. G. Kolumban, M.P. Kennedy, L.O. Chua, The role of synchronization in digital communications using chaos—part II: chaotic modulation and chaotic synchronization, *IEEE Trans. Circuits Syst. I* 45 (11) (1998) 1129–1140.
2. L.M. Pecora, T.L. Carroll, Driving Systems with chaotic signals, *Phys. Rev. A*, 44(4), pp. 2374–2383, 1991.
3. L.M. Pecora, T.L. Carroll, Synchronization in Chaotic Systems, *Phys. Rev. Lett.*, 64(8), pp.821–824, 1990.
4. M.N. Lorenzo, V. Perez-Munuzuri, V. Perez-Villar, Noise performance of a synchronization scheme through compound chaotic signal, *Int. J. Bifurcation Chaos* 10 (12) (2000) 2863–2870.
5. M. Murali, M. Lakshmanan, Drive-response scenario of chaos synchronization in identical nonlinear systems, *Phys. Rev. E* 49 (5) (1994) 4882–4885.
6. L.M. Pecora, T.L. Carroll, Synchronization in chaotic systems, *Phys. Rev. Lett.* 64 (8) (1990) 821–823.
7. A. Pikovsky, M. Rosenblum, J. Kurths, Synchronization: a Universal Concept in Nonlinear Sciences, first paperback ed., The Cambridge Nonlinear Science Series, vol. 12, Cambridge University Press, Cambridge, 2003.
8. E. Sanchez, M.A. Matias, V. Perez-Munuzuri, Analysis of synchronization of chaotic systems by noise: an experimental study, *Phys. Rev. E* 56 (4) (1997) 4068–4071.
9. M. Wang, Z. Hou, H. Xin, Internal noise-enhanced phase synchronization of coupled chemical chaotic oscillators, *J. Phys. A* 38 (1) (2005) 145–152.
10. X. Yang, T.X. Wu, D.L. Jaggard, Synchronization recovery of chaotic wave through an imperfect channel, *IEEE Antennas Wireless Propag. Lett.* 1 (2002) 154–156.
11. G. Chen, Control and Synchronization of chaotic Systems (a bibliography), <ftp.erg.uh.edu/pub/TeX/chaos.tex>, University of Houston, Houston, TX, USA.
12. L. Kocarev, U. Parlitz, General approach for chaotic synchronization with applications to communication, *Phys. Rev. Lett.*, 4, p.5028, 1994.
13. G. Mycolaitis, A. Tamaševičius, A. Cenys, A. Namajunas, K. Navionis, A.N. Anagnostopoulos, Globally synchronizable non-autonomous chaotic oscillator, in: *Proceedings of Seventh International Workshop on Nonlinear Dynamics of Electronic Systems*, Denmark, July 1999, pp.277–280.
14. M. P. Kennedy, Robust op amp realization of Chua's circuit, *Frequenz*, 46, no. 3–4, p66–88, 1992.
15. Xian-Feng Li, Yan-Dong Chu, Jian-Gang Zhang, Ying-Xiang Chang, Nonlinear dynamics and circuit implementation for a new Lorenz-like attractor, *Chaos, Solitons & Fractals* (2008), doi:10.1016/j.chaos.2008.09.011
16. Chil-Min Kim, Sunghwan Rim, Won-Ho Kye, Jung-Wan Ryu, Young-Jai Park, Anti-synchronization of chaotic oscillators, *Physics Letters A* 320 (2003) 39–46.

## Experimental In-Out Synchronization- Intermittency between two bidirectionally coupled circuits

I.M. Kyprianidis<sup>(1)</sup>, Ch.K. Volos<sup>(1)</sup>, S.G. Stavriniades<sup>(1)</sup>,  
I.N. Stouboulos<sup>(1)</sup>, A.N. Anagnostopoulos<sup>(1)</sup> and A.N. Miliou<sup>(2)</sup>

<sup>(1)</sup>Physics Dept., Aristotle University of Thessaloniki, GR-54124, Greece.

<sup>(2)</sup>Dept. of Informatics, Aristotle University of Thessaloniki, GR-54124, Greece.

March 5, 2010

In this paper the in-out intermittent synchronization of two coupled, nonlinear, double-scroll, chaotic operating, circuits is experimentally studied. The synchronized circuits are bidirectionally coupled via a linear resistor. In order to determine the kind of intermittency demonstrated laminar lengths versus the deviation of the control parameter from its critical value, and the mean laminar length distribution, are studied<sup>1</sup>.

### 1 Introduction

Research activities in chaotic circuits and systems, resulted in a lot of publications on the related phenomena that such systems exhibit [1], [2]. Since the introduction of the notion of chaotic synchronization by Pecora and Carroll [3], the topic of coupled chaotic circuit synchronization has been studied intensely, with numerous interesting applications, such as broadband communications systems [4]-[7] and cryptography [9]-[13], coming out of this research.

An important issue on the synchronization of chaotic systems is the way that it is established. In most cases, when the coupling factor falls short of a critical value, the synchronized state becomes unstable and characteristic intermittent dynamics are observed. The difference between two signals from each subsystem blows occasionally from its almost zero value, demonstrating instant desynchronization. This kind of transition is termed “On-Off Intermittency” and its dynamics are quite different from those of the three classic intermittency types (scenarios) observed in chaotic systems [14]-[16]. Such intermittent behaviour is observed both in unidirectional and bidirectional coupling.

---

<sup>1</sup> This work was partly presented in the “3rd International Interdisciplinary Symposium on Chaos and Complex Systems – CCS2010”

There have been also reports of another type of intermittent behavior known as “In-Out intermittency” [17], [18]. This kind of intermittency is a more general version of “On-off intermittency” [19], appearing most frequently in chaotic synchronization of bidirectional coupled circuits and systems [20], [21]. In the case of “In-Out intermittency”, trajectories also escape occasionally from the relatively steady synchronized state to irregular “burst” states and then quickly return back to the synchronization. As a result, the system attractor blows out from a lower dimensional subspace in a random-like way, due to transverse instability [18].

The route from synchronization to desynchronization has been experimentally studied for two coupled, double-scroll circuits for the case of a certain parameter set set both bidirectionally [22] and unidirectionally coupled [23]. At those papers it was shown that the statistics obeyed the laws describing On-Off Intermittency. In the present paper, the same resistively coupled double scroll circuits are experimentally studied employing another set of parameters. With this configuration the system undergoes the transition from synchronization to desynchronization of the In-Out Intermittency type.

## 2 The coupled double-scroll circuit

The system that is formed by the bidirectional resistive coupling of two identical nonlinear double-scroll circuits, appears in Fig. 1. Both circuits are trimmed to

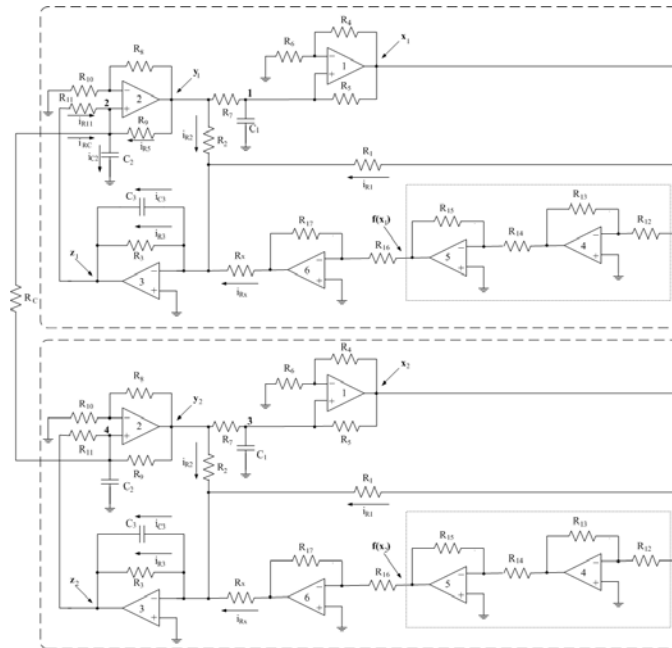


**Figure 1:** The  $v_{c2}$ -bidirectionally coupled (y-coupled) double-scroll circuits.

operate in a chaotic mode. The normalized set of state equations that govern the two subcircuit system dynamics is:

$$\begin{cases} \dot{x}_1 = y_1 \\ \dot{y}_1 = z_1 + \xi \cdot (y_2 - y_1) \\ \dot{z}_1 = -\alpha \cdot x_1 - \alpha \cdot y_1 - b \cdot z_1 + c \cdot f(x_1) \\ \dot{x}_2 = y_2 \\ \dot{y}_2 = z_2 + \xi \cdot (y_1 - y_2) \\ \dot{z}_2 = -\alpha \cdot x_2 - \alpha \cdot y_2 - b \cdot z_2 + c \cdot f(x_2) \end{cases} \quad (1)$$

The first three equations of system (1) describe the first of the two coupled identical double-scroll circuits, while the other three describe the second one. Signals  $x_{1,2}$ ,  $y_{1,2}$ , and  $z_{1,2}$ , represent the voltages at the outputs of the operational amplifiers (LF411) 1, 2 and 3 respectively, as it is shown in Fig. 1. Saturation function  $f(x_{1,2})$ , used in Eq. (1) is defined by the expression of Eq. (2):

$$f(x) = \begin{cases} 1, & \text{if } x \geq k \\ \frac{1}{k}x, & \text{if } -k \leq x < k \\ -1, & \text{if } x < -k \end{cases} \quad (2)$$

This implementation  $f(x_{1,2})$  is implemented in such a way that the saturation plateaus are at  $\pm 1$  and the slope of the linear region is  $1/k$ . Since the coupling of the two circuits is bidirectional, the coupling coefficient  $\xi = R/2R_C$  is present at the equations of both circuits.

Resistance and capacitor values were:  $R=R_4=R_5=R_6=R_7=R_8=R_9=R_{10}=R_{11}=20\text{k}\Omega$ , and  $C_1=C_2=C_3=1\text{nF}$ . The saturated circuit was implemented with the operational amplifiers (LF411) numbered 4 and 5, where  $R_{12}=25\text{k}\Omega$ ,  $R_{13}=R_{15}=1\text{k}\Omega$ , and  $R_{14}=14.3\text{k}\Omega$ . It should be mentioned that the operational amplifier 6 implements the function  $-f(x)$ . Using  $R_{16}=R_{17}=1\text{k}\Omega$ ,  $R_1=20\text{k}\Omega$ ,  $R_2=14.4\text{k}\Omega$ ,  $R_3=20.4\text{k}\Omega$  and  $R_X=12.5\text{k}\Omega$ , we defined  $\alpha$ ,  $b$ ,  $c$  and  $k$  as follows:

$$\alpha = \frac{1}{R_1 \cdot C_3}, \quad b = \frac{1}{R_3 \cdot C_3}, \quad c = \frac{1}{R_X \cdot C_3}, \quad k = \frac{R_2}{R_3} \quad (3)$$

In contrast to Refs [22] and [23] where  $c=1$ , in the present report the normalized value of  $c$  was:  $c=0.8$ . Parameters  $\alpha$  and  $b$  and  $k$  were set again to  $\alpha=0.5$ ,  $b=0.5$ ,  $k=0.7$ , so each of sub-circuit, operates in a chaotic mode and exhibits a double scroll attractor as shown in Fig. 2.

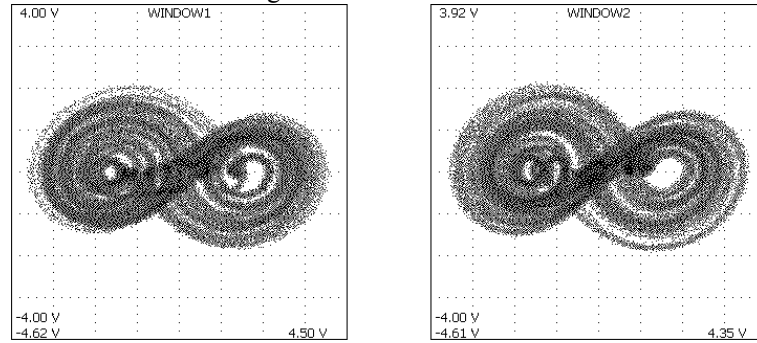


**Figure 2:** The double-scroll attractors of each circuit when they operate independently.

### 3 Experimental Results

Resistance  $R_C$  in the denominator of coupling coefficient  $\xi$  served as the system's control parameter and its value was changed from almost 9 k $\Omega$  down to almost 7 k $\Omega$ . Although, in this region each circuit remained chaotic, the coupled system underwent a transition from full to incomplete synchronization.

Signals  $x_1$ ,  $x_2$  and  $y_1$ ,  $y_2$  in both circuits were monitored by a four channel digital oscilloscope (Yokogawa DL9140), so that the time-series  $y_1$ ,  $y_2$ , their difference ( $y_1 - y_2$ ), the synchronization phase portrait ( $y_1$  vs.  $y_2$ ) and each separate circuit phase portrait ( $x_1$  vs.  $y_1$  and  $x_2$  vs.  $y_2$ ) could be simultaneously displayed and registered.

A second digital oscilloscope (Tektronix TDS1002B), further connected to a laptop, was used to register the difference signal ( $y_1 - y_2$ ), in order to perform the statistics of the results. During measurements the oscilloscope was controlled by the laptop connected to it. For this reason a customized acquisition setup, based on NI's LabView, was built [24].

As long as  $R_C$  was below the critical value  $R_{C-crit} = 8.7\text{k}\Omega$ , the two identical double-scroll circuits remained synchronized. For values of  $R_C$  lower than 8.5k $\Omega$  the two circuits began to demonstrate incomplete (intermittent) synchronization.

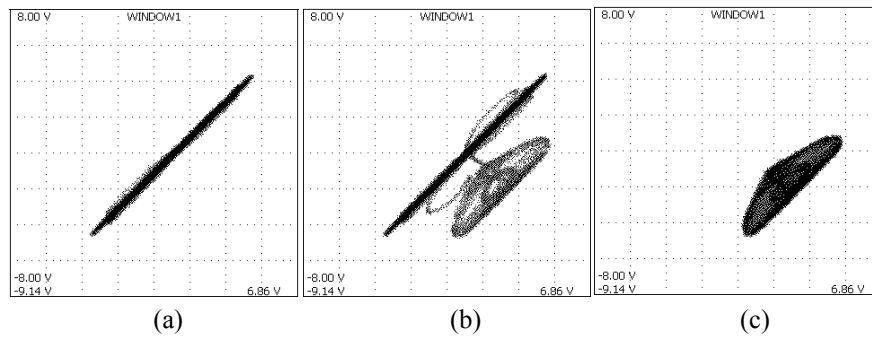


**Figure 3:** Synchronization phase portraits ( $y_1$  vs  $y_2$ ) in the case of: (a) full synchronization ( $R_C=8.8\text{k}\Omega$ ), (b) intermittent synchronization ( $R_C=7.9\text{k}\Omega$ ) and (c) desynchronization ( $R_C=7.1\text{k}\Omega$ ).

This behaviour was exhibited in the range  $8.7\text{k}\Omega \geq R_C \geq 7.1\text{k}\Omega$ , and with decreasing  $R_C$  the incomplete synchronization became stronger. The corresponding synchronization phase portraits ( $y_1$  vs  $y_2$ ) depict the transition from synchronization to desynchronization as follows:

In Fig. 3(a) the synchronization phase portrait for  $R_C=8.8\text{k}\Omega$  is shown. As expected in the case of synchronization, the trajectory remains along the diagonal.

In Fig. 3(b) - for  $R_C=7.9\text{k}\Omega$  - the corresponding phase portrait consists of both the diagonal and a wing-like structure below the diagonal. This behaviour of the trajectory is expected in the case of incomplete synchronization, with the diagonal corresponding to synchronized mode of operation and the escapes to the wing to desynchronization bursts. What is remarkable in these bursts is that they are spatially limited within the appearing wing-like structure.

In the phase portrait in Fig. 3(c) ( $R_C=7.1\text{k}\Omega$ ) the diagonal disappears and only the wing-like structure remains. Thus, desynchronization prevails and the

trajectory, is always out of the diagonal. However the desynchronization is spatially limited and the trajectory remains strictly within the wing-like structure. In Figs. 4(a)-4(c) three representative cases of the intermittent synchronization for

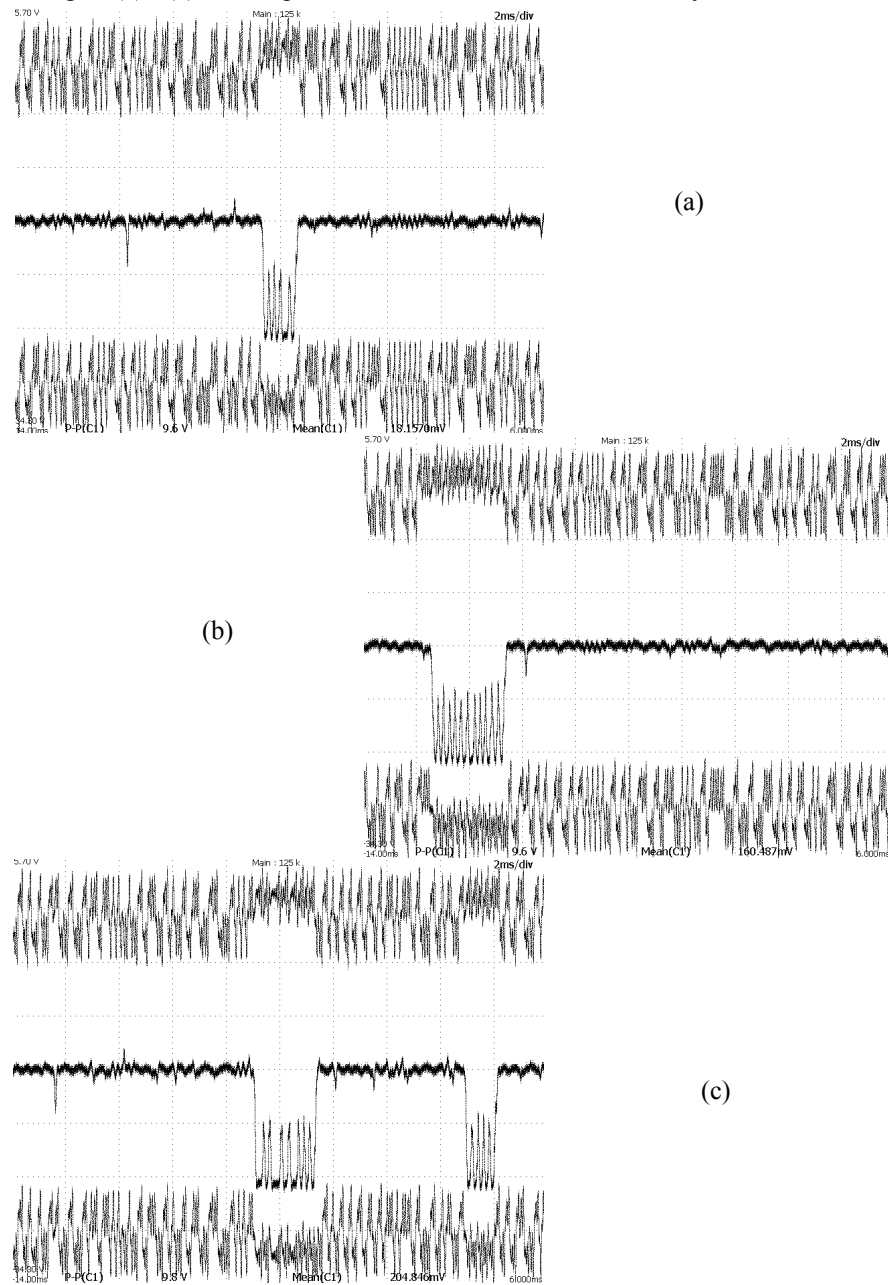


**Figure 4:** Time-series of  $y_1$  (upper side) and  $y_2$  (lower side) and their difference (in the middle), in three typical cases of intermittent synchronization: (a)  $R_C=8.2\text{k}\Omega$ , (b)  $R_C=8.0\text{k}\Omega$  and (c)  $R_C=7.8\text{k}\Omega$ .

decreasing values of the control parameter  $R_C$  are presented. The time-series  $y_1$ ,  $y_2$  of each individual circuit (top and bottom timeseries), together with the difference signal ( $y_1 - y_2$ ) (middle timeseries), are presented. The appearing bursts in the difference signal indicate escapes from the diagonal to the wing-like structure appearing in Fig 3(b). Obviously, these bursts become of longer duration and appear more frequently, with decreasing values of  $R_C$ .

## 4 Evaluation

The evolution of the intermittent behavior as suggested by the curves of Figs. 3(a)-3(c) and 4(a)-4(c), i.e. the route from synchronization to desynchronization between the two identical, coupled, double-scroll circuits, has the characteristics of intermittency [14], [15], [18]. In order to determine the kind of intermittency exhibited in the studied case, laminar length distributions and the scaling of the mean laminar lengths according to the difference of the control parameter from its critical value ( $R_C - R_{C-crit}$ ), were measured and evaluated.

In Fig. 5, a representative distribution  $P(\tau)$  of durations  $\tau$  of laminar lengths (synchronized state) of the difference signal, for  $R_C = 7.9 \text{ k}\Omega$  is presented in a

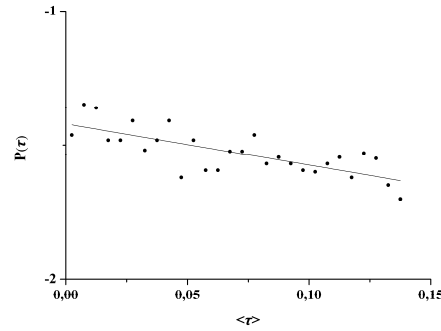


**Figure 5:** A typical semi logarithmic plot  $P(\tau)$  vs.  $\tau$  in the case of  $R_C = 7.9 \text{ k}\Omega$ .

-logarithmic plot. The curve of this plot consists of a linear part with slope  $\beta$  equal to -1.499. Similar distributions for other values of control parameter  $R_C$  gave slopes  $\beta$  not substantially deviating from -1.50. Apparently, these distributions follow the theoretically predicted law [25]:

$$P(\tau) \propto \tau^\beta \quad (4)$$

that holds for exponent  $\beta = -1.50$ . In the mentioned case of  $R_C = 7.9 \text{ k}\Omega$ ,  $\beta$  deviates from this predicted value, only by 0.07%. Taking into account the estimated value of  $\beta$  and the fact that the bursts correspond to jumps between two different manifolds (the diagonal and wing-like structure, respectively), the classification of this intermittency as one of the “In-Out” kind, can be safely supported [18].

Furthermore, mean duration  $\langle \tau \rangle$  of laminar lengths versus the difference ( $R_C - R_{C-crit}$ ), is presented in a double logarithmic plot, in Fig. 6. A linear fitting of the experimental data results to a straight line with a slope  $\gamma$  equal to -1.051, clearly confirming that a power law of the following form holds:

$$\langle \tau \rangle \propto (R_C - R_{C-crit})^\gamma \quad (5)$$

According to this law  $\langle \tau \rangle$  scales with the difference  $(R_C - R_{C-crit})$  with an exponent  $\gamma = -1.0$ . Our value for  $\gamma$ , deviates by 5.10% from the predicted one, further confirming the “In-Out” classification of the observed intermittency [18], [33].

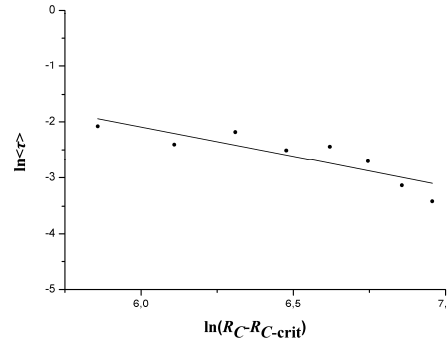


**Figure 6:** Double logarithmic plot of  $\langle \tau \rangle$  vs.  $(R_C - R_{C-crit})$ . The line stands for the fitting of Eq 5.

## 5 Discussion

In this report the transition from synchronization to desynchronization of two identical double-scroll circuits, bidirectionally coupled, was experimentally studied and classified as one of the *in-out intermittency*.

According to the measured timeseries of Figs 4(a)-4(c) the bursts, appearing in the difference signal  $(y_1 - y_2)$ , result from corresponding jumps in the time-series  $y_1(t)$ ,  $y_2(t)$ . What is remarkable is that these jumps happened almost always in opposite directions. This is a consequence of the behaviour of the trajectories in the phase-portraits of each double scroll circuit. As long as the two sub-circuits

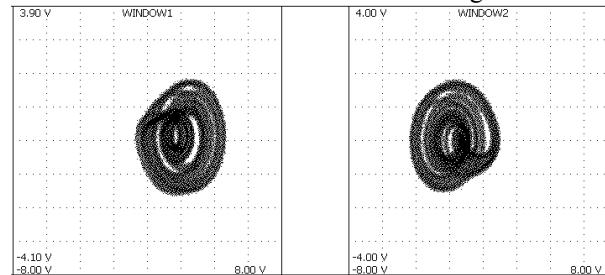


**Figure 7:** The attractors of each double scroll circuit when the circuits are desynchronized.

remain synchronized, their trajectories describe identical double scroll attractors. However, during the jumps each of the original double-scroll attractors limits itself to only one of its scrolls but in a complementary way as shown in Fig. 7. It should be interesting to further investigate the conditions which lead to this behaviour and if the inverse effect is also taking place.

## Acknowledgements

The authors would like to thank the referees for their valuable comments.



## References

- [1] G. Chen and X. Dong (eds), *From Chaos to Order: Methodologies, Perspectives and Applications*, World Scientific, Singapore, 1998.
- [2] G. Chen and X. Yu (eds.), *Chaos Control: Theory and Applications*, Springer-Verlag, Berlin-Heidelberg, 2003.
- [3] L.M. Pecora and T.L. Carroll, Synchronization in chaotic systems, *Phys Rev Lett*, 64, 821-824 (1990).
- [4] M.P. Kennedy, R. Rovatti, G. Setti (eds), *Chaotic Electronics in Communications*, CRC Press, 2000.
- [5] L. Kocarev, U. Parlitz, General approach for chaotic synchronization with applications to communications, *Phys Rev Lett*, 74, 5028-5031 (1995).
- [6] G. Kolumban, M.P. Kennedy L.O. Chua, The role of synchronization in digital communications using chaos – Part I: Fundamentals of digital communications, *IEEE Trans Circ Syst I*, 44, 927-936 (1997).
- [7] A.S. Dmitriev, A.V. Kletsov, A.M. Laktushkin, A.I. Panas, S.O. Starkov, Ultrawideband wireless communications based on dynamic chaos, *Uspekhi sovremennoi radioelektroniki*, 1, 4-16 (2008).
- [8] G. Alvarez, F. Montoya, M. Romera and G. Pastor, Chaotic cryptosystems, in: *Proceedings of 33rd Annual 1999 International Carnahan Conference on Security Technology*, (L. D. Sanson, Ed.) 332-338, (1999).
- [9] C.P. Silva and A.M. Young, Introduction to Chaos-based Communications and Signal Processing, *Procs IEEE Aerospace Conference*, 279-299, (2000).
- [10] L. Kocarev, Chaos-based cryptography: A brief Overview, *IEEE Circuits and Systems Magazine*, 1, 6-21 (2001).
- [11] C. K. Tse and F. C. M. Lau (eds.), *Chaos-based digital communication systems: operating principles. Analysis Methods and Performance Evaluation*, Springer-Verlag, Berlin-Heidelberg, 2003.
- [12] A.N. Miliou, S.G. Stavriniades, A.P. Valaristos A.N. Anagnostopoulos, Nonlinear electronic circuit-PART II: Synchronization in a chaotic MODEM scheme (Review) *Nonlinear Analysis* 71, e21-e31 (2009).
- [13] S.G. Stavriniades, A.N. Anagnostopoulos, A.N. Miliou, A. Valaristos, L. Magafas, K. Kosmatopoulos, S. Papaioannou, A digital chaotic synchronized communication system, *J. of Eng Sci Rev*, 2(1), 82-86 (2009).
- [14] N. Platt, E.A. Spiegel, C. Tresser, On-Off Intermittency: A Mechanism for Bursting,” *Phys. Rev. Lett.*, 70, 279-282 (1993).
- [15] J.F. Heagy, N. Platt, S.M. Hammel, Characterization of On-Off Intermittency, *Phys. Rev. E*, 49, 1140-1150 (1994).
- [16] C. Toniolo, A. Provenzale, E.A. Spiegel, Signature of on-off intermittency in measured signals, *Phys. Rev. E*, 66, 066209 (2002).
- [17] P. Ashwin, E. Covas and R. Tavakol, Influence of noise on scaling for in-out intermittency, *Phys. Rev. E*, 64, 066204 (2001).
- [18] Q. Chen, Y. Hong, G. Chen, D.J. Hill, Intermittent phenomena in switched systems with high coupling strengths, *IEEE Trans on CAS-I*, 53(12), 2692-2704 (2006).
- [19] P.W. Hammer, N. Platt, S.M. Hammel, J.F. Heagy, B.D. Lee, Experimental Observation of On-Off Intermittency, *Phys. Rev. Lett.*, 73, 1095-1098 (1994).
- [20] Y.H. Yu, K. Kwak, T.K. Lim, On-Off Intermittency in an Experimental Synchronization Process, *Phys. Lett. A*, 198, 34-38 (1995).
- [21] A. Cenys, A. Namajunas, A. Tamacevicius, T. Schneider, On-Off Intermittency in Chaotic Synchronization Experiment, *Phys. Lett. A*, 213, 259-264 (1996).
- [22] I.M. Kyprianidis, Ch.K. Volos, S.G. Stavriniades, I.N. Stouboulos, A.N. Anagnostopoulos, On-off intermittent synchronization between two bidirectionally coupled double scroll circuits, *Commun Nonlinear Sci Numer Simulat*, 15, 2192–2200 (2010).
- [23] I.M. Kyprianidis, Ch.K. Volos, S.G. Stavriniades, I.N. Stouboulos and A.N. Anagnostopoulos, Master-Slave double-scroll circuit incomplete synchronization, *J. of Eng Sci Rev*, accepted for publication (2009).
- [24] S.G. Stavriniades, Th. Laopoulos, A.N. Anagnostopoulos A. Valaristos, An Automated Acquisition setup for the Evaluation of Intermittency Statistics, *Procs IEEE IDAACS'09*, Cosenza (Rende), Italy, 111-116 (2005).
- [25] E. Ott, *Chaos in Dynamical Systems*-2nd Edition, in Cambridge University Press (Eds.) (2002).

# Spectral Analysis and Allan Variance Calculation in the case of Phase Noise

Georgakaki D.<sup>1\*</sup>, Mitsas C.<sup>2\*\*</sup>, Polatoglou H.M.<sup>1\*\*\*</sup>

March 7, 2010

<sup>1</sup>Physics Department, Solid State Physics Section, Aristotle University of Thessaloniki,  
54124, Thessaloniki, Greece

<sup>2</sup>Mechanical Measurements Dept., Hellenic Institute of Metrology, 57022, Thessaloniki,  
Greece

\*georgakd@auth.gr, \*\*chris.mitsas@eim.gr, \*\*\*hariton@auth.gr

## Abstract

In this work, time series analysis techniques are used to analyze sequential, equi-spaced mass measurements of a Si density artifact, collected from an electromechanical transducer. Specifically, techniques such as Power Spectral Density, Bretthorst periodogram, Allan variance and Modified Allan variance can provide much insight regarding the stochastic correlations that are induced on the outcome of an experiment by the measurement system and establish criteria for the limited use of the classical variance in metrology. These techniques are used in conjunction with power law models of stochastic noise in order to characterize time or frequency regimes by pointing out the different types of frequency modulated (FM) or phase modulated (PM) noise. In the case of phase noise, only Modified Allan variance can tell between white PM and flicker PM noise. Oscillations in the system can be detected accurately with the Bretthorst periodogram. Through the detection of colored noise, which is expected to appear in almost all electronic devices, a lower threshold of measurement uncertainty is obtained and the white noise model of statistical independence can no longer provide accurate results for the examined data set.

**Key words:** phase noise, time-series analysis, Fourier analysis, Bretthorst method, Allan variance

## 1 Introduction

Finding correlations in time series of measurements and defining the type of stochastic noise apparent in the measured signal remain very crucial issues for modern metrology. According to Zhang, when measurements are autocorrelated, the use of classical variance for the estimation of type A uncertainty of a data set, leads to wrong results [1]. Moreover, power law models of the type  $1/f^\alpha$  [2] are necessary to describe the type of stochastic noise that characterizes the system, which produces the time series.

In most cases, due to colored noise generation, the Frequency Modulated White Noise model (White-FM) fails to describe the system. An additional problem is Phase Modulated Noise (PM), apparent in all electrical oscillators [3] and more complex devices, as thoroughly reviewed and analyzed by Rubiola [4]. PM Noise is attributed to the phase fluctuations (or frequency fluctuations) of a signal produced by a real, non-ideal oscillator. In this oscillator the frequency of oscillation is modulated by electronic noise, inevitably leading to random frequency fluctuations in time and thus affecting the performance of the system that uses the oscillator. A list of reasons for the PM Noise generation is given by Howe [5] but still its origin remains a controversy issue in the areas of metrology.

Generally there have been utilized several methods from both time and frequency domain, in order to best analyze the response of metrological instruments, electromechanical transducers in our case study. In this paper we will focus on Allan and Modified Allan variance (time domain) as well as Schuster and Bretthorst periodograms (frequency domain).

Allan variance, initially introduced by Allan in time and frequency metrology [6], is an alternative approach for the variance calculation of autocorrelated measurements and has been thoroughly used by Witt in the area of electrical measurements [7]. Because of the fact that this method cannot tell the difference between White PM Noise and Flicker PM Noise, the Modified Allan variance has been used instead [8].

In the frequency domain, Fast Fourier Transform and Schuster periodograms remain the most widely used tools for evaluating the different types of noise in the signal's Power Spectrum. Schuster periodograms can detect oscillations in the signal and interpret them as individual peaks. Due to the limitations and in certain occasions misleading results of the Discrete Fourier Transform, an alternative method is proposed, based on Bayesian analysis: the Bretthorst periodogram [9]. This method also identifies oscillations in a signal and can distinguish between two very close frequency peaks that FFT treats as one.

The data on which the above methods will be tested, was obtained from characterization experiments of a newly commissioned 1kg/ 10mg resolution mass comparator at the Hellenic Institute of Metrology density laboratory. The principle function of this comparator will be the measurement of mass in air of Si and ceramic density artifacts of mass ca. 1kg in the form of spheres through comparative weighing. It should be noted that these methods can be applied to any electromechanical transducer system equally well with similar results.

## 2 General Considerations

Let's consider an input signal of the following simple sinusoidal form

$$V_{in}(t) = V_c \sin(2\pi f_c t) \quad (1)$$

The output of a non-ideal oscillator will be of the form

$$V_{out}(t) = (V_c + \varepsilon(t)) \sin(2\pi f_c + \phi(t)) \quad (2)$$

where the time variations in amplitude are included into  $\varepsilon(t)$  and the frequency deviation from the fundamental one is described by  $\varphi(t)$ , called the phase fluctuations of the output signal. Ignoring amplitude variations and changing to frequency regime, phase fluctuations with a spectral density  $S_\phi(f)$  and frequency fluctuations with a spectral density  $S_y(f)$ , are described with equations (3) and (4), with  $h_i$  representing the intensity coefficients of each power law noise contribution and  $\alpha, \beta$  are the spectral exponents:

$$S_y(f) = \sum_{a=-2}^{+2} h_a f^a \quad (3)$$

$$S_\phi(f) = \sum_{\beta=-4}^0 h_\beta f^\beta, \beta = a - 2 \quad (4)$$

### 3 Computational Methods

#### 3.1 Fourier Spectral Analysis

The Discrete Fourier Transform is one of the most powerful tools in signal analysis and thoroughly used in many physical systems. The periodogram was introduced by Schuster, as a method of detecting periodicities and estimating their frequencies and is essentially the squared magnitude of the discrete fourier transform of the data. In 1965, Cooley and Tukey introduced the Fast Fourier Transform, a method that led to more efficient computer calculations and is considered nowadays an optimal frequency and power spectral estimator.

By plotting  $S(f) - f$  in a log-log diagram, the different noise levels in the power spectrum can be estimated from the adjustment of equation (3) to the log-log plot. The calculation of the spectral exponent  $\alpha$ , leads to the identification of white noise ( $\alpha=0$ ), flicker noise ( $\alpha=-1$ ), random walk noise ( $\alpha=-2$ ) or any intermediate case  $-2 < \alpha < 2$  of colored noise [7].

Unfortunately, the Discrete Fourier Transform will provide accurate frequency estimates only when the following conditions are met [9,10]: 1) the length of the data series  $N$  is sufficiently large, 2) the data series is stationary, 3) there is no evidence of low frequency existence, 4) the data contain one stationary frequency, 5) the noise is white. When one or more of the above conditions is violated (the last one in our work) an alternative method is proposed, based on Bayesian Analysis, called the Bretthorst Periodogram.

#### 3.2 Bretthorst Periodogram

Bayesian Probability Theory defines a probability of occurrence as a reasonable degree of belief, given some prior information of the data. In our example the probability distribution of a frequency of oscillation  $\omega$  is computed conditional on the data  $D$  and the prior information  $I$ , abbreviated as the posterior probability  $P(\omega|D,I)$ . To calculate this one must find the direct probability (or likelihood function)  $P(D|\omega,I)$ , the prior probability  $P(\omega|I)$ , the probability  $P(D|I)$  (in parameter estimation problems it is a simple normalization constant) and eliminate the nuisance parameters.

$$P(\omega|D, I) = \frac{P(D|\omega, I) \cdot P(\omega|I)}{P(D|I)} \quad (5)$$

Based simply on Bayes product and sum rules [11] one can obtain the posterior probability of the frequency with or without prior knowledge of the noise variance  $\sigma^2$  in the signal, concluding to equations (6a) and (6b) correspondingly. Specifically (6b) is the well-known t-student distribution. An analytical proof of these relations can be found in [9, 10].  $C(\omega)$  is the Schuster periodogram and  $\bar{d}^2$  is the observed mean-square data value.

$$P(\omega|D, \sigma, I) \propto \exp(C(\omega)/\sigma^2) \quad (a) \quad P(\omega|D, I) \propto [1 - \frac{2C(\omega)}{N\bar{d}^2}] \quad (b) \quad (6)$$

Basically, the above equations give evidence that a single stationary frequency is present in the data and because of the processing in equations (6a-6b), all details of the periodogram are suppressed except the frequency peak, observed as a single spike in the Bretthorst periodogram.

### 3.3 Allan Variance

The Allan variance or Two-sample variance was first introduced by David W. Allan for the evaluation of the stability of time and frequency standards [6]. As well established, the most common measure of dispersion is the classical variance, whose value decreases as the number of data points included in the calculations, increases. Unfortunately this is only true in the case of truly random processes, where the variance of the mean decreases with the number  $N$  of data points as  $\text{var}(X) = \frac{\sigma^2}{N}$ .

Allan stated that in the case of autocorrelated data the above equation does not apply since there exists a possibility that the estimated variance will diverge as the number of data points increases [12]. So, we create a high-pass filter by extracting each  $k+1$  value from its previous one  $k$  and thus we remove any possible trends, fast fluctuations or other peculiar characteristics. The Allan variance  $\sigma_y^2(\tau)$  is estimated at time intervals  $\tau = m\tau_0$ , where  $\tau_0$  is a minimum sampling time and  $m$  is usually chosen to denote powers of two.

$$\sigma_y^2(\tau) = \frac{1}{2(N-1)} \sum_{k=1}^{N-1} (y_{k+1}(\tau) - y_k(\tau))^2 \quad (7)$$

From the resulting plot of  $\sigma_y^2(\tau) \cdot \tau$  one can estimate the cut-off value after which the inclusion of more data points does not lead to the decrease of the variance. In a log-log plot the Allan variance is proportional to  $\tau^\mu$  and  $\mu = -\alpha - 1$ , where  $\alpha$  is the spectral exponent appearing in equation (3). Special cases [6,7] are:  $\mu=1$  (random walk noise),  $\mu=0$  (flicker noise) and  $\mu=-1$  (white noise).

### 3.4 Modified Allan Variance

This variance was first introduced in the domain of optics because it divides white phase noise from flicker phase noise by the different dependence on gate time. More specifically, ModVar is proportional to  $\tau^{-3}$  for the former and  $\tau^{-2}$  for the latter and ModStd is proportional to  $\tau^{-3/2}$  and  $\tau^{-1}$  correspondingly [13]. Given an infinite sequence  $\{x_k\}$  of samples evenly spaced in time with sampling period  $\tau_0$ , the ModVar is defined as

$$Mod\sigma_y^2(\tau) = \frac{1}{2n^4\tau_0^2(N-3n+1)} \sum_{j=1}^{N-3n+1} \left[ \sum_{i=j}^{n+j-1} (x_{i+2n}(\tau) - 2x_{i+n}(\tau) + x_i(\tau)) \right]^2 \quad (8)$$

where  $n=1,2,\dots,N/3$ . The MVar obeys to a power law of the observation time  $\tau$  of the form  $Mod\sigma_y^2 \sim k\tau^\mu$  where  $\mu = -3 - a$  [14].

## 4 Results

After removing the deterministic component (linear trend because of the ambient temperature) of the data with the application of a first difference filter, the resulting series is carefully examined for correlations and noise. The lag plot and autocorrelation function of the first-differenced time series are presented below, in fig. (1) and fig. (2) correspondingly.

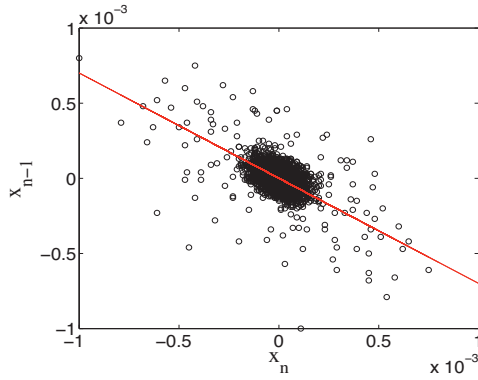


Figure 1. Lag Plot with negative correlations.

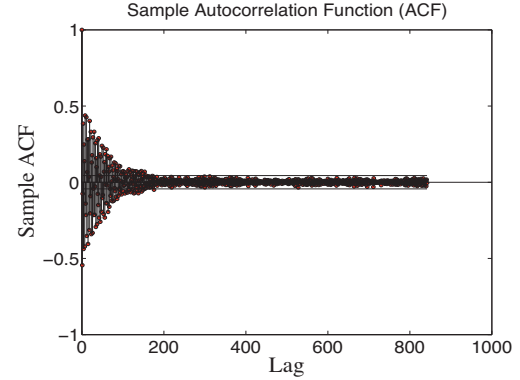


Figure 2. Autocorrelation function with oscillatory behavior.

The lag plot reveals negative correlations between successive data points with lag=1 but is unable to tell between White and Flicker PM Noise. Moreover, the autocorrelation function changes between positive and negative values for the first 200 lags (strong correlations) and afterwards, the data become statistically independent falling well within the 95% confidence bands of  $\pm \frac{2}{\sqrt{N}}$ , implying that the white noise model is now sufficient to describe the measurements. In order to determine safely whether or not to use Allan Variance, additional information is needed from the frequency domain analysis. The Schuster periodogram and the Power Spectrum of the data are shown in the following figures.

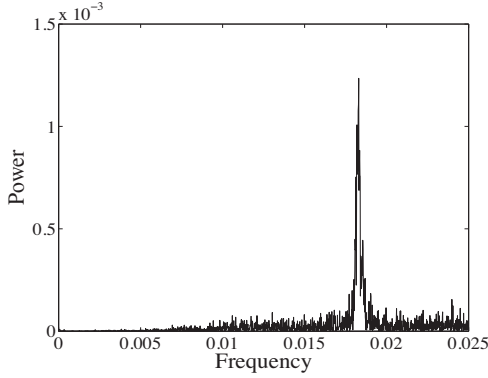


Figure 3. Periodogram with a single peak.

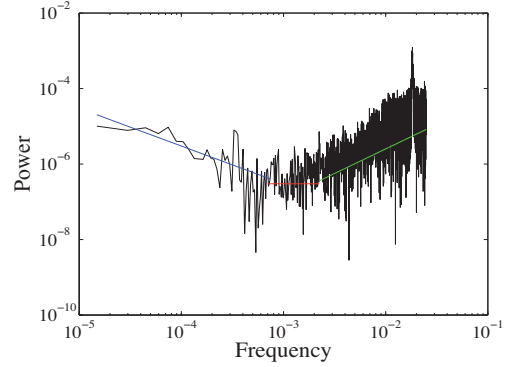


Figure 4. Power Spectrum with three different noise regions.

The periodogram reveals a strong oscillation at approximately 0.0183 Hz (or 54.64 sec). The power spectrum in a log-log scale, seems to be divided in three regions: at lower frequencies the blue line indicates a power law model of the form  $1/f$  (Flicker FM Noise), the red line indicates that the White FM Noise model is adequate to describe the data and finally at higher frequencies the green line indicates a power law model  $1/f^{-1}$  or  $1/f^{-2}$  (PM Noise). Thus, there exist two cut-off frequencies at which evident changes in slope occur, revealing the different noise areas. The total power spectrum is given by the equation  $S_y(f) = h_0 f_0 + h_{-1} f_{-1} + h_1 f_1$  (or  $h_2 f_2$ ), where  $h_i$  are the intensity coefficients. In order to be sure for the oscillation that FFT revealed, we apply the Bretthorst methodology and according to theory we expect a single spike at the frequency of 0.0183 Hz. In order to keep the same quantities of measurement we will calculate  $P(f|D, I)$ . As can be observed in fig. (5), the single spike (red line) confirms the existence of  $f_{osc} = 0.0183$  Hz and as predicted by theory all the other information of the periodogram (black diagram) is suppressed to a uniform plateau of zero slope.

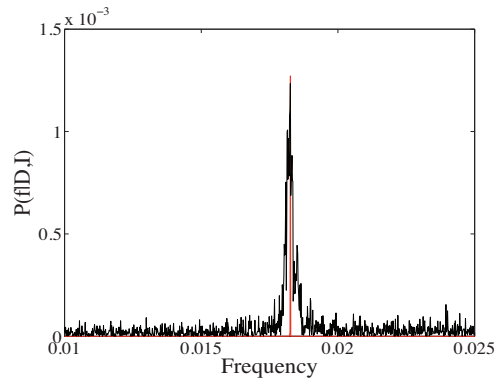


Figure 5. Comparison of Schuster and Bretthorst periodogram

From all the above, it is obvious that the use of classical variance for the calculation of type A uncertainty is inadequate and Allan variance will be used instead. In addition, Modified Allan variance will give a straightforward answer for the phase noise characterization problem in our data set. Fig. (6) below, gives the dependence of the Allan deviation over time. Clearly, there exist three different regions, in accordance with the power spectrum of fig. (4): the phase noise region  $\mu=-1$  (or  $\mu=-2$  for the Allan Variance) indicated by the blue line, the white FM noise area  $\mu=-0.5$  (or  $\mu=-1$  for the Allan variance) adjusted by the red line and finally the flicker FM floor ( $\mu=0$ ). For  $\tau=256$ ,  $\sigma(\tau)=1.9 \cdot 10^{-6}$  in contrast to classical std which estimates  $\sigma=9.57 \cdot 10^{-5}$ . Note that the last two points are not included in the calculation. Probable causes of the flicker floor are power supply voltage fluctuations, changes in the components of the artifact and microwave power changes. Fig. (7) gives the dependence of the Modified Allan deviation over time. The slope of the blue fitted line is  $-3/2$ , which indicates that white PM Noise appears at small times and correspondingly high frequencies, as already observed in the power spectrum.

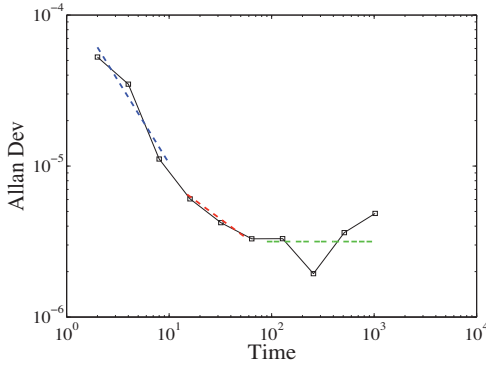


Figure 6. Allan variance.

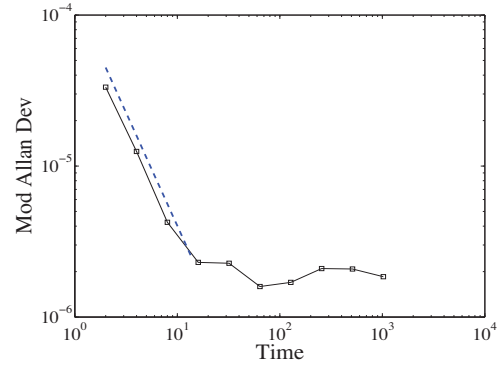


Figure 7. Modified Allan variance.

## 5 Conclusions

The main purpose of this work is to point out the importance of considering measurement results as time series and of using the time series analysis methods to test for correlations and underlying stochastic noise. Only in the absence of correlation the use of the expression  $\sigma/\sqrt{N}$  is appropriate to characterize the random uncertainty. Otherwise, the Allan variance is an alternate, more appropriate tool to characterize the dispersion of a set of experimental results.

In the case of phase noise, only Modified Allan variance provides accurate results and discriminates flicker from white PM noise. Bretthorst periodogram is a powerful tool of bayesian spectral analysis which detects oscillations in an output signal and identifies peaks at a very close distance. For the case study of mass measurements we consider here, all the above techniques give consistent results.



## References

- [1] N.F. Zhang, Calculation of the uncertainty of the mean of autocorrelated measurements, *Metrologia*, 43, S276-S281 (2006).
- [2] N.J. Kasdin, Discrete simulation of colored noise and stochastic processes and  $1/f^\alpha$  power law noise generation, *Proceedings of the IEEE*, 83 (5), 802-827 (1995).
- [3] A. Hajimiri and T.H. Lee, A general theory of phase noise in electrical oscillators, *IEEE Journal of Solid-State Circuits*, 33 (2), 179-194 (1998).
- [4] E. Rubiola and V. Giordano, Oscillators and the characterization of frequency stability: an introduction, Phase noise metrology in *Noise, Oscillators and Algebraic Randomness* (M. Planat, eds.), Springer, Chapelle des Bois France, 1999, 175-215.
- [5] D.A. Howe et al, Vibration-Induced PM Noise in Oscillators and Measurements of Correlation with Vibration Sensors in *Proceedings of the 36th Annual Precise Time and Time Interval (PTTI) Systems and Applications Meeting*, (L. Breakiron ed.), Washington D.C., 2005, 494-498
- [6] D.W. Allan, Should the Classical Variance Be Used As a Basic Measure in Standards Metrology?, *IEEE Transactions on Instrumentation and Measurement*, IM-36, No 2, 646-654 (1987).
- [7] T.J. Witt, Testing for Correlations in Measurements, *Advanced Mathematical and Computational Tools in Metrology IV*, World Scientific Publishing Company, 273-288 (2000).
- [8] D.W. Allan and J.A. Barnes, A Modified "Allan Variance" with Increased Oscillator Characterization Ability, *Proceedings of the 35th Annual Frequency Control Symposium*, 470-475 (1981).
- [9] G.L. Bretthorst, An introduction to parameter estimation using Bayesian Probability Theory in *Maximum entropy and Bayesian methods*, (P.F. Fougere ed.), Kluwer Academic Publishers, The Netherlands, 1990, 53-79.
- [10] G.L. Bretthorst, *Bayesian Spectrum Analysis and Parameter Estimation*, (J. Kimmel ed.), Springer-Verlag, Berlin Heidelberg, 1988.
- [11] A. Gelman et al, *Bayesian Data Analysis*, (2nd ed), Chapman & Hall/CRC, Boca Raton, Florida, 2004.
- [12] J. Jespersen, Introduction to the time domain characterization of frequency standards, *Tutorials from the Annual Precise Time and Time Interval (PTTI) applications and Planning Meeting* (23rd), Pasadena, California, 1991.
- [13] Won-Kyu Lee et al, The uncertainty associated with the weighted mean frequency of a phase-stabilized signal with white phase noise, *Metrologia*, 47, 24-32 (2010).
- [14] S. Bregni, The Modified Allan Variance as Time-Domain Analysis Tool for Estimating the Hurst Parameter of Long-Range Dependent Traffic, *Proceedings of the IEEE Global Telecommunications Conference*, 3, 1406-1410 (2004).

---

**Instructions to Contributors**  
**Journal of Concrete and Applicable Mathematics**  
A quarterly international publication of Eudoxus Press, LLC, of TN.

**Editor in Chief: George Anastassiou**  
Department of Mathematical Sciences  
University of Memphis  
Memphis, TN 38152-3240, U.S.A.

**1. Manuscripts hard copies in triplicate, and in English, should be submitted to the Editor-in-Chief:**

**Prof. George A. Anastassiou**  
Department of Mathematical Sciences  
The University of Memphis  
Memphis, TN 38152, USA.  
Tel. 901.678.3144  
e-mail: [ganastss@memphis.edu](mailto:ganastss@memphis.edu)

**Authors may want to recommend an associate editor the most related to the submission to possibly handle it.**

**Also authors may want to submit a list of six possible referees, to be used in case we cannot find related referees by ourselves.**

**2. Manuscripts should be typed using any of TEX, LaTeX, AMS-TEX, or AMS-LaTeX and according to EUDOXUS PRESS, LLC. LATEX STYLE FILE. (Click [HERE](#) to save a copy of the style file.) They should be carefully prepared in all respects. Submitted copies should be brightly printed (not dot-matrix), double spaced, in ten point type size, on one side high quality paper 8(1/2)x11 inch. Manuscripts should have generous margins on all sides and should not exceed 24 pages.**

**3. Submission is a representation that the manuscript has not been published previously in this or any other similar form and is not currently under consideration for publication elsewhere. A statement transferring from the authors (or their employers, if they hold the copyright) to Eudoxus Press, LLC, will be required before the manuscript can be accepted for publication. The Editor-in-Chief will supply the necessary forms for this transfer. Such a written transfer of copyright, which previously was assumed to be implicit in the act of submitting a manuscript, is necessary under the U.S. Copyright Law in order for the publisher to carry through the dissemination of research results and reviews as widely and effectively as possible.**

**4. The paper starts with the title of the article, author's name(s) (no titles or degrees), author's affiliation(s) and e-mail addresses. The affiliation should comprise the department, institution (usually university or company), city, state (and/or nation) and mail code.**

**The following items, 5 and 6, should be on page no. 1 of the paper.**

**5. An abstract is to be provided, preferably no longer than 150 words.**

**6. A list of 5 key words is to be provided directly below the abstract. Key words should express the precise content of the manuscript, as they are used for indexing purposes.**

**The main body of the paper should begin on page no. 1, if possible.**

**7. All sections should be numbered with Arabic numerals (such as: 1. INTRODUCTION) .**

**Subsections should be identified with section and subsection numbers (such as 6.1. Second-Value Subheading).**

**If applicable, an independent single-number system (one for each category) should be used to label all theorems, lemmas, propositions, corrolaries, definitions, remarks, examples, etc. The label (such as Lemma 7) should be typed with paragraph indentation, followed by a period and the lemma itself.**

**8. Mathematical notation must be typeset. Equations should be numbered consecutively with Arabic numerals in parentheses placed flush right, and should be thusly referred to in the text [such as Eqs.(2) and (5)]. The running title must be placed at the top of even numbered pages and the first author's name, et al., must be placed at the top of the odd numbed pages.**

**9. Illustrations (photographs, drawings, diagrams, and charts) are to be numbered in one consecutive series of Arabic numerals. The captions for illustrations should be typed double space. All illustrations, charts, tables, etc., must be embedded in the body of the manuscript in proper, final, print position. In particular, manuscript, source, and PDF file version must be at camera ready stage for publication or they cannot be considered.**

**Tables are to be numbered (with Roman numerals) and referred to by number in the text. Center the title above the table, and type explanatory footnotes (indicated by superscript lowercase letters) below the table.**

**10. List references alphabetically at the end of the paper and number them consecutively. Each must be cited in the text by the appropriate Arabic numeral in square brackets on the baseline.**

**References should include (in the following order):  
initials of first and middle name, last name of author(s)  
title of article,**

name of publication, volume number, inclusive pages, and year of publication.

Authors should follow these examples:

### **Journal Article**

1. H.H.Gonska, Degree of simultaneous approximation of bivariate functions by Gordon operators, (journal name in italics) *J. Approx. Theory*, 62,170-191(1990).

### **Book**

2. G.G.Lorentz, (title of book in italics) *Bernstein Polynomials* (2nd ed.), Chelsea, New York, 1986.

### **Contribution to a Book**

3. M.K.Khan, Approximation properties of beta operators, in (title of book in italics) *Progress in Approximation Theory* (P.Nevai and A.Pinkus, eds.), Academic Press, New York, 1991, pp.483-495.

11. All acknowledgements (including those for a grant and financial support) should occur in one paragraph that directly precedes the References section.

12. Footnotes should be avoided. When their use is absolutely necessary, footnotes should be numbered consecutively using Arabic numerals and should be typed at the bottom of the page to which they refer. Place a line above the footnote, so that it is set off from the text. Use the appropriate superscript numeral for citation in the text.

13. After each revision is made please again submit three hard copies of the revised manuscript, including in the final one. And after a manuscript has been accepted for publication and with all revisions incorporated, manuscripts, including the TEX/LaTeX source file and the PDF file, are to be submitted to the Editor's Office on a personal-computer disk, 3.5 inch size. Label the disk with clearly written identifying information and properly ship, such as:

Your name, title of article, kind of computer used, kind of software and version number, disk format and files names of article, as well as abbreviated journal name.

Package the disk in a disk mailer or protective cardboard. Make sure contents of disks are identical with the ones of final hard copies submitted!

Note: The Editor's Office cannot accept the disk without the accompanying matching hard copies of manuscript. No e-mail final submissions are allowed! The disk submission must be used.

14. Effective 1 Nov. 2009 for current journal page charges, contact the Editor in Chief. Upon acceptance of the paper an invoice will be sent to the contact author. The fee payment will be due one month from the invoice date. The article will proceed to publication only after the fee is paid. The charges are to be sent, by money order or certified check, in US dollars, payable to Eudoxus Press, LLC, to the address shown on

the Eudoxus [homepage](#).

No galley proofs will be sent and the contact author will receive one(1) electronic copy of the journal issue in which the article appears.

15. This journal will consider for publication only papers that contain proofs for their listed results.

# TABLE OF CONTENTS, JOURNAL OF CONCRETE AND APPLICABLE MATHEMATICS, VOL. 9, NO. 3, 2011

Applied Chaos: Linearizing Multibit DS Converters for Telecom Applications, K. Papathanasiou et al,.....	197
Chaos Synchronization and its Application to Secure Communication, M.S. Papadopoulou et al ,.....	205
Strict stability criteria of unperturbed Systems with initial time difference, COSKUN YAKAR and MUSTAFA BAYRAM GÜCEN,.....	213
Boundedness and Lagrange Stability of Fractional Order Differential Equations in Caputo's Sense with Initial Time Difference, Coskun YAKAR and Muhammed ÇIİÇEK,.....	223
Monotone Technique in Terms of Two Monotone Functions in Finite System, Coskun YAKAR, Bircan BAL and Ali YAKAR,.....	233
Dynamical Analysis and Electronic Implementation of A New Chaotic Attractor, İhsan Pehlivan <b>et al</b> .....	240
Testing stability and robustness in three cryptographic chaotic systems, N.A. Anagnostopoulos et al,.....	247
Experimental In-Out Synchronization-Intermittency between two bidirectionally coupled circuits,I.M. Kyprianidis et al,.....	262
Spectral Analysis and Allan Variance Calculation in the case of Phase Noise, Georgakaki.D et al,.....	270

**VOLUME 9, NUMBER 4      OCTOBER 2011**

**ISSN:1548-5390 PRINT,1559-176X ONLINE**



**JOURNAL  
OF CONCRETE  
AND APPLICABLE  
MATHEMATICS**

**EUDOXUS PRESS,LLC**

**SCOPE AND PRICES OF THE JOURNAL**  
**Journal of Concrete and Applicable Mathematics**

A quartely international publication of **Eudoxus Press,LLC**

**Editor in Chief: George Anastassiou**  
Department of Mathematical Sciences,  
University of Memphis  
Memphis, TN 38152, U.S.A.  
ganastss@memphis.edu

The main purpose of the "Journal of Concrete and Applicable Mathematics" is to publish high quality original research articles from all subareas of Non-Pure and/or Applicable Mathematics and its many real life applications, as well connections to other areas of Mathematical Sciences, as long as they are presented in a Concrete way. It welcomes also related research survey articles and book reviews. A sample list of connected mathematical areas with this publication includes and is not restricted to: Applied Analysis, Applied Functional Analysis, Probability theory, Stochastic Processes, Approximation Theory, O.D.E, P.D.E, Wavelet, Neural Networks, Difference Equations, Summability, Fractals, Special Functions, Splines, Asymptotic Analysis, Fractional Analysis, Inequalities, Moment Theory, Numerical Functional Analysis, Tomography, Asymptotic Expansions, Fourier Analysis, Applied Harmonic Analysis, Integral Equations, Signal Analysis, Numerical Analysis, Optimization, Operations Research, Linear Programming, Fuzzyness, Mathematical Finance, Stochastic Analysis, Game Theory, Math. Physics aspects, Applied Real and Complex Analysis, Computational Number Theory, Graph Theory, Combinatorics, Computer Science Math. related topics, combinations of the above, etc. In general any kind of Concretely presented Mathematics which is Applicable fits to the scope of this journal. Working Concretely and in Applicable Mathematics has become a main trend in many recent years, so we can understand better and deeper and solve the important problems of our real and scientific world. "Journal of Concrete and Applicable Mathematics" is a peer-reviewed International Quarterly Journal. We are calling for papers for possible publication. The contributor should send three copies of the contribution to the editor in-Chief typed in TEX, LATEX double spaced. [ See: Instructions to Contributors]

**Journal of Concrete and Applicable Mathematics(JCAAM)**  
**ISSN:1548-5390 PRINT, 1559-176X ONLINE.**

is published in January, April, July and October of each year by

**EUDOXUS PRESS,LLC,**  
1424 Beaver Trail Drive, Cordova, TN38016, USA,  
Tel.001-901-751-3553  
anastassioug@yahoo.com  
<http://www.EudoxusPress.com>.

**Visit also [www.msci.memphis.edu/~ganastss/jcaam](http://www.msci.memphis.edu/~ganastss/jcaam).**  
**Webmaster: Ray Clapsadle**

**Annual Subscription Current Prices:** For USA and Canada, Institutional: Print \$400, Electronic \$250, Print and Electronic \$450. Individual: Print \$150, Electronic



\$80,Print &Electronic \$200.For any other part of the world add \$50 more to the above prices for Print.

Single article PDF file for individual \$15.Single issue in PDF form for individual \$60.

No credit card payments.Only certified check,money order or international check in US dollars are acceptable.

Combination orders of any two from JoCAAA,JCAAM,JAFA receive 25% discount,all three receive 30% discount.

**Copyright**©2011 by Eudoxus Press,LLC all rights reserved.JCAAM is printed in USA.

**JCAAM is reviewed and abstracted by AMS Mathematical Reviews,MATHSCI,and Zentralblatt MATH.**

It is strictly prohibited the reproduction and transmission of any part of JCAAM and in any form and by any means without the written permission of the publisher.It is only allowed to educators to Xerox articles for educational purposes.The publisher assumes no responsibility for the content of published papers.

***JCAAM IS A JOURNAL OF RAPID PUBLICATION***

---

## Editorial Board

### Associate Editors

---

#### Editor in -Chief:

George Anastassiou  
Department of Mathematical Sciences  
The University Of Memphis  
Memphis, TN 38152, USA  
tel. 901-678-3144, fax 901-678-2480  
e-mail ganastss@memphis.edu  
www.msci.memphis.edu/~anastasg/anlyjour.htm  
Areas: Approximation Theory,  
Probability, Moments, Wavelet,  
Neural Networks, Inequalities, Fuzzyness.

#### Associate Editors:

1) Ravi Agarwal  
Florida Institute of Technology  
Applied Mathematics Program  
150 W. University Blvd.  
Melbourne, FL 32901, USA  
agarwal@fit.edu  
Differential Equations, Difference  
Equations,  
Inequalities

2) Drumi D. Bainov  
Medical University of Sofia  
P.O. Box 45, 1504 Sofia, Bulgaria  
drumibainov@yahoo.com  
Differential Equations, Optimal Control,  
Numerical Analysis, Approximation Theory

3) Carlo Bardaro  
Dipartimento di Matematica & Informatica  
Universita' di Perugia  
Via Vanvitelli 1  
06123 Perugia, ITALY  
tel. +390755855034, +390755853822,  
fax +390755855024  
bardaro@unipg.it ,  
bardaro@dipmat.unipg.it  
Functional Analysis and Approximation Th.,  
Summability, Signal Analysis, Integral  
Equations,  
Measure Th., Real Analysis

4) Francoise Bastin  
Institute of Mathematics  
University of Liege  
4000 Liege

21) Gustavo Alberto Perla Menzala  
National Laboratory of Scientific Computation  
LNCC/MCT  
Av. Getulio Vargas 333  
25651-075 Petropolis, RJ  
Caixa Postal 95113, Brasil  
and

Federal University of Rio de Janeiro  
Institute of Mathematics  
RJ, P.O. Box 68530 Rio de Janeiro, Brasil  
perla@lncc.br and perla@im.ufrj.br  
Phone 55-24-22336068, 55-21-25627513 Ext 224  
FAX 55-24-22315595  
Hyperbolic and Parabolic Partial Differential  
Equations,  
Exact controllability, Nonlinear Lattices and  
Global  
Attractors, Smart Materials

22) Ram N. Mohapatra  
Department of Mathematics  
University of Central Florida  
Orlando, FL 32816-1364  
tel. 407-823-5080  
ramm@pegasus.cc.ucf.edu  
Real and Complex analysis, Approximation Th.,  
Fourier Analysis, Fuzzy Sets and Systems

23) Rainer Nagel  
Arbeitsbereich Funktionalanalysis  
Mathematisches Institut  
Auf der Morgenstelle 10  
D-72076 Tuebingen  
Germany  
tel. 49-7071-2973242  
fax 49-7071-294322  
rana@fa.uni-tuebingen.de  
evolution equations, semigroups, spectral th.,  
positivity

24) Panos M. Pardalos  
Center for Appl. Optimization  
University of Florida  
303 Weil Hall  
P.O. Box 116595  
Gainesville, FL 32611-6595  
tel. 352-392-9011  
pardalos@ufl.edu  
Optimization, Operations Research

BELGIUM

f.bastin@ulg.ac.be  
Functional Analysis,Wavelets

5) Yeol Je Cho  
Department of Mathematics Education  
College of Education  
Gyeongsang National University  
Chinju 660-701

KOREA

tel.055-751-5673 Office,  
055-755-3644 home,  
fax 055-751-6117  
yjcho@nongae.gsnu.ac.kr  
Nonlinear operator Th.,Inequalities,  
Geometry of Banach Spaces

6) Sever S.Dragomir  
School of Communications and Informatics  
Victoria University of Technology  
PO Box 14428  
Melbourne City M.C  
Victoria 8001,Australia  
tel 61 3 9688 4437,fax 61 3 9688 4050  
sever.dragomir@vu.edu.au,  
sever@sci.vu.edu.au  
Math.Analysis,Inequalities,Approximation  
Th.,  
Numerical Analysis, Geometry of Banach  
Spaces,  
Information Th. and Coding

7) Angelo Favini  
Università di Bologna  
Dipartimento di Matematica  
Piazza di Porta San Donato 5  
40126 Bologna, ITALY  
tel.++39 051 2094451  
fax.++39 051 2094490  
favini@dm.unibo.it  
Partial Differential Equations, Control  
Theory,  
Differential Equations in Banach Spaces

8) Claudio A. Fernandez  
Facultad de Matematicas  
Pontificia Universidad Católica de Chile  
Vicuna Mackenna 4860  
Santiago, Chile  
tel.++56 2 354 5922  
fax.++56 2 552 5916  
cfernand@mat.puc.cl  
Partial Differential Equations,  
Mathematical Physics,  
Scattering and Spectral Theory

25) Svetlozar T.Rachev  
Dept.of Statistics and Applied Probability  
Program

University of California,Santa Barbara  
CA 93106-3110,USA  
tel.805-893-4869  
rachev@pstat.ucsb.edu

AND

Chair of Econometrics and Statistics  
School of Economics and Business Engineering  
University of Karlsruhe  
Kollegium am Schloss,Bau II,20.12,R210  
Postfach 6980,D-76128,Karlsruhe,Germany  
tel.011-49-721-608-7535  
rachev@lsoe.uni-karlsruhe.de  
Mathematical and Empirical Finance,  
Applied Probability, Statistics and Econometrics

26) John Michael Rassias  
University of Athens  
Pedagogical Department  
Section of Mathematics and Infomatics  
20, Hippocratous Str., Athens, 106 80, Greece

Address for Correspondence

4, Agamemnonos Str.  
Aghia Paraskevi, Athens, Attikis 15342 Greece  
jrassias@primedu.uoa.gr  
jrassias@tellas.gr  
Approximation Theory,Functional Equations,  
Inequalities, PDE

27) Paolo Emilio Ricci  
Universita' degli Studi di Roma "La Sapienza"  
Dipartimento di Matematica-Istituto  
"G.Castelnuovo"  
P.le A.Moro,2-00185 Roma,ITALY  
tel.++39 0649913201,fax ++39 0644701007  
riccip@uniroma1.it,Paoloemilio.Ricci@uniroma1.it  
Orthogonal Polynomials and Special functions,  
Numerical Analysis, Transforms,Operational  
Calculus,  
Differential and Difference equations

28) Cecil C.Rousseau  
Department of Mathematical Sciences  
The University of Memphis  
Memphis,TN 38152,USA  
tel.901-678-2490,fax 901-678-2480  
ccrousse@memphis.edu  
Combinatorics,Graph Th.,  
Asymptotic Approximations,  
Applications to Physics

29) Tomasz Rychlik

- 9) A.M.Fink  
Department of Mathematics  
Iowa State University  
Ames, IA 50011-0001, USA  
tel.515-294-8150  
fink@math.iastate.edu  
Inequalities, Ordinary Differential Equations
- 10) Sorin Gal  
Department of Mathematics  
University of Oradea  
Str.Armatei Romane 5  
3700 Oradea, Romania  
galso@uoradea.ro  
Approximation Th., Fuzzyness, Complex Analysis
- 11) Jerome A. Goldstein  
Department of Mathematical Sciences  
The University of Memphis,  
Memphis, TN 38152, USA  
tel.901-678-2484  
jgoldste@memphis.edu  
Partial Differential Equations, Semigroups of Operators
- 12) Heiner H. Gonska  
Department of Mathematics  
University of Duisburg  
Duisburg, D-47048  
Germany  
tel.0049-203-379-3542 office  
gonska@informatik.uni-duisburg.de  
Approximation Th., Computer Aided Geometric Design
- 13) Dmitry Khavinson  
Department of Mathematical Sciences  
University of Arkansas  
Fayetteville, AR 72701, USA  
tel.(479)575-6331, fax(479)575-8630  
dmitry@uark.edu  
Potential Th., Complex Analysis, Holomorphic PDE,  
Approximation Th., Function Th.
- 14) Virginia S. Kiryakova  
Institute of Mathematics and Informatics  
Bulgarian Academy of Sciences  
Sofia 1090, Bulgaria  
virginia@diogenes.bg  
Special Functions, Integral Transforms, Fractional Calculus
- 15) Hans-Bernd Knoop  
Institute of Mathematics  
Polish Academy of Sciences  
Chopina 12, 87100 Torun, Poland  
T.Rychlik@impan.gov.pl  
Mathematical Statistics, Probabilistic Inequalities
- 30) Bl. Sendov  
Institute of Mathematics and Informatics  
Bulgarian Academy of Sciences  
Sofia 1090, Bulgaria  
bsendov@bas.bg  
Approximation Th., Geometry of Polynomials, Image Compression
- 31) Igor Shevchuk  
Faculty of Mathematics and Mechanics  
National Taras Shevchenko  
University of Kyiv  
252017 Kyiv  
UKRAINE  
shevchuk@univ.kiev.ua  
Approximation Theory
- 32) H.M. Srivastava  
Department of Mathematics and Statistics  
University of Victoria  
Victoria, British Columbia V8W 3P4  
Canada  
tel.250-721-7455 office, 250-477-6960 home,  
fax 250-721-8962  
harimsri@math.uvic.ca  
Real and Complex Analysis, Fractional Calculus and Appl.,  
Integral Equations and Transforms, Higher Transcendental Functions and Appl., q-Series and q-Polynomials, Analytic Number Th.
- 33) Stevo Stevic  
Mathematical Institute of the Serbian Acad. of Science  
Knez Mihailova 35/I  
11000 Beograd, Serbia  
sstevic@ptt.yu; sstevo@matf.bg.ac.yu  
Complex Variables, Difference Equations, Approximation Th., Inequalities
- 34) Ferenc Szidarovszky  
Dept. Systems and Industrial Engineering  
The University of Arizona  
Engineering Building, 111  
PO.Box 210020  
Tucson, AZ 85721-0020, USA  
szidar@sie.arizona.edu  
Numerical Methods, Game Th., Dynamic Systems,

Institute of Mathematics  
 Gerhard Mercator University  
 D-47048 Duisburg  
 Germany  
 tel.0049-203-379-2676  
 knoop@math.uni-duisburg.de  
 Approximation Theory, Interpolation

16) Jerry Koliha  
 Dept. of Mathematics & Statistics  
 University of Melbourne  
 VIC 3010, Melbourne  
 Australia  
 koliha@unimelb.edu.au  
 Inequalities, Operator Theory,  
 Matrix Analysis, Generalized Inverses

17) Mustafa Kulenovic  
 Department of Mathematics  
 University of Rhode Island  
 Kingston, RI 02881, USA  
 kulenm@math.uri.edu  
 Differential and Difference Equations

18) Gerassimos Ladas  
 Department of Mathematics  
 University of Rhode Island  
 Kingston, RI 02881, USA  
 gladas@math.uri.edu  
 Differential and Difference Equations

19) V. Lakshmikantham  
 Department of Mathematical Sciences  
 Florida Institute of Technology  
 Melbourne, FL 32901  
 e-mail: lakshmik@fit.edu  
 Ordinary and Partial Differential  
 Equations,  
 Hybrid Systems, Nonlinear Analysis

20) Rupert Lasser  
 Institut für Biomathematik & Biomertie, GSF  
 -National Research Center for environment  
 and health  
 Ingolstaedter landstr.1  
 D-85764 Neuherberg, Germany  
 lasser@gsf.de  
 Orthogonal Polynomials, Fourier Analysis,  
 Mathematical Biology

Multicriteria Decision making,  
 Conflict Resolution, Applications  
 in Economics and Natural Resources  
 Management

35) Gancho Tachev  
 Dept. of Mathematics  
 Univ. of Architecture, Civil Eng. and Geodesy  
 1 Hr. Smirnenski blvd  
 BG-1421 Sofia, Bulgaria  
 gtt\_fte@uacg.bg  
 Approximation Theory

36) Manfred Tasche  
 Department of Mathematics  
 University of Rostock  
 D-18051 Rostock  
 Germany  
 manfred.tasche@mathematik.uni-rostock.de  
 Approximation Th., Wavelet, Fourier Analysis,  
 Numerical Methods, Signal Processing,  
 Image Processing, Harmonic Analysis

37) Chris P. Tsokos  
 Department of Mathematics  
 University of South Florida  
 4202 E. Fowler Ave., PHY 114  
 Tampa, FL 33620-5700, USA  
 profcpt@math.usf.edu, profcpt@chumal.cas.usf.edu  
 Stochastic Systems, Biomathematics,  
 Environmental Systems, Reliability Th.

38) Lutz Volkmann  
 Lehrstuhl II für Mathematik  
 RWTH-Aachen  
 Templergraben 55  
 D-52062 Aachen  
 Germany  
 volkm@math2.rwth-aachen.de  
 Complex Analysis, Combinatorics, Graph Theory

# Particles Flow on the Regular Polygon

Alexander P. Buslaev , Alexander G. Tatashev

Department of Mathematics

The Moscow State Automobile and Road Technical University

125319, Leningradskii pr.,64, Moscow, Russia

apal2006@yandex.ru

**AMS 2000 Mathematics Subject Classification:** 34B45, 60G50, 60J10, 37B99, 37B15.

**Key words and phrases:** Mathematical model, random walking, steady probabilities, average velocity.

## Abstract

A random walking of particles on the closed sequence of cells is studied. At the current time the particle occupies some cell. The transition of particle occurs at the integer time with a given probability provided that the cell, following the cell occupied by the particle, is free. The steady probabilities of system states and the average individual velocity of particles have been found.

## 1. Introduction. Formulation of the problem

The closed sequence of  $n$  cells is studied. There are  $m$  particles,  $0 < m < n$ . At the current time the particle occupies some cell. No more than one particle occupies the cell. The cell  $i + 1$  follows the cell  $i$ ,  $i = 1, 2, \dots, n - 1$ . The cell 1 follows the cell  $n$ . The transitions of particle occur at the integer time  $1, 2, 3, \dots$ . If at the integer time the cell following the cell, which is occupied by the particle, is free then the transition of the particle occurs with the probability  $p$ ,  $0 < p < 1$ , independent of the behaviour of the other particles.

The discrete time models, which describe the movement of particles on the discrete lattice, are investigated in [1–5].

In [1] the lattice on the straight line, in which a random walking describes the traffic flow, has been considered. Each position of the lattice contains not more than one particle. It is not permissible for the distance between two neighbouring particles to be less than the minimum permissible value. If the neighbouring right particle approaches to the left one and the distance between the particles becomes less than the minimum permissible

distance then the left particle has to move aside to the left to keep the necessary distance. If the distance between the particle and the neighbouring one is more than the minimum permissible distance then at discrete time the particle moves with given probabilities to the right or to the left. We suppose that the probability of moving to the right is more than the probability of moving to the left. The case of two particles and the general case have been considered. *It has been proved for the system of two particles that the distance between particles has in the steady state the geometrical distribution with the parameter depending on the parameters of particles movement.* This result can be considered as follows. If the velocity of the leader is less than the velocity of that moving behind then the movement is synchronized at the steady state with the movement of the leader and the distance between the leader and the particle moving behind is distributed geometrically. It has been proved for the common case that the number of particles of a batch has the geometrical distribution with the parameter depending on the probabilities of particles movement. Model considered in [1] describes approximately such phenomena as reaching of the maximum capacity, appropriate to the optimal density of the traffic flow, and the traffic jam occurrence.

In [2] the model of work [1] has been generalized for the velocity of the car depending on the velocity of the car going ahead. Different kinds of dependences of the traffic intensity on the density have been found for the different parameters. It is shown that abrupt decrease of the intensity can be modelled for the case of the traffic density exceeding the optimal value.

The theory of Markov chains was used in [1] and [2] for investigation of the random walking [6].

In [3] it has been found by means of the dual mapping the accurate results on several models of traffic flows. The descriptions of limit configurations have been obtained for these models. These results are used in [3] for investigation of a fast particle, which moves in the direction of the particles flow or against the direction of the particles flow.

In [4] it has been studied by means of a new variation approach the ergodic properties of a model of a multi-lane traffic flow, considered as a deterministic walking of particles on an infinite lattice. For a class of initial configurations of particles the description of their limit behaviour is obtained, as well as estimates of the transient period. Statistical quantities describing limit configurations are obtained also.

In [5] a closed chain of cells, on which particles move, has been considered. The model time is continuous. Every particle can move with a given intensity for one cell forward remaining on its lane. If the appropriate cell is busy and the two neighbouring cells on the other lane are free, then the particle moves for one cell forward and comes to the other lane. The approximate method has been worked out for the calculation of the traffic flow velocity. The method is based on use of a Markov chain. This chain describes the behaviour of four neighbouring cells. It is assumed for the Markov chain that probabilities of transitions can be calculated as each of the four cells, neighbouring for the four considered cells, were busy with the probability equal to the flow density and *were not independent on the states of the other cells*.

Some physical formulation and investigation of traffic models by simulation method have been represented in [7], [8].

The system, considered in our work, is described by the Markov chain. The chain states are characterized by the disposition of the particles. The number of the chain states equals the number  $C_n^m$  of combinations of  $m$  elements from  $n$  ones, where  $n$  is the number of cells and  $m$  is the number of particles. Let  $N$  be the number of chain states.

*Lemma 1. The considered Markov chain is irreducible.*

*Proof.* It is one and only one system state of the system corresponds to each binary  $n$ -valued integer number containing  $m$  "ones" and  $n - m$  "zeros" in their records. Besides it is possible, shifting "ones" to the neighbouring position with zeros, to come for a finite number of transitions from every state to every other state. Really, we can collect all the "ones" so that they made up a cluster, beginning from the most right position, and then we can arrange the "ones" appropriately.

Let the chain states be numbered arbitrarily. Let  $p_i$  be stationary probability of the  $i$ -th state,  $i = 1, \dots, N$ . Let  $p_{ij}$  be the probability of the transition from the state  $i$  to the state  $j$ ,  $i, j = 1, \dots, N$ .

The steady states probabilities of the chain satisfies the system of equations

$$p_i \sum_{j=1}^N p_{ij} = \sum_{j=1}^N p_j p_{ji}, \quad i = 1, \dots, N, \quad (1)$$

$$\sum_{j=1}^N p_j = 1. \quad (2)$$

Let  $k(i)$  be the number of clusters for the  $i$ -th state of the chain. We call "cluster"



the batch of the neighboring cells busy with particles and isolated each from other by the free cells. If the  $i$ -th state is the current state of the chain then the number of particles, which are able to move, equals the number of clusters for this state, i.e. this number is equal to  $k(i)$ ,  $0 \leq k(i) \leq m$ . There are  $2^{k(i)}$  states to which the chain can pass from state  $i$ . Let  $l(i, j)$  be the number of particles that move if the chain passes from the state  $i$  to the state  $j$ ,  $1 \leq k(i) \leq m + 1$ . Then

$$p_{ij} = p^{l(i,j)}(1-p)^{k(i)-l(i,j)}, \quad l(i, j) = 0. \quad (3)$$

The probability, that the chain does not leave the  $i$ -th state at the current time, is equal to the probability that all the  $k(i)$  particles do not move. This probability equals  $p_{ii} = (1-p)^{k(i)}$ . By this reason and in accordance with (2)

$$\sum_{j=1, j \neq i} p_{ij} = 1 - (1-p)^{k(i)}.$$

*There exist steady probabilities of the considered Markov chain and these probabilities are unique.* It follows from the known theorem of the theory of Markov chains. In accordance with this theorem, if it is possible to come from an arbitrary state to the other arbitrary state for a finite number of transitions (it is equivalent to that all the elements of some power of the transition matrix are positive i.e. the Markov chain corresponding to this matrix is irreducible) then system (1)–(2) has a solution and the solution is unique, [6].

## 2. States with a given number of clusters

Let  $S(k, n, m)$  be the number of  $k$  clusters states for number of cells equal to  $n$  and number of particles equal to  $m$ .

Lemma 2. *The equality is true*

$$S(k, n, m) = \begin{cases} \frac{n}{k} C_{m-1}^{k-1} C_{n-m-1}^{k-1}, & k \leq \min(m, n-m); \\ 0, & k > \min(m, n-m). \end{cases} \quad (4)$$

*Proof.* Let  $R(k, m)$  be the number of ways to represent the number  $m$  as sum of  $k$  items provided the order of the items is taken into account

( $k \leq \min(m, n-m)$ ). It is the number of ways to take  $k-1$  elements from  $m-1$  ones:

$$R(k, m) = C_{m-1}^{k-1}. \quad (5)$$

Let us find the number  $A(k, n, m)$  of the elements of the set  $A$  of states with  $k$  clusters and for that cell 1 is free and cell 2 is busy. This number equals to the number of ways to distribute  $m$  particles on  $k$  clusters (this number equals  $R(k, m)$ ) multiplied by the number of ways to choose the lengths of  $k - 1$  gaps (this number equals  $R(k, n - m)$ ). So we have for  $k \leq \min(m, n - m)$

$$A(k, n, m) = R(k, m)R(k, n - m). \quad (6)$$

It follows from (5) and (6) that

$$A(k, n, m) = C_{m-1}^{k-1} C_{n-m-1}^{k-1}. \quad (7)$$

Let state  $a = (i_1, \dots, i_n)$  be an element of set  $A$ . Let  $b(a, d)$  be the state that is attended from the state  $a$  by turning, provided the  $i$ -th cell  $i$  comes to the position, that was occupied by the  $(i + d)$ -th cell, i.e.

$b(a, d) = (i_{n-d+1}, i_{n-d+2}, \dots, i_n, i_1, \dots, i_{n-d})$ . Every  $k$  clusters chain states can be represented as  $b(a, d)$  for  $k$  different ordered pairs  $(a, d)$ , where  $a$  is some element of set  $A$  and  $d$  is one of the number  $0, 1, \dots, n - 1$ . There exist  $nA(k, n, m)$  non-identical pairs  $(a, d)$ . So

$$S(k, n, m) = \frac{n}{k} A(k, n, m). \quad (8)$$

Equation (4) follows from (7) and (8). Lemma has been proved.

### 3. Steady probabilities of states

*Theorem 1. The solution of the system (1)–(2) is*

$$p_i = \frac{C}{(1 - p)^{k(i)-1}}, \quad i = 1, \dots, N, \quad (9)$$

where

$$C = \left( \sum_{k=1}^{\min(m, n-m)} \frac{n}{k} \cdot C_{m-1}^{k-1} C_{n-m-1}^{k-1} \frac{1}{(1 - p)^{k-1}} \right)^{-1}. \quad (10)$$

*Proof.* Let us write system (1) as

$$\sum_{j=1}^N p_i p_{ij} = \sum_{j=1}^N p_j p_{ji}, \quad i = 1, \dots, N. \quad (11)$$

Let  $F(i)$  be the set of states to that it is possible to come from state  $i$  at ones. Let  $F(i, l)$  be the subset of set  $F(i)$  containing the states to that it is possible to come from

the state  $i$  by transitions of  $l$  particles. Let  $B(i)$  be the set of states from that it is possible to come to state  $i$  at ones. Let  $B(i, l)$  be the subset of  $B(i)$  containing the states from that it is possible to come to state  $i$  by transitions of  $l$  particles.

We have

$$p_{ij} = \begin{cases} 0, & j \notin F(i), \quad i, j = 1, \dots, N, \\ p^l(1-p)^{k(i)-l}, & j \in F(i, l), \quad i, j = 1, \dots, N, \quad l = 1, \dots, k(i), \end{cases} \quad (12)$$

$$p_{ji} = \begin{cases} 0, & j \notin B(i), \quad i, j = 1, \dots, N, \\ p^l(1-p)^{k(j)-l}, & j \in B(i, l), \quad i, j = 1, \dots, N, \quad l = 1, \dots, k(i). \end{cases} \quad (13)$$

Taking into account (12) and (13) we can write (11) as

$$\sum_{l=1}^{k(i)} \text{card}(F(i, l)) p_i p^l (1-p)^{k(i)-l} = \sum_{l=1}^{k(i)} \sum_{j \in B(i, l)} p_j p^l (1-p)^{k(j)-l}, \quad i = 1, \dots, N. \quad (14)$$

We use the designation  $\text{card}(A)$  for the number of the elements of set  $A$ .

Substituting (9) to (14) we can write (14) as

$$\sum_{l=1}^{k(i)} \text{card}(F(i, l)) p^l (1-p)^{1-l} = \sum_{l=1}^{k(i)} \text{card}(B(i, l)) p^l (1-p)^{1-l}, \quad i = 1, \dots, N. \quad (15)$$

Because of the symmetry  $\text{card}(B(i, l)) = \text{card}(F(i, l))$ ,  $l = 1, \dots, k(i)$ ,

$i = 1, \dots, N$ .

So solution (9) satisfies equation (11) and therefore it satisfies system (1).

Equation (10) for  $C$  follows from (2), (9) and Lemma 2.

Theorem 1 has been proved.

## 4. The average velocity of particles

Let us call the quantity of movement the number of particles moving at the current time.

Let us call the average velocity of particle the ratio of the quantity of movement to the total number of particles.

For the quantity of movement we have

$$Q = \sum_{i=1}^N p_i k(i) p. \quad (16)$$

*Theorem 2.*

*For the average velocity of particles  $v$  the equation is true*

$$v = \frac{1}{m} Q = \frac{n}{m} \sum_{k=1}^{\min(m, n-m)} \frac{C p}{(1-p)^{k-1}} C_{m-1}^{k-1} C_{n-m-1}^{k-1}.$$

*Proof.* The statement of Theorem 2 follows from Theorem 1, Lemma 2 and equation (16).

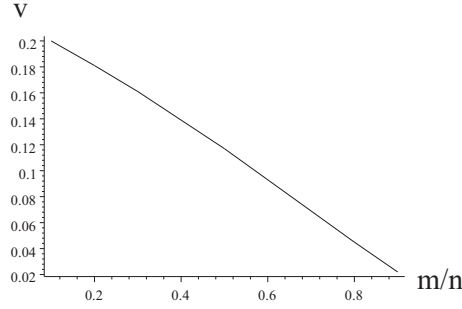


Figure 1: Dependence of the average velocity  $v$  on the flow density  $\rho$ ,  $n = 10$ ,  $p = 0.2$ .

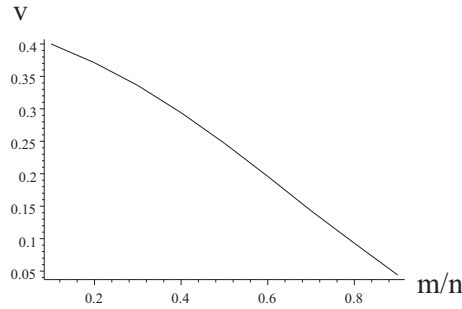


Figure 2: Dependence of the average velocity  $v$  on the flow density  $\rho$ ,  $n = 10$ ,  $p = 0.4$ .

*Lemma 3.*

- (1) *The average velocity of particle is an increasing function on parameter  $p$ .*
- (2)  *$v = p(1 - r)$ , where  $r$  is the probability that the cell following a busy cell is busy also.*

*Proof.* Statement (1) is a consequence of equation (16) and Theorem 1 in accordance with that the probabilities of the states, for that the number of clusters is larger, increases and the probabilities of the states, for that the number clusters is smaller, decreases.

It is true for the quantity  $Q$  of movement

$$Q = np(1 - r). \quad (17)$$

From (17) and equation

$$v = \frac{Q}{m}$$

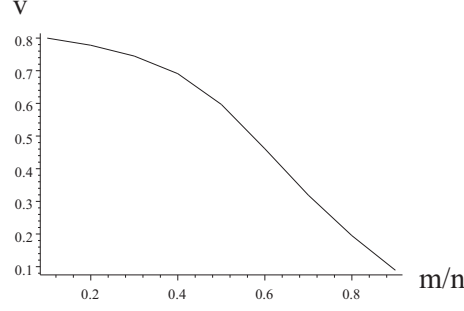


Figure 3: Dependence of the average velocity  $v$  on the flow density  $\rho$ ,  $n = 10$ ,  $p = 0.8$ .

statement (2) follows. Lemma 3 has been proved.

The dependence of the average velocity of particles on the density of particles flow  $\rho = \frac{m}{n}$  is represented in Fig. 1–3 for  $m = 10$  and  $p = 0.2, 0.4, 0.8$ .

## 5. Analysis of the case of the probability of transition close to 0

We have from (9) that

$$p_i = C + O(p), \quad p \sim 0, \quad i = 1, \dots, N. \quad (18)$$

We have from (2) and (18)

$$p_i = \frac{1}{N} + O(p), \quad p \sim 0, \quad i = 1, \dots, N. \quad (19)$$

*Lemma 4.* The equality is true for  $p \sim 0$

$$r = \frac{m-1}{n-1} + O(1).$$

*Proof.* Probability that a given cell is busy can be represented as  $\frac{1}{N}C_{n-1}^{m-1}$  for  $p_i = \frac{1}{N}$ ,  $i = 1, \dots, N$ . Probability, that the cell following the given cell is busy also, is equal to  $\frac{1}{N}C_{n-2}^{m-2}$ . The ratio of  $\frac{1}{N}C_{n-2}^{m-2}$  to  $\frac{1}{N}C_{n-1}^{m-1}$  equals  $r$ . Calculating this ratio we get the lemma statement.

*Theorem 3.*

1) It is true for  $i = 1, \dots, N$

$$p_i = \frac{1}{N} + O(p), \quad p \sim 0.$$

2) The average velocity of particle equals

$$v = p \cdot \frac{n-m}{n-1} + o(p), \quad p \sim 0.$$

*Proof.* The statement follows from equation (19), equation  $v = p(1-r)$  and Lemma 4.

## 6. Analysis of the case of the probability of transition close to 1

Let  $K(n, m)$  be the maximum possible number of clusters for given  $m$  and  $n$ . Equation (9) can be written as

$$p_i = A(1-p)^{K(n,m)-k(i)}, \quad (20)$$

where  $A$  is the probability of state with  $K(n, m)$  clusters.

We have from (20) that

$$p_i = o(1-p), \quad k(i) < K(n, m), \quad p \sim 1.$$

Hence

$$Q = K(n, m) + o(1-p), \quad p \sim 1.$$

Taking into account that

$$K(n, m) = \begin{cases} m \leq \frac{n}{2}, \\ n-m, \quad m > \frac{n}{2}, \end{cases}$$

we have

$$Q = \begin{cases} m + o(1-p), \quad m \leq \frac{n}{2}, \\ n-m + o(1-p), \quad m > \frac{n}{2}. \end{cases} \quad (21)$$

Let us define  $\rho$  as

$$\rho = \frac{m}{n}. \quad (22)$$

It follows from (21) and (22) that

$$v = \begin{cases} 1 + o(1-p), \quad \rho \leq \frac{1}{2}, \\ \frac{1}{\rho} - 1 + o(1-p), \quad \rho > \frac{1}{2}. \end{cases} \quad (23)$$

Equation (23) corresponds to the results of the work [3], where it was considered a similar model for the case of the probability of the transition of particle close to 1.

## 7. Exact solution for the quadrangle

Let us consider the case  $n = 4, m = 2$ . There are four one cluster chain states and two clusters chain states.

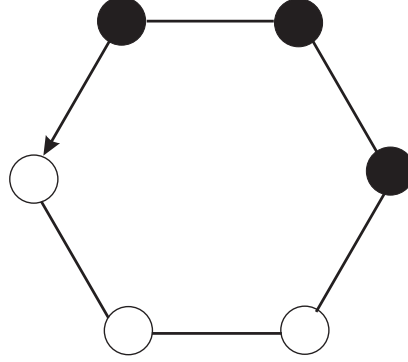


Figure 4: One cluster chain state

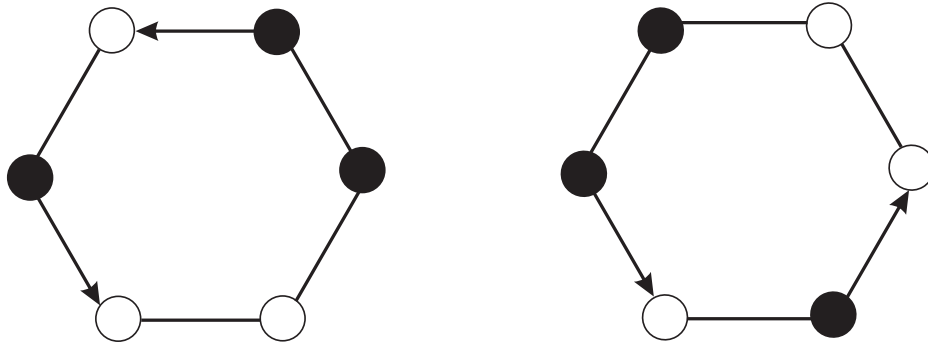


Figure 5: Two clusters chain states

We have from (9)

$$p_i = \frac{1-p}{6-4p}, \quad k(i) = 1,$$

and

$$p_i = \frac{1}{6-4p}, \quad k(i) = 2.$$

For the average velocity of particles we have

$$v = \frac{2p - p^2}{3 - 2p}.$$

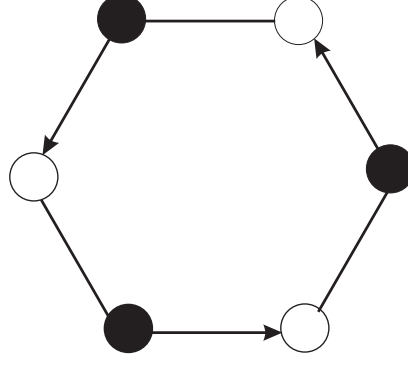


Figure 6: Three clusters chain state

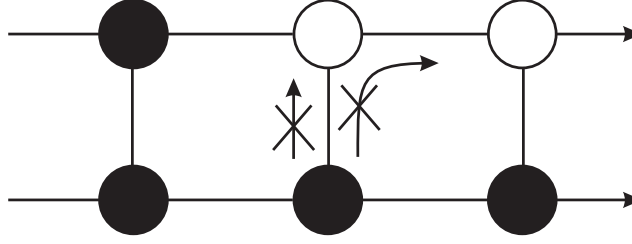


Figure 7: Pass to the other lane is forbidden

## 8. Exact solution for the hexagon

Let us designate the state of chain by sequence of zeros and ones. One on the  $i$ -th place means that for this state there is particle in the  $i$ -th cell.

Let us consider the case  $n = 6$ ,  $m = 3$ . There are 20 states of the chain. Among them there are 6 one cluster states. These states are

$(1, 1, 1, 0, 0, 0)$ ,  $(0, 1, 1, 1, 0, 0)$ ,  $\dots$ ,  $(0, 0, 0, 1, 1, 1)$  (Fig. 4). There are 2 three clusters states.

They are  $(1, 0, 1, 0, 1, 0)$ ,  $(0, 1, 0, 1, 0, 1)$  (Fig. 6). And there are 12 two clusters states (Fig. 5).

In accordance with Theorem 1 we have

$$p_i = \frac{1 - 2p + p^2}{20 - 24p + 6p^2}, \quad k(i) = 1,$$

$$p_i = \frac{1 - p}{20 - 24p + 6p^2}, \quad k(i) = 2,$$

$$p_i = \frac{1}{20 - 24p + 6p^2}, \quad k(i) = 3.$$



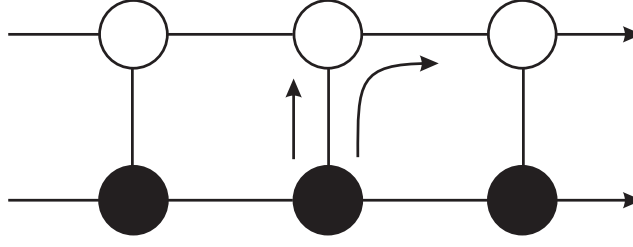


Figure 8: Pass to the other lane with moving ahead

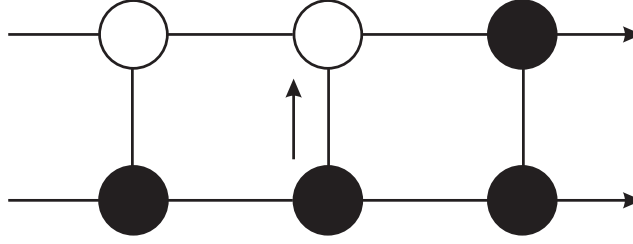


Figure 9: Pass to the other lane without moving ahead

## 9. Generalization for the case of the multi-lane movement of particles

Let us describe the model in which the movement of particles on two lanes occurs in accordance with the rules analogous to rules described in [5].

Let us consider two closed chain of cells (two lanes). There are  $n$  cells on every lane. Each cell corresponds to pair of numbers  $(i, j)$ , where  $j$  is the number of the lane ( $j = 1, 2$ ), and  $i$  is the number of the cell on the lane,  $i = 1, \dots, n$ . The movement of particles occurs in accordance with the following rule.

If the cell, following the cell containing the particle, is free then the particle comes to the following cell with probability  $p$ .

If the cell, following the cell containing the particle, is busy and it is busy also the cell of the other lane being behind then at the current time the particle does not move (Fig. 7).

If the cell, following the cell containing the particle, is busy and three neighbouring cells on the other lane are free then the particle passes to the other lane moving forward to the next cell (Fig. 8).

If the cell, following the cell containing the particle, is busy and two cells behind are free then the particle passes to the other lane without moving forward (Fig. 9).

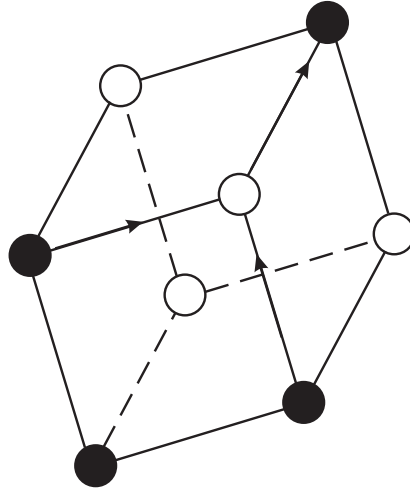


Figure 10: Two-channel quadrangle

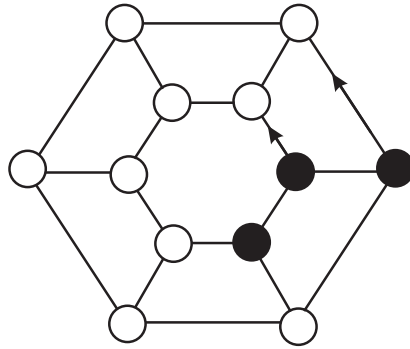


Figure 11: Two-channel hexagon

We can formulate the problem of investigation of this model. In particular we can formulate the problem of calculation of the average velocity of particle for the mode.

The analogous model has been considered in [5]. The difference is that particles cannot pass to the other lane without moving forward and, if there are two free cells on the other lane, the particle passes to the other lane either the cell on the other lane behind is busy or it is free. It has been worked out in [5] an approximate method that can be used for calculation of characteristics of the system described in this section.

The formulated problem can be interpreted as the problem of the random walking of particles on a polyhedron (Fig. 10,11).

The analogous generalization of the problem can be formulated for the case when the number of lanes is more than two.

## References

- [1] Belyaev, Ju.K. On the simplified model of movement without overtake / Izv. AN SSSR. Techn. kibernet, N 3, 17–21 ,1969, (in Russian) .
- [2] Zele, U. Generalized model of movement without overtake / Izv. AN SSSR. Techn. kibernet, N 5, 100–103 ,1972, (in Russian) .
- [3] Blank, M.L. Exact analysis of the dynamic systems, occurring in traffic flow modelling/ UMN ,2000, 55: 3 (333), 167–168 ,(in Russian) .
- [4] Blank M.L. Dynamics of traffic jams: order and chaos /Mosc. Math. J., 2001, v. 1, N 1, 1–26.
- [5] Belyaev, Ju.K., Buslaev, A.P., Seleznyov, O.V., Tatashev, A.G., Yashina, M.V. Markov approximation of the stochastic models of two-lane movement /Moscow State Automobile and Road Technical University, Dep. VINITI 03.07.2002 , N 1234–, V 2002,Moscow ,2002, (in Russian) .
- [6] Borovkov, A.A. Probability theory / Nauka, Moscow ,1976, (in Russian) .
- [7] Nagel, K., Schreckenberg M. A cellular automation model for traffic / J. Physique I. ,1992, 2 , 2221–2229.
- [8] Belitsky, V., Krug, J., Jordano Neves E., Shultz G. A A cellular automation model for two-lane traffic / Stat. Phys.,2001, 103:5/6 , 945–971.

## NOTES ON ABSOLUTE SUMMABILITY FACTORS

W. T. Sulaiman

Department of Computer Engineering

College of Engineering

University of Mosul, Iraq.

[waadsulaiman@hotmail.com](mailto:waadsulaiman@hotmail.com)

**Abstract.** In the present paper we prove a result concerning absolute summability of an infinite series. This result improved a previous result due to Rhoades and Savas[2]

## 1. Introduction

Let  $T$  be a lower triangular matrix,  $(s_n)$  a sequence, and

$$T_n := \sum_{v=0}^n t_{nv} s_v. \quad (1.1)$$

A series  $\sum a_n$  is said to be summable  $|T|_k$ ,  $k \geq 1$ , if

$$\sum_{n=1}^{\infty} n^{k-1} |\Delta T_{n-1}|^k < \infty. \quad (1.2)$$

Given any lower triangular matrix  $T$  one can associate the matrices  $\bar{T}$  and  $\hat{T}$ , with entries defined by

$$\bar{t}_{nv} = \sum_{i=v}^n t_{ni}, \quad n, i = 0, 1, 2, \dots, \quad \hat{t}_{nv} = \bar{t}_{nv} - \bar{t}_{n-1,v}$$

respectively. With  $s_n = \sum_{i=0}^n a_i \lambda_i$ ,

$$t_n = \sum_{v=0}^n t_{nv} s_v = \sum_{v=0}^n t_{nv} \sum_{i=0}^v a_i \lambda_i = \sum_{i=0}^n a_i \lambda_i \sum_{v=i}^n t_{nv} = \sum_{i=0}^n \bar{t}_{ni} a_i \lambda_i. \quad (1.3)$$

$$Y_n := t_n - t_{n-1} = \sum_{i=0}^n \bar{t}_{ni} a_i \lambda_i - \sum_{i=0}^{n-1} \bar{t}_{n-1,i} a_i \lambda_i = \sum_{i=0}^n \hat{t}_{ni} a_i \lambda_i, \quad \text{as } \bar{t}_{n-1,n} = 0. \quad (1.4)$$

$$X_n := u_n - u_{n-1} = \sum_{i=0}^n \hat{u}_{ni} a_i \mu_i. \quad (1.5)$$

We call  $T$  a triangle if  $T$  is lower triangular and  $t_{nn} \neq 0$  for all  $n$ . A triangle  $A$  is called factorable if its nonzero entries  $a_{mn}$  can be written in the form  $b_m c_n$  for each  $m$  and  $n$ .

If we assumed that  $T$  to be factorable, then  $t_{nv} = a_n b_v$ , and therefore we have

$$\bar{t}_{nv} = \sum_{r=v}^n t_{nr} = a_n \sum_{r=v}^n b_r := a_n B_r \quad (1.6)$$

$$\begin{aligned}\hat{t}_{nv} &= \bar{t}_{nv} - \bar{t}_{n-1,v} = a_n B_v - a_{n-1} \sum_{r=v}^{n-1} b_r = a_n B_v - a_{n-1} B_v + a_{n-1} b_n \\ &= a_n B_v - a_{n-1} B_v = -\Delta a_{n-1} B_v, \text{ as } a_{n-1} b_n = t_{n-1,n} = 0.\end{aligned}\quad (1.7)$$

Also, we have  $\Delta B_v = b_v$ ,  $B_n = b_n$ .

We also assume that  $(p_n)$  is a positive sequences of numbers such that

$$P_n = p_0 + p_1 + \dots + p_n \rightarrow \infty, \text{ as } n \rightarrow \infty,$$

A positive sequence  $(a_n)$  is said to be *almost increasing* if there exist a positive increasing sequence  $(b_n)$  and two positive constants  $A$  and  $B$  such that (see[1]),  $Ab_n \leq a_n \leq Bb_n$ .

The series  $\sum a_n$  is said to be summable  $|R, p_n|_k$ ,  $k \geq 1$ , if

$$\sum_{n=1}^{\infty} n^{k-1} |T_n - T_{n-1}|^k < \infty,$$

where

$$T_n = \frac{1}{P_n} \sum_{v=0}^n p_v s_v.$$

Rhoads and Savas[2] have used the notation  $|\bar{N}, p_n|_k$  in order to denote the  $|R, p_n|_k$  - summability. They have proved the following result

**Theorem 1.1.** *Let  $A$  be a lower triangular matrix with non-negative entries satisfying*

- (i)  $a_{n0} = 1$   $n=0,1,\dots$ ,
- (ii)  $t_{n-1,v} \geq t_{nv}$  for  $n \geq v+1$ ,
- (iii)  $na_{nn} = O(1)$ ,  $1 = O(na_{nn})$ , and
- (iv)  $\sum_{v=1}^{n-1} a_{nv} |\hat{a}_{n,v+1}| = O(a_{nn})$

If  $(X_n)$  is a positive non- decreasing sequence such that

- (v)  $\lambda_m X_m = O(1)$ ,
- (vi)  $\sum_{n=1}^m (nX_n) |\Delta^2 \lambda_n| = O(1)$ , and
- (vii)  $\sum_{n=1}^m a_{nn} |t_n|^k = O(X_m)$ , where  $t = \frac{1}{n+1} \sum_{k=1}^n ka_k$ ,

then the series  $\sum a_n \lambda_n$  is summable  $|A|_k$ ,  $k \geq 1$ .

The aim of this paper is to improve the above result by weakening the condition (vii), and to deal with a general matrix  $T$  whose elements are positive or negative as, well as to study the new case in which the matrix  $T$  is factorable.

## 2. Results

**Lemma 2.1[1].** Let  $(X_n)$  be almost increasing sequence satisfying (v) and (vi). Then

$$\sum_{n=1}^{\infty} X_n |\Delta \lambda_n| < \infty \quad (2.1)$$

$$n X_n |\Delta \lambda_n| < \infty. \quad (2.2)$$

**Lemma 2.2.** the condition

$$\sum_{n=1}^m \frac{|t_{nn}|}{X_n^{k-1}} |t_n|^k = O(X_m) \quad (2.3)$$

is weaker than (vii) .

**Proof.** If (vii) holds, then we have

$$\sum_{n=1}^m \frac{|t_{nn}| |t_n|^k}{X_n^{k-1}} = O\left(\frac{1}{X_1^{k-1}}\right) \sum_{n=1}^m |t_{nn}| |t_n|^k = O(X_m),$$

while if (2.3) is satisfied then,

$$\begin{aligned} \sum_{n=1}^m |t_{nn}| |t_n|^k &= \sum_{n=1}^m \frac{|t_{nn}|}{X_n^{k-1}} |t_n|^k X_n^{k-1} \\ &= \sum_{n=1}^{m-1} \left( \sum_{v=1}^n \frac{|t_{nv}|}{X_v^{k-1}} \right) \Delta X_n^{k-1} + \left( \sum_{n=1}^m \frac{|t_{nn}|}{X_n^{k-1}} \right) X_m^{k-1} \\ &= O(1) \sum_{n=1}^{m-1} X_n |\Delta X_n^{k-1}| + O(X_m) X_m^{k-1} \\ &= O(X_{m-1}) \sum_{n=1}^{m-1} (X_{n+1}^{k-1} - X_n^{k-1}) + O(X_m^k) \\ &= O(X_{m-1}) (X_m^{k-1} - X_1^{k-1}) + O(X_m^k) \\ &= O(X_m^k). \end{aligned}$$

Therefore (viii) implies (2.3) but not conversely .

The following is our main result

**Theorem 2.3.** Let  $(X_n)$  be an almost increasing sequence . Let  $(\lambda_n)$  be sequences of numbers satisfying (v) and (vi), . Let  $T = (t_{nv})$  be a factorable matrix,  $t_{nv} = a_n b_v$  satisfying

$$\sum_{n=1}^m \frac{|a_n b_n| |t_n|^k}{X_n^{k-1}} = O(X_m) \quad (2.4)$$

$$n |a_n b_n| = O(1), \quad 1 = O(n |a_n b_n|), \quad (2.5)$$

$$\sum_{v=0}^{n-1} |\Delta a_{n-1} b_v| = O(|a_n b_n|), \quad (2.6)$$

$$\sum_{n=v+1}^m |\Delta a_{n-1} b_v| = O(|a_v b_v|), \quad (2.7)$$

$$\sum_{n=v+1}^m n^{k-1} |a_n b_n|^{k-1} |\Delta a_{n-1} B_{v+1}|^k = O(1), \quad (2.8)$$

$$\sum_{v=0}^{n-1} |a_v b_v| |\Delta a_{n-1} B_{v+1}| = O(|a_n b_n|), \quad (2.9)$$

then the series  $\sum a_n \lambda_n$  is summable  $|T|_k$ ,  $k \geq 1$ .

**Proof.** We have

$$\begin{aligned} Y_n &:= \sum_{v=1}^n \hat{t}_{nv} v a_v \lambda_v v^{-1} \\ &= \sum_{v=1}^{n-1} \left( \sum_{r=1}^v r a_r \right) \Delta_v (\hat{t}_{nv} \lambda_v v^{-1}) + \left( \sum_{v=1}^n v a_v \right) \hat{t}_{nn} \lambda_n n^{-1} \\ &= \sum_{v=0}^{n-1} (v+1) t_v (\Delta \hat{t}_{nv} \lambda_v v^{-1} + \hat{t}_{n,v+1} \frac{1}{v(v+1)} \lambda_v + \hat{t}_{n,v+1} \frac{1}{v+1} \Delta \lambda_v) + \frac{n+1}{n} t_n t_{nn} \lambda_n \\ &= \sum_{v=0}^{n-1} (v+1) t_v \left( -v^{-1} \Delta a_{n-1} b_v \lambda_v - \frac{1}{v(v+1)} \Delta a_{n-1} B_{v+1} \lambda_v - \frac{1}{v+1} \Delta a_{n-1} B_{v+1} \Delta \lambda_v \right) \\ &\quad + \frac{n+1}{n} t_n a_n b_n \lambda_n \\ &= Y_{n1} + Y_{n2} + Y_{n3} + Y_{n4}. \end{aligned}$$

In order to prove the Theorem, By Minkowski's inequality, it is sufficient to show that

$$\sum_{n=1}^m n^{k-1} |Y_{ni}| < \infty, \quad i = 1, 2, 3.$$

Applying Holder's inequality, we have

$$\begin{aligned} \sum_{n=1}^m n^{k-1} |Y_{n1}|^k &= \sum_{n=1}^m n^{k-1} \left| \sum_{v=0}^{n-1} \frac{v+1}{v} t_v \Delta a_{n-1} b_v \lambda_v \right|^k \\ &\leq \sum_{n=1}^m n^{k-1} \sum_{v=0}^{n-1} |t_v|^k |\Delta a_{n-1} b_v| |\lambda_v|^k \left( \sum_{v=1}^{n-1} |\Delta a_{n-1} b_v| \right)^{k-1} \\ &= O(1) \sum_{n=1}^m (n |a_n b_n|)^{k-1} \sum_{v=0}^{n-1} |t_v|^k |\Delta a_{n-1} b_v| |\lambda_v|^k \\ &= O(1) \sum_{n=1}^m O(1) \sum_{v=0}^{n-1} |t_v|^k |a_{n-1} b_v| |\lambda_v|^k \end{aligned}$$

$$\begin{aligned}
&= O(1) \sum_{v=0}^m |t_v|^k |\lambda_v|^k \sum_{n=v+1}^m |\Delta a_{n-1} b_v| \\
&= O(1) \sum_{v=0}^m |t_v|^k |\lambda_v|^k |a_v b_v| \\
&= O(1) \sum_{v=1}^m \frac{|t_v|^k}{X_v^{k-1}} |\lambda_v|^{k-1} X_v^{k-1} |\lambda_v| \\
&= O(1) \sum_{v=1}^m \frac{|t_v|^k}{X_v^{k-1}} |\lambda_v| \\
&= O(1) \sum_{v=1}^{m-1} \left( \sum_{r=1}^v \frac{|t_r|^k}{X_r^{k-1}} \right) |\Delta \lambda_v| + O(1) \left( \sum_{v=1}^m \frac{v^k |t_v|^k}{X_v^{k-1}} \right) |\lambda_m| \\
&= O(1) \sum_{v=1}^{m-1} X_v |\Delta \lambda_v| + O(1) X_m |\lambda_m| \\
&= O(1) \sum_{v=1}^{m-1} X_v \beta_v + O(1) X_m |\lambda_m| \\
&= O(1). \\
\sum_{n=1}^m n^{k-1} |Y_{n2}|^k &= \sum_{n=1}^m n^{k-1} \left| \sum_{v=0}^{n-1} v^{-1} t_v \Delta a_{n-1} B_{v+1} \lambda_v \right|^k \\
&= O(1) \sum_{n=1}^m n^{k-1} \left| \sum_{v=0}^{n-1} a_v b_v t_v \Delta a_{n-1} B_{v+1} \lambda_v \right|^k \\
&= O(1) \sum_{n=1}^m n^{k-1} \sum_{v=0}^{n-1} |t_v|^k |\lambda_v|^k |a_v b_v| |\Delta a_{n-1} B_{v+1}| \left( \sum_{v=0}^{n-1} |a_v b_v| |\Delta a_{n-1} B_{v+1}| \right)^{k-1} \\
&= O(1) \sum_{v=0}^m |a_v b_v| |t_v|^k |\lambda_v|^k \sum_{n=v+1}^m n^{k-1} |a_n b_n|^{k-1} |\Delta a_{n-1} B_{v+1}| \\
&= O(1) \sum_{v=1}^m \frac{|a_v b_v| |t_v|^k |\lambda_v|}{X_v^{k-1}} (X_v |\lambda_v|)^{k-1} \\
&= O(1) \sum_{v=1}^m \frac{|a_v b_v| |t_v|^k |\lambda_v|}{X_v^{k-1}} \\
&= O(1) \sum_{v=1}^{m-1} \left( \sum_{r=1}^v \frac{|a_r b_r| |t_r|^k}{X_r^{k-1}} \right) |\Delta \lambda_v| + O(1) \left( \sum_{v=1}^m \frac{|a_v b_v| |t_v|^k}{X_v^{k-1}} \right) m |\lambda_m| \\
&= O(1) \sum_{v=1}^m X_v |\Delta \lambda_v| + O(1) m X_m |\lambda_m| \\
&= O(1).
\end{aligned}$$

$$\sum_{n=1}^m n^{k-1} |Y_{n3}|^k = \sum_{n=1}^m n^{k-1} \left| \sum_{v=0}^{n-1} t_v \Delta a_{n-1} B_{v+1} \Delta \lambda_v \right|^k$$



$$\begin{aligned}
&\leq \sum_{n=1}^m n^{k-1} \sum_{v=0}^{n-1} \frac{|t_v|^k}{X_v^{k-1}} |\Delta a_{n-1} B_{v+1}|^k |\Delta \lambda_v| \left( \sum_{v=0}^{n-1} |\Delta \lambda_v| X_v \right)^{k-1} \\
&= O(1) \sum_{v=0}^m \frac{|a_v b_v| |t_v|^k}{X_v^{k-1}} |\Delta \lambda_v| \sum_{n=v+1}^m |\Delta a_{n-1} B_{v+1}|^k \\
&= O(1) \sum_{v=0}^m \frac{|a_v b_v| |t_v|^k}{X_v^{k-1}} |\Delta \lambda_v| \\
&= O(1) \sum_{v=0}^{m-1} \left( \sum_{r=0}^v \frac{|a_r b_r| |t_r|^k}{X_r^{k-1}} \right) \Delta |\Delta \lambda_v| + O(1) \left( \sum_{v=0}^m \frac{|a_v b_v| |t_v|^k}{X_v^{k-1}} \right) |\Delta \lambda_m| \\
&= O(1) \sum_{v=0}^{m-1} v X_v |\Delta^2 \lambda_v| + O(1) X_m |\Delta \lambda_m| \\
&= O(1).
\end{aligned}$$

$$\begin{aligned}
\sum_{n=1}^m n^{k-1} |Y_{n4}|^k &= \sum_{n=1}^m n^{k-1} |t_n a_n b_n \lambda_n|^k \\
&= O(1) \sum_{n=1}^m (n |a_n b_n|)^{k-1} |a_n b_n| \frac{|t_n|^k}{X_n^{k-1}} (X_n |\lambda_n|)^{k-1} |\lambda_n| \\
&= O(1) \sum_{n=1}^m \frac{|a_n b_n| |t_n|^k}{X_n^{k-1}} |\lambda_n| \\
&= O(1), \text{ as in the case of } Y_{n2}.
\end{aligned}$$

The proof of the Theorem is complete.

**Corollary 2.4.** *Let  $(X_n)$  be an almost increasing sequence. Let  $(\lambda_n)$  be sequences of numbers satisfying (v) and (vi), . Let  $T = (t_{nv})$  be a factorable matrix,  $t_{nv} = p_v / P_n$  satisfying (2.4) and*

$$n p_n = O(P_n), \quad P_n = O(np_n), \quad (2.10)$$

$$\sum_{n=v+1}^m \left( \frac{p_n}{P_n P_{n-1}} \right)^k (P_n - P_v)^k = O(1), \quad (2.11)$$

$$\sum_{v=0}^n \frac{p_v}{P_v} = O(1), \quad (2.12)$$

then the series  $\sum a_n \lambda_n$  is summable  $|R, p_n|_k$ ,  $k \geq 1$ .

## References

- [1] H. Bor, An application of almost increasing sequences, *Int. J. Math. Math. Sci.*, 22 (2000), 859-863.
- [2] B. E. Rhoades and E. Savas, A note on absolute summability factors , *Periodica Mathematica Hungarica* 51 (1), (2005), 53-60.

# Necessary and Sufficient Conditions for Inclusion Relations for Absolute Summability of Infinite Series

W. T. Sulaiman

*Department of Computer Engineering,  
College of Engineering  
University of Mosul, Iraq.  
waadsulaiman@hotmail.com*

**Abstract.** We obtain the necessary and sufficient conditions for  $|U|_k$  summability of  $\sum a_n \mu_n$  to imply  $|T|_s$  summability of  $\sum a_n \lambda_n$ ,  $1 < k \leq s < \infty$ . Other results are also obtained.

2000 (MSC) : 40F05, 40D25, 40G99.

Key words : Absolute summability, weight mean matrix, Holder's inequality.

## 1. INTRODUCTION

Let  $T$  be a lower triangular matrix,  $(s_n)$  a sequence, then

$$T_n := \sum_{v=0}^n t_{nv} s_v. \quad (1)$$

A series  $\sum a_n$  is said to be summable  $|T|_k$ ,  $k \geq 1$ , if

$$\sum_{n=1}^{\infty} n^{k-1} |\Delta T_{n-1}|^k < \infty. \quad (2)$$

Given any lower triangular matrix  $T$  one can associate the matrices  $\bar{T}$  and  $\hat{T}$ , with entries defined by

$$\bar{t}_{nv} = \sum_{i=v}^n t_{ni}, \quad n, v = 0, 1, 2, \dots, \quad \hat{t}_{nv} = \bar{t}_{nv} - \bar{t}_{n-1,v}$$

respectively. With  $s_n = \sum_{i=0}^n a_i \lambda_i$ ,

$$t_n = \sum_{v=0}^n t_{nv} s_v = \sum_{v=0}^n t_{nv} \sum_{i=0}^v a_i \lambda_i = \sum_{i=0}^n a_i \lambda_i \sum_{v=i}^n t_{nv} = \sum_{i=0}^n \bar{t}_{ni} a_i \lambda_i. \quad (3)$$

$$Y_n := t_n - t_{n-1} = \sum_{i=0}^n \bar{t}_{ni} a_i \lambda_i - \sum_{i=0}^{n-1} \bar{t}_{n-1,i} a_i \lambda_i = \sum_{i=0}^n \hat{t}_{ni} a_i \lambda_i, \quad \text{as } \bar{t}_{n-1,n} = 0. \quad (4)$$

$$X_n := u_n - u_{n-1} = \sum_{i=0}^n \hat{u}_{ni} a_i \mu_i. \quad (5)$$

We call  $T$  a triangle if  $T$  is lower triangular and  $t_{nn} \neq 0$  for all  $n$ . A triangle  $A$  is called factorable if its nonzero entries  $a_{mn}$  can be written in the form  $b_m c_n$  for each

$m$  and  $n$ . We also assume that  $U = (u_{ij})$  is a triangle.  $(p_n), (q_n)$  are assumed to be positive sequences of numbers such that

$$\begin{aligned} P_n &= p_0 + p_1 + \dots + p_n \rightarrow \infty, \quad \text{as } n \rightarrow \infty, \\ Q_n &= q_0 + q_1 + \dots + q_n \rightarrow \infty, \quad \text{as } n \rightarrow \infty. \end{aligned}$$

If we assumed that  $T$  and  $U$  to be factorable, then  $t_{nv} = a_n b_v$  and  $u_{nv} = c_n d_v$ , and therefore we have

$$\bar{t}_{nv} = \sum_{r=v}^n t_{nr} = a_n \sum_{r=v}^n b_r := a_n B_r \quad (6)$$

$$\begin{aligned} \hat{t}_{nv} &= \bar{t}_{nv} - \bar{t}_{n-1,v} = a_n B_v - a_{n-1} \sum_{r=v}^{n-1} b_r = a_n B_v - a_{n-1} B_v + a_{n-1} b_n \\ &= a_n B_v - a_{n-1} B_v = -\Delta a_{n-1} B_v, \quad \text{as } a_{n-1} b_n = t_{n-1,n} = 0. \end{aligned} \quad (7)$$

Also, we have

$$\Delta B_v = b_v, \quad \Delta D_v = d_v, \quad \Delta D_v^{-1} = -\frac{d_v}{D_v D_{v+1}}, \quad B_n = b_n \text{ and } D_n = d_n.$$

$(p_n), (q_n)$  are assumed to be positive sequences of numbers such that

$$\begin{aligned} P_n &= p_0 + p_1 + \dots + p_n \rightarrow \infty, \quad \text{as } n \rightarrow \infty, \\ Q_n &= q_0 + q_1 + \dots + q_n \rightarrow \infty, \quad \text{as } n \rightarrow \infty. \end{aligned}$$

The series  $\sum a_n$  is said to be summable  $|R, p_n|_k$ ,  $k \geq 1$ , if

$$\sum_{n=1}^{\infty} n^{k-1} |\Delta z_{n-1}|^k < \infty,$$

where

$$z_n = \sum_{i=0}^n p_i s_i.$$

In their paper, Rhoades and Savas [2] have used the notation  $|\bar{N}, p_n|_k$  to denote the  $|R, p_n|_k$  summability. They proved the following result.

**Theorem 1.1.** *Let  $(p_n)$  and  $(q_n)$  be positive sequences,  $1 < k \leq s < \infty$ . Then*

$$|N, p_n|_k \Rightarrow |N, q_n|_s$$

iff

$$n^{1/k-1/s} \frac{q_n P_n}{p_n Q_n} = O(1), \quad (8)$$

$$\left( \sum_{n=m}^{\infty} \left( n^{1-1/s} \frac{q_n}{Q_n Q_{n-1}} \right)^s \right)^{1/s} \left( \sum_{v=1}^m \left| Q_v - \frac{q_v P_v}{p_v} \right|^{k^*} \frac{1}{v} \right)^{1/k^*} = O(1), \quad (9)$$

where  $k^*$  denote the conjugate index of  $k$ , i.e.,  $1/k + 1/k^* = 1$ .

The aim of this paper is to present the following generalization

## 2. RESULTS

The following is our main result

**Theorem 2.1.** Let  $1 < k \leq s < \infty$ ,  $(\lambda_n), (\mu_n)$  be sequences of constants. Let  $T$  and  $U$  be factorable triangles with bounded entries  $tt_{nv} = a_n b_v, u_{nv} = c_n d_v$ . Then the implication

$$\sum a_n \mu_n \text{ summable } |U|_k \Rightarrow \sum a_n \lambda_n \text{ summable } |T|_s$$

holds iff the following holds

$$n^{1/k-1/s} \left( \frac{\Delta a_{n-1} b_n \lambda_n}{\Delta c_{n-1} d_n \mu_n} \right) = O(1), \quad (10)$$

$$\left( \sum_{n=m}^{\infty} \left| n^{1-1/s} \Delta a_{n-1} \right|^s \right)^{1/s} \left( \sum_{v=1}^m \left| \frac{1}{\Delta c_{v-1}} \left( -\frac{d_v}{D_v D_{v+1}} B_v \frac{\lambda_v}{\mu_v} + \frac{1}{D_{v+1}} B_v \Delta \left( \frac{\lambda_v}{\mu_v} \right) + \frac{b_v}{D_{v+1}} \frac{\lambda_{v+1}}{\mu_{v+1}} \right) \right|^{k^*} \right)^{1/k^*} = O(1). \quad (11)$$

**Proof.** Let  $(u_n)$  and  $(t_n)$  denote the  $n$ th terms of the  $|U|$  and  $|T|$  transforms of

$\sum_{j=0}^n a_j \mu_j$  and  $\sum_{j=0}^n a_j \lambda_j$  respectively. Then

$$X_n := u_n - u_{n-1} = \sum_{i=0}^n \hat{u}_{ni} a_i \mu_i = -\Delta c_{n-1} \sum_{i=0}^n D_i a_i \mu_i.$$

$$Y_n := y_n - y_{n-1} = \sum_{i=0}^n \hat{t}_{ni} a_i \lambda_i = -\Delta a_{n-1} \sum_{i=0}^n B_i a_i \lambda_i.$$

By Abel's transformation, we have

$$\begin{aligned}
Y_n &= -\Delta a_{n-1} \sum_{v=1}^n D_v a_v \mu_v \frac{B_v \lambda_v}{D_v \mu_v} \\
&= -\Delta a_{n-1} \sum_{v=1}^{n-1} \left( \sum_{r=1}^v D_r a_r \mu_r \right) \Delta_v \left( \frac{B_v \lambda_v}{D_v \mu_v} \right) - \Delta a_{n-1} \left( \sum_{v=1}^n D_v a_v \mu_v \right) \frac{b_n \lambda_n}{d_n \mu_n} \\
&= -\Delta a_{n-1} \sum_{v=1}^{n-1} \frac{X_v}{\Delta c_{v-1}} \left( \Delta(D_v^{-1}) B_v \frac{\lambda_v}{\mu_v} + \frac{B_v}{D_{v+1}} \Delta \left( \frac{\lambda_v}{\mu_v} \right) + \frac{b_v}{D_{v+1}} \frac{\lambda_{v+1}}{\mu_{v+1}} \right) - \Delta a_{n-1} \left( \frac{b_n \lambda_n}{\Delta c_{n-1} d_n \mu_n} \right) X_n \\
&= -\Delta a_{n-1} \sum_{v=1}^{n-1} \frac{1}{\Delta c_{v-1}} \left( -\frac{d_v}{D_v D_{v+1}} B_v \frac{\lambda_v}{\mu_v} + \frac{1}{D_{v+1}} B_v \Delta \left( \frac{\lambda_v}{\mu_v} \right) + \frac{b_v}{D_{v+1}} \frac{\lambda_{v+1}}{\mu_{v+1}} \right) X_v - \left( \frac{\Delta a_{n-1} b_n \lambda_n}{\Delta c_{n-1} d_n \mu_n} \right) X_n
\end{aligned}$$

.Define

$$X_n^* = n^{1-1/k} X_n, \quad Y_n^* = n^{1-1/s} Y_n,$$

then, we have

$$\begin{aligned}
Y_n^* &= -n^{1-1/s} \Delta a_{n-1} \sum_{v=1}^{n-1} \frac{1}{\Delta c_{v-1}} \left( -\frac{d_v}{D_v D_{v+1}} B_v \frac{\lambda_v}{\mu_v} + \frac{1}{D_{v+1}} B_v \Delta \left( \frac{\lambda_v}{\mu_v} \right) + \frac{b_v}{D_{v+1}} \frac{\lambda_{v+1}}{\mu_{v+1}} \right) X_v \\
&\quad - n^{1/k-1/s} \left( \frac{\Delta a_{n-1} b_n \lambda_n}{\Delta c_{n-1} d_n \mu_n} \right) X_n.
\end{aligned}$$

Therefore

$$Y_n^* = \sum_{v=1}^n a_{nv} X_v^*,$$

where

$$a_{nv} = \begin{cases} -n^{1-1/s} \frac{\Delta a_{n-1}}{\Delta c_{n-1}} \left( -\frac{d_v}{D_v D_{v+1}} B_v \frac{\lambda_v}{\mu_v} + \frac{1}{D_{v+1}} B_v \Delta \left( \frac{\lambda_v}{\mu_v} \right) + \frac{b_v}{D_{v+1}} \frac{\lambda_{v+1}}{\mu_{v+1}} \right), & 1 \leq v < n \\ -n^{1/k-1/s} \left( \frac{\Delta a_{n-1} b_n \lambda_n}{\Delta c_{n-1} d_n \mu_n} \right), & v = n \\ 0, & v > n. \end{cases}$$

(12)

Then  $|U|_k$  of  $\sum a_n \mu_n$  implies  $|T|_s$  of  $\sum a_n \lambda_n$  is equivalent to

$$\sum |X_n^*|^k < \infty \Rightarrow \sum |Y_n^*|^s < \infty.$$

The above means that  $A: l^k \rightarrow l^s$ , where  $A$  is the matrix whose entries are defined by (12). We may write  $A = B + C$ , where

$$b_{nv} = \begin{cases} a_{nv}, & 1 \leq v < n, \\ 0, & \text{otherwise} \end{cases}$$

and  $C$  is the diagonal matrix with  $c_{nn} = a_{nn}$ .

From Theorem 2(ii) of [1], a factorable matrix with nonzero entries  $a_{nv} = b_n c_v$  is a bounded operator from  $l^k$  to  $l^s$  iff

$$\left( \sum_{n=m}^{\infty} b_n^s \right)^{1/s} \left( \sum_{v=1}^m c_v^{k^*} \right)^{1/k^*} = O(1), \quad (13)$$

where  $k^*$  is the conjugate index of  $k$ .

By applying (13) to  $B$ , using (12) we obtain  $B: l^k \rightarrow l^s$  iff

$$\left( \sum_{n=m}^{\infty} \left( -n^{1-1/s} \frac{\Delta a_{n-1}}{\Delta c_{n-1}} \right)^s \right)^{1/s} \left( \sum_{v=1}^m \left| -\frac{d_v}{D_v D_{v+1}} B_v \frac{\lambda_v}{\mu_v} + \frac{1}{D_{v+1}} B_v \Delta \left( \frac{\lambda_v}{\mu_v} \right) + \frac{b_v}{D_{v+1}} \frac{\lambda_{v+1}}{\mu_{v+1}} \right|^{k^*} \right)^{1/k^*} = O(1). \quad (14)$$

Now we have to show that for  $k \leq s$ ,  $C = (c_{nn}): l^k \rightarrow l^s$  iff  $(c_{nn})$  is bounded.

As  $k \leq s$ ,  $C: l^k \rightarrow l^s$ . That is

$$\left( \sum_{n=1}^{\infty} |c_{nn} s_n|^s \right)^{1/s} < \infty, \text{ for every } (s_n) \in l^k. \quad (15)$$

From (15), we conclude that  $(c_{nn}) \in l^{s^*}$ , where  $s^*$  is the conjugate of  $s$ . This shows that  $(c_{nn})$  is bounded. Conversely, if  $(c_{nn})$  is bounded, since  $k \leq s$ , we get  $C: l^k \rightarrow l^s$ .

Therefore  $A = (a_{nv}): l^k \rightarrow l^s$  iff (10) and (11) holds. This completes the proof of the Theorem.

**Remark.** It may be mentioned that Theorem 1.1 follows from Theorem 2.1 by putting

$$\hat{t}_{nv} = \frac{q_n Q_{v-1}}{Q_n Q_{n-1}}, \quad \hat{u}_{nv} = \frac{p_n P_{v-1}}{P_n P_{n-1}}, \quad \lambda_n = \mu_n = 1 \text{ for all } n.$$

### 3. APPLICATIONS

**Corollary 3.1.** Let  $1 < k \leq s < \infty$ ,  $(\lambda_n)$  be a sequence of constants. Let  $T$  and  $U$  be factorable triangles with bounded entries  $\hat{t}_{nv} = a_n b_v, \hat{u}_{nv} = c_n d_v$ . Then the implication

$$\sum a_n \text{ summable } |U|_k \Rightarrow \sum a_n \lambda_n \text{ summable } |T|_s$$

holds iff the following holds

$$n^{1/k-1/s} \left( \frac{\Delta a_{n-1} b_n \lambda_n}{\Delta c_{n-1} d_n} \right) = O(1), \quad (16)$$

$$\left( \sum_{n=m}^{\infty} \left| n^{1-1/s} \Delta a_{n-1} \right|^s \right)^{1/s} \left( \sum_{v=1}^m \left| \frac{1}{\Delta c_{v-1}} \left( -\frac{d_v}{D_v D_{v+1}} B_v \lambda_v + \frac{1}{D_{v+1}} B_v \Delta \lambda_v + \frac{b_v}{D_{v+1}} \lambda_{v+1} \right) \right|^k \right)^{1/k^*} = O(1). \quad (17)$$

**Proof.** Follows from Theorem 2.1 by putting  $\mu_n = 1$ , for all  $n$ .

**Corollary 3.2.** Let  $1 < k \leq s < \infty$ ,  $(\mu_n)$  be sequences of constants. Let  $T$  and  $U$  be factorable triangles with bounded entries  $t_{nv} = a_n b_v, u_{nv} = c_n d_v$ . Then the implication

$$\sum a_n \mu_n \text{ summable } |U|_k \Rightarrow \sum a_n \text{ summable } |T|_s$$

holds iff the following holds

$$n^{1/k-1/s} \left( \frac{\Delta a_{n-1} b_n}{\Delta c_{n-1} d_n \mu_n} \right) = O(1), \quad (18)$$

$$\left( \sum_{n=m}^{\infty} \left| n^{1-1/s} \Delta a_{n-1} \right|^s \right)^{1/s} \left( \sum_{v=1}^m \left| \frac{1}{\Delta c_{v-1}} \left( -\frac{d_v}{D_v D_{v+1}} B_v \frac{1}{\mu_v} + \frac{1}{D_{v+1}} B_v \Delta \left( \frac{1}{\mu_v} \right) + \frac{b_v}{D_{v+1}} \frac{1}{\mu_{v+1}} \right) \right|^k \right)^{1/k^*} = O(1). \quad (19)$$

**Proof.** Follows from Theorem 2.1 by putting  $\lambda_n = 1$  for all  $n$ .

**Corollary 3.3.** Let  $1 < k \leq s < \infty$ ,  $(\lambda_n), (\mu_n)$  be sequences of constants. Let  $T$  and  $U$  be factorable triangles with bounded entries  $t_{nv} = a_n b_v, u_{nv} = c_n d_v$ . Then the implication

$$\sum a_n \mu_n \text{ summable } |U|_k \Rightarrow \sum a_n \lambda_n \text{ summable } |T|_s$$

holds iff the following holds

$$\frac{\Delta a_{n-1} b_n}{\Delta c_{n-1} d_n \mu_n} = O(1), \quad (20)$$



$$\left( \sum_{n=m}^{\infty} \left| n^{1-1/k} \Delta a_{n-1} \right|^k \right)^{1/k} \left( \sum_{v=1}^m \left| \frac{1}{\Delta c_{v-1}} \left( -\frac{d_v}{D_v D_{v+1}} B_v \frac{\lambda_v}{\mu_v} + \frac{1}{D_{v+1}} B_v \Delta \left( \frac{\lambda_v}{\mu_v} \right) + \frac{b_v}{D_{v+1}} \frac{\lambda_{v+1}}{\mu_{v+1}} \right) \right|^{k^*} \right)^{1/k^*} = O(1). \quad (21)$$

**Proof.** Follows from Theorem 2.1 by putting  $s = k$ .

**Corollary 3.4.** Let  $1 < k \leq s < \infty$ ,  $(\lambda_n)$  be a sequence of constants. Let  $U$  be a factorable triangle with bounded entries  $\hat{u}_{nv} = c_n d_v$ . Then the implication

$$\sum a_n \text{ summable } |U|_k \Rightarrow \sum a_n \lambda_n \text{ summable } |R, q_n|_s$$

holds iff the following holds

$$n^{1/k-1/s} \left( \frac{q_n \lambda_n}{Q_n \Delta c_{n-1} D_n} \right) = O(1), \quad (22)$$

$$\left( \sum_{n=m}^{\infty} \left| n^{1-1/s} \frac{q_n}{Q_n Q_{n-1}} \right|^s \right)^{1/s} \left( \sum_{v=1}^m \left| \frac{1}{\Delta c_{v-1}} \left( -\frac{d_v}{D_v D_{v+1}} Q_{v-1} \lambda_v + \frac{Q_{v-1}}{D_{v+1}} \Delta \lambda_v - \frac{q_v}{D_{v+1}} \lambda_{v+1} \right) \right|^{k^*} \right)^{1/k^*} = O(1). \quad (23)$$

**Proof.** Follows from Corollary 3.1 by putting

$$T \equiv (R, q_n), \quad \Delta a_{n-1} = \frac{q_n}{Q_n Q_{n-1}}, \quad B_v = Q_{v-1}.$$

**Corollary 3.5.** Let  $1 < k \leq s < \infty$ ,  $(\mu_n)$  be a sequence of constants. Let  $T$  be a factorable triangle with bounded entries,  $\hat{t}_{nv} = a_n b_v$ . Then the implication

$$\sum a_n \mu_n \text{ summable } |U|_k \Rightarrow \sum a_n \text{ summable } |T|_s$$

holds iff the following is satisfied

$$n^{1/k-1/s} \left( \frac{\Delta a_{n-1} b_n P_n}{p_n \mu_n} \right) = O(1), \quad (24)$$

$$\left( \sum_{n=m}^{\infty} \left| n^{1-1/s} \Delta a_{n-1} \right|^s \right)^{1/s} \left( \sum_{v=1}^m \left| \frac{P_v P_{v-1}}{P_v} \left( \frac{p_v}{P_v P_{v-1}} \frac{B_v}{\mu_v} + \frac{B_v}{P_v} \Delta \left( \frac{1}{\mu_v} \right) + \frac{b_v}{P_v} \frac{1}{\mu_{v+1}} \right) \right|^{k^*} \right)^{1/k^*} = O(1). \quad (25)$$

**Proof.** Follows from Corollary 3.2 by putting

$$U \equiv (R, p_n), \quad \Delta c_{n-1} = -\frac{p_n}{P_n P_{n-1}}, \quad D_v = P_{v-1}.$$

## RERERENCES

- [1] G. Bennett, Some elementary inequalities, Quart. J. Math. Oxford 38 (1987), 401-425.
- [2] B. E. Rhoades and E. Savas, Necessary and sufficient conditions for inclusion relations for absolute summability, Proc. Indian Acad. Sci (Math. Sci) 113 (2003), 243-250.

# On A Characterization Of Absolute Summability Factors

W. T. Sulaiman

Department of Computer Engineering, College of  
Engineering, University of Mosul, Iraq.  
waadsulaiman@hotmail.com

2000 Mathematics subject classification : 40F05, 40D25.

Key words : absolute summability, summability factor.

**Abstract.** In this paper we give two general results concerning absolute summability by using matrices  $T$  and  $U$  and a sequence of numbers  $(\lambda_n)$ . In fact we give the following :

Characterization of the series  $\sum a_n \lambda_n$  to be summable  $|T|_k$   $(|T|)$  whenever  $\sum a_n \mu_n$  is summable  $|U|$   $(|U|_k)$ ,  $k \geq 1$ .

## 1. Introduction

Let  $T$  be a lower triangular matrix,  $(s_n)$  a sequence, then

$$(1) \quad T := \sum_{v=0}^n t_{nv} s_v.$$

A series  $\sum a_n$  is said to be summable  $|T|_k$ ,  $k \geq 1$ , if

$$(2) \quad \sum_{n=1}^{\infty} n^{k-1} |\Delta T_{n-1}|^k < \infty.$$

Given any lower triangular matrix  $T$  one can associate the matrices  $\bar{T}$  and  $\hat{T}$ , with entries defined by

$$\bar{t}_{nv} = \sum_{i=v}^n t_{ni}, \quad n, v = 0, 1, 2, \dots, \quad \hat{t}_{nv} = \bar{t}_{nv} - \bar{t}_{n-1, v}$$

respectively. With  $s = \sum_{i=0}^n a_i \lambda_i$ ,

$$(3) \quad t_n = \sum_{v=0}^n t_{nv} s_v = \sum_{v=0}^n t_{nv} \sum_{i=0}^v a_i \lambda_i = \sum_{i=0}^n a_i \lambda_i \sum_{v=i}^n t_{nv} = \sum_{i=0}^n \bar{t}_{ni} a_i \lambda_i.$$

$$(4) \quad Y_n := t_n - t_{n-1} = \sum_{i=0}^n \bar{t}_{ni} a_i \lambda_i - \sum_{i=0}^{n-1} \bar{t}_{n-1, i} a_i \lambda_i = \sum_{i=0}^n \hat{t}_{ni} a_i \lambda_i, \quad \text{as } \bar{t}_{n-1, n} = 0.$$

$$(5) \quad X_n := u_n - u_{n-1} = \sum_{i=0}^n \hat{u}_{ni} a_i \mu_i,$$

we also have  $\hat{t}_{vv} = t_{vv}$ ,  $\hat{u}_{vv} = u_{vv}$ .

We call  $T$  a triangle if  $T$  is lower triangular and  $t_{nn} \neq 0$  for all  $n$ . A triangle  $A$  is called factorable if its nonzero entries  $a_{mn}$  can be written in the form  $b_m c_n$  for each  $m$  and  $n$ . We assume that  $U = (u_{nv})$  is a factorable triangle,  $u_{nv} = c_n d_v$ . We have

$$\bar{u}_{nv} = \sum_{r=v}^n u_{nr} = c_n \sum_{r=v}^n d_r := c_n D_v \quad (6)$$

$$\begin{aligned} \hat{u}_{nv} &= \bar{u}_{nv} - \bar{u}_{n-1,v} = c_n D_v - c_{n-1} \sum_{r=v}^{n-1} d_r = c_n D_v - c_{n-1} D_v + c_{n-1} d_n \\ &= c_n D_v - c_{n-1} D_v = -\Delta c_{n-1} D_v, \text{ as } c_{n-1} d_n = u_{n-1,n} = 0. \end{aligned} \quad (7)$$

Also, we have

$$\Delta D_v = d_v, \quad \Delta D_v^{-1} = -\frac{d_v}{D_v D_{v+1}}, \quad D_n = d_n.$$

$(p_n), (q_n)$  are assumed to be positive sequences of numbers such that

$$\begin{aligned} P_n &= p_0 + p_1 + \dots + p_n \rightarrow \infty, \quad \text{as } n \rightarrow \infty, \\ Q_n &= q_0 + q_1 + \dots + q_n \rightarrow \infty, \quad \text{as } n \rightarrow \infty. \end{aligned}$$

The series  $\sum a_n$  is said to be summable  $|R, p_n|_k$ ,  $k \geq 1$ , if

$$\sum_{n=1}^{\infty} n^{k-1} |\Delta z_{n-1}|^k < \infty,$$

where

$$z_n = \sum_{i=0}^n p_i s_i.$$

Some authors used the notation  $|\bar{N}, p_n|_k$  in order to mean  $|R, p_n|_k$ , that is the two summabilities are exactly the same. The notation  $\lambda \in (A, B)$ , where  $A$  and  $B$  are two summabilities, means that  $\sum a_n$  summable  $A$  implies that  $\sum a_n \lambda_n$  is summable  $B$ .

Recently, Rhoades and Savas [2] established the following results concerning characterizations of some absolute summabilities.

**Theorem 1.1.** Let  $1 \leq k < \infty$ . Then  $\lambda \in (\bar{N}, p_n|_k, |T|_k)$  iff  $T$  satisfies the following

- (i)  $|t_{vv} \lambda_v| \frac{P_v}{p_v} = O(v^{1/k-1})$
- (ii)  $\left( \sum_{n=v+1}^{\infty} n^{k-1} |\Delta_v(\hat{t}_{nv} \lambda_v)|^k \right)^{1/k} = O\left(\frac{P_v}{p_v}\right)$

$$(iii) \quad \left( \sum_{n=v+1}^{\infty} n^{k-1} |\hat{t}_{n,v+1} \lambda_{v+1}|^k \right)^{1/k} = O(1).$$

**Theorem 1.2.** Let  $1 \leq k < \infty$ . Suppose that  $T$  satisfies

$$(6) \quad \sum_{n=v+1}^{\infty} |\hat{t}_{nv}| \text{ converges for each } v=1,2,\dots$$

$$(7) \quad \sum_{n=v+1}^{\infty} |\hat{t}_{n,v+1}| \text{ converges for each } v=1,2,\dots$$

Then  $\lambda \in (N, p_n|_k, |T|)$  iff

$$(i) \quad \sum_{v=1}^{\infty} \frac{1}{v} \left| \sum_{n=v+1}^{\infty} \frac{P_v}{p_v} \Delta_v(\hat{t}_{nv} \lambda_v) + \hat{t}_{n,v+1} \lambda_{v+1} \right|^{k'} < \infty$$

$$(ii) \quad \sum_{v=1}^{\infty} \frac{1}{v} \left| \frac{t_{vv} P_v \lambda_v}{p_v} \right|^{k'} < \infty,$$

where  $k'$  is the conjugate index of  $k$ .

The following Lemma is needed for our aim

**Lemma 1.3 [1].** Let  $1 \leq k < \infty$ . Then an infinite matrix  $T : l \rightarrow l^k$  iff

$$\sup_v \sum_{n=1}^{\infty} |t_{nv}|^k < \infty.$$

and  $U = (u_{nv})$ . In fact we intend to prove the following

## 2. Results

**Theorem 2.1.** Let  $1 \leq k < \infty$ . Let the matrix  $U = (u_{nv})$  is factorable, that is  $u_{nv} = c_n d_v$ . Let

$$(8) \quad \sum_{n=v+1}^{\infty} |\Delta c_{n-1} d_v| = O(|\Delta c_{v-1} D_v|).$$

Then the implication

$$\sum a_n \text{ is summable } |U| \Rightarrow \sum a_n \lambda_n \text{ is summable } |T|_k$$

holds iff

$$(i) \quad |\hat{t}_{vv} \lambda_v| = O(v^{1/k-1} |\Delta c_{v-1} D_v|)$$

$$(ii) \quad \sum_{n=v+1}^{\infty} n^{k-1} |\Delta_v(\hat{t}_{nv} \lambda_v)|^k = O(|\Delta c_{v-1} D_v|^k)$$

$$(iii) \quad \sum_{n=v+1}^{\infty} n^{k-1} |\hat{t}_{n,v+1} \lambda_{v+1}|^k = O \left( \left| D_{v+1} \right| \sum_{n=v+1}^{\infty} |\Delta c_{n-1}| \right)^k.$$

**Proof.** By (4) and (5), in order to prove the theorem, we have to show that

$$(9) \quad \sum_{n=1}^{\infty} n^{k-1} |Y_n|^k < \infty$$

whenever

$$(10) \quad \sum_{n=1}^{\infty} |X_n| < \infty.$$

For  $k \geq 1$  define

$$B = \left\{ (a_i) : \sum a_i \text{ is summable } |U| \right\}$$

$$C = \left\{ (a_i) : \sum a_i \lambda_i \text{ is summable } |T|_k \right\}.$$

These are Banach spaces, if normed by

$$(11) \quad \|X\| = \sum_n |X_n|,$$

$$(12) \quad \|Y\| = \left( |Y_0|^k + \sum_n n^{k-1} |Y_n|^k \right)^{1/k}.$$

Since  $\sum a_n \mu_n$  is summable  $|U|$  implies that  $\sum a_n \lambda_n$  is summable  $|T|_k$ , by the Banach-Steinhaus theorem, there exists a constant  $N > 0$  such that

$$(13) \quad \|Y\| \leq N \|X\|$$

for all sequences satisfying (10).

Now, applying (3) and (4) to the sequence

$$a_v = e_v, \quad a_{v+1} = -e_{v+1}, \quad a_n = 0 \text{ otherwise},$$

when  $e_v$  is the  $v$ -th coordinate sequence, we get

$$X_n = \begin{cases} 0, & n < v, \\ -\Delta c_{v-1} D_v, & n = v, \\ -\Delta c_{n-1} d_v, & n > v, \end{cases}$$

Using (11) and (12),

$$\|X\| = |\Delta c_{v-1} D_v| + \sum_{n=v+1}^{\infty} |\Delta c_{n-1} d_v|,$$

$$\|Y\| = \left( v^{k-1} |\hat{t}_{vv} \lambda_v|^k + \sum_{n=v+1}^{\infty} n^{k-1} |\Delta_v (\hat{t}_{nv} \lambda_v)|^k \right)^{1/k}.$$

Therefore, it follows from (13) that

$$v^{k-1} |\hat{t}_{vv} \lambda_v|^k + \sum_{n=v+1}^{\infty} n^{k-1} |\Delta (\hat{t}_{nv} \lambda_v)|^k \leq N^k \left( |\Delta c_{v-1} D_v| + \sum_{n=v+1}^{\infty} |\Delta c_{n-1} d_v| \right)^k.$$

As the above inequality holds for every  $v \geq 1$ , we obtain, by (8)

The above inequality is true iff each term of the left side is  $O(\hat{u}_{vv}^k)$ .

The left term gives

$$v^{k-1} |\hat{t}_{vv} \lambda_v|^k = O(|\Delta c_{v-1} D_v|^k),$$

or

$$|\hat{t}_{vv} \lambda_v| = O(v^{1/k-1} |\Delta c_{v-1} D_v|),$$

that is

$$|\hat{t}_{vv} \lambda_v| = O(v^{1/k-1} |\Delta c_{v-1} D_v|).$$

Therefore (i) is necessary. On taking the second term, we obtain

$$\sum_{n=v+1}^{\infty} n^{k-1} |\Delta(\hat{t}_{nv} \lambda_v)|^k = O(|\Delta c_{v-1} D_v|^k),$$

which is condition (ii).

It remains to prove the necessity of (iii), we again apply (3) and (4), to the sequence with  $a_v = e_{v+1}$  to obtain

$$X_n = \begin{cases} 0, & n < v+1 \\ -\Delta c_{n-1} D_{v+1}, & n \geq v+1 \end{cases}$$

$$Y_n = \begin{cases} 0, & n < v+1, \\ \hat{t}_{n,v+1} \lambda_{v+1}, & n \geq v+1. \end{cases}$$

By using again (11) and (12), we obtain

$$\|X\| = \sum_{n=v+1}^{\infty} |\Delta c_{n-1} D_{v+1}|,$$

$$\|Y\| = \left( \sum_{n=v+1}^{\infty} n^{k-1} |\hat{t}_{n,v+1} \lambda_{v+1}|^k \right)^{1/k}.$$

From (13), it follows that

$$\sum_{n=v+1}^{\infty} n^{k-1} |\hat{t}_{n,v+1} \lambda_{v+1}|^k = O\left( \sum_{n=v+1}^{\infty} |\hat{u}_{n,v+1}| \right)^k = O\left( \sum_{n=v+1}^{\infty} |\Delta c_{n-1} D_{v+1}| \right)^k$$

$$= O\left( |D_{v+1}| \sum_{n=v+1}^{\infty} |\Delta c_{n-1}| \right)^k.$$

which is the necessity of (iii).

In order to prove the conditions sufficient, we have from (4)

$$\begin{aligned}
 Y_n &= \sum_{v=1}^n D_v a_v \frac{\hat{t}_{nv} \lambda_v}{D_v} \\
 &= \sum_{v=1}^{n-1} \left( \sum_{r=1}^v D_r a_r \right) \Delta_v \left( \frac{\hat{t}_{nv} \lambda_v}{D_v} \right) + \left( \sum_{v=1}^n D_v a_v \right) \frac{\hat{t}_{nn} \lambda_n}{D_n} \\
 &= - \sum_{v=1}^{n-1} \frac{X_v}{\Delta c_{v-1}} \left( \frac{1}{D_v} \Delta_v (\hat{t}_{nv} \lambda_v) + \frac{d_v}{D_v D_{v+1}} \hat{t}_{n,v+1} \lambda_{v+1} \right) - \frac{X_n \hat{t}_{nn} \lambda_n}{\Delta c_{n-1} d_n}.
 \end{aligned}$$

Set  $Y_n^* = n^{1-1/k} Y_n$ . Then we have

$$- \left( \frac{n^{1-1/k} \hat{t}_{nn} \lambda_n}{\Delta c_{n-1} D_n} \right) X_n.$$

We are writing  $Y_n^* = \sum_{v=1}^n a_{nv} X_v$ , where

$$a_{nv} = \begin{cases} - \frac{n^{1-1/k}}{\Delta c_{v-1}} \left( \frac{1}{D_v} \Delta_v (\hat{t}_{nv} \lambda_v) + \frac{d_v}{D_v D_{v+1}} \hat{t}_{n,v+1} \lambda_{v+1} \right), & \text{if } 1 \leq v \leq n-1, \\ - v^{1-1/k} \frac{\hat{t}_{vv} \lambda_v}{\Delta c_{v-1} D_v}, & \text{if } n = v, \\ 0, & \text{if } n > v \end{cases}$$

The statement that  $\sum a_n \lambda_n$  is summable  $|T|_k$ ,  $k \geq 1$  whenever  $\sum a_n$  is summable  $|U|$  is equivalent to

$$\sum |Y_n^*|^k < \infty \quad \text{whenever} \quad \sum |X_n| < \infty,$$

or equivalently

$$\sup_v \sum_n |a_{nv}|^k < \infty.$$

By Lemma 1.3, it follows that

$$\begin{aligned}
 \sum_{n=v}^{\infty} |a_{nv}|^k &= v^{k-1} \left| \frac{\hat{t}_{vv} \lambda_v}{\Delta c_{v-1} D_v} \right|^k \\
 &\quad + \sum_{n=v+1}^{\infty} n^{k-1} \left| \frac{1}{\Delta c_{v-1}} \left( \frac{1}{D_v} \Delta_v (\hat{t}_{nv} \lambda_v) + \frac{d_v}{D_v D_{v+1}} \hat{t}_{n,v+1} \lambda_{v+1} \right) \right|^k.
 \end{aligned}$$

Clearly conditions (8), (i)-(iii), via minkowski's inequality implies that

$$\sum_{n=v}^{\infty} |a_{nv}|^k = O(1),$$

as  $v \rightarrow \infty$ . The proof is complete.



**Theorem 2.2.** Let  $1 < k < \infty$ . Let  $T$  satisfies (6) and (7) and  $U$  is factorable triangle,  $u_{nv} = c_n d_v$ , and

$$(14) \quad v^{1/k-1} \left| \frac{\lambda_v}{\Delta c_{v-1} D_v} \right| = O(1), \quad \frac{d_v}{D_v D_{v+1}} = O(|\Delta c_{v-1}|).$$

Then the implication

$$\sum a_n \mu_n \text{ is summable } |U|_k \Rightarrow \sum a_n \lambda_n \text{ is summable } |T|$$

holds iff

$$(i) \quad \sum_{v=1}^{\infty} \frac{1}{v} \left| \sum_{n=v+1}^{\infty} \frac{1}{\Delta c_{v-1}} \left( \frac{1}{D_v} \Delta_v(\hat{t}_{nv} \lambda_v) + \frac{d_v}{D_v D_{v+1}} \hat{t}_{n,v+1} \lambda_{v+1} \right) \right|^{k'} < \infty$$

$$(ii) \quad \sum_{v=1}^{\infty} \frac{1}{v} \left| \frac{\hat{t}_{vv} \lambda_v}{\Delta c_{v-1} D_v} \right|^{k'} < \infty,$$

where  $k'$  is the conjugate index of  $k$ .

**Proof.** As before, we have

$$Y_n = - \sum_{v=1}^{n-1} \frac{1}{\Delta c_{v-1}} \left( \frac{1}{D_v} \Delta_v(\hat{t}_{nv} \lambda_v) + \frac{d_v}{D_v D_{v+1}} \hat{t}_{n,v+1} \lambda_{v+1} \right) X_v - \left( \frac{\hat{t}_{nn} \lambda_n}{\Delta c_{n-1} d_n} \right) X_n$$

$$\text{Set } X_n^* = n^{1-1/k} X_n, \quad Y_n = \sum_{v=1}^n a_{nv} X_v^*,$$

where

$$a_{nv} = \begin{cases} - \frac{v^{1/k-1}}{\Delta c_{v-1}} \left( \frac{1}{D_v} \Delta_v(\hat{t}_{nv} \lambda_v) + \frac{d_v}{D_v D_{v+1}} \hat{t}_{n,v+1} \lambda_{v+1} \right), & \text{if } 1 \leq v \leq n-1, \\ - v^{1/k-1} \frac{\hat{t}_{vv} \lambda_v}{\Delta c_{v-1} D_v}, & \text{if } n = v, \\ 0, & \text{if } n > v \end{cases}$$

The condition that  $\sum a_n \lambda_n$  is summable  $|T|$  whenever  $\sum a_n$  is summable  $|U|_k$  is equivalent to  $\sum |Y_n| < \infty$  whenever  $\sum |X_n^*|^k < \infty$ . The necessary and sufficient conditions for this implication are

$$(15) \quad \sum_{n=v}^{\infty} a_{nv} z_v < \infty \text{ for each bounded sequence } z = (z_v), \quad v = 1, 2, \dots$$

and

$$(16) \quad \sum_{v=1}^{\infty} \left| \sum_{n=v}^{\infty} a_{nv} z_v \right|^{k'} < \infty \quad \text{for each bounded sequence } z.$$

To verify (15), we have

$$\sum_{n=v}^{\infty} a_{nv} z_v = -v^{1/k-1} \frac{\hat{t}_{vv} \lambda_v}{\Delta c_{v-1} D_v} z_v - \sum_{n=v+1}^{\infty} \frac{v^{1/k-1}}{\Delta c_{v-1}} \left( \frac{1}{D_v} \Delta_v (\hat{t}_{nv} \lambda_v) + \frac{d_v}{D_v D_{v+1}} \hat{t}_{n,v+1} \lambda_{v+1} \right) z_v$$

Now,

$$\begin{aligned} & \sum_{n=v+1}^{\infty} \left| \frac{v^{1/k-1}}{\Delta c_{v-1}} \left( \frac{1}{D_v} \Delta_v (\hat{t}_{nv} \lambda_v) \right) z_n \right| \\ & \leq N \frac{v^{1/k-1}}{|\Delta c_{v-1} D_v|} \sum_{n=v+1}^{\infty} |\hat{t}_{nv} \lambda_v - \hat{t}_{n,v+1} \lambda_{v+1}| \\ & \leq N \frac{v^{1/k-1}}{|\Delta c_{v-1} D_v|} \left( |\lambda_v| \sum_{n=v+1}^{\infty} |\hat{t}_{nv}| + |\lambda_{v+1}| \sum_{n=v+1}^{\infty} |\hat{t}_{n,v+1}| \right) \\ & = O(1), \end{aligned}$$

by (6) and (7), where  $M$  is bounded for  $z$ . Also

$$\begin{aligned} & \sum_{n=v+1}^{\infty} \left| \frac{v^{1/k-1}}{\Delta c_{v-1}} \left( \frac{d_v}{D_v D_{v+1}} \hat{t}_{n,v+1} \lambda_{v+1} \right) z_n \right| \\ & \leq N v^{1/k-1} \left| \frac{d_v \lambda_{v+1}}{\Delta c_{v-1} D_v D_{v+1}} \right| \sum_{n=v+1}^{\infty} |\hat{t}_{n,v+1}| \\ & = O(1), \end{aligned}$$

we obtain (15) satisfied.

From (16), the necessary and sufficient conditions for the inclusion of the theorem is

$$(17) \quad \sum_{n=1}^{\infty} \left| v^{1/k-1} \frac{\hat{t}_{vv} \lambda_v}{\Delta c_{v-1} D_v} z_v - \sum_{n=v+1}^{\infty} \frac{v^{1/k-1}}{\Delta c_{v-1}} \left( \frac{1}{D_v} \Delta_v (\hat{t}_{nv} \lambda_v) + \frac{d_v}{D_v D_{v+1}} \hat{t}_{n,v+1} \lambda_{v+1} \right) z_v \right|^{k'} < \infty$$

For each bounded sequence  $z$ . From (17) by choosing  $z_n = 1$  for each  $n$  it follows that

$$(18) \quad \sum_{v=1}^{\infty} \left| v^{1/k-1} \frac{\hat{t}_{vv} \lambda_v}{\Delta c_{v-1} D_v} \right|^{k'} = O(1)$$

$$(19) \quad \sum_{v=1}^{\infty} \left| \sum_{n=v+1}^{\infty} \frac{v^{1/k-1}}{\Delta c_{v-1}} \left( \frac{1}{D_v} \Delta_v (\hat{t}_{nv} \lambda_v) + \frac{d_v}{D_v D_{v+1}} \hat{t}_{n,v+1} \lambda_{v+1} \right) \right|^{k'} = O(1),$$

which are conditions (i) and (ii).

(i) and (ii) are also sufficient via using Minkowski's inequality along with (18) and (19), since (17) holds for every bounded sequence  $z = (z_n)$ .

**Remark 2.3.** The two results of [2] can be obtained from theorems 2.1 and 2.2 by putting

$$U \equiv (\bar{N}, p_n), \quad \hat{u}_{nv} = \frac{p_n P_{v-1}}{P_n P_{n-1}}, \quad -\Delta c_{n-1} = \frac{p_n}{P_n P_{n-1}}, \quad D_v = P_{v-1}.$$

**Corollary 2.4.** Let  $1 \leq k < \infty$ . Let the matrix  $U = (u_{nv})$  is factorable, that is  $u_{nv} = c_n d_v$ . Let (8) be satisfied. Then the implication

$$\sum a_n \text{ is summable } |U| \Rightarrow \sum a_n \text{ is summable } |T|_k$$

holds iff

- (i)  $|\hat{t}_{nv}| = O\left(v^{1/k-1} |\Delta c_{v-1} D_v|\right)$
- (ii)  $\sum_{n=v+1}^{\infty} n^{k-1} |\Delta_v(\hat{t}_{nv})|^k = O\left(|\Delta c_{v-1} D_v|^k\right)$
- (iii)  $\sum_{n=v+1}^{\infty} n^{k-1} |\hat{t}_{n,v+1}|^k = O\left(|D_{v+1}| \sum_{n=v+1}^{\infty} |\Delta c_{n-1}|\right)^k.$

**Proof.** The proof follows from theorem 2.1 by putting  $\lambda_n = 1, \forall n$ .

**Remark 2.5.** Concerning the summabilities  $|\bar{N}, p_n|_k, |\bar{N}, q_n|_k$ , it may be mentioned that many other results can be obtained from theorems 2.1 and 2.2 by putting  $T \equiv (\bar{N}, p_n)$  and  $U \equiv (\bar{N}, q_n)$ .

## References

- [1]. I. J. Maddox, Elements of Functional Analysis, Cambridge Univ. Press, Cambridge, (1970).
- [2] B. E. Rhoades and E. Savas, A characterization of absolute summability factors, Taiwanese Journal of Mathematics, 8(3), (2004), 453-465.

# A Summability Factor Theorem For Absolute Summability Involving quasi $\beta$ -Power Increasing Sequences

W. T. Sulaiman

Department of Computer Engineering, College of  
Engineering, University of Mosul, Iraq  
waadsulaiman@hotmail.com

**Abstract.** In this note we generalize and improve a result of Savas [2] concerning a summability factor theorem for summability  $|T, \delta|_k$ , where T is triangular matrix.

2000 Mathematics Subject Classification : 40F05, 40D25.

Key words : Absolute summability, almost increasing sequence.

## 1. Introduction

Let T be a lower triangular matrix, and  $(s_n)$  a sequence. Then

$$(1) \quad T_n := \sum_{v=0}^n t_{nv} s_v.$$

A series  $\sum a_n$  with partial sums  $s_n$  is said to be summable  $|T|_k$ ,  $k \geq 1$ , if

$$(2) \quad \sum_{n=1}^{\infty} n^{k-1} |T_n - T_{n-1}|^k < \infty,$$

and it is said to be summable  $|T, \delta|_k$ ,  $k \geq 1$ ,  $\delta \geq 0$ , if

$$\sum_{n=1}^{\infty} n^{\delta k + k - 1} |T_n - T_{n-1}|^k < \infty.$$

With T, two lower triangular matrices  $\bar{T}$  and  $\hat{T}$  are associated as follows

$$(3) \quad \begin{aligned} \bar{t}_{nv} &= \sum_{r=v}^n t_{nr} \quad n, v = 0, 1, 2, \dots, \\ \hat{t}_{nv} &= \bar{t}_{nv} - \bar{t}_{n-1, v} \quad n = 1, 2, \dots. \end{aligned}$$

we may write

$$(4) \quad T_n = \sum_{v=0}^n t_{nv} \sum_{r=0}^v a_r \lambda_r = \sum_{r=0}^n a_r \lambda_r \sum_{v=r}^n t_{nv} = \sum_{r=0}^n \bar{t}_{nr} a_r \lambda_r.$$

Thus

$$(5) \quad \begin{aligned} T_n - T_{n-1} &= \sum_{v=0}^n t_{nv} a_v \lambda_v - \sum_{v=0}^{n-1} t_{n-1, v} a_v \lambda_v \\ &= \sum_{v=0}^n \hat{t}_{nv} a_v \lambda_v \quad (t_{n-1, n} = 0) \end{aligned}$$

$$\begin{aligned}
&= \sum_{v=0}^{n-1} \left( \sum_{r=0}^v a_r \right) \Delta_v (\hat{t}_{nv} \lambda_v) + \left( \sum_{v=0}^n a_v \right) t_{nn} \lambda_n \quad (\hat{t}_{nn} = t_{nn}) \\
&= \sum_{v=0}^{n-1} s_v (\Delta_v \hat{t}_{nv} \lambda_v + \hat{t}_{n,v+1} \Delta \lambda_v) + s_n t_{nn} \lambda_n \\
&= T_{n1} + T_{n2} + T_{n3}.
\end{aligned}$$

Let  $(p_n)$  be a sequence of positive numbers such that

$$P_n = p_0 + p_1 + \dots + p_n \rightarrow \infty \text{ as } n \rightarrow \infty, \quad p_{-1} = P_{-1} = 0.$$

In the special case when  $t_{nv} = p_v / P_n$ , the summability  $|T|_k$  is called  $|R, p_n|_k$ .

A positive sequence  $(a_n)$  is said to be almost increasing if there exists a positive increasing sequence  $(b_n)$  and two positive constants  $A$  and  $B$  such that

$$Ab_n \leq a_n \leq Bb_n \quad \text{for each } n.$$

A positive sequence  $(\gamma_n)$  is said to be quasi  $\beta$ -power increasing sequence if there is a constant  $K = K(\beta, \gamma) \geq 1$  such that  $K n^\beta \gamma_n \geq m^\beta \gamma_m$  holds for all  $n \geq m \geq 1$ . It should be mentioned that every almost increasing sequence is quasi  $\beta$ -power increasing sequence for any  $\beta > 0$ , while the converse need not be true as for example  $\gamma_n = n^{-\beta}$ ,  $\beta > 0$ .

By a triangle we mean a lower triangular matrix with all principal diagonal entries non zero.

Concerning almost increasing sequences, Savas [2] gave the following result

**Theorem 1.1.** Let  $(X_n)$  be an almost increasing sequence and let  $(\beta_n)$  and  $(\lambda_n)$  be sequences such that

$$(6) \quad |\Delta \lambda_n| \leq \beta_n,$$

$$(7) \quad \lim_n \beta_n = 0,$$

$$(8) \quad \sum_{n=1}^{\infty} n |\Delta \beta_n| X_n < \infty,$$

$$(9) \quad |\lambda_n| X_n = O(1),$$

are satisfied. Let  $T$  be a triangular matrix with non-negative entries satisfying

$$(10) \quad n t_{nn} = O(1)$$

$$(11) \quad t_{n-1,v} \geq t_{nv} \quad \text{for } n \geq v+1,$$

$$(12) \quad \bar{t}_{n0} = 1 \quad \text{for all } n,$$

$$(13) \quad \sum_{v=1}^{n-1} t_{vv} \hat{t}_{n,v+1} = O(t_{nn}),$$

$$(14) \quad \sum_{n=v+1}^{m+1} n^{\delta_k} |\Delta_v \hat{t}_{nv}| = O(v^{\delta_k} t_{vv}),$$

$$(15) \quad \sum_{n=v+1}^{m+1} n^{\delta k} \hat{t}_{n,v+1} = O(v^{\delta k}), \text{ and}$$

$$(16) \quad \sum_{n=1}^m n^{\delta k-1} |s_n|^k = O(X_m),$$

then the series  $\sum a_n \lambda_n$  is summable  $|T, \delta|_k$ ,  $k \geq 1$ ,  $0 \leq \delta < 1/k$ .

Since quasi  $\beta$ -power ( $0 < \beta < 1$ ) increasing sequences are weaker than almost increasing sequences, it is true, in order to have better results, replacing almost increasing sequences by quasi  $\beta$ -power increasing sequences. Not only that, in fact our aim is to improve as well as generalized the result [2] in the following sense

1. Our result deal with a general series  $\sum a_n$  with negative and positive terms
2. The condition imposed on  $(X_n)$  is weaker.

## 2. Results.

**Lemma 2.0.** *Conditions (6)-(8) imply*

$$\sum_{n=1}^{\infty} \beta_n X_n = O(1).$$

**Proof. Method 1.** Since  $\beta_n \rightarrow 0$ , then, we have

$$\begin{aligned} \sum_{n=1}^{\infty} \beta_n X_n &= \sum_{n=1}^{\infty} X_n \sum_{v=n}^{\infty} \Delta \beta_v = \sum_{v=1}^{\infty} \Delta \beta_v \sum_{n=1}^v n^{\beta} X_n n^{-\beta} \\ &= O(1) \sum_{v=1}^{\infty} |\Delta \beta_v| v^{\beta} X_v \sum_{n=1}^v n^{-\beta} \\ &= O(1) \sum_{v=1}^{\infty} |\Delta \beta_v| v^{\beta} X_v \int_0^v u^{-\beta} du \\ &= O(1) \sum_{v=1}^{\infty} v |\Delta \beta_v| X_v = O(1). \end{aligned}$$

**Method 2.** As

$$\begin{aligned} m X_m \beta_m &= m X_m \sum_{n=m}^{\infty} \Delta \beta_n = m^{1-\beta} m^{\beta} X_m \sum_{n=m}^{\infty} \Delta \beta_n = O(1) m^{1-\beta} \sum_{n=m}^{\infty} n^{\beta} X_n |\Delta \beta_n| \\ &= O(1) \sum_{n=m}^{\infty} n^{1-\beta} n^{\beta} X_n |\Delta \beta_n| = O(1), \text{ then} \\ \sum_{n=1}^m \beta_n X_n &= \sum_{n=1}^{m-1} \left( \sum_{v=1}^n X_v \right) \Delta \beta_n + \left( \sum_{n=1}^m X_n \right) \beta_m \\ &= \sum_{n=1}^{m-1} \left( \sum_{v=1}^n v^{\beta} X_v v^{-\beta} \right) \Delta \beta_n + \left( \sum_{n=1}^m n^{\beta} X_n n^{-\beta} \right) \beta_m \\ &= O(1) \sum_{n=1}^m n^{\beta} X_n \left( \sum_{v=1}^n v^{-\beta} \right) \Delta \beta_n + O(1) m^{\beta} X_m \left( \sum_{n=1}^m n^{-\beta} \right) \beta_m \end{aligned}$$

$$= O(1) \sum_{n=1}^m n X_n |\Delta \beta_n| + O(1) m X_m \beta_m = O(1).$$

We state and prove the main result

**Theorem 2.1.** *Let  $(X_n)$  be a quasi  $\beta$ -power increasing sequence,  $0 < \beta < 1$ , and let  $(\beta_n)$  and  $(\lambda_n)$  be sequences satisfying (6)-(9). Let  $T$  be a triangular matrix satisfying*

$$(17) \quad n |t_{nn}| = O(1),$$

$$(18) \quad \sum_{n=v+1}^{\infty} n^{\delta k + k - 1} |t_{nn}|^{k-1} |\Delta_v \hat{t}_{nv}| = O(v^{\delta k} |t_{vv}|),$$

$$(19) \quad \sum_{n=v+1}^{\infty} n^{\delta k + k - 1} |\hat{t}_{n,v+1}|^k = O(v^{\delta k}),$$

$$(20) \quad \sum_{v=0}^{n-1} |\Delta_v \hat{t}_{nv}| = O(|t_{nn}|), \text{ and}$$

$$(21) \quad \sum_{n=1}^m n^{\delta k - 1} \frac{|s_n|^k}{X_n^{k-1}} = O(X_m).$$

Then the series  $\sum a_n \lambda_n$  is summable  $|T, \delta|_k$ ,  $k \geq 1$ ,  $0 \leq \delta < 1/k$ .

In addition, the following shows that condition (21) is weaker than (16) whenever  $(X_n)$  is almost increasing. For if (16) holds,

then, we have

$$\sum_{n=1}^m n^{\delta k - 1} \frac{|s_n|^k}{X_n^{k-1}} = O\left(\frac{1}{X_1^{k-1}}\right) \sum_{n=1}^m n^{\delta k - 1} |s_n|^k = O(X_m),$$

while if (21) is satisfied we have

$$\begin{aligned} \sum_{n=1}^m n^{\delta k - 1} |s_n|^k &= \sum_{n=1}^m n^{\delta k - 1} \frac{|s_n|^k}{X_n^{k-1}} X_n^{k-1} \\ &= \sum_{n=1}^{m-1} \left( \sum_{v=1}^n v^{\delta k - 1} \frac{|s_v|^k}{X_v^{k-1}} \right) \Delta X_n^{k-1} + \left( \sum_{n=1}^m n^{\delta k - 1} \frac{|s_n|^k}{X_n^{k-1}} \right) X_m^{k-1} \\ &= O(1) \sum_{n=1}^{m-1} X_n |\Delta X_n^{k-1}| + O(X_m) X_m^{k-1} \\ &= O(X_{m-1}) \sum_{n=1}^{m-1} (X_{n+1}^{k-1} - X_n^{k-1}) + O(X_m^k) \end{aligned}$$

$$\begin{aligned}
&= O(X_{m-1})(X_m^{k-1} - X_1^{k-1}) + O(X_m^k) \\
&= O(X_m^k).
\end{aligned}$$

Therefore (16) implies (21) but not conversely

**Proof of Theorem 2.1.** It is sufficient, by (5), and Minkowski's inequality, to show that

$$\sum_{n=1}^m n^{k-1} |T_{nj}|^k < \infty, \quad j=1,2,3.$$

Applying Holder's inequality, we have

$$\begin{aligned}
\sum_{n=1}^{m+1} n^{\delta k + k - 1} |T_{n1}|^k &\leq \sum_{n=1}^{m+1} n^{\delta k + k - 1} \left( \sum_{v=0}^{n-1} |\Delta_v \hat{t}_{nv}| |\lambda_v| |s_v| \right)^k \\
&\leq \sum_{n=1}^{m+1} n^{\delta k + k - 1} \left( \sum_{v=0}^{n-1} |\Delta_v \hat{t}_{nv}| |\lambda_v|^k |s_v|^k \right) \left( \sum_{v=0}^{n-1} |\Delta_v \hat{t}_{nv}| \right)^{k-1} \\
&= \sum_{n=1}^{m+1} n^{\delta k + k - 1} |t_{nn}|^{k-1} \sum_{v=0}^{n-1} |\Delta_v \hat{t}_{nv}| |\lambda_v|^k |s_v|^k \\
&= O(1) \sum_{v=0}^m |s_v|^k |\lambda_v|^k \sum_{n=v+1}^{m+1} n^{\delta k + k - 1} |t_{nn}|^{k-1} |\Delta_v \hat{t}_{nv}| \\
&= O(1) \sum_{v=0}^m v^{\delta k} |s_v|^k |\lambda_v|^k |t_{vv}| \\
(22) \quad &= O(1) \sum_{v=0}^m v^{\delta k - 1} |s_v|^k |\lambda_v|^k \\
&= O(1) \sum_{v=0}^m v^{\delta k - 1} \frac{|s_v|^k}{X_v^{k-1}} (X_v |\lambda_v|)^{k-1} |\lambda_v| \\
&= O(1) \sum_{v=0}^{m-1} \left( \sum_{r=0}^v r^{\delta k - 1} \frac{|s_r|^k}{X_r^{k-1}} \right) \Delta |\lambda_v| + \left( \sum_{v=0}^m v^{\delta k - 1} \frac{|s_v|^k}{X_v^{k-1}} \right) |\lambda_m| \\
&= O(1) \sum_{v=0}^{m-1} X_v |\Delta \lambda_v| + O(1) X_m |\lambda_m| \\
&= O(1) \sum_{v=0}^{m-1} X_v \beta_v + O(1) \\
&= O(1),
\end{aligned}$$

$$\begin{aligned}
\sum_{n=1}^{m+1} n^{\delta k + k - 1} |T_{n2}|^k &\leq \sum_{n=1}^{m+1} n^{\delta k + k - 1} \left( \sum_{v=0}^{n-1} |\hat{t}_{n,v+1}| |\Delta \lambda_v| |s_v| \right)^k \\
&\leq \sum_{n=1}^{m+1} n^{\delta k + k - 1} \left( \sum_{v=0}^{n-1} |\hat{t}_{n,v+1}| |s_v| \beta_v \right)^k \\
&\leq \sum_{n=1}^{m+1} n^{\delta k + k - 1} \sum_{v=0}^{n-1} |\hat{t}_{n,v+1}|^k \frac{|s_v|^k}{X_v^{k-1}} \beta_v \left( \sum_{v=0}^{m-1} \beta_v X_v \right)^{k-1}
\end{aligned}$$



$$\begin{aligned}
&= O(1) \sum_{v=0}^m \frac{|s_v|^k}{X_v^{k-1}} \beta_v \sum_{n=v+1}^{m+1} n^{\delta k+k-1} |\hat{t}_{n,v+1}|^k \\
&= O(1) \sum_{v=0}^m v^{\delta k-1} \frac{|s_v|^k}{v X_v^{k-1}} v \beta_v \\
&= O(1) \sum_{v=0}^{m-1} \left( \sum_{r=0}^v r^{\delta k-1} \frac{|s_r|^k}{X_r^{k-1}} \right) |\Delta(v \beta_v)| + O(1) \left( \sum_{v=0}^m v^{\delta k-1} \frac{|s_v|^k}{X_v^{k-1}} \right) m \beta_m \\
&= O(1) \sum_{v=0}^{m-1} X_v (-\beta_v + (v+1) \Delta \beta_v) + O(1) m \beta_m X_m \\
&= O(1) \sum_{v=0}^m \beta_v X_v + O(1) \sum_{v=0}^m v |\Delta \beta_v| X_v + O(1) m \beta_m X_m \\
&= O(1).
\end{aligned}$$

Finally,

$$\begin{aligned}
\sum_{n=1}^m n^{\delta k+k-1} |T_{n3}|^k &\leq \sum_{n=1}^m n^{\delta k+k-1} (|t_{nn}| |\lambda_n| |s_n|)^k \\
&= O(1) \sum_{n=1}^m n^{\delta k-1} |\lambda_n|^k |s_n|^k \\
&= O(1),
\end{aligned}$$

as in the case of (22). This completes the proof of the theorem.

If Theorem 2.1 is restricted to a series of positive terms, then the result can be stated as the following

**Theorem 2.2.** Let  $(X_n)$  be a quasi  $\beta$ -power increasing sequence and let  $(\beta_n)$  and  $(\lambda_n)$  be sequences satisfying (6)-(9). Let  $T$  be a triangular matrix with non-negative entries satisfying (10)-(12) and let (14), (21), and

$$(23) \quad \sum_{n=v+1}^{\infty} n^{\delta k+k-1} |\hat{t}_{n,v+1}|^k = O(v^{\delta k}),$$

be satisfied. Then the series  $\sum a_n \lambda_n$  is summable  $|T, \delta|_k$ ,  $k \geq 1$ ,  $0 \leq \delta < 1/k$ .

By making a comparison between Theorems 2.2 and 1.1, we have

1. Condition (21) is weaker than (16),
2. Condition (23) replaces the two conditions (13) and (15).

This probably implies that this special case of Theorem 2.1 is better than Theorem 1.1.

**Proof of Theorem 2.2.** It is sufficient to consider  $I_1$  only. Observe that conditions

$$(11)-(12) \text{ imply } \sum_{v=0}^{n-1} |\Delta \hat{t}_{nv}| = O(t_{nn}) \text{ (see [2])}.$$

$$\begin{aligned}
\sum_{n=1}^{m+1} n^{\delta k+k-1} |T_n|^k &\leq \sum_{n=1}^{m+1} n^{\delta k+k-1} \left( \sum_{v=0}^{n-1} |\Delta_v \hat{t}_{nv}| |\lambda_v| |s_v| \right) \\
&\leq \sum_{n=1}^{m+1} n^{\delta k+k-1} \left( \sum_{v=0}^{n-1} |\Delta_v \hat{t}_{nv}| |\lambda_v|^k |s_v|^k \right) \left( \sum_{v=0}^{n-1} |\Delta_v \hat{t}_{nv}| \right)^{k-1} \\
&= \sum_{n=1}^{m+1} n^{\delta k+k-1} (nt_{nn})^{k-1} \sum_{v=0}^{n-1} |\Delta_v \hat{t}_{nv}| |\lambda_v|^k |s_v|^k \\
&= O(1) \sum_{v=0}^m |s_v|^k |\lambda_v|^k \sum_{n=v+1}^{m+1} n^{\delta k} |\Delta_v \hat{t}_{nv}| \\
&= O(1) \sum_{v=0}^m v^{\delta k} |s_v|^k |\lambda_v|^k t_{vv} \\
&= O(1) \sum_{v=0}^m v^{\delta k-1} |s_v|^k |\lambda_v|^k \\
&= O(1),
\end{aligned}$$

as has been done before .

**Theorem 2.3.** Let  $(X_n)$  be a quasi  $\beta$ -power increasing sequence and let  $(\beta_n)$  and  $(\lambda_n)$  be sequences satisfying (6)-(9) . Let  $T$  be a triangular matrix satisfying (20)-(21), and

$$(24) \quad \sum_{n=v+1}^{\infty} n^{k-1} |t_{nn}|^{k-1} |\Delta_v \hat{t}_{nv}| = O(|t_{vv}|),$$

$$(25) \quad \sum_{n=v+1}^{\infty} n^{k-1} |\hat{t}_{n,v+1}|^k = O(1).$$

Then the series  $\sum a_n \lambda_n$  is summable  $|T|_k$ ,  $k \geq 1$ .

**Proof.** The proof follows from Theorem 2.1 by putting  $\delta = 0$ .

**Corollary 2.4.** Let  $(X_n)$  be a quasi  $\beta$ -power increasing sequence . If  $(\lambda_n)$  and  $(\beta_n)$  satisfy conditions (6)-(9), and if  $(p_n)$  is a sequence satisfying

$$(26) \quad n p_n = O(P_n),$$

$$(27) \quad \sum_{n=v+1}^{\infty} n^{\delta k-1} \frac{1}{P_{n-1}} = O\left(v^{\delta k} \frac{1}{P_v}\right),$$

then the series  $\sum a_n \lambda_n$  is summable  $|R, p_n|_k$ ,  $k \geq 1$ .

**Proof.** With  $T \equiv (R, p_n)$ , that is  $t_{nv} = \frac{p_v}{P_n}$ , and  $\hat{t}_{nv} = \frac{p_n P_{v-1}}{P_n P_{n-1}}$ , all of the conditions of

Theorem 2.2 are satisfied . In fact

$$\sum_{n=v+1}^m n^{\delta k+k-1} |\hat{t}_{n,v}|^k = \sum_{n=v+1}^m n^{\delta k+k-1} \left( \frac{p_n P_v}{P_n P_{n-1}} \right)^k = O(1) p_v^k \sum_{n=v+1}^m n^{\delta k-1} \frac{1}{P_{n-1}^k}$$

$$\begin{aligned}
O(1) \frac{p_v^k}{P_v^{k-1}} \sum_{n=v+1}^m n^{\delta_k-1} \frac{1}{P_{n-1}} &= O\left(v^{\delta_k} \frac{p_v^k}{P_v^k}\right) = O(v^{\delta_k}). \\
\sum_{n=v+1}^m n^{\delta_k+k-1} |t_{nm}|^{k-1} |\Delta \hat{t}_{nv}| &= \sum_{n=v+1}^m n^{\delta_k+k-1} \left(\frac{p_n}{P_n}\right)^{k-1} \frac{p_n p_v}{P_n P_{n-1}} \\
&= O(1) p_v \sum_{n=v+1}^m n^{\delta_k-1} \frac{1}{P_{n-1}} = O\left(v^{\delta_k} \frac{p_v}{P_v}\right) = O(v^{\delta_k} t_{vv}).
\end{aligned}$$

**Note.** Concerning Corollary 2.4, a similar result has been obtained in [2], using the condition

$$(28) \quad \sum_{n=v+1}^{m+1} n^{\delta_k} \left| \frac{p_n}{P_n P_{n-1}} \right| = O\left(\frac{v^{\delta_k}}{P_v}\right).$$

But condition (27) is weaker than (28). (The two summabilities  $|\overline{N}, p_n|_k$  and  $|R, p_n|_k$  are the same).

## References

- [1] H. Bor, An application of almost increasing sequences, Int. J. Math. Math. Sci. 23 (2000) no.12, 859-863.
- [2] E. Savas, On almost increasing sequences for generalized absolute summability, Math. Ineq. Appl., 9 (4) (2006), 717-723.

# Tail behavior for nonstationary moving averages with random coefficients

Aliou DIOP , Saliou DIOUF

January 7, 2010

LERSTAD, UFR de sciences Appliquées et de Technologies, B.P 234,  
Université Gaston Berger, Saint-Louis, Sénégal.  
alioudiop52@yahoo.fr, saliou\_diouf@yahoo.fr

## Abstract

We consider a class of nonstationary time series defined by  $Y_t = \mu_t + \sum_{j=0}^{\infty} C_{t,j} \sigma_{t-j} \eta_{t-j}$  where  $\{\eta_t; t \in \mathbf{Z}\}$  is sequence of iid random variables with regularly varying tail probabilities,  $\sigma_t$  is a scale parameter and  $\{C_{t,j}, t \in \mathbf{Z}, j > 0\}$  an infinite array of random variables identically distributed. We study an asymptotic tail behavior for  $(Y_t)$ .

**Key words and phrases :** Tail behavior, Regular varying function, Nonstationary process.

**AMS 2000 Mathematics Subject Classification :** 62G32, 62G30, 62F12.

## 1 Introduction

In recent years, modeling extremes of environmental time series has been the purpose of many investigations because of its wide applicability to the analysis of phenomenon such as extreme temperature, flood, storm winds and extreme ozone concentrations. See Horowitz ([6]) who considered the following model for daily ozone maxima  $\{Y_t\}$ :

$$\log(Y_t) = f(t) + \zeta_t$$

where  $f(t)$  is a deterministic part, such as a seasonal component or trend, and  $\zeta_t$  is a normal stationary autoregressive process. Ballerini and McCormick ([1]) studied the limit theory for processes of the form  $Y_t = f(t) + h(t)\zeta_t$  where  $h(\cdot)$  is positive and periodic and  $\{\zeta_t\}$  is a stationary process satisfying certain mixing conditions. Niu ([8]) studied the limit theory for extreme values of a class of nonstationary time series with the following form

$$Y_t = \mu_t + X_t, \quad X_t = \sum_{k=0}^{\infty} c_k \eta_{t-k} \sigma_{t-k} \quad (1.1)$$

where  $\sigma_t$  is a non random positive constant and  $\{\zeta_t\}$  is a sequence of iid random variables with regularly varying tail probabilities.

In this paper, we are interested in a nonstationary moving average process with random coefficients. The object of the paper is the determination of the tail behavior of the process  $(X_t)_t$  and appears as a direct extension of the results of Resnick and Willekens ([12]) and Kulik ([7]).

The exposition proceeds as follows. Section 2 describes the model, gives some examples and assumptions are provided. Section 3 contains the tail behavior of the process  $(X_t)_t$ . The marginal distribution of  $(X_t)_t$  has Pareto-like tails.

## 2 The model

Some extreme value data, especially in environmental contexts, often exhibit some stylized facts (see Coles([3]), Eastoe and Tawn ([5])):

- dependence on covariate effects
- short term dependence (storms for example)
- seasonality (due to the annual cycle in meteorology)
- long-trends (due to gradual climatic change)
- other forms of non-stationarity (switching regime due to weather regimes)

To take into account these facts, we introduce a class of nonstationary time series defined by the following relations

$$Y_t = \mu_t + X_t, \quad X_t = \sum_{k=0}^{\infty} C_{t,k} \eta_{t-k} \sigma_{t-k} \quad (2.2)$$

where  $\{\eta_t; t \in \mathbf{Z}\}$  is sequence of iid random variables with regularly varying tail probabilities,  $\sigma_t$  is a scale parameter and  $\{C_{t,k}, t \in \mathbf{Z}, k > 0\}$  an infinite array of random variables identically distributed called weights. Our goal is to study the tail behavior of the process defined in (2.2).

We may give an example of model (2.2) for, say, ground-level ozone data  $\{X_t\}$  defined by the following relation

$$X_t = \begin{cases} \phi_1 X_{t-1} + \sigma_{1t} \eta_t^{(1)}, & \text{if } W_{t-\delta} > \tau, \\ \phi_2 X_{t-1} + \sigma_{2t} \eta_t^{(2)}, & \text{if } W_{t-\delta} \leq \tau, \end{cases} \quad (2.3)$$

where  $\tau$  and  $\phi_i$  are non random constants and with threshold variable  $W_{t-\delta}$ . The sequences  $\eta_t^{(i)}, i = 1, 2$  are sequence of iid random variables with regularly

varying tail probabilities. The ground level ozone process has piecewise linear structure. It switches between two first order autoregressive process according to meteorological conditions, including daily temperature, relative humidity and wind speed and direction, which play an important role in determining the severity of ozone concentration.

In hydrological framework where the water level  $\{X_t\}$  is observed at a given location,  $W_{t-\delta}$  could be interpreted as threshold level upstream from that location and  $\delta$  the delay (in terms of days, hours, for instance) for the raw wave to reach that location.

- The dependence on covariates effects can also be modeled by considering the scale parameters  $\sigma_{it}$ ,  $i = 1, 2$  as a nonlinear function of meteorological variables of the form

$$\sigma_{it} = \exp \left\{ \beta_{i0} + \sum_{j=1}^m \beta_{ij} x_{tj} \right\}.$$

- To allow for a seasonal component (annual for instance) in the variance, we could use

$$\sigma_{it} = \exp \left\{ \alpha_{i0} + \sum_{j=1}^m \alpha_{ij} \cos \left( \frac{2\pi jt}{365} \right) + \beta_{ij} \sin \left( \frac{2\pi jt}{365} \right) \right\}.$$

- To allow for long trends due to gradual climatic change, we could use  $\mu_t = a_0 + a_1 t$ .

We define  $I_{1t} = \mathbf{1}_{\{W_{t-\delta} > \tau\}}$ ,  $I_{2t} = 1 - I_{1t}$ . The model (2.3) can be written as

$$X_t = \phi_{(t)} X_{t-1} + Z_t \quad (2.4)$$

where

$$\phi_{(t)} = \phi_1 I_{1t} + \phi_2 I_{2t} \quad \text{and} \quad Z_t = \sigma_{1t} \eta_t^{(1)} I_{1t} + \sigma_{2t} \eta_t^{(2)} I_{2t}.$$

The equation (2.4) is a stochastic difference equation where the pairs  $(\phi_{(t)}, Z_t)_t$  are sequences of independent and not identically distributed  $\mathbb{R}^2$ -valued random variables. The solution of (2.4) can be written as

$$X_t = \sum_{j=0}^{\infty} \left( \prod_{k=0}^{j-1} \phi_{(t-k)} \right) Z_{t-j} \quad (2.5)$$

We will use the following assumptions. We assume that the absolute value of each weight  $C_{t,k}$  has an upper endpoint  $c_k$  defined by

$$c_k = \sup\{c : \mathbb{P}(|C_{t,k}| \leq c) < 1\}, \quad k = 1, 2, \dots$$

Assume the following conditions hold:

**H<sub>1</sub>**– The sequence of random variables  $\{\eta_t, t \in \mathbb{Z}\}$  is a sequence of independent, identically distributed (i.i.d.) random variables and satisfy:

$$\mathbb{P}(|\eta_1| > x) = x^{-\alpha} L(x), \quad \alpha > 0 \quad (2.6)$$

and

$$\lim_{x \rightarrow \infty} \frac{\mathbb{P}(\eta_1 > x)}{\mathbb{P}(|\eta_1| > x)} = \pi_0, \quad \lim_{x \rightarrow \infty} \frac{\mathbb{P}(\eta_1 < -x)}{\mathbb{P}(|\eta_1| > x)} = 1 - \pi_0. \quad (2.7)$$

where  $\alpha > 0$ ,  $0 < \pi_0 \leq 1$  and  $L$  is a slowly varying function at infinity that is  $\lim_{x \rightarrow \infty} \frac{L(tx)}{L(x)} = 1$ .

Let  $a_n$  be the  $(1 - n^{-1})$  quantile of  $|\eta_1|$

$$a_n = \inf\{x : \mathbb{P}(|\eta_1| \leq x) \geq 1 - n^{-1}\} \quad (2.8)$$

**H<sub>2</sub>**– For all fixed  $t$  and  $k$ , random variables  $C_{t,k}$  and  $\eta_{t-k}$  are independent.

**H<sub>3</sub>**– For some,  $\delta > 0$   $\sum_{k=1}^{\infty} c_k^{1-\delta} < \infty$  and  $\sum_{k=1}^{\infty} \sigma_k^{\alpha} c_k^{\delta\alpha} < \infty$ .

**H<sub>4</sub>**–

$$\frac{1}{n} \sum_{j=1}^n \sigma_j^{\alpha} \rightarrow \sigma^{\alpha} \quad \text{as } n \rightarrow \infty. \quad (2.9)$$

### 3 Tail asymptotics

Throughout, all limit relationships are for  $x \rightarrow \infty$  unless otherwise specified. For two positive functions  $a(\cdot)$  and  $b(\cdot)$ , we write  $a(x) \lesssim b(x)$  if  $\limsup a(x)/b(x) \leq 1$ , write  $a(x) \gtrsim b(x)$  if  $\liminf a(x)/b(x) \geq 1$ , and write  $a(x) \sim b(x)$  if both. The asymptotic tail behaviors for  $(X_t)$  defined in (2.2) are given by the following theorems.

**Theorem 3.1** *Suppose that the conditions  $H_1 - H_3$  hold. Then the tail behavior distribution of  $(X_t)_t$  defined in (2.2) is :*

$$\lim_{x \rightarrow \infty} \frac{\mathbb{P}(|\sum_{k=0}^{\infty} C_{t,k} \sigma_{t-k} \eta_{t-k}| > x)}{\mathbb{P}(|\eta_1| > x)} = \sum_{k=0}^{\infty} \mathbb{E}[|\sigma_{t-k} C_{1,k}|^{\alpha}]. \quad (3.10)$$

**Theorem 3.2** *Suppose that the conditions  $H_1 - H_3$  hold. Then the tail behavior distribution of  $(Y_t)_t$  defined in 2.2 is :*

$$\lim_{x \rightarrow \infty} \frac{\mathbb{P}(\sum_{k=0}^{\infty} C_{t,k} \sigma_{t-k} \eta_{t-k} > x)}{\mathbb{P}(|\eta_1| > x)} = \sum_{k=0}^{\infty} \pi_0 \mathbb{E}[|\sigma_k C_{1,k}|^{\alpha}]. \quad (3.11)$$

$$\lim_{x \rightarrow \infty} \frac{\mathbb{P}(\sum_{k=0}^{\infty} C_{t,k} \sigma_{t-k} \eta_{t-k} < -x)}{\mathbb{P}(|\eta_1| > x)} = \sum_{k=0}^{\infty} (1 - \pi_0) \mathbb{E}[|\sigma_k C_{1,k}|^{\alpha}]. \quad (3.12)$$

We now begin the proof with two lemmas, the first is due to Cline ([2]), the second one is inspired by Lemma 3.1 in Resnick and Van Den Berg ([11])

**Lemma 3.3** Consider  $Z$  a random variable satisfying (2.6) and (2.7), and  $Y$  is another random variable independent of  $Z$  and satisfying  $\mathbb{E}[|Y|^\delta] < \infty$  for some  $\delta > \alpha$ . Then

$$\mathbb{P}(ZY > x) \sim \pi_0 \mathbb{E}[|Y|^\alpha] \mathbb{P}(|Z| > x) \quad (3.13)$$

and

$$\mathbb{P}(ZY < -x) \sim (1 - \pi_0) \mathbb{E}[|Y|^\alpha] \mathbb{P}(|Z| > x). \quad (3.14)$$

**Lemma 3.4** Suppose that  $U_0, \dots, U_m$  are random variables,  $F$  is a distribution function such that  $1 - F(x) = \mathbb{P}(U_0 > x) = x^{-\alpha} L(x)$ . Suppose

$$\lim_{x \rightarrow \infty} \frac{\mathbb{P}(U_k > x)}{1 - F(x)} = p_k c_k, \quad k = 0, \dots, m, \quad 0 \leq p_k \leq 1, \quad (3.15)$$

and

$$\lim_{x \rightarrow \infty} \frac{\mathbb{P}(U_k < -x)}{1 - F(x)} = (1 - p_k) c_k, \quad (3.16)$$

(a) If

$$\lim_{x \rightarrow \infty} \frac{\mathbb{P}(|U_k| > x, |U_l| > x)}{1 - F(x)} = 0, \quad k \neq l, \quad (3.17)$$

then

$$\lim_{x \rightarrow \infty} \frac{\mathbb{P}(|\sum_{k=0}^m U_k| > x)}{1 - F(x)} = \sum_{k=0}^m c_k. \quad (3.18)$$

(b) If

$$\lim_{x \rightarrow \infty} \frac{\mathbb{P}(U_k > x, U_l > x)}{1 - F(x)} = 0, \quad k \neq l, \quad (3.19)$$

then

$$\lim_{x \rightarrow \infty} \frac{\mathbb{P}(\sum_{k=0}^m U_k > x)}{1 - F(x)} = \sum_{k=0}^m p_k c_k. \quad (3.20)$$

$$\lim_{x \rightarrow \infty} \frac{\mathbb{P}(\sum_{k=0}^m U_k < -x)}{1 - F(x)} = \sum_{k=0}^m (1 - p_k) c_k. \quad (3.21)$$

### Proof

For the proof of (a) see [11].

(b) The proof is analogous to that of Lemma 2.1 in [4].

We begin by showing that

$$\lim_{x \rightarrow \infty} \frac{\mathbb{P}(U_1 + U_2 > x)}{1 - F(x)} = p_1 c_1 + p_2 c_2.$$

Define  $a_n$  such that  $n(1 - F(a_n)) \rightarrow 1, n \rightarrow \infty$  and on  $[-\infty, +\infty]$  define the measure  $\nu_i$  by

$$\nu_i(dx) = p_i x^{-\alpha-1} \mathbb{1}_{(x>0)} dx + (1 - p_i) (-x)^{-\alpha-1} \mathbb{1}_{(x<0)} dx.$$



The definition of  $a_n$ , (3.15) and (3.16) implies

$$\begin{aligned} n\mathbb{P}(a_n^{-1}Y_i \in \cdot) &\rightarrow_v c_i\nu_i \\ n\mathbb{P}(a_n^{-1}(Y_1, Y_2) \in (\cdot, \cdot)) &\rightarrow_v \mu \end{aligned} \quad (3.22)$$

where  $\mu$  concentrates on  $[-\infty, \infty]^2/\{\emptyset\}$  and for all  $x > 0$

$$\begin{aligned} \mu\{(y, 0) : y > x\} &= p_1 c_1 x^{-\alpha} \quad \text{and} \quad \mu\{(0, y) : y > x\} = p_2 c_2 x^{-\alpha} \\ \mu\{(y, 0) : y < -x\} &= (1 - p_1) c_1 x^{-\alpha} \quad \text{and} \quad \mu\{(0, y) : y < -x\} = (1 - p_2) c_2 x^{-\alpha}. \end{aligned}$$

Now let  $(Y'_n, Y''_n)$  be iid copies of  $(Y_1, Y_2)$  and applying Proposition 3.21 in [9] to (3.22) gives

$$\xi_n = \sum_{k=0}^{\infty} \varepsilon_{(\frac{k}{n}, a_n^{-1}(Y'_k, Y''_k))} \Rightarrow \xi = \sum_{k=0}^{\infty} \varepsilon_{(t'_k, (j'_k, 0))} + \sum_{k=0}^{\infty} \varepsilon_{(t'_k, (0, j''_k))} \quad (3.23)$$

on  $M_p([0, \infty) \times ([-\infty, \infty]^2/\{\emptyset\}))$  where the limit is Poisson random measure (PRM) on  $[0, \infty) \times ([-\infty, \infty]^2/\{\emptyset\})$  with mean measure  $dt \times d\mu$ .

Now we define the map  $T : [0, \infty) \times ([-\infty, \infty]^2/\{\emptyset\}) \rightarrow [-\infty, \infty]/\{0\}$  by  $T(t, x, y) = x + y$ . It is obvious the  $T$  is vaguely continuous, so Proposition 3.18 of [9] may be applied to (3.23) to obtain

$$\xi_n \circ T^{-1} = \sum_{k=0}^{\infty} \varepsilon_{(\frac{k}{n}, a_n^{-1}(Y'_k + Y''_k))} \Rightarrow \xi \circ T^{-1} = \sum_{k=0}^{\infty} \varepsilon_{(t'_k, j'_k)} + \sum_{k=0}^{\infty} \varepsilon_{(t'_k, j''_k)},$$

where the limit PRM concentrates on  $[0, \infty) \times ([-\infty, \infty] \setminus \{0\})$  with mean measure  $\mu \circ T^{-1}$ .

To evaluate  $\mu \circ T^{-1}$  we compute for  $z > 0$

$$\mu \circ T^{-1}(z) = \mu\{(x, y) : x + y > z\}$$

and because  $\mu$  concentrates on  $[-\infty, \infty]^2/\{0\}$  this equals

$$\mu\{(x, 0) : x + 0 > z\} + \mu\{(0, y) : 0 + y > z\} = p_1 c_1 z^{-\alpha} + p_2 c_2 z^{-\alpha}.$$

Applying again Proposition 3.21 in [9], we have

$$n\mathbb{P}(a_n^{-1}(Y_1 + Y_2) > x) \rightarrow_v (p_1 c_1 + p_2 c_2) x^{-\alpha}.$$

This proves the result for  $m = 2$ , the case for general  $m$  follows by induction. Analogously (3.21) is handled very similarly as (3.20)

### Proof of Theorem 3.1

First, we shall show that

$$\lim_{x \rightarrow \infty} \frac{\mathbb{P}(|\sum_{k=0}^m C_{t,k} Z_{t-k}| > x)}{\mathbb{P}(|\eta_1| > x)} = \sum_{k=0}^m \mathbb{E}[|C_{1,k} \sigma_{t-k}|^\alpha] \quad \text{where} \quad Z_k = \sigma_{t-k} \eta_k. \quad (3.24)$$

By Lemma 3.3 we have

$$\lim_{x \rightarrow \infty} \frac{\mathbb{P}(C_{t,k}Z_{t-k} > x)}{\mathbb{P}(|\eta_1| > x)} = \pi_0 \mathbb{E}[|C_{t,k}\sigma_{t-k}|^\alpha]. \quad (3.25)$$

Let  $\varepsilon > 0$  and  $k \neq l$

$$\begin{aligned} \mathbb{P}(|C_{t,k}Z_{t-k}| > x, |C_{t,l}Z_{t-l}| > x) &\leq \mathbb{P}(|C_{t,k}Z_{t-k}| \mathbb{I}_{\{|C_{t,k}| > \varepsilon\}} > x) + \mathbb{P}(|C_{t,l}Z_{t-l}| \mathbb{I}_{\{|C_{t,l}| > \varepsilon\}} > x) \\ &\quad + \mathbb{P}(|C_{t,k}| \leq \varepsilon, |C_{t,l}| \leq \varepsilon, |C_{t,k}Z_{t-k}| > x, |C_{t,l}Z_{t-l}| > x) \\ &\leq \mathbb{P}(|C_{t,k}Z_{t-k}| \mathbb{I}_{\{|C_{t,k}| > \varepsilon\}} > x) + \mathbb{P}(|C_{t,l}Z_{t-l}| \mathbb{I}_{\{|C_{t,l}| > \varepsilon\}} > x) \\ &\quad + \mathbb{P}(|\eta_{t-k}| > x(\sigma_{t-k}\varepsilon)^{-1}, |\eta_{t-l}| > x(\sigma_{t-l}\varepsilon)^{-1}) \\ &= I_1 + I_2 + I_3. \end{aligned}$$

By Lemma 3.3 and using Fatou's lemma, we have

$$\lim_{x \rightarrow \infty} \frac{I_1}{\mathbb{P}(|\eta_1| > x)} = \mathbb{E}[|C_{t,k}\sigma_{t-k}|^\alpha \mathbb{I}_{\{|C_{t,k}| > \varepsilon\}}] \rightarrow 0 \quad \text{as } \varepsilon \rightarrow \infty. \quad (3.26)$$

The proof of  $I_2$  is similar to  $I_1$ .

Since  $\eta_{t-k}$  and  $\eta_{t-l}$  are independent, we have

$$I_3 = o(\mathbb{P}(|\eta_1| > x)). \quad (3.27)$$

Combining (3.26) and (3.27), we get

$$\lim_{x \rightarrow \infty} \frac{\mathbb{P}(|C_{t,k}Z_{t-k}| > x, |C_{t,l}Z_{t-l}| > x)}{\mathbb{P}(|\eta_1| > x)} = 0. \quad (3.28)$$

The convergence (3.24) follows from Lemma 3.4.

Secondly, to establish (3.10), we shall prove that

$$\frac{\mathbb{P}(|\sum_{k=0}^{\infty} C_{t,k}Z_{t-k}| > x)}{\mathbb{P}(|\eta_1| > x)} \gtrsim \sum_{k=0}^{\infty} \mathbb{E}(|C_{1,k}\sigma_{t-k}|^\alpha). \quad (3.29)$$

and

$$\frac{\mathbb{P}(|\sum_{k=0}^{\infty} C_{t,k}Z_{t-k}| > x)}{\mathbb{P}(|\eta_1| > x)} \lesssim \sum_{k=0}^{\infty} \mathbb{E}(|C_{1,k}\sigma_{t-k}|^\alpha). \quad (3.30)$$

Set

$$S_m = \sum_{k=0}^m C_{t,k}Z_{t-k} \quad \text{and} \quad R_m = \sum_{k=m+1}^{\infty} C_{t,k}Z_{t-k}.$$

Notice that

$$\begin{aligned} \mathbb{P}(|S_m + R_m| > x) &\geq \mathbb{P}(|S_m| > x(1 + \varepsilon), |R_m| < x\varepsilon) \\ &\geq \mathbb{P}(S_m > x(1 + \varepsilon)) - \mathbb{P}(|R_m| \geq x\varepsilon) \end{aligned} \quad (3.31)$$

and

$$\mathbb{P}(|S_m + R_m| > x) \leq \mathbb{P}(|S_m| > x(1 - \varepsilon)) + \mathbb{P}(|R_m| \geq x\varepsilon) \quad (3.32)$$

From (3.24),

$$\lim_{x \rightarrow \infty} \frac{\mathbb{P}(|S_m| > x(1 + \varepsilon))}{\mathbb{P}(|\eta_1| > x)} = (1 + \varepsilon)^{-\alpha} \sum_{k=0}^m \mathbb{E}(|C_{1,k} \sigma_{t-k}|^\alpha).$$

Letting  $m \rightarrow \infty$  and  $\varepsilon \rightarrow 0$  it gives

$$\lim_{x \rightarrow \infty} \frac{\mathbb{P}(|S_m| > x(1 + \varepsilon))}{\mathbb{P}(|\eta_1| > x)} = \sum_{k=0}^{\infty} \mathbb{E}(|C_{1,k} \sigma_{t-k}|^\alpha). \quad (3.33)$$

Now we have to establish that

$$\lim_{x \rightarrow \infty} \frac{\mathbb{P}(|R_m| \geq \varepsilon x)}{\mathbb{P}(|\eta_1| > x)} \rightarrow 0. \quad (3.34)$$

$$\begin{aligned} \mathbb{P}(|R_m| \geq \varepsilon x) &= \mathbb{P}\left(\left|\sum_{k=m+1}^{\infty} C_{t,k} Z_{t-k}\right| > x\varepsilon\right) \\ &\leq \mathbb{P}\left(\sum_{k=m+1}^{\infty} |C_{t,k} Z_{t-k}| > x\varepsilon\right) \\ &\leq \mathbb{P}\left(\sum_{k=m+1}^{\infty} c_k |Z_{t-k}| > x\varepsilon\right) \\ &\leq \mathbb{P}\left(\sum_{k=m+1}^{\infty} c_k |Z_{t-k}| > x\varepsilon \sum_{k=m+1}^{\infty} c_k^{1-\delta}\right) \\ &\leq \sum_{k=m+1}^{\infty} \mathbb{P}(|Z_{t-k}| > x c_k^{-\delta} \varepsilon) \\ &\leq \sum_{k=m+1}^{\infty} \mathbb{P}(|\eta_1| > x \sigma_{t-k}^{-1} c_k^{-\delta} \varepsilon) \end{aligned}$$

Hence

$$\lim_{x \rightarrow \infty} \frac{\mathbb{P}(|R_m| \geq \varepsilon x)}{\mathbb{P}(|\eta_1| > x)} \leq \sum_{k=m+1}^{\infty} (\sigma_{t-k}^{-1} c_k^{-\delta} \varepsilon)^{-\alpha}$$

By  $H_3$ , we obtain (3.34). Combining (3.31) (3.33) and (3.34), we obtain (3.29). (3.30) follows from (3.32) (3.33) and (3.34). The theorem is entirely demonstrated.

### Proof of Theorem 3.2

First, we shall show that

$$\lim_{x \rightarrow \infty} \frac{\mathbb{P}(\sum_{k=0}^m C_{t,k} Z_{t-k} > x)}{\mathbb{P}(|\eta_1| > x)} = \sum_{k=0}^m \pi_0 \mathbb{E}[|C_{1,k} \sigma_{t-k}|^\alpha] \quad \text{where } Z_k = \sigma_k \eta_k. \quad (3.35)$$

By Lemma 3.3, we have

$$\begin{aligned} \lim_{x \rightarrow \infty} \frac{\mathbb{P}(C_{t,k}Z_{t-k} > x)}{\mathbb{P}(|\eta_1| > x)} &= \pi_0 \mathbb{E}[|C_{t,k}\sigma_{t-k}|^\alpha]. \\ \lim_{x \rightarrow \infty} \frac{\mathbb{P}(C_{t,k}Z_{t-k} > x, C_{t,l}Z_{t-l} > x)}{\mathbb{P}(|\eta_1| > x)} &\rightarrow 0 \end{aligned} \quad (3.36)$$

because

$$\mathbb{P}(C_{t,k}Z_{t-k} > x, C_{t,l}Z_{t-l} > x) \leq \mathbb{P}(|C_{t,k}Z_{t-k}| > x, |C_{t,l}Z_{t-l}| > x) \rightarrow 0$$

By Lemma 3.4, we get (3.35).

Notice that

$$\begin{aligned} \mathbb{P}(S_m + R_m > x) &\geq \mathbb{P}(S_m > x(1 + \varepsilon), |R_m| < x\varepsilon) \\ &\geq \mathbb{P}(S_m > x(1 + \varepsilon)) - \mathbb{P}(|R_m| \geq x\varepsilon) \end{aligned} \quad (3.37)$$

and

$$\mathbb{P}(S_m + R_m > x) \leq \mathbb{P}(S_m > x(1 - \varepsilon)) + \mathbb{P}(|R_m| \geq x\varepsilon) \quad (3.38)$$

Combining (3.37), (3.38), (3.34) and (3.35) we have

$$\frac{\mathbb{P}(\sum_{k=0}^{\infty} C_{t,k}Z_{t-k} > x)}{\mathbb{P}(|\eta_1| > x)} \gtrsim \sum_{k=0}^{\infty} \pi_0 \mathbb{E}(|C_{1,k}\sigma_{t-k}|^\alpha). \quad (3.39)$$

and

$$\frac{\mathbb{P}(\sum_{k=0}^{\infty} C_{t,k}Z_{t-k} > x)}{\mathbb{P}(|\eta_1| > x)} \lesssim \sum_{k=0}^{\infty} \pi_0 \mathbb{E}(|C_{1,k}\sigma_{t-k}|^\alpha). \quad (3.40)$$

Combining (3.39) and (3.40), (3.11) follows analogously.

## Acknowledgements :

These results were obtained thanks to the support of AIRES-Sud, a programme from the French Ministry of Foreign and European Affairs implemented by the Institut de Recherche pour "le Développement (IRD-DSF)". The authors acknowledge grants from "Ministère de la Recherche Scientifique" of Senegal.

## References

- [1] R. Ballerini and W. P. McCormick. Extreme value theory for processes with periodic variances. *Comm. Statist. Stoch. Models*, **5**, 45-51 (1989).
- [2] D. Cline, Estimation and linear prediction for regression, autoregression and ARMA with infinite variance data. PhD thesis, departement of statistics, Colorado State University, Ft. Collins, CO 80521 USA, 1983.

- [3] S. Coles, *An Introduction to Statistical Modeling of Extreme Values*. Springer, London, 2001.
- [4] R.A. Davis and S.I. Resnick, Limit theory for bilinear processes with heavy-tailed noise. *Ann. Appl. Prob.* **6**, 1191-1210 (1996).
- [5] E.F. Eastoe and J.A. Tawn, Modelling non-stationary extremes with to surface level ozone. *J. R. Stat. Soc., Ser. C, Appl. Stat.* **58**, 25-45 (2009).
- [6] J. Horowitz, Extreme values for a nonstationary stochastic process : an application to air quality analysis. *Technometrics*, **22**, 469-478 (1980).
- [7] R. Kulik, Limit theorem for moving average with random coefficients and heavy tailed noise. *J. Appl. Probab.* **43**, 245-256 (2006).
- [8] X-F. Niu, Extreme value theory for a class of nonstationary time series with applications. *Ann. Appl. Prob.* **7**, 508-522 (1997).
- [9] S.I. Resnick, Point processes, regular variation and weak convergence. *Adv. in Appl. Probab.* **18**, 66-138 (1986).
- [10] S.I. Resnick, *Extreme values, Regular Variation and Point Process*. Springer, New york, 1987.
- [11] S. I. Resnick and E. Van Den Berg, Sample correlation behavior for the heavy tailed general bilinear process. *Commun. Statist. Stoch. models* **16**, nr 2, 233-258 (2000).
- [12] S.I. Resnick, and E. Willekens, Moving averages with random coefficients and random coefficient autoregressive models. *Commun. Statist. Stoch. models* **7**, 511-525 (1991).

# **RELATIVE CONTROLLABILITY OF PERTURBED INFINITE NEUTRAL DIFFERENTIAL SYSTEMS**

**DAVIES IYAI**

Department of Mathematics and computer Science,  
Rivers State University of Science and Technology,  
P.M.B 5080, Port Harcourt, Rivers State, Nigeria.  
email:davsdone@yahoo.com

## **Abstract**

The purpose of this paper is to establish condition for the relative controllability of a perturbed infinite neutral differential systems with the perturbation function having implicit derivative, and multiple lumped time varying delays in the control. Our aim is achieved by defining the appropriate control and its corresponding solution by an integral equation. We then obtain the solution by applying the Schauder fixed point theorem. Some special cases of the perturbation function are also discussed.

2000 Mathematics subject classification: Primary 93B05; Secondary 34H05

Keywords: Controllability, neutral system, infinite delay, relative controllability, perturbation.

## **1. INTRODUCTION**

In Davies [3], the importance of delays in differential equations were discussed and the emphasis was on neutral functional differential equation (one in which the derivatives of the past history or derivatives of functional of the past history are involved as well as the present states of the system); because of its theoretical and

practical interest. For example, neutral functional differential equations are natural models for voltage and current fluctuations in problems arising in transmission lines, they also appear in the study of population dynamics, vibrating mass attached to an elastic bar etc. Remarkable contributors in this area of study include Hale and Verduyn Lunel [6], Kuang and Feldstein [16], Park [4], Xu et al [10] etc. Several authors Chukwu [2], Fu [15], Gahl [14], Balachandran and Anandhi [12]; Mahmudov and Zorlu [13] have investigated the controllability of neutral functional differential equation and results obtained through fixed point approaches, the choice of fixed point depends on the type of nonlinearity in the state equation. The control equation of neutral functional differential equation has applications in ecology, epidemics, population growth and in some complex economic studies etc . (see Onwuatu [9])

For controllability of neutral functional differential equations with implicit derivative in the perturbation function, very little attention has been drawn. Here, the problem is made more complex with the difficulty of making the right conditions to suit the fixed point of interest. However, Gahl [14]; Balachandran and Balasubramaniam [11] have illustrated the controllability of such systems. In [11], Balachandran and Balasubramaniam studied the controllability of nonlinear neutral Volterra integrodifferential systems with implicit derivative through the notions of condensing map and measure of noncompactness of a set by the use of Sadovskii fixed point theorem.

Our objective in this research is to extend the result in Gahl [14] by studying the relative controllability of a more general class of infinite neutral functional differential systems with the perturbation function having implicit derivative, and multiple lumped time varying delays in the control. Our method of approach shall be to define the appropriate control and its corresponding solution by an integral equation. We then obtain the solution by applying the Schauder fixed point theorem. Some special cases of the perturbation function are also discussed.

## 2. BASIC NOTATIONS, PRELIMINARIES AND DEFINITIONS

Suppose  $h > 0$  is a given number,  $E = (-\infty, \infty)$ ,  $E^n$  is a real  $n$ -dimensional Euclidean space with norm  $|\cdot|$ .  $C = C([-h, 0], E^n)$  is the space of continuous function mapping the interval  $[-h, 0]$  into  $E^n$  with the norm  $\|\cdot\|$  where

$\|\phi\| = \sup_{-h \leq s \leq 0} |\phi(s)|$ , for  $\phi \in C$ . Let  $\tau \in E$ ,  $a > 0$  and  $x \in C([\tau - h, \tau + a], E^n)$ , then

given  $t \in [\tau, \tau + a]$ , we define the symbol  $x_t$  by  $x_t(s) = x(t + s)$ ,  $-h \leq s < 0$ .

Let  $g$  be a bounded linear operator taking  $[\tau, \infty] \times C \rightarrow E^n$ , we define the functional difference operator  $D(\cdot): [\tau, \infty] \times C \rightarrow E^n$  by

$$D(t)\phi = \phi(0) - g(t, \phi) \quad (2.1)$$

for  $t \in [\tau, \infty]$ ,  $\phi \in C$ , we now define a neutral functional differential equation to be a system of the form

$$\frac{d}{dt} D(t) x_t = f(t, x_t) \quad (2.2)$$



where  $x_t \in C$ , and  $f$  is a continuous function from  $(\tau, \infty) \times C$  into  $E^n$ , we say that  $x$  is a solution of (2.2) with initial value  $\phi$  at  $\sigma$  if there exists  $a \in [\tau, \infty]$ ,  $a > 0$  such that  $x \in C([\sigma - h, \sigma + a], E^n)$ ,  $x_0 = \phi$ ,  $D(t)x_t$  is continuously differentiable on  $(\sigma, \sigma + a)$  and (2.2) is satisfied on  $(\sigma, \sigma + a)$ .

We shall consider perturbed neutral control systems of the form

$$\begin{aligned} \frac{d}{dt} D(t)x_t = & L(t, x, u) + \int_{-\infty}^0 A(\theta)x(t + \theta)d\theta \\ & + f(t, x(t), \dot{x}(t), u(w_0(t)), u(w_1(t)), \dots, u(w_j(t)), \dots, u(w_N(t))) \end{aligned} \quad (2.3)$$

its linear base control system

$$\frac{d}{dt} D(t)x_t = L(t, x, u) \quad (2.4)$$

and its free system

$$\frac{d}{dt} D(t)x_t = L(t, x, 0) + \int_{-\infty}^0 A(\theta)x(t + \theta)d\theta \quad (2.5)$$

where  $D(t)x_t = x(t) - Ax(t-1)$ ,  $L(t, x, \bar{u}) = Gx(t) + Bx(t-1) + Fu(t) + Hu(t-h)$ .

$A, B, G$  are  $n \times n$  matrices,  $F, H$  are  $n \times m$  matrices.  $A(\theta)$  is an  $n \times n$  matrix

whose elements are square integrable on  $(-\infty, 0]$ . If  $\phi \in C([-h, 0], E^n)$ ,  $x \in E^n$ , the

function  $f : E \times M_1 \times M_2 \times M_3 \rightarrow E^n$  (where  $M_1$  is the space of continuous

$n$ -vector functions on  $[0, t_1]$ ,  $M_2$  is the space of continuous  $n$ -vector functions

on  $[0, t_1] - S_3$  with finite left and right limits on  $S_3$ ; and  $M_3$  is the space of

admissible controls on  $[1-h, t_1]$ ). The continuous strictly increasing functions

$w_j(t) : [0, t_1] \rightarrow E$ ,  $j = 0, 1, 2, \dots, N$ , represent deviating arguments in the control,

that is,  $w_j(t) = t - h_j(t)$ , where  $h_j(t)$  are lumped time varying delays for

$j = 0, 1, 2, \dots, N$ . We assume also that the functions  $w_j(t) : [0, t_1] \rightarrow E$ ,

$j = 0, 1, 2, \dots, N$  are twice continuously differentiable and strictly increasing in  $[0, t_1]$ .

Further,  $w_j(t) \leq t$  for  $t \in [0, t_1]$ ,  $j = 0, 1, 2, \dots, N$ . We introduce the time lead

function (see[5])

$r_j(t) : [w_j(t_0), w_j(t_1)] \rightarrow [0, t_1]$ ,  $j = 0, 1, 2, \dots, N$ , such that  $r_j(w_j(t)) = t$  for  $t \in [0, t_1]$ .

Without loss of generality, we assume that  $h_0(t) = t$  and the following inequality

holds for  $t = t_1$

$$\begin{aligned} h &= w_N(t_1) \leq w_{N-1}(t_1) \leq \dots \leq w_{N+1}(t_1) \leq t_0 = \\ &w_N(t_1) < w_{N-1}(t_1) \leq \dots \leq w_j(t_1) \leq w_0(t_1) = t_1 \end{aligned}$$

Let  $X(t)$  be the unique  $n \times n$  constant matrix function with the following properties

- a)  $X(t) = 0$ , for  $t < 0$
- b)  $X(t) = I$  the identity matrix
- c)  $X(t) - AX(t-1)$  is continuous on  $[0, \infty]$
- d)  $X(t)$  satisfies  $\dot{X}(t) - A\dot{X}(t-1) = L(t, x, 0)$

for  $t \in (0, \infty) - S_2$ , where  $S_2$  is the set of non-negative integers.

Then a unique solution of (2.4) exist on  $[1, t]$  satisfying  $x_L(t, u) = \phi(t)$  for  $t \in [0, 1]$

and by Gahl [14], this solution is given by

$$\begin{aligned} x_L(t, u) &= X(t-1)\phi(1) - X(t-2)\phi(1) + \int_1^t X(t-s-1)[A\phi(s) + B\phi(s)]ds \\ &\quad + \int_1^t X(t-s)[Fu(s) + Hu(s-h)]ds \end{aligned} \tag{2.6}$$

for all  $t \in [1, t_1]$ .  $x_L(t, u)$  is a continuous function which satisfies (2.4) on  $J = [1, t_1]$  except for a finite number of points which are contained in the set

$$S_3 = S_2 \{t : t = t_1 \pm h + I; \ t \neq k \text{ or } h \neq I, \text{ for } k \in S_2\}$$

Define the matrix functions  $Z$  by

$$Z(t, s) = X(t - s)F + X(t - s - h)H$$

Then it follows immediately that

$$x_L(t, u) = x_L(t, 0) + \int_1^t Z(t, s)u(s)ds \quad (2.7)$$

We note from remarks in [14] that since  $\dot{X}(t)$  is continuous and bounded on  $[0, t_1] - S_2$

$$\frac{\partial}{\partial t} Z(t, s) = \dot{X}(t - s)F + \dot{X}(t - s - h)H$$

Then, the corresponding solution of (2.3) following the methods of Gahl [14] and Sinha [1] is given by

$$\begin{aligned} x(t, \phi, u, f) &= x_L(t, u) + q(t, s, \theta) \\ &+ \int_1^t X(t, s)f(s, x(\cdot), \dot{x}(\cdot), u(w_0(\cdot)), u(w_1(\cdot)), \dots, u(w_j(\cdot)), \dots, u(w_N(\cdot)))ds \end{aligned}$$

or

$$\begin{aligned} x(t, \phi, u, f) &= x_L(t, 0) + q(t, s, \theta) + \int_1^t Z(t, s)u(s)ds \\ &+ \int_1^t X(t - s)f(s, x(\cdot), \dot{x}(\cdot), u(w_0(\cdot)), u(w_1(\cdot)), \dots, u(w_j(\cdot)), \dots, u(w_N(\cdot)))ds \end{aligned} \quad (2.8)$$

for  $t \in J$ , so that  $x(t, \phi, u, f)$  satisfies (2.3) on  $J - S_3$ ,

where

$$q(t, s, \theta) = \int_1^t X(t-s) \int_{-\infty}^0 A(\theta) x(t+\theta) d\theta ds$$

Here the control of interest are all functions  $u$  with  $u(t) = 0$  for  $t < 1$  which are also piecewise continues and bounded on  $J$  with all points of discontinuity contained in the set

$$S_1 = \{1, t_1 - 1, t_1 - 2, \dots, t_1 - h - 1, t_1 - h - 2, \dots\} \cap J$$

and being of simple type yielding finite jumps in  $u$ .

We now give some definitions upon which our study hinges.

### Definition 2.1

The system (2.3) is said to be relatively controllable on  $J$  if, for every function  $\phi \in C$ , and every  $x_1 \in E^n$ , there exists an admissible control function  $u$  such that the solution of the system (2.3) satisfies  $x(t_1) = x_1$ .

### Definition 2.2

The controllability matrix of (2.3) will be given by

$$W = \int_1^t Z(t, s) Z^T(t, s) ds$$

where  $Z^T$  is the transpose of  $Z$ .

## 3. CONTROLLABILITY RESULTS

Here we state theorem which summarize the main results of this section.

**Theorem 3.1.** The system (2.4) is relative controllable on  $J$  if and only if  $W$  is nonsingular.

**Proof:** The proof can be observed from Proposition 3.1 of Dauer and Gahl [8]

### MAIN RESULT OF THIS PAPER

We are now ready to obtain our main result of this paper which extends those of Gahl [14] and Davies [3] to the relative controllability of infinite neutral functional differential systems with perturbation function having implicit derivative, and multiple lumped time varying delays in the control.

Let  $Q$  be the Banach space of all functions  $(x, u): [0, t_1] \times [1-h, t_1] \rightarrow E^n \times E^m$ , where  $x$  is in  $M_1$ ,  $\dot{x}$  is in  $M_2$ , and  $u$  is in  $M_3$ . The norm on  $Q$  is

$$\|(x, u)\| = \|x\| + \|u\| + \|\dot{x}\|$$

where

$$\|x\| = \sup |x(t)| \text{ for } t \in [0, t_1],$$

$$\|\dot{x}\| = \sup |\dot{x}(t)| \text{ for } t \in [0, t_1] - S_3,$$

$$\|u\| = \sup |u(t)| \text{ for } t \in [1-h, t_1].$$

That  $Q$  is a Banach space follows with the aid of the fact that if  $\{x_n(t)\}$  is a uniformly convergent sequence on a bounded interval converging to some function  $x(t)$  and if  $\{\dot{x}_n(t)\}$  is also uniformly convergent, then  $\{\dot{x}_n(t)\}$  converges uniformly to  $\dot{x}(t)$ .

For system (2.3), take

$$k = (x, u) \in E^n \times E^n \times E^{(N+1)m}$$

and let

$$|k| = |x| + |\dot{x}| + |u_0| + |u_1| + \dots + |u_j| + \dots + |u_N|,$$

where  $|\cdot|$  denotes the standard norm in the finite dimensional Euclidean space

We now assume the following conditions on  $f$  :

$$H_0: \sup \left\{ \left| f(t, x(\cdot), \dot{x}(\cdot), u(w_0(\cdot)), u(w_1(\cdot)), \dots, u(w_j(\cdot)), \dots, u(w_N(\cdot))) \right| : t \in J - S_3 \right\} \leq G(r) < \infty$$

$$\text{For all } (x, u) \in Q \text{ such that } |k| \leq r, \text{ where } \lim_{r \rightarrow \infty} \frac{G(r)}{r} = 0$$

$H_1$ : Let  $\{(x_n, u_n)\} \in C_n[t_0, t_1] \times C_m[t_0, t_1]$  be a bounded sequence such that

$$\{(u_n(t-h))\}, \{u_n(t)\}, \{x_n(t)\} \text{ and } \{x_n(t-1)\} \text{ are each equicontinuous for}$$

$$t \in [a, b] \subseteq J. \text{ Then } \{f(t, x(\cdot), \dot{x}(\cdot), u(w_0(\cdot)), u(w_1(\cdot)), \dots, u(w_j(\cdot)), \dots, u(w_N(\cdot)))\} \text{ is}$$

equicontinuous on  $[a, b]$ .

**Theorem 3.2.** Let  $f$  be continuous on  $J - S_3 \times M_1 \times M_2 \times M_3$  with finite left and right limits on  $S_3$  and assume  $f$  satisfies conditions  $H_0$  and  $H_1$ . If system (2.4) is relatively controllable on  $J$ , then system (2.3) is relatively controllable on  $J$ .

**Proof:** By Theorem 3.1  $W^{-1}$  exists. Let  $\phi$  be an  $n$ -vector function on  $[0, 1]$  of class

$M_1$ , and  $x_1 \in E^n$ . We define an operator  $T$  on  $Q$  by  $T(x, u) = (y, v)$ , where

$$v(t) = Z^T(t, s)W^{-1}(t, s) \left[ x_1 - x_L(t, 0) - q(t, s, \theta) - \int_1^t X(t-s)f(s, x(\cdot), \dot{x}(\cdot), u(w_0(\cdot)), u(w_1(\cdot)), \dots, u(w_j(\cdot)), \dots, u(w_N(\cdot)))ds \right]$$

for  $t \in J$ , and  $v(t) = 0$  for  $t < 1$ ;

$$y(t) = x_L(t;0) + q(t,s,\theta) + \int_1^t Z(t_1,s)v(s)ds \\ + \int_1^t X(t-s)f(s,x(\cdot),\dot{x}(\cdot),u(w_0(\cdot)),u(w_1(\cdot)),\dots,u(w_j(\cdot)),\dots,u(w_N(\cdot)))ds$$

for  $t \in J$ , and  $y(t) = \phi(t)$  for  $0 \leq t < 1$ .

We show that  $T:Q \rightarrow Q$ . By the definition of  $Z(t,s)$  and the remarks following in section 2,  $v(t)$  is an admissible control function. Since  $x_L(1,0) = \phi(1)$ ,  $y(t)$  is continuous on  $[0, t_1]$ . In order to show that  $(y, v) \in Q$ , it remains to establish that  $\dot{y}(t) \in M_2$ . Let  $t \in J - S_3$ . To obtain an expression for  $\dot{y}(t)$  we use the fact that  $Z(t,s)$  is discontinuous on  $J$  for

$s = t, t-1, \dots, t-h, t-h-1, \dots$  and  $X(t-s)$  is discontinuous for  $s = t, t-1, \dots$ . Then

$$\int_1^t Z(t,s)v(s)ds = \sum_{j=1}^{p(t)} \left( \int_{t-a_j}^{t-a_{j+1}} Z(t,s)v(s)ds + \int_1^{t-a_1} Z(t,s)v(s)ds \right)$$

where  $t-a_j$ ,  $j=1, \dots, P(t)+1$ , are the points of discontinuity in  $s$  of  $Z(t,s)$  for  $s \in [1, t]$ . Using  $-$  and  $+$  to denote left and right limits respectively,

$$\frac{d}{dt} \int_1^t Z(t,s)v(s)ds = \int_1^t \frac{\partial Z}{\partial t}(t,s)v(s)ds \\ + \sum_{j=1}^{p(t)} [Z(t, (t-a_{j+1})^-) \cdot v(t-a_{j+1}) - Z(t, (t-a_j)^+) \cdot v(t-a_j)] \\ + Z(t, (t-a_1)^-) \cdot v(t-a_1)$$

We are also using here the fact that the points  $t-a_j$  are points of continuity of  $v$ , since, if  $t-a_j \in S_1$  then  $t \in S_3$ . By the definition of  $Z(t,s)$

$$\frac{d}{dt} \int_1^t Z(t,s)v(s)ds = \int_1^t (\dot{X}(t-s)F + X(t-s-h)H)v(s)ds + \sum_{j=0}^{p(t)} R_j(t)$$

where

$$R_j(t) = [X(a_{j+1}^+)F + X((a_{j+1}-h)^+)H]v(t-a_{j+1}) - [X(a_j^-)F + X((a_j-h)^-)H]v(t-a_j)$$

$a_0 = 0$ , and recall that  $X(0^-) = 0$ . We note that a similar derivation is needed to show that the expression for  $x_L(t;u)$  in equation (2.6) satisfies (2.4) on  $J$  except for points where  $t-a_j \in S_1$  or  $t \in S_2$ . Thus, the defined structure of  $S_3$  is necessary.

Similarly, for  $t \in J - S_3$ ,

$$\begin{aligned} & \frac{d}{dt} \int_1^t X(t-s)f(s, x(\cdot), \dot{x}(\cdot), u(w_0(\cdot)), u(w_1(\cdot)), \dots, u(w_N(\cdot)))ds \\ &= \int_1^t \dot{X}(t-s)f(s, x(\cdot), \dot{x}(\cdot), u(w_0(\cdot)), u(w_1(\cdot)), \dots, u(w_N(\cdot)))ds \\ &+ \sum_{i=1}^{[t]-1} \left[ \begin{aligned} & X((i-1)^+)f(t-i+1, x(\cdot), \dot{x}(\cdot), u(w_0(\cdot)), u(w_1(\cdot)), \dots, u(w_N(\cdot))) \\ & - X(i^-)f(t-1, x(\cdot), \dot{x}(\cdot), u(w_0(\cdot)), u(w_1(\cdot)), \dots, u(w_N(\cdot))) \end{aligned} \right] \\ &+ X([t]-1)^+f(t-[t]+1, x(\cdot), \dot{x}(\cdot), u(w_0(\cdot)), u(w_1(\cdot)), \dots, u(w_N(\cdot))) \end{aligned}$$

where  $[t]$  is the largest integer  $\leq t$  and if  $[t]=1$  the sum is empty. We are also using here the fact that if  $t \in J - S_3$  then  $t-i \in J - S_3$  for  $i=1, 2, \dots, [t]-1$ , along with the continuity assumption on  $f$ . Rearranging terms we have

$$\begin{aligned} & \frac{d}{dt} \int_1^t X(t-s)f(s, x(\cdot), \dot{x}(\cdot), u(w_0(\cdot)), u(w_1(\cdot)), \dots, u(w_N(\cdot)))ds \\ &= \int_1^t \dot{X}(t-s)f(s, x(\cdot), \dot{x}(\cdot), u(w_0(\cdot)), u(w_1(\cdot)), \dots, u(w_N(\cdot)))ds + \sum_{i=0}^{[t]-1} P_i(t) \end{aligned}$$

where



$$P_i(t) = \left[ X(i^+) - X(i^-) \right] f(t-i, x(\cdot), \dot{x}(\cdot), u(w_0(\cdot)), u(w_1(\cdot)), \dots, u(w_j(\cdot)), \dots, u(w_N(\cdot)))$$

Then for  $t \in J - S_3$  we have

$$\begin{aligned} \dot{y}(t) = & \dot{x}_L(t; 0) + q(t, \dot{s}, \theta) + \int_1^t (\dot{X}(t-s)F + \dot{X}(t-s-h)H)v(s)ds + \sum_{j=0}^{p(t)} R_j(t) \\ & + \int_1^t \dot{X}(t-s) f(s, x(\cdot), \dot{x}(\cdot), u(w_0(\cdot)), u(w_1(\cdot)), \dots, u(w_j(\cdot)), \dots, u(w_N(\cdot))) ds \\ & + \sum_{i=0}^{[t]-1} P_i(t) \end{aligned} \quad (3.1)$$

Since  $\dot{y}(t)$  is continuous on  $J - S_3$  and has finite left and right limits on

$$S_3, \dot{y}(t) \in M_2 \text{ and } T: Q \rightarrow Q. \text{ Where } q(t, \dot{s}, \theta) = \int_1^t \dot{X}(t, s) \int_{-\infty}^0 A(\theta)x(t+\theta) d\theta ds$$

Let us introduce the following notations

$$a_1 = \sup |Z(t, s)| \text{ for } 1 \leq s \leq t \leq t_1$$

$$a_2 = |W^{-1}(t, s)|$$

$$a_3 = \sup (|x_L(t; 0)| + |q(t, s, \theta)| + |x_1|) \text{ for } t \in J$$

$$a_4 = \sup |X(t)| \text{ for } 0 \leq t \leq t_1$$

$$a_5 = \sup |\dot{X}(t)| \text{ for } t \in [0, t_1] - S_2$$

$$a_6 = \sup (|\dot{x}_L(t; 0)| + |q(t, \dot{s}, \theta)|) \text{ for } t \in J - S_2$$

$$a_7 = |F| + |H|$$

$$b = \max \{(t_1 - 1) a_1, 1, (t_1 - 1) a_5 a_7 + 2(p(t_1) + 1) a_4 a_7\}$$

$$c_1 = (2N + 6)ba_1a_2a_4(t_1 - 1)$$

$$c_2 = (2N + 6)a_4(t_1 - 1)$$

$$c_3 = (2N + 6)[2[t_1]a_4 + (t_1 - 1)a_5]$$

$$d_1 = (2N + 6)a_1a_2a_3b$$

$$d_2 = (2N + 6)a_3$$

$$d_3 = (2N + 6)a_6$$

$$c = \max\{c_1, c_2, c_3\}$$

$$d = \max\{d_1, d_2, d_3\}$$

$$\sup|f| = \sup\left|f(s, x(\cdot), \dot{x}(\cdot), u(w_0(\cdot)), u(w_1(\cdot)), \dots, u(w_j(\cdot)), \dots, u(w_N(\cdot)))\right| \text{ for } S \in J - S_3$$

Since  $\phi$  is of class  $M_1$  on  $[0, 1]$  and  $\lim_{r \rightarrow \infty} \frac{G(r)}{r} = 0$ , by Proposition 3.1 in Dauer [7],

$f$  satisfies the following condition: for each pair of positive constants  $c$  and  $d$ ,

there exists a positive constant  $r$  such that if  $|k| \leq r$ , then

$$cG(r) + d \leq r \quad (3.2)$$

Also, for given  $c$  and  $d$ , if  $r$  is a constant such that (3.2) is satisfied, then any  $r_1$  such that  $r < r_1$  will also satisfy (3.2). Now take  $c$  and  $d$  as given above, and let  $r$  be chosen so that (3.2) is satisfied and  $\sup|\phi(t)|$  for  $t \in [0, 1] \leq r(N+3)^{-1}$ ,  $\sup|\dot{\phi}|$  for  $t \in [0, 1] \leq r(N+3)^{-1}$ .

Therefore, if

$$\|x\| \leq r(N+3)^{-1}, \quad \|u\| \leq r(N+3)^{-1}, \text{ and } \|\dot{x}\| \leq r(N+3)^{-1}$$

Then

$$|k| = |x(s)| + \sum_{j=0}^N |u(w_j(s))| \leq r \quad \text{for all } s \in J.$$

It follows from property  $H_0$  that if  $|k| \leq r$ , then  $c \sup |f| + d \leq r$ . Now let

$$Q(r) = \{(x, u) \in Q : \|(x, u)\| \leq r\},$$

and let  $(x, u) \in Q(r)$ . Then

$$\begin{aligned} |v(t)| &\leq a_1 a_2 [a_3 + (t_1 - 1)a_4 \sup |f|] \leq d_1 [(2N + 6)b]^{-1} + c_1 \sup |f| [(2N + 6)b]^{-1} \\ &\leq (d + c \sup |f|) [(2N + 6)b]^{-1} \leq r [(2N + 6)b]^{-1} \leq r (2N + 6)^{-1} \text{ for all } t \in J \end{aligned}$$

Similarly,

$$\begin{aligned} |y(t)| &\leq a_3 + (t_1 - 1)a_1 \|v\| + (t_1 - 1)a_4 \sup |f| \leq d_2 (N + 3)^{-1} + b \|v\| + c_2 \sup |f| (2N + 6)^{-1} \\ &\leq r (2N + 6)^{-1} + (d + c \sup |f|) (2N + 6)^{-1} \leq r (N + 3)^{-1} \end{aligned}$$

for all  $t \in J$

Using equation (3.1) and the expressions for  $R_j(t)$  and  $P_i(t)$  and letting  $t \in J - S_3$ ,

$$\begin{aligned} |\dot{y}(t)| &\leq a_6 + (t_1 - 1)a_5 a_7 \|v\| + 2(P(t_1) + 1)a_4 a_7 \|v\| + ((t_1 - 1)a_5 + 2[t_1]a_4) \sup |f| \\ &\leq d_3 (2N + 6)^{-1} + b \|v\| + [c_3 \sup |f|] (2N + 6)^{-1} \\ &\leq r (2N + 6)^{-1} + [d + c \sup |f|] (2N + 6)^{-1} \\ &\leq r (N + 3)^{-1} \end{aligned}$$

Hence  $\|(y, v)\| \leq r$ , and  $T : Q(r) \rightarrow Q(r)$

By the continuity assumption on  $f$ ,  $T$  is continuous on  $Q$ . Now let  $P(r)$  be closed convex hull of  $T(Q(r))$ , and we show that  $T$  has a fixed point in  $P(r)$ . Since  $Q(r)$  is closed, bounded and convex in  $Q$  and  $T : Q(r) \rightarrow Q(r)$ ;  $P(r)$  is also closed, bounded, and convex in  $Q(r)$  and  $T : P(r) \rightarrow P(r)$ . In order to apply the schauder fixed point theorem it remains to show that  $T$  is completely continuous on  $P(r)$ .

Let  $\{(y_n, v_n)\}_{n=1}^{\infty}$  be a sequence in  $T(P(r))$ , and we show that it has a convergent subsequence in  $Q$ . Let  $(y_n, v_n) = T(x_n, u_n)$  for some  $(x_n, u_n) \in P(r)$ . Since  $\|(y_n, v_n)\| \leq r$  for all  $n$ , the sequence  $\{y_n(t)\}$ ,  $\{\dot{y}_n(t)\}$ , and  $\{v_n(t)\}$  are each uniformly bounded on the sets  $[0, t_1]$ ,  $[0, t_1] - S_3$ , and  $[1-h, t_1]$  respectively. Further, by the boundedness assumption on  $f$  and since  $P(r)$  is contained in  $Q(r)$ , the sequence  $\{y_n(t)\}$  is equicontinuous on  $[0, t_1]$ . Also since  $Z^T(t_1, s)$  has a continuous extension on the closure of each subinterval of  $[1-h, t_1] - S_1$ , the sequence  $\{v_n(t)\}$  can be extended to be equicontinuous on the closure of each of these subintervals. We note that the equicontinuity holds for all member of  $T(Q(r))$ . Hence it holds for the limit points in  $Q$  of all convex combinations of members of  $T(Q(r))$  and, therefore, it holds for all members of  $P(r)$ . Thus  $\{x_n(t)\}$  is equicontinuous on  $[0, t_1]$  and  $\{u_n(t)\}$  can be extended to be equicontinuous on the closure of each subinterval of  $[1-h, t_1] - S_1$ .

We now apply property  $H_1$  in order to show that  $\{\dot{y}_n(t)\}$  can be extended to be equicontinuous on the closure of each subinterval of  $[0, t_1] - S_3$ . For  $t \in J - S_3$ , it follows that  $t - i \in [0, t_1] - S_3$  and  $t - h - i \in [1-h, t_1] - S_1$ , for  $i = 0, 1, 2, \dots, [t]$ .

Therefore, each of the sequences  $\{u_n(t-i)\}$ ,  $\{u_n(t-h-i)\}$ ,  $\{x_n(t-i)\}$ , and  $\{x_n(t-i-1)\}$ , for  $i = 0, 1, 2, \dots, [t] - 1$  can be extended to be equicontinuous on the closure of each subinterval of  $J - S_3$ . By property  $H_1$  the sequence

$\{f(t-i, x_n(\cdot), \dot{x}_n(\cdot), u_n(w_0(\cdot)), u_n(w_1(\cdot)), \dots, u_n(w_j(\cdot)), \dots, u_n(w_N(\cdot)))\}$  is equicontinuous on

the closure of each of these subintervals for  $i=0,1,2,...,[t]-1$ . It follows from equation (3.1) that the sequence  $\{\dot{y}_n(t)\}$  can be extended to be equicontinuous on the closure of each subinterval of  $[0,t_1]-S_3$ . Now by successive applications of Ascoli's theorem we obtain a convergent subsequence of  $Q$  of  $\{(y_n, v_n)\}$ . Hence,  $T(P(r))$  is sequentially compact and, therefore, its closure is also sequentially compact. This implies that  $T$  is completely continuous on  $P(r)$ .

By the Schauder fixed point theorem  $T$  has a fixed point in  $P(r)$ , call it  $(x,u)$ .

Therefore

$$\begin{aligned} x(t) &= x_L(t,0) + q(t,s,\theta) + \int_1^t Z(t,s)u(s)ds \\ &+ \int_1^t X(t-s)f(s,x(\cdot),\dot{x}(\cdot),u(w_0(\cdot)),u(w_1(\cdot)),\dots,u(w_j(\cdot)),\dots,u(w_N(\cdot)))ds \end{aligned}$$

for  $t \in J$ , and  $x(t) = \phi(t)$  for  $t \in [0,1]$ .

Also

$$\begin{aligned} x(t_1) &= x_L(t_1;0) + q(t,s,\theta) + \int_1^t Z(t_1,s)Z^T(t_1,s) \times \\ &W^{-1}(t,s,u) \left( \begin{aligned} &x_1 - x_L(t_1;0) - q(t,s,\theta) \\ &- \int_1^t X(t-s)f(s,x(\cdot),\dot{x}(\cdot),u(w_0(\cdot)),u(w_1(\cdot)),\dots,u(w_j(\cdot)),\dots,u(w_N(\cdot)))ds \end{aligned} \right) ds \\ &+ \int_1^t X(t-s)f(s,x(\cdot),\dot{x}(\cdot),u(w_0(\cdot)),u(w_1(\cdot)),\dots,u(w_j(\cdot)),\dots,u(w_N(\cdot)))ds = x_1 \end{aligned}$$

This completes the proof, since  $x(t)$  is the desired solution.

#### 4. EXAMPLES

In the sequel, we shall consider some examples of the function  $f$  which satisfies the hypothesis of Theorem 3.2

##### Example 4.1

Let

$$f = k(t, x(t), x(t-1), u(w_0(t)), u(w_1(t)), \dots, u(w_j(t)), \dots, u(w_N(t))) + \int_1^t g(s, x(s), x(s-v(s)), \dot{x}(s), \dot{x}(s-\theta(s)), u(w_0(s)), u(w_1(s)), \dots, u(w_j(s)), \dots, u(w_N(s))) ds$$

where  $w_j(t)$  is as defined in Section 2,  $v$  and  $\theta$  are nonnegative measurable functions; and the  $n$ -vector functions  $k$  and  $g$  are defined on the appropriate  $E^n$  spaces as in  $H_0$ . It should be noted that term of the form  $\int_1^t g(x(s)) ds$  are of the so called renewal type and are included in systems treated by Dauer and Gahl [8].

##### Example 4.2

Take  $g = 0$  in Example 1. Then note that  $f$  is independent of  $\dot{x}(\cdot)$  and has an  $E^n$  space domain, which is a characteristic of perturbation functions used in other treatments of controllability. But, if  $f$  depends on  $\dot{x}(\cdot)$  then in order to satisfy condition  $H_1$ , we must include function spaces in the domain of  $f$ , which is a characteristic of the perturbation functions treated in Gahl [14].

## CONCLUSION

We have studied the relative controllability of perturbed infinite neutral differential system with perturbation function having implicit derivative, and multiple lumped time varying delays in the control using the Schauder fixed point theorem. It was shown that, if the linear control system is relatively controllable, then the nonlinear system is relatively controllable provided that the perturbation function whose domain contains appropriate function spaces satisfies certain growth and continuity conditions.

## REFERENCES

1. A. S. C. Sinha, "Null controllability of nonlinear infinite delay systems with restrained control", *Int. J. Control* **42** (3) 735-741 (1985)
2. E. N. Chukwu, "Control in  $W_2^{(1)}$  of nonlinear interconnected systems of neutral type", *J. Austral. Math. Soc. Series B* **36** 286 – 312 (1994)
3. I. Davies, "Euclidean null controllability of infinite neutral differential systems", *ANZIAM J.* **48** 1-9 (2006)
4. J. H. Park, "Simple criteria for stability of interval neutral delay differential system", *Applied Mathematics Letter* **16**(7) 1063-1068 (2003)
5. J. Klamka, "Relative controllability of nonlinear systems with delays in control", *Automatica*, **12**(6) 633-634 (1976)
6. J. K. Hale and S.M. Verduyn Lunel, *Introduction to Functional Differential Equations* (Applied Mathematical Sciences Volume 99). Springer-Verlag, New York, 1993.
7. J. P. Dauer, "Nonlinear perturbations of Quasi-linear control systems", *J. Math. Anal. Appl.* **54** 717-725 (1976)
8. J. P. Dauer and R.D Gahl, "Controllability of nonlinear delay systems", *Journal of Optimization Theory and Application* **21**(1) 59-70 (1977).
9. J. U. Onwuatu, "Null controllability of nonlinear infinite neutral systems", *Kybernetika* **29** 325-336 (1993)
10. J. Xu, Z. Wang and Z. Zheng, "On the existence of almost periodic solutions of neutral functional differential equations", *EJQTDE* **4** 1-9 (1998)
11. K. Balachandran and P. Balasubramaniam, "Controllability of nonlinear neutral Volterra integrodifferential systems", *J. Austral. Math. Soc. Ser. B* **36** 107-116 (1994)
12. K. Balachandran and E. R. Anandhi, "Controllability of neutral functional integrodifferential infinite delay systems in Banach Spaces", *Taiwanese Journal of Mathematics* **8** (4) 689 – 702 (2004)



13. N. I. Mahmudov and S. Zorlu, "Approximate controllability of semilinear neutral systems in Hilbert spaces", *J. Applied Mathematics and Stochastic analysis*, **16** 233-242 (2003)
14. R. D. Gahl, "Controllability of nonlinear system of neutral type", *Journal of Mathematical Analysis and Applications* **63** 33 – 42 (1978).
15. X. Fu, "Controllability of neutral functional differential systems in abstract space," *J. Applied Mathematics and Computation* **141** 281-296 (2003)
16. Y. Kuang and A. Feldstein, "Boundedness of solutions of nonlinear non-autonomous neutral delay equation", *Journal of Mathematical Analysis and Application* **156** 293 - 304 (1991).

---

**Instructions to Contributors**  
**Journal of Concrete and Applicable Mathematics**  
A quarterly international publication of Eudoxus Press, LLC, of TN.

**Editor in Chief: George Anastassiou**  
Department of Mathematical Sciences  
University of Memphis  
Memphis, TN 38152-3240, U.S.A.

**1. Manuscripts hard copies in triplicate, and in English, should be submitted to the Editor-in-Chief:**

**Prof. George A. Anastassiou**  
Department of Mathematical Sciences  
The University of Memphis  
Memphis, TN 38152, USA.  
Tel. 901.678.3144  
e-mail: [ganastss@memphis.edu](mailto:ganastss@memphis.edu)

**Authors may want to recommend an associate editor the most related to the submission to possibly handle it.**

**Also authors may want to submit a list of six possible referees, to be used in case we cannot find related referees by ourselves.**

**2. Manuscripts should be typed using any of TEX, LaTeX, AMS-TEX, or AMS-LaTeX and according to EUDOXUS PRESS, LLC. LATEX STYLE FILE. (Click [HERE](#) to save a copy of the style file.) They should be carefully prepared in all respects. Submitted copies should be brightly printed (not dot-matrix), double spaced, in ten point type size, on one side high quality paper 8(1/2)x11 inch. Manuscripts should have generous margins on all sides and should not exceed 24 pages.**

**3. Submission is a representation that the manuscript has not been published previously in this or any other similar form and is not currently under consideration for publication elsewhere. A statement transferring from the authors (or their employers, if they hold the copyright) to Eudoxus Press, LLC, will be required before the manuscript can be accepted for publication. The Editor-in-Chief will supply the necessary forms for this transfer. Such a written transfer of copyright, which previously was assumed to be implicit in the act of submitting a manuscript, is necessary under the U.S. Copyright Law in order for the publisher to carry through the dissemination of research results and reviews as widely and effectively as possible.**

**4. The paper starts with the title of the article, author's name(s) (no titles or degrees), author's affiliation(s) and e-mail addresses. The affiliation should comprise the department, institution (usually university or company), city, state (and/or nation) and mail code.**

**The following items, 5 and 6, should be on page no. 1 of the paper.**

**5. An abstract is to be provided, preferably no longer than 150 words.**

**6. A list of 5 key words is to be provided directly below the abstract. Key words should express the precise content of the manuscript, as they are used for indexing purposes.**

**The main body of the paper should begin on page no. 1, if possible.**

**7. All sections should be numbered with Arabic numerals (such as: 1. INTRODUCTION) .**

**Subsections should be identified with section and subsection numbers (such as 6.1. Second-Value Subheading).**

**If applicable, an independent single-number system (one for each category) should be used to label all theorems, lemmas, propositions, corrolaries, definitions, remarks, examples, etc. The label (such as Lemma 7) should be typed with paragraph indentation, followed by a period and the lemma itself.**

**8. Mathematical notation must be typeset. Equations should be numbered consecutively with Arabic numerals in parentheses placed flush right, and should be thusly referred to in the text [such as Eqs.(2) and (5)]. The running title must be placed at the top of even numbered pages and the first author's name, et al., must be placed at the top of the odd numbed pages.**

**9. Illustrations (photographs, drawings, diagrams, and charts) are to be numbered in one consecutive series of Arabic numerals. The captions for illustrations should be typed double space. All illustrations, charts, tables, etc., must be embedded in the body of the manuscript in proper, final, print position. In particular, manuscript, source, and PDF file version must be at camera ready stage for publication or they cannot be considered.**

**Tables are to be numbered (with Roman numerals) and referred to by number in the text. Center the title above the table, and type explanatory footnotes (indicated by superscript lowercase letters) below the table.**

**10. List references alphabetically at the end of the paper and number them consecutively. Each must be cited in the text by the appropriate Arabic numeral in square brackets on the baseline.**

**References should include (in the following order):  
initials of first and middle name, last name of author(s)  
title of article,**

name of publication, volume number, inclusive pages, and year of publication.

Authors should follow these examples:

### **Journal Article**

1. H.H.Gonska, Degree of simultaneous approximation of bivariate functions by Gordon operators, (journal name in italics) *J. Approx. Theory*, 62,170-191(1990).

### **Book**

2. G.G.Lorentz, (title of book in italics) *Bernstein Polynomials* (2nd ed.), Chelsea, New York, 1986.

### **Contribution to a Book**

3. M.K.Khan, Approximation properties of beta operators, in (title of book in italics) *Progress in Approximation Theory* (P.Nevai and A.Pinkus, eds.), Academic Press, New York, 1991, pp.483-495.

11. All acknowledgements (including those for a grant and financial support) should occur in one paragraph that directly precedes the References section.

12. Footnotes should be avoided. When their use is absolutely necessary, footnotes should be numbered consecutively using Arabic numerals and should be typed at the bottom of the page to which they refer. Place a line above the footnote, so that it is set off from the text. Use the appropriate superscript numeral for citation in the text.

13. After each revision is made please again submit three hard copies of the revised manuscript, including in the final one. And after a manuscript has been accepted for publication and with all revisions incorporated, manuscripts, including the TEX/LaTeX source file and the PDF file, are to be submitted to the Editor's Office on a personal-computer disk, 3.5 inch size. Label the disk with clearly written identifying information and properly ship, such as:

Your name, title of article, kind of computer used, kind of software and version number, disk format and files names of article, as well as abbreviated journal name.

Package the disk in a disk mailer or protective cardboard. Make sure contents of disks are identical with the ones of final hard copies submitted!

Note: The Editor's Office cannot accept the disk without the accompanying matching hard copies of manuscript. No e-mail final submissions are allowed! The disk submission must be used.

14. Effective 1 Nov. 2009 for current journal page charges, contact the Editor in Chief. Upon acceptance of the paper an invoice will be sent to the contact author. The fee payment will be due one month from the invoice date. The article will proceed to publication only after the fee is paid. The charges are to be sent, by money order or certified check, in US dollars, payable to Eudoxus Press, LLC, to the address shown on

the Eudoxus [homepage](#).

No galley proofs will be sent and the contact author will receive one(1) electronic copy of the journal issue in which the article appears.

15. This journal will consider for publication only papers that contain proofs for their listed results.

# TABLE OF CONTENTS, JOURNAL OF CONCRETE AND APPLICABLE MATHEMATICS, VOL. 9, NO. 4, 2011

<b>Particles Flow on the Regular Polygon,</b> Alexander P. Buslaev , Alexander G. Tatashev,.....	290
Notes on absolute summability factors, W. T. Sulaiman,.....	304
Necessary and Sufficient Conditions for Inclusion Relations for Absolute Summability of Infinite Series, W. T. Sulaiman,.....	311
On A Characterization Of Absolute Summability Factors, W. T. Sulaiman,.....	319
A Summability Factor Theorem For Absolute Summability Involving quasi $\beta$ -Power Increasing Sequences, W. T. Sulaiman,.....	328
Tail behavior for nonstationary moving averages with random coefficients, Aliou Diop , Saliou Diouf,.....	336
Relative controllability of perturbed infinite Neutral differential systems, Davies Iyai,.....	346